

Activation and Inactivation of the Complement
Anaphylatoxins During Chronic Neutrophilic
Inflammation of the Cystic Fibrosis Airway

Matthew Stott BSc

Thesis submitted for the Degree of Doctor of Philosophy
September 2018

Institute of Infection and Immunity
Cardiff University
School of Medicine
Heath Park
Cardiff
CF14 4XN

DECLARATION

This work has not been submitted in substance for any other degree or award at this or any other university or place of learning, nor is being submitted concurrently in candidature for any degree or other award.

Signed (candidate) Date
.....

STATEMENT 1

This thesis is being submitted in partial fulfillment of the requirements for the degree of(insert MCh, MD, MPhil, PhD etc, as appropriate)

Signed (candidate) Date
.....

STATEMENT 2

This thesis is the result of my own independent work/investigation, except where otherwise stated, and the thesis has not been edited by a third party beyond what is permitted by Cardiff University’s Policy on the Use of Third Party Editors by Research Degree Students. Other sources are acknowledged by explicit references. The views expressed are my own.

Signed (candidate) Date
.....

STATEMENT 3

I hereby give consent for my thesis, if accepted, to be available online in the University’s Open Access repository and for inter-library loan, and for the title and summary to be made available to outside organisations.

Signed (candidate) Date
.....

STATEMENT 4: PREVIOUSLY APPROVED BAR ON ACCESS

I hereby give consent for my thesis, if accepted, to be available online in the University’s Open Access repository and for inter-library loans **after expiry of a bar on access previously approved by the Academic Standards & Quality Committee.**

Signed (candidate) Date
.....

Dedication

I would like to dedicate this thesis to my wife Frankie, who gave me unwavering support and encouragement from beginning to end. Her calming influence has kept me positive and focused throughout, thank you.

Acknowledgements

I wish to thank Dr. Eamon McGreal for his supervision throughout my project. He has been and will continue to be an excellent role model and mentor who has continually supported and challenged me.

I would like to thank Dr. Carmen van den Berg who initially introduced me to the laboratory 10 years ago and encouraged me to apply for this project. Her encouragement and guidance throughout my PhD will always be greatly appreciated.

I would like to thank Prof. Paul B. Morgan who gave me crucial feedback throughout my study. He invited me to join his laboratory and the Complement Biology Group and gave me the opportunities to progress my development.

Thank you to Dr. Julian Forton for collecting the patient samples and providing expertise on cystic fibrosis.

Thank you to Dr. Peter Monk for the RBL-C5aR1 and RBL-C3aR cell lines that were crucial for this project.

I would like to thank Complement UK for the opportunity to study for a PhD in complement biology. I also wish to thank Alexion for my funding via their educational grant.

I would like to thank Dr. Samuel Touchard for his expertise in statistics. I wish to thank James Wheeldon for his critical feedback and encouragement during my time in the Henry Wellcome Building. Thank you to the members of the Complement Biology Group, particularly Dina Fathalla, David Walters and Wiola Zelek, for their help and feedback over the past 4 years.

Summary

Cystic fibrosis (CF) is a fatal genetic disease that affects 1/2500 people in the UK. Mutations in the cystic fibrosis transmembrane conductance regulator (CFTR) cause dehydration of mucosal membranes, leading to mucus obstruction of the small airways. The CF lungs are susceptible to recurrent infection promoting chronic neutrophilic inflammation. Neutrophils recruited to the CF lungs become dysfunctional and are ineffective at clearing pathogens, perpetuating inflammation. Neutrophil serine proteases (NSPs) released by neutrophils collaterally remodel the airway, reducing lung function and causing mortality.

The complement anaphylatoxins (C5a and C3a) are important mediators of inflammation. C5a and C3a are chemotactic for monocytes and granulocytes, they also stimulate degranulation and the generation of reactive oxygen species (ROS). C5a is particularly potent towards neutrophils and is critical for orchestrating their response towards pathogens. C5a and C3a are elevated in the CF airway. Furthermore, in addition to complement activation these anaphylatoxins can be generated by non-complement proteases including NSPs. The mechanisms by which C5a and C3a promote chronic neutrophilic inflammation in the CF airways are not fully understood.

In my study I show that C5a and C3a correlate with markers of neutrophilic inflammation (neutrophil count and CXCL8) in bronchoalveolar lavage (BAL) fluid from paediatric CF patients. I further characterise the generation of functionally active C5a-like and C3a-like forms by NSPs. Moreover, I demonstrate that atypical C5a production by NSPs cannot be prevented by therapeutic complement inhibitors. I show for the first time that NSP-generated C5a-like fragments are resistant to inactivation by carboxypeptidase B, an important regulator of C5a activity.

I also further characterise the interaction between C5a and soluble glycosaminoglycans (GAGs), these are abundant during chronic neutrophilic inflammation of the CF airway. Additionally, I show that GAG interaction influences C5a activity. In conclusion, the CF airway environment modifies C5a function; these mechanisms could promote chronic neutrophilic inflammation.

Abbreviations

A. fumigatus - *Aspergillus fumigatus*

AAT – alpha-1-anti-trypsin

ABPA – allergic bronchopulmonary aspergillosis

ACP - acylation-stimulating protein

aHUS - atypical hemolytic uremic syndrome

AMD - age-related macular degeneration

ARDS – acute respiratory distress syndrome

BAL – bronchoalveolar lavage

BCA - bicinchoninic acid

BLTR – leukotriene receptor

BMI – body mass index

BN-PAGE – blue native PAGE

BSA – bovine serum albumin

C – complement component (e.g. C5a)

CaCC – calcium activated chloride channel

C. albicans - *Candida albicans*

CAR - coxsackie and adenovirus receptors

CD – cluster of differentiation (e.g. CD44)

CDR – complementarity determining region

CF – cystic fibrosis

CFTR - cystic fibrosis transmembrane conductance regulator

CG – cathepsin G

CHIPS - chemotaxis inhibitory protein expressed by *Staphylococcus aureus*

COPD – chronic obstructive pulmonary disease

CPB – carboxypeptidase B

CPN – carboxypeptidase N

CR – complement receptor

CS – chondroitin sulphate

CT - computerised tomography

C3aR – C3a receptor

C5aR – C5a receptor

C/EBPa - (CCAAT/ enhancer binding protein a)

Da - dalton

DAMP – damage associated molecular pattern

DNA – deoxyribonucleic acid

ECL – enhanced chemiluminescence substrate
ECM – extracellular matrix
EGTA - ethylene glycol-bis(β -aminoethyl ether)-N,N,N',N'-tetraacetic acid
ELISA – enzyme linked immunosorbent assay
ENaC – epithelial sodium channel
ER – endoplasmic reticulum
ERS – European Respiratory Society
FasL – first apoptosis signal ligand
FcR – fragment crystallisable region receptor
FEV1 – forced expiratory volume in 1 second
fMLP – formyl-Met-Leu-Pro
FPR – formyl peptide receptor
FRET - Forster resonance energy transfer
ESL-1 - E-selectin-ligand
g - gram
GAG - glycosaminoglycan
GI – gastrointestinal
GPI - Glycosylphosphatidylinositol
HA – hyaluronic acid
HMGB - high mobility group box 1 protein
HRP – horse radish peroxidase
HS – heparan sulphate
HTA – Human Tissue Act
ICAM - intercellular adhesion molecules
Ig - immunoglobulin
IL – interleukin
ITAMs - immunoreceptor tyrosine-based activation motifs
JAM - junctional adhesion molecule
k – kilo (10^3) (prefix)
L – litre
LFA - lymphocyte function-associated antigen-1
LPS – lipopolysaccharide
LTB₄ – leukotriene B₄
m – metre (unit)
m – milli (10^{-3}) (prefix)
M - Molar
M – mega (10^6) (prefix)

MAC – membrane attack complex
MAPK - mitogen-activated protein kinase
MASP - mannose-binding lectin associated protease
MBL – mannose binding lectin
MCP-1 – macrophage chemoattractant protein-1
MES - 2-(N-morpholino)ethanesulfonic acid
MG – alpha-2-macroglobulin
MHC – major histocompatibility complex
MMP – matrix metalloprotease
MMR – macrophage mannose receptor
MPO – myeloperoxidase
n – nano (10^{-9}) (prefix)
NADPH - Nicotinamide adenine dinucleotide phosphate
nC5a – native human C5a (generated by C5-convertase)
NE – human neutrophil elastase
NET – neutrophil extracellular trap
NLR – NOD-like receptor
NMR - nuclear magnetic resonance spectroscopy
NOD - nucleotide-binding oligomerisation domain
NRA - orphan nuclear receptor
NSP – neutrophil serine protease
ORAI - calcium release-activated calcium channel protein
p – pico (10^{-12}) (prefix)
P. aeruginosa – *Pseudomonas aeruginosa*
Pa - pascal
PAF – platelet activating factor
PAFR – protease activated receptor
PAGE – polyacrylamide gel electrophoresis
PAMP – pathogen associated molecular pattern
PAR - protease activated receptor
PBS – phosphate buffered saline
PCR – polymerase chain reaction
PGP - Pro-Gly-Pro
PI3K - phosphatidylinositol 3-kinase
PK3 – Protein kinase 3
PLC - phospholipase C
PMA - phorbol 12-myristate 13-acetate

PMN – polymorphonuclear leukocyte
PNH - paroxysmal nocturnal hemoglobinuria
PRR – pathogen recognition receptor
PR3 – proteinase 3
PSGL-1 - P-selectin glycoprotein ligand-1
RBL – rat basophil leukaemia
rhC5a – recombinant human C5a
RIA – radio immunoassay
RIP - receptor-interacting serine-threonine protein kinase
ROS – reactive oxygen species
RPM – revolutions per minute
rRNA – ribosomal ribonucleic acid
SDS - sodium dodecyl sulphate
SD75 – Superdex 75
siRNA – small interfering RNA
SLPI – secretory leukocyte protease inhibitor
STIM - stromal interaction molecules
TEMED - tetramethylethylenediamine
TGF β – transforming growth factor β
Th – T helper cell
TLR – toll-like receptor
TMB - 3,3',5,5'-Tetramethylbenzidine
TNF α - tumour necrosis factor alpha
TNF β - tumour necrosis factor β
TRAF - TNF receptor associated factors
TRIS - 2-Amino-2-(hydroxymethyl)-1,3-propanediol
UK – United Kingdom
 μ - micro (10^{-6}) (prefix)
VLA - very late antigen

Table of Contents

1. Introduction	11
1.1. Clinical description of CF	11
1.2. Pathogens in the CF airway	16
1.3. Inflammation	19
1.3.1. Inflammation in the normal airway	22
1.3.2. Inflammation in the CF airway	27
1.4. Biology of neutrophils	30
1.4.1. Differentiation	30
1.4.2. Effector functions	31
1.4.3. Neutrophil cell surface receptors	32
1.4.4. Neutrophil chemotaxis	40
1.4.5. Phagocytosis	48
1.4.6. ROS production	49
1.4.7. Degranulation	49
1.4.8. NET formation	55
1.5. Neutrophilic inflammation in CF airway	57
1.5.1. Neutrophil PPR expression in the CF airway	57
1.5.2. NSPs in the CF airway	58
1.5.3. Dysfunction in ROS in the CF airway	60
1.5.4. NSP inhibitors in the CF airway	61
1.5.5. NETs	62
1.5.6. Resolution of inflammation	63
1.5.7. GAGs in the CF airway	64
1.5.8. Neutrophil recruitment in the CF airway	66
1.6. The Complement system	68
1.6.1. Initiation and activation.	69
1.6.2. Complement effector functions	71
1.6.3. Regulation of complement	72
1.6.4. Non-canonical activation of complement by endogenous and exogenous proteases	73
1.6.5. Complement in disease	73
1.6.6. Complement and inflammation	75
1.7. C5a	76
1.7.1. C5a structure	76
1.7.2. Regulation of C5a activity	76
1.7.3. Receptors for C5a / C5adesArg	78

1.7.4.	C5a Function	81
1.7.5.	Pathogenic roles of C5a.....	83
1.7.6.	C5a in the CF airway	85
1.8.	C3a.....	87
1.8.1.	Structure and regulation.....	87
1.8.2.	Receptors for C3a / C3adesArg	88
1.8.3.	The pathogenic roles of C3a	90
1.8.4.	C3a in the CF airway	92
1.9.	Summary and background to the project.....	93
1.10.	Hypothesis	94
1.11.	Aims	94
2.	Materials and methods.....	95
2.1.	Buffers and solutions	95
2.1.1.	Phosphate buffered saline (PBS), pH 7.4.....	95
2.1.2.	PBS-tween (PBS-T), pH 7.5.....	95
2.1.3.	Bovine serum albumin (BSA)	95
2.1.4.	1 M trisamino(hydroxy)methane (TRIS), pH 7.5	95
2.1.5.	1 M NaCl.....	96
2.1.6.	NE activity buffer.....	96
2.1.7.	Carbonate buffer (2%) – ELISA capture antibody diluent	96
2.1.8.	0.1 M Citrate buffer for β -hexosaminidase release experiments	96
2.1.9.	Solid phase binding assay buffer	97
2.1.10.	Complement haemolysis assay buffer	97
2.2.	Complement proteins, Proteases, Protease inhibitors, glycosaminoglycans	98
2.3.	Antibodies	99
2.4.	BAL fluid sample processing	100
2.5.	CF cohort characterisation	101
2.5.1.	Differential cell counts.....	101
2.5.2.	NE activity assay	105
2.5.3.	CXCL8	105
2.5.4.	Complement Meso Scale Discovery (MSD) multiplex platforms	106
2.6.	C5 ELISA.....	107
2.6.1.	C3a ELISA.....	108
2.6.2.	C5a ELISAs	109
2.6.3.	Total protein.....	110
2.6.4.	CPB and CPN activity assay.....	111
2.6.5.	Dimethyl methylene blue staining – GAG quantification	111

2.7.	Protease cleavage experiments	112
2.7.1.	Proteolysis of C3a or C5a by proteases present in CF BAL fluid.....	112
2.7.2.	Generation of C3a and C5a by proteases present in CF BAL fluid.....	113
2.7.3.	Generation of C3a and C5a by purified NSPs.....	113
2.7.4.	Inactivation of C3a and C5a by porcine CPB	113
2.8.	Polyacrylamide gel electrophoresis (PAGE).....	114
2.8.1.	SDS-PAGE	114
2.8.2.	Native PAGE.....	114
2.8.3.	Blue native-PAGE (BN-PAGE).....	115
2.8.4.	Silver staining	115
2.8.5.	Western blotting.....	115
2.9.	Cell reporter assays	117
2.9.1.	Cell culture.....	117
2.9.2.	Intracellular calcium signalling assay	117
2.10.	Classical pathway complement haemolysis assay	119
2.10.1.	Sheep erythrocyte sensitisation.....	119
2.10.2.	Haemolysis assay	119
2.11.	Fluid-phase column chromatography	120
2.11.1.	Size exclusion chromatography.....	120
2.11.2.	Affinity chromatography.....	120
2.12.	Solid phase binding assay: C5a – GAG interaction.....	121
2.12.1.	Biotinylation of HS.....	121
2.13.	Solid phase binding assay	121
2.14.	Statistics	122
3.	Characterising C3a and C5a in bronchoalveolar lavage fluid from a cohort of CF patients	123
3.1.	Background to the study	123
3.1.1.	Fluid sampling in airway disease and CF	124
3.1.2.	Using airway fluid to investigate neutrophilic inflammation in the CF airway	131
3.1.3.	Investigating the role of complement in promoting neutrophilic inflammation in the CF airway.....	132
3.2.	Hypothesis.....	135
3.3.	Aims	135
3.4.	Airway sampling and correcting for repeated measures.....	136
3.5.	Clinical description of the CF cohort.....	138
3.6.	Characterising neutrophilic inflammation in CF BAL fluid	140
3.7.	Complement in the CF airway.....	142
3.7.1.	Developing an in-house ELISA for the detection of C5.....	143

3.7.2.	Correlating complement with markers of neutrophilic inflammation	144
3.7.3.	Assessing the relative levels of complement in CF BAL fluid	146
3.8.	Correlating C3a with markers of neutrophilic inflammation in the CF airway	149
3.9.	Correlating C5a with markers of neutrophilic inflammation in the CF airway	153
3.10.	Stratification of the CF cohort for further analysis of C3a and C5a as pathogenic factors	155
3.11.	Discussion	159
3.12.	Conclusion to the chapter	167
4.	Generation of C5a and C3a by neutrophil serine proteases in the CF airway.....	168
4.1.	Background to the study	168
4.1.1.	Atypical generation of C3a and C5a by non-complement proteases	168
4.1.2.	Generation of functional forms of C3a and C5a by NSPs.....	170
4.1.3.	Generation of C3a and C5a by proteases present during airway disease	171
4.1.4.	Generation of C5a by proteases present in the CF airway	171
4.2.	Hypothesis.....	173
4.3.	Chapter aims	173
4.4.	Evidence of C3a and C5a generation by NSPs in the CF airway.	174
4.4.1.	Evidence of complement activation and generation of C3a and C5a.....	174
4.4.2.	Evidence for the generation of C3a and C5a by NE in the CF airway	176
4.5.	Degradation of C5a and C3a by proteases present in the in the CF airway	177
4.5.1.	Optimising the visualisation of C5a on SDS-PAGE.	178
4.5.2.	Proteolysis of C5a by purified NSPs	179
4.5.3.	Degradation of C5a by proteases in CF BAL fluid	181
4.5.4.	C3a proteolysis by purified NSPs.....	182
4.6.	Generation of C3a and C5a by proteases present in CF BAL fluid.....	184
4.7.	Generation of functional C5a-like fragments by purified NSPs	186
4.7.1.	Visualising NSP-generated C5a by SDS-PAGE and Western blot	186
4.7.2.	Assessing the functional activity of NSP-generated C5a-like fragments using a U937-C5aR1 reporter cell line.....	188
4.7.3.	Comprehensive analysis of C5a-like fragments generated by NSPs.....	191
4.8.	C3a generation by NSPs.....	200
4.8.1.	Optimisation of a C3a activity assay for measuring the activity of C3-like fragments.....	202
4.8.2.	Activity of C3a-like fragments generated by NSPs	203
4.9.	Functional differences in alternatively generated forms of C3a and C5a	206
4.9.1.	Measuring CPB and CPN activity in CF BAL fluid.	206
4.9.2.	A RBL-C5aR1 reporter cell line for measuring C5a activity	207
4.9.3.	Inactivation of native C3a and C5a by porcine CPB.....	209

4.9.4.	CPB inactivation of C3a and C5a forms generated by NSPs	209
4.10.	Discussion	213
4.10.1.	Evidence for C3a and C5a generation by NSPs in the CF airway.....	213
4.10.2.	Comparing NSP proteolysis of recombinant and native C5a forms.....	214
4.10.3.	Generation of C3a-like and C5a-like fragments by proteases present in CF BAL fluid	214
4.10.4.	Generation of functional C3a-like forms by purified NSPs	216
4.10.5.	Generation of functional C5a-like forms by purified NSPs	217
4.10.6.	Assessing C5 function following exposure to purified NSPs	217
4.10.7.	Investigating CPB inactivation of C3a-like and C5a-like fragments.....	218
4.11.	Conclusion to the chapter	223
5.	Generation of C5a-like fragments by neutrophil serine proteases in the presence of C5 cleavage inhibitors	224
5.1.	Background to the chapter	224
5.2.	Hypothesis	229
5.3.	Aims	229
5.4.	Comparison of the activity of four therapeutic C5 cleavage inhibitors using a haemolysis assay	230
5.5.	Generation of C5a by NSPs in the presence of four C5 cleavage inhibitors	231
5.5.1.	Visualising C5a-like fragments generated by NSPs	232
5.5.2.	Quantifying the generation of C5a by NSPs in the presence of therapeutic C5 cleavage inhibitors	234
5.5.3.	Assessing the activity of C5a-like fragments generated by NSPs in the presence of therapeutic C5-cleavage inhibitors.....	236
5.6.	Investigating inactivation of therapeutic C5 cleavage inhibitors by NE	238
5.7.	Susceptibility of therapeutic C5 cleavage inhibitors to proteolysis by NE	239
5.8.	Discussion	241
5.9.	Conclusion to the chapter	246
6.	Characterising interactions between C5a and glycosaminoglycans.....	247
6.1.	Background to the chapter	247
6.1.1.	Structure of GAGs and their diversity	247
6.1.2.	Functional roles of GAGs in inflammation	249
6.1.3.	The role of GAGs in the CF airway	250
6.1.4.	Interaction between CXCL8 and GAGs in the CF airway	253
6.1.5.	Interactions between C5a and GAGs.....	254
6.2.	Hypothesis	255
6.3.	Aims for this chapter	255
6.4.	Sulphated GAG expression in the CF airway	256
6.4.1.	Quantifying soluble GAGs in CF BAL fluid	256

6.4.2.	Correlations between GAGs and markers of neutrophilic inflammation in CF BAL fluid	258
6.5.	Characterisation of C5a-GAG interactions by PAGE	259
6.5.1.	Resolving nC5a and rhC5a by native-PAGE and BN-PAGE	259
6.5.2.	Separating C5a and C5a-GAG complexes using BN-PAGE	261
6.6.	Using size exclusion chromatography to characterise C5a-GAG complexes.....	262
6.6.1.	Optimising an in-house ELISA for detection of C5a in column eluate	262
6.6.2.	Separating C5a-GAG complexes using a SD75 column	265
6.6.3.	Investigating low C5a recovery from SD75 column	265
6.6.4.	Separating C5a-GAG complexes on a Superose 6 column.....	269
6.7.	Characterising C5a-GAG interaction using a heparin-sepharose affinity column.	270
6.8.	Solid phase plate assay for detection of C5a-GAG binding	272
6.8.1.	Optimisation of solid phase C5a-GAG binding assay	273
6.8.2.	Characterisation of C5a-GAG binding using solid phase plate assay	275
6.8.3.	Investigating binding of HS to other complement components	278
6.9.	Functional significance of C5a-HS interaction	279
6.9.1.	Effects of HS binding on C5a function.....	280
6.9.2.	Testing the ability of HS to protect C5a from degradation by NE.....	280
6.9.3.	Influence of HS on the inactivation of C5a by CPB	283
6.10.	Discussion	285
6.11.	Conclusion to the chapter	290
7.	Final summary	291
7.1.	Limitations to the study	291
7.2.	What does my research mean for CF?.....	294
7.3.	CF therapeutics – what is the future?.....	296
7.4.	Do we need to research the roles C5a (and C3a) in CF pathogenesis?.....	297
7.5.	The importance of Complement.....	298
7.6.	Immune modulation by NSPs.....	300
7.7.	Conclusion to the chapter	301
7.8.	Key findings from my study	302
7.9.	Future Work.....	302
8.	References	303

List of figures

Figure 1-1: Diagram of hydration in normal and CF airways.....	11
Figure 1-2: UK CF population by age.....	14
Figure 1-3: Diagram of different organs where CF pathology manifests.....	15
Figure 1-4 Bacterial infections in the UK CF population.....	17
Figure 1-5: Diagram of the normal healthy airway.....	23
Figure 1-6 Diagram of neutrophil transendothelial and transepithelial migration.....	24
Figure 1-7 Diagram representing some of roles for the different cell types in the CF airway and how they contribute to CF airway pathology.....	29
Figure 1-8: Diagram of neutrophil differentiation and granulopoiesis.....	31
Figure 1-9 Neutrophil effector functions.....	32
Figure 1-10: G-protein couple receptor signalling pathways and functions.....	33
Figure 1-11: Diagram of G-protein coupled receptor internalisation.....	34
Figure 1-12: Cytokine receptor signalling pathways and functions.....	37
Figure 1-13: Pattern recognition receptor signalling pathways and functions.....	39
Figure 1-14: Diagram of neutrophil polarisation during chemotaxis.....	41
Figure 1-15: Arachidonic metabolites and their receptors.....	46
Figure 1-16 Diagram of the process of phagocytosis.....	48
Figure 1-17: Protease and anti-protease balance in the normal and chronically inflamed airway.....	61
Figure 1-18: Overview of the reported mechanisms of neutrophil dysfunction in the CF airway.....	65
Figure 1-19 Diagram of the complement system and its functions and regulation.....	70
Figure 1-20: Diseases where complement has been reported to contribute to pathogenesis.....	74
Figure 1-21: Amino acid sequence and secondary structure of C5a/C5adesArg.....	77
Figure 1-22: N-glycosylation of C5a/C5adesArg.....	78
Figure 1-23: Amino acid sequences and structures of C5aR1 and C5aR2.....	79
Figure 1-24 Comparing tertiary structures of C5a and C3a.....	87
Figure 1-25: Amino acid sequence and secondary structure of C3a.....	88
Figure 1-26: Functions of C3a are dependent on cell type.....	89
Figure 2-1: A typical example of a captured field from a cytopins.....	104
Figure 3-1: Diagram of the lobes in the human lungs.....	125
Figure 3-2: Effect of repeated measures on sample population levels of CXCL8.....	137
Figure 3-3: Analysis of clinical parameters and neutrophilic inflammation in the CF cohort.....	139
Figure 3-4: Influence of a serine protease inhibitor on CXCL8 levels measured by ELISA.....	140
Figure 3-5: Correlations between markers of neutrophilic inflammation measured in CF BAL fluid.....	141
Figure 3-6: Developing a sensitive ELISA for the quantification of C5 in CF BAL fluid.....	143
Figure 3-7: Correlations between markers of neutrophilic inflammation and complement component measured in CF BAL fluid.....	145
Figure 3-8: The relationship between C3a and neutrophilic inflammation in CF BAL fluid.....	150
Figure 3-9: Comparing quantification of C3a measured by singleplex (ELISA) and multiplex (MSD) platforms.....	152
Figure 3-10: The relationship between C5a and neutrophilic inflammation in CF BAL fluid.....	154
Figure 3-11: Comparing neutrophilic inflammation and complement following stratification of the CF cohort.....	157
Figure 3-12: Median percentage predicted FEV1 in CF patients over 6 years.....	160
Figure 4-1: Evidence of C3a and C5a generation in BAL fluid from the CF airway.....	174

Figure 4-2: Evidence of normal complement activity in BAL fluid from the CF cohort	175
Figure 4-3: Correlation of C3 and C5 proteolysis by NE in BAL fluid from CF patients.	176
Figure 4-4: Evidence of C3a and C5a generation by NE in BAL fluid from CF patients.	177
Figure 4-5: Recombinant C5a and native C5a separation and detection by SDS-PAGE and Western blot.....	178
Figure 4-6: Proteolysis of C5a by purified NSPs.....	180
Figure 4-7: Degradation of C5a by proteases present in BAL fluid from CF patients.	181
Figure 4-8: Proteolysis of C3a by purified NSPs.....	183
Figure 4-9: C3a and C5a generation by proteases expressed in BAL fluid from the CF cohort.....	184
Figure 4-10: Generation of C5a-like fragments by NSPs.....	186
Figure 4-11: Optimising a U937-C5aR1 C5a reporter assay.	189
Figure 4-12: Assessing the activity of NSP-generated C5a using U937-C5aR1 cells.	190
Figure 4-13: Quantification of C5a generation by NSP proteolysis of C5.....	192
Figure 4-14: Simplified structural diagram of C5.....	193
Figure 4-15: Quantification of C5 following exposure to NSPs.	194
Figure 4-16: Percentage conversion of C5 to C5a and other non-C5a intermediates.	195
Figure 4-17: Determining the concentration of C5 required for 50% lysis in 1 % C5-depleted serum.....	197
Figure 4-18: Assessing C5 activity following exposure to NSP.....	198
Figure 4-19: Generation of C3a-like fragments by purified NSPs.	200
Figure 4-20: Resolving NSP-generated C3a fragments on 20% polyacrylamide gels.....	201
Figure 4-21: Example of a standard curve for RBL-C3aR β -hexosaminidase reporter assay.	203
Figure 4-22 Assessing the activity of C3a-like fragments generated by NSP.	204
Figure 4-23: Quantifying CPB and CPN activity in CF BAL fluid.....	206
Figure 4-24: Optimisation of RBL-C5aR1 C5a reporter assay.....	208
Figure 4-25: Inactivation of native C5a and C3a by porcine CPB.....	209
Figure 4-26: Inactivation of NSP-generated C5a-like fragments by porcine CPB.	210
Figure 4-27: Inactivation of CG-generated C3a-like fragments by porcine CPB.	212
Figure 4-28: Diagram of the role of NSP-generated C5a in the CF airway.	219
Figure 4-29: Amino acid sequence of C5a and predicted preferential cleavage sites for NE and PR3.....	220
Figure 4-30: Amino acid sequence C3a and predicted preferential cleavage site of CG and PR3.....	221
Figure 5-1: Complement therapeutics, their target pathway and phase in clinical trial.	225
Figure 5-2: Structures of OmCI and RaCI complexes and reported binding sites of Eculizumab and SKY59.	227
Figure 5-3: Comparing the activity of therapeutic C5 cleavage inhibitors.....	231
Figure 5-4: Visualising C5a-like fragments generated by NSPs when in the presence of therapeutic C5 cleavage inhibitors.	232
Figure 5-5: Quantifying NSP-generation of C5a-like fragments when in the presence of therapeutic C5 cleavage inhibitors.	234
Figure 5-6: Activity of C5a-like fragments generated by NSPs in the presence of therapeutic C5 cleavage inhibitors.....	236
Figure 5-7: Impact of NE on the function of therapeutic C5 cleavage inhibitors.....	238
Figure 5-8: Visualising degradation of therapeutic C5 cleavage inhibitors following exposure to NE.....	239
Figure 5-9: Diagram of the mechanisms by which NE could bypass C5 cleavage inhibitors.	244
Figure 6-1: Diagram of the carbohydrate composition of GAGs.	248

Figure 6-2: Proteoglycan cores and associated GAGs.....	249
Figure 6-3: Processing of HA during inflammation.	250
Figure 6-4: Chemotactic role of GAGs in the airway.....	253
Figure 6-5: Dimethyl-methylene blue stain assay for quantifying sulphated GAGs in CF BAL fluid.....	256
Figure 6-6: Soluble GAG concentration in CF BAL fluid.	257
Figure 6-7: Spearman rank correlation analysis of GAGs and markers of neutrophilic inflammation in CF BAL fluid.....	258
Figure 6-8: Comparing PAGE techniques for resolution of C5a and C5a-GAG complexes.	260
Figure 6-9: C5a and C5a-GAG complexes resolved by BN-PAGE.....	261
Figure 6-10: Diagram C5a ELISA and the antibodies used.	263
Figure 6-11: Optimisation of C5a ELISA to quantify C5a in column chromatography fractions.	264
Figure 6-12: A tube-based ELISA to detect C5a.....	266
Figure 6-13: Separation of nC5a and nC5a-HS complexes on SD75 column.....	267
Figure 6-14: Separation of C5a and C5a-GAG complexes by a Superose 6 column.....	269
Figure 6-15: Assessing binding of nC5a and nC5a-GAG complexes to a heparin affinity column.	271
Figure 6-16: Optimisation of solid phase binding assay.....	273
Figure 6-17: Influence of NaCl on C5a-HS interaction.....	275
Figure 6-18: Competition for nC5a-bioinylated-HS binding using unlabeled GAGs.	276
Figure 6-19: Comparing the binding of different complement components to HS.	278
Figure 6-20: Influence of HS on C5a activity.	280
Figure 6-21: Influence of HS of C5a inactivation by NE.	281
Figure 6-22: Quantifying NE proteolysis of C5a when in complex with HS.	282
Figure 6-23: Influence of HS on inactivation of C5a by CPB.....	283
Figure 6-24: Amino acid sequence of nC5a and rhC5a.....	286

List of tables

Table 1-1: <i>Cftr</i> mutation classes I-VI and diagrams describing phenotypes.....	13
Table 1-2: Diversity of pathogens associated with pulmonary infection in the CF airway.....	16
Table 1-3: Immune cells and their roles in inflammation.....	20
Table 1-4 Cell populations observed during chronic inflammation of the CF airway	27
Table 1-5: Neutrophil granules, the function of their contents.....	50
Table 1-6 Role of C5a in disease	83
Table 1-7 Quantification of C5a/C5adesArg in airway diseases	84
Table 1-8: Quantification of C3a/C3adesArg in airway diseases.	91
Table 2-1: Other reagents used in this study, where they came from, stock concentrations and storage conditions	98
Table 2-2: Antibodies used throughout project.	99
Table 2-3: Typical examples of cells identified in CF BAL fluid.....	103
Table 3-1 Control population used in studies reporting on BAL fluid.....	127
Table 3-2: Advantages and disadvantages of the different techniques used to sample the CF airway	130
Table 3-3: Uses of CF BAL fluid in this study.	134
Table 3-4: Clinical description of the CF cohort.....	138
Table 3-5: Comparing complement levels in CF BAL fluid with plasma from normal plasma.	147
Table 3-6: Justification for stratification of well and unwell CF patients	155
Table 3-7: Reported means of neutrophil count, NE activity and CXCL8 in CF BAL fluid. .	161
Table 4-1: List of exogenous and endogenous proteases that have been reported to generate C3a-like and C5a-like fragments.	169
Table 4-2 Summary of experiments exposing complement components to NSPs	222
Table 6-1: Comparison of structure and function of GAGs expressed in the CF airway.....	252

1. Introduction

1.1. Clinical description of CF

CF is the most prevalent fatal genetic disease in Europe and the USA, affecting 1/2500 births in the United Kingdom (UK). CF patients have poor quality of life and despite improved disease management, the median age of mortality is 31 years (UK CF registry 2016). Multiple therapeutic avenues are being explored to increase life expectancy yet, we lack understanding of the precise mechanisms of how the disease manifests, particularly in the airway. A consequence of the gap in our knowledge is that new therapeutics in CF only marginally improve patient health (Elborn 2016). In this review I will discuss driving factors behind neutrophilic inflammation in the CF airway and the rationale behind investigating the role of the complement anaphylatoxins in promoting CF pathogenesis.

CF is a recessive autosomal disorder caused by mutation of the CFTR, a chloride channel essential for maintaining hydration of mucosal membranes throughout the body (figure 1-1) (Haq et al. 2016).

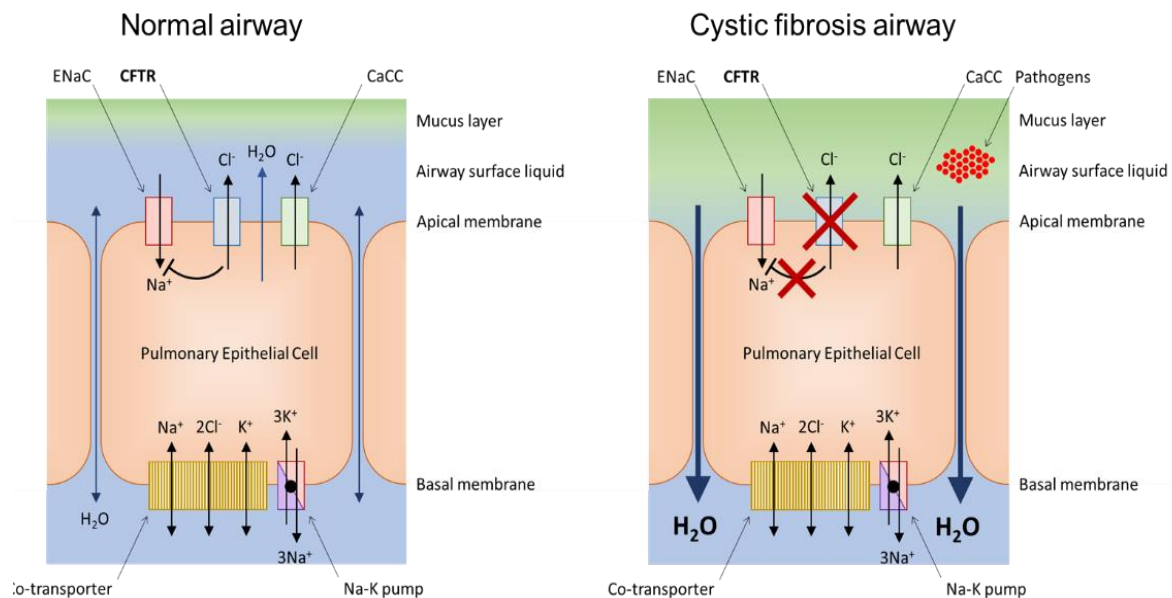


Figure 1-1: Diagram of hydration in normal and CF airways. Airway hydration in the normal airway (left) compared to the CF airway (right). Adapted from Haq et al. 2016 (Haq et al. 2016). Loss of CFTR or reduced activity reduces airway surface liquid volume and accumulation of thick mucus. CFTR-inhibition of ENaC is also reduced leading to unregulated absorption of sodium.

Water homeostasis by epithelial cells is regulated at the apical membrane by absorption of Na^+ by epithelial Na^+ channels (ENaCs) and secretion of Cl^- by CFTR (Haq et al. 2016). To hydrate mucosal surfaces, Cl^- is pumped out of epithelial cells and Na^+ is pumped in, facilitating the movement of water through gap junctions in the epithelium (Haq et al. 2016). As well as functioning as a Cl^- channel, CFTR also regulates ENaCs via an intracellular feedback loop (Haq et al. 2016). Along mucosal membranes of CF patients, reduced Cl^- secretion by CFTR induces Na^+ resorption from the mucosal layer by ENaCs and subsequently Na^+ secretion across the basolateral membrane (Donaldson and Boucher 2007). Consequently, water is drawn from the mucosal layer through cell gap junctions causing dehydration of the mucosal surface (Donaldson and Boucher 2007). Expression of Ca^{2+} activated Cl^- channels (CaCC) on the apical surface of epithelial cells, enables CF patients, with reduced CFTR activity, to maintain a level of hydration that enables people without CFTR-mediated Cl^- activity to survive (Donaldson and Boucher 2007). In support of the necessity of CaCC for survival in CF patients, it was shown that there was greater disease pathology in mice with genetically reduced CaCC expression (Clarke et al. 1994).

Since 2007, all new-born babies in the UK are genetically screened for CF by heel prick test (UK CF registry 2016). Positive cases from the heel prick test undergo further confirmation by a sweat test whereby conductivity of sweat is measured. Those with defective CFTR have a high NaCl concentration due to the inability to resorb Cl^- in sweat glands. The clinical threshold for normal sodium concentration in sweat is 30 mM; subjects with >30 mM sodium are likely to have CF and those above 60 mM are positive for the disease (LeGrys *et al.* 2007). The *cftr* alleles for each suspected positive case are sequenced and compared with over 1000 *cftr* genotypes that have been genetically characterised (Sosnay *et al.* 2013). The phenotypes of these mutations have been categorised into six classes, with the severity of CF disease being dependent on which alleles a patient has; the different categories have been listed in table 1-1 (Elborn 2016).

Normal	I	II	III	IV	V	VI
CFTR defect	No functional CFTR protein	CFTR trafficking defect	Defective channel regulation	Decreased channel conductance	Reduced synthesis of CFTR	Decreased CFTR stability
Type of mutations	Nonsense; frameshift; canonical splice	Missense; aminoacid deletion	Missense; aminoacid change	Missense; aminoacid change	Splicing defect; missense	Missense; aminoacid change
Specific mutation examples	Gly542X (3.6%) Trp1282X Arg553X 621+1G→T	Phe508del (90.9%) Asn1303Lys Ile507del Arg560Thr	Gly551Asp (5.9%) Gly178Arg Gly551Ser Ser549Asn	Arg117His (5.1%) Arg347Pro Arg117Cys Arg334Trp	3849+10kbC→T 2789+5G→A 3120+1G→A 5T	4326delTC Gln1412X 4279insA

Disease severity

High

Low

Sweat chloride

60 - 100 mmol/L

30 - 60 mmol/L

Table 1-1: *Cftr* mutation classes I-VI and diagrams describing phenotypes, adapted from Elborn 2016 (Elborn 2016). Molecular impact of each mutation class and effect on CFTR function or expression. Example of genotypes for each class and percentage prevalence of the most common (red) alleles in the UK for each class. Disease severity decreases from class I (high) to class VI (low). Sweat chloride range for each class set by the UK CF registry (Fogarty *et al.* 2012)

The most common *cftr* genotype is $\Delta F508\text{Del}$; 90.9% people diagnosed carry at least one $\Delta F508\text{Del}$ allele and 50.2% are homozygous (UK CF registry 2016). The $\Delta F508\text{Del}$ allele is lacking a phenylalanine at amino acid position 508 of 1480 (of the wild type allele) and causes a missense translation of the CFTR. The phenotype of the $\Delta F508\text{Del}$ mutation is a misfolded CFTR that is targeting for degradation in the endoplasmic reticulum (ER) and, is therefore not expressed on the apical membrane of the epithelium (Jensen *et al.* 1995). This means that the majority of patients have a *cftr* phenotype that is indicative of severe disease, accounting for the low median age of death (figure 1-2). Consequently, due to the severity of disease in these cases, CF is predominantly a paediatric disease; however, patients diagnosed with less severe disease alleles live into their 60s or older (figure 1-2)(UK CF registry 2016).

There is no difference in allele distribution between males and females yet, the median predicted life expectancy of females is significantly lower (UK CF registry 2016). For example, males and females with CF registered in the UK between 2012-2016 have a median predicted survival age of 47.9 and 44.2 years respectively. This difference in life expectancy has been attributed to elevated oestradiol (oestrogen steroid hormone) in women that correlates with the presence of biofilm forming strains of *Pseudomonas aeruginosa* (*P. aeruginosa*), a bacterial pathogen that causes pulmonary exacerbation in CF patients (Chotirmall *et al.* 2012).

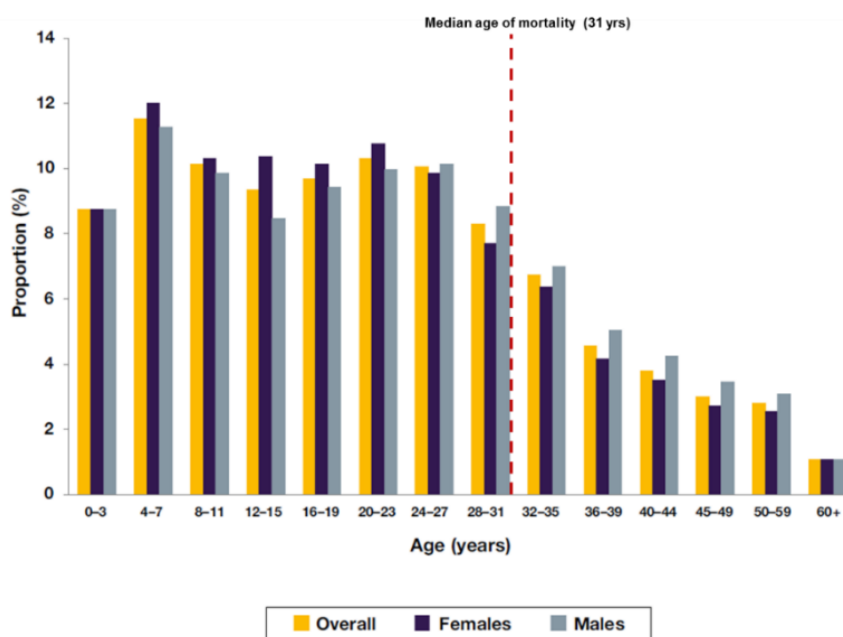


Figure 1-2: UK CF population by age, adapted from UK CF registry 2016. Proportion of both sexes (yellow), females (purple) and males (grey) with CF. The median age of mortality has been annotated by a red dashed line (n=9695).

The CFTR is expressed on epithelia throughout the body and therefore the disease affects multiple organs (figure 1-3) (Xue *et al.* 2016). Expression of CFTR is not limited to epithelial tissue and has been demonstrated on immune cells such as monocytes, macrophages, alveolar macrophages and neutrophils (Yoshimura *et al.* 1991). Due to expression throughout epithelial tissues, CF patients can suffer multiple complications including in the gastrointestinal (GI) tract. At birth blockage of the intestines can prevent passage of meconium, known as meconium ileus (Xue *et al.* 2016). Dehydration and obstruction of the pancreatic and bile ducts can also lead to malnutrition, reducing development and causing osteoporosis. Consequently, body mass index (BMI) is routinely used as a measure of disease progression (Kerem *et al.* 2014). In severe cases, reduced function in the pancreas caused by insufficient hydration and mucus blockage and consequent insulin deficiency that can induce CF-related diabetes (Frost *et al.* 2018).

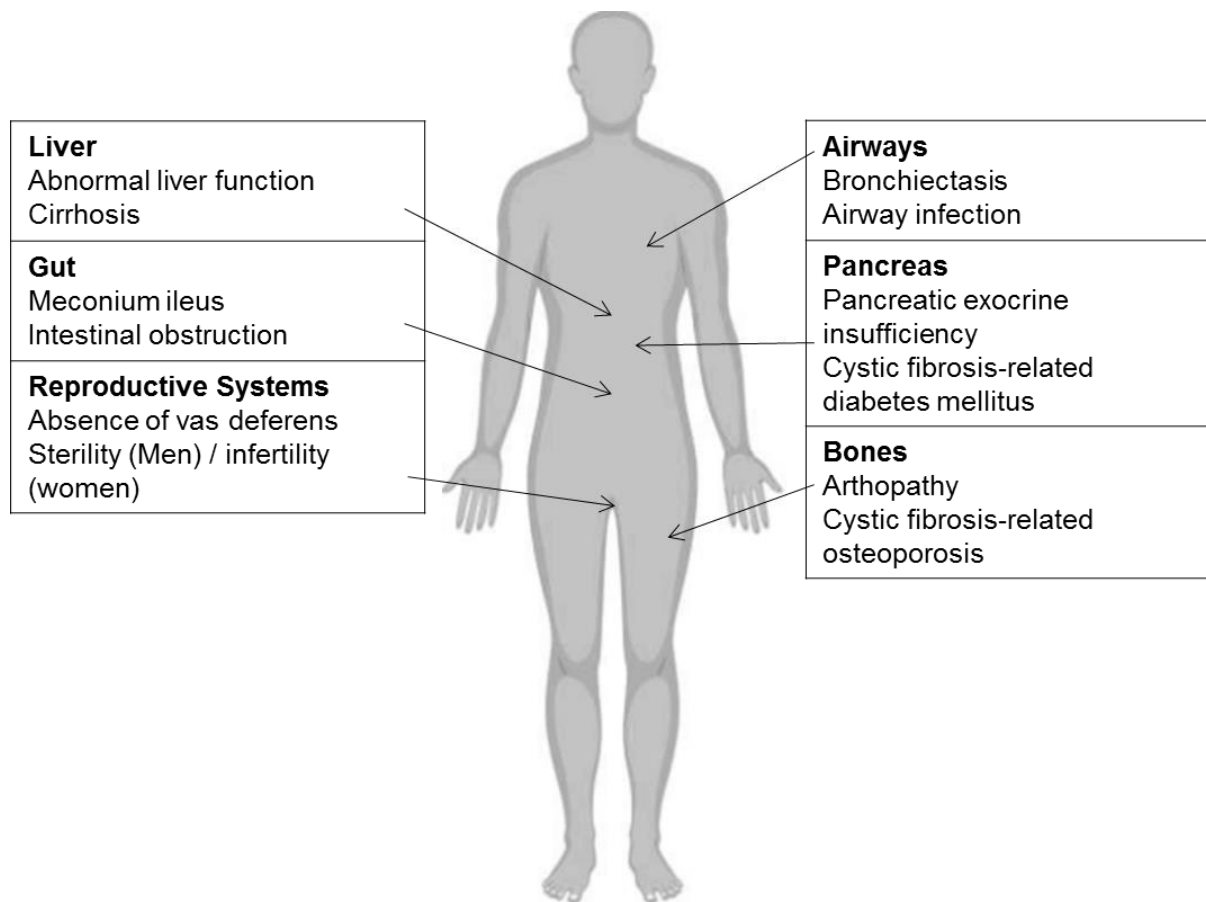


Figure 1-3: Diagram of different organs where CF pathology manifests
CFTR dysfunction in several organs can lead to well-characterised pathologies in CF patients.

The reproductive organs are also affected by dehydration of mucosal surfaces, causing sterility in men and infertility in women (Ahmad *et al.* 2013). Despite system-wide complications, airway disease in CF is the primary cause of morbidity and mortality, this is due

to continual exposure of the airway to the external environment. Therefore, reduced lung function is the predominant cause of morbidity and mortality in CF patients (Elborn 2016). In the remainder of the introduction I will focus on CF in the airway and the driving forces behind pathogenesis.

1.2. Pathogens in the CF airway

The lungs are constantly being exposed to the external environment by inhalation of debris and pathogens. Mucociliary clearance is critical for removing foreign material, keeping the airway clear and preventing infection. In CF, dehydration and depleted airway surface liquid volume reduces mucociliary clearance, causing accumulation of viscous mucus that obstructs the small airways and harbours pathogens (Hoegger *et al.* 2014). Opportunistic bacterial and fungal pathogens that would normally be cleared in healthy lungs, establish chronic infection in the CF airway and cause pulmonary exacerbations. Pathogens that have been identified in CF airway during pulmonary exacerbation are listed in (table 1-2). CF Patients are frequently hospitalised and intravenous antibiotics are administered to fight the infection. The frequency of hospitalisation increases with patient age, furthermore chronic infection and the consequent inflammation can irreversibly remodel the CF airway, reducing lung function that eventually leads to mortality (UK CF registry 2016).

Pathogens in the CF airway

Bacterial (Gram positive)	Bacterial (Gram negative)	Fungal	Viral
<i>Staphylococcus aureus</i> (inc. methicillin resistant)	<i>Pseudomonas aeruginosa</i>	<i>Aspergillus fumigatus</i>	Influenza
<i>Mycobacterium spp.</i> (nontuberculous)	<i>Burkholderia cenocepacia</i> complex	<i>Candida albicans</i>	Adenovirus
	<i>Stenotrophomonas maltophilia</i>	<i>E. dermatiditis</i>	Rhinovirus
	<i>Achromobacter spp.</i>		Metapneumovirus
	<i>Haemophilus influenzae</i>		Picornavirus

Table 1-2: Diversity of pathogens associated with pulmonary infection in the CF airway.

Pathogens that have been identified during pulmonary exacerbation in CF patients. Pathogens in bold are reported to be opportunistic pathogens in the CF airway (de Vrankrijker *et al.* 2010).

Identifying pathogenic microbes is critical for monitoring and preventing pulmonary exacerbation by administering the most effective antimicrobial, whilst maintaining a healthy lung flora (Chmiel *et al.* 2013). Early antibiotic intervention reduces the risk of permanent lung function loss and mortality; however, prophylactic administration of antibiotics is controversial, with some reports suggesting antibiotic prophylaxis can cause proliferation of bacterial strains

associated with infection, such as *P. aeruginosa* (Chmiel *et al.* 2013; Smyth and Walters 2014). This is because some strains of *P. aeruginosa* can form biofilms protecting them from eradication by antibiotics (Parkins and Floto 2015).

Identification of bacterial pathogens has been dramatically improved by sensitive and quantitative molecular analysis, such as sequencing 16S rRNA. A longitudinal study by Stokell *et al.* measured bacterial diversity in CF sputum. They observed that pulmonary exacerbation onset by *P. aeruginosa* and *B. cenocepacia* reduced bacterial diversity, suggesting that there was proliferation of single strains (Stokell *et al.* 2015). *P. aeruginosa*, *B. cenocepacia* and *S. aureus* are the most prevalent exacerbating pathogens in CF and correlate with the decline in lung function (Parkins and Floto 2015). In particular, biofilm forming strains of *P. aeruginosa* are notoriously difficult to eradicate and can cause multiple hospitalisations annually in individual patients (Parkins and Floto 2015). Biofilms are an extracellular matrix of carbohydrates, protein and DNA that prevent immune cells and their antimicrobial agents from reaching the pathogens.

P. aeruginosa can colonise the airways within the first three years of life; however, only 6.4% of the UK CF population below 16 years old have chronic infections (UK CF registry 2016). The UK CF registry has reported that during adolescence *P. aeruginosa* infection rates dramatically increase (figure 1-4), with 54.6% of 32 to 35-year olds having a chronic *P. aeruginosa* infection (UK CF registry 2016).

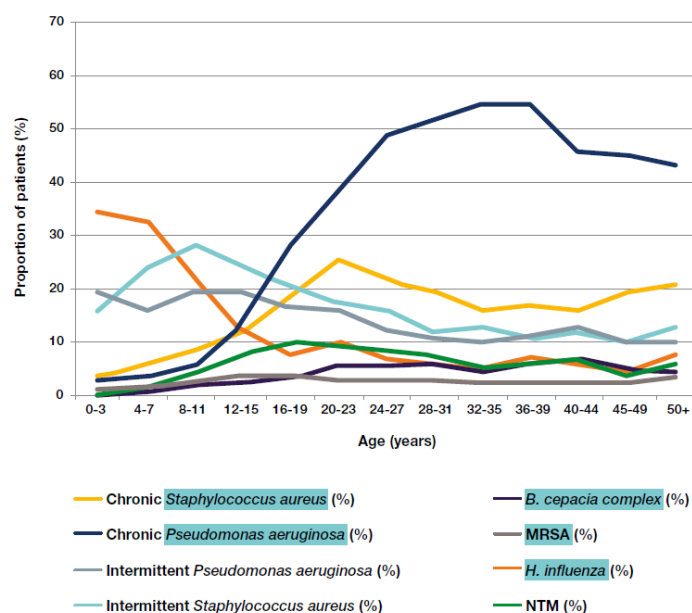


Figure 1-4 Bacterial infections in the UK CF population, extracted from UK CF registry 2016. Percentage of the UK CF population that had at least one positive pathogen identification in 12 months. MRSA – methicillin resistant *staphylococcus aureus*, NTM – non-tuberculous mycobacteria (n=9695.)

Successful colonisation by *P. aeruginosa* is due to a large genome that possesses survival genes enabling host immune evasion (Stover *et al.* 2000). It has been hypothesised that *P. aeruginosa* is prolific in the CF airway because of the absence of CFTR in neutrophil phagosomes, reducing myeloperoxidase-mediated killing (Painter *et al.* 2006). As well as the secretion of proteases, haemolysins and exotoxins, *P. aeruginosa* can switch to less motile and more mucoid strains in the CF airway preventing eradication by antibiotics (Smith *et al.* 2017). In evidence, 44% of paediatric CF patients (< 5 years) in Australia and New Zealand reacquired *P. aeruginosa* within a median follow-up time of 2.8 years (Kidd *et al.* 2015). Therefore, several anti-pseudomonal therapies are being developed to target biofilm formation and are currently undergoing clinical trials (Kidd *et al.* 2015).

Notably, antibiotics such as tobramycin and ceftazidime that are effective at targeting *P. aeruginosa* have also been reported to enable proliferation of anaerobic *Streptococci spp.* (Tunney *et al.* 2011). Although anaerobic bacteria have been found to be pathogenic in other lung diseases, such as non-CF bronchiectasis, it is unclear whether their presence is detrimental in CF (Tunney *et al.* 2011).

Pathogen identification in the CF airway can also vary depending on the airway sampling technique. There are three methods for sampling airway fluid for pathogen screening; cough swabs, induced sputum and BAL fluid. Cough swabs are cotton swabs placed in, but not touching, the posterior pharynx whilst the patient is encouraged to cough. Induced sputum is performed by inhalation of hypertonic saline and physiotherapy to encourage the production of mucus that can be used for analysis. Finally, BAL is an invasive procedure that requires sedation of the patient. A flexible bronchoscope is inserted into the infected portion of the airway (determined by computerised tomography (CT)) and saline is instilled then sucked back up for analysis. These airway sampling procedures and their advantages and disadvantages will be discussed in the background to chapter 3.

Fungal pathogens have been isolated from the CF airway during pulmonary exacerbation, yet it is not clear whether a particular species, at one time, is responsible for driving pathogenesis or whether it is just present (Middleton *et al.* 2013). For example, in one clinic, a study of *Aspergillus fumigatus* (*A. fumigatus*) reported that *Candida albicans* (*C. albicans*) and bacterial pathogen *P. aeruginosa*, were also isolated from the same sputum samples (50.5 and 64.2 % respectively) (Bakare *et al.* 2003). *C. albicans* and *A. fumigatus* have both been shown to co-colonise CF the airway with *P. aeruginosa*; however, it was unclear whether the presence of fungi was a pathogenic factor or a consequence of advancing disease (Chotirmall and McElvaney 2014). If misdiagnosed (e.g. mistaken for *S. aureus* in a chest X-ray) *A.*

fumigatus can colonise the lungs causing allergic bronchopulmonary aspergillosis (ABPA), a hyper-responsiveness to *Aspergillus spp.* allergens (Chotirmall and McElvaney 2014). ABPA, typically induces wheezing and pulmonary exacerbation, chronic infection can cause bronchiectasis, lung fibrosis and mortality through respiratory failure.

A. fumigatus produces small spores called conidia that are ubiquitous in the environment. In healthy lungs these do not pose any risk and are cleared; however, in the compromised CF airway conidia germinate producing hyphae and establishing colonies. Detection rates of *A. fumigatus* in CF patients is between 6 and 60%, but not all patients go on to develop ABPA and it is not always a reliable predictor of worsening disease (Singh *et al.* 2018). *C. albicans* is a skin commensal but can cause candidiasis in immunocompromised individuals and CF patients (Navarro *et al.* 2001). Despite the *C. albicans* detection rate ranging from 35 to 93% in CF patients, its detection only correlated with a small reduction of lung function, 5 – 10% FEV₁ (Navarro *et al.* 2001; Singh *et al.* 2018). FEV₁ (forced expiratory volume in one second), is the volume of air that can be forcibly expelled in a spirometer in the first second after a deep breath. FEV₁ is usually calculated as a percentage predicted according to the median FEV₁ for people of the same gender, height and mass.

Viruses have also been detected in CF patients but a longitudinal study using nasal swabs found that there was no difference in prevalence compared to healthy controls; however, acute respiratory illnesses lasted longer in CF patients and viral infections may predispose to infection by *P. aeruginosa*, precipitating pulmonary exacerbation (van Ewijk *et al.* 2008).

The primary response to infection in the airway is inflammation. I will continue with a general overview of inflammation but will continue to focus on inflammation in the airway leading to chronic neutrophilic inflammation of the CF airway.

1.3. Inflammation

Inflammation is an evolutionally ancient immune response to trauma; the predominant characteristic of inflammation is the recruitment of leukocytes that stop infection, clear affected tissue and prevent systemic damage. It was first described in 30-38 B.C by the Roman, Celsus, that four signs of acute injury were: redness, swelling, heat and pain. A fifth sign, loss of function was later described by Galen, 132-200 A.D (Punchard *et al.* 2004). Whilst our understanding of the mechanisms behind inflammation has progressed significantly, inflammation is not a simple process and therefore the immune response varies depending on the tissue and type of trauma (i.e. whether this is sterile or non-sterile) (Robb *et al.* 2016).

Furthermore, there is a spectrum of inflammation ranging from acute, lasting a few hours or at the other extreme it can be chronic and consequently pathological (such as CF) (Robb *et al.* 2016).

Inflammation is the immune response to damage, it is primarily an innate immune response; however, both innate and adaptive immune cells are involved (table 1-3 for lung specific cells). The complement system also plays a significant part by bridging the innate and adaptive immune systems together enabling efficient resolution through the clearance of pathogens and dead cells (Ricklin and Lambris 2013). The complement system will be discussed in greater depth in section 1.6.

Cell	Role in inflammation	References
Innate Immune cells		
Polymorphonuclear leukocytes		
Neutrophils	Phagocytosis of pathogens, release of enzymes, ROS and neutrophil extracellular traps.	(Robb <i>et al.</i> 2016)
Eosinophils	Release eosinophilic granules, eosinophil extra cellular traps	(Felton <i>et al.</i> 2014)
Basophils	Release cytokines, enzymes and histamines	(Robb <i>et al.</i> 2016)
Monocyte/macrophages		
Alveolar macrophages	Release pro-inflammatory mediators, suppress hyper-responsiveness	(Hussell and Bell 2014)
Macrophages	Release pro-inflammatory mediators, ROS and protease Important for resolution, apoptosis of neutrophils.	(Shapouri-Moghaddam <i>et al.</i> 2018)
Other innate immune cell		
Mast cells	Release histamines, enzymes and cytokines that induce mucus release from goblet cells, increase endothelial permeability and recruit PMNs.	(Felton <i>et al.</i> 2014)
Stromal cells		
Epithelial cells	Produce mucus, release pro-inflammatory mediators, express adhesion molecules for leukocyte transmigration	(Parkos 2016)
Endothelial cells	Release pro-inflammatory mediators, express adhesion molecules for leukocyte transmigration	(Parkos 2016)
Adaptive immune cells		
Dendritic cells	Phagocytic, relay antigens to lymph nodes, stimulate innate lymphoid cell recruitment, stimulate B-cell IgE response to allergens (via naïve T-cells)	(Condon <i>et al.</i> 2011; Felton <i>et al.</i> 2014)
NK cells	Pro-inflammatory and tissue-protective roles by releasing cytokines and cytolytic granules	(Culley 2009)
Innate lymphoid cells	Pro-inflammatory (TNF, IL-17) and pro-resolution (IL-22) roles by releasing cytokines	(Sonnenberg and Artis 2015)
Naive T-cells	Present antigens to B-cells	(Felton <i>et al.</i> 2014)
CD4 ⁺ T-helper cells	Release pro-inflammatory cytokines	(Lloyd and Saglani 2013)

Table 1-3: Immune cells and their roles in inflammation

Inflammation can be initiated by the recognition of damage-associated molecular patterns (DAMPs). These endogenous factors are released by necrotic or damaged cells following trauma (Rock *et al.* 2011). Examples of DAMPs are uric acid, heat shock protein 70, fibrinogen domain A, fragments of GAGs and CpG-rich deoxyribonucleic acid (DNA) regions (Rock *et al.* 2011). Exogenous factors released by pathogens also stimulate the immune system and stromal cells, these have been termed pathogen-associated molecular patterns (PAMPs); examples of PAMPs are: bacterial components such as lipopolysaccharide (LPS), flagellin, peptidoglycans and unmethylated DNA (Tang *et al.* 2012). DAMPs and PAMPs are recognised by pattern-recognition receptors (PRRs) that are expressed on the surface and within the cytosol of immune cells such as T-cells, B-cells, NK-cells, dendritic cells, macrophages, and polymorphonuclear leukocytes (PMNs)(Tang *et al.* 2012).

PRRs have distinct functions that orchestrate inflammation through initiation, amplification and resolution (Tang *et al.* 2012). For instance, toll-like receptors (TLRs) such as TLR1, TLR2, TLR4 and TLR5 recognise bacterial components and up-regulate the expression and release of pro-inflammatory cytokines such as interleukin-1 β (IL-1 β) and tumor necrosis factor- α (TNF α) (Tang *et al.* 2012). IL-1 β is a key pro-inflammatory mediator that is released through the activation of cytosolic complexes termed “inflammasomes” (Lamkanfi 2011). Inflammasomes are centered around NOD (nucleotide-binding oligomerisation domain) -like receptors (NLRs), that can be primed and activated through stimulation of PRRs by DAMPs and PAMPs (Lamkanfi 2011). A major process of NLRP activation is the expression of pro-IL-1 β that undergoes cleavage and activation to IL-1 β by caspase 1. IL-1 β is an essential pro-inflammatory cytokine that, in-turn, stimulates the release of other pro-inflammatory mediators, amplifying inflammation (Lamkanfi 2011). Pro-inflammatory mediators such as cytokines (as well as lipid mediators such as leukotrienes) act by recruiting leukocytes to the trauma site, activating effector cell functions such as the generation of ROS and upregulating phagocytic receptors for phagocytosis of pathogens and debris.

A crucial phase of inflammation is repair and resolution. Macrophages are a key cell type in the resolution of inflammation; they phagocytose cell debris and dead cells and also have a critical role in the efferocytosis of neutrophils (Shapouri-Moghaddam *et al.* 2018). Macrophages also release IL-10 and transforming growth factor- β (TGF- β), that simulate collagen expression in fibroblasts, establishing the extra cellular matrix (ECM), the scaffolding that connects tissue structure. (Shapouri-Moghaddam *et al.* 2018). IL-10 also suppresses and dampens inflammation. Oneway IL-10 achieves this is by inhibiting pro-inflammatory TLRs through upregulation of microRNA that target MyD88-dependent signaling, an important signaling pathways for TLRs and G-protein coupled receptors (Mittal and Roche 2015).

If inflammation is not resolved, it can become chronic and cause permanent tissue damage, this is because long term exposure of tissue to proteases and ROS released by PMNs and macrophages can collaterally remodel tissue (Braga *et al.* 2015). Furthermore, over-stimulated fibroblasts can lead to fibrosis and the generation of scar tissue, altering the normal structure of organs leading to loss of function (Shapouri-Moghaddam *et al.* 2018). Examples of fibrotic diseases that occur are diabetes mellitus, liver cirrhosis, cardiovascular disease and plaque formation, kidney disease and lung diseases, such as bronchiectasis and CF (Braga *et al.* 2015).

Having broadly discussed inflammation, I will continue by focusing on airway inflammation and the key cells that are involved.

1.3.1. Inflammation in the normal airway

The airway lining is comprised of different epithelial cells. The epithelial lining of the smaller airways is composed of mucus producing goblet cells and epithelial cells (figure 1-5). Epithelial cells are further divided into type I ciliated epithelial cells (pneumocytes) that primarily facilitate gas exchange and, type II epithelial cells. They are also important for immune surveillance (Hussell and Bell 2014; Robb *et al.* 2016). The mucosal barrier lining the lungs is constantly absorbing and clearing debris and pathogens that have been inhaled. Mucociliary clearance by epithelial cells removes organic and inorganic particulates from the airway to maintain gas exchange and lung function. If the mucosal barrier is breached, pathogens can establish colonies causing infection; this initiates an inflammatory response in reaction to the release of DAMPs (by damaged epithelial cells) and PAMPs (by the pathogens).

DAMPs and PAMPs are recognised by PRRs expressed on the surface of epithelial cells and resident alveolar macrophages. Alveolar macrophages are unique to the airway. They are essential for the phagocytosis of debris and surveillance of the airway lumen (Hussell and Bell 2014). Interestingly, they need to be responsive to pathogens but also suppressive and not become over-activated by the multitude of different debris and stimulants they encounter (Hussell and Bell 2014). This dichotomy is facilitated through the normal expression of PRRs (in comparison with circulating macrophages) but lower expression of major histocompatibility complexes (MHC). They also release TGF β that suppresses T-cell activation (Roth and Golub 1993; Hussell and Bell 2014). Alveolar macrophages also migrate and present antigen in

draining lymph nodes, although this role is primarily performed by dendritic cells (Kirby *et al.* 2009).

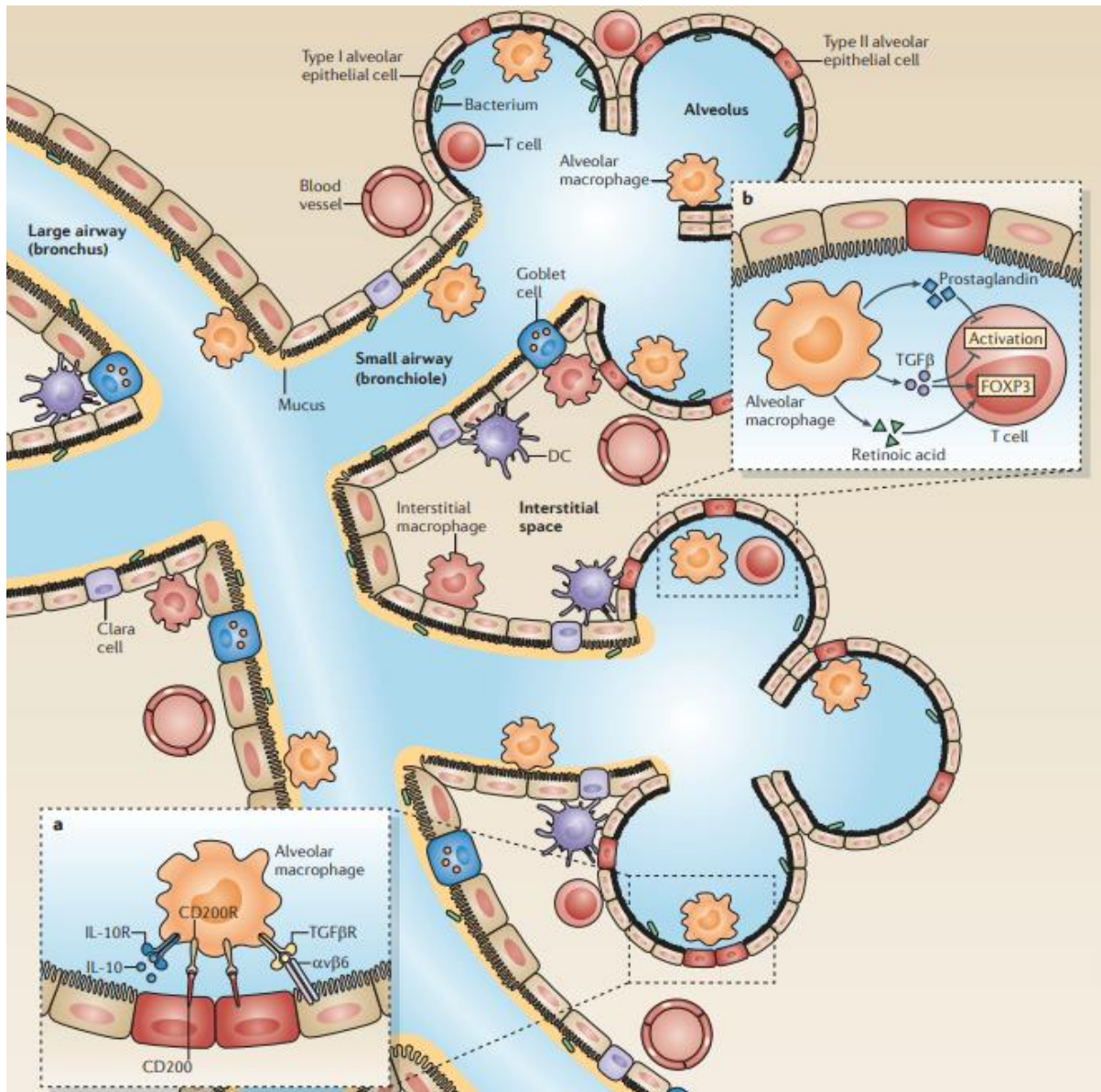


Figure 1-5: Diagram of the normal healthy airway, extracted from Hussell and Bell (Hussell and Bell 2014). The airway is separated into the large airway, small airways, alveolar space (alveolus), and the interstitial space. The epithelial lining comprises of ciliated type I epithelial cells (tan), type II epithelial cells (red), goblet cells (blue), clara cells (light purple). Cells present in the airway are alveolar macrophages (orange) and small numbers of T-cells (light red). The epithelium is covered in a layer of mucus (yellow) that prevents infection of the large and small airways by pathogens (green). The boxes demonstrate the immuno-suppressive roles that alveolar macrophages have towards **A)** epithelium and **B)** T-cells.

Following the initiation and amplification of an immune response, alveolar macrophages and epithelial cells release pro-inflammatory cytokines and chemokines; that facilitate extravasion of circulating neutrophils to the airway lumen and site of infection (figure 1-6). Pro-inflammatory cytokines up-regulate expression of adhesion molecules on capillary endothelial cells that supply the alveoli. Specifically, E-selectin expressed on endothelial cells bind to neutrophils via complementary receptors these are O-glycosylated carbohydrate ligands such as cluster of differentiation-44 (CD44), E-selectin ligand-1 and P-selectin glycoprotein ligand-1 (PSGL-1) (Voisin and Nourshargh 2013). Neutrophil migration to the airway lumen is also enabled by the cytokine-mediated relaxation of epithelial tight-junctions by inducing the internalisation and disassociation of junction proteins such as occludin and claudin (Parkos 2016).

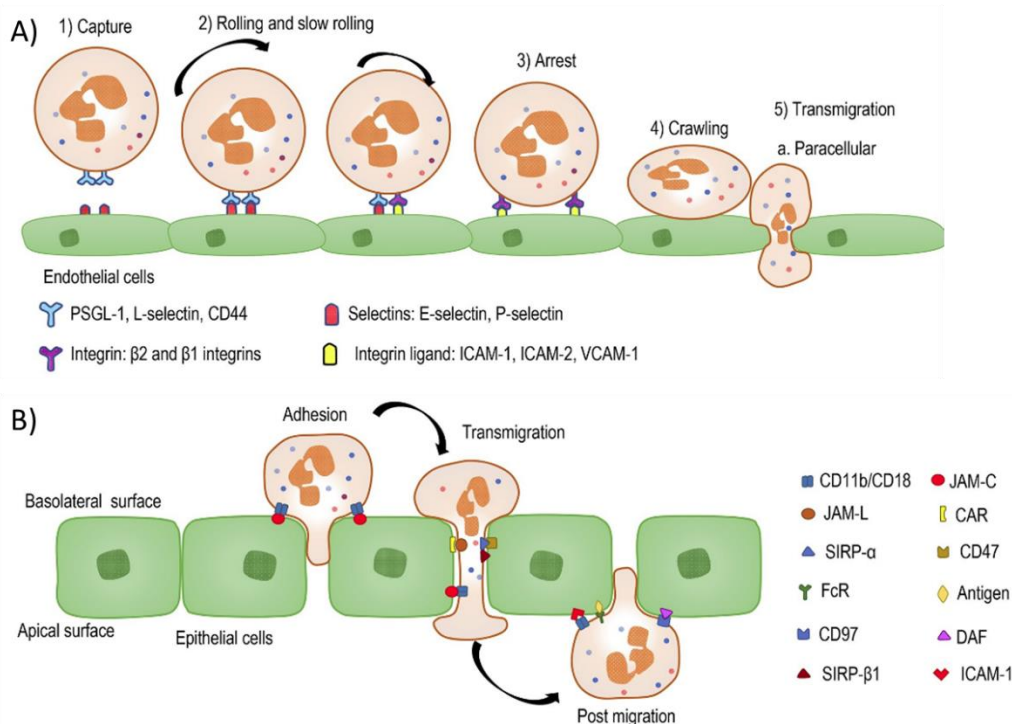


Figure 1-6 Diagram of neutrophil transendothelial and transepithelial migration, extracted from Zhou *et al.* (Zhou et al. 2018). **A)** Neutrophil transendothelial migration is a multistep process that involves capturing and slowing neutrophil movement in blood, by expression of adhesion molecules by both neutrophils and endothelial cells. Firmly arrested neutrophils transmigrate through gap junctions in the lumen and pericytes via adhesion of ICAMs and VCAMs expressed on the luminal endothelial surface. **B)** Neutrophil transepithelial migration from the basolateral surface to the apical surface (airway lumen) is mediated by array of JAMs, CARs and Fc receptors.

Neutrophil migration from the circulation to the airway lumen is a complex step-wise process that involves a multitude of adhesion molecules expressed on the surfaces of neutrophils, endothelial cells, pericytes and airway epithelial cells (figure 1-6A). The first step in transendothelial migration is to tether circulating neutrophils, slowing fluid-phase movement.

Weak interactions between L-selectins on neutrophils surfaces with PSGL-1 on the endothelial lumen reduce the movement of neutrophils in the bloodstream (McEver 2002; Zarbock *et al.* 2011).

Further adhesion of neutrophils to the endothelium is mediated via interactions between intercellular adhesion molecules (ICAMs) and vascular cell adhesion protein-1 (VCAMs) on endothelial cells with lymphocyte function-associated antigen-1 (LFA-1) and very late antigen-4 (VLA-4) respectively; these molecules reduce neutrophil movement to a slow roll or crawl (Zarbock *et al.* 2011). Transendothelial migration occurs through gaps between the endothelial cells and pericytes, this step requires tight interaction between the neutrophils and lumen and is mediated through the expression of junctional adhesion molecules (JAMs) on endothelial cells (Voisin and Nourshargh 2013). Neutrophils undergo actin cytoskeletal rearrangement, polarising the cell to produce protrusions (lamellipodia) in order to squeeze between gap junctions and migrate through the interstitial space (Voisin and Nourshargh 2013).

Neutrophil epithelial migration from the basolateral membrane (airway interstitial space) to the apical membrane (alveolar space) is a three-step process; adhesion, transmigration and post migration (figure 1-6B). Neutrophil transepithelial migration also involves interaction between JAMs and integrins such as CD11b (complement receptor 3) and CD18 as well as coxsackie and adenovirus receptors (CARs) (Parkos 2016).

Upon infiltration into the airway, neutrophils have several effector functions: phagocytosis, generation of ROS, release of proteases (and antimicrobial peptides) and neutrophil extracellular trap (NET) formation; these functions will be discussed in section 1.4.8. Macrophages also have a crucial role in orchestrating and resolving inflammation. As well as the presence of resident alveolar macrophages, circulatory monocytes are recruited into the airway where they differentiate into macrophages. Chemotaxis of macrophages is mediated by macrophage chemoattractant protein-1 (MCP-1) and CXCL8 upregulation of adhesion molecules expressed on the macrophage surface, allowing firm adhesion to the endothelium and transmigration to the airway lumen (Mantovani *et al.* 2004).

The function of macrophages can be manipulated by their environment and has been broadly categorized into two phenotypes: M1 macrophages are proinflammatory and release proinflammatory mediators such as TNF α , IL-1 β , IL-6 and chemokines: they can also release proteases, generate ROS, and stimulate Th-1 T-cells (Shapouri-Moghaddam *et al.* 2018). M2 macrophages are anti-inflammatory or pro-resolution, they have been further characterised

into M2a (tissue remodeling), M2b (immunoregulation), M2c (phagocytosis of apoptotic cells) and M2d (angiogenesis) (Shapouri-Moghaddam *et al.* 2018). Categorisation of M1 and M2 is based on expression of surface and soluble markers: M1 macrophages express IL-1R, TLRs (pro-inflammatory TLR2, TLR4) and MHCII but release low levels of IL-10 (Shapouri-Moghaddam *et al.* 2018). M2 macrophages (generally across the sub-classes) produce arginase-1, an inhibitor of ROS production, they also express macrophage mannose receptor (MMR, CD206) (Salam *et al.* 2011; Shapouri-Moghaddam *et al.* 2018). MMR is a c-type lectin that recognises pathogen-associated carbohydrate structures but are also important for removing neutrophil anti-microbial glycoproteins that could damage self-tissue, such as myeloperoxidase (MPO), a co-factor for ROS production (Gazi and Martinez-Pomares 2009).

An important step in the resolution of airway inflammation (and inflammation in general) is the switching of macrophage phenotype from the pro-inflammatory M1 state to pro-resolution M2 types. There are a range of stimulants and receptors that promote macrophage phenotype switching, these include: cytokines (IL-4, IL-10, TGF- β), TLRs (TLR7, TLR8, TLR9) (Tang *et al.* 2012; Shapouri-Moghaddam *et al.* 2018)

Phenotype switching of macrophages to M2 promotes efferocytosis of neutrophils by upregulation of first apoptosis signal ligand (FasL) and phosphatidylserine ligands on neutrophils. The removal of apoptotic neutrophils is essential to prevent damage to tissue by factors released by neutrophils such as proteases and ROS (Shapouri-Moghaddam *et al.* 2018). Macrophages present an array of scavenger and apoptotic receptors on their surfaces for the clearance neutrophils such as FasR, phosphatidylserine receptor, CD36, CD14, β -integrins (complement receptors) and collectins (Vandivier *et al.* 2002b). As well as, facilitating uptake of apoptotic neutrophils, ligation of the above receptors stimulates the release of pro-resolution cytokines such as IL-10 and TGF- β ; they also suppress expression of pro-inflammatory cytokines like CXCL8 and TNF- α (Vandivier *et al.* 2002b).

Over stimulation of immune cells by pro-inflammatory cytokines or ineffective clearance of pathogens can lead to chronic inflammation of the airway. Chronic inflammation in the lungs is particularly detrimental because enzymes released by macrophages and PMNs can collaterally degrade and remodel the small airways, reducing lung function (Robb *et al.* 2016). Examples of chronic inflammatory diseases in the airway are asthma, chronic obstructive pulmonary disease (COPD) and CF (Robb *et al.* 2016). In the next section I will discuss inflammation in the CF lung.

1.3.2. Inflammation in the CF airway

In CF, the inflammatory response to infection is characterised by an overwhelming influx of neutrophils to the airway lumen. Therefore, neutrophilic inflammation is strongly associated with pulmonary exacerbation and decline in lung function (Sagel *et al.* 2012). Despite neutrophil domination of the CF airway, other innate and adaptive immune cells are also elevated and may contribute to disease progression (Table 1-4) and (figure 1-7).

Cell	Function	Reference
Lymphocytes (sub-epithelial tissue)		
CD4+ Th2	Release pro-inflammatory cytokines (IL-4, IL-5 and IL-3). Co-ordinate eosinophil activity during allergic in asthma and ABPA in CF	(Knutsen <i>et al.</i> 2004)
CD4+ Th17	Release IL-17 that stimulates chemokine secretion. IL-17 is reported to be elevated during <i>P. aeruginosa</i> infection	(Bayes <i>et al.</i> 2014)
CD4+ Th22	Pseudomonal-specific Th22 cells release IL-22 that in turn induce repair and regeneration of epithelial cells	(Bayes <i>et al.</i> 2014)
Natural Killer cells	Release interferon- γ , that mediate clearance of <i>P. aeruginosa</i> . Impaired function in fibrotic lung disease	(Culley 2009)
Monocytes		
Macrophages (lung parenchyma)	Excessive neutrophilic inflammation suggests efferocytosis may be impaired. Contribute to fibrosis. M1 and M2 phenotypes observed.	(Vandivier <i>et al.</i> 2002a; Bruscia and Bonfield 2016)
Alveolar Macrophages (airway lumen)	Upregulation of pro-inflammatory cytokine release, impaired function	(Hussell and Bell 2014)
Dendritic cells		
Polymorphonuclear leukocytes and mast cells		
Mast cells	Cause bronchoconstriction during allergen response. Source of pro-inflammatory cytokines and can induce fibroblast proliferation	(Andersson <i>et al.</i> 2011)
Eosinophils	Elevated eosinophil cationic protein and myeloperoxidase in CF airway but contribution to disease is unclear	(Koller <i>et al.</i> 1994; Eltboli <i>et al.</i> 2014)
Basophils	Basophil activation tests in blood used to diagnose ABPA in CF. Source of IL-4 stimulating CD4+ T-cell differentiation	(Gernez <i>et al.</i> 2016)
Neutrophils	Most prominent cell type during inflammation of the CF airway. Chronic neutrophilic inflammation collaterally causes airway remodelling and irreversible loss of lung function	(Sagel <i>et al.</i> 2012)

Table 1-4 Cell populations observed during chronic inflammation of the CF airway

1.3.2.a. T-Cells in the CF airway

The presence of a sub-set of cells does not necessarily imply a pathogenic role. In asthma, T-helper 2 (Th2), and more recently reported Th17 and Th22 cells, are reported to play an important role in hyper-responsiveness through recruitment of eosinophils (Lloyd and Hessel 2010). Moreover, it is hypothesised that the multiple-factorial causes of asthma may not be based on single sub-set of cells but dysfunctional communication between structural cells and cells from adaptive and innate lineages (Lloyd and Saglani 2013). CF patients also have varying degrees of asthma and elevated T-cell populations, particularly Th-17 cells (Bayes *et al.* 2014). Unlike allergenic (eosinophilic) asthma, the CF airway is dominated by neutrophils. Th17 cells in CF are characterised by the release of IL-17, a pro-inflammatory cytokine that stimulates the release of neutrophil chemoattractants from macrophages, epithelial cells and endothelial cells (figure 1-7) (Tan *et al.* 2011; Bayes *et al.* 2014). It has been reported that IL-17 is elevated in the CF airway and may contribute to chronic neutrophilic inflammation in the CF airway (Tan *et al.* 2011; Bayes *et al.* 2014).

1.3.2.b. Macrophages in the CF airway

The role of macrophages in promoting CF disease progression has been studied intensely (Bruscia and Bonfield 2016). Elevated macrophage numbers are observed in the CF airway and correlate with concentrations of CCL2 (macrophage chemoattractant) in CF BAL fluid (Bruscia and Bonfield 2016). Despite this, characterising macrophage populations in the CF airway has been challenging due to dynamic stimulatory environment that could favour both M1 and M2 phenotypes (Bruscia and Bonfield 2016). For instance, levels of IL-4 and IL-13 are elevated in BAL fluid from CF patients; these cytokines promote polarisation of macrophages to the M2 phenotype (Hartl *et al.* 2006). Contrary to this, pro-inflammatory cytokines that are indicative of M1 phenotype polarisation (IL-6, CXCL8 and TNF α) have also been reported to be elevated (Bonfield *et al.* 1995). Therefore, it is difficult to attribute disease progression to either phenotype. None the less, there is evidence of over-activation of both; this is supported by elevated pro-inflammatory cytokines (M1) and fibrosis (M2) (Bruscia and Bonfield 2016).

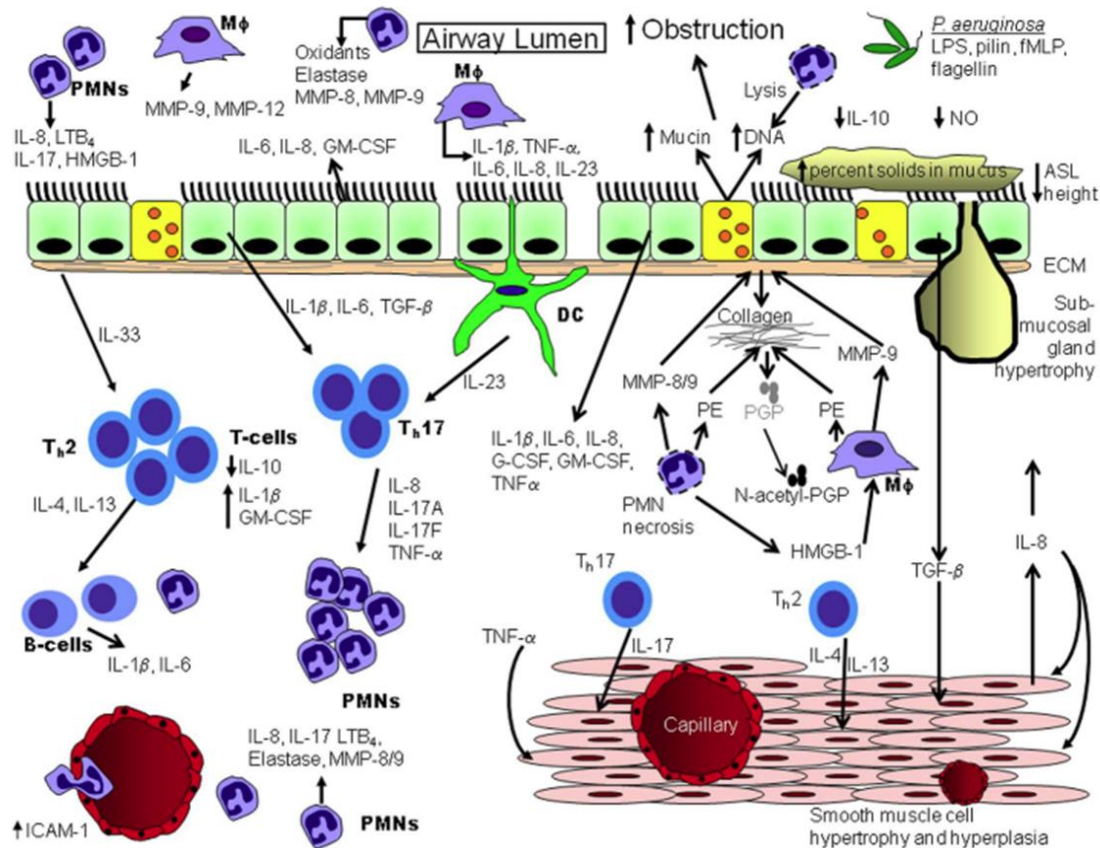


Figure 1-7 Diagram representing some of roles for the different cell types in the CF airway and how they contribute to CF airway pathology, extracted from Nichols *et al.* (Nichols and Chmiel 2015). The interaction of immune and stromal cells in the CF is complex owing to a plethora of cytokines, lipid mediators, enzymes and ECM fragments. The production of pro-inflammatory cytokines ($TNF\alpha$, $IL-1\beta$, $IL-18$, $IL-6$) by epithelial cells and macrophages stimulate the release of chemoattractants such as CXCL8 ($IL-8$) by other epithelial cells and macrophages but also T-cells. Recruitment of neutrophil to the interstitial tissue and release of matrix metalloproteases generates N-acetyl-PGP, recruiting more neutrophils. Necrotic neutrophils, not cleared by macrophages, lyse and release DNA, protease and ROS that promote airway obstruction and remodel the airway causing a loss of lung function.

Phagocytosis of apoptotic and necrotic immune cells by macrophages (efferocytosis) is essential for resolution of inflammation and prevents prolonged exposure to proteases that are released by dying neutrophils. Inefficient efferocytosis leads to degradation of structural cells and the surrounding ECM, promoting small airway remodelling and consequently irreversible loss of lung function (Robb *et al.* 2016). Since discovering CFTR expression on macrophages it has been hypothesised that the CFTR may be important for clearance of pathogens and apoptotic neutrophils (Painter *et al.* 2006). Di Pietro *et al.* have shown that TLR4 is dysregulated in the absence of CFTR (Di Pietro *et al.* 2017). The authors show that TLR4 expression is dependent on the heme oxygenase 1/carbon monoxide pathway, a process that is interrupted without CFTR (Di Pietro *et al.* 2017). They summarise by hypothesising that the abundance of LPS during bacterial infection causes the over-activation of macrophages (Di Pietro *et al.* 2017). Moreover, Di *et al.* have investigated the role of CFTR

in the acidification of endocytic compartments following phagocytosis of bacteria. Autonomous integration of CFTR during endocytosis promotes acidification by accumulating Cl⁻, generating a large enough counterion conductance to maintain H⁺ gradients (Di *et al.* 2006). Di *et al.* showed that internalised CFTR be detected in non-CF alveolar macrophages and that macrophages from *cftr* ^{-/-} mice failed to acidify endosome to a bactericidal pH (Di *et al.* 2006).

Another proposed mechanism of macrophage dysfunction is the cleavage of PRRs by proteases released by neutrophils; this will be discussed in detail in section 1.5.2. It is clear that delineating the roles of different immune cells in disease progression is complicated due to heterogeneity in the airway of CF patients.

Despite elevated numbers of macrophages, Th cells and other PMNs neutrophils make up >70% of the cells in the airway during pulmonary exacerbation and are directly responsible for irreversible loss of lung function. Therefore, better understanding of neutrophil dysfunction may improve effectiveness of therapeutics targeting inflammation.

1.4. Biology of neutrophils

Neutrophils are the first line of defense during infection. They are highly responsive to their environment and possess an armory of effector functions that allow them to eradicate pathogens. In this section I discuss the mechanisms that enable neutrophils to efficiently clear infection and maintain homeostasis.

1.4.1. Differentiation

Neutrophils are released as terminally differentiated cells from the bone-marrow at a steady state of $1 - 2 \times 10^{11}$ cells/day (Borregaard 2010). Neutrophils start as a common progenitor myeloblast, similar to erythrocytes, granulocytes and monocytes. They differentiate to myeloblasts, then promyelocytes and subsequently neutrophils; this is in response differential cues such as CCAAT/enhancer binding protein a (C/EBPa) and PU.1 (figure 1-8) (Borregaard 2010). The release of neutrophils from the bone marrow is mediated by the ligand CXCL12 and the regulated expression of its receptors, CXCR2 (retention in the bone marrow) and CXCR4 (release)(Borregaard 2010; Kruger *et al.* 2015).

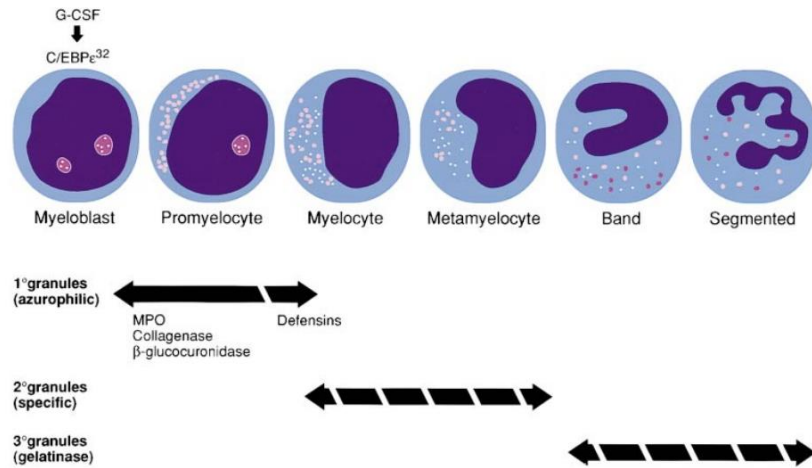


Figure 1-8: Diagram of neutrophil differentiation and granulopoiesis, extracted from Lekstrom-Himes et al. (Lekstrom-Himes *et al.* 1999). Neutrophils differentiate in the marrow and mature through stimulation by differential cues. Neutrophil granules develop sequentially in a process called granulopoiesis.

1.4.2. Effector functions

The primary role of neutrophils is to infiltrate damaged tissue and fight pathogens. If neutrophils do not encounter pro-inflammatory signals or signals to prolong life, they undergo apoptosis within days of release from the bone marrow (Geering and Simon 2011). Neutrophils infiltrate the infected tissue by transmigration through the endothelium and epithelium, as described in section 1.3.1. Arriving at the site of infection, neutrophils have four main effector functions that facilitate the clearance of pathogens and promote further neutrophil recruitment, these are: phagocytosis, ROS production, degranulation and neutrophil extracellular trap (NET) formation (figure 1-9).

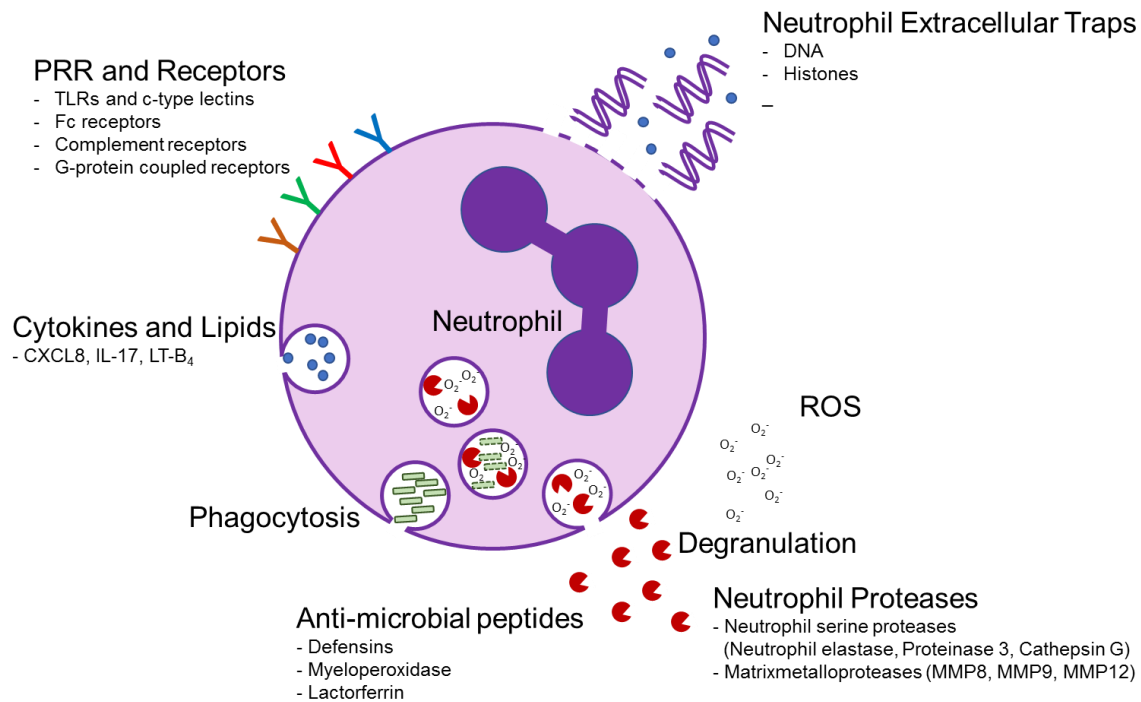


Figure 1-9 Neutrophil effector functions

1.4.3. Neutrophil cell surface receptors

For neutrophils to respond to infection appropriately, they possess an array of surface (and cytosolic) molecules and receptors that are regulated by the expression of cytokines and other stimulatory factors released by other neutrophils and other cells at the infection site. Important cell surface receptors expressed on neutrophils are G-protein-coupled receptors, adhesion molecules, cytokine receptors, Fcγ-receptors (FcγRs) and PRRs, I will briefly discuss each of these in turn (Futosi *et al.* 2013).

1.4.3.a. G-protein coupled receptors

G-protein-coupled receptors are critical for neutrophil function during an inflammatory insult; they facilitate chemotaxis by responding to ligands released by resident tissue cells. Examples of molecules that are chemotactic for neutrophils are: chemokines (via CXCR1, CXCR2, CCR1 and CCR2), formyl-peptides released by bacteria (via FPR1, FPRL1 and, FPRL2), leukotriene B₄ (via BLT1 and BLT2), platelet activating factor (via PAFR) and, complement anaphylatoxin C5a (C5aR1). The biology of these chemoattractants will be discussed in section 1.4.4 (Futosi *et al.* 2013). As well as mediating chemotaxis, G-protein-

coupled receptors also have important functions in inducing ROS production, degranulation, priming and up-regulation of other receptors.

Upon ligand binding, signal is transduced via pertussis toxin-sensitive heteromeric G-proteins (figure 1-10). The $G\alpha$ subunit and β -arrestins disassociate from the G-protein-coupled receptor and bind Src-family kinases, a pathway that stimulates neutrophil degranulation (Fumagalli *et al.* 2007). Specifically, the Src-kinases, Hck, Fgr and Lyn have been shown to be essential for neutrophil degranulation (Mocsai *et al.* 1999; Mocsai *et al.* 2000; Fumagalli *et al.* 2007). The $G\alpha$ subunit (as well as $G\beta\gamma$ subunits) can also activate phospholipases $C\beta$ (PLC β 1, PLC β 2 and PLC β 3); these produce inositol 1,4,5-trisphosphate, a signalling mediator important for chemotaxis, ROS production and NET release (Smrcka and Sternweis 1993; Li *et al.* 2000; Nguyen *et al.* 2017). Along with diacylglycerol, inositol 1,4,5-trisphosphates induce the release of calcium from the ER by diffusing through the ER membrane and binding to inositol 1,4,5-trisphosphate receptors, ligand-gated calcium channels (Smrcka and Sternweis 1993; Clemens and Lowell 2015).

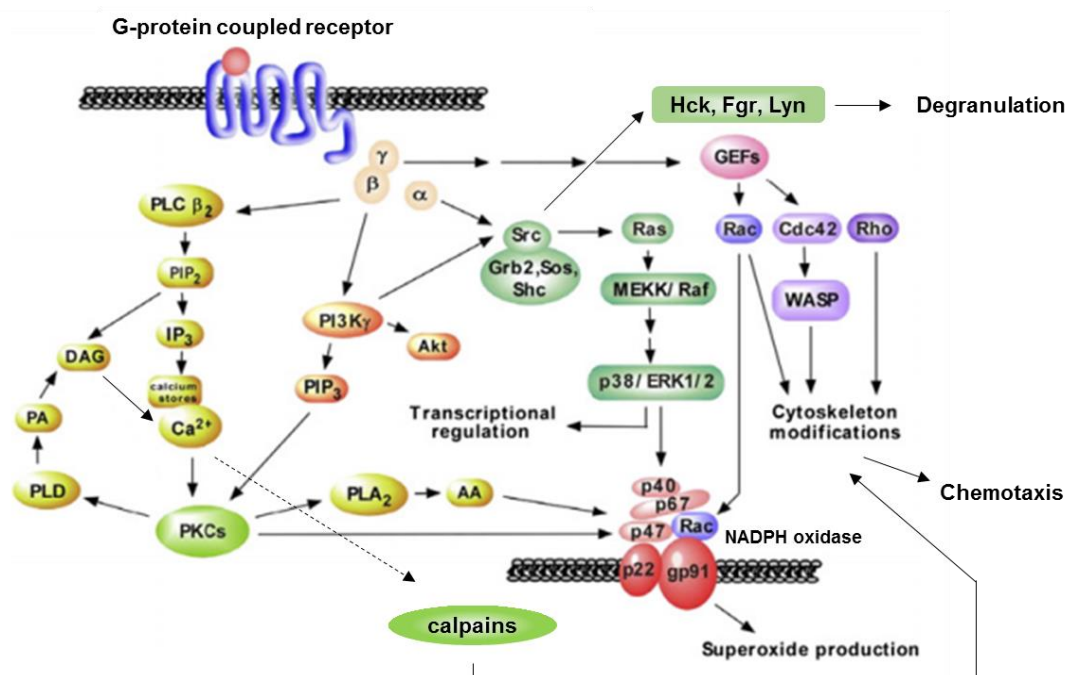


Figure 1-10: G-protein couple receptor signalling pathways and functions, adapted from Rabiet *et al.* (Rabiet *et al.* 2007). Following ligand binding, G-proteins $G\beta\gamma$ and $G\alpha$ can initiate several pathways that trigger neutrophil functions. $G\alpha$ subunits bind Src that induces ROS production and upregulation of pro-inflammatory mediators through Ras and p38/ ERK pathways. Src activates Src family kinases that induce degranulation. G-protein subunits also activate phospholipase C and via inositol 1,4,5-trisphosphate (IP3) and diacylglycerol, inositol 1,4,5-trisphosphates (DAG) induce Ca²⁺ release and protein kinase C (PKC) activation. PKC phosphorylates p47 and p40 to form facilitate formation of NADPH oxidase.

Interestingly, secondarily to ER calcium release, further calcium can be pumped into neutrophils from the extracellular space via calcium release-activated calcium channel protein (ORAI) following stimulation by stromal interaction molecules (STIM) located in the membrane of the ER (Clemens and Lowell 2015). Calcium mediates calcium-dependent protein kinase C phosphorylation of p47^{phox} and p40^{phox}, both are subunits of NADPH oxidase, the catalyst for ROS production (see section 1.4.6) (El-Benna *et al.* 2016; Nguyen *et al.* 2017). Intracellular calcium also binds calpains, cysteine proteases that aid actin polymerisation and actin- β -integrin cross-linking, important for chemotaxis and granule mobilisation (Tian *et al.* 2004).

G-protein subunits $\beta\gamma$ also bind and activate phosphatidylinositol 3-kinases (PI3K) that in turn activate the ERK-Akt pathway and p38 mitogen-activated protein kinase (MAPK) pathways, these up-regulate adhesion molecules, enabling neutrophil chemotaxis (Kim and Haynes 2013).

A crucial part of G-protein-coupled receptor signalling is regulation, this has two steps: desensitisation, mediated by β -arrestins, that uncouple G-proteins by phosphorylating the receptors (Magalhaes *et al.* 2012). The second subsequent step is internalisation or endocytosis of the receptors, a process that is facilitated again by β -arrestins that interact with clathrin (figure 1-11) (Magalhaes *et al.* 2012).

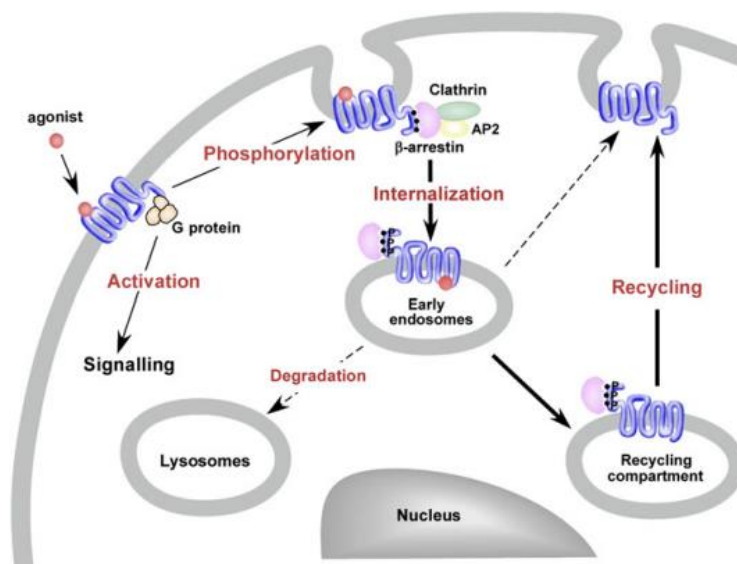


Figure 1-11: Diagram of G-protein coupled receptor internalisation, extracted from Rabiet *et al.* (Rabiet *et al.* 2007) Following ligand binding, G-protein coupled receptors are phosphorylated and bound by β -arrestins that form complexes with clathrin and AP2, facilitating internalisation. They can either fuse with lysosomes, degrading the G-protein receptors or be re-phosphorylated and recycle to the cell surface.

Endosomal compartments can merge with lysosomes whereby G-protein coupled receptors are degraded; however, the majority of internalised receptors are desensitised and recycled to the cell surface (Magalhaes *et al.* 2012). Internalisation is determined by the level of phosphorylation of the receptor in the seventh transmembrane domain (Oakley *et al.* 2000). G-protein-coupled receptors that do not internalise are de-phosphorylated and re-sensitised (Magalhaes *et al.* 2012).

Interestingly, the association with β -arrestins allows cross-desensitisation between CXCRs and also heterologous desensitisation by other β -arrestin-associated G-protein coupled receptors on neutrophils such as C5aR1 and formyl-peptide receptor 1 (Heit *et al.* 2002; Sogawa *et al.* 2011). This is because the same β -arrestins that mediate desensitisation are used by all of above the receptors. Furthermore, C5a and fMLP desensitisation is not reciprocated by CXCLs revealing a hierarchy of desensitisation in response to different neutrophils chemoattractants (Heit *et al.* 2002; Sogawa *et al.* 2011).

1.4.3.b. Adhesion molecules

Neutrophils express L-selectin and integrins on their cell surface to facilitate endothelial and epithelial transmigration (Futosi *et al.* 2013). They also present glycoproteins, PSGL-1, CD44 and E-selectin-ligand (ESL-1), as well as glycosphingolipids, that bind E-selectins, expressed on endothelial cells to arrest neutrophil movement through blood vessels (Hidalgo *et al.* 2007; Nimrichter *et al.* 2008). The expression of integrins is also important for neutrophil transmigration, specifically neutrophils express LFA-1 (CD11a/CD18), Mac-1 (CD11b/CD18; CR3 (complement receptor 3)), integrin α X (CD11c, CD18, CR4) and, VLA-4 that bind to ICAMs or VCAMs on the endothelial luminal surface.

Interestingly, PSGL-1 and integrin binding to endothelial receptors (E-selectin and ICAMs respectively) induces intracellular signalling cascades through interaction with co-receptors such as immunoreceptor tyrosine-based activation motifs (ITAMs) and Fc γ R/DAP12 (Mocsai *et al.* 2006). ITAM-mediated signalling stimulates syk activation and up-regulation of integrins, generation of cytokines as well as ROS production. ROS production via syk signalling is triggered through phospholipase C- γ (PLC- γ), that increases intracellular calcium concentration and subsequently, ROS production (Berton *et al.* 2005; Mocsai *et al.* 2006; Nguyen *et al.* 2017). Signalling in this manner enables communication between neutrophils and the endothelium.

The integrin Mac-1 is also known as CR3. As well as binding to ICAMs, CR3 also recognises β -glucans, the most abundant component of fungal cell walls; however, fungal recognition by CR3 does not induce ROS production (Wright and Silverstein 1983; Thornton *et al.* 1996). Furthermore, CR3 also binds to the complement opsonin iC3b (inactivated C3b) and consequently CR3 can recognise both opsonised and non-opsonised yeasts (Netea *et al.* 2008). CR4, also recognises iC3b, together expression of CR3 and CR4 are important for neutrophil phagocytosis of opsonised and non-opsonised pathogens (Ren *et al.* 2004; Netea *et al.* 2008).

There are two other complement receptors, CR1 and CR2. Neutrophils do not express CR2, but it has important roles in activation of B-cells, acting as a B-cell co-receptor via interaction with IgM immunocomplexes and C3d (Boackle *et al.* 1998). CR1 binds several complement proteins, such as C3b (and lesser extent iC3b), C4b, C1q and mannose-binding lectin. Therefore, because mannose-binding-lectin and C3b opsonise yeasts (and other pathogens) CR1 is an important phagocytic receptor (Li *et al.* 2012). CR1 is also a complement regulator, it is a co-factor with factor I for inactivation of C3b (to iC3b), iC3b (to C3f and C3d,g) and, C4b (to C4c and C4d)(Ross *et al.* 1983). The complement system will be described in further detail in section 1.6.

1.4.3.c. Cytokine receptors

Cytokine receptors are divided into four subsets: type I and type II cytokine receptors, IL-1 family receptors and the TNF receptor family. Neutrophils express Type I cytokine receptors such as IL-4R, IL-6R, IL-12R, IL-15R, G-CSFR and GM-CSFR (Futosi *et al.* 2013). The Type II cytokine receptors expressed by neutrophils are interferon receptors (IFNAR (IFN- α/β , IFNGR (IFN- γ)) and IL-10R (Ellis and Beaman 2004; Bazzoni *et al.* 2010). Type I and type II receptors activate transcription factors via the JAK/STAT pathway. They are split into two classes because Type I cytokine receptors are generally pro-inflammatory, whereas type II cytokine receptor are associated with pro-resolution cytokines (figure 1-12)(Futosi *et al.* 2013). The two receptor classes are associated with different isotypes of JAK and STAT so that pro-inflammatory or pro-resolution genes can be differentially activated (O'Shea and Plenge 2012).

Neutrophils express receptors for IL-1 α and IL-1 β (IL-1RI/IL-1R3) as well as IL-18 (IL-1R5/IL-1R7(IL18RAP)) (Futosi *et al.* 2013). Ten IL-1 family receptors and co-receptors have been identified; these are structurally more similar to TLRs than they are to type I and type II cytokine

receptors, in that they possess an extracellular immunoglobulin-like domain (O'Neill 2008; Dinarello 2018). IL-1RI is the receptor for IL-1 α and IL-1 β , IL-1 β is a potent pro-inflammatory cytokine but, despite expression of IL-1RI, the only stimulatory effect on neutrophils is promoting survival (Colotta *et al.* 1993; Mitroulis *et al.* 2010). IL1-RII, a decoy receptor lacking a cytoplasmic signalling domain, it is highly expressed on neutrophils and is thought to be important for regulating IL-1 β stimulation of resident cells and macrophages (Futosi *et al.* 2013). IL-18 is a neutrophil stimulant, promoting survival and inducing cytokine release and ROS production (Leung *et al.* 2001). IL-1 β or IL-18 stimulation of IL-1RI/IL-1R3 and IL-1R5/IL-1R7 induces signalling via MyD88-IRAK kinase family pathway and activation of transcription factors (NF- κ B) (Fortin *et al.* 2009).

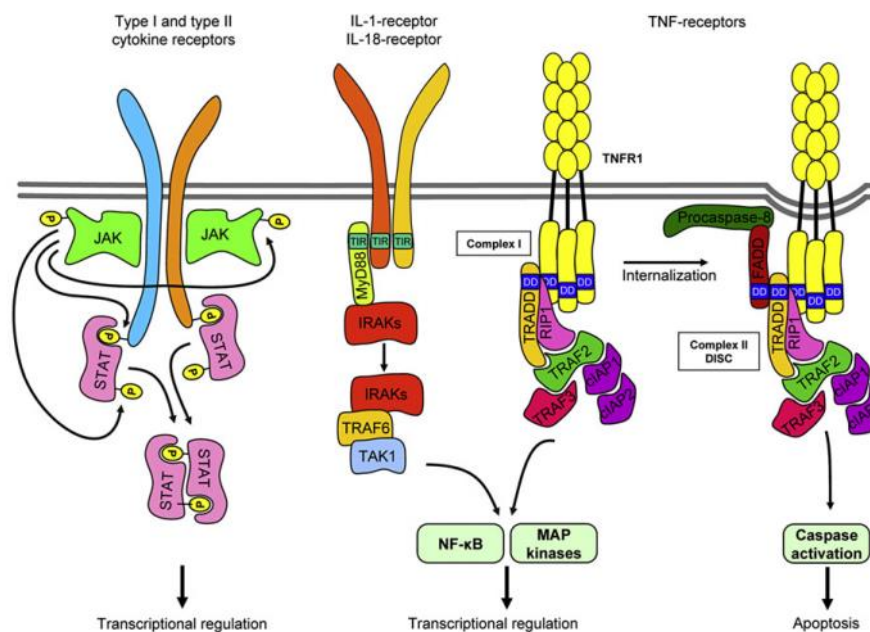


Figure 1-12: Cytokine receptor signalling pathways and functions, extracted from Futosi *et al.* (Futosi *et al.* 2013). Cytokine type I and II receptors signal via JAK / STAT pathways following ligand-mediated phosphorylation. IL-1 family receptors signal via MyD88 pathways using TIR located within the intracellular domains. TNF-family receptors signal via RIP and TRAF complexes; however, differential TRAF interaction facilitates alternative functions such as MAP kinase activation (pro-inflammatory gene expression) or caspase activation (apoptosis).

Neutrophils also express TNF-family receptors, these can be divided in-two by the possession of an intracellular death-domain (Futosi *et al.* 2013). For instance, TNFR-1, TRAIL-R2 and, Fas receptor are death receptors and promote neutrophil apoptosis (O'Donnell *et al.* 2015). TNF α is a potent activator of neutrophils by inducing ROS production (Dri *et al.* 1999). TNF-family receptors signal via receptor-interacting serine-threonine protein kinase (RIP1) and TNF receptor associated factors (TRAF); however, alternative TRAF complexes are used to differentiate the pro-inflammatory and pro-resolution signals that these receptors transmit (Futosi *et al.* 2013).

1.4.3.d. Pattern recognition receptors

Neutrophils express an array of PRRs that trigger activation upon recognising DAMPs and PAMPs (Tang *et al.* 2012). Humans express 11 TLRs that recognise a range of DAMPs and PAMPs, such as bacterial membrane components like peptidoglycans (TLR2), LPS (TLR4) or, flagellin (TLR5) (Takeuchi and Akira 2010; Futosi *et al.* 2013). They also recognise danger cues from host cells such as DNA (TLR5), heat-shock-protein 70 (TLR2), GAG fragments (TLR4) (Zhang and Schluesener 2006; Tang *et al.* 2012). Neutrophils express all known TLRs, except TLR3. Activation of TLRs upon ligand binding can induce cytokine release and promote survival (Hayashi *et al.* 2003; Koller *et al.* 2009). As mentioned, TLRs belong to the same family of receptors as IL-1R and therefore, like IL-1R1 signal via MyD88-IRAK pathways, leading activation of NF- κ B transcription factors (figure 1-13) (O'Neill 2008). One function of TLRs is to induce the generation of proIL-1 β that is cleaved by caspase-1 following inflammasome activation via secondary signals such as an increase in intracellular calcium or ROS (Lamkanfi 2011).

Neutrophils also express C-type lectins, these are fundamental for recognition of fungal pathogens such as *Candida albicans* and *Aspergillus fumigatus* (Steele *et al.* 2005). C-type lectins such as Dectin-1 (CLEC7A), recognise β -glucans on the surface of *A. fumigatus* (and *Candida spp*), whereas, Dectin-2 (CLEC2) binds mannose disaccharides and also recognises *C. albicans* (Steele *et al.* 2005; Feinberg *et al.* 2017; Griffiths *et al.* 2018). Another C-type lectin, Mincle (CLEC4E) recognises α -mannose structures on the cell walls of *Malassezia spp.*; these are responsible for causing skin lesions but can also cause sepsis in immunocompromised patients (Yamasaki *et al.* 2009).

Neutrophils also express other C-type lectins such as MDL-1 (CLEC5A) and Mcl (CLEC4D) (Futosi *et al.* 2013). C-type lectins signal via ITAMs; however, Dectin-1 and Dectin-2 only possess half an ITAM (hemITAM) and therefore, it has been suggested that homo-dimerisation with TLRs is required for signal activation (Hughes *et al.* 2010).

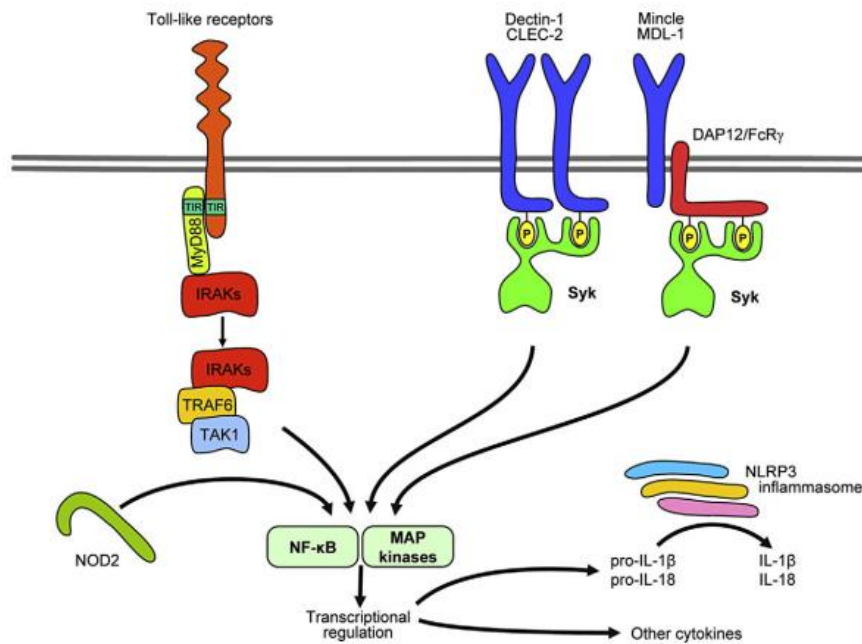


Figure 1-13: Pattern recognition receptor signalling pathways and functions, extracted from Futosi et al. (Futosi et al. 2013). Surface expressed TLRs signal via MyD88 and TIR located in cytoplasmic domains (like TNF-family receptors (figure 1-12)). TLR activation activates MAP kinases and NF-κB transcription factors that upregulate transcription of pro-inflammatory cytokines, particularly IL-1 β , this becomes activated by NLRP3 inflammasome. Dectin-1 and 2 and Mincle recognise pathogen surface molecules, these trigger signaling through Syk and, like TLRs, stimulates NF-κB and Map kinase transcription factors.

As for, PSGL-1 and Fc γ R signalling, C-type lectin signalling is mediated by interaction with co-receptors ITAMs and Fc γ R/DAP12 that lead to activation of the syk pathway and cytokine transcription via NF-κB (Gross *et al.* 2006). The syk signal pathway also triggers intracellular calcium via activation of PLC- γ , the consequent increase in calcium causes ROS production, NET release and degranulation (Berton *et al.* 2005).

1.4.3.e. Fc γ receptors

Fc γ Rs bind to the fragment crystallisable (Fc) tail regions of immunoglobulins and facilitate the recognition and opsonisation of immunoglobulin targeted pathogens (Karsten and Kohl 2012). Seven Fc γ R subclasses have been identified; each have been reported to have different affinities for IgG subclasses. For instance, Fc γ RI has been reported to have the highest affinity for IgG, whereas the other Fc γ R classes have much lower affinity for IgGs but can differentially bind to different IgG subclasses (IgG1-4) (Karsten and Kohl 2012). There are two low-affinity Fc γ R that are crucial for immunoglobulin recognition by neutrophils, these are Fc γ RIIA and Fc γ RIIIB. Moreover, both are required for receptor activation and signal transduction (Futosi *et al.* 2013). The current model of activation of these receptors is that

FcγIIIB binds first, but because FcγIIIB is glycosylphosphatidylinositol (GPI)-anchored and does not possess an intracellular signalling domain it requires FcγIIA to function (Futosi *et al.* 2013). Signalling of FcγRs is mediated via a γ-accessory protein that is associated with ITAMs and induces signal via the syk-pathway and subsequent ROS production (Karsten and Kohl 2012).

Not all FcγR induce a pro-inflammatory signal. FcγRIIB is anti-inflammatory and has been shown to associate with dectin-1 when FcγRIIB recognises highly glycosylated immunoglobulins (Karsten *et al.* 2012). Dectin-1 signalling via syk, promotes phosphorylation of Src homology 2 domain-containing inositol phosphatase on FcγRIIB with the downstream affects inhibiting complement C5a receptor 1 (C5aR1) stimulation and neutrophil activation (Karsten *et al.* 2012).

In this section I have discussed some of the key molecules and receptors that regulate the functions of neutrophils. Neutrophils are the first line of response during inflammation and migrate to the infection site by transmigration following gradients of chemotactic molecules that are released by resident cells (and infiltrating neutrophils) upon sensing danger signals. In the next section I will discuss the range of molecules with chemotactic activity for neutrophils, with particular emphasis on those that have been found elevated in the CF airway.

1.4.4. Neutrophil chemotaxis

Neutrophil chemotaxis requires both neutrophils and tissue cells to display adhesion molecules to facilitate transmigration from the circulation through the vascular endothelium to the infected tissue. Furthermore, chemotaxis requires significant changes in neutrophil morphology for adherence and migration which I will briefly discuss.

Neutrophils express chemotactic G-protein-coupled receptors that as well as mediating ROS production and degranulation also induce neutrophil chemotaxis (Futosi *et al.* 2013). There is a range of neutrophil chemoattractants that elicit a response via G-protein-coupled receptors. A detailed account of several chemoattractants important in the airway will be in the next section. Upon activation of chemotactic G-protein-coupled receptors on neutrophils, G-protein subunits, G α G $\beta\gamma$, trigger various signalling cascades, such as PI3K activation. PI3K and its products, phosphatidylinositol (3,4,5)-trisphosphate, stimulate Rac GEFs (Guanine nucleotide exchange factors) and, in turn, Rac GTPases (Mocsai *et al.* 2015). This signalling pathway promotes neutrophil polarisation by inducing actin polymerisation and myosin mobilisation that

produce lamellipodia, an extension of the neutrophil leading edge (figure 1-14) (Mocsai *et al.* 2015).

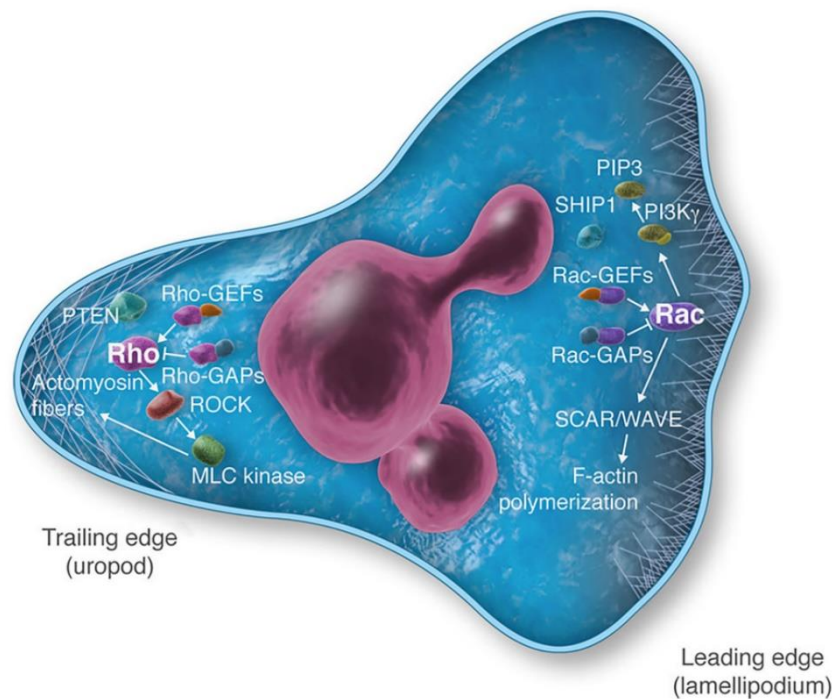


Figure 1-14: Diagram of neutrophil polarisation during chemotaxis, extracted from Mocsai *et al.* (Mocsai *et al.* 2015). Neutrophil polarisation facilitates migration towards chemotactic gradients by generation of a leading edge. The leading edge is formed by dynamic actin polymerisation following activation of Rac by PI3K. At the trailing edge PI3K stimulate Rho-mediated stabilisation of actin to form a uropod.

At the opposite end, the trailing edge, the actin-myosin arrangements are stable and form a uropod, a process that involves disassociation of actin with the cellular cytoskeleton (Mocsai *et al.* 2015). The formation of the uropod is mediated by phosphatidylinositol activation of Rho (Ras homolog gene)(Mocsai *et al.* 2015). It has been shown that neutrophil polarisation does not change distribution of G-protein-coupled receptors and therefore, migration of neutrophils is facilitated by dynamic changes in morphology towards the chemotactic gradient (Ku *et al.* 2012). This is because at the leading edge chemotactic receptors will become activated; whereas at the trailing edge there will be less receptor activity. Therefore, the difference in receptor activation across the cell, rather than receptor mobility, is important for chemotaxis (Ku *et al.* 2012).

Our understanding of neutrophil homing and accumulation at the inflammation site has been improved by the recent development of intravital imaging in mice (Lämmerman *et al.* 2015). Here neutrophils are labelled and their movement is followed through membranous

translucent tissue; for instance in the GI tract or skin (Lämmerman *et al.* 2015). From these experiments it has been observed that neutrophils accumulate *en masse* in a process that is called neutrophil swarming (Lämmerman *et al.* 2015). Two types of neutrophil swarming events have been observed: transient swarms and persistent swarms (Lämmerman *et al.* 2015). Transient swarms are formed by coordinated groups of 10 – 150 neutrophils; these typically disperse within 40 minutes and are associated with minor trauma (Lämmerman *et al.* 2015). Persistent swarms are formed by an assembly of greater than 300 neutrophils that sustain recruitment for periods longer than 40 minutes (Lämmerman *et al.* 2015). Furthermore, large persistent swarms can form by merging together multiple smaller groups. (Lämmerman *et al.* 2015)

In skin it has been shown that neutrophil swarming is initiated by “pioneer” neutrophils drawn in to the tissue by DAMPs, PAMPs and chemotactic molecules released by damaged tissue. Neutrophil recruitment and swarming is subsequently amplified by the release of leukotriene B₄ (LTB₄, see section 1.4.4e) by pioneer neutrophils (Lämmerman *et al.* 2015). However, LTB₄ is not solely responsible for neutrophil swarming and other chemotactic molecules may also be important for driving neutrophil swarming (Lämmerman *et al.* 2015). The process of neutrophil swarming also differs on the tissue; the ECM density is a key factor in governing the rate of neutrophil swarming (Lämmerman *et al.* 2015)

In the following sections I will discuss the range of neutrophil chemoattractants and their relative potencies (where investigated).

1.4.4.a. Major neutrophil chemoattractants

There are several different forms of neutrophil chemoattractants, most of which are released by host cells following stimulation by DAMPs, PAMPs and cytokines (e.g. chemokines and leukotriene B₄). However, some are derived from bacterial components (e.g. fMLP), ECM components (e.g. Pro-Gly-Pro, PGP) or the complement cascade (C5a). A similarity between them all is that they induce chemotaxis through G-protein coupled receptors (Futosi *et al.* 2013). I will briefly discuss each chemoattractant individually, apart from C5a which will be discussed in section 1.7.

1.4.4.b. Pro-Gly-Pro

PGP and acetyl-PGP are chemotactic peptides released from the ECM following degradation of collagen by neutrophil matrix metalloproteases (MMPs), MMP8 and MMP9, during

inflammation (Abdul Roda *et al.* 2015). PGP is directly generated by collagen degradation, but acetyl-PGP is a secondary product following acetylation by acrolein (which is found in cigarette smoke and is a by-product of glycerol breakdown during heating) (Abdul Roda *et al.* 2015). It has been shown that PGPs bind and activate CXCR2, inducing ROS production and inhibiting neutrophil apoptosis (Kim *et al.* 2011). PGPs are degraded during inflammation by leukotriene A₄ hydrolase; however, in cases of chronic inflammation such as in COPD or CF there is an imbalance of ECM degradation / PGP generation and inactivation by leukotriene A₄ hydrolase (Snelgrove *et al.* 2010). Therefore, PGPs are elevated in these diseases and could be used as biomarkers of airway inflammation and remodelling (Abdul Roda *et al.* 2015).

1.4.4.c. High mobility group box 1 protein (HMGB1)

HMGB1 is a DNA binding molecule that facilitates and interacts with transcription factors and histones (Yang *et al.* 2013). It is released by necrotic cells during inflammation and therefore could be considered a DAMP (Yang *et al.* 2013). HMGB1 has three cysteine residues that when reduced can modify interaction with cytokines allowing it to bind external receptors and induce intracellular signals (Yang *et al.* 2013). For examples, partial reduction of HMGB1 enables interaction with MD-2, an adapter protein for TLR4 that can stimulate TLR4 and consequent pro-inflammatory cytokine release (Yang *et al.* 2013). If all three cysteine residues are reduced however, HMGB1 binds the chemokine CXCL12 modulating chemotactic activity via CXCR4 (Venereau *et al.* 2012). Of further interest, HMGB1 can also bind complement C1q, activating the classical pathway and complement cascade, promoting cell lysis by the membrane attack complex, driving further HMGB1 release and generating the neutrophil chemoattractant C5a (Kim *et al.* 2018).

1.4.4.d. CXCL8

CXCL8 (also known as IL-8) is a member of the chemokine family; these are categorised by conserved N-terminal cysteine residues. Four sub-families have been established: C, CC, CXC and CX₃C. CXC Chemokines have a low molecular weight between 8-9 kDa (Walz *et al.* 1987). They can be further subdivided by the presence of a Glu-Leu-Arg (ELR) binding domain located before the above conserved cysteine residues; CXCL8 is ELR-positive (Hebert *et al.* 1991).

In the airway, chemokines can be produced by alveolar macrophages, epithelial, and endothelial cells upon stimulation by DAMPs, PAMPs and cytokines (Hartl *et al.* 2012). A list

of characterised chemokines that have been isolated in the CF lung can be found in Hartl *et al.* but, for the remainder of this review I will focus on CXCL8 (Hartl *et al.* 2012). Two different length forms CXCL8 exist, CXCL8(77) and a more active truncated form, CXCL8(72) (Padrines *et al.* 1994). CXCL8(77) is released by non-immune cells whereas CXCL8(72) is secreted by immune cells (Padrines *et al.* 1994).

Furthermore, CXCL8(77) is subsequently proteolytically modified by NSPs and other proteases to create the more potent CXCL8(72) form (Padrines *et al.* 1994). Pre-term infants have a higher prevalence of CXCL8(77); however, pre-term infants that went on to develop bronchopulmonary dysplasia (an airway condition that can afflict pre-term children) had higher expression of the more potent CXCL8(72) form (Chakraborty *et al.* 2014). Using patient BAL fluid, Chakraborty *et al.* showed that CXCL8(77) activation was mediated through cleavage by neutrophil proteases present in the airway. The authors also noted that over extended periods, CXCL8 was susceptible to degradation beyond the N-terminus resulting in loss of function (Chakraborty *et al.* 2014).

At low concentrations soluble CXCL8 is monomeric; however, oligomerisation of CXCL8 (and other chemokines) allows stronger initial chemotactic attraction to high concentrations of CXCL8 (Das *et al.* 2010). Furthermore, positively charged epitopes located on the C-terminal α -helix and proximal loop at residues 18-23, encourage binding to non-sulphated and sulphated GAGs such as heparan sulphate (HS) and hyaluronic acid (HA) (Kuschert *et al.* 1999). Soluble GAGs, released by degradation of the ECM during chronic inflammation, can inhibit CXCL8 binding to CXCR1 (Pichert *et al.* 2012b; Schlorke *et al.* 2012). Conversely, cell surface GAGs facilitate ligand binding of dimerized CXCL8 establishing chemotactic gradients within tissue and upregulating the production of ROS in neutrophils (Pichert *et al.* 2012b; Schlorke *et al.* 2012).

CXCL8 binds to receptors via a sterically protected ELR motif adjacent to the N-terminus (Gerber *et al.* 2000). CXCL8 has been shown to have affinity towards three receptors: CXCR1, CXCR2 and the Duffy antigen receptor (Stillie *et al.* 2009). The latter has been shown to facilitate transmigration of neutrophils to sites of infection and is also upregulated in the lung during infection by pneumonitis (Lee *et al.* 2003). CXCR1 and CXCR2 share 77% homology but CXCR1 only binds CXCL6 and CXCL8 (Stillie *et al.* 2009). On the other hand, CXCR2 binds CXCL6 and CXCL8 as well as the remaining CXCL family. This divergence in binding of different CXCL chemokines has an important functional role; this is because the signalling pathways differ between the two receptors (Stillie *et al.* 2009). CXCR1 signalling is mediated via phospholipase D1 and induces NADPH oxidase activation and ROS release, whereas both

CXCR1 and CXCR2 can signal via phospholipase D2. This pathway has shown to be important for chemotaxis as well as ROS production and degranulation (Lehman *et al.* 2006).

1.4.4.e. Leukotriene B₄

Since their characterisation in the 1980s, leukotrienes have been reported to have diverse functions beyond leukocyte activation and chemotaxis such as vascular homeostasis and cell proliferation. See Brink *et al.* for an extensive list of functions (Brink *et al.* 2003). LTB₄ is a derivative of leukotriene A₄, an eicosanoid metabolite of arachidonic acid break-down that is mediated by 5-lipoxygenase, a lipase produced by granulocytes and macrophages (Brink *et al.* 2003). Therefore, LTB₄ is generated following recruitment of leukocytes to the site of inflammation (Yokomizo 2011; Sadik and Luster 2012).

LTB₄ binds to two rhodopsin family G-protein coupled receptors, BLT₁R and BLT₂R; however, LTB₄ has higher affinity to BLT₁R than BLT₂R (Yokomizo *et al.* 1997; Yokomizo *et al.* 2000; Brink *et al.* 2003). They are both highly expressed in leukocyte populations as well as endothelial and vascular smooth cells (Brink *et al.* 2003). Neutrophil chemotaxis is induced upon LTB₄ ligand binding to BLT₁R or BLT₂R (Yokomizo *et al.* 1997). Murine models lacking BLT₁R or BLT₂R have revealed that LTB₄, more so than the other arachidonic acid derivatives, play an important role in the development of inflammatory conditions such as rheumatoid arthritis and asthma (Mathis *et al.* 2010).

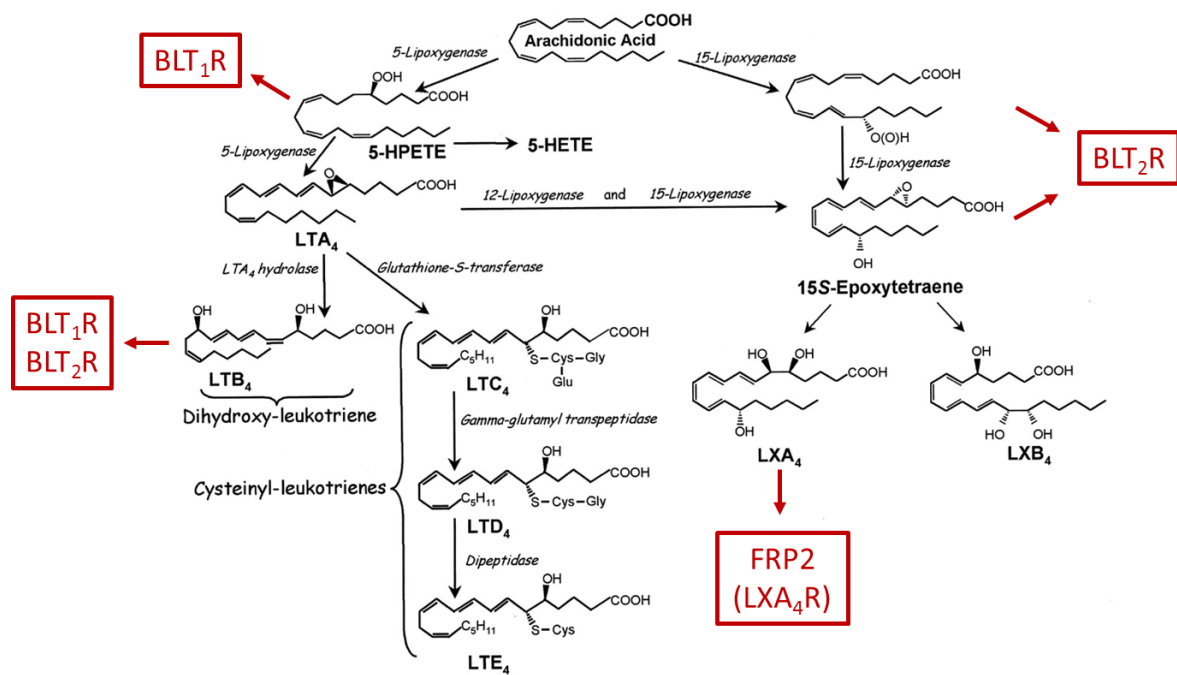


Figure 1-15: Arachidonic metabolites and their receptors, adapted from Brink *et al.* (Brink *et al.* 2003). Leukotriene B₄ is produced from leukotriene A₄ by LTA₄ hydrolase. Leukotriene B₄ binds with high affinity to BLT₁R and with low affinity to BLT₂R. 5-HETE and other arachidonic acid metabolites generated by cyclooxygenases can also bind BLT₂R. Lipoxin A₄, binds FRP2 or LXA₄R, inhibiting neutrophil chemotaxis.

A number of arachidonic acid derived lipid mediators compete for BLT₁R binding. These include: 12(S)-HETE, 12(S)-HpETE and 15(S)-HETE whereas 12(S)-Hydroxyheptadeca-5Z, 8E, and 10E-trienoic acid(12-HHT), derived through cyclooxygenase, have high affinity for BLT₂R (figure 1-15) (Okuno *et al.* 2008). The relevance of these other lipid competitors is not fully understood but it has been shown they may be important macrophage chemoattractants and encourage wound healing (Liu *et al.* 2014). Furthermore, ibuprofen, a cyclooxygenase inhibitor, may slow wound healing (Liu *et al.* 2014). This is also important for CF because some clinics prescribe high doses of ibuprofen as a non-steroidal anti-inflammatory drug.

1.4.4.f. Formyl-Met-Leu-Phe

During the 1980s *Escherichia coli* culture filtrates were found to possess chemotactic properties. Chromatography identified heterogeneous peptides specifically formyl-methionyl products from N-terminal regions (Marasco *et al.* 1984). Formyl-methionyl products are generated through bacterial protein synthesis and trafficking (Ye *et al.* 2009). Membrane-bound bacterial proteins that possess transporter signal peptides are cleaved by signal peptidases releasing peptide fragments into the extracellular space (Ye *et al.* 2009). The released peptides are anionic, ranging in molecular weights between 0.15 - 1.5 kDa;

furthermore, the chemotactic potency varies between peptide fractions generated by different bacterial species (Ye *et al.* 2009). The 440 Da tripeptide formyl-Met-Leu-Phe has been shown to be the most potent (Marasco *et al.* 1984). Formyl-peptides can also be endogenous to cells, originating from damaged mitochondria, specifically NADPH dehydrogenase subunit I (Shawar *et al.* 1995). During infection necrotic cells release DAMPs, including those produced by mitochondria, enhancing chemotaxis towards to tissue trauma (Shawar *et al.* 1995).

Studying formyl peptide receptors has highlighted a range of ligands from formyl to non-formyl peptides. Le *et al.* have reviewed these extensively (Le *et al.* 2002). Three pertussis sensitive G-protein coupled receptors for formyl-peptides have been identified; formyl peptide receptor (FPR), FPR2 and FPR3 (Ye *et al.* 2009). FPR and FPR2 are highly expressed on monocytes and neutrophils whereas FPR3 mRNA has solely been detected in monocytes and mature dendritic cells (Durstin *et al.* 1994; Yang *et al.* 2002). Furthermore, FPR3 is restricted to binding non-formylated proteins such as host acute phase proteins and amyloid- β (Le *et al.* 2002). FPR2 and FPR3 share 69% and 56% identity to FPR respectively; sequence divergence is most common in the receptor carboxyl tails required for signalling, whereas amino acid sequence is most conserved in the cytoplasmic loops (Ye *et al.* 2009). FPR2 has a low affinity to fMLP but high affinity to the lipid mediator lipoxin A₄, therefore FPR2 is also known as LXA₄R (Fiore *et al.* 1994). None the less both FPR and FPR2 are “promiscuous” receptors and bind a growing list pathogen and host derived peptides (Rabiet *et al.* 2007).

1.4.4.g. Comparison of neutrophil chemoattractants

Interestingly, several groups have compared neutrophil chemotaxis when stimulated simultaneously by opposing gradients of different chemotactic molecules (Lin *et al.* 2005; Kim and Haynes 2012). Here, microfluidic platforms were used to precisely compare the potency of chemotactic molecules (Lin *et al.* 2005; Kim and Haynes 2012). Initial reports by Lin *et al.* examining CXCL8 and LTB₄ showed that CXCL8 is 4 to 5-fold more potent when used to induce chemotaxis at the same molar ratio (Lin *et al.* 2005). Additionally, Lin *et al.* show that at high LTB₄ concentrations CXCL8 promoted LTB₄-mediated stimulation (Lin *et al.* 2005).

Chemoattractants also have different roles within the different stages of chemotaxis. It has been demonstrated that CXCL8 and LTB₄ draw neutrophils from circulation to the affected tissue; whereas, fMLP and C5a are important for end-stage chemotaxis, directing neutrophil to the infection or trauma locus (Heit *et al.* 2002). Heit *et al.* found that the p38 MAPK signalling pathway used by fMLP and C5a receptors could inhibit PI3K/Akt signalling by induced CXCL8

and LTB₄ (Heit *et al.* 2002). Therefore, C5a and fMLP can override other chemoattractants. Kim and Haynes later investigated the potency of host-derived and pathogen-derived stimulants by comparing fMLP, CXCL8, CXCL2 and LTB₄ in a series of pairwise tug of wars. They established a hierarchy of chemotaxis showing that fMLP > CXCL8 > CXCL2 > LTB₄ confirming the initial reports by Heit *et al.* Kim and Hayes also noted that the above molecules had functions in addition to chemotaxis as determined by signalling pathways, such as priming, stimulating degranulation, cytokine release and upregulation of opsonic receptors. In their summary Kim and Haynes reflected on the complex local environment in disease which is difficult *in vitro* (Kim and Haynes 2012).

1.4.5. Phagocytosis

Following transmigration to the affected tissues, neutrophils recognise pathogens using PPRs. These simulate the release of chemoattractants and pro-inflammatory cytokines as well as facilitating phagocytosis. Neutrophils are phagocytic and possess opsonic receptors (CR1, CR3, CR4) that bind complement proteins (C3b, C4b, C1q, mannan-binding protein, iC3b), they also express Fc receptors for phagocytosis of pathogens opsonised with immunoglobulins (Futosi *et al.* 2013). The process of phagocytosis requires mobility of phagocytic/opsonic receptors (figure 1-16).

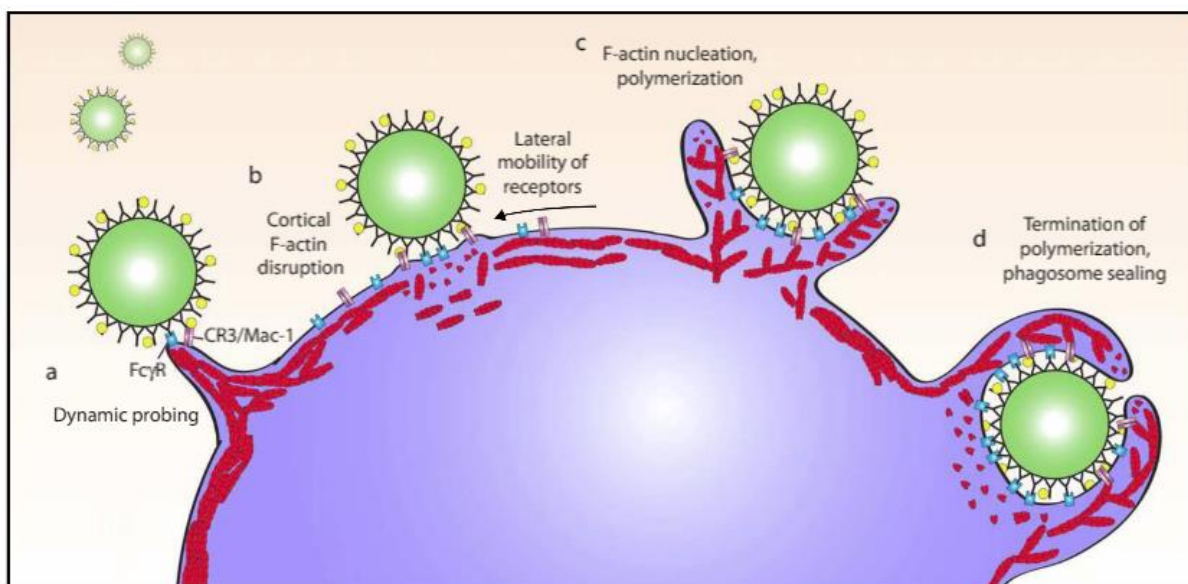


Figure 1-16 Diagram of the process of phagocytosis, extracted from Freeman and Grinstein (Freeman and Grinstein 2014) a) Phagocytes probe the environment by projecting phagocytic and opsonic receptors on pseudopods. b) Mobility of receptors is increased by debranching and severing actin. c) Actin polymerisation projects pseudopods around pathogen. d) Membrane merges and seals the phagosome.

Upon binding pathogens, actin is debranched by coronins and severed by cofilin and gelsolin so that further receptors can localise and enable the pathogen to be engulfed (Freeman and Grinstein 2014). Activation of pro-inflammatory FcγRs and C-type lectins induces signalling via ITAM and the syk-pathway, this recruits WASP and Arp2/3 complexes that promote actin polymerisation and myosin mobilisation of actin to extend the membranes into pseudopods (Freeman and Grinstein 2014). The final step is termination of actin polymerisation and fusing of the membrane to envelope the pathogen into the phagosome (Freeman and Grinstein 2014).

1.4.6. ROS production

Endosomal compartments containing pathogens fuse with granules containing anti-microbial agents and proteases such as lactoferrin, mediators of ROS production (such as MPO and flavocytochrome) as well as NSPs (Cowland and Borregaard 2016). ROS are generated by NADPH oxidase that reduce NADPH, donating the electron to oxygen, the by-product, H₂O₂, is subsequently converted to hypochlorous acid by MPO (El-Benna *et al.* 2016). In combination O₂⁻, H₂O₂ and hypochlorous acid are antimicrobial agents that destabilise and rupture cell membranes of phagocytosed pathogens within cytosolic compartments. The dependence on ROS for combating pathogens is highlighted in chronic granulomatous disease, whereby patients can have one of five mutations in the gene for NADPH oxidase; these lead to reduced ROS production (Roos and de Boer 2014). Consequently, people with chronic granulomatous disease have recurrent infections caused by pathogens such as *Burkholderia cepacia*, *Staphylococcus aureus* and *A. fumigatus* (Roos and de Boer 2014).

1.4.7. Degranulation

Activation of neutrophils by factors such as fMLP and C5a, through their respective G-protein coupled receptors, induces a process called degranulation, whereby neutrophil granules fuse with the cell membrane and their contents (enzymes, anti-microbial peptides and ROS) are released into the extracellular environment. Degranulation is not just important for clearance of pathogens but enables migration of neutrophils through the ECM, by degradation of the dense network of collagen fibres that support tissue structure. Here, degranulation is induced by the interaction between β-integrins and ICAMs (Mocsai *et al.* 1999; Mocsai *et al.* 2000; Fumagalli *et al.* 2007).

It has been found that neutrophils degranulate sequentially in response to different cues. For example, during extravasation, or prolonged stimulation by cytokines. However, overstimulation and inefficient phagocytosis of apoptotic neutrophils can result in an uncontrolled release of proteases (Cowland and Borregaard 2016).

Three granule types have been described: Primary, secondary and tertiary granules and in addition secretory vesicles (table 1-5).

Granule		Component	Function
Primary	Neutrophil serine proteases	Neutrophil Elastase	Antimicrobial, immune activation, zymogen and cytokine activation, NET localisation
		Cathepsin G	
		Proteinase 3	
		Azurocidin	Epithelial tissue permeability (family member but not protease)
	Acid hydrolases	β -glucuronidase α -fucosidase α -mannosidase	ECM breakdown
	Cationic Proteins	Defensins	Pattern recognition molecule
		MPO	ROS production
Lysozyme		Bacterial cell wall breakdown	
Secondary	Lactoferrin	Iron-sequestering, biofilm breakdown	
	Collagenase (MMPs)	ECM breakdown	
	Lysozyme	See above	
	Flavocytochrome	NADPH oxidase component	
Tertiary (Gelatinase)	Gelatinase Collagenase	ECM breakdown	
Secretory vesicles	fMLP receptor	PRR, chemotaxis, degranulation	
	CR3	C3b (opsonin) receptor	
	CR1	C4b (opsonin) receptor	
	Flavocytochrome	See above	

Table 1-5: Neutrophil granules, the function of their contents, adapted from Cowland and Borregaard 2016 (Cowland and Borregaard 2016).

The three types of neutrophil granules contain proteases that are relevant to function. A fourth type, secretory vesicles, enable quick mobilisation of PRRs and Fc γ R receptors to the cell surface (Cowland and Borregaard 2016). Upon diapedesis from the circulation, tertiary granules release gelatinase and collagenase that break down ECM allowing access to infection site (Cowland and Borregaard 2016). Whereas primary and secondary granules contain anti-microbial molecules and proteases (Cowland and Borregaard 2016).

Proteases are kept physically separate to prevent protease-protease degradation. For example, neutrophil gelatinase-associated lipocalin, can be degraded by neutrophil elastase (NE) (Le Cabec *et al.* 1997). For the same reason, NSPs such as NE and cathepsin G (CG), are stored as precursors and require proteolytic activation by cathepsin C (Lindmark *et al.* 1994).

1.4.7.a. Neutrophil serine proteases

NSPs are instrumental in the lysosomal degradation of phagocytosed pathogens and local breakdown of ECM. The three proteases with highest granular expression are NE, CG, and proteinase 3 (PR3) (Cowland and Borregaard 2016). NSPs are homologous and belong to the chymotrypsin super family. NE and PR3 share 53% sequence homology and their genes are located proximally on chromosome 19. Coding for CG is found on chromosome 14 alongside genes for chymase and granzyme H (Zimmer *et al.* 1992). NSPs contain a serine residue within the active site that acts upon carbonyl bonds within substrate peptides. Substrate specificity is determined by amino acid sequence of the active site and the surrounding surface loops. The active sites of NE and PR3 are similar due to shared homology; they are hemispherical and hydrophobic. The active site of CG is larger than either NE or PR3. It is separated into two compartments, with the lowest section carrying a negative charge. All three NSPs preferentially cleave hydrophobic residues. In particular, CG is characterised by chymotrypsin-like and trypsin-like activity, cleaving larger hydrophobic sequences (Korkmaz *et al.* 2010).

NSPs are readily ensnared in NETs (section 1.4.8) due their positive charge, and the negative charge of the released DNA. Using a panel of random fluorescently tagged peptides O'Donoghue *et al.* determined the proteolytic profile for the trapped proteases. NE was shown to be the most active and have the most diverse substrate specificity, followed by CG and PR3 respectively. However, the majority of substrates were cleaved by all three NSPs (O'Donoghue *et al.* 2013). It is therefore not surprising that NSPs have a wider role, not only as antimicrobial agents, but more widely in immune modulation.

NSPs can also degrade ECM substrates such as elastin, fibronectin and collagen (Kelly *et al.* 2008). However, if there is unregulated release of NSPs then tissue is susceptible to remodelling causing a loss of organ function, a particular issue in airway diseases such as asthma, COPD and CF (Kelly *et al.* 2008).

NSPs have been reported to cleave bacterial cell components such as protein A on Gram negative bacteria and flagellin on *P aeruginosa* (Belaouaj *et al.* 2000; Lopez-Boado *et al.* 2004). By generating NE deficient mice, Belaouaj *et al.* showed a dependence on NE to eradicate bacterial infection during peritoneal infection. More specifically, Gram-negative bacteria such as *Klebsellia pnemoniae* and *Escherichia coli*, but not Gram-positive pathogens such as *Staphylococcus aureus* (Belaouaj *et al.* 1998). With greater relevance to CF pathogens, Vethanayagam *et al.* determined the contribution of NE, CG and ROS to fighting bacterial pathogen *Burkholderia cenocepacia* and fungal pathogen, *A. fumigatus*. Interestingly, mice deficient in NADPH oxidase subunit p47^{phox} were unable to clear *A. fumigatus* inoculated via the airway. Yet, those deficient in NE and CG but not p47^{phox} recovered quickly. The authors concluded that the host requires multiple antimicrobial agents in addition to NSPs, for clearance of bacterial and fungal pathogens (Vethanayagam *et al.* 2011).

NSPs also have immunomodulatory roles such as activating inflammatory molecules from their pro- forms. For example, IL-1 β is an important stimulant for pro-inflammatory cytokines release (Joosten *et al.* 2009). It is classically activated via inflammasome protease caspase-1; however, PR3 has also been shown to cleave pro-IL-1 β into the active form in capase-1 deficient mice (Joosten *et al.* 2009). This additional mechanism of activation has cast doubt on the efficacy of caspase-1 inhibitors to treat elevated IL-1 β in rheumatoid arthritis, an autoimmune disease that is characterised by neutrophilic inflammation of joints (Joosten *et al.* 2009).

As well as activation of pro-inflammatory cytokines, NSPs have been reported to promote inflammation via modulation of immune receptors. Reports investigating NE function suggest that NE can upregulate expression of CXCL8 through induction of TLR4 signalling pathways (Devaney *et al.* 2003). As a consequence, cells become more sensitive to LPS and release CXCL8. Using PI-phospholipase, David *et al.* have demonstrated that PR3 binds GPI-anchored Fc γ RIIIb (CD16) and NADPH oxidase located on neutrophil cell membranes, these interactions were shown to mediate induction of respiratory bursts (David *et al.* 2005).

NSPs are also able to activate protease activated receptors (PAR). PARs are G-protein coupled receptors that are activated upon binding of the ligand that, until cleaved, is fixed and distal from the signalling domain (Mercer *et al.* 2014). They are expressed on myocytes, neurons, platelets and endothelial cells; they are well-documented for activation by thrombin (Mercer *et al.* 2014). NSP modulation of PARs has been investigated. It has been found that

NE cleavage sites on PAR-1 inactivates the receptor (Mercer *et al.* 2014). Conversely, PR3 cleaves PAR-2 stimulating CXCL8 release and an increase in endothelial permeability (Kuckleburg and Newman 2013). In addition, NE has been shown to induce PAR-2 mediated release of MU5AC using goblet-like Calu-3 cells (Zhou *et al.* 2013a). Therefore, because there is neutrophilic inflammation in the CF airway, NSPs could be important for elevated mucus production in this disease (Zhou *et al.* 2013a).

1.4.7.b. Neutrophil serine protease inhibitors

Host-derived protease inhibitors regulate protease function to prevent tissue damage. Several inhibitors control NSP activity in the lung, these are: α 1-anti-trypsin (AAT), Serpin B (including proteinase inhibitor 6 and proteinase inhibitor 9), secretory leukocyte protease inhibitor (SLPI) and elafin (Korkmaz *et al.* 2010). I will discuss AAT, SLPI and elafin in more detail as these have been shown to be the most significant inhibitors of NSPs in the CF airway (Korkmaz *et al.* 2010).

AAT is an inhibitor of NE, CG, MMP-12, trypsin and plasmin (Korkmaz *et al.* 2010). AAT is from a family of proteinase inhibitors called serpins. AAT is produced by the liver (acute phase), but it has also been shown to be produced by neutrophils (stored in granules), macrophages as well as epithelial cells (du Bois *et al.* 1991; Twigg *et al.* 2015). AAT is a 52 kDa glycoprotein, and therefore, because of its size, cannot easily diffuse from the circulation. This means that isolated tissues rely upon local production to maintain regulation of NE (and CG) activity (du Bois *et al.* 1991). AAT binds irreversibly to NE and CG (and other proteases) at a ratio of 1:1. During the interaction between NSP and AAT the peptide bond Met358-Ser359 on AAT is cleaved by the protease causing a conformational change (Korkmaz *et al.* 2010).

An interesting secondary function of AAT is that it has been shown to bind the lipid chemoattractant LTB₄ via protein-lipid hydrophobic interactions. This prevents LTB₄ from interacting with the chemotactic receptor BLT₁R (O'Dwyer *et al.* 2015). Furthermore, the interaction with LTB₄ does not affect the inhibitory function of AAT towards NE (O'Dwyer *et al.* 2015).

To highlight the importance of AAT and NSP regulation, genetic mutations in the *serpina1* gene can lead to airway diseases that manifest as symptomless to severe pulmonary disease such as COPD (Janciauskiene *et al.* 2018). Moreover, mutant "Z" variants of AAT (Glu to Lys

at position 342) can form polymers that have been shown to be chemotactic for neutrophils, driving pulmonary disease further (Janciauskiene *et al.* 2018).

SLPI, is smaller than AAT (11.7 kDa), but like AAT SLPI is also produced by neutrophils and macrophages. Additionally, in the lungs it can be generated by mucosal glands, alveolar macrophages and epithelial cells through stimulation by cytokines and LPS (Saitoh *et al.* 2001; Twigg *et al.* 2015). SLPI is inhibitory towards NE, CG, trypsin and chymotrypsin (Saitoh *et al.* 2001). Despite homology with NE, the active site of PR3 has an isoleucine residue at position 190 (compared to valine in NE), this one amino acid difference means that the PR3 active site is slightly smaller and therefore, cannot bind SLPI (Fujinaga *et al.* 1996). Unlike AAT, the interaction between SLPI and target proteases is reversible, this is because binding is mediated via 6 hydrogen bonds rather than conformational changes, as shown for AAT (Koizumi *et al.* 2008).

An important structural property of SLPI is that it is small and, therefore, can diffuse more efficiently through tissue, protecting the ECM from excessive degradation (Korkmaz *et al.* 2010). As well as NSP inhibition, SLPI has also been demonstrated to have anti-inflammatory functions by dampening the response of monocytic cells to CXCL8, TNF α and to bacterial components such as LPS and lipoteichoic acid (Taggart *et al.* 2005). The mechanism behind these anti-inflammatory functions are intracellular. SLPI can enter the nucleus of monocytic cells and bind NF-kB, preventing pro-inflammatory cytokine transcription (Taggart *et al.* 2005).

Elafin is also small (6 kDa) and shares 40% homology with SLPI; however, a significant structural difference is that elafin can be released as a pre-cursor molecule (pre-elafin or trappin-2) that possesses a transglutaminase substrate in the N-terminal (Schalkwijk *et al.* 1999). The importance of this N-terminal tail is that it facilitates incorporation of elafin into the lung ECM by a process called interstitial transglutamination (Schalkwijk *et al.* 1999). Like SLPI, a small molecular weight and immobilisation in the ECM are crucial for protecting tissue remodelling by proteases (Korkmaz *et al.* 2010). Interestingly, chimeric inhibitors combining the inhibitory specificity of SLPI and elafin have been recombinantly produced as a potential therapeutic for targeting all three major NSPs (NE, CG and PR3) (Zani *et al.* 2009).

Similar to SLPI, elafin too has anti-inflammatory properties that work in the same way. It has been shown that elafin inhibits NF-kB activation in monocytes reducing production of TNF α and macrophage inhibitory protein-2 (Butler *et al.* 2006). Additionally, due to its cationic charge, elafin also has anti-microbial activity, binding several bacterial pathogens such as *Staphylococcus aureus*, *P. aeruginosa* and the fungal pathogen *C. albicans* (Bellemare *et al.*

2010). Furthermore, elafin has been shown to accumulate in the cytosol of *P. aeruginosa*, bind DNA and interfere with the expression of virulence factors, such as biofilm production (Bellemare *et al.* 2010). This is of particular interest to CF because the above pathogens are prevalent in the CF airway.

1.4.8. NET formation

A final arm of the neutrophil arsenal against pathogens in the release of DNA to form NETs, a process that can be likened to a self-destruct mechanisms (Brinkmann 2018). NETs form three-dimensional structures that ensnare Gram-positive, Gram-negative bacteria as well as yeast and hyphal forms of fungi (Branzk *et al.* 2014; Brinkmann 2018). The negative charge of DNA within NETs captures anti-microbials, proteases and ROS that are released simultaneously with NETs (Brinkmann 2018). NETs and their captured components, breakdown and kill the ensnared pathogens preventing them from spreading infection throughout tissue (Urban *et al.* 2009). Complement proteins have also been detected in NETs. It has been shown that both the classical and alternative pathways can be activated using complement components ensnared in NETs (Wang *et al.* 2015a). Despite this, it is unclear how significant the relationship between complement and NETs is for clearing infection or promoting pathogenesis during inflammation (Wang *et al.* 2015a).

The process of generating NETs (NETosis) has been described as a death pathway that is not necrosis or apoptosis. Furthermore, there is an element of control that dictates how much DNA is released meaning NETosis is not necessarily suicide (Brinkmann 2018). NETosis has been shown to be induced by a list of mediators, such as: pathogen components (bacterial, fungal and viral), CXCL8, activated platelets, complement and ROS (Brinkmann 2018). The pathways that lead to NETosis have been studied in most detail using phorbol 12-myristate 13-acetate (PMA), a compound that is used throughout cell-biology to stimulate signal transduction via protein kinase 3 (PK3) (Fuchs *et al.* 2007). The subsequent generation of cytosolic ROS disintegrates mitochondria and the nucleus and increases intracellular calcium (Fuchs *et al.* 2007). Rising calcium concentration activates peptidyl-arginine 4, facilitating the unravelling of chromatin, this is in tandem with NE degradation of histones (Neeli *et al.* 2009; Papayannopoulos *et al.* 2010). Together, nuclear membrane break-down and expansion of chromatin changes the appearance of neutrophil nucleus from lobular to a round mass, prior to cell rupture (Fuchs *et al.* 2007).

There are also reports that neutrophils can undergo non-suicidal apoptosis, whereby mitochondrial, but not nuclear DNA, was released from vesicles (Yipp *et al.* 2012). Yipp *et al.* showed using knockout mice that C3 and TLR2 were essential for this process with preliminary analysis suggesting that C3a, and to a lesser extent C5a, were “vital NETosis” mediators. The authors go on to conclude that it makes sense that neutrophils should be able release NETs but still maintain other antimicrobial mechanisms such as phagocytosis and ROS (Yipp *et al.* 2012).

I have briefly discussed the key effector mechanisms of neutrophils for the clearance of pathogens; however, neutrophils have also been reported to contribute to resolution by releasing annexins and pro-resolving lipid mediators such as lipoxin A₄ (Jones *et al.* 2016b). Annexin-1 binds phospholipase A₂, inhibiting neutrophil and macrophage responses to pro-inflammatory cytokines and enzymes associated with nitric oxide synthesis (nitric oxide synthase) (Minghetti *et al.* 1999). Lipoxin A₄ reduces neutrophil chemotaxis by working as an antagonist against other pro-inflammatory lipids (leukotrienes), preventing upregulation of adhesion molecules and therefore slowing neutrophil migration to the site of inflammation (Papayianni *et al.* 1996; Scannell and Maderna 2006).

In summary, neutrophils are essential for the clearance of pathogens and a key component of inflammation; however, if inflammation becomes chronic due to persistent infection or over-stimulation, neutrophils can become pathological. ROS and protease release can collaterally damage host tissue causing tissue remodelling, fibrosis and loss of function. Diseases where neutrophils contribute chronic inflammation and tissue damage are: rheumatoid arthritis, cardiovascular disease, nephritis (Kruger *et al.* 2015). Furthermore, neutrophils contribute to the pathology of several lung diseases such as pneumonia, COPD, asthma and CF (Kruger *et al.* 2015). In the next section, I will discuss the role of neutrophil pathogenesis in the CF airway, particularly how neutrophils become dysfunctional and contribute to remodelling of the airway

1.5. Neutrophilic inflammation in CF airway

The CF airway is characterised by chronic neutrophilic inflammation yet, despite their numbers, neutrophils are ineffective at clearing infection and are therefore considered dysfunctional. Consequently, it has been well established that neutrophil count correlates with a decline in lung function, measured by FEV₁ (Hartl *et al.* 2012). The phenomenon of neutrophil dysfunction is not unique to CF and has also been described in sepsis or systemic infection (Delano and Ward 2016). Here, neutrophils are overwhelmed by pro-inflammatory signals and chemotactic molecules sending them into a state of “shock” (Delano and Ward 2016). In that condition, over-activation of neutrophils together with recruitment of immature neutrophils from the bone marrow leads to ineffective pathogen clearance and consequently, mortality (Delano and Ward 2016). The mechanisms behind neutrophil dysfunction in CF are poorly understood. To understand neutrophil dysfunction in CF we need to answer: 1) Why does the CF airway become dominated by neutrophils? 2) Despite their number, why are they so ineffective at clearing pathogens? I will address these questions by going through the key aspects of neutrophil dysfunction and how this has been shown to contribute to CF airway pathogenesis.

1.5.1. Neutrophil PRR expression in the CF airway

TLR2, TLR4 and TLR5 have been studied in depth with respect to expression in the CF airway (Hartl *et al.* 2012). Neutrophils in the CF airway highly express TLR5, which recognises bacterial flagellin. Using confocal microscopy and flow cytometry Koller *et al.* analyse neutrophils isolated from CF BAL fluid, there was significantly increased TLR5 expression compared to other TLRs and, there was significantly elevated expression on neutrophils in CF BAL fluid compared to healthy blood donors and non-CF bronchiectasis patients (Koller *et al.* 2008). Koller *et al.*, also showed that TLR5 correlated with the detection of flagellated bacteria in these patients demonstrating that TLR5 is important for response to pathogens. Furthermore, high levels of circulating oestrogen have been shown to impede NF- κ B activation, a transcription factor important in TLR signalling (Chotirmall *et al.* 2010). This consequently leads to reduced cytokine expression in female CF patients, shedding light onto the gender gap with regards to reduced lung function in CF (Chotirmall *et al.* 2010).

Neutrophils also store and degranulate pentraxin 3, an opsonic soluble PRR that recognises *A. fumigatus* and *P. aeruginosa* (Doni *et al.* 2016). Pentraxin 3 has high affinity to complement

C1q, enhancing complement activation and opsonisation of pathogen surfaces (Gaziano *et al.* 2004; Moalli *et al.* 2011; Doni *et al.* 2016). Expression of pentraxin 3 is elevated in COPD, correlating with neutrophilic inflammation and decline in lung function. However, this correlation does not necessarily imply a causal relationship (Van Pottelberge *et al.* 2012). Pentraxin 3 expression has also been studied in the CF airway; Hamon *et al.* reported that pentraxin 3 concentration in CF sputum is lower than that of COPD and healthy controls (Hamon *et al.* 2013). In explanation, the same authors demonstrate that proteases in the CF airway degrade pentraxin 3, particularly proteases released by *A. fumigatus* and therefore, degradation of pentraxin 3 may be a defence mechanism for this pathogen (Hamon *et al.* 2013). In conclusion, degradation of pentraxins by pathogen-derived and host-derived protease could be a contributing factor to poor pathogen clearance in the CF airway (Hamon *et al.* 2013).

1.5.2. NSPs in the CF airway

There have been numerous investigations into the dysfunction of neutrophil effector functions; however, there is not one single aspect of neutrophil dysfunction that is responsible for CF pathogenesis (Hartl *et al.* 2012). None the less, NSPs have been identified as a major contributor to neutrophil dysfunction through the cleavage of cell surface receptors and cytokines (Twigg *et al.* 2015). Furthermore, they have also been shown to promote non-canonical activation of cytokines (such as CXCL8, see section 1.4.7a) and other proteases (Twigg *et al.* 2015). In this section I will briefly discuss some of the substrates for NSPs that have been associated with neutrophil dysfunction in the CF airway.

NSPs, as well as ROS, are critical for killing pathogens following phagosome-lysosome fusion (Cowland and Borregaard 2016). NSPs and MMPs are also important for degradation of ECM, facilitating transmigration of leukocytes (Cowland and Borregaard 2016). In the CF airway, excessive neutrophil activation and reduced clearance of late apoptotic and necrotic neutrophils causes the unregulated release of neutrophil proteases into the airway (Hartl *et al.* 2012). Neutrophils generate different classes of proteases during granulopoiesis (table 1-5), but NSPs contribute widely to degradation of the ECM and, with relevance to neutrophil dysfunction, immune molecules and receptors (Hartl *et al.* 2012; Twigg *et al.* 2015; Cowland and Borregaard 2016).

1.5.2.a. Dysfunction in phagocytosis in the CF airway

In section 1.4.3 I discussed the array of phagocytic receptors on neutrophil cell surface. It has been shown that several of these phagocytic receptors are susceptible to cleavage by NSPs (Hartl *et al.* 2012). Tosi *et al.* have shown that FcγRIIIB but not FcγRIIB is susceptible to cleavage by NE, reducing, but not completely abrogating, *P. aeruginosa* phagocytosis (Tosi and Berger 1988). The same group also has shown that CR1, but not CR3, was susceptible to degradation; however, exposure to NE continued to prevent *P. aeruginosa* phagocytosis (Tosi *et al.* 1990). Tosi *et al.* went on to demonstrate that *P. aeruginosa*-bound iC3b could be also cleaved by both NE and pseudomonas proteases, inhibiting pathogen uptake (Tosi *et al.* 1990). More recently, our group has shown that Dectin-1 is also susceptible to degradation by NE and proteases expressed by *A. fumigatus*, reducing macrophage uptake of zymosan particles (Griffiths *et al.* 2018). In these experiments Dectin-1 cleavage was observed when exposed to CF BAL fluid with detectable NE activity, suggesting a role for impaired pathogen uptake in CF (Griffiths *et al.* 2018).

1.5.2.b. C5aR1 inactivation

C5aR1 is a G-protein coupled receptor that binds to the chemotactic complement fragment C5a (will be discuss in detail in section 1.7.3). It has been shown by our group that NSPs, present in the CF airway, can cleave and inactivate C5aR1 (van den Berg *et al.* 2014). This does not mean that C5a is not an important chemoattractant and inflammatory mediator in the CF airway. It was hypothesised that the C5a/C5aR1 axis contributes to the influx of neutrophils to the CF lumen; however, upon infiltration to the chronically inflamed airway NSPs cleave C5aR1 rendering it unresponsive to stimulation (van den Berg *et al.* 2014). As will be discussed later, C5a is not just a potent chemoattractant but critical for upregulation of PRRs and therefore, recognition and killing of pathogens (Hunniger *et al.* 2015).

1.5.2.c. Mucociliary clearance

PR3 has been shown to cleave and activate PAR-2 stimulating CXCL8 release and an increase in endothelial permeability (Kuckleburg and Newman 2013). In addition, NE has been shown to induce PAR-2 mediated release of MUC5AC using goblet-like Calu-3 cells (Zhou *et al.* 2013a). MUC5AC is a mucin that is elevated during chronic airway inflammation in

COPD and CF. Increased expression of mucins leads to airway obstruction causing infection and reducing lung function (Kreda *et al.* 2012).

NSP-mediated damage to cilia has also been investigated. Amitani *et al.* have shown using human tissue that NSP cause epithelial disruption by detachment from the basal membrane however, there was no evidence that NE (or Pseudomonas elastase from *P. aeruginosa*) were able to degrade cilia (Amitani *et al.* 1991).

Airway surfactants are important in reducing airway surface tension to facilitate gas exchange and prevent air collapse. Surfactant protein-A and surfactant protein-D are collectins (collagenous lectins); they are like C-type lectins but are soluble PRRs that opsonise pathogens for phagocytosis by neutrophils. It has been shown that both surfactant protein A and D concentrations are decreased in the CF airway compared to healthy controls (Postle *et al.* 1999). In explanation, it has been shown that both surfactant protein-A and D are susceptible to degradation by NSPs, preventing the role of opsonising pathogens (Rubio *et al.* 2004; Duvoix *et al.* 2011).

1.5.3. Dysfunction in ROS in the CF airway

ROS production is critical for pathogen killing, but it can also be detrimental towards host cells and can cause significant collateral damage when released in an unregulated manner, as observed in the CF airway (McGrath *et al.* 1999). It was demonstrated by Starosta *et al.* that oxidation of pulmonary proteins by ROS may promote pathogenesis (Starosta *et al.* 2006). Specifically, the authors found that protein carbonyls were elevated in CF patients with predicted lung function (FEV₁) less than <80%. Carbonyl groups (CO, aldehydes and ketones) are generated on protein side chains, especially during oxidation of amino acids such as proline, arginine and threonine (Dalle-Donne *et al.* 2003; Starosta *et al.* 2006). Furthermore, it has been proposed that malabsorption of anti-oxidants by individuals with CF hinders the ability to counteract excessive ROS release (Skov *et al.* 2015). To restore redox balance, two anti-oxidant derivatives, N-acetylcysteine and ascorbic acid, have been administered to CF patients in a trial (Skov *et al.* 2015). Skov *et al.* measured efficacy by monitoring lung function and urine oxidation markers over a three-month period. Despite observing encouraging trends, the authors concluded that the study was underpowered and could not confidently suggest routinely administering anti-oxidants (Skov *et al.* 2015).

1.5.4. NSP inhibitors in the CF airway

NSP inhibitors such as AAT, SLPI and elafin are essential for regulating NSP-mediated degradation; however, during excessive neutrophilic inflammation these inhibitors can be overwhelmed by the excessive release of NSPs themselves (figure 1-17). Proteolysis of ECM components such as, elastin, collagen and fibronectin remodels the airway, reducing lung function. Furthermore, the broad range and specificity of NSPs means that they can also activate PARs, cleave cytokines from pro-forms and inactivate phagocytic receptors and receptors that orchestrate neutrophilic inflammation, such as C5aR1 (Twigg *et al.* 2015).

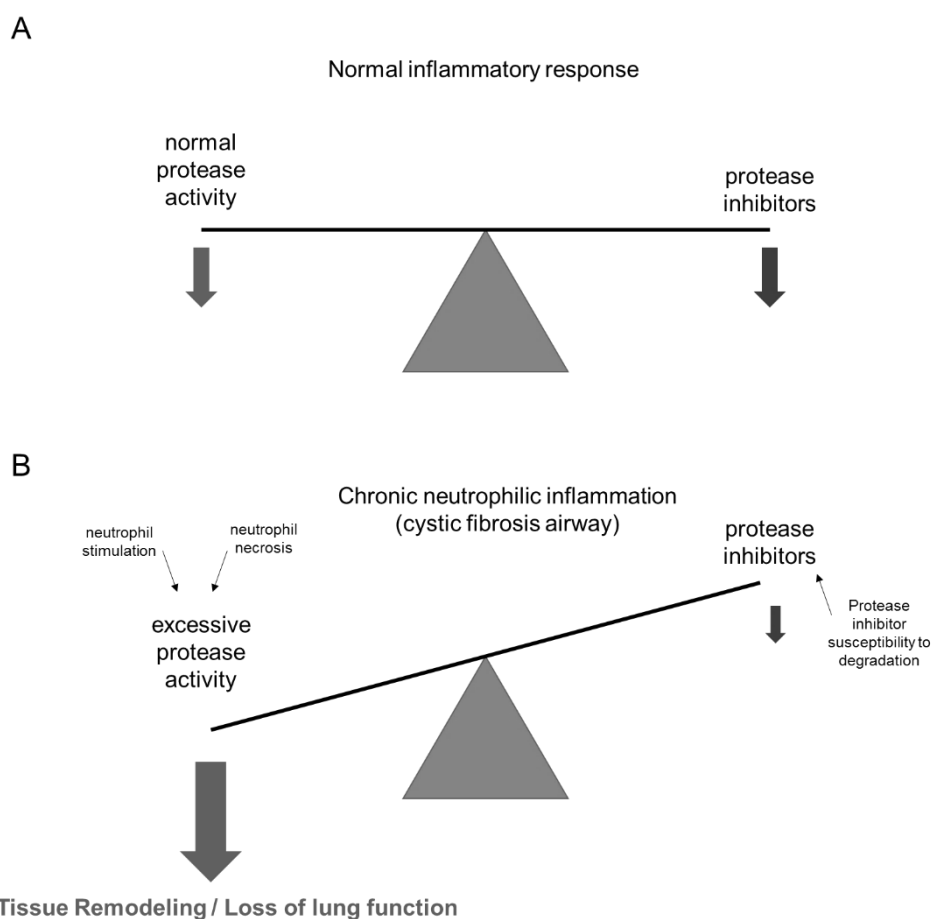


Figure 1-17: Protease and anti-protease balance in the normal and chronically inflamed airway. During a normal inflammatory response protease activity is regulated by protease inhibitors that are released by neutrophils, macrophages and resident lung cells. **B)** During chronic neutrophilic inflammation inefficient clearance of apoptotic neutrophils and stimulation of neutrophils causes the excessive release of NSPs into airway that overwhelm protease inhibitors. The fine balance protease/anti-protease balance is tipped and there is ECM degradation, tissue remodeling and consequently loss of lung function.

As well as there being an excess of proteases to inhibitors, it has also been shown that the inhibitors too are susceptible to degradation, reducing their activity towards proteases. It has been observed that SLPI is inversely proportional to pseudomonas elastase and NE in BAL fluid from CF patients (Weldon *et al.* 2009). Further investigation showed that NE could inactivate SLPI, cleaving at two different sites however, NE-degraded SLPI retained some inhibitory activity towards NE (Weldon *et al.* 2009). Degradation of SLPI has also been demonstrated using cathepsins S, L and B cysteines released by macrophages and lung epithelial cells (Taggart *et al.* 2001). As demonstrated for SLPI, Elafin can also be proteolytically inactivated by NE, as well as pseudomonas elastase (Guyot *et al.* 2008; Guyot *et al.* 2010). Cleavage of the elafin protease-binding loop by NE did not reduce the anti-microbial activity (Guyot *et al.* 2008). In contrast, AAT is resistant to proteolytic degradation by NE (and the other NSPs); however, inactivation by MMP-8 released by neutrophils has been demonstrated (Michaelis *et al.* 1990).

1.5.5. NETs

NETs entrap proteases and pattern recognition molecules such as collectins, ficolins and pentraxins; in turn these degrade or tag pathogens for phagocytosis (Brinkmann 2018). Due to their size fungal pathogens such as *C. albicans* and *A. fumigatus* are readily trapped in NETs (Parks *et al.* 2009). Conversely to the bactericidal function of NETs, *P. aeruginosa* can utilise DNA scaffolding in NETs to form biofilms, preventing recognition by the immune system (Parks *et al.* 2009). In CF, extracellular DNA inversely correlates with pulmonary function suggesting that neutrophil necrosis and NET assembly contributes to pathogenesis. However, bacterial lysis will also contribute to extracellular DNA (Lethem *et al.* 1990). To counteract the detrimental effects of NETs, a trial of DNase was administered to children with CF (Ratjen *et al.* 2005). Decreased DNA concentration was observed over 18 months, whilst neutrophil numbers were not significantly different to the placebo group (Ratjen *et al.* 2005). The authors state that DNase is not directly anti-inflammatory; however, reviews of the long-term impact of this treatment on lung function suggest it is more beneficial for the most unwell patients (Konstan and Ratjen 2012).

1.5.6. Resolution of inflammation

Efferocytosis of apoptotic neutrophils is an important initiator of inflammatory resolution. Neutrophils have a short life span in circulation (8 to 20 hours) and longer life span in tissue (1 to 4 days) (Greenlee-Wacker 2016). Neutrophils are highly adaptive to their local environment allowing them to rapidly respond to infection or damage but also respond to pro-resolution cues that prevent them causing collateral damage of tissue (Prince *et al.* 2017). In a recent report investigating important pathways in neutrophil survival, Prince *et al.* stimulated neutrophils *in vitro* with several pro-survival cues (cAMP (protein kinase A agonist), GM-CSF, LPS, conditioned (LPS-treated) monocyte media, hypoxia (Prince *et al.* 2017). Messenger RNA transcripts were quantified. Interestingly, a combination of two PKA agonists (N6/8-AHA) upregulated an intriguing apoptosis pathway that involved transcription of nuclear receptors, *NR4A2* and *NR4A3* (Prince *et al.* 2017). Further experimentation in murine cells knocking down expression of *NR4A2* and *NR4A3* using siRNA, revealed that *NR4A2* but not *NR4A3* was important for neutrophil survival.

Apoptosis of neutrophils can be triggered intrinsically or extrinsically with respect to the cell (Moriceau *et al.* 2010). For example, ROS-induced disruption to mitochondrial membrane potential or ER can induce apoptosis intrinsically (Moriceau *et al.* 2010). Neutrophil apoptosis can be triggered extrinsically by Fas via Fas receptors and tumour necrosis factor alpha (TNF α) via TNF-R1. Moriceau *et al.* have demonstrated delayed neutrophil apoptosis in $\Delta F508$ *cftr* heterozygotes and homozygotes in comparison to healthy controls (Moriceau *et al.* 2010). It was hypothesised that reduced glutathione, an important cellular anti-oxidant, may delay Fas-mediated apoptosis in CF patients due to deficiencies in the CFTR, but they recognised that other unknown factors could be responsible (Moriceau *et al.* 2010).

Macrophages are essential for the efferocytosis of apoptotic neutrophils. It has been shown that the phosphatidylserine receptor expressed on monocyte-derived macrophages is susceptible to NE and CG cleavage reducing uptake of apoptotic Jurkat cells (T-cell line) (Vandivier *et al.* 2002b). In the same report it was shown that surfactant protein-D, found reduced in the CF airway and airway disease, is critical for clearance of apoptotic neutrophils through binding to MPO. Later insight into surfactant protein D deficiency in the CF airway has revealed susceptibility to cleavage mediated by NE and CG (Duvoix *et al.* 2011). Investigation into the role of surfactant protein D in the CF airway by our group also revealed, that the level of surfactant protein D oligomerisation is important for function. Particularly,

lower levels of surfactant protein D oligomerisation, as found in the CF airway, were less capable of binding zymosan (Kotecha *et al.* 2013).

1.5.7. GAGs in the CF airway

GAGs are linear repeats of heterogenous polysaccharides that are expressed on the cell surface and are important constituents of the ECM, particularly in the alveolar epithelium and subepithelial tissue of the airways (Reeves *et al.* 2011a). GAGs have multiple homeostatic functions in cell migration, differentiation, adhesion, wound healing and inflammation (Reeves *et al.* 2011a). The structural properties and function of GAGs in the airway will be discussed in greater detail in chapter 6 as part of the background to the study. However, I will briefly cover some of the major aspects of GAGs and their role in pathogenesis of the CF airway.

As well as protease inhibitors, GAGs, such as HS, play an important role in regulating NE activity (Reeves *et al.* 2011a). The mechanism here is that HS is generated in large arrays with a protein core (such as syndecan). During an inflammatory response NE can cleave syndecan releasing soluble HS (Spencer *et al.* 2006). In turn, soluble HS inhibits NE activity, regulating activity and preventing extensive damage to the ECM or affecting the inflammatory process (Spencer *et al.* 2006). However, during chronic neutrophilic inflammation of the airway, such as in CF, NE degrades HS proteoglycans, but the high NE activity overwhelms the above feedback mechanism, leading to tissue degradation (Spencer *et al.* 2006; Reeves *et al.* 2011a).

Soluble GAGs, released by degradation of the ECM, have been shown to bind with multiple chemokines and anti-microbial peptides modifying their functions both positively and negatively (Reeves *et al.* 2011a). For example, LL-37 (also known as cathelicidin) is an anti-microbial protein that binds LPS, it is also chemotactic for neutrophils and induces degranulation and ROS production via stimulation of FPR2 (Zanetti 2004; Bergsson *et al.* 2009). Binding of LL-37 to GAGs reduces antimicrobial activity furthermore, GAGs prevent degradation of LL-37 allowing it to accumulate in the CF airway (Bergsson *et al.* 2009).

CXCL8 is another important example of the immunomodulatory effects of soluble GAG binding in the CF airway (Reeves *et al.* 2011b). It has been shown that several different GAGs bind to CXCL8. Furthermore, it has been hypothesised that these interactions are important for establishing chemotactic gradients within tissue, such as the lungs (Pichert *et al.* 2012b). CXCL8, is elevated in the CF airway, despite susceptibility to degradation by NSPs (Dean *et*

al. 1993; Leavell *et al.* 1997). It has been shown that when in complex with GAGs CXCL8 is resistant to degradation by NSPs (Reeves *et al.* 2011b). Unlike LL-37, GAG interaction with CXCL8 does not alter function however, in both the case of LL-37 and CXCL8, hypertonic saline, a mucolytic therapy in CF, disrupts GAG interactions increasing susceptibility to degradation (Bergsson *et al.* 2009; Reeves *et al.* 2011b; Schlorke *et al.* 2012).

Neutrophil Dysfunction in the CF airway

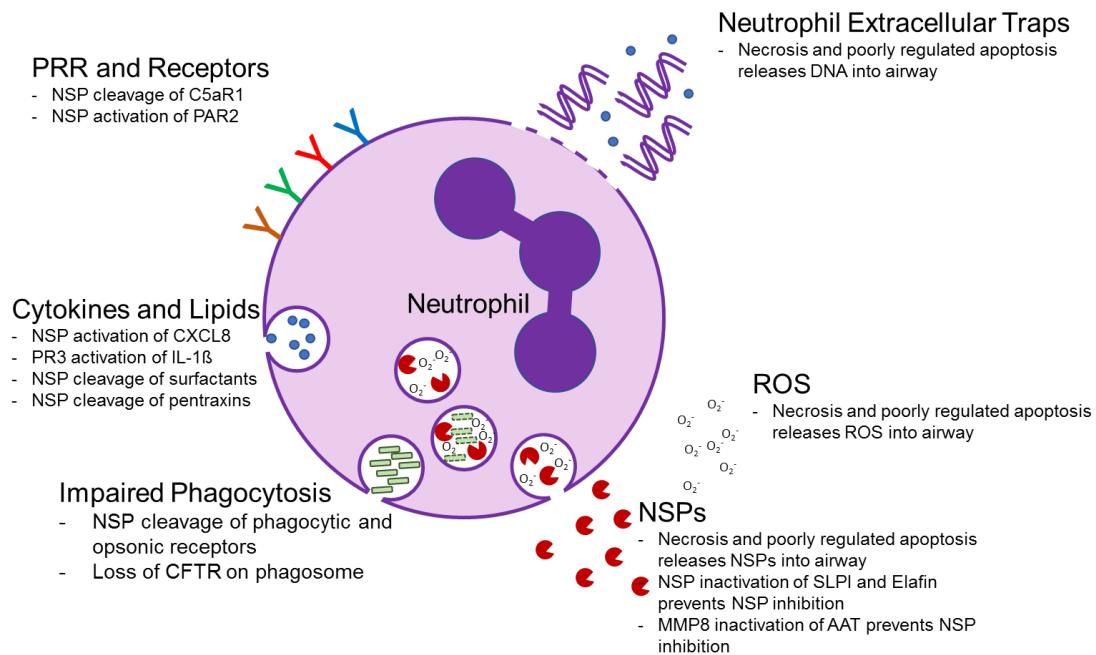


Figure 1-18: Overview of the reported mechanisms of neutrophil dysfunction in the CF airway

In this section I have discussed several aspects of neutrophil dysfunction that drive pathogenesis in the CF airway (summarised in figure 1-18). Impaired neutrophil function during chronic neutrophilic inflammation sheds light on why they might be ineffective at clearing pathogens; however, understanding the factors underpinning excessive PMN recruitment to the CF airway is crucial. Investigating the conundrum of excessive neutrophil recruitment to the CF airway has been approached in two ways 1) characterising neutrophil chemoattractants that are elevated in the CF airway 2) Assessing defects in neutrophil efferocytosis. Investigation of how neutrophilic inflammation is initiated and resolved in the CF airway has revealed that there is dysregulation in both (Hartl *et al.* 2012). I have briefly discussed dysfunction in the clearance of apoptotic neutrophils in the CF airway in the previous section. In the next section I will focus on the chemoattractants that have been found

elevated in the CF airway and how they individually contribute to pathogenesis in the CF airway.

1.5.8. Neutrophil recruitment in the CF airway

Neutrophil chemoattractants have been found elevated in the CF airway and are thought to be a major contributing factor to disease progression through neutrophil recruitment (Sagel *et al.* 2007; Mackerness *et al.* 2008). The most intensively investigated chemoattractant is CXCL8; however LTB₄, fMLP, platelet activation factor (PAF) and C5a have also been reported to be elevated (Mackerness *et al.* 2008). Mackerness *et al.* used CF sputum to stimulate neutrophil migration and assessed the significance of each of the above chemotactic molecules using inhibitory antibodies or receptor antagonists (Mackerness *et al.* 2008). They showed that inhibition of CXCL8 significantly reduced neutrophil chemotaxis towards sputum from 13 CF patients. Additionally, only by including inhibitors of LTB₄, fMLP, PAF and C5a or receptor antagonists could chemotaxis be fully arrested. Furthermore, using flow cytometry they show that neutrophil shape change, an indicator of chemotaxis, following incubation with CF sputum could be partially arrested by pre-incubating sputum with inhibitors for CXCL8, LTB₄, and fMLP. C5a and PAF receptor inhibitors were additionally required to completely prevent any shape change (Mackerness *et al.* 2008).

This important study highlights the fact that, despite CXCL8 being highly cited as the most significant factor contributing to neutrophil recruitment and activation, there are additional potent mediators that may also play a critical role in CF pathogenesis (Mackerness *et al.* 2008). We need to understand the function of each molecule and their role in CF pathogenesis before confidently pursuing them as therapeutic targets. I will discuss the significance of CXCL8, LTB₄ and fMLP in the CF airway (as well as other airway diseases) and, where appropriate, therapeutics that have been developed to reduce their pathogenesis.

1.5.8.a. CXCL8 in the CF airway

CXCL8 is a member of the chemokine family and is a potent chemoattractant (Griffith *et al.* 2014). Several groups have measured CXCL8 in CF airway samples such as BAL fluid or sputum and reported that it is significantly elevated compared to healthy or non-diseased controls. Furthermore, it is well established that CXCL8 correlates with neutrophilic count and markers of neutrophilic inflammation, such as NE activity (Dean *et al.* 1993; Richman-Eisenstat *et al.* 1993; Sagel *et al.* 2001). Due to the strong correlations reported between

CXCL8 and neutrophil count, CXCL8 is routinely used a marker of neutrophilic inflammation when investigating factors that promote neutrophilic inflammation or assessing the influence of therapeutics on CF airway inflammation (Ratjen *et al.* 2016; Barnaby *et al.* 2018).

As mentioned in section 1.5.7, CXCL8 (and other chemokines) have been shown to bind to GAGs and this is an interesting field within CF pathology. CXCL8, in complex with soluble GAGs, is protected from proteolysis by NSPs thereby, increasing its half-life within the CF airway. In CF clinics, nebulised hypertonic saline is administered to patients followed by a vigorous physiotherapy routine. Nebulised saline reduces mucus viscosity and alongside physiotherapy helps to free obstruction of the small airways. Reeves *et al.* demonstrated that hypertonic saline could be used to disrupt ionic bonds between CXCL8 and GAGs, facilitating the proteolytic cleavage of free CXCL8 by proteases present in the airway (Reeves *et al.* 2011b). McElvaney *et al.* have more recently engineered a compound, PA401, that could compete with CXCL8 for GAG-binding, therefore leaving CXCL8 susceptible to proteolysis by proteases (McElvaney *et al.* 2015). It was shown using CF BAL fluid, that increasing the concentration of PA401 could prevent CXCL8-GAG binding leaving the free CXCL8 susceptible to degradation by the constituent proteases however, the authors noted that PA401 was also susceptible to degradation by proteases (McElvaney *et al.* 2015). This mechanisms of promoting degradation CXCL8 by NSPs could help reduce CXCL8 levels in the CF airway and reduce the recruitment of neutrophils (McElvaney *et al.* 2015).

1.5.8.b. Leukotriene B₄ in the CF airway

LTB₄ is lipid neutrophil chemoattractant derived from arachidonic acid (Brink *et al.* 2003). LTB₄ is elevated in CF patient sputum and correlates with increased expression of TNF α , an important pro-inflammatory cytokine that upregulates the LTB₄-generating enzyme, 5-LOX (Greally *et al.* 1993). Characterisation of LTB₄ in CF BAL fluid revealed a 30-fold increase compared to healthy controls. Increased concentrations of less potent eicosanoids such as prostaglandins and thromboxane were also noted; these have functions including bronchoconstriction (Konstan *et al.* 1993). Despite high concentrations of LTB₄, chemotaxis of neutrophils was shown to be reduced in sputum from CF patients that were positive for *P. aeruginosa*, and in the presence of other chemotactic stimuli (fMLP), raising questions about cross-receptor inactivation or desensitisation (Lawrence and Sorrelli 1992).

In light of the elevated levels of LTB₄ in the CF airway, a double-blind clinical trial was carried out on a cohort of CF patients using a LTB₄ antagonist, BIIL-284 BS, a BLT₁R antagonist (Birke *et al.* 2001). Children and adults with CF were treated orally with a placebo or the

antagonist over a 24-week period. The trial was terminated prematurely following a significant increase in serious adverse events, such as pulmonary exacerbation resulting in admission to hospital (Konstan *et al.* 2014). In a separate study, the same group investigated the mechanism behind the adverse events in the BIIL-284 BS trial and found that inhibiting LTB₄-mediated neutrophil chemotaxis induced *P. aeruginosa* bacteraemia in mice (Doring *et al.* 2014). The BIIL-284 BS trial is further reason why we need to better understand the complex roles of the range of chemotactic and pro-inflammatory molecules in the CF airway before undergoing intervention.

1.5.8.c. fMLP in the CF airway

Formyl-Met-Leu-Pro is a by-product of bacterial protein synthesis. Recognition by surface receptors induces a potent chemotactic response and also stimulates degranulation and ROS production (Ye *et al.* 2009). In COPD, like CF, neutrophil inflammation promotes disease progression (Hoenderdos and Condliffe 2013). CXCL8 correlates with neutrophil recruitment during pulmonary exacerbation in COPD; however, fMLP-mediated ROS production plays an important role in pathogenesis, reducing lung function (Jones *et al.* 2016a). Quantification of formyl peptides and small host derived peptides such as DAMPs in the CF literature is not well-documented. Mackerness *et al.* identified formyl peptides in CF sputum using, ion-exchange chromatography. Furthermore, they used a FPR receptor antagonist, Boc-Met-Leu-Phe, to inhibit fMLP-mediated chemotaxis in CF BALF, demonstrating that fMLP contributes to neutrophil stimulation in the CF airway (Mackerness *et al.* 2008).

Complement C5a has also been identified as an important mediator of neutrophilic inflammation in the CF airway (Fick *et al.* 1986; Sass *et al.* 2015; Hair *et al.* 2017). In the next chapter I will discuss the complement system with particular focus on the complement anaphylatoxins, C3a and C5a, and their potential role in CF disease pathogenesis.

1.6. The Complement system

Complement is an evolutionary ancient arm of the immune system and crucial for the clearance of pathogens, necrotic cells and other foreign bodies (Ricklin and Lambris 2013). Throughout its evolution in humans complement has bridged adaptive and innate immune responses allowing specific targeting of pathogens via antibody complexes (Ricklin and Lambris 2013). Complement is essentially a cascade of proteases that cleave fluid phase mediators, the products of which assemble to produce other proteases with alternative

substrate specificity (Ricklin and Lambris 2013). There are three effector products of the complement system: the membrane attack complex (MAC), opsonins and the complement anaphylatoxins (figure 1-19). The main source of complement proteins is the liver; however, local generation of complement components is widely reported as a source of complement in tissue (Li *et al.* 2007).

1.6.1. Initiation and activation.

There are two activation pathways, classical and lectin, with a third pathway, or amplification loop, that rapidly upregulates complement activation (also known as the alternative pathway)(Ricklin and Lambris 2013). The classical pathway is predominantly initiated through C1q binding to immunoglobulins (IgG and IgM) on pathogen surfaces, or host cells in the case of auto-immune diseases such as systemic lupus erythematosus (Ricklin and Lambris 2013; Leffler *et al.* 2014).

Upon binding immunoglobulins (and pentraxin 3), C1q forms complexes with proteases C1r and C1s that cleave C4 and C2 into C4a and C4b or C2a and C2b respectively (Ricklin and Lambris 2013). C4b binds to cell surfaces and forms (with C2b) the C3 convertase (C4bC2b), a proteolytic complex central to the complement system (Ricklin and Lambris 2013).

The lectin pathway is initiated by mannose-binding lectin (MBL), ficolins and collectins that bind to mannose and other carbohydrates on the surfaces of pathogens and host cells (Ricklin and Lambris 2013; Farrar *et al.* 2016). Mannose-binding lectin associated proteases (MASPs) form complexes with MBL, ficolins and collectins and, like the C1 complex, cleave C2 and C4 to help assemble the C4bC2b C3 convertases (Ricklin and Lambris 2013)

The amplification loop is based around the principle that C3 can be spontaneously hydrolysed (C3(H₂O)) in blood by surfaces of particles, lipids, platelets and gas bubbles (Nilsson and Nilsson Ekdahl 2012). Factor D cleaves factor B into Bb, this binds with C3(H₂O) on cell surfaces to form a C3(H₂O)Bb C3 convertase (Nilsson and Nilsson Ekdahl 2012). C3 convertases (both C4bC2b and C3(H₂O)Bb) cleave C3 into C3a and C3b, C3b drives generation of more C3 complexes (C3bBb) (Nilsson and Nilsson Ekdahl 2012).

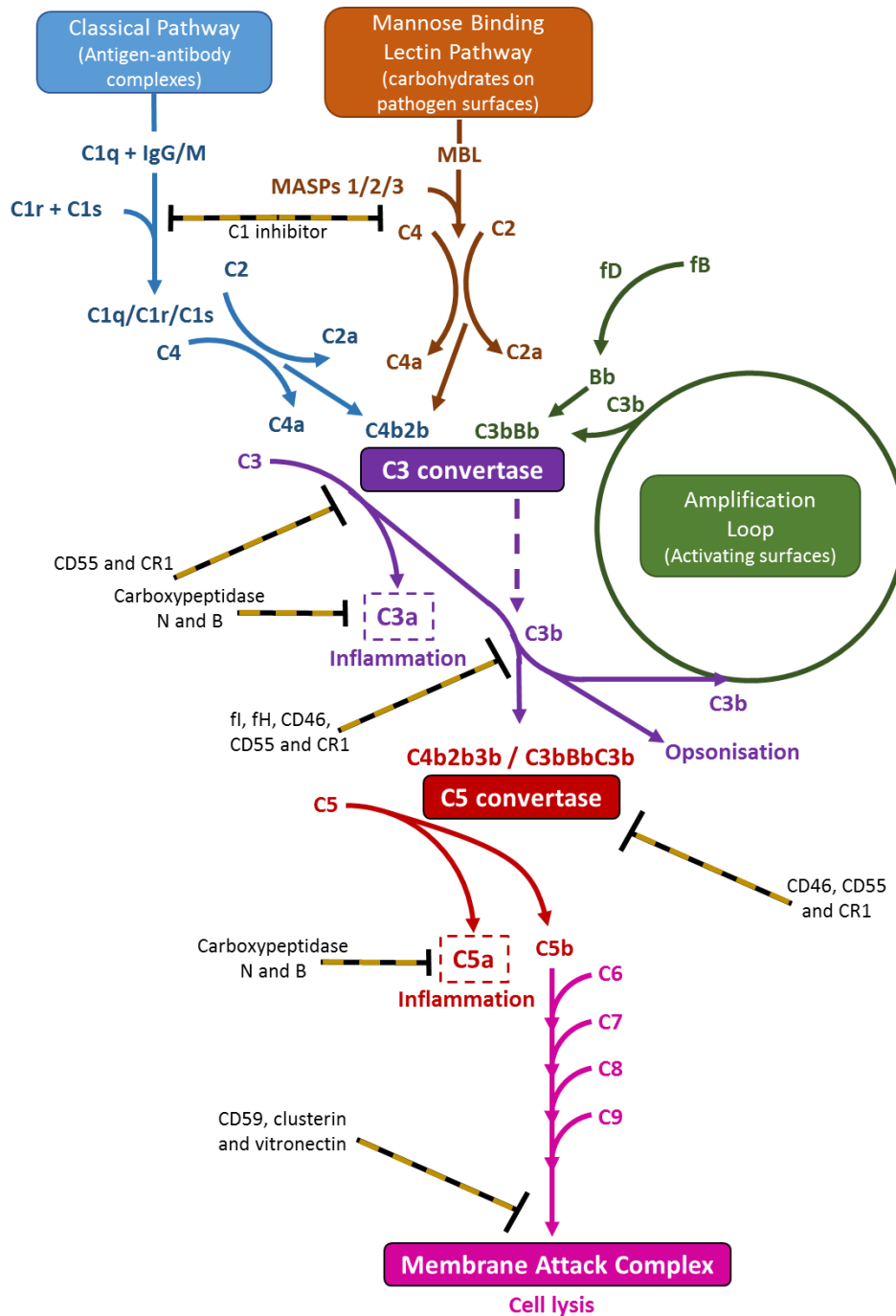


Figure 1-19 Diagram of the complement system and its functions and regulation.

The complement system is activated by two initiation pathways, classical (blue) and mannose binding lectin (orange). Activation can also be regulated via the amplification loop (green) also known as the alternative pathway. Complement activation converges on the assembly of C3 convertase (purple), cleavage of C3 produces C3b and C3a. C3b opsonises pathogen and host surfaces and those of foreign bodies such as debris or cholesterol crystals. The majority of C3b is inactivated or hydrolysed (iC3b) but this is still a functional opsonin. C3b can further drive complement activation via the amplification loop or bind to C3 convertase forming C5 convertase (red). C5 is cleaved by C5 convertase producing C5b and C5a. C5b inserts into cell surfaces and with the terminal components forms the membrane attack complex (pink). C3a and C5a are also produced by their respective convertases and have multiple pro-inflammatory functions. Complement is tightly regulated by complement regulators (black/yellow) that inhibit activation (C1 inhibitor), destabilise convertases (CR1, CD46, CD55, factor H and factor I) and prevent MAC formation (CD59, clusterin, vitronectin). The complement anaphylatoxins are inactivated by carboxypeptidases N and B.

1.6.2. Complement effector functions

The cleavage of C3 by C3 convertases produces C3a and C3b. As well as forming new C3 convertases, C3b can bind with C3 convertases to assemble C5 convertases (C4bC2bC3b and C3bBbC3b) (Ricklin and Lambris 2013). C5 convertases cleave C5 into C5a and C5b, with C5b interacting with C6 to form C5bC6. C5bC6 binds to cell surfaces and forms a larger assembly with C7 that inserts into the cell membrane (Ricklin and Lambris 2013). The final step is the binding of C8 and >20 C9 components to C5b6-9 to form a pore in the cell membrane called MAC, through which there is free movement of water and ions across the membrane (Serna *et al.* 2016). A threshold of multiple MACs on a cell surface are required to lyse pathogen and host cell membranes, below this threshold cell integrity is maintained, a phenomenon known as sub-lytic MAC formation (Triantafilou *et al.* 2013). The diffusion of ions into the cell through MAC still occurs and, in particular, the flow of calcium ions into host cells like monocytes and neutrophils has been reported to induce intracellular calcium signalling pathways, triggering inflammasome activation and IL-1 β production (Triantafilou *et al.* 2013).

C3b covalently binds hydroxyl groups on cell surfaces. These are mainly carbohydrates but can include protein amine groups (Ricklin and Lambris 2013). C3b on cell surfaces not only facilitates the assembly of C5 convertases and MAC formation but is also an opsonin for phagocytes through recognition by CR1 (Ricklin and Lambris 2013). C3b is predominantly found in an inactivated form (iC3b) following inactivation by Factor I and co-factors (Ricklin and Lambris 2013). Inactivated C3b cannot form C5 convertase but, along with other complement break-down products (such as C3d), can be recognised by complement receptors (CR1, CR2, CR3 (main iC3b receptor) and CR4) and therefore, iC3b is also opsonic (Ricklin and Lambris 2013). Opsonic recognition by complement is essential for clearance of pathogens and necrotic cells during infection (Freeman and Grinstein 2014).

The complement cascade also generates three anaphylatoxins, C3a, C4a and C5a (Ricklin and Lambris 2013). C5a and C3a are important orchestrators of inflammation that induce chemotaxis, degranulation and ROS production in monocytes and neutrophils; they will be discussed in greater depth in sections 1.7 and 1.8 respectively. The role of C4a in inflammation is not clear. A receptor for C4a has only recently been described, before then no function had been assigned. Wang *et al.* investigated C4a signalling using a screen of cells transfected with individual G-protein coupled receptors (Wang *et al.* 2017). The authors observed that C4a induced intracellular calcium flux via PAR 1 and 4 on endothelial cells, increasing

permeability. Despite intriguing results, these preliminary data require further investigation as the authors could only speculate on a role in disease (Wang *et al.* 2017).

1.6.3. Regulation of complement

Complement is important for clearance of pathogens as well as immune complexes, apoptotic and necrotic host cells; however, tight regulation is required to maintain homeostasis and prevent pathogenesis (Ricklin and Lambris 2013). The human complement system has several regulators that control activation and prevent MAC-mediated lysis of self-cells (Ricklin and Lambris 2013). C1 esterase inhibitor is a serine protease inhibitor that prevents activation of complement by binding to C1r and C1s, it can also inhibit proteases in the coagulation pathway and MASPs (Riedl 2015). Genetic deficiency in C1 esterase inhibitor causes hereditary angioedema, activation of complement and generation of complement anaphylatoxins (C3a and C5a) that consequently induce inflammation in the skin leading to swelling (Riedl 2015).

Complement regulation is also maintained by several cell surface molecules that either prevent MAC formation (CD59), prevent the formation of convertases (CD35/CR1) or act as co-factors for factor I-mediated inactivation of C3b (CD35/CR1, CD46, CD55) (Ricklin and Lambris 2013). CD59 is a glycoposphatidylinositol cell-surface anchored protein that prevents MAC formation by blocking C9 polymerisation on the C5b6-8 terminal pathway complex (Hillmen *et al.* 2006). The significance of CD59 in restricting MAC deposition is highlighted in paroxysmal nocturnal haemoglobinuria (PNH), a complement-mediated disease that is caused by mutation in GPI, required for CD59 (and CD55) presentation on cell surfaces (Hillmen *et al.* 2006). Erythrocytes only possess GPI-anchored cell surface complement regulators (CD59 and CD55) and therefore, are susceptible to lysis by MAC (Hillmen *et al.* 2006). As well as surface-bound MAC regulators, soluble MAC formation inhibitors, clusterin and vitronectin, bind to C7-C9 preventing MAC assembly and cell lysis (Ricklin *et al.* 2010).

CD55 (or decay accelerating factor, DAF) is a membrane bound regulator that dissociates C3-convertase (both C4b2b and C3bBb) and thereby prevents C5 convertase formation (Ricklin *et al.* 2010). CR1 also has decay accelerating function as well as being a phagocytic receptor for C3b (Ricklin *et al.* 2010). CR1 binds C3b and C4b acting as a cofactor for factor I-mediated inactivation to iC3b and iC4b; these inactivated fragments are unable to form convertases. Other regulators that act as cofactors for factor I are CD46 (membrane bound) and soluble

regulators such as factor H and factor H-like proteins, that interact with factor I and aid factor I mediated cleavage and inactivation of C3b, generating iC3b.

Finally, C3a and C5a are potent mediators of inflammation and therefore require tight regulation. C3a and C5a are rapidly inactivated by carboxypeptidase N (CPB) and B (CPB) through cleavage of the arginine C-terminal residue (Campbell *et al.* 2002). The products, C3adesArg and C5adesArg have substantially reduced activity (Campbell *et al.* 2002).

1.6.4. Non-canonical activation of complement by endogenous and exogenous proteases

An area of complement biology that has growing appreciation is the activation and regulation of complement by non-complement enzymes. These include, proteases from the coagulation system, NSPs released by neutrophils and also exogenous sources such as bacteria, fungi and protease from parasites such as dust mites (Brozna *et al.* 1977; Wetsel and Kolb 1983; Robbins *et al.* 1991; Giles *et al.* 2015). In particular, the generation of the complement anaphylatoxins C3a and C5a from their parent molecules (C3 and C5) during infection and inflammation (Huber-Lang *et al.* 2012; Yuan *et al.* 2015; Hooshmand *et al.* 2017). However, despite our knowledge of non-canonical C3a and C5a generation, our understanding of how much they contribute to disease pathology is unclear and will be discussed in much greater depth as part of the background to chapter 4.

1.6.5. Complement in disease

The complement system has important roles in homeostasis, development and immunity. Consequently, genetic deficiency in some complement components can lead to specific pathologies or susceptibility to infection (figure 1-20) (Ricklin and Lambris 2013). As mentioned above, mutations in GPI and cell membrane anchors can lead to PNH through lack of CD59 and CD55 expressions on erythrocytes (Hillmen *et al.* 2006).

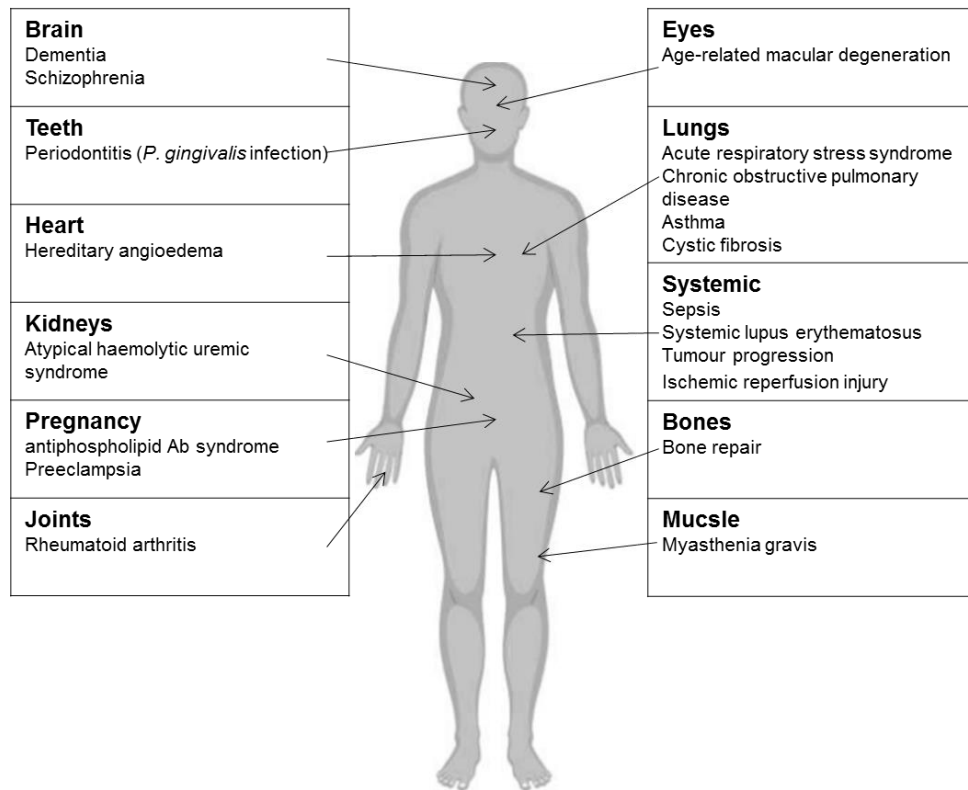


Figure 1-20: Diseases where complement has been reported to contribute to pathogenesis.

Another well-characterised disease where complement plays a major pathogenic role is atypical haemolytic uremic syndrome (aHUS), an auto-immune disease caused by auto-antibodies targeting factor H or mutation in genes coding for factor H (Wong *et al.* 2013). aHUS predominantly manifests in the kidneys whereby, over-activation of platelets or endothelial cell damage causes a loss of kidney function and leads to mortality through end-stage renal disease (Wong *et al.* 2013). To further highlight the importance of complement in host defence, there are rare cases of human genetic (homozygous) C3 deficiency (Botto *et al.* 2009). These patients have recurrent bacterial infections at a young age suggesting that complement plays an important role in host defence prior to establishing adaptive antibody repertoire (Botto *et al.* 2009). These patients also shed light on to the role of C3 in adaptive immune response and development of B cell memory (Botto *et al.* 2009; Ricklin *et al.* 2010).

A characteristic of many complement disorders is inflammation, a consequence of complement activation and generation of pro-inflammatory anaphylatoxins C3a and C5a, which recruit and stimulate migrating immune cells (Ricklin *et al.* 2010).

1.6.6. Complement and inflammation

Inflammation is a pathogenic factor in many complement-mediated diseases. Age-related macular degeneration (AMD) is a disease that causes a loss of vision in elderly people (Ricklin *et al.* 2010). The causes of AMD are currently still under investigation; however, mutation in complement components such as C3, factor B and factor H are reported to be risk factors (Kauppinen *et al.* 2016). AMD is a slow-acting disease driven and perpetuated by an imbalance in complement activation that promotes inflammation and damage of subretinal tissue (Kauppinen *et al.* 2016). This damage is thought to be mediated by activation of monocytes, macrophages and neutrophils through the release of ROS (Kauppinen *et al.* 2016).

Dementia has become increasingly accepted as an inflammatory disease, with complement playing a role in promoting pathogenesis (Morgan and Harris 2015). C1q has been shown to be elevated in brain tissue from Alzheimer's patients and is thought to be important in synaptic pruning (selective killing of synapses) and neurodegeneration (Morgan and Harris 2015). The role of C1q in synaptic pruning has been further elucidated in mice whereby C1q deficient mice were unable to efficiently clear inactive synapses (Morgan and Harris 2015; Hong *et al.* 2016). Alzheimer's disease is characterised by the formation of amyloid- β plaques and cytosolic Tau tangles (Pimplikar 2014). It is hypothesised that amyloid- β plaques can activate the classical pathway leading to the generation of C3a and C5a, these consequently stimulate microglia (macrophages in the brain) to release pro-inflammatory cytokines that can promote tissue damage (Morgan and Harris 2015).

Complement activity has also been implicated in inflammatory airway diseases such as acute respiratory distress syndrome, asthma, COPD and CF (Pandya and Wilkes 2014). The complement system is critical for eradication of airway pathogens. C3-deficiency increases susceptibility to *Streptococcus pneumoniae* and *P. aeruginosa*, pathogens associated with pneumonia (Pandya and Wilkes 2014). Exposing the lungs of mice and rats to LPS (simulating bacterial infection) has demonstrated that complement is important for opsonisation of pathogens (Bolger *et al.* 2007). Furthermore, LPS-induced lung injury elevated the expression of complement components (C1q, C1r, C1s, C2, C4, C3, C5, C6, factor B, and factor H) in the airways of these animals (Bolger *et al.* 2007). Despite reliance on complement for clearing pathogens associated with pulmonary infection, complement activation has also been reported to be a contributing factor to airway inflammation through the generation of C3a and

C5a (Fick *et al.* 1986; Marc *et al.* 2010). In the next sections, I will discuss in depth the structure, function and pathogenic roles of C5a and C3a, focussing on the CF airway.

1.7. C5a

1.7.1. C5a structure

C5 convertase cleaves the C5 alpha-chain subunit to produce C5b, that through assembly with C6-9, form MAC on opsonised cell surfaces (Ricklin *et al.* 2010). The by-product, C5a, is a 10.4 kDa glycoprotein comprised of 74 amino acids (Cook *et al.* 2010). Nuclear magnetic resonance spectroscopy (NMR) reveals that the tertiary structure of C5a comprises a core of four α -helices, held in tight formation by three disulphide bridges, a disordered fifth helix on the C-terminus contains a pentapeptide receptor activation domain (figure 1-21) (Cook *et al.* 2010). The C5a structure has been determined using crystals of C5a dimers; however, it is not clear whether C5a functions as a dimer *in vivo*, or if this phenomenon is due to the methodology used to crystallise the proteins (Cook *et al.* 2010). Interestingly, dimer formation has been shown to be important for CXCL8 function, which like C5a, is a low molecular weight potent chemoattractant (Das *et al.* 2010).

1.7.2. Regulation of C5a activity

C5a is a potent chemoattractant, but its activity *in vivo* is difficult to measure because it is rapidly inactivated by carboxypeptidases through cleavage of the C-terminal arginine to form C5a-desArg (Campbell *et al.* 2002). Furthermore, no commercially available antibodies can differentiate between C5a and C5a-desArg and therefore, it is assumed that the majority of C5a quantified in serum is in the C5adesArg form (Campbell *et al.* 2002). Throughout this thesis C5a *in vivo* or *ex vivo* will be called C5a, despite knowledge that the majority of the C5a is presumably C5adesArg. Two carboxypeptidases have been reported to inactivate C5a: Zinc metalloprotease CPN and thrombin-activated pro-enzyme carboxypeptidase B2 (also known as CPB) (Campbell *et al.* 2002). Expression of CPN is constitutive whereas, CPB requires activation meaning its function can be regulated and therefore, in turn, controls the activity of C5a (Morser *et al.* 2018).

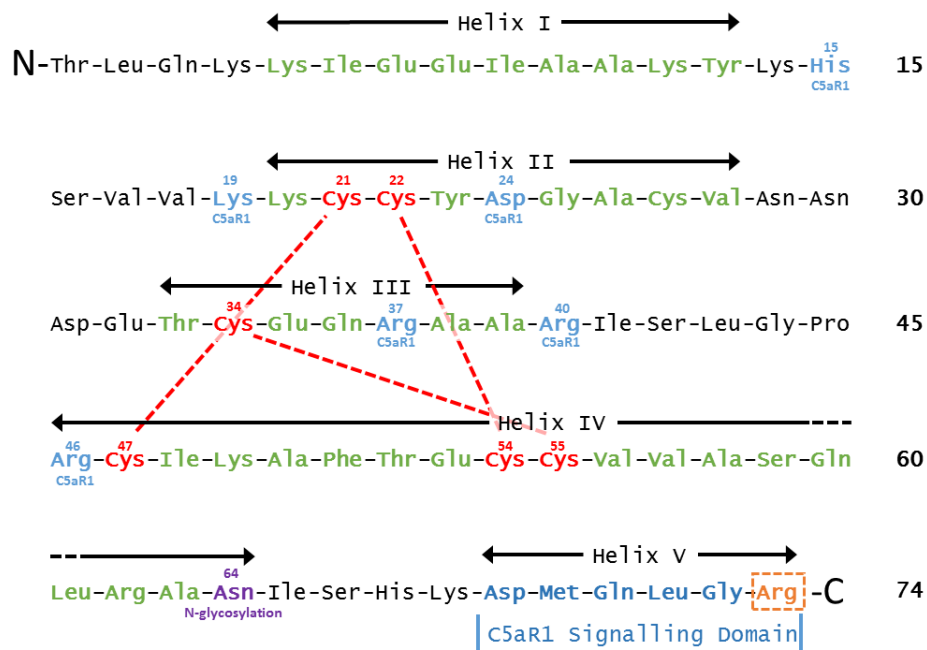


Figure 1-21: Amino acid sequence and secondary structure of C5a/C5adesArg. Helices I-V are marked out by black arrows, constituent amino acids are in green, connecting loop amino acids are in black. Cysteine residues and their sequence position are in red, dashed red lines are disulphide bonds. Documented C5aR1 binding residues are in blue, terminal arginine is in orange within a dashed box. N-glycosylation at asparagine-64 is highlighted in purple.

Morser *et al.* used *cpb2*^{-/-} and *cpn*^{-/-} mice to investigate C5a regulation in a model of aHUS. They showed that *cpb2*^{-/-}, but not *cpn*^{-/-}, mice were more susceptible to aHUS compared to wild type mice (Morser *et al.* 2018). Interestingly, when injected with cobra venom factor, a protease able to cleave C5 into functional C5b and C5a, *cpn*^{-/-} mice had a reduced renal function compared to *cpb2*^{-/-} (Morser *et al.* 2018). These experiments demonstrate that in mice CPN is constitutively expressed and required for acute challenges whereas, CPB is protective in more long-term conditions such as aHUS (Morser *et al.* 2018). It should be noted that C5a is not the only substrate for CPN and CPB, they also facilitate clot regulation via the cleavage of terminal lysine on fibrin that prevent clot formation by plasmin (Kovacs *et al.* 2014). Exogenous enzymes expressed by invading pathogens have also been reported to cleave C5a C-terminal arginine (Klos *et al.* 2013). For example, metalloproteases, such as those released by parasitic nematodes, C5a peptidases released by *Streptococcus pyogenes* and Scp A peptidases secreted by enterobacterium *Serratia marcescens* (Klos *et al.* 2013).

C5a-desArg binds C5aR1, with 100-fold less affinity than C5a; furthermore, the binding orientation is altered when C-terminal Arg74 is removed (Nikiforovich *et al.* 2008). In particular removing C-terminal arginine from C5a has been shown to reduce interaction between C5aR1 residues Arg206 and Arg200 with the C5a residue Asp69 (Nikiforovich *et al.* 2008). When the

C-terminal arginine of C5a is cleaved by CPN/B, the C5a C-terminal alpha helix becomes flexible, extruding or merging with the second alpha helix, reducing functional activity via C5aR1 (Schatz-Jakobsen *et al.* 2014).

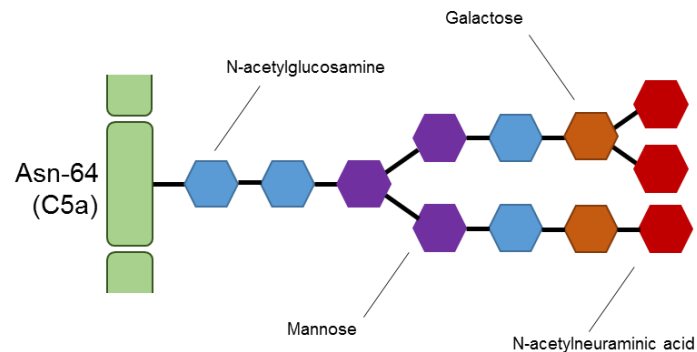


Figure 1-22: N-glycosylation of C5a/C5adesArg, C5a based on data from Fernandez *et al.* (Fernandez and Hugli 1976). N-glycosylation accounts for up to 25% of the total C5a molecular weight. C5a is glycosylated at Asn-64, the N-glycosylation is biantennary structure comprised of N-acetylglucosamine (blue), mannose (purple), galactose (orange) and N-acetylneuraminic acid (red).

Another structural feature of C5a is an N-glycosylation site at Asn64 (figure 1-22). The glycosylation of C5a increases the molecular weight by 25% and influences function (Gerard and Hugli 1981). Glycosylation of C5a has been shown to significantly inhibit activity of C5ades-Arg form, this has been demonstrated by comparing to porcine C5a-desArg which, lacks N-glycosylation (Gerard and Hugli 1981).

1.7.3. Receptors for C5a / C5adesArg

There are two known C5a receptors, C5aR1 and C5aR2 (Klos *et al.* 2013); both receptors belong to the G-protein coupled receptor superfamily however, C5aR2 does not bind G-proteins (Klos *et al.* 2013).

1.7.3.a. C5aR1

C5aR1 is expressed in most tissues throughout the body, The highest expression is observed on monocytes, macrophages and PMNs such as eosinophils, basophils and neutrophils (Karsten *et al.* 2015). However, expression of C5aR1 on cells of lymphoid origin is controversial (Klos *et al.* 2013). Migration of B and T cells towards C5a has been demonstrated and there has also been extensive research investigating reduced apoptosis of T cells in response to C5a (Strainic *et al.* 2008). Yet, another study report that C5aR1 is expressed in a small population of T cells (CD3+) and can induce chemotaxis (Nataf *et al.*

1999). Non-immune cells have also been shown to express C5aR, such as neurons, astrocytes and cells from major organs (lungs, liver and heart) (Zwirner *et al.* 1999; Karsten *et al.* 2015).

C5aR1 signal activation is induced via the C-terminal pentapeptide of C5a, inducing signal via acidic residues on the C5aR1 extracellular N-terminus (figure 1-23) (Nikiforovich *et al.* 2008). Interestingly, flexibility in the C5aR1 N-terminus may indicate different binding configurations for C5a and C5adesArg and may explain the difference in affinity for the two forms (Nikiforovich *et al.* 2008).

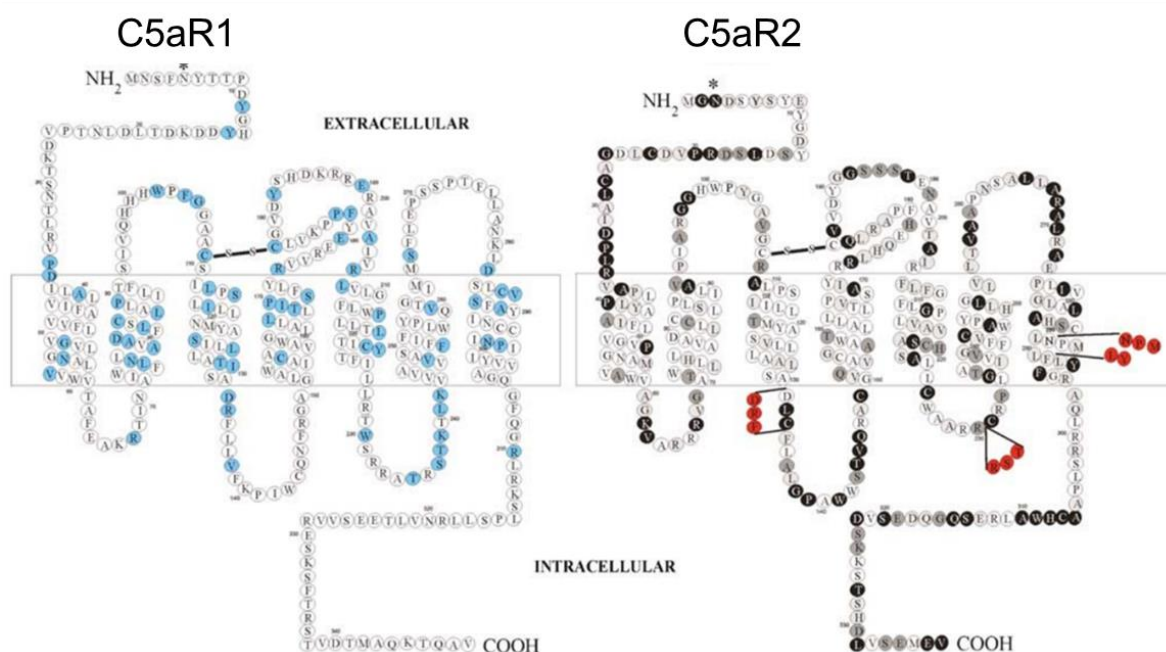


Figure 1-23: Amino acid sequences and structures of C5aR1 and C5aR2, extracted from Monk *et al.* (Monk *et al.* 2007). There is 35% amino acid conservation between C5aR1 and C5aR2; conserved residues in C5aR2 are shaded (dark grey on C5aR2). Site-directed mutagenesis has revealed many C5aR1 residues that are important for ligand binding and signal transduction (blue). The amino acids essential for G-protein signalling in C5aR1 but are missing in C5aR2 (red).

A study using site-directed mutagenesis or chimeric C5aR1 and fMLP receptors (FPR1 and FPR2) report that there are multiple C5a binding sites located within the connecting loops of C5aR1 transmembrane domains (loops) (Pease *et al.* 1994). Furthermore, recombinant C5a (rhC5a), that has been genetically engineered to lack the C-terminal signalling domain, can bind but not activate C5aR1 (Nikiforovich *et al.* 2008). More recent studies have demonstrated that C5a binds C5aR1 in a step-wise manner with the receptor undergoing a series of conformational changes, whereby receptor binding and activation occurring separately (Sahoo *et al.* 2018).

Investigation into receptor binding sites has also revealed that there are at least three additional naturally occurring agonists for the C5aR1: outer-membrane protein H, a porin from *Salmonella spp*, *Escherichia spp* and *Yersinia spp* (Jia *et al.* 2010), a homodimer of ribosome S19 from apoptotic cells (Yamamoto 2000) and chemotaxis inhibitory protein expressed by *Staphylococcus aureus* (CHIPS) (Wright *et al.* 2007). Interestingly, Wright *et al.* have shown that CHIPS is an agonist of FRP1 but an antagonist of C5aR1; however, CHIPS is also highly immunogenic and induces the production of specific antibodies (Wright *et al.* 2007).

C5aR1 is coupled to pertussis-toxin sensitive G proteins α_{i2} ; however, unlike most G-protein receptors the G-proteins are pre-coupled allowing rapid signal activation that override other G-protein coupled receptors such as CXCR1 (Klos *et al.* 2013). Signal activation of C5aR1 induces intracellular calcium release, MAPK, and PI3K γ activation (Klos *et al.* 2013). The type of response depends on the cell type expressing C5aR1. For instance, neutrophils release calcium from intracellular stores whereas monocytes rely upon extracellular calcium (Monk and Partridge 1993; Ibrahim *et al.* 2004). In neutrophils, C5a-C5aR1 binding induces chemotaxis, degranulation, ROS production and NET release. C5a, acting via C5aR1, is also important for upregulation of phagocytic receptors such as CR3 and Fc γ R receptors (Hunniger *et al.* 2015). Priming by C5a is also important for inflammasome activation and the release of IL-1 β and IL-18 (An *et al.* 2014; Grailer *et al.* 2014).

1.7.3.b. C5aR2

The function of C5aR2 (previously known as C5L2) is the subject of debate: the most popular hypothesis is that C5aR2 is a decoy receptor that removes fluid phase C5a or C5a des-Arg (Klos *et al.* 2013). This hypothesis is supported by evidence that C5a/C5adesArg binds C5aR2 with equal affinity whereas, C5a binds C5aR1 with higher affinity than C5adesArg (Scola *et al.* 2009). C5aR2 is a seven-transmembrane receptor that lacks the ability to couple G-proteins, a characteristic also observed with other decoy receptors such as IL1RII (Futosi *et al.* 2013). C5aR2 is highly expressed on cells of myeloid origin; however, studying PMNs suggests that basal expression is low and requires activation (Cain and Monk 2002). C5aR2 does not undergo ligand-induced internalisation but does cycle between the cell surface and intracellular compartments allowing sequestering and lysosomal degradation of C5a or C5adesArg (Cain and Monk 2002). This recycling function of C5aR2 has been shown to be more efficient for C5a-desArg than C5a (Scola *et al.* 2009).

1.7.3.c. C5aR1 and C5aR2 cross-talk

C5aR1 can form homodimers, as well as heterodimers with CCR5, enabling co-internalisation when under at equivocal states of phosphorylation (Huttenrauch *et al.* 2005). It is not fully understood whether hetero-dimerisation occurs between other G-protein coupled receptors and C5aR2; however, it has been speculated that dimerisation may enable differential signalling between G-protein dependent and β -arrestin-mediated pathways and could reveal additional functions of C5aR2 (Defea 2008; Rabiet *et al.* 2008). Further cross-communication between receptors may occur between C5aR2 and non-G protein-coupled receptor such as TLRs and therefore, C5aR2 could have regulatory function towards C5aR1 and TLRs (Raby *et al.* 2011).

1.7.4. C5a Function

C5a has multiple functions; these are dependent on cell type and expression of C5aR1. C5a activation of C5aR1 on PMNs and monocytes in the airway can trigger three functions (Hunniger *et al.* 2015);

- 1) Increased expression of β -integrins allowing adherence to the vascular endothelium and transmigration to affected tissue.
- 2) Activation of granulocytes inducing degranulation, ROS production and pro-inflammatory cytokine release.
- 3) Priming by upregulation of pathogen recognition receptors allowing efficient targeting and phagocytosis of pathogens.

These functions are critical for an inflammatory response to infection or trauma. For example, Hunniger *et al.* used neutrophils isolated from healthy blood to demonstrate the dependence on C5a to orchestrate response to *C. albicans* infection (Hunniger *et al.* 2015). By inhibiting either C5aR1 or C5a Hunniger *et al.* showed that C5a was required for a rapid response, occurring within 10 minutes; however, other factors, such as CXCL8, were necessary for a sustained response (Hunniger *et al.* 2015). Additionally, the authors showed that C5a primed neutrophils by upregulating CR3 (CD11b), Fc receptors (CD16) and L-selectin (CD62L) (Hunniger *et al.* 2015). Supporting this, other groups have observed that C5a is required for efficient clearance of bacterial pathogens such as *Staphylococcus aureus* and *Escherichia coli* (Mollnes *et al.* 2002; Skjeflo *et al.* 2014).

In particular, Skjeflo *et al.* used a micro-sphere array to detect cytokine expression during a blood infection induced using lipoteichoic acid (bacterial cell wall component). They demonstrated that blockade of C5a generation or activity using eculizumab, compstatin, or a C5aR1 antagonist significantly reduced the expression of IL-1 β , TNF α , IL-6, and CXCL8. With greater relevance to the CF airway, Höpken *et al.* intratracheally infected *C5ar1*^{-/-} mice with *P. aeruginosa* (Hopken *et al.* 1996). The authors observed that 10 out of 11 C5aR1 deficient mice died within two days of the challenge, whereas all wild type mice survived over a six-day period. Interestingly, they also show elevated neutrophil numbers in the lungs of *C5ar1* knockout mice, meaning that C5a may not be crucial for recruitment to the lung but, it is essential for clearance of *P. aeruginosa* from the airway (Hopken *et al.* 1996). However, *P. aeruginosa* is an opportunistic pathogen in diseases such as COPD and CF wherein, the role of C5a is more complex and can promote pathogenesis. This will be discussed in the next section.

The upregulation of Fc γ Rs is critical for phagocytic cells to fight infection however, the relationship between the C5a/C5aR1 axis and Fc γ Rs is not simple (Karsten *et al.* 2012). Cross-talk between C5aR1 and Fc γ Rs enables heightened response to pathogens but also regulation. This function is mediated through the differential expression of activating Fc γ Rs and inhibitory Fc γ RIIB (Karsten *et al.* 2012). Karsten *et al.* used Fc γ RI knockout mice to demonstrate the inhibitory effect of Fc γ RIIB on C5aR1-mediated chemotaxis of neutrophils and macrophages. Following injection of C5a into mouse peritonea, they observed that there was significantly reduced chemotaxis of neutrophils in activating-Fc γ R knockout mice (Karsten *et al.* 2012). In explanation, Karsten *et al.* show that immune complexes inhibited chemotaxis of wild type neutrophils. This effect was reversed by administering an inhibitory antibody towards Fc γ RIIB in mice. The result of these experiments was that Fc γ RIIB blocks C5aR1 mediated ERK1/2 phosphorylation and intracellular calcium release. Further investigation by the authors using Förster resonance energy transfer (FRET) demonstrated that Fc γ RIIB associates with dectin-1; an interaction that was dictated by the glycosylation state of the IgG. For example, highly glycosylated IgGs promoted Fc γ RIIB-dectin-1 association, although interaction was not through direct binding of glycosylated IgG with dectin-1. In conclusion, Karsten *et al.*, reported strong evidence demonstrating that glycosylation of IgG can regulate cellular responses to C5a during inflammation and that this may play an important inflammatory role during autoimmune disease where self-antibodies are not glycosylated (Karsten *et al.* 2012).

1.7.5. Pathogenic roles of C5a

The potency of C5a to induce inflammatory response in multiple cell types also means that it is a contributing factor to inflammatory disorders whereby dysregulation of C5a activity contributes to pathogenesis (Klos *et al.* 2013). Elevated C5a is a contributing pathogenic factor in many inflammatory diseases, listed in table 1-6.

Disease	Role of C5a in disease	Reference
Sepsis	Systemic infection leading to organ failure, high mortality rate associated with exaggerated inflammatory response. C5aR1 and C5aR2 inversely proportional to disease severity reflecting neutrophil activation by C5a.	(Xu <i>et al.</i> 2016)
ischemia-reperfusion injury	Inflammation following prolonged tissue hypoxia caused by myocardial infarction, stroke or organ transplant. Complement activation leading to MAC deposition and generation of C5a. C5a associated with chemotaxis of monocytes and PMNs to hypoxic tissue leading to further tissue damage. C5a induction of cytokine release by epithelial and endothelial cells.	(Peng <i>et al.</i> 2012)
Glomerulonephritis	Assembly of autoimmune complexes in the glomerulus following chronic serum sickness. Complement activation generates C5a leading to macrophage inflammation of endocapillaries.	(Alexander <i>et al.</i> 2015)
Rheumatoid Arthritis	Assembly of autoimmune complexes within the synovium causes complement activation and inflammation. Activation and degranulation of granulocytes leads to joint degradation.	(Jose <i>et al.</i> 1990)
Neuromyelitis Optica	Assembly of autoimmune complexes against aquaporin-4, a water pore within astrocytes of the CNS. Complement activation promoting lysis and targeting of astrocytes within the optic nerve and spinal cord.	(Kuroda <i>et al.</i> 2013)
Airway Disorders		
Acute lung injury/ respiratory distress syndrome (ARDS)	Inflammation of the airway in response to airborne particles or microorganisms. Complement activation generates C5a promoting influx of PMNs and monocytes. Poorly regulated inflammation leads to tissue damage. C5a plays pivotal role in lung damage during ARDS, growing evidence supporting the role of C5a in pathogenesis of influenza A viruses	(Wang <i>et al.</i> 2015b)
Chronic Obstructive Pulmonary Disease (COPD)	Long term exposure to air pollution such as smoking. Shortness of breath caused by emphysema, inflammation induced bronchoconstriction. Inflammation and activation of granulocytes driven by C5a.	(Marc <i>et al.</i> 2010)
Asthma	In allergic asthma the airway is hyper-responsive to environmental stimulants. C5a induces the release of pro-inflammatory cytokines (IL-4, IL-5 and IL-13) by Th2 cells.	(Khan <i>et al.</i> 2015)

Table 1-6 Role of C5a in disease

In blood, C5a is responsible for an exaggerated inflammatory response during sepsis and ischemia-reperfusion injury (Scola *et al.* 2007; Xu *et al.* 2016). As a result, C5b (MAC formation) and C5a generation are therapeutic targets and have led to the development of numerous agonists, antagonists and monoclonal antibodies (Morgan and Harris 2015).

Eculizumab is a humanised mouse anti-C5 monoclonal antibody primarily designed to prevent C5 cleavage by C5 convertase, inhibiting MAC formation and C5a generation. It was designed as a therapeutic for patients with aHUS or PNH. Administration of eculizumab has been successful in treating these diseases over the last 15 years (Hillmen *et al.* 2006; Zuber *et al.* 2012). Neutrophil activation by C5a causes the release of MPO and PR3 during necrotizing and crescentic glomerulonephritis; CCX168 is a C5aR antagonist that is currently in phase II clinical trials to reduce disease severity (Bekker *et al.* 2016). Specifically targeting C5a, a pre-clinical trial of IFX-1 has been shown to be effective against influenza A induced acute lung injury in African green monkeys (Sun *et al.* 2015).

There are few reports of C5a quantification in airway disorders including CF; therefore, the role of C5a in promoting pathogenesis in these diseases is unclear. C5a correlates with a decline in clinical scoring particularly in asthma, acute lung injury, COPD and CF (see table 1-7).

Disease	Sample type	C5a Median (ng/mL)	C5a Range (ng/mL)	Sample size	Immunoassay	Reference
Cystic Fibrosis	sputum	1.0	0 – 3.0	15	ELISA R&D systems OR ELISA BD biosciences	(Sass <i>et al.</i> 2015)
Cystic Fibrosis	BAL fluid	258	0 – 590	9	RIA Upjohn diagnostics	(Fick <i>et al.</i> 1986)
Asthma	BALF Fluid (allergen challenge)	16.4	1.0 – 54.0	14	Affinity Chromatography	(Krug <i>et al.</i> 2001)
Asthma	sputum	1.2	0.2 – 5.8	10	Cytometric Bead array BD sciences	(Marc <i>et al.</i> 2004)
COPD	sputum	1.6	0.2 – 6.5	7	Cytometric Bead array BD sciences	(Marc <i>et al.</i> 2004)
COPD	sputum	1.2	0.4 – 1.9	13	Cytometric Bead array BD sciences	(Marc <i>et al.</i> 2010)
COPD	Sputum (during exacerbation)	1.19	0.5 – 50.7	24	ELISA BD biosciences	(Westwood <i>et al.</i> 2016)
Normal plasma		8.0	7.0 – 9.0	53	Cytometric Bead array BD sciences	(Strey <i>et al.</i> 2009)

Table 1-7 Quantification of C5a/C5adesArg in airway diseases

In the asthmatic airway, C5a stimulates mast cells to release histamine causing smooth muscle contraction along the vasculature and increases permeability to migrating cells by inducing the relaxation tight junctions between cells (Khan *et al.* 2015). *C5ar1* knock-out mice have also been used to demonstrate the role of C5a in orchestrating dendritic cell modulation of T-helper cells in asthma (Khan *et al.* 2015). C5a activation of conventional pulmonary dendritic cells induces the expression of IL-17 and IL-22, promoting Th2 adaptive immunity in the asthmatic airway (Khan *et al.* 2015). Furthermore, inducing allergenic asthma symptoms in patients using ovalbumin elevated C5a and neutrophil influx, suggesting that it is an important contributor to inflammation (Khan *et al.* 2015).

The role of C5a/C5aR1 in driving disease progression has added complexity in that it has been shown to be dependent on the stage of disease (Staab *et al.* 2014). *C5aR1* knock-out mice and a C5aR1 antagonist, PMX205, have been used to show that C5aR1 has a protective role during the sensitising stage of asthma; here there is initial contact between the allergen and dendritic cells and the subsequent interaction with Th-2 cells.. It was found that C5aR1 expression on both cell types was important for controlling the response (Kohl *et al.* 2006). In contrast once an allergic response has been established (following allergen exposure) C5a signalling accentuates hyper-responsiveness by driving eosinophilic inflammation (Kohl *et al.* 2006; Staab *et al.* 2014).

In COPD, BAL fluid C5a levels correlated negatively with lung function and were associated with disease progression (Marc *et al.* 2010). There was no significant difference in plasma C5a between patients and the controls group, supporting evidence that complement activation occurs locally in the airway (Marc *et al.* 2010).

1.7.6. C5a in the CF airway

C5a has also been reported to contribute to disease progression in the CF airway (Fick *et al.* 1986; Sass *et al.* 2015; Hair *et al.* 2017). Fick *et al.* report elevated C5a in CF BAL fluid compared to healthy volunteers, the authors also showed that elevated C5a correlated positively with PMNs in these patients. It was hypothesised by Fick *et al.* that, C5a was generated through C5 proteolysis by proteases expressed in the lung, rather than complement activation and production of C5a by C5 convertase (Fick *et al.* 1986). As mentioned in section 1.6.4, several endogenous and exogenous non-complement proteases have been shown to generate functional C3a and C5a-like anaphylatoxins. Fick *et al.* showed that inhibition of serine proteases and *P. aeruginosa* metalloproteases in BAL fluid *ex vivo* reduced C5a

production from purified C5, suggesting that these proteases contribute to elevated C5a in the CF airway (Fick *et al.* 1986).

More recently, Sass *et al.* measured C5a in CF sputum during an investigation comparing generation of C5a by protease from *Staphylococcus aureus* and complement activation (Sass *et al.* 2015). They reported that proteases released by dead and living pathogens were able to generate C5a; however, they concluded that complement activation, rather than non-canonical generation, was responsible for elevated C5a in the CF airway (Sass *et al.* 2015). The same group also published a longitudinal study measuring elevation of C5a in sputum during pulmonary exacerbation (Hair *et al.* 2017). They observed that C5a concentrations spiked during exacerbation, hypothesising that C5a is a driving factor behind neutrophilic inflammation in the airway (Hair *et al.* 2017).

Our group has shown that C5aR1 is susceptible to proteolysis and subsequent inactivation by serine proteases expressed in CF BAL fluid (van den Berg *et al.* 2014). This was replicated by exposing C5aR1 to supernatant from primary neutrophils following stimulation with C5a (van den Berg *et al.* 2014). Inactivation of C5aR1 was confirmed by exposing U937 monocytes transfected with C5aR1 to purified NSPs. The conclusion to this work was that, loss of C5aR1 during chronic neutrophilic inflammation of the CF airway disorients neutrophils, preventing communication between innate immune cells and neighbouring epithelial cells. Consequently, clearance of pathogens is inefficient, prolonging infection and inflammation leading to the loss of lung function (van den Berg *et al.* 2014).

1.8. C3a

C3a is produced by cleavage of the C3 alpha chain by C3 convertases (C4bC2b and C3bBb) also generating C3b, an important opsonin and component for the assembly of further convertases for the assembly of MAC (Ricklin and Lambris 2013). C3a shares structural and sequence (35%) homology with C5a however, there are subtle differences as well as differential receptor expression that means their roles in inflammation are quite distinctive (Klos *et al.* 2013).

1.8.1. Structure and regulation

C3a is a 77 amino acid protein and, like C5a, the structure forms a four-helix core with signal activity residing in the C-terminus (figure 1-24 and 1-25) (Caporale *et al.* 1980; Muto *et al.* 1987). The NMR structure of C3a has been compared with C5a (Cook *et al.* 2010). Cook *et al.* showed that the alpha helices of C3a are on average shorter than C5a; however, they do not comment on how this relates to function (Cook *et al.* 2010). Furthermore, C3a and C5a NMR structures were performed on dimerised proteins, but C3a was dimerised via the C-terminus whereas C5a was dimerised through core arginine residue at position 40 and 46 (Cook *et al.* 2010). Cook *et al.*, speculated that the significance of different dimerisation sites is that C5a could function as a dimer as the C-terminal signalling domains remain exposed, unlike C3a where dimers form via the C-terminal (Cook *et al.* 2010).

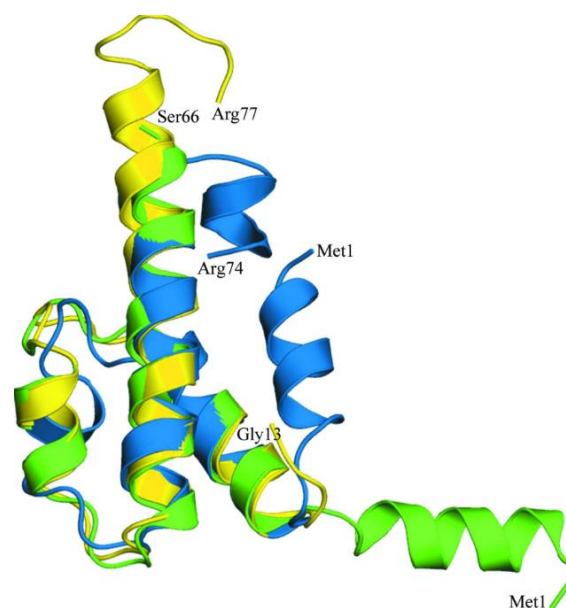


Figure 1-24 Comparing tertiary structures of C5a and C3a

Extracted from Cook *et al.* 2010. Superimposition of C5a NMR structure (blue), C5a X-ray structure (green) and C3a NMR structure (yellow). Terminal amino acids have been annotated.

Another structural dissimilarity between C3a and C5a is that C3a is not glycosylated (Caporale *et al.* 1980). Cleavage of C-terminal arginine by CPB or CPN prevents receptor binding suggesting that both binding and signalling activity is located within the C-terminus (Caporale *et al.* 1980). C3a / C3aR binding and activation has been shown using a pentapeptide construct of the signalling domain, Leu-Gly-Leu-Ala-Arg. Caporle *et al.* showed that this construct retained 0.2% molar activity in stimulating smooth muscle contraction compared to full-length C3a, but when inducing mast cell degranulation of histamine this construct had 10% activity (Caporale *et al.* 1980). Additionally, longer C-terminal constructs possess greater activity: 21 amino acid C3a constructs (C3a c-terminal residues 57-77) retain 100% function, meaning that the majority of the C3a N-terminal is redundant for function (Huey *et al.* 1984).

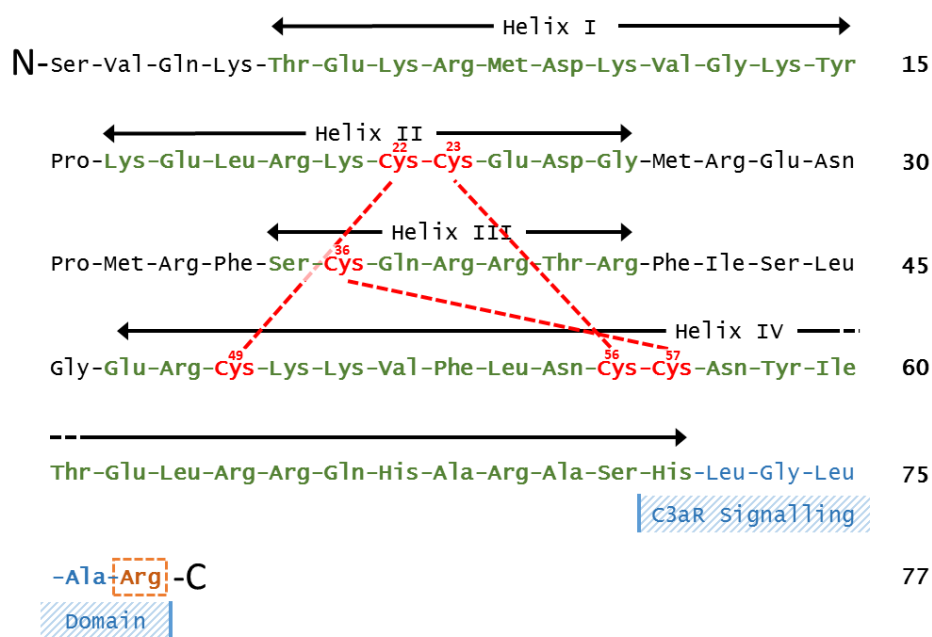


Figure 1-25: Amino acid sequence and secondary structure of C3a. Helices I-V are marked out by black arrows, constituent amino acids are in green, connecting loop amino acids are in black. Cysteine residues and their sequence position are in red, dashed red lines are represent disulphide bonds. Signalling domain is in blue, terminal arginine is in orange within a dashed box.

1.8.2. Receptors for C3a / C3adesArg

C3a binds C3aR, a seven transmembrane G-protein coupled receptor (Klos *et al.* 2013). Expression of C3aR has been detected in most human tissues including on epithelial and endothelial cells as well as astrocytes and smooth muscle cells (Klos *et al.* 2013). Unlike C5aR1, C3aR expression on leukocytes, such as neutrophils, is low and there is no basal expression on lymphocytes, unless stimulated with interferon- γ (Werfel *et al.* 2000). None the

less, C3aR has been detected on monocytes, macrophages, microglia and, mast cells (Klos *et al.* 2013).

Expression of C3aR on neutrophils is controversial (Klos *et al.* 2013). Those that have shown C3aR expression suggest that it stimulates calcium flux, as observed for other granulocytes (figure 1-26) (Norgauer *et al.* 1993; Vibhuti *et al.* 2011).

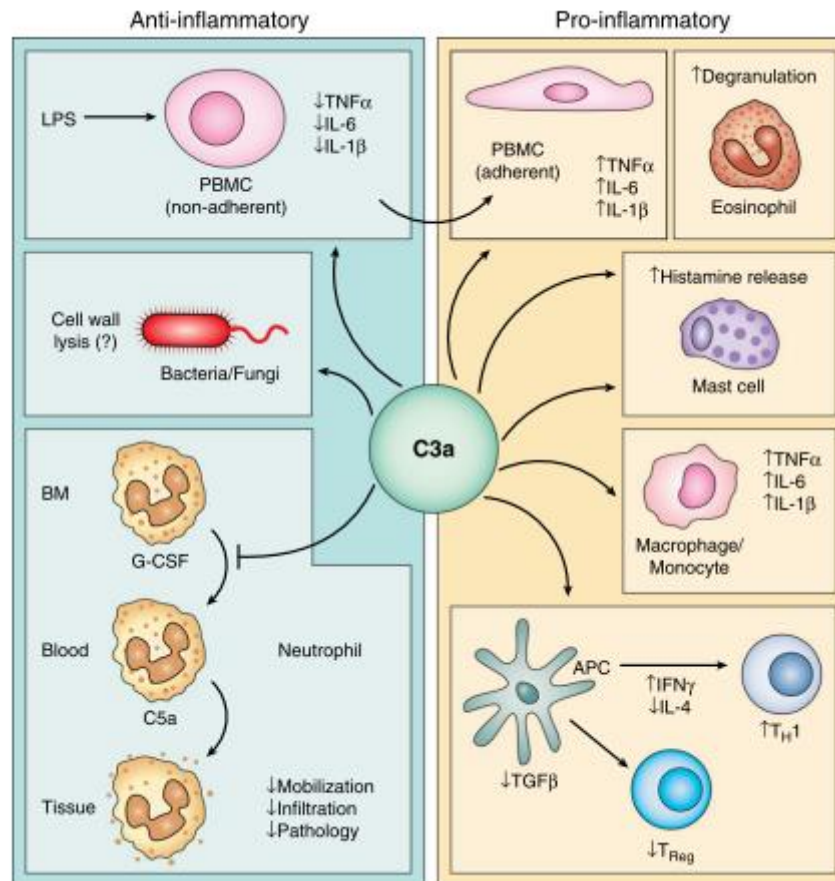


Figure 1-26: Functions of C3a are dependent on cell type, extracted from Coulthard *et al.* (Coulthard and Woodruff 2015). C3a has pro and anti-inflammatory affects upon binding C3aR but function depends on cell type. C3a induces eosinophil degranulation and histamine release from mast cells. In monocyte/macrophage C3aR-mediated inflammasome causes the release of IL-1 β . T-cell expression of C3aR is controversial however, it has been reported that C3a suppresses T-regulatory cell production and prevents polarisation of Th1 cells to Th2 phenotypes. C3aR expression on neutrophils is also controversial but it has been proposed that C3a inhibits neutrophil release from the bone marrow. C3a itself also has microbial properties.

Those who doubt C3aR expression in neutrophils suggest that the cells used for the above experiments were contaminated with other granulocytes (Klos *et al.* 2013). Despite this, Wu *et al.* used *C3ar* $-/-$ mice to propose a role for C3a suppression of neutrophil migration from bone marrow into circulation during their maturation (Wu *et al.* 2013). The authors observed that mice lacking C3aR had elevated neutrophil influx during ischemic reperfusion injury of the

intestines compared to wild type mice. Wu *et al.* used a C3a “super agonist” (WWGKKYRASKLGLAR), previously reported to have 2 to 15-fold higher activity over native C3a, to reduce neutrophil migration to circulation (Ember *et al.* 1991; Wu *et al.* 2013). In conclusion, the authors suggested that C3a may have a therapeutic role to prevent neutrophil migration from bone marrow in ischemic reperfusion.

Activation of C3aR induces calcium response although, in comparison to C5a, such activation is weaker than that triggered by C5aR1 activation (Norgauer *et al.* 1993). Degranulation of mast cells is induced via ERK 1/2 pathway activation. β -arrestins may also have an important role in C3aR signalling beyond desensitisation and internalisation (Vibhuti *et al.* 2011). For example, silencing β -arrestin 1 prevented degranulation of mast cells in response to C3a (Vibhuti *et al.* 2011). As well as degranulation in mast cells, C3a has been shown to induce IL-1 β from monocytes and macrophages by priming the NLRP3 inflammasome (Asgari *et al.* 2013). Therefore, binding of C3a to C3aR has been shown to have both anti-inflammatory (neutrophils, anti-microbial) and pro-inflammatory (mast cells, eosinophils, monocytes/macrophages) functions depending on cell type (Coulthard and Woodruff 2015).

Interestingly, C3adesArg has been shown to be identical to acylation-stimulating protein (ACP), a mediator of triglyceride synthesis that may be important for metabolic and immune function (Cianflone 2003). It has been suggested that C5aR2 on adipocytes binds ACP however, despite several publications, this topic remains highly controversial (Cianflone 2003; Klos *et al.* 2013). Yet, C5aR2 knock-out mice have been shown to have macrophage inflammation in adipose tissue, and the same mice were more susceptible to developing insulin resistance when fed a diabetes-inducing diet (Fisette *et al.* 2013). However, these experiments do not prove that ACP is a ligand for C5aR2 and these could be explained by possible hetero-dimerisation between C5aR2 and C5aR1 or C3aR (Zhang *et al.* 2017).

1.8.3. The pathogenic roles of C3a

C3adesArg has very little or no affinity for C3aR which means that C3adesArg is not cleared from the circulation/tissue (Klos *et al.* 2013). Consequently, C3adesArg can accumulate to greater concentrations than C5a/C5adesArg during complement activation because C5a/C5adesArg can be removed by internalisation of C5aR1 and C5aR2 (Klos *et al.* 2013). Additionally, C3 concentrations are 10-fold higher than C5 in blood and therefore, there is greater capacity to generate C3a. Consequently C3a/C3adesArg concentration in plasma is approximately 50 ng/mL compare to 5 ng/mL for C5a/C5adesArg (Barnum and Schein 2018).

Accumulation of C3adesArg in disease as a result of reduced clearance means that it can be a good candidate biomarker of complement activation and has been used to indicate infection, inflammation and tumour growth; an extensive list of these diseases can be found in Klos *et al.* 2013 (Klos *et al.* 2013).

C3a, like C5a, is thought to contribute to pathogenesis in inflammatory airway diseases such as asthma, COPD and CF (table 1-8) (Krug *et al.* 2001; Marc *et al.* 2004; Sass *et al.* 2015). C3a has been shown to be elevated during hyper-allergenic response in asthma; furthermore, the role of C3a in the asthmatic lung may be multi-factorial (Engelke *et al.* 2014). C3a is known to induce mast cell and eosinophil degranulation; both these cells types are found elevated in the asthmatic airway during an allergenic challenge (Engelke *et al.* 2014). Furthermore, C3a has been shown to induce smooth muscle contraction, a symptom of asthma (Humbles *et al.* 2000). Increased mucus production has also been reported. In explanation, Dillard *et al.* hypothesise that C3a stimulates Clara cell MUC5A production, an important constituent of mucus (Dillard *et al.* 2007). Wild type and C3 knock-out mice were compared and it was demonstrated that wild type mice had increased mucus production and airway obstruction during hyper-allergenic challenge (Dillard *et al.* 2007). However, neutrophils have not been shown to contribute to any of these C3a-mediated pathogenic factors in asthma, which is likely to be due to low or absent of C3aR expression on the neutrophil cell surface (Dillard *et al.* 2007; Klos *et al.* 2013).

Disease	Sample type	Median (ng/mL)	Range (ng/mL)	Sample size	Immunoassay	Reference
Cystic Fibrosis	sputum	15.0 (approx.)	0 – 170 (approx.)	14	ELISA systems R&D OR ELISA BD biosciences	(Sass <i>et al.</i> 2015)
Asthma	BALF Fluid (allergen challenge)	29.0	3.9 - 854	14	Affinity Chromatography	(Krug <i>et al.</i> 2001)
Asthma	sputum	2.12	0.14 – 50.1	10	Cytometric Bead array BD sciences	(Marc <i>et al.</i> 2004)
COPD	sputum	0.67	0.5 – 8.7	7	Cytometric Bead array BD sciences	(Marc <i>et al.</i> 2004)
COPD	Sputum (during exacerbation)	15.4	1.5 - 30.8	24	ELISA BD biosciences	(Westwood <i>et al.</i> 2016)
Normal plasma		33.0	28.5 – 37.5	53	Cytometric Bead array BD sciences	(Strey <i>et al.</i> 2009)

Table 1-8: Quantification of C3a/C3adesArg in airway diseases.

A recent short abstract by Westwood *et al.* describe elevated C3a and C5a in sputum from a cohort of 24 COPD patients (Westwood *et al.* 2016). Both complement factors correlated with increased recovery time following exacerbation however, the authors could not attribute pathogenesis to either C5a or C3a (Westwood *et al.* 2016). Marc *et al.* have also measured C3 in COPD (and asthma) and performed correlations with disease progression; however, despite elevated C3a in the airway, there were no significant correlations (Marc *et al.* 2010). The authors concluded that C5a has a more significant role in disease progression in COPD and the asthmatic airway.

1.8.4. C3a in the CF airway

In CF, Sass *et al.*, observed elevated C3a compared to healthy controls (and C5a, as described above) and, unlike C5a, C3a correlated with reduced inflammation and improved lung function (Sass *et al.* 2015). Furthermore, C3a inversely correlated with neutrophil count supporting evidence that C3a may be an important regulator of neutrophil migration from the bone marrow (Wu *et al.* 2013; Sass *et al.* 2015); however, because there is controversy over the expression of C3aR on neutrophils, further investigation is required to confirm a role of C3a in regulation of neutrophilic inflammation in the CF airway.

1.9. Summary and background to the project

In this literature review I have described the current understanding of neutrophil biology and how their dysfunction promotes pathogenesis in the CF airway. C5a and C3a are important mediators of lung inflammation and have been associated with disease progression including airway disorders such as asthma, COPD and CF. Despite recent publications, the precise mechanisms by which they promote CF pathogenesis are not well understood. Our group has recently shown that C5aR1 is susceptible to cleavage by NSPs during chronic neutrophilic inflammation disarming neutrophils. Despite this, there may be functional modifications of C5a and C3a mediated by the CF airway environment that also contribute to pathogenesis in this disease; this will be the focus of investigation in this thesis.

It has been shown in three reports (Fick *et al.* 1986; Sass *et al.* 2015; Hair *et al.* 2017) that C3a and C5a is elevated in the CF airway and that C5a (and C3a) correlates with neutrophilic inflammation and loss of lung function. Despite higher levels of C5a and C3a in the CF airway, there is inefficient pathogen clearance and consequently chronic neutrophilic inflammation that contributes to loss of lung function and mortality. There is growing evidence suggesting that non-complement proteases can generate functional forms of C3a and C5a. Yet, it is not known whether there are functional differences between the *de novo* C3a and C5a forms compared to their native convertase generated counterparts. The functional differences in C3a and C5a generated by NSPs will be investigated as part of this project.

There is also evidence that the abundance of soluble GAG released through degradation of the airway ECM can modify inflammation in the CF airway, specifically through interaction with CXCL8. There is evidence suggesting that C5a can bind to GAGs; however, it is not fully understood if these interactions modify C5a activity and promote CF pathogenesis as a consequence. As well as characterising the generation of C5a in the CF airway I will also investigate the influence of GAGs on C5a function.

1.10. Hypothesis

I hypothesise that during chronic neutrophilic inflammation of the CF airway, alternative forms of C3a and C5a are generated by NE, CG and PR3 which have modified function over their convertase-produced counterparts. In addition, I hypothesise that current complement therapeutics that inhibit C5a conversion by C5 convertase are ineffective at preventing C5a generation by NSPs. I also hypothesise that C5a (and C3a) interact with GAGs in the local lung environment also modifying their function. Together, C3a and C5a interaction with the local lung environment modifies their activity and promotes pathogenesis in the CF airway.

1.11. Aims

1. Characterise C3a and C5a in BAL fluid from a cohort of 33 paediatric CF patients and correlate with markers of neutrophilic inflammation (CXCL8, NE activity neutrophil count) and disease progression (lung function; FEV₁).
2. Investigate non-canonical *ex vivo* generation of C5a (and C3a) by proteases present in CF BAL fluid. Further, functionally characterise C5a-like and C3a-like fragments generated by NSPs using C5aR1 and C3aR transfected cell lines.
3. Assess the effectiveness of complement therapeutic C5 convertase-inhibiting monoclonal antibodies at preventing non-canonical C5a generation by NSPs. Quantify generation and measure activity of C5a-like fragments generated by NSPs whilst in the presence of therapeutic C5 cleavage inhibitor.
4. Investigate interaction between C5a and soluble GAGs that have been shown to be elevated in during neutrophilic inflammation of the CF airway. Assess the functional significance of C5a-GAG complexes by measuring activity using RBL-C5aR1 cell line following exposure to either CPN/B and NSPs.

2. Materials and methods

2.1. Buffers and solutions

2.1.1. Phosphate buffered saline (PBS), pH 7.4

Fresh PBS was prepared before each experiment. PBS was prepared by diluting 10X stock solution (Fisher Scientific, Loughborough, UK) 1 in 10 in de-ionised H₂O to produce a 1X PBS solution. For cell work, a sterile 10X PBS (for cell culture) stock solution (Fisher Scientific, Loughborough, UK) was used and diluted in sterile H₂O in a tissue culture hood.

2.1.2. PBS-tween (PBS-T), pH 7.5

Fresh sterile PBS-T was prepared before each experiment however, for ELISAs PBS-T was not sterile and prepared in a 1 L bottle and was prepared when required. PBS-T was prepared by adding 0.05% (v/v) tween-20 (Fisher Scientific, Loughborough, UK) to 1X PBS.

2.1.3. Bovine serum albumin (BSA)

Fresh BSA was prepared for each experiment. 1% (w/v) BSA solution (typical concentration, unless stated otherwise) was prepared by weighing out 10 mg protease-free BSA (Sigma Aldrich, Dorset, UK) and dissolving in a 30 mL universal container with 1 mL PBS and mixing by vortex. These amounts were scaled up for larger quantities.

2.1.4. 1 M trisamino(hydroxy)methane (TRIS), pH 7.5

60.57 g TRIS (Fisher Scientific, Loughborough, UK) was weighed out in a 250 mL capacity weigh-boat and added to a 0.5 L glass bottle. De-ionised H₂O was added to approximately 450 mL and mixed by magnetic follower. 0.5 M HCl was added by Pasteur pipette and pH measured by bench pH meter with TRIS compatible probe, until pH reached 7.5. Solution was transferred to a 0.5 L measuring cylinder and de-ionised H₂O was added until the solution reached the 0.5 L mark. 1 M TRIS stock solution was stored in a glass bottle at 4°C. For β -hexosaminidase assays, 1 M TRIS was prepared but at pH 9.0.

2.1.5. 1 M NaCl

58.44 g NaCl (Fisher Scientific, Loughborough, UK) was weighed out in a 250 mL capacity weigh-boat and added to a 1 L glass bottle. De-ionised H₂O was added to approximately 950 mL and mixed by magnetic follower, solution was transferred to a 1 L measuring cylinder and de-ionised H₂O was added until the solution reached the 1 L mark. 1 M NaCl stock solution was stored in a glass bottle at 4°C.

2.1.6. NE activity buffer

Activity buffer was prepared fresh for each experiment, 4 mL de-ionised H₂O, 5 mL 1 M NaCl, 1 mL 1 M TRIS (pH 7.5), 50 µL Triton X-100 (Fisher Scientific, Loughborough, UK) were added to 30 mL universal container and vortexed for 5 seconds until Triton had diluted. Activity buffer was stored at room temperature until used.

2.1.7. Carbonate buffer (2%) – ELISA capture antibody diluent

Sodium bicarbonate (2g) was weighed and dissolved in approximately 90 mL de-ionised H₂O in a glass bottle on a stirrer with magnetic follower. Once dissolved solution was transferred to a 100 mL measuring cylinder and H₂O added to make 100 mL, solution was returned to the glass bottle and stored at room temperature. Required volume of carbonate buffer was filtered through 0.2 µm filter before each use.

2.1.8. 0.1 M Citrate buffer for β-hexosaminidase release experiments

0.2 M citric acid solution was prepared by dissolving 1.92 g citric acid in 50 mL de-ionised H₂O. 0.24 M tri-sodium citrate solution was prepared by dissolved 1.58 g tri-sodium citrate in 40 mL de-ionised H₂O. The 50 mL 0.2M citric acid and 0.24 M tri-sodium citrate were combined and 0.5 M NaOH was added by Pasteur pipette slowly, pH was monitored by bench top pH meter. 0.5 M NaOH was added until pH reached pH 4.5. Solution was transferred to 100 mL measuring cylinder and made up to 100 mL with de-ionised H₂O. 0.1 M citrate buffer was aliquoted into volumes of 20 mL in universal containers and stored at -20°C until use.

2.1.9. Solid phase binding assay buffer

50 mM Sodium acetate, 100 mM NaCl, 0.1% tween-20, pH 6.0. NaCl (2.92 g) was weighted out and added to 0.5 mL bottle with 8.33 mL 3 M sodium acetate (Fisher Scientific, Loughborough, UK). Approximately 400 mL de-ionised H₂O was added and solution was stirred by magnetic follower until NaCl had dissolved. 0.5 mL tween-20 was added and stirred until dissolved. Using a pH meter, pH was corrected to 6.0 using a Pasteur pipette to slowly add 0.5 M NaOH. Solution was transferred to a 0.5 L measuring cylinder and H₂O added to a volume of 0.5 L. Solution was returned to the glass bottle and stored at 4°C until use.

2.1.10. Complement haemolysis assay buffer

One complement fixation test tablet (Oxoid, Hampshire, UK) was added to 100 mL de-ionised H₂O in a 0.25 L glass bottle and stirred by magnetic follower until dissolved. Solution was stored at room temperature. The final solution is 3 mM barbitone, 154 mM NaCl, 1.8 mM MgCl₂, 2.5 mM CaCl₂ at pH 7.2.

2.2. Complement proteins, Proteases, Protease inhibitors, glycosaminoglycans

Reagent	Manufacturer	Typical Stock Concentration	Storage
Complement Proteins			
C3	Complement technology, Texas, US	1 mg/mL	-80°C
C5	Complement technology, Texas, US	1 mg/mL	-80°C
C3a	Complement technology, Texas, US	100 µg/mL	-80°C
C5a (native, purified from human blood)	Complement technology, Texas, US	100 µg/mL	-80°C
Recombinant C5a (produced in <i>E. coli</i>)	Hycult Technology, Uden, Netherlands	100 µg/mL	-80°C
Proteases/peptidases			
Neutrophil Elastase	Athens research, Georgia, US	500 µg/mL (16.9 µM)	-20°C
Cathepsin G	Athens research, Georgia, US	500 µg/mL (16.9 µM)	-20°C
Proteinase 3	Athens research, Georgia, US	1000 µg/mL (34 µM)	-20°C
Porcine Carboxypeptidase B	Sigma Aldrich, Dorset, UK	1 mg/mL	-20°C
Protease Inhibitors			
Phenylmethylsulfonyl fluoride (PMSF)	Sigma Aldrich, Dorset, UK	100 mM solution	4°C
4-(2-Aminoethyl)benzenesulfonyl fluoride hydrochloride (AEBSF)	Sigma Aldrich, Dorset, UK	10 µg/mL	-20°C
Alpha-1-antitrypsin (AAT)	Sigma Aldrich, Dorset, UK	2 mg/mL	-20°C
Glycosaminoglycans			
Heparan sulphate sodium salt from bovine kidney	Sigma Aldrich, Dorset, UK	1 mg/mL	-20°C
Chondroitin sulphate from shark cartilage	Sigma Aldrich, Dorset, UK	3 mg/mL	-20°C
Hyaluronic acid from Rooster comb	Sigma Aldrich, Dorset, UK	3 mg/mL	-20°C
Complement Inhibitors			
SKY59 (monoclonal antibody)	Roche, Basel, Switzerland	10 mg/mL	-80°C
Eculizumab (monoclonal antibody)	Gift from Santiago Rodrigues de Cordoba, Madrid, Spain	10 mg/mL	-80°C
OmCI	Gift from Paul Morgan, Cardiff, UK	8.4 mg/mL	-80°C
RaCI	Gift from Matthijs Jore, Oxford, UK	0.8 mg/mL	-80°C

Table 2-1: Other reagents used in this study, where they came from, stock concentrations and storage conditions

2.3. Antibodies

Target	Host species	Type (Isotype)	Clone	Manufacturer	Dilution used
Human C5a/C5a des-Arg	Mouse	Monoclonal (IgG1)	2952	Hycult Biotechnology	2 µg/mL [C5a-IH E]
Human C5/C5a (C5 alpha chain)	Mouse	Monoclonal (IgG2a)	557	Hycult Biotechnology	0.2 µg/mL [WB] 1 µg/mL [C5 E] 2 µg/mL [C5a-IH E]
Human C5	Mouse (humanised)	Monoclonal (IgG4)	SKY59	Roche	1 µg/mL [C5 E]
Human C5 (C5 Beta chain)	Mouse	Monoclonal (IgG1)	2D5	In-house	1 µg/mL [C5 E]
Human C3/C3a	Mouse	Monoclonal (IgG1)	2898	Hycult Biotechnology	0.2 µg/mL [WB]
Human C3a/C3a-desArg	Rabbit	Polyclonal	N/A	Complement Technology	40 µg/mL (total protein) [WB]
Mouse IgG	Goat	HRP-conjugate	N/A	Stratech Scientific Ltd	37.5 ng/mL [WB] 60 ng/mL [C5 E]
Mouse IgG2a	Goat	HRP-conjugate	N/A	Stratech Scientific Ltd	50 ng/mL [WB] 160 ng/mL [C5a-IH E]
Rabbit IgG	Donkey	HRP-conjugate	N/A	Stratech Scientific Ltd	100 ng/mL [WB]

Table 2-2: Antibodies used throughout project. Antibodies used throughout this project, their target, the species they were produced in, the class of the antibody, clone if applicable, manufacturer and the concentration they were diluted to for each application: E – ELISA, WB – western blot, IH – in-house. HRP-horseradish peroxidase (HRP).

2.4. BAL fluid sample processing

BAL fluid samples were collected by Dr. Julian Forton as part of a separate study investigating airway microbiome in the CF airway (Ronchetti *et al.* 2018). Ethical approval was obtained from the Research Ethics Committee, Cardiff & Vale University Health Board, Cardiff, UK. Written informed consent was obtained by parents or legal guardians. The cohort in this study had 32 CF patients however, there were 41 sampling events in total because repeated measures were taken for 7 patients; 5 patients had 2 recorded events and 2 patients had 3 recorded events. Following my analysis (section 3.4), I determined that repeated measures would be included in the population and therefore, there were 41 events in total. BAL was performed by clinicians in accordance with guidelines published in the ERS (European Respiratory Society) Task Force on BAL in children (de Blic *et al.* 2000). A flexible bronchoscope is inserted into the right middle lobe and 0.9% sterile saline is instilled at a volume of 3 mL/Kg to a maximum volume of 20 mL. Following collection, BAL fluid was immediately placed on ice until collection for processing.

BAL fluid was processed within 1 hour of collection. The volume of each sample was determined by weight, using the assumption that 1 g = 1 mL BAL fluid. Cells were removed from suspension by centrifugation at 500 x g for 5 minutes at 4°C, the supernatant was aliquoted and immediately stored at -80°C. Cell pellets were resuspended in 1-3 mL 10 mM EDTA/PBS, depending on pellet size, and cells counted using a haemocytometer, cells were further diluted in trypan blue at a 1:1 ratio so that dead cells (positively stained) could be omitted from the count, an approximation of percentage dead cells was recorded. Cells were diluted to 1×10^6 cells/mL in 10 mM EDTA/PBS and 50 μ L (50,000 cells) were fixed to polylysine slides by cytofuge (centrifuge for slides) at 500 x g for 5 minutes, room temperature. Slides were dried in air for 24 hours then stored at -20°C in slide cassettes wrapped in foil. All BAL fluid aliquots and cytopsin slides numbers were recorded as part of the human tissue act (HTA) 2004 (<https://www.legislation.gov.uk/ukpga/2004>).

2.5. CF cohort characterisation

2.5.1. Differential cell counts

2.5.1.a. Cytospin staining

Cytospins were removed from -20°C and thawed at room temperature. Slides were stained with Hemacolor® (Merck Millipore, UK) as recommended by the manufacturer. In brief, each slide was submerged in a fix stain containing methanol for 1 minute then blotted dry. Stain and drying was repeated for an eosinophilic stain (granular stain) followed by the azure nuclear stain. Slides were dried for at least one hour at room temperature. A coverslip was fixed using DPX mounting medium (Fisher Scientific, Loughborough, UK) and left to solidify for at least one hour. Slides were stored in a locked cupboard, as directed by HTA guidelines, at room temperature prior to microscopy.

2.5.1.b. Microscopy

Microscopy was performed on a Leica microscope at 20X magnification, at least four spatially separate fields were captured for each slide, ensuring not to capture the same cells in multiple fields. For some samples, cell counts were low and therefore up to eight fields were captured. Using Microsoft Paint, cell types were counted and marked. At least 300 cells were counted for each sample; however, for six samples between <300 cells were counted because of low cell numbers in the BAL fluid, analysis was performed on all data.

2.5.1.c. Differential cell count and calculation

Cells were identified as polymorphonuclear leukocytes (PMNs), “mononuclear”, or, “cellular” but not enough evidence to determine cell type. For mononuclear cells, cell types were further differentiated into monocytes (including macrophages and lipid laden macrophages), squamous epithelial cells and monocyte other (lymphocytes) (figure 2-1). Due to subjective nature of differential cell counting a selection of five slides from five different BAL fluids that were considered difficult to count were also counted by my supervisor, Dr. Eamon McGreal, to compare and validate counting technique. Where cell counts differed by more than 10% (2 samples), a mean between our two counts was used, for differences <10% I used my counts in the analysis. An example of the cells counted and three typical CF cytopins from my study can be found (table 2-3 and figure 2-1). Neutrophil count was calculated assuming that PMNs were predominantly neutrophils. The percentage of each cell type was calculated for each

slide, by dividing the number of that type of cells (in all the fields for that sample) by the total amount cells included in the count (in all fields for that sample) and multiplying by 100. The neutrophil count for each sample was calculated by multiplying the cell count (haemocytometer) by the percentage of neutrophils (PMNs) for that sample.

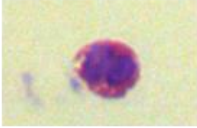
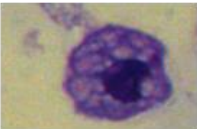
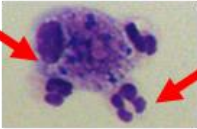
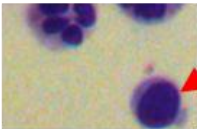
Cell type	Example from CF BAL slides
Polymorphonuclear Leukocytes	
Polymorphonuclear Leukocytes (PMN)	
Basophil	
Mononuclear Cells	
Monocytes	
Lipid-laden macrophage	
Neutrophil-macrophage interaction	<div style="display: flex; align-items: center;"> <div style="margin-right: 10px;">Macrophage</div>  <div style="margin-left: 10px;">PMN</div> </div>
Epithelial Cell	<div style="display: flex; align-items: center;"> <div style="margin-right: 10px;">Cilia</div>  </div>
Lymphocyte	

Table 2-3: Typical examples of cells identified in CF BAL fluid. Polymorphonuclear leukocytes are round, smaller than monocyte/macrophages, and had multilobular nuclei. Basophils were rare (2 counted in over 180 slides), they were similar to PMNs, but positively stained red. Monocyte/macrophages were typically large and had a “fried-egg” appearance. Lipid-laden macrophage were similar to monocyte/macrophages but contained light patches. Epithelial cells were distinctive with a rectangular shape and a “fuzzy” patch of cilia at the apical membrane. Suspected lymphocytes were smaller than PMNs and a nucleus that occupied most of the cell.

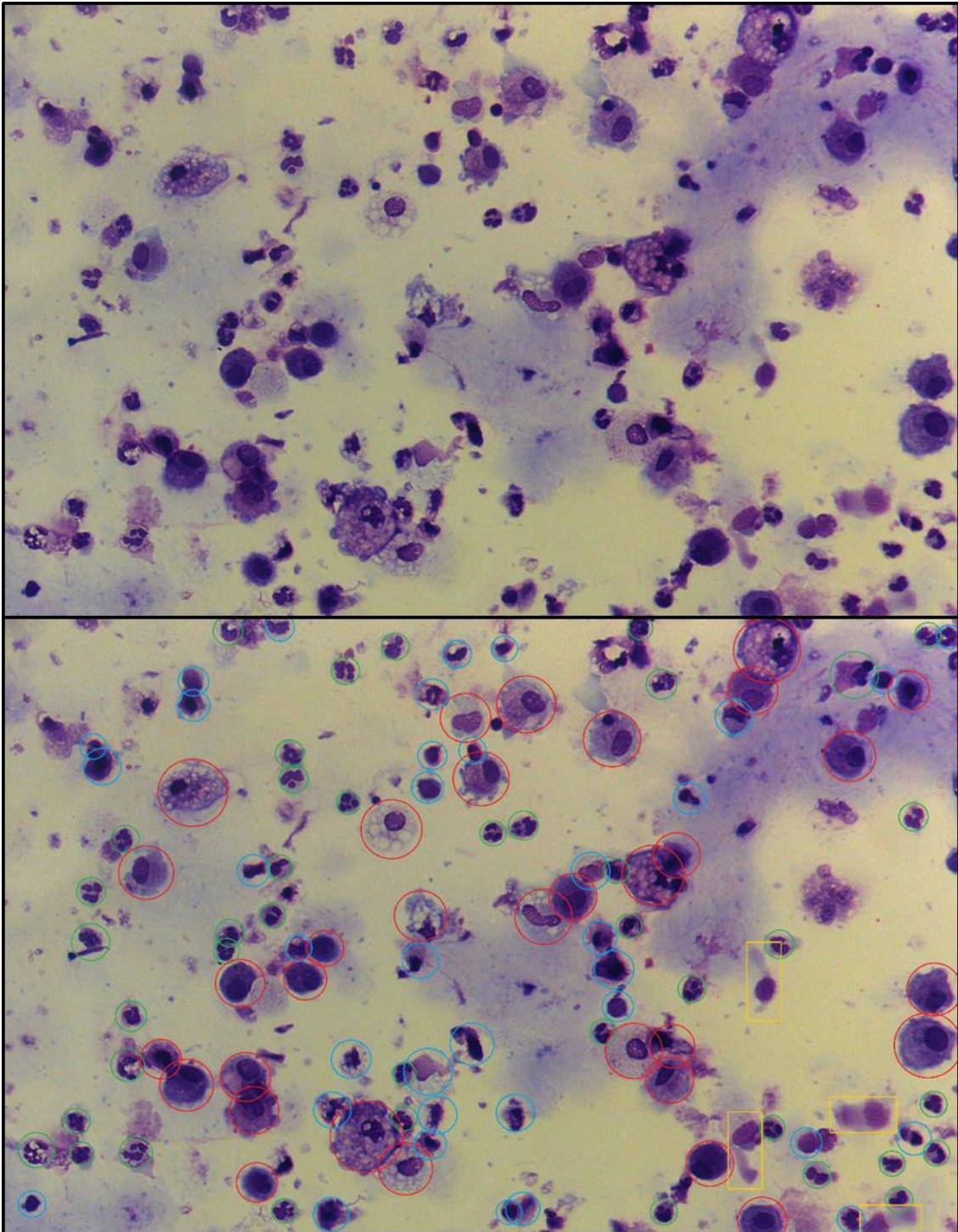


Figure 2-1: A typical example of a captured field from a cytopspins. Top) unannotated field B) Annotated to show which cells were included in the differential count. Monocyte/macrophages were circled in red, PMNs were circled in green, lung epithelial cells are in yellow rectangles and other non-identified cells (but would have been included in the haemocytometer count) were circled in blue.

2.5.2. NE activity assay

CF BAL fluid (50 μ L) was removed from -80°C and thawed on ice, prior to use BAL fluid was centrifuged 10,000 RPM for 1 min at room temperature in a microfuge. Initially, BAL fluid was diluted 1:3 using activity buffer (100 mM TRIS, 500 mM NaCl, 0.05% (v/v) Triton X-100, pH7.5), further dilutions were made depending on activity of the sample. For example; samples that had low activity a dilution of no less than 1:1 was used, or if samples had activity higher than the standard curve then BAL fluid was diluted further. For standards, purified human NE was diluted serially in activity buffer to give a range of 80nM to 1.125nM. Activity buffer without NE was used as a negative control.

For the assay, 50 μ L diluted BAL fluid or standard was added to a 96-well plate in duplicate. 50 μ L protease-specific chromogenic substrate (2 mM Suc-Ala-Ala-Pro-Val-pNA in activity buffer, Bachem, Cambridge, UK) was added to each well to start the assay. Absorbance from each well was read at 405nm using a spectrophotometer, a protocol was programmed to take a reading every minute for 20 minutes. Protease activity was quantified by calculating the mean change in absorbance over time (20 minutes). NE activity in CF BAL fluid was interpolated from a quadratic curve generated from change in absorbances of the purified NE standards, these was calculated in Graphpad Prism 7. The interpolated NE activity was multiplied by the dilution factor for each respective BAL fluid sample. The limit of detection for this assay was between 80 and 1.125 nM NE however, 16 out of 41 samples had no detectable NE activity; however, these data still provide valuable information about inflammation. I consulted our group statistician (Dr. Samuel Touchard), he advised that rather than omitting them from the data set, these samples were given the value half-way (mean) between the limit of detection (1.125 nM) and zero, so 0.563 nM.

2.5.3. CXCL8

Duo-set CXCL8 ELISA (R&D systems, Abingdon, UK) was performed as recommended by the manufacturer. A 96-well Maxisorb plate (NUNC (Fisher Scientific, Loughborough, UK)) was coated with 100 μ L 4 μ g/mL capture antibody in PBS and incubated overnight at room temperature. Coated wells were washed three times with 250 μ L PBS-tween20 (0.05% (v/v)) and blotted dry on paper towel. Wells were blocked with 200 μ L reagent diluent (1% BSA/PBS (w/v), prepared in-house) and incubated for 60 minutes at room temperature. Wells were washed, and 100 μ L standard or sample loaded in duplicate. For standards, CXCL8 (provided) was diluted serially in 2-fold increments from 2000 pg/mL to 31.123 pg/mL in

reagent diluent. CF BAL fluid was removed from -80°C, thawed and kept on ice, prior to use BAL fluid was centrifuged 10,000 RPM for 1 min at room temperature in a microfuge. BAL fluid was diluted 1 in 3 with reagent diluent. BAL fluid with high NE activity, indicative of neutrophilic inflammation, were diluted 1 in 10. The plate was incubated for 2 hours at room temperature. Wells were washed and 100 µL 1.2 µg/mL detection antibody in reagent diluent was added. The plate was incubated for 2 hours at room temperature. Wells were washed and 100 µL streptavidin-HRP conjugate (diluted 1 in 40, as specified by the manufacturer) was added. The plate was incubated for 20 minutes at room temperature. Wells were washed and 100 µL 3,3',5,5'-Tetramethylbenzidine (TMB) substrate was added. Colour (blue) was allowed to develop for 2-3 minutes until standards were visible. Reaction was stopped immediately by adding 50 µL 2 N sulphuric acid to each well. Optical absorbance was measured for each well at 450 nm with 570 nm reference filter using a spectrophotometer (Dynex, Worthing, UK). CXCL8 concentration in BAL fluid was interpolated from a sigmoidal curve using log₁₀ standard concentrations, calculations were performed by Graphpad Prism® 7. The interpolated value for each BAL fluid sample was multiplied by the dilution factor for that sample. The limits of detection for this assay were between 2000 to 31.125 pg/mL. As for NE activity, any samples that had no detectable CXCL8 were given the value 15.56 pg/mL, the mean of the lower limit of detection and zero.

2.5.4. Complement Meso Scale Discovery (MSD) multiplex platforms

Antibody pairings for the MSD platform were optimised in-house by Dr. Rowan Orme as part of several studies measuring complement in disease (Kopczynska *et al.* 2017; Kopczynska *et al.* 2018). The majority of the antibodies used for the detection of analytes using this platform were developed in-house under the supervision of Prof. B. Paul Morgan. Plates were coated and prepared by MSD using a combination of commercial and in-house antibody pairings. Complement components were organised onto two plates depending on the dilution factor required for detection and quantification from the standard curve. The activation plates measured C3, C5, factor H, factor B, factor I, and iC3b. Due to issues with detection, C5 data were excluded from these plates and were measured by ELISA (see C5 ELISA). The second plate measured C5b-9 (terminal complement complex) factor Bb, C5a, C3a, and factor D. Due to technical issues with C5a standards, C5a data were excluded from these plates and were measured by commercial C5a ELISA.

For MSD assay, wells were blocked with 150 µL 3% BSA in PBS (w/v) and incubated at room temperature for 2 hours on an orbital shaker (600 RPM). Blocking solution was removed by

blotting on paper towel. In duplicate, 25 μ L standards or sample was added to the plate and incubated for 1 hour at room temperature on shaker. For standards, a pre-made master mix prepared for each plate type was diluted 1 in 10 or 1 in 20 for activation and regulator plates respectively. Both standard sets were serially diluted 5-fold in 1% BSA (w/v)/10mM EDTA/PBS to give a 7-point standard curves for each analyte. CF BAL fluid was removed from -80°C, thawed and kept on ice, prior to use BAL fluid was centrifuged 10,000 RPM for 1 min at room temperature in a microfuge. BAL fluid was diluted in 1% BSA (w/v)/10mM EDTA/PBS, 1:1 for activation plates or 1/2000 for regulator plate. Wells were washed four times with 200 μ L tween-20/PBS (0.05%, v/v) and blotted dry on paper towel. For detection, a SULFO-tag conjugated antibody mix specific to each plate was diluted to 1 μ g/mL in 1% BSA/10mM EDTA/PBS and 25 μ L added to each well. The plate was incubated for 1 hour at room temperature on shaker. Plate was washed and blotted dry, then 150 μ L read buffer (provided by MSD) was diluted 1:1 with H₂O and added to each well. Plate was immediately read using MSD plate reader. Data was analysed using MSD workbench® v4.0 and a template protocol that was programmed to interpolate values from each standard curve. Each analyte was multiplied by the dilution factor for that BAL fluid sample; a factor of 2 for the activators plate and a factor of 2000 for the regulators plate. Any analytes below the lower limits of detection were not included in the analysis.

2.6. C5 ELISA

A C5 ELISA was developed and optimised in-house, (section 3.7.1) Maxisorb 96-well plates were coated with 50 μ L/well 1 μ g/mL SKY59 (Roche Pharmaceuticals, Basel, Switzerland) humanised mouse anti-human C5 monoclonal antibody in 2% carbonate buffer (w/v) and incubated 60 minutes at 37°C. Wells were washed three times with 200 μ L PBS-Tween20 (0.05%, v/v) and blotted dry on paper towel. Wells were blocked with 250 μ L 1% BSA/PBS (w/v) and incubated for 60 minutes at 37°C. Plate was washed, 50 μ L standards or sample was added in duplicate and incubated for 60 minutes at 37°C. For standards, purified C5 from human serum (Complement Technology, Texas, US) was diluted 5-fold serially in 1% BSA/PBS from 1000 to 0.064 μ g/mL (v/v). For cohort characterisation CF BAL fluid was removed from -80°C, thawed and kept on ice, prior to use BAL fluid was centrifuged 10,000 RPM for 1 min at room temperature in a microfuge, samples were then diluted 1 in 2 with 1% (w/v) BSA/PBS. For quantification of C5 in C5a generation experiments (section 4.7.3), samples were diluted 1 in 5000 in 1% BSA/PBS. After incubation with standards or samples, plates were washed then, 50 μ L mouse anti-human C5/C5a antibody clone 557 (Hycult Biotech, Uden, Netherlands) in 1% BSA/PBS was added to each well and incubated for 60 minutes at 37°C. Plate was washed, 50 μ L 60 ng/mL goat anti-mouse IgG-HRP conjugate

antibody (Stratech Scientific Ltd, Suffolk, UK) was added and incubated for 60 minutes at 37°C. Plate was washed and 50 µL TMB substrate was added to each well and colour was allowed to develop (up to 5 minutes) until standards were visible. To stop reaction, 25 µL 1 N (4%) hydrochloric acid was added to each well. Optical absorbance at 450nm with 570 nm reference filter, was measured on a spectrophotometer. C5 concentration in samples was interpolated from a sigmoidal curve using Graphpad Prism® 7. Interpolated C5 concentration was multiplied by the dilution factor for that sample. The detection range for this assay was 1000 to 0.064 ng/mL. For a single CF BAL fluid sample, the C5 concentration was detectable but >3 standard deviations below the mean and therefore, regarded as an outlier and omitted from the data set.

Two versions of the C5 ELISA were used for detection of C5 during C5a generation experiments. These versions either used different detection antibodies: Hycult anti-C5/C5a antibody, as described above, or an in-house monoclonal antibody, 2D5 (Giles *et al.* 2015). Both antibodies were used at the same concentration and all other conditions remained the same.

2.6.1. C3a ELISA

C3a Microvue™ ELISA (Quidel®, San Diego, US) was performed as recommended by the manufacturer, all reagents were provided by the manufacturer. Briefly, 100 µL standard or sample was added in duplicate to pre-coated 96-well plates and incubated at room temperature for 60 minutes. For standards, ready-to-use dilutions were used, these had been made from dilutions of human serum. CF BAL fluid was removed from -80°C, thawed and kept on ice, prior to use BAL fluid was centrifuged 10,000 RPM for 1 min at room temperature in a microfuge. For sample dilution, BAL fluid was diluted 1 in 20 with sample diluent (“buffered protein base” in 0.035% (w/v) ProClin®) however, BAL fluid that had high C5a concentrations (C5a was quantified in samples before C3a), indicative of anaphylatoxin generation, were diluted 1 in 30. After incubation with standards or samples, wells were washed twice with wash 300 µL 1X wash solution (PBS, 1% tween-20, and 0.035% (w/v) ProClin® 300, made fresh by diluted 20X stock solution 1 in 20 in de-ionised H₂O) using a wash bottle and blotted dry on paper towel. For detection, 100 µL conjugate antibody was added and incubated for 60 minutes at room temperature. Wells were washed four times and 100 µL substrate solution added to each well and incubated at room temperature. Colour was allowed to develop until the standard curve was visible (up to 15 minutes). Reaction was stopped with 100 µL stop solution (1 N HCl) and optical absorbance was measured at 450 nm using a

spectrophotometer. C3a concentration in CF BAL fluid was interpolated from a sigmoidal curve using Graphpad Prism® 7. Interpolated values were multiplied by the dilution factor for that sample. The detection range for this assay was 4810 to 50 pg/mL. 3 samples out of 41 had no detectable C3a, like NE and CXCL8, these were given an arbitrary value halfway between the lower detection limit and zero, 25 pg/mL.

2.6.2. C5a ELISAs

Two different C5a ELISAs were used as part of this study; a commercial C5a ELISA and one that was developed in-house. The commercial ELISA was used for quantification of C5a where C5 might also be present such as CF BAL fluid and C5a generation experiments (using purified C5). The in-house ELISA was used for quantification of C5a when no C5 was used in the experiment, such as quantifying C5a in gel chromatography experiments.

2.6.2.a. Commercial C5a ELISA

C5a Microvue™ ELISA (Quidel®, San Diego, US) was performed as recommended by the manufacturer, all reagents were provided by the manufacturer. Pre-coated 96-well plates were hydrated with 300 µL 1X wash solution (PBS, 1% tween-20, and 0.035% ProClin® 300, made fresh by diluted 20X stock solution 1 in 20 in de-ionised H₂O) and incubated at room temperature for 2 minutes. Wells were washed twice with wash solution using a wash bottle and blotted dry on paper towel. 100 µL standard or sample was added to the plate and incubated at room temperature for 60 minutes for standards, ready-to-use dilutions were added, these were provided by the manufacturer and made from dilutions of human serum. For CF samples, CF BAL fluid was removed from -80°C, thawed and kept on ice, prior to use BAL fluid was centrifuged 10,000 RPM for 1 min at room temperature in a microfuge. BAL fluid was diluted 1 in 3 with sample diluent (PBS, 0.05% tween-20, 2.5% “protein stabilisers”, and 0.035% ProClin) however, CF BAL fluid with high CXCL8 concentrations, indicative of inflammation, were diluted 1 in 4. For C5a generation experiments in section 4.7.1, samples were diluted 1 in 5000. After incubation with standards or samples, wells were washed five times and then 100 µL conjugate antibody was added and incubated for 60 minutes at room temperature. Wells were washed five times and 100 µL substrate solution added to each well and incubated at room temperature. Colour was allowed to develop until the standard curve was visible (up to 15 minutes). Reaction were arrested with 100 µL stop solution (1 N Hydrochloric acid) and optical absorbance was measured at 450 nm using a spectrophotometer. C5a concentration in samples was interpolated from a linear curve using

Graphpad Prism® 7. The C5a value was multiplied by the dilution factor for that sample to calculate C5a concentration. The detection range for this assay was 953 to 10 pg/ml. There was no detectable C5a in 8 out of 41 CF samples. As mentioned above for another analytes, these samples were given values between the lower detection limit and zero, in this case 5 pg/mL. There are no commercially available ELISAs that can distinguish between C5a and C5adesArg. Therefore measurement of C5a/C5adesArg in BAL fluid in this study is referred to as C5a; however, it is assumed that the majority of this C5a is actually C5adesArg.

2.6.2.b. In-house C5a ELISA

Maxisorb 96-well plates were coated with 50 µL 2 µg/mL mouse anti-human C5a neo epitope monoclonal antibody clone 2952 (Hycult Biotechnology, Uden, Netherlands) diluted in 2% (w/v) carbonate buffer and incubated overnight at room temperature. Wells were washed three times with 200 µL PBS-tween20 (0.05%, v/v) and blotted dry on paper towel. Plates were blocked with 150 µL 1% semi-skimmed milk (Sigma, Dorset, UK)/ PBS and incubated for 60 minutes at room temperature. Wells were washed, and 50 µL standard or sample were added in duplicate and incubated for 90 minutes at room temperature. For standards, purified native C5a was diluted serially 2-fold from 16 ng/mL to 0.5 ng/mL in 1% milk / PBS. For C5a quantification in column chromatography fractions, samples were diluted 1/2.5 in 1% milk / PBS. Wells were washed, and 50 µL 2 µg/mL mouse anti-human C5/C5a in 1% milk / PBS (Hycult Biotechnology, Uden, Netherlands) was added and incubated for 60 minutes at room temperature. Plates were washed, and 50 µL 160 ng/mL goat anti-mouse Ig2a HRP-conjugated antibody (Stratech Scientific Ltd, Suffolk, UK) in 1% milk /PBS and incubated 60 minutes at room temperature. Wells were washed, and 50 µL TMB substrate was added and the plate was incubated for 20-30 minutes at room temperature in the dark. Reaction was stopped with 50 µL 5% HCl (v/v). Optical absorbance was measured at 450 nm with 570 nm reference filter using a spectrophotometer. C5a concentration in samples was interpolated from a linear curve using GraphPad Prism® 7, interpolated values were multiplied by the dilution factor (2.5). The detection range for this assay was 16 ng/mL to 0.5 ng/mL.

2.6.3. Total protein

Bicinchoninic acid (BCA) assay (Fisher Scientific, Loughborough, UK) was used to measure total protein in CF BAL fluid. BSA protein standard (Fisher Scientific, Loughborough, UK) was diluted 2-fold serially in PBS from 200 to 1.25 µg/mL. CF BAL fluid was removed from -80°C, thawed and kept on ice, prior to use BAL fluid was centrifuged 10,000 RPM at room

temperature in a microfuge. For quantification of total protein CF BAL fluid was diluted 1 in 3 in PBS. For the assay, 75 μ L of standard or sample was added in duplicate to a sterilin™ 96-well plate. To each well 75 μ L a BCA solution containing 25 parts reagent A, 24 parts reagent B and 1 part reagent C was added. The plate was incubated for 3 hours at 37°C. Optical absorbance was measured at 570 nm using a spectrophotometer. Total protein concentration in CF BAL fluid was interpolated from a sigmoidal curve using Graphpad Prism® 7, the interpolated values were multiplied by the dilution factor for that CF sample to give the total protein concentration. The detection range for this assay was 200 to 1.25 μ g/mL. For 2 out of 41 samples total protein was not quantified because only a small volume of BAL fluid was recovered from these patients and characterisation of total protein was considered not to be a priority.

2.6.4. CPB and CPN activity assay

Protocol for the quantification of CPB and CPN activity was adapted from Mueller-Ortiz *et al.* (Mueller-Ortiz *et al.* 2009). CPB/N activity was quantified using a specific chromogenic substrate, furylacryloyl-Ala-Lys (Bachem, Cambridgeshire, UK). For standards, porcine CPB was diluted 2-fold serially in PBS from 15 μ g/mL to 0.94 μ g/mL. For CF samples, CF BAL fluid was removed from -80°C, thawed and kept on ice, prior to use BAL fluid was centrifuged 10,000 RPM for 1 min at room temperature in a microfuge, BAL fluid was diluted 1 in 4 in PBS. For experiments investigating the influence of factors on porcine CPB activity, 15 μ g/mL porcine CPB was incubated 1:1 with the experimental sample (section 6.9.3). For the assay, 100 μ L standard or sample (in duplicate) was pipetted into a sterilin™ 96-well plate, followed by 150 μ L 833 μ M substrate (solubilised in activity buffer (0.1 M HEPES, 0.5 M NaCl at pH 7.8)). The plate was loaded onto FluorSTAR® Omega plate reader (BMG labtech, Aylesbury, UK). Change in optical absorbance at 336 nm was measured over time for no more than 25 minutes. Activity in samples was interpolated from the change in absorbance of the standards, calculated using a linear curve in GraphPad Prism® 7. Interpolated values were multiplied by the dilution factor for those samples. The detection range for this assay was 15 to 0.94 μ g/mL.

2.6.5. Dimethyl methylene blue staining – GAG quantification

Dimethyl-methylene blue (Sigma, Dorset, UK) was used to quantify soluble sulphated GAGs in CF BAL fluid, the protocol was adapted from Stone *et al.* (Stone *et al.* 1994). Stain was prepared by dissolving 8 mg/mL dimethyl-methylene blue in a stain solution of 40.5 mM

glycine and 625 mM NaCl, pH 4.0. The stain was filtered through 0.2 µm filter and stored at 4°C. For standards, HS was diluted 2-fold serially from 200 to 6.25 µg/mL in PBS. For samples, CF BAL fluid was removed from -80°C, thawed and kept on ice, prior to use BAL fluid was centrifuged at 10,000 RPM for 1 min at room temperature in a microfuge. BAL fluid was diluted 1:1 in PBS. For the assay, 20 µL of standard or sample was loaded onto a sterilin® 96-well plate, in duplicate. To each well 200 µL dimethyl methylene blue stain was added, optical absorbance was measured at 570 nm on a spectrophotometer. GAG concentration was interpolated from a sigmoidal curve using Graphpad Prism® 7, the interpolated values were multiplied by the dilution factor for those samples. The detection range for this assay was 200 to 6.25 ng/ml. Dimethyl methylene blue stains sulphated GAGs and therefore, although a HS standard curve was used in this assay, other GAGs may have been detected as several different GAGs have been shown to be present in the CF airway (table 6-1). Therefore, GAG concentration is relative to HS.

Dimethyl methylene blue was also used to quantify purified GAG concentration in elute from chromatography columns. Quantification of GAGs in fractions was performed on samples that had been diluted for the in-house C5a ELISA therefore, the dilution factor was 1 in 2.5. Assay was performed as for quantification of GAGs in CF BAL fluid.

2.7. Protease cleavage experiments

2.7.1. Proteolysis of C3a or C5a by proteases present in CF BAL fluid

Aliquots were removed from -80°C and thawed on ice. Prior to use BAL fluid was centrifuged 10,000 RPM for 1 min at room temperature in a microfuge. Supernatant was carefully removed and diluted 1:1 in cold PBS-T. Purified C3a or C5a were removed from -80°C and diluted to 10 µg/mL in cold PBS-T. In 0.5 mL Eppendorf tubes, the above complement components were exposed to an equal volume of CF BAL fluid and incubated at 37°C (water bath) for 60 minutes. Following exposure, tubes were centrifuged at 10,000 RPM for 15 seconds to reduce sample loss in condensate. Proteolytic activity from serine proteases was inhibited using 5 mM PMSF or 20 µg/mL AAT (inhibitor use is specified in respective figure legends). 5X Laemmli buffer (10% sodium dodecyl sulphate (w/v), 50% glycerol (v/v), 0.001% (w/v)) bromophenol blue was added to each sample at a ratio of 1:4, and samples were stored at -20°C prior to SDS-PAGE.

2.7.2. Generation of C3a and C5a by proteases present in CF BAL fluid

CF BAL fluid aliquots were removed from -80°C and thawed on ice. Prior to use BAL fluid was centrifuged 10,000 RPM at room temperature in a microfuge. Supernatant was carefully removed and diluted 1:1 in cold PBS-T. Purified C5 and C3 were removed from -80°C and diluted to 300 µg/mL in cold PBS-T. In 0.5 mL Eppendorf tubes, the above complement components were exposed to an equal volume of CF BAL fluid and incubated at 37°C (water bath) for 60 minutes. Following exposure, tubes were centrifuged at 10,000 RPM for 15 seconds to reduce sample loss in condensate. Proteolytic activity from serine proteases was inhibited using 5 mM PMSF or 20 µg/mL AAT (inhibitor use is specified in respective figure legends). 5X Laemmli buffer was added to each sample at a ratio of 1:4, and samples were stored at -20°C prior to SDS-PAGE.

2.7.3. Generation of C3a and C5a by purified NSPs.

Purified C5 and C3 were removed from -80°C and diluted to 300 µg/mL in cold PBS-T. Purified NSPs were removed from -20°C and diluted from stock solutions of 17 µM (NE, CG) or 34 µM (PR3) using PBS-T, unless specified NSPs were diluted to a final concentration of 420 nM. In 0.5 mL Eppendorf tubes, C5 or C3 were exposed to an equal volume of individual protease and incubated at 37°C for the time limits described in the figure legends. Following exposure, tubes were centrifuged at 10,000 RPM for 15 seconds to reduce sample loss in condensate. Proteolytic activity from serine proteases was inhibited using 5 mM PMSF or 20 µg/mL AAT (inhibitor use is specified in respective figure legends). For SDS-PAGE (section 2.8.1), 5X Laemmli buffer was added to each sample at a ratio of 1:4, and samples were stored at -20°C. For quantification of C5 or C5a, 1 µL of sample was removed at diluted 1 in 5000 in the dilution buffers required for the respective ELISAs. For C3a or C5a activity assays (section 2.9.2), samples were diluted 1 in 10 in phenol red-free DMEM. For complement haemolysis assays, samples were diluted 1 in 47 in complement fixation buffer (section 2.1.10).

2.7.4. Inactivation of C3a and C5a by porcine CPB

Purified C3a (1.5 µg/mL) or C5a (2.5 µg/mL) or the C3a-like or C5a-like fragments generated by NSPs (section 2.7.3) were incubated with an equal volume of 30 µg/mL (final concentration 15 µg/mL) porcine CPB at 37°C for 60 minutes. Following exposure, tubes were centrifuged

at 10,000 RPM for 15 seconds to reduce sample loss in condensate. For activity assays, samples were diluted 1 in 10 in phenol red-free medium.

2.8. Polyacrylamide gel electrophoresis (PAGE)

2.8.1. SDS-PAGE

Different gel types were used for resolution of the different proteins investigated in this study, these have been specified in the figure legends. Bis-Tris (37:5:1) gels were cast using Mini-Protean® hand-cast system (Bio-Rad, Hertfordshire, UK). Running gel contained 94 mM TRIS, 1% SDS (w/v), acrylamide (concentrations as stated in legends), 0.1% ammonium persulphate (w/v), and 0.1% Tetramethylethylenediamine (TEMED, v/v) at pH 8.8. Stacking gels consisted of 120mM Tris, 1% SDS, 4% acrylamide, 0.1% APS, and 0.1% TEMED at pH 6.8. For western blots analysis 1.5 mm gels were cast, 1 mm gels were cast for silver staining.

Pre-cast 0.75mm gradient gels, 4-20% Tris-glycine (SDS-free) (ThermoFisher, Loughborough, UK), were used to resolve C3 and C5 cleavage fragments and were used in native-PAGE and blue native-PAGE experiments.

Electrophoresis of both gel types were carried out in 25 mM Tris, 0.1% SDS, and 192 mM glycine. Fixed concentration gels were run at 40 mA(constant) per gel for approximately 45 minutes at room temperature. Gradient gels were run at 80 V (constant) for 2 h at room temperature. Samples were loaded using a pipette and loading tips, volume loaded was 10 µl for 1 mm gels and 15 µl for 1.5 mm gels. For reference 2.5 µl of either 2 – 40 kDa ladder (Fisher Scientific, Loughborough, UK) or EZ-Run 11 - 170 kDa (Fisher Scientific, Loughborough, UK) protein ladder was loaded. Blank wells were loaded with the dilution buffer of the samples that had been diluted in 5X Laemmli buffer.

2.8.2. Native PAGE

For native PAGE (SDS-free), pre-cast 4-20% gradient gels were used. Samples were diluted in 5X SDS-free loading buffer that contained 500 mM TRIS, 50% glycerol (v/v), 1% bromophenol blue (w/v) at pH 8.6. For resolution, 10 µL sample was loaded per well, gels were submerged in native running buffer containing 25 mM TRIS and 192 mM glycine at pH 8.3. Electrophoresis was performed at 100V for 2 h, tank was cooled by placing in ice on a magnetic stirrer.

2.8.3. Blue native-PAGE (BN-PAGE)

BN-PAGE protocol was developed from Fiala *et al.* (Fiala *et al.* 2011). For native BN-PAGE (SDS-free), pre-cast 4-20% gradient gels were used. Coomassie blue G-250 was used as a protein charge carrier instead of SDS or the native charge of the proteins. Samples were diluted in a SDS-free loading buffer similar to that used for native-PAGE (section 2.8.2) however, in addition, 0.1% (v/v) Coomassie blue R-250 (Fisher Scientific, Loughborough, UK) was added. For resolution, 10 μ L sample was loaded per well, gels were submerged in native running buffer containing 25 mM TRIS, 192 mM glycine and 0.02% (v/v) coomassie blue R-250 (pH 8.3). Electrophoresis was performed at 100V for 2 h, tank was cooled by placing in ice on a magnetic stirrer.

2.8.4. Silver staining

Protocol for silver staining was adapted from Shevchenko *et al.* 1996 (Shevchenko *et al.* 1996). All washes and stains were performed using sterile H₂O in 250 mL capacity weigh boats. Following electrophoresis gels were immediately fixed in 50% methanol (v/v) / 5% acetic acid (v/v) in sterile water for 20 minutes on a rocker at room temperature. Gels were washed twice in 50% methanol for 10 minutes followed by two 60 second rinses in H₂O. Gels were sensitised in 0.02% sodium thiosulphate (w/v) for 60 seconds and rinsed twice in H₂O. Gels were stained with cold 0.1% silver nitrate (w/v) for 45 minutes at 4°C. Stain was discarded, and gels were rinsed twice in H₂O. To develop, gels were washed in cold 0.04% formalin (v/v) / 2% sodium carbonate (w/v) until protein bands were visible (~30 minutes). Developing was stopped by discarding formalin solution and washing in 5% acetic acid (v/v) for at least 5 minutes, at room temperature. For imaging gels were soaked in 20% glycerol (v/v) overnight and dried between dialysis membranes. Dried gels were scanned and annotated using Corel Graphics Suite X5 v15.2.0.661.

2.8.5. Western blotting

2.8.5.a. Antibody staining

Proteins resolved by electrophoresis on polyacrylamide gels were transferred to nitrocellulose membranes (Pall Life Sciences, Hampshire, UK) in 25 mM TRIS, 192 mM glycine, 20% methanol (v/v) at 100 V (fixed) for 60 minutes, cooled by ice block on a magnetic stirrer. For visualisation of fragments generated by the proteolysis of C3 or C5, membranes were cut in-

two along the line of the 56 kDa protein reference ladder. All membranes were treated the same during the following steps. Membranes were blocked in 5% semi-skimmed milk (Sigma, Dorset, UK) (w/v) / PBS for at least 30 minutes at room temperature. For staining blots were incubated in 2.5 mL antibody / 5% milk (See antibody table 2-2 for antibody dilutions) in 60 mL falcon tubes overnight on rollers at room temperature. Blots were washed three times with 15 mL PBS-T and once with 15 mL PBS for at least 15 minutes each, at room temperature on rollers. Membranes were stained with respective HRP-conjugate antibody in 2.5 mL / 5% milk for 60 minutes at room temperature on rollers. Blots were washed three times in both PBS-T then PBS as above.

2.8.5.b. Developing western blots

For developing, membranes were incubated with 250 μ L enhanced chemo-luminescent substrate (ECL) for 2 minutes, three levels of ECL sensitivity were available high, medium or, low (ECL select (GE Lifesciences, Buckinghamshire, UK), ECL prime (GE Lifesciences, Buckinghamshire, UK) or Pierce ECL (Fisher Scientific, Loughborough, UK)). In a dark room, Super RX Fuji X-ray film (VWR, Leicestershire, UK) was exposed to membranes for 2 minutes (typical length of time) and subsequently developed by submerging in developer for 1 minute (or as long as it takes to visualise bands), washing in tap water and finally in fixer for at least 30 seconds. The ECL sensitivity or exposure time were varied for each blot so that different aspects of the gel could be visualised. For example, for C5 and C3 cleavage experiments blots were cut in two and incubated with different ECLs, as described in figure legends. This was because the large amounts of C3 or C5 that had been resolved on the gels meant that blots became over-exposed when they were developed. Exposed films were scanned and annotated using Corel Graphics Suite X5 v15.2.0.661. Figures showing western blots represented all the bands that could be visualised, unless stated otherwise.

2.9. Cell reporter assays

2.9.1. Cell culture

2.9.1.a. U937-C5aR1

U937-C5aR1 monocytes (A gift from Prof. Eric Prossnitz, New Mexico, USA) were cultured in 10% (v/v) FCS (Fisher Scientific, Loughborough, UK), 5000 U/mL penicillin-streptomycin (Fisher Scientific, Loughborough, UK), 2 mM L-glutamine in RPMI1640 (Fisher Scientific, Loughborough, UK). Cells were cultured at 37°C 5% CO₂ in 50 mL flasks and passaged every 3-4 days when confluent.

2.9.1.b. RBL-C3aR and RBL-C5aR1

Rat basophil leukaemia (RBL-2H3) cells transfected with C5aR1 (RBL-C5aR1) and RBL-C3aR (both cell lines were gifts from Dr. Peter Monk, Sheffield University, UK) adherent cell lines were cultured in 10% (v/v) FCS, 5000 U/mL penicillin-streptomycin, 4 mM L-glutamine in DMEM (Fisher Scientific, Loughborough, UK). Cells were cultured at 37°C 5% CO₂ in 50 mL flasks and passaged by trypsinisation every 3-4 days when confluent.

2.9.2. Intracellular calcium signalling assay

2.9.2.a. Cell preparation

U937-C5aR1 were cultured until exponential growth phase. When confluent, cells were poured into a 30 mL universal container and centrifuged at 500 x g for 3 minutes at room temperature. Supernatant was discarded, and cell pellet resuspended in sterile 0.9% saline and then centrifuged a second time. Cell pellet was resuspended in 2-3 mL saline, a 20 µL sample was removed and added to an equal volume of trypan blue, to check for dead cells. Cells were counted using a haemocytometer under 20X magnification. Following counting, cell suspension was topped up to 20 mL with saline and centrifuged. Supernatant was discarded, and pellet was resuspended at 1×10^7 cells/mL in culture medium. Cells were incubated with 2 µM Fura-2-AM in culture medium for 30 minutes at room temperature. Following incubation, cells were washed in saline, centrifuged and resuspended at 5×10^6 cells/mL in Krebs / HEPES buffer (120mM NaCl, 25mM HEPES, 4.8 mM KCl, 1.2 mM KH₂PO₄ and, 1.2 mM MgSO₄, 1.3mM CaCl₂, pH 7.4).

2.9.2.b. Calcium flux assay

U937-C5aR1 Cells (5×10^6) were seeded in a 96-well plate and placed in a FLUOstar Omega microplate reader set at 37°C and acclimatised for 5 minutes. Cells were stimulated with 10 μ L sample, this was either purified C5a or cleavage fragments diluted 1 in 10 in Krebs-HEPES. Intracellular calcium release was quantified by measuring emission from Fura-2 at 510 nm when excited at 340 nm and 380nm. The ratio of fluorescent intensity was calculated for maximum and minimum calcium release by adding 0.5% (v/v) triton X-100 or 0.08 M ethylene glycol tetraacetic acid (EGTA) respectively. Calcium release upon stimulation was quantified by the following equation: $Ca^{2+} = K(R - R_{min}) / (R_{max} - R)$ where $K = 0.2865 \mu$ M and R is the ratio of fluorescence (340/380) as described by Al-Mohanna and Hallett (Al-Mohanna and Hallett 1988).

For C5aR1 inhibition, U937-C5aR1 cells were pre-incubated with 80 μ M AS-65121 C5aR1 antagonist (Cambridge Bioscience Ltd, Cambridge, UK) for 10 minutes at 37°C. Cells were seeded, and assay performed as above.

2.9.2.c. β -hexosaminidase release assay

RBL-C3aR and RBL-C5aR1 were cultured until in exponential growth phase. When confluent, supernatant was discarded and cells trypsinised in 5mL 0.11 mM Trypsin, 0.91 mM EDTA for 10 minutes at 37°C 5% CO₂. Trypsin was neutralised by adding an equal volume of culture media. Cells were centrifuged 500 x g for 3 minutes at room temperature, supernatant was discarded, and cells were resuspended in 2-3 mL media. A 20 μ L sample was removed and added to an equal volume of trypan blue. Cells were counted using a haemocytometer under 20X magnification. Cells were diluted to 5×10^5 cells/mL in medium and 50,000 cells were seeded into a sterile 96-well plate and allowed to adhere overnight at 37°C 5% CO₂. Supernatant was discarded using a pipette and cells were washed with 150 μ L sterile PBS. Saline was immediately removed, and cells were stimulated with 50 μ L sample for 30 minutes at 37°C 5% CO₂. For reference in assays using RBL-C5aR1, purified native C5a was diluted 5-fold in series using phenol red free medium from 250 to 0.4 ng/mL C5a. For reference in assays using RBL-C3aR, purified native C3a was diluted 2-fold in series using phenol red free medium from 250 to 15.63 ng/mL. Experimental samples were diluted at least 1/10 in DMEM prior to stimulation (see figure legends). After stimulation, supernatant was immediately removed and added to 50 μ L β -hexosaminidase substrate (1 mM 4-Nitrophenyl N-acetyl- β -D-glucosaminide in 0.1 M citrate buffer (pH4.5)) and incubated for 3 hours at 37°C. Colour

change was induced by addition of 150 μ L 1M TRIS (pH 9), absorbance was measured at 405nm on a spectrophotometer. C5a or C3a activity in samples was interpolated from a sigmoidal curve generated using reference standards (purified C3a and C5a), curve was calculated using Graphpad Prism® 7. Cell stimulation could also be quantified as a percentage of maximum β -hexosaminidase, released by inducing lysis by incubating the cells with 50 μ L 0.1% (v/v) triton X-100.

2.10. Classical pathway complement haemolysis assay

2.10.1. Sheep erythrocyte sensitisation

One millilitre sheep erythrocytes (TCS Bio-science, Botolph Claydon, UK) were washed three times in 20 mL PBS by centrifugation at 872 x g for 5 minutes at 4°C, supernatant was removed using a 20 mL syringe and kwill. After the final wash step the pellet was unsettled by gentle tapping against the hand and 200 μ L erythrocytes from the residual volume were sensitised in 10 mL 1 in 4000 sheep anti-sera (Siemens Healthcare, Marburg, Germany) in complement fixation at room temperature for 30 minutes on rollers. Sensitised sheep erythrocytes were washed three times in PBS, as above, and resuspended in 10 mL complement fixation buffer

2.10.2. Haemolysis assay

In a U-bottomed 96-well plate 50 μ L sensitised sheep erythrocytes were added to 90 μ L 1% C5-depleted normal human serum (in-house). 10 μ L 1.81 μ g/ml C5 (following cleavage experiments in detailed in section 4.7.3) was added and incubated for 45 minutes at 37°C. The plate was centrifuged at 500 x g for 5 minutes at room temperature. 50 μ L erythrocyte supernatant was transferred to 100 μ L H₂O in a flat-bottomed plate and optical absorbance was measured at 405nm using a spectrophotometer. Sheep erythrocytes lysis was calculated as a percentage of the positive control (erythrocytes lysed with 100 μ L H₂O) minus negative control (erythrocytes incubated with complement fixation buffer only) for example: % lysis = ((sample absorbance – negative control absorbance) / (positive control absorbance – negative control absorbance)) x 100.

2.11. Fluid-phase column chromatography

2.11.1. Size exclusion chromatography

Superdex 75 (SD75) or Superose 6 columns (GE Lifesciences, Buckinghamshire, UK) were attached to AKTA prime FPLC (GE Lifesciences, Buckinghamshire, UK), washed with two column volumes of H₂O and, equilibrated in PBS. All washes and gel filtration were performed at 4°C, 0.3 mL / min flowrate and back pressure did not exceed 0.8 MPa. All buffers were filtered through 0.2 µm filters prior to use. Volume, flowrate, conductivity and ultra violet (UV) were continually recorded throughout all experiments.

Purified native C5a (10 µg/mL) was incubated for 2 h at 37°C with 500 µg/mL HS sodium salt from bovine kidney or chondroitin sulphate (CS) sodium salt from shark cartilage (Sigma Aldrich, Dorset, UK) diluted in H₂O. Two hundred microliters sample was loaded onto columns via a 200 µL induction loop. For each run the induction loop was washed with 5 mL PBS, the loop was then bypassed for the remainder of the run; in total, during each run, the columns had a one column volume of PBS flowed through. Fractions were collected in 12mm polystyrene tubes from 5 mL onwards, 0.5 mL fractions were collected into an equal volume of 2% semi-skimmed milk powder (w/v) / 0.1% tween-20 (v/v) / PBS at 4°C. Fractions were stored at 4°C until C5a quantification. Due to the limit of sensitivity in the UV spectrometer, C5a concentration was measured by in-house C5a ELISA (section 2.6.2b).

2.11.2. Affinity chromatography

A heparin 1 mL HiTrap affinity column (GE Lifesciences, Buckinghamshire, UK) was attached to AKTA prime and washed with 15 mL (15 column volumes) H₂O, followed by 1 M NaCl in PBS until conductivity plateaued. Column was re-equilibrated in PBS (154 mM NaCl). All washes and gel filtration were performed at 4°C, 0.5 mL / min flowrate and back pressure did not exceed 0.3 MPa.

Purified native C5a was incubated with GAGs as described for experiments using size exclusion chromatography. Two hundred microliters sample was loaded via a 200 µl induction loop. For each run the induction loop was washed with 2 mL PBS, the loop was bypassed and a further 5 mL PBS run through the column. The material on the column was eluted with a gradient of NaCl / PBS from 154 mM to 1000 mM that increased at a rate of 10% / min, real-time conductivity was recorded as a measure of increasing NaCl concentration. Fractions

were collected in 1.5 mL Eppendorf tubes throughout entire run, until buffer reached 100% 1000 mM NaCl / PBS. Fraction volumes of 0.5 mL were collected into an equal volume of 2% semi-skimmed milk powder (w/v) / 0.1% tween-20 (v/v) / PBS. C5a concentration in fractions was measured by in-house C5a ELISA.

2.12. Solid phase binding assay: C5a – GAG interaction

2.12.1. Biotinylation of HS

Method for biotinylation of HS was adapted from Clark *et al.* (Clark *et al.* 2006). One milligram lyophilised HS sodium salt from bovine kidney was reconstituted in 126 μ L 0.1 M (2-(N-morpholino) ethanesulfonic acid, MES). Biotinylation was carried out by adding 3.6 μ L 18.55 mg/mL biotin / DMSO (ThermoFisher) and 1.6 μ L 0.522 M 1-ethyl-3-(3-dimethylaminopropyl) carbodiimide hydrochloride in 0.1 M MES. Reagents were incubated at room temperature overnight. Biotinylated-HS was concentrated on Vivaspin protein concentrator spin column (GE life sciences, Buckinghamshire, UK) with a molecular weight cut off of 10 kDa. Spin-columns were centrifuged at 13,000 RPM for 10 minutes in a microfuge cooled to 4°C. Run-through was discarded, and columns were washed twice with 500 μ L sterile PBS with centrifugation at 13,000 RPM for 10 minutes, 4°C. Biotinylated-HS retained on the column was reconstituted with 1 mL PBS and stored at 4°C. For long-term storage, biotinylated HS was added to 50% glycerol and stored at -20°C.

2.13. Solid phase binding assay

Protocol for solid phase binding assay was adapted from Clark *et al.* (Clark *et al.* 2006). Maxisorb 96-well plates were coated with 150 μ L purified C5a, C3a, C3 or C5 in sterile PBS or PBS only (negative control) at concentrations stated in figure legends for respective experiments. Coated plates were sealed and incubated at 37°C, overnight. Plates were washed with 300 μ L assay buffer (50 mM sodium acetate, 100mM NaCl, 0.1 % tween-20 (v/v) pH 6.0) three times, blotting dry on paper towel between washes. Plates were blocked with 200 μ L 1% (w/v) BSA / assay buffer and incubated for at least 90 minutes at 37°C. After blocking plates were washed a further three times in 300 μ L assay buffer. To each well, 150 μ L 1 μ g/mL biotinylated HS in assay buffer was added and incubated for 3 h at 37°C. For competition experiments, varying concentrations of non-biotinylated HS, CS or HA were added to biotinylated HS maintaining a final concentration of 1 μ g/mL biotinylate-HS. After incubation with biotinylated-HS plates were washed three times and blotted dry, 150 μ L 25 ng/mL streptavidin-HRP was added to each well and incubated for 30 minutes at 37°C. Plates

were washed three times, blotted dry, and 150 μ L TMB substrate was added to each well. Colour was allowed to develop for up to 15 minutes, reaction was arrested using 4% HCl. Absorbance of each well was read by spectrophotometer at 450 nm. For figures, data is either plotted as absorbance values however, for competition experiments data was calculated as percentage absorbance of positive controls (biotinylated-HS).

2.14. Statistics

All statistical analyses were performed by Graphpad Prism 7, apart from the correlation matrix in figure 3.7 whereby analyses were performed in GraphPad prism, but matrix was drawn by Dr. Samuel Touchard using the statistic software R (<https://www.r-project.org/>).

All statistical tests were performed on data with $n \geq 3$, significance was reported when $p < 0.05$. All statistical analyses were reported in figure legends. Reporting of statistical outcomes in figures uses the following annotation ns – non-significant, * $p < 0.05$, ** $p < 0.01$, *** $p < 0.001$ and $P < 0.0001$.

When tested, there was not enough evidence to suggest that all data from the CF cohort had a Gaussian distribution and therefore, non-parametric tests were performed to analyse correlations between variables (Spearman rank correlation) and difference in medians (Wilcoxon paired t-test). The data population from the CF cohort contained seven patients that had repeated measures. After analysis (section 3.4), I determined that it was not appropriate to correct for repeated measures. For the correlation matrix in figure 3.7, testing for multiple comparisons was performed using the Holm-Bonferroni test for multiple comparisons (Holm 1979). Correlation analysis and presentation of Cohort data was performed on data transformed by log 10.

For dose-response and time-course experiments means were compared by two-way ANOVA with correction for multiple comparisons by Tukey's multiple comparisons test. Data in figures for experimental data was plotted as means with standard deviation. For preliminary data where $n < 3$ data was presented as the mean.

3. Characterising C3a and C5a in bronchoalveolar lavage fluid from a cohort of CF patients

3.1. Background to the study

The CF airway is a complex environment containing host-cells, pathogens and a multitude of endogenous and exogenous factors that continuously stimulate and regulate the immune system (Sagel *et al.* 2007; Sly *et al.* 2013). For example: DNA, cytokines, chemotactic molecules, endotoxins (PAMPs) and DAMPs have been investigated in the CF airway (Mackerness *et al.* 2008; Hartl *et al.* 2012; Kruger *et al.* 2015). Despite identification and quantification of these factors, the full picture of their roles in disease pathogenesis is very much incomplete.

Reflecting on our lack of understanding of the complex inflammatory environment in the CF airway, many anti-inflammatory therapeutics targeting single molecules in the CF airway have been mostly ineffective, or any modest benefits could not be measured over short trial periods (Cantin *et al.* 2015). Examples of pro-inflammatory molecules that have either been trialed or identified as therapeutic targets in the CF airway are: CXCL8, LTB₄, CXCR2 and IL-17/IL-17R (McAllister *et al.* 2005; Moss *et al.* 2013; Konstan *et al.* 2014; McElvaney *et al.* 2015). Furthermore, ibuprofen is the only anti-inflammatory drug that slows decline in lung function and is prescribed for long-term management (Konstan *et al.* 2007). Yet, only 10% patients are prescribed ibuprofen for long-term use (Konstan *et al.* 2007). This is due to concern over adverse effects in the GI tract, owing to high doses combined, with dehydration of the CF GI tract (Konstan *et al.* 2007; Mogayzel *et al.* 2013). Instead, over 50% of CF patients (including children) are given long-term courses of inhaled corticosteroids, despite reports that they only deliver modest improvements in lung function and concern that they may cause adverse developmental effects in paediatric patients (Lai *et al.* 2000; Mogayzel *et al.* 2013; Balfour-Lynn and Welch 2016). The mechanism of corticosteroid function is not well-defined but, it is reported that they prevent the release of pro-inflammatory cytokines through inhibition of NF- κ B transcription factors (de Benedictis and Bush 2012). The effects of corticosteroids are not limited to inhibiting pro-inflammatory cytokine release, other reported effects of corticosteroids are decreased mucus production, accelerated eosinophil apoptosis but the promoting of neutrophil survival (Saffar *et al.* 2011; de Benedictis and Bush 2012).

To improve understanding of inflammation in the CF airway there needs to more comprehensive characterisation of the different factors involved in promoting disease. This

can be an issue because laboratories have access to different types of airway fluid samples. These may only represent a small section of the airway or make assumptions that inflammation is spread throughout the airway. More recently, there is growing appreciation of the fact that infection and inflammation maybe localised throughout the airway (McNally *et al.* 2017; McElvaney *et al.* 2018). In this background section I will discuss the types of samples used to characterise inflammatory mediators and what has previously been reported on C3a and C5a using clinical samples.

3.1.1. Fluid sampling in airway disease and CF

One of the primary reasons for sampling the CF airway is because a patient has symptoms of pulmonary exacerbation such as difficulty breathing, chronic cough or wheezing (de Blic *et al.* 2000). Airway fluid is sampled to identify pathogens and enable the administration of the most effective antibiotics. A follow-up examination is performed after a course of antibiotics to confirm eradication of the infection (Brennan *et al.* 2008). Airway fluid samples are also essential for research, such as monitoring the efficacy of a therapeutic during a trial or, like myself, characterising pro-inflammatory mediators in the CF airway. There are three types of sampling techniques that can be used for lower airway sampling these are: BAL, induced sputum or cough swab. There is an ongoing debate about which of these is most appropriate for identifying pathogens and pathogenic factors. The advantages and disadvantages of each technique will be discussed below and are summarised in table 3-2.

3.1.1.a. Bronchoalveolar lavage

The ERS has published several guidelines on pathogen surveillance in CF; they state that BAL is “gold standard” for identification of pathogens in the CF airway (de Blic *et al.* 2000; Brennan *et al.* 2008). BAL is an invasive procedure that involves inserting a flexible fiberoptic bronchoscope into the airway whilst the patient is sedated. Due to the fact that patients have to be sedated, BAL may also be performed on CF patients whilst undergoing other surgery that also requires anesthetic; this allows further opportunity for surveillance of the airway. An example of such surgery is the insertion of a portacath; these to allow antibiotics to be directed straight into the circulation (Ronchetti *et al.* 2018).

When performing BAL, the bronchoscope is primarily positioned in the right middle lobe (figure 3-1); this is because this site is most straight forward to access. The left lung is more difficult to access due to a more acute angle in the left primary bronchus; this is skewed because of

the location of the heart. The “gold-standard” for performing BAL on CF patients for the detection of pathogens is to sample from the right middle lobe followed by the left lower lobe or infection site depending on imaging availability (figure 3-1) (Brennan *et al.* 2008). Moreover, a recent study suggests that a six-site sampling technique is most effective for comprehensive detection of pathogens (Ronchetti *et al.* 2018). The six-sites in the study by Ronchetti *et al.* were sampled in the same order for each patient: right middle lobe, left lingular, right lower lobe, right upper lobe, left lower lobe, and left upper lobe.

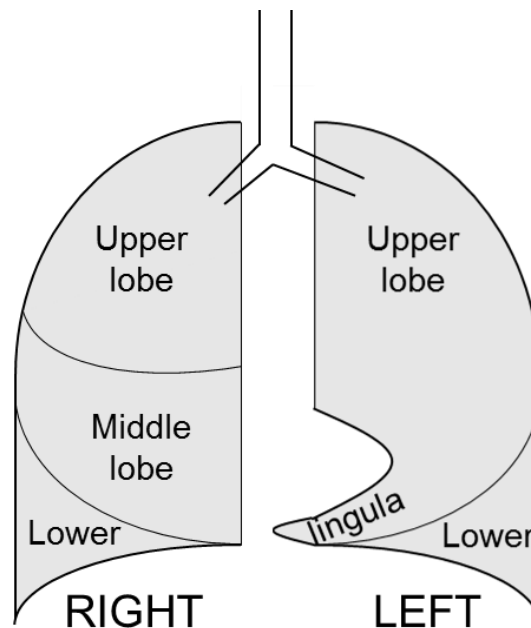


Figure 3-1: Diagram of the lobes in the human lungs. The human airway is separated into two lungs (left and right), these are further divided into upper, middle and lower however, the left middle lobe (lingula or tongue) is small and has a notch to accommodate the heart. Standard procedure for 2-lobe bronchoalveolar lavage is to sample from the right middle lobe followed by the left lower lobe.

Once the bronchoscope is situated at the correct sample site, saline is instilled at a volume proportional to the patient weight (recommended: 3 mL/Kg to a maximum of 20 mL)(de Blic *et al.* 2000). A syringe attached to the end of the tubing is used to aspirate fluid, along with cells, pathogens and debris, back out so that they can be analysed in the laboratory. It should be noted that, due to mucus obstruction in the airway not all the volume of saline instilled is recovered. The ERS guidelines for performing BAL on the CF airways state that recovery of greater than 40% of the instilled volume is acceptable (de Blic *et al.* 2000).

The identification of pathogens in BAL (and from sputum or cough swabs) is performed using positive selection culture media for known pathogenic strains in CF (de Blic *et al.* 2000; Bakare *et al.* 2003; de Vrankrijker *et al.* 2010). A disadvantage of using growth cultures is the time it

takes for pathogens to grow (48 hours), particularly if laboratories are sub-culturing strains and testing antibiotic susceptibility as this can take a further 48 hours (Burns and Rolain 2014). Culture media are specific for the detection of *Haemophilus influenzae*, *Staphylococcus aureus*, methicillin-resistant *Staphylococcus aureus* (MRSA), *P. aeruginosa*, *Burkholderia cepacia* complex species, non-tuberculous Mycobacterium species, *Achromobacter xylosoxidans*, *Stenotrophomonas maltophilia*, and *Klebsiella pneumoniae* (Ronchetti et al. 2018). Polymerase chain reaction (PCR) based assays that sequence 16S rRNA are becoming more routine; PCR is quicker than culture growth, but despite several reports, it is not clear whether PCR is more advantageous than growth cultures for pathogen identification (Miles 2010). A further method of identifying pathogens is to use mass spectrometry, this is quick and has shown to be 98% successful at identifying pathogens at the genus level using growth cultures as a reference (Desai et al. 2012).

As well as the identification of pathogens there are also guidelines for processing BAL fluid for analysis of cells and supernatant (de Blic et al. 2000). The ERS recommends that BAL fluid should be stored on ice until processed and, that samples should be processed within 30 minutes and stored at -70°C or below. The report also states that, further “processing” is not standardised and, that BAL fluid “should be optimised for the particular questions being asked” (de Blic et al. 2000).

A controversial issue with BAL (and other airway fluid sampling techniques) is that when reporting on CF fluid constituents (cells, cytokines and other factors), concentration should be reported as concentration per millilitre (de Blic et al. 2000; Brennan et al. 2008). Reporting concentration in this way is in contrast to other tissue fluid samples whereby concentrations are standardised to total protein or albumin. Correcting for total protein cannot be performed on airway samples due to capillary leakage in the airway during inflammation (de Blic et al. 2000). Other methods of standardising BAL fluid have been investigated, such as using secreted components of IgA and Urea. Secreted components of IgA are complexes of polymeric immunoglobulin receptors and IgA that protect IgA from degradation (Kaetzel et al. 1991). They are released by epithelial tissue and have not been reported to be influenced by lung injury or lung permeability (Watts and Bruce 1995). Urea is a product of mammalian metabolism and is ubiquitous throughout the cardiovascular system. Urea has been used to standardise the measurement of airway surface hydration and mucin concentration (Esther et al. 2017). The problem with standardising using urea, is that with each successive aliquot of BAL fluid removed from the airway the urea concentration increases, a consequence of urea leakage from circulation (Marcy et al. 1987). For the same reason, the ERS recommend that pathogen identification is performed on the first aliquot removed during each BAL procedure

(Brennan *et al.* 2008). Despite the above attempts to standardise the reporting of airway fluid constituents, the ERS recommends that analytes should be stated as grams per millilitre (de Blic *et al.* 2000; Brennan *et al.* 2008).

A disadvantage of BAL sampling is that it is an invasive procedure that requires sedation of the patient. None the less, the ethical issues of using of BAL to sample the CF airway are outweighed by the necessity to identify pathogens. Despite this, the invasiveness of BAL is a problem for clinical trials requiring longitudinal monitoring of a patient. Moreover, it is ethically inappropriate to perform an invasive technique such as BAL on healthy patients therefore, control populations for reporting in CF BAL use other non-CF patient populations that also undergo BAL, these are summarised in table 3-1. Despite identification of control populations that can be used as “healthy” controls for studies investigating CF, many non-CF conditions that require BAL are caused by infection (Brennan *et al.* 2008). Therefore, it cannot be guaranteed that healthy controls are free from pathogens. Consequently if studying inflammatory markers in the airway, concentrations of analytes may not represent the normal airway (Ringholz *et al.* 2014).

In summary, performing BAL in the CF airway is an invasive but effective and well-established technique for the identification of pathogens; however, there can be a lack of standardisation in processing and concentration reporting across different laboratories that makes it difficult to make comparisons of the constituent components.

Disease	Cause	Limitations in use as a control population for CF	Reference of use in CF study
Tonsillectomy	Recurrent infections of the tonsils – surgical removal of tonsils	No guarantee that the patient is healthy or free of airway infection Tonsillectomy is being phased out as a treatment for tonsillitis	(McGreal <i>et al.</i> 2010; Kotecha <i>et al.</i> 2013)
Primary ciliary dyskinesia	Genetic defect that reduces motility of flagella	Recurrent infections Pulmonary obstruction	(Ringholz <i>et al.</i> 2014)
Structural airway abnormalities (Stridor – blockage of the larynx)	Infection, blockage (foreign bodies), tumour or laryngospasm	Recurrent infection Inflammation	(Armstrong <i>et al.</i> 2005; Brennan <i>et al.</i> 2008)
Severe recurrent wheezy bronchitis	Neutrophil mediated inflammation	Controls for defects in cellular function through loss of CFTR Not necessarily “healthy” control and some patients may have some degree of neutrophilic inflammation	(Le Bourgeois <i>et al.</i> 2002)

Table 3-1 Control population used in studies reporting on BAL fluid.

One important advantage of BAL over induced sputum and cough swabs is that it can be performed on young paediatric CF patients; this is because it does not require any degree of cooperation between patient and clinician due to the anaesthesia (de Blic *et al.* 2000). This is an important advantage because it allows the identification of airway risk factors from an early age giving insight into the initial stages of lung inflammation (Sly *et al.* 2013). This is integral for developing therapeutics to prevent decline in lung function in CF patients from birth. I will now discuss other methods of airway fluid sampling in CF such as induced sputum and cough swabs.

3.1.1.b. Induced sputum

Older CF patients can often produce sputum spontaneously; however, with paediatric patients it can be difficult to get a patient to cooperate or understand instruction. Furthermore, disease severity is less advanced in paediatric CF patients and therefore, there is less mucus to expectorate (Forton 2015). In order to obtain airway samples from paediatric patients more consistently, sputum can also be induced. The induced sputum procedure involves inhaling nebulised saline (as with spontaneous sputum sampling) but in addition patients are given vigorous physiotherapy to help produce a sample. Physiotherapy is routinely given to CF patients to help free up obstruction and mucus in the airway; it involves percussion (tapping on the back), vibration and active breathing cycles to help produce sputum (Ronchetti *et al.* 2018).

In comparison to BAL, induced sputum is relatively inexpensive and easy to perform, it does not require sedation or invasive insertion of a bronchoscope. A disadvantage of sputum sampling is that, unlike BAL there is no guarantee or standardisation over where in the airway the sample originates. In BAL, the bronchoscope is directed to the same locations in the airway; however, in sputum the sample could be a pool of material from several locations (Forton 2015). The use of induced sputum to detect pathogens in the CF airway has been compared with BAL fluid; Jung *et al.* compared *P. aeruginosa* isolates in cough swabs, sputum and BAL fluid from 38 stable CF patients (Jung *et al.* 2002). The authors found that sputum was as effective as BAL fluid at detecting *P. aeruginosa* in the CF airway, but there was a greater diversity in strains detected in sputum than BAL fluid; this is further evidence that sputum is heterogenous. In a more comprehensive study comparing CF airway fluid sampling techniques, Ronchetti *et al.* report that 6-lobe BAL and 2-lobe BAL (ERS recommended) detects a greater bacterial diversity than sputum and cough swabs (Ronchetti *et al.* 2018). Despite this, the authors found that there were some pathogen isolates detected in sputum

that were not found in BAL fluid. In conclusion, Ronchetti *et al.* state that even though sputum was not as sensitive as BAL they recommend sputum sampling becomes common practice for frequent surveillance of pathogens in the lower airway. If a patient presents with chronic cough and wheezing, an indication of pulmonary exacerbation, then BAL is performed for more sensitive identification of pathogens (Ronchetti *et al.* 2018).

As well as pathogen surveillance, and with greater relevance to my own study, quantification of inflammatory markers such as NE activity and CXCL8 have been compared in sputum and BAL fluid from CF patient. It was shown by McElvaney *et al.* that although there are correlations between inflammatory markers and lung function in sputum and BAL fluid from the CF airway, these associations are stronger in BAL fluid (McElvaney *et al.* 2018). A reason for this is that the reducing agent dithiothreitol is routinely added to the sputum during processing of the samples to release cells from mucus to facilitate differential cell counts (McElvaney *et al.* 2018). It has been shown that dithiothreitol reduces sensitivity for the detection of IL-6, macrophage migration inhibitory factor and MPO in sputum compared to addition of BSA (Pignatti *et al.* 2002). Recently, McElvaney *et al.* have modified sputum collection, so that it no longer requires dithiothreitol and show that the new method improves detection of inflammatory markers in the CF airway to comparable levels as BAL fluid (McElvaney *et al.* 2018). The authors promote cell release from mucus plugs through washes with PBS and centrifugations rather than adding dithiothreitol; this relatively simple modification improved detection of NE activity and IL-1 β quantification to the same level as BAL fluid. In light of the Ronchetti *et al.* study comparing pathogen isolates in sputum and in BAL fluid, the detection of pathogens was not compared using the modified sputum processing (Ronchetti *et al.* 2018). This new method of processing sputum studied by McElvaney *et al.* is an important step forward that enables non-invasive sampling of the CF airway for assessing inflammation in the laboratory (McElvaney *et al.* 2018).

3.1.1.c. Cough swabs

Cough swabs are also used to identify pathogens in the CF airway. Swabbing can be performed on young paediatric patients that cannot expectorate sputum. The cough swab procedure involves placing a cotton-tipped swab into the posterior pharynx. It is critical that the swab does not touch the posterior pharynx as it will become contaminated by bacterial species on the surface and would therefore not represent the lower airways (Maiya *et al.* 2004). As for sputum and BAL fluid, pathogens isolated from cough swabs are identified using growth cultures, and more recently PCR and 16S RNA (Ronchetti *et al.* 2018).

An initial report comparing cough swabs and sputum in non-CF and CF patients with symptoms indicating airway infection found that for 92% of CF patients cough swabs led to the same choice of antibiotics as would have been made with sputum (Equi *et al.* 2001). Despite this, the authors raised the issue that cough swabs only had 34% sensitivity compared to sputum and therefore, there was a high chance of not detecting pathogens in symptomatic patients (false negatives). As discussed above, Ronchetti *et al.* compared the presence of CF pathogens in cough swabs, sputum and BAL fluid; their study supported data from Equi *et al.* showing that sputum detected more pathogen isolates than cough swabs (Equi *et al.* 2001; Ronchetti *et al.* 2018). None the less, as already mentioned, Ronchetti *et al.* found that BAL was the most sensitive procedure for identifying exacerbation-causing pathogens (Ronchetti *et al.* 2018).

Procedure	Advantages	Disadvantages
Bronchoalveolar lavage	<ul style="list-style-type: none"> - Samples specific sites - Best procedure for identifying pathogens - Can be performed on paediatric patients 	<ul style="list-style-type: none"> - Invasive - Requires sedation - Unethical to perform on healthy volunteers - expensive
Induced sputum	<ul style="list-style-type: none"> - Non-invasive - Inexpensive - Does not require specialist equipment - Good detection rates of pathogens - Can be performed frequently 	<ul style="list-style-type: none"> - Difficult to acquire samples from paediatric patients - No guarantee of origin of sample and therefore there is a risk of error (false negatives) - Addition of dithiothreitol may affect characterisation of airway fluid components
Cough swab	<ul style="list-style-type: none"> - Non-invasive - Inexpensive - Does not require specialist equipment - Can be performed frequently 	<ul style="list-style-type: none"> - Easily contaminated - Pathogen detection not as good as other sampling methods

Table 3-2: Advantages and disadvantages of the different techniques used to sample the CF airway

3.1.2. Using airway fluid to investigate neutrophilic inflammation in the CF airway

I have summarised the use of three sampling techniques that are commonly used for detection of pathogens in the lower airway of CF patients with symptoms of pulmonary exacerbation. Airway fluid sampling is critical for monitoring the lower airway for pathogens but can also provide valuable information about inflammation and other biological processes. Several inflammatory markers have been reported to be risk factors for pulmonary exacerbation; Sly *et al.* used BAL fluid, CT and, clinical scores to identify predictors of bronchiectasis (airway remodelling) in paediatric (3 months to 3 years) CF patients (Sly *et al.* 2013). The authors found that NE activity was highly predictive of airway disease. Others have also shown that the presence of neutrophils and NE activity correlates with loss of lung function (Konstan *et al.* 1994; McElvaney *et al.* 2018). A comprehensive longitudinal study of inflammatory biomarkers in CF sputum by Sagel *et al.* found that as well neutrophil count and NE activity, other factors were associated with decline in lung function; these were CXCL8, IL-6, IL-1 β and MMP-9 (Sagel *et al.* 2012).

It is important to establish markers of neutrophilic inflammation in the CF airway so that pathogenic factors can be investigated and targeted therapeutically. Furthermore, markers such as neutrophil count, NE activity and CXCL8 are also important for monitoring the effect of therapeutics on inflammation during trials and treatment courses (Ratjen *et al.* 2016; Barnaby *et al.* 2018; Sagel *et al.* 2018). For example, Lumacaftor is a CF therapeutic that facilitates CFTR transport to the apical membrane of airway epithelial cells (Elborn *et al.* 2016). Lumacaftor is administered to CF patients with a *cftr* phenotype that is characterised by CFTR mis-folding or reduced transport to the apical membrane of the epithelial cells, such as Δ F508Del (see table 1-1) (Elborn *et al.* 2016). Several trials have shown that Lumacaftor slows the decline in lung function and reduces rates of pulmonary exacerbations in CF patients; however, only more recently have groups investigated the effects on inflammatory markers (Barnaby *et al.* 2018). Lumacaftor has been trialled in combination with a similar therapeutic that facilitates CFTR function, ivacaftor, that is given to patients with CFTR mutations such as G551D (Wainwright *et al.* 2015). A significant finding by Barnaby *et al.* was that ivacaftor, when used in combination with lumacaftor, reduced phagocytosis of *P. aeruginosa* by monocyte-derived macrophages by reducing cytokine release. Therefore, the authors suggested that patients that are prescribed this drug combination might be more at risk of infection by *P. aeruginosa*. The study by Barnaby *et al.* highlights the importance of

measuring inflammation during drug trials in CF patients in order to better understand the effects on the immune system.

3.1.3. Investigating the role of complement in promoting neutrophilic inflammation in the CF airway

Establishing markers of neutrophilic inflammation in the CF airway is also important for investigating other mechanisms of neutrophil dysfunction and contributors to pathogenesis. The complement anaphylatoxins have been shown to contribute to airway diseases such as asthma and COPD (Marc *et al.* 2004; Khan *et al.* 2015), as discussed in sections 1.7 and 1.8. A mass-spectrometry proteomic analysis of CF BAL fluid showed that several complement components were less abundant in the airway CF patients (n=8) compared to non-CF controls (asthma, n=4), these include; C1q, C2, C4b, C5 and C6 (Gharib *et al.* 2009). Interestingly, computational analysis by Gharib *et al.* found that the comparative levels of these complement components were associated with proteases such as MMP8 and MMP9 as well as adhesion molecules. A similar analysis by Pattison *et al.* investigated the proteomic profile in sputum from CF patients (n=12) infected with *P. aeruginosa* (Pattison *et al.* 2017). Using two-dimensional liquid chromatography and mass-spectrometry, the authors found a relative decrease in complement component C3 compared to non-smoking healthy controls (n=12). The relationships between complement, particularly C3a and C5a, and pathways associated with neutrophilic inflammation were not reported on in the study by Pattison *et al.* as they were by Gharib *et al.* Despite this, leukocyte extravasion and Fc γ -mediated phagocytosis pathways (protein pathway configured set by Ingenuity Pathway Analysis) were significantly upregulated; these are both pathways that complement anaphylatoxins, such as C5a, have critical roles in promoting (Hunniger *et al.* 2015; Pattison *et al.* 2017). The above proteomic analyses give insight into the most significant pathways that are upregulated in the samples tested but they do not provide specific information on mechanism and therefore, the extent to which C3a and C5a contribute to CF disease pathology is not fully understood.

Elevated levels of C3a and C5a have been reported in the CF airway (Fick *et al.* 1986; Sass *et al.* 2015; Hair *et al.* 2017). Together with the mass spectrometry studies above (that show decreased C3 and C5), increased C3a and C5a suggest that there is increased complement activation in the CF airway. It has been shown that C5a correlates negatively with lung function (FEV1) (Fick *et al.* 1986; Sass *et al.* 2015; Hair *et al.* 2017). Furthermore, Hair *et al.* have reported that C5a levels in CF sputum spike during pulmonary exacerbation; however, is not clear whether elevated C5a is a consequence or cause of exacerbation (Hair *et al.* 2017). As

well as association with clinical makers, the importance of C5a in promoting neutrophilic inflammation has been investigated in relation to other chemotactic molecules (Mackerness *et al.* 2008).

For my project, I am interested in the mechanisms by which C5a (and C3a) contribute to pathogenesis in CF. In particular, I am interested in the non-canonical generation of C5a and C3a in the CF airway by NSPs. In addition, I am also interested in how interaction with the local lung environment modifies C5a function. As part of this study, I have processed BAL fluid from a cohort of CF patients and used it to both characterise C3a and C5a as mechanisms of neutrophil inflammation in the CF airway, in addition to exploring mechanisms of C3a and C5a generation. In this first chapter, I will characterise neutrophilic inflammation in CF BAL fluid and explore the relationships between inflammation and complement components, particularly the complement anaphylatoxins C3a and C5a. This is primarily to assess whether there is any evidence in the CF cohort to suggest that C3a and C5a contribute to chronic neutrophilic inflammation in the CF airway (table 3-3).

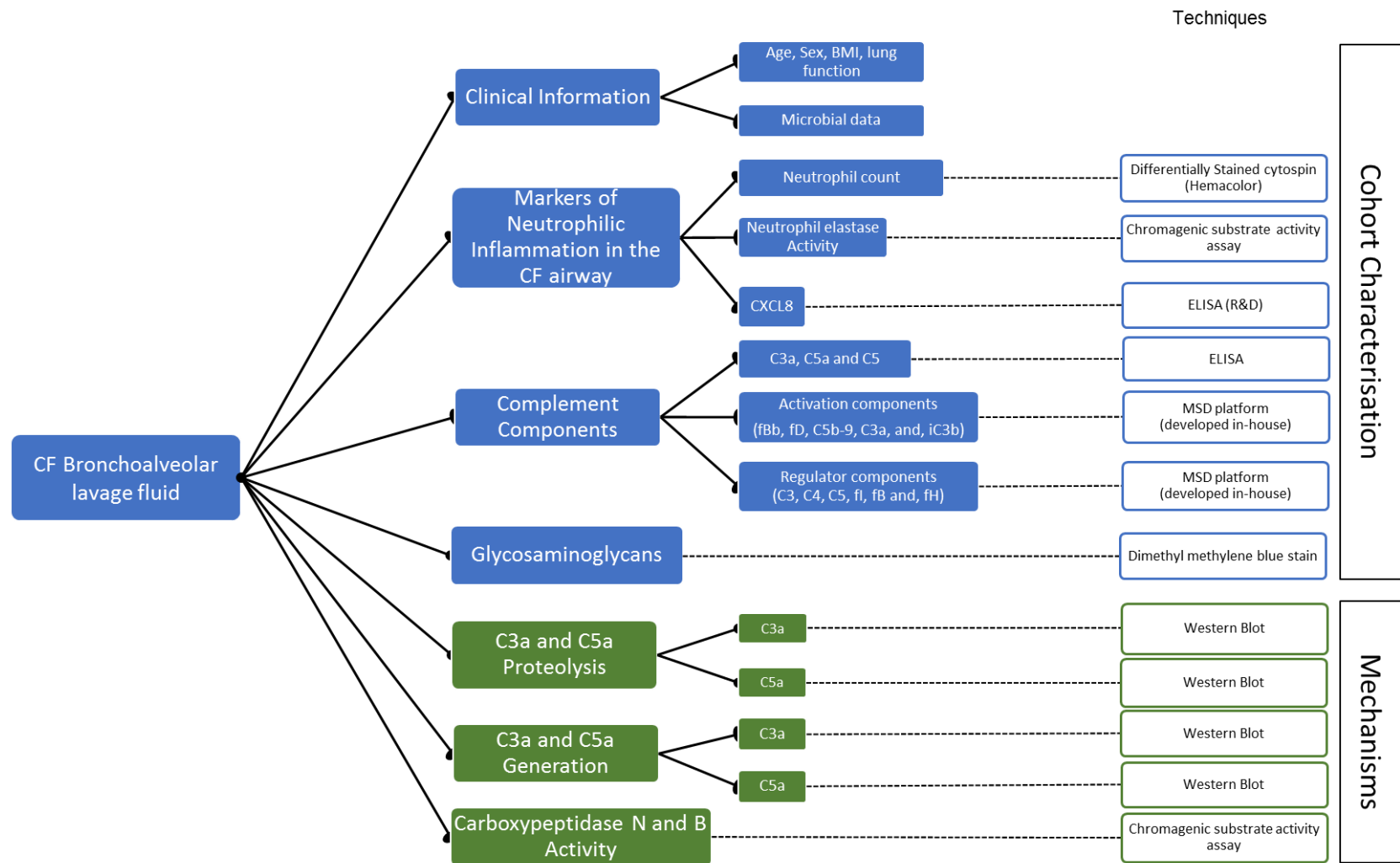


Table 3-3: Uses of CF BAL fluid in this study. CF BAL fluid was used to characterise (blue) neutrophilic inflammation, complement components and soluble GAG concentration. CF BAL fluid was also used to study mechanisms (green) in which the local lung environment modifies the activity of C3a and C5a. Techniques performed are linked by dashed lines to each corresponding component.

3.2. Hypothesis

I hypothesise that complement C3a and C5a correlate with markers of neutrophilic inflammation in CF BAL fluid and clinical markers of disease progression.

3.3. Aims

The aim of this section is to investigate the relationships between complement and neutrophilic inflammation in the CF airway, with particular focus on the complement anaphylatoxins, C3a and C5a.

1. Assess the clinical characteristics of the CF cohort, including lung function, BMI and age.
2. Measure well-established markers of neutrophilic inflammation in CF such as neutrophil count, NE activity and CXCL8 concentration in BAL fluid from the CF cohort.
3. Investigate the role of complement in promoting neutrophilic inflammation by measuring complement components in CF BAL fluid using multiplex and singleplex ELISA-style platforms. Perform correlation analyses between complement components and markers of neutrophilic inflammation in the CF airway.
4. Further characterise the role of C3a and C5a in driving neutrophilic inflammation in the CF airway by performing correlation analyses against markers of neutrophilic inflammation and clinical makers of disease progression (lung function and BMI)

3.4. Airway sampling and correcting for repeated measures

As part of a separate study, Dr. Julian Forton performed BAL on CF patients attending the Children's Hospital for Wales (Cardiff, UK). The procedure was carried out on patients that were admitted for chest exacerbation, attending an annual review or those under general anaesthetic for routine surgery. BAL fluid from the right middle lobe (figure 3-1) was sampled with a total of 41 sampling events; however, from 32 individual CF patients over the study period. Therefore, for seven patients repeated measures were taken; five patients had two recorded events and two patients had three recorded events. As discussed in the background to the study, there are a number of reasons for performing BAL on a CF patient and therefore, repeated measures could have been recorded for a number of reasons. I did not categorise patients into "reasons for lavage" because this will reduce population size and consequently lower power of statistical analyses. The issue that arises from using repeated measures is that data from the same patients are not independent and therefore, could skew the population data set. Therefore, I assessed whether data from repeated measures could be included as part of my population. The effect of repeated measures was investigated by testing two variables; NE activity and CXCL8 concentration, these are well-established markers of neutrophil inflammation in the CF airway (McElvaney *et al.* 2018). The overall aim of this analysis was to determine whether the data required standardisation as a consequence of the repeated measures (figure 3-2).

Initially I reviewed the time interval between recorded events for each patient that had repeated measures taken (figure 3-2A). This was to assess whether events were measured within quick succession; a factor that might reduce variation between events and therefore skew the data. For example, if the time interval is short between recording events, it could indicate that airway surveillance is being performed to monitor worsening condition and therefore, inflammatory markers could be elevated in these samples. The mean time between sampling from the same patients was 1.69 years, the greatest time between samples was 3.39 years and the least time between samples was 0.12 years. Considering that all but one of the time intervals between sampling were greater than one year, I did not have any evidence to suggest that time interval between repeated measures had any influence on these data.

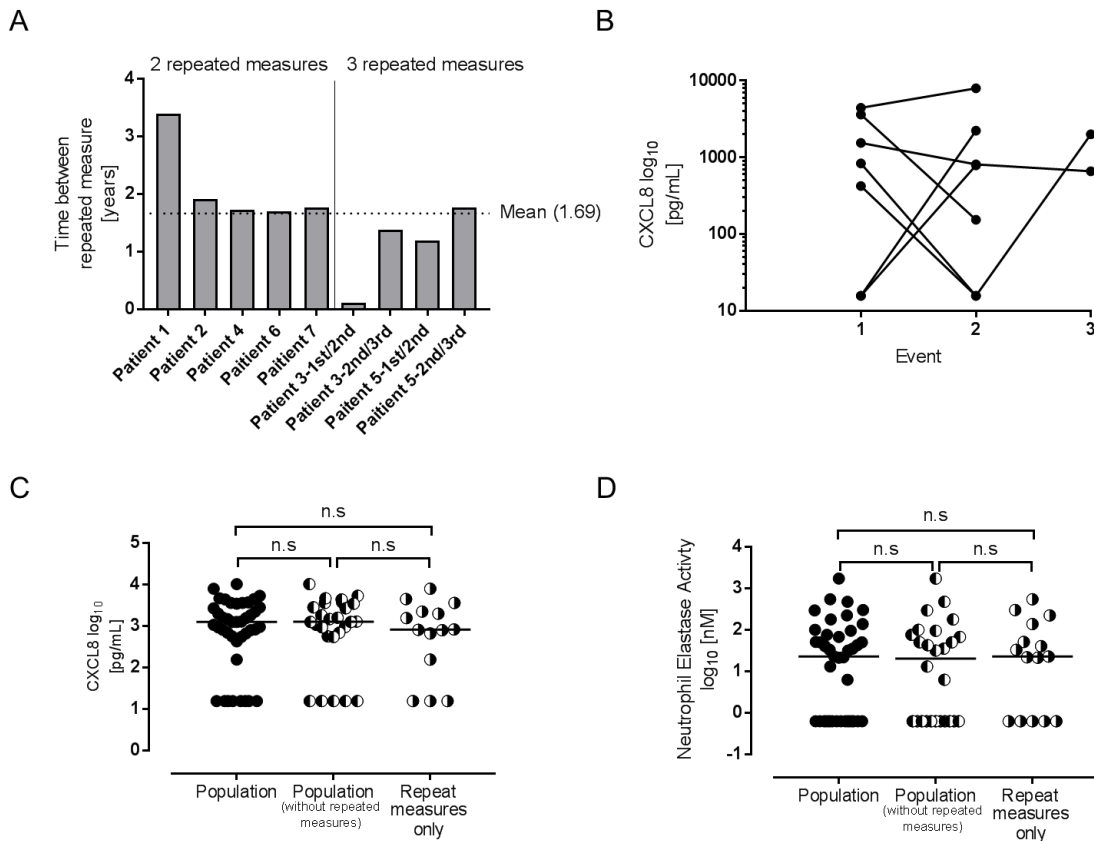


Figure 3-2: Effect of repeated measures on sample population levels of CXCL8. **A)** Interval between repeated measures for each patient where two or three events were recorded. Dotted line represents the mean interval between repeated measures. **B)** CXCL8 concentration in BAL fluid for each patient between sampling. **C)** CXCL8 concentration and **D)** NE activity in BAL fluid from all events (n=41, black circles) or without repeated measures (n=26, half-filled circles (filled left), or repeated measures only (n=15, half-filled circles (filled right) medians are plotted for each (solid black line). Comparison of medians by Non-parametric t-tests (Mann-Whitney).

To further support the inclusion of repeated measures in the cohort data set, CXCL8 concentration recorded in each event for each patient (with repeated measures) was plotted (figure 3-2B). The mean change in CXCL8 between recording events for each patient (regardless of increase or decrease) was 1566 pg/mL CXCL8. This demonstrates that there is variation between repeated measures and therefore, provides more evidence to support that each event is independent of the one before it.

Finally, the mean CXCL8 concentration or median NE activity was compared between a population including all data, a population without any patients with repeated measures or the repeated measures only (figure 3-2C and 3-2D). There were no statistical differences between the medians in these populations for either variable when compared by one-way ANOVA (Kruskal-Wallis). From these analyses I determined that there was no conclusive evidence to suggest that I could not include these data as separate events in my population. Therefore, any further analysis will describe a population of 41 events, unless stated otherwise.

3.5. Clinical description of the CF cohort

To begin characterising the CF cohort I have collated clinical data about the patients, table 3-4 is a clinical description of the population in this study. Importantly, this population is young; it has a median age of 8.3 years enabling me to investigate early stages of neutrophilic inflammation in the CF airway. The proportion of this population that has at least one $\Delta F508Del$ allele is 90.2% which, is similar to the UK average 90.9% (UK CF registry 2016). Three of the four patients that did not possess at least one $\Delta F508Del$ (class II) mutation had at least one R709X (class I) allele: class I and II mutations have severe disease phenotypes (see table 1-1 for description of classes, R709X not listed due to low prevalence in UK population) (Elborn 2016). BMI is used as a measure of malnutrition, a symptom of poor nutrient uptake due to reduced pancreatic secretion and bile duct blockade. The median body mass index was 17.7 Kg/m², this is below the “normal” classification (18.5 to 25 Kg/m²) moreover, 70% (26/37 patients with recorded BMI) had a BMI that was sub-normal.

Number of events (patients)		41 (33)
Repeated measures		26 patients with 1 measure 5 patients with 2 measures 2 patients with 3 measures
Gender % Male / Female		53.7 / 46.7
Median Age, (range)		8.3 (1.0 – 17.7) decimal years
Cftr genotype $\Delta F508Del$	% homozygous	43.9
	% heterozygous	46.3
	% non - $\Delta F508Del$	9.8
Median Body Mass Index (range) n=37		17.7 (10.6 – 21.4) Kg/cm ²
Median FEV₁ (range) % predicted n=29		80 (41 – 110.0)
Median FEC (range) % predicted n=29		83.5 (52 – 121.0)
Percentage <i>P. aeruginosa</i> colonisation within the last 3 years		46.2

Table 3-4: Clinical description of the CF cohort

FEV₁ and FVC are measures of lung function and capacity respectively, these require co-operation with the clinician and therefore are difficult to perform on paediatric patients (below 5 years old). In my cohort FEV₁ and FVC were recorded for 29 out of 41 events, 12 of the events that did not have these variables recorded were because the patient was five years old

or younger. The percent predicted FEV₁ for the population had a range of 40 – 110%, demonstrating that my population represents a spectrum of well and unwell patients.

Neutrophilic inflammation is a pathogenic factor for reducing lung function in the CF airway, therefore correlation analyses were performed between age, lung function (FEV₁) and BAL fluid neutrophil count (figure 3-3).

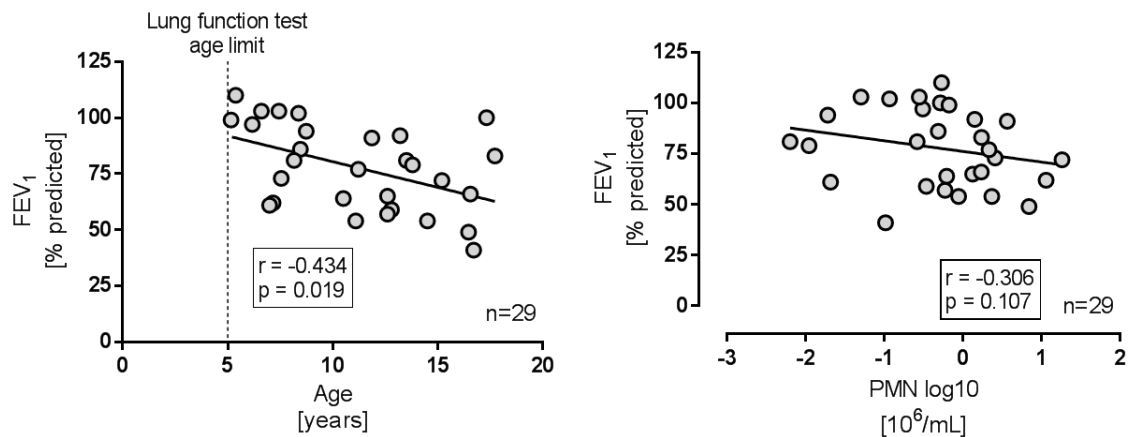


Figure 3-3: Analysis of clinical parameters and neutrophilic inflammation in the CF cohort.

A) Percentage predicted FEV₁ (y-axis) was correlated with Age (x-axis), a linear regression was fitted (solid line) and Spearman rank statistical outcomes (r and p values) in black box. Vertical dashed lines marks where FEV₁ data is unlikely to be obtained due to the age of the patient. **B)** Percentage predicted FEV₁ (y-axis) was correlated with polymorphonuclear leukocyte (PMN) count in BAL fluid from CF cohort (PMN, x-axis). A linear regression was fitted (solid line) and Spearman rank statistical outcomes (r and p values) in black box.

These data support a consensus on CF pathology in that as a patient ages there is a decline in lung function (figure 3-3A) (UK CF registry 2016). A negative trend was observed between neutrophil counts, from differential stains of cytopspins and lung function however, this trend was not statistically significant (figure 3-3B). These analyses were performed to investigate the associations between neutrophilic inflammation and the collateral loss of lung function in the CF cohort; however, Spearman rank correlation analyses do not prove a causal relationship.

Clinical data, as well as variables in BAL fluid such as neutrophil count, show that the CF cohort in this study reflects general trends that have been observed in the UK CF population (UK CF registry 2016). Therefore, data from my cohort is a suitable platform for analysis of neutrophil inflammation and the role of complement anaphylatoxins in promoting pathogenesis.

3.6. Characterising neutrophilic inflammation in CF BAL fluid

CF is characterised by neutrophilic inflammation of the airway. To investigate inflammation, neutrophil count, NE activity and CXCL8 are routinely used by researchers as markers of neutrophilic inflammation (McElvaney *et al.* 2018). Furthermore, they are also used in clinical trials to assess changes in neutrophilic inflammation in response to therapy (Dittrich *et al.* 2018). To investigate neutrophilic inflammation in the CF cohort, I performed correlations between the above variables.

Neutrophil counts were performed on differentially stained cytopspins produced using CF BAL fluid. NE activity in CF BAL fluid was measured using a chromogenic substrate that is specific to NE, quantifying against a standard curve of NE purified from primary human neutrophils. CXCL8 was measured by commercial ELISA.

It has been reported that CXCL8 and IgGs can be degraded by serine proteases present in CF airway fluid (Prince *et al.* 1979; Leavell *et al.* 1997); therefore, I investigated whether the addition of a serine protease inhibitor (AEBSF) improved quantification of CXCL8. To each sample (n=13), I added either 10 mM AEBSF in assay diluent (1% BSA) or the equivalent volume of diluent without the inhibitors, the ELISA was performed as recommended by the manufacturer.

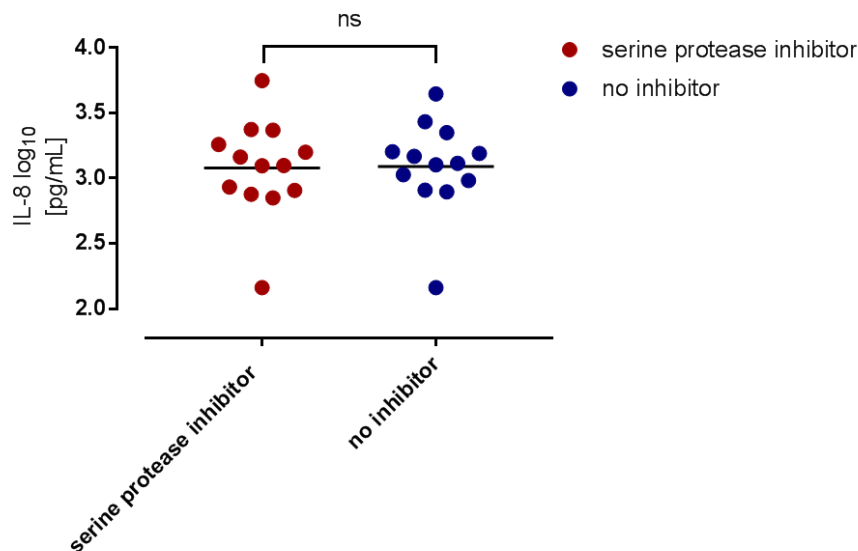


Figure 3-4: Influence of a serine protease inhibitor on CXCL8 levels measured by ELISA.

CF BAL fluid samples were diluted 1 in 10 in 1% BSA (protease free)(blue) or serine protease inhibitor (AEBSF (10mM)) in 1% BSA (red) and incubated for 15 minutes at room temperature, CXCL8 ELISA was performed as instructed by the manufacturer. Values were interpolated from a standard curve of purified CXCL8 (without inhibitor) and multiplied by the dilution factor (10). Median CXCL8 (y-axis) for both conditions was compared by Wilcoxon matched pairs t-test ($p = 0.519$)

There was no statistical difference in the median CXCL8 concentration when CF BAL fluid was incubated with or without a serine protease inhibitor (figure 3-4). I concluded from this experiment that even though it is reported that CXCL8 and IgG are susceptible to proteolysis by NSPs, this phenomenon is not significant enough to influence quantification of CXCL8 by ELISA (Prince *et al.* 1979; Leavell *et al.* 1997). I continued to compare markers of neutrophilic inflammation in the CF airway (figure 3-5).

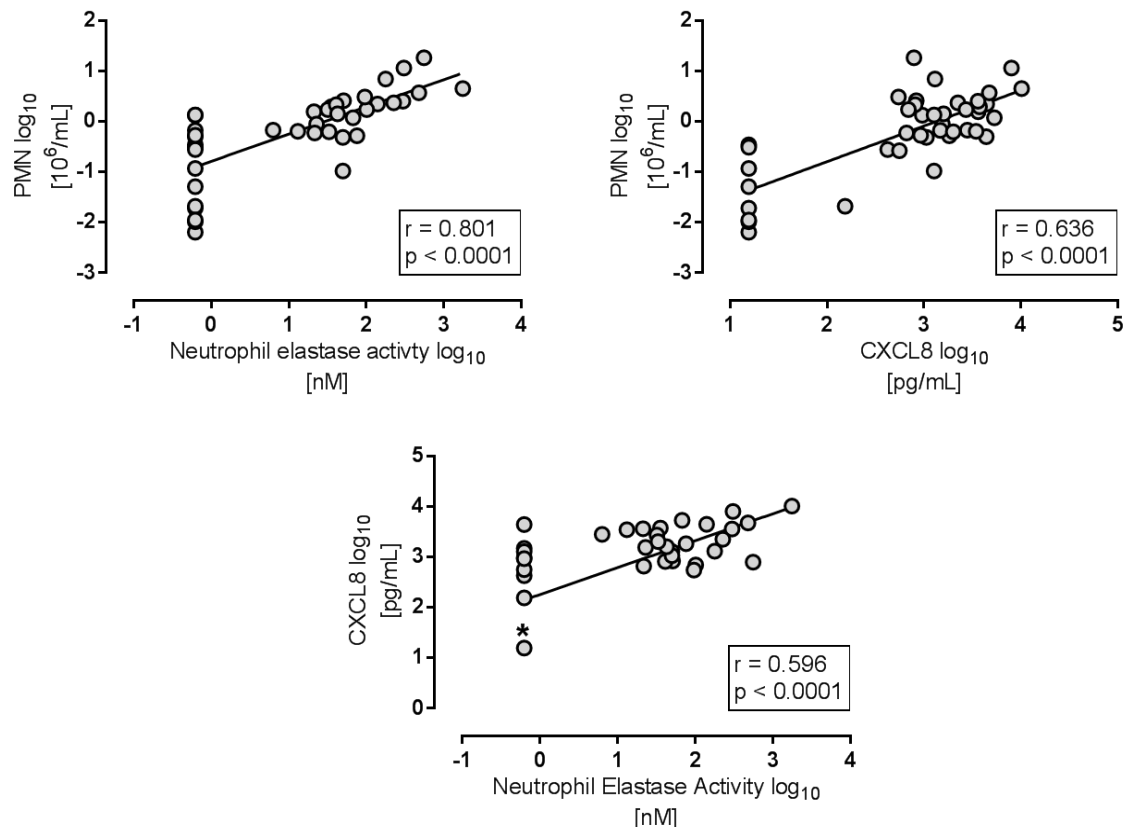


Figure 3-5: Correlations between markers of neutrophilic inflammation measured in CF BAL fluid. Variables were analysed using Spearman rank correlation analysis, statistical outcomes (r and p values) for each test are in boxes on the respective plots. Correlations were performed between **A**) Neutrophil count and neutrophil elastase activity, **B**) neutrophil count and CXCL8, and **C**) between neutrophil elastase activity and CXCL8. In “C” the asterisk highlights six overlapping data points where data were assigned a value halfway between zero and the limit of detection for both parameters (see methods). N=41.

Neutrophil count had a statistically significant, positive correlation with NE activity and supports neutrophils as a major source of NE in the CF airway (figure 3-5A)(Hartl *et al.* 2012). NE activity is quantified in CF airway fluid rather than NE concentration, this is because NE activity is a better indicator of potential airway remodeling (Sagel *et al.* 2012).

Neutrophil count also positively correlated with CXCL8 concentration, a well-characterised neutrophil chemoattractant that is found elevated in the CF airway (Dean *et al.* 1993) (figure 3-5B). Finally, NE activity positively correlated with CXCL8 (figure 3-5C). The statistical outcomes from these three plots support the use of neutrophil count, NE activity and CXCL8 to measure neutrophilic inflammation in the CF airway.

So far, I have shown that the CF cohort used in this study reflects the clinical nature of CF by demonstrating that lung function is negatively correlated with neutrophil count (Sagel *et al.* 2012). I have also demonstrated that markers of neutrophilic inflammation in the CF airway strongly correlate with each other. From these data I can be confident that observations made from my study also reflect what is happening in the CF population as a whole, and not just an isolated cohort. I continued to investigate the relationship between neutrophilic inflammation and complement in CF BAL fluid.

3.7. Complement in the CF airway

The role of complement in promoting pathogenesis in the CF airway is not clear. Proteomic analysis by Gharib *et al.* has previously identified that several complement components (C1q, C2, C4b, C5, C6, C2) are significantly reduced in CF BAL fluid compared to non-CF controls (Gharib *et al.* 2009). Two multiplex platforms were developed by our group. These platforms used a combination of commercial and in-house antibodies. The MSD platforms were optimised for measuring complement components in serum but were sensitive enough to quantify analytes in other tissues as well as BAL fluid. Complement components were separated onto two plates: one that measured factor Bb, factor D, C5b-9 complex, C3a, C5a and iC3b and the other plate measured C3, C4, C5, factor I, factor B and factor H.

A technical problem with the standards meant that C5 and C5a could not be measured using the MSD platform; therefore, C5a and C5 were measured using single-plex ELISAs. This problem did not affect quantification of the other components. C3a was detectable by the MSD platform; however, I also quantified C3a by ELISA. C3a and C5a were measured by separate commercial ELISAs (Quidel), this manufacturer was carefully selected as some commercial C5a ELISAs reported cross-reactivity to C5. In serum, the molar concentration of C5 is between 200-1000-fold that of C5a therefore, any cross-reactivity with C5 in an ELISA would skew C5a quantification (Barnum and Schein 2018).

3.7.1. Developing an in-house ELISA for the detection of C5

Commercial C5 ELISAs are available; however, the group I was working with specialised in developing antibodies for measuring complement components. Therefore, an in-house C5 ELISA was developed for sensitive quantification of C5. Three monoclonal anti-C5 antibodies were compared to assess which ELISA pairing combination was most sensitive for quantification of C5. The three antibodies were: An in-house mouse monoclonal anti-C5 antibody (2D5), a commercial monoclonal mouse anti-C5/C5a antibody (Hycult-577) and a commercial humanized antibody from Roche that is not available on the market (SKY59). Antibody pairings compared the use of different antibodies for capture and detection. Not all pairings were tested because the appropriate HRP-conjugated tertiary antibodies were not available. Appropriate HRP-conjugated tertiary antibodies were commercially available but were not required because preliminary experiments showed that the pairings used were suitable for C5 quantification (see below). The monoclonal antibodies and HRPO-conjugated antibodies pairings were compared using a dilution series of C5 ranging from 250 to 1000 ng/mL (figure 3-6).

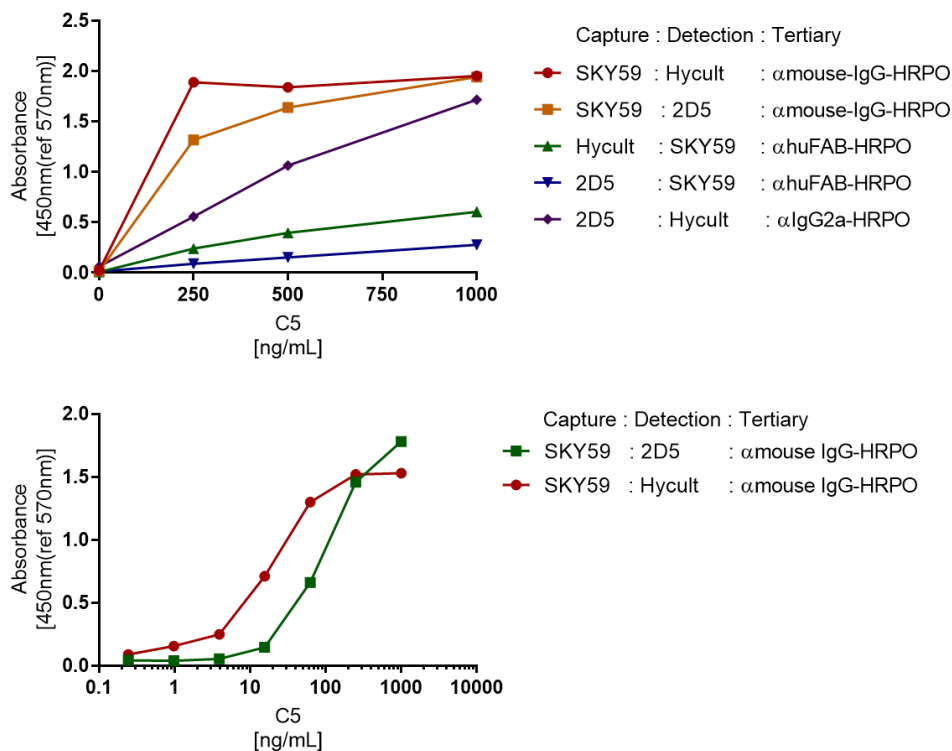


Figure 3-6: Developing a sensitive ELISA for the quantification of C5 in CF BAL fluid.

Comparison of three mouse anti-C5 antibodies, using each in different combinations as either capture or detection. Antibodies were compared using a titration of C5 from 1000 to 250 ng/mL (x-axis) in 1% BSA/PBS. Different tertiary antibodies were required for quantification, these were either: goat anti-mouse IgG HRPO, goat anti-mouse IgG2a HRPO or donkey anti-human FAB fragment HRPO. **B)** Sensitivity of SKY59:Hycult (red) (capture: detection) and SKY59:2D5 (green) pairings using a titration of C5 from 0.24 to 1000 ng/mL (x-axis). n=1.

Each of the antibody combinations used produced an absorbance curve for the concentrations of C5 tested (figure 3-6A). The best sensitivity for the detection of C5 was obtained using SKY59 as the capture antibody, therefore further comparisons were made between C5 ELISA antibody combinations using SKY59 as a capture antibody and either 2D5 or the Hycult antibody for detection. It has previously been shown that C5 is almost depleted in CF BAL fluid compared to asthmatic controls (Gharib *et al.* 2009). For this reason, I assessed the limit of detection for SKY59:2D5 and SKY59:Hycult ELISA pairings. Sensitivity was compared for the above two pairings by titrating C5 from 1000 ng/mL to 0.24 ng/mL in a 4-fold dilution series (figure 3-6B).

The SKY59:Hycult pairing was more sensitive at measuring low concentrations of C5 than the SKY59:2D5 pairing. For instance, there was a discernable difference in signal at 0.98 ng/mL C5 between the two antibody pairings with SKY59:hycult having a higher absorbance value, this was not tested statistically because it was an optimisation experiment. In the same experiment, cross-reactivity with C5a, C3a and C3 was assessed, none of the above components had any detectable signal when tested at equimolar concentrations to 1000 ng/mL C5 (5.26 nM) (not shown). Despite only performing a single experiment, from these data I decided that the SKY59:Hycult C5 ELISA pairing would be most suitable for measuring C5 concentrations in CF BAL fluid. The use of the different pairing to those I tested (SKY59:polyclonal anti-C5) has recently been reported by our lab (Zepek *et al.* 2018). Having optimised and developed a sensitive ELISA for the detection of C5, I went on to measure C5 and the other complement components (that I had platforms for) in CF BAL fluid.

3.7.2. Correlating complement with markers of neutrophilic inflammation

Complement components were quantified in CF BAL fluid. Values for these components were correlated against neutrophil counts, NE activity and CXCL8 using Spearman rank analyses and the outcomes combined in a matrix (figure 3-7). This was to give an overview of the relationship between complement and neutrophilic inflammation of the CF airway. Not all CF BAL fluid samples measured on the MSD platform were used in the analysis due to variation within the duplicates. This was because of technical error handling small sample volumes and sensitivity of the plates to user error. Due to availability of the plates these samples could not be re-tested. This meant that for Bb, factor D, C5b-9 complex, C3a (MSD), C5a (MSD) and iC3b the sample size was reduced to 28 from a total of 41. As mentioned above, C5a and C3a were also quantified by commercial ELISA and therefore these analytes were not affected. Analytes measured on the second complement component plate (C3, C4, C5, factor

I, factor B and factor H) were not affected and therefore sample number on this plate was n=41.

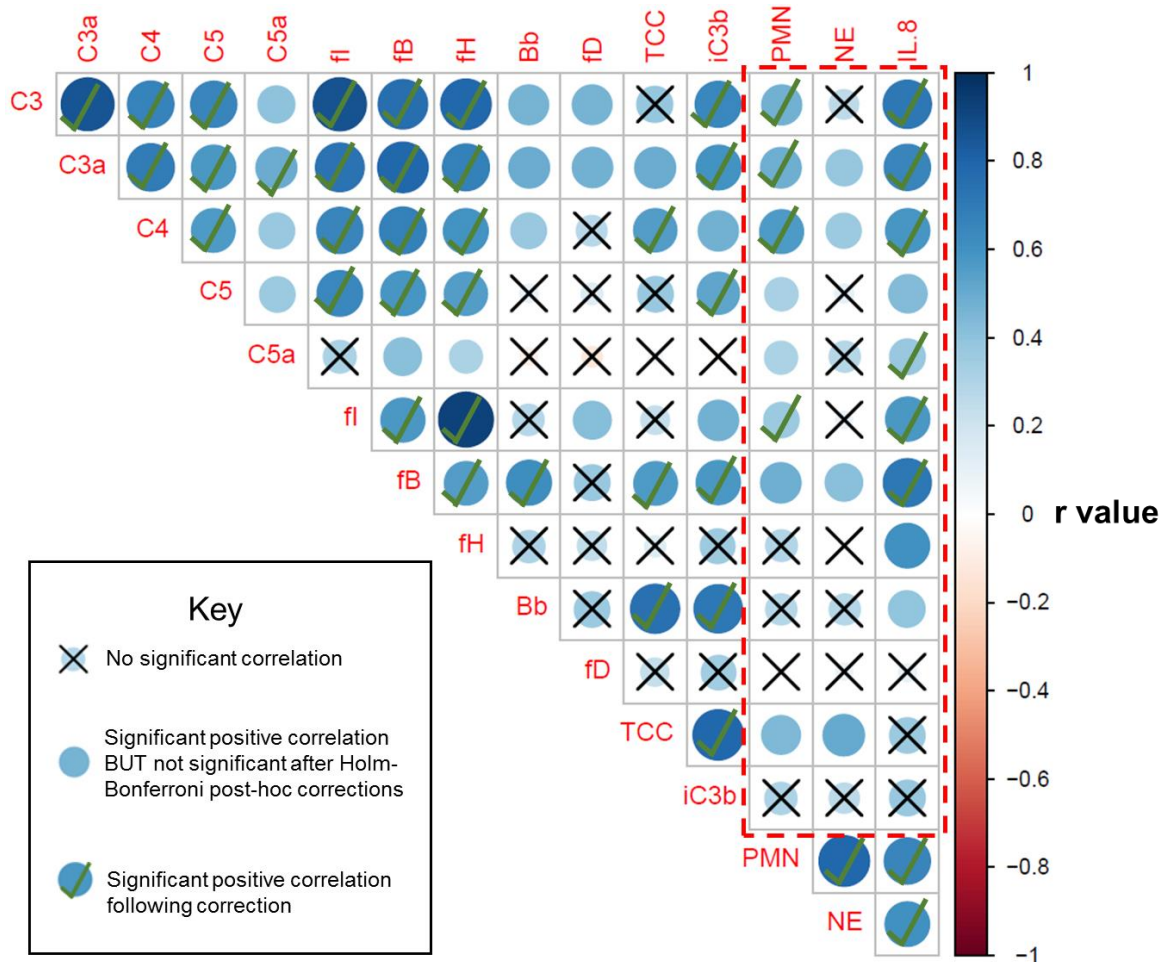


Figure 3-7: Correlations between markers of neutrophilic inflammation and complement component measured in CF BAL fluid. C3a, C5a and C5 were quantified by individual ELISAs; all other complement components were measured by MSD platforms. C5b-9 “TCC”. CXCL8 “IL.8”, neutrophil elastase activity, and neutrophil count used the data from figure 3-5. All variables were analysed using Spearman rank correlations, the strength of the correlations (r values) are signified by circle shade (using the scale to the right of the chart) and circle size. For example, a strong positive correlation will have a large deep blue circle. Analyses that were not statistically significant were labelled with a black cross. Red dashed box indicates correlations between complement and markers of neutrophilic inflammation. Post-hoc Holm-Bonferroni analysis for multiple comparisons (Holm 1979) was performed on ranked p-values, correlations that remained statistically significant after corrections for multiple comparisons are annotated with a green tick (see key).

Spearman rank correlation analysis was performed to test the relationships between the 14 analytes tested. Further post-hoc analysis was performed by Holm-Bonferroni test for multiple comparisons (Holm 1979). Holm-Bonferroni analysis is less conservative than traditional Bonferroni post-hoc analysis. This is because for significance at $p = 0.05$, the Bonferroni test for multiple comparison requires the p values of each corresponding correlation to be less than 0.05 (significance level) divided by the number of comparisons made (105). In the case of my analysis this would mean that there would be statistical significance at $p < 0.05 / 105 = 0.00047$. The Holm-Bonferroni test is similar; however, the correlations are ranked by their p values from lowest to highest. Therefore, the most significant p value (lowest) would be ranked 1 and least significant p value (highest) would be 105. Each respective correlation is significant if the p value for that test is less than 0.05 (significance level) divided by number of tests (105) minus the rank of the p value (1 to 105). This means that correlations with less statistically significant p values are less likely to be discarded. In comparison, without correcting for multiple comparisons there were 68/105 statistically significant correlations at $p=0.05$. Correcting using the Bonferroni method there would have been 8/105 significant correlation; however, with the method I performed (Holm-Bonferroni), there were 36/105 significant correlations. Therefore, I have corrected using a less conservative method that reduces the number of false-negatives.

My first observation was that analytes from the complement component plate measuring Bb, factor D, C5b-9 complex, and iC3b, had more non-significant outcomes than the other analytes. This could reflect lower sample sizes, a consequence of technical error. Before correction for multiple comparisons, there are a striking number of statistically significant positive relationships between complement components and three markers of neutrophilic inflammation (neutrophil count, NE activity and CXCL8 concentration). After correction for multiple comparisons Holm-Bonferroni, the strongest correlations were between the three markers of neutrophilic inflammation. There were also positive relationships between C3, C3a, C4 and, factor I with either neutrophil count and CXCL8. A significant positive correlation was also observed between C5a and CXCL8.

3.7.3. Assessing the relative levels of complement in CF BAL fluid

As well as investigating the relationship between complement and neutrophilic inflammation, I also compared complement in BAL fluid from the CF airway to the levels that have been reported in the plasma from healthy normal control (Barnum and Schein 2018). As mentioned

above, Gharib *et al.* have reported that the relative levels of several complement components are reduced in the CF airway compared to healthy controls (Gharib *et al.* 2009). Despite proteomic analysis of BAL fluid, comprehensive quantification of complement in CF or normal BAL fluid has not previously been performed. In my study, I did not have a healthy control population and therefore, I cannot make the same comparisons as Gharib *et al.* As a method of investigating the levels of complement components in BAL fluid from CF airway without a control population, I standardised the mean of each component in CF BAL fluid against C3, a component that is abundant in plasma and central to complement activity. For comparison with normal plasma, I performed the same standardisation on the mean concentrations of complement components in plasma from healthy donors that have been reported in the “Complement facts book”, a collaborative review of complement dogma that includes reported concentrations in normal plasma (Barnum and Schein 2018). The values for the complement components from BAL fluid or plasmaplasm were divided by the respective C3 measured in those samples.

	Mean [ng/ml]		C3 to component ratio	
	CF BAL fluid	Normal plasma	CF BAL fluid	Normal plasma
C3	60387	1250000		
C3a	1.7	50	36160	25000
C4	762	600000	79	2
C5	27	75000	2212	17
C5a	0.06	10	1041155	125000
C5b-9	20.0	100	3025	12500
iC3b	189.2	N/A	319	N/A
fI	11.2	35000	5392	35.7
fD	86.6	2000	697	625
fB	227	200000	266	6.3
Bb	30.4	400	1988	3125
fH	114	192500	530	6.5

Table 3-5: Comparing complement levels in CF BAL fluid with plasma from normal plasma.

The mean complement concentrations from CF BAL fluid were calculated from measurements made by MSD platforms and ELISAs. The mean concentrations of components in plasma were collated from the Complement Facts Book (Barnum and Schein 2018). Complement components were standardised against mean C3 concentration for CF BAL fluid (grey) and plasma (white) respectively.

In table 3-5 I have collated the mean complement components measured in CF BAL fluid and the mean of those that have been reported in normal plasma (Barnum and Schein 2018). Before I assessed complement to C3 ratios, I made a visual comparison of complement

component concentrations between CF BAL fluid and normal plasma. The concentration of complement components in CF BAL fluid is less than what has been reported in normal plasma (Barnum and Schein 2018). The main source of complement components in plasma is the liver however, cells from various tissues have been also shown to produce complement components locally (Li *et al.* 2007). Furthermore, local generation of complement may be an important source of complement in the airway (Hetland *et al.* 1986). Although complement component levels in CF BAL fluid are lower than in normal plasma this does not necessarily mean that complement is not functioning and therefore, a pathogenic factor in the CF airway. In addition to comparing the levels, complement components were also standardised with C3 as a method of comparing the relative levels of complement between the CF airway and plasma.

As mentioned above, I standardised the complement component concentrations by calculating the C3 to complement component ratio. Then, I used normal plasma as a reference of functional complement to investigate whether there was any evidence that complement is dysfunctional in the CF airway. Interestingly, the C3 to other component ratios between components such as Factor Bb, Factor D and C3a are not too dissimilar when comparing normal plasma and CF BAL fluid; however, other components generally had a higher C3 to complement component ratio in CF BAL fluid than compared to normal plasma (table 3-5). This could either imply that complement components in CF BALF fluid are less abundant in relation to C3 than those in normal plasma or C3 is elevated in the CF airway compared to other components. With particular interest to this project, the C3 to C5 ratio in CF BAL fluid was over 100-fold of that in normal plasma. C5 is essential for activation of the terminal complement cascade and in turn important for the elimination of pathogens. Unlike the majority of the other components, the terminal complement complex (C5b-9) had a lower ratio to C3 in BAL fluid than in normal plasma. This means that there is more C5b-9 in CF BAL fluid compared to normal plasma, relative to C3, and therefore, suggests that there is more terminal complement activation. Furthermore, markers of complement activation, such as C3a and C5a, did not correspond with each other when comparing the ratio with C3 between CF BAL fluid and normal plasma. Specifically, there is a 10-fold reduction in the ratio of C3 to C5a in the CF BAL fluid compared to normal plasma but, there was a 1.5-fold increase in the C3 to C3a ratio.

The above analysis has been performed with the assumption that plasma concentrations are correct. In summary, there appears to be more terminal complement activation in the CF airway than normal plasma, reflecting that complement is more active. In addition, C5 is very low, almost depleted, suggesting that it is being consumed. This hypothesis is supported by

the increase in terminal complement pathway activation (C5b-9). C5a is also very low, particularly when comparing the C3 to C5a and C3 to C3a ratios.

From my analysis of complement in CF BAL fluid, I have found that concentrations of several complement components measured positively correlate with markers of neutrophilic inflammation. Furthermore, in comparison, levels of complement components in CF BAL fluid are lower than normal plasma and, when standardised against C3, there are clear differences in the relative abundance of some components, particularly C5. These data are descriptive and have not been statistically analysed. This because data was compared to the literature and not to data from my own study or measured by the same platforms. Therefore, any conclusions from these data are speculative. Nevertheless, it does indicate that there are perturbations in complement and relative levels in the CF airway.

The main aim of this chapter was to use CF BAL fluid to investigate whether C3a and C5a contribute to CF pathogenesis by driving neutrophilic inflammation. In the next sections I will analyse the relationships between the complement anaphylatoxins, C3a and C5a, and neutrophilic inflammation individually.

3.8. Correlating C3a with markers of neutrophilic inflammation in the CF airway

The analysis in figure 3-7 indicated that C3a positively correlated with markers of neutrophilic inflammation in CF BAL fluid. C3a is elevated in CF sputum (Sass *et al.* 2015). Furthermore, it has been shown by Sass *et al.* that C3a concentration in CF sputum positively correlated with lung function. This led the authors to suggest that there is a protective role for C3a in the CF airway (Sass *et al.* 2015). Furthermore the same group later reported that C3a in CF sputum positively correlated with markers of neutrophilic inflammation in the CF airway such as NE activity, MPO and DNA (Hair *et al.* 2017). To further examine the relationship between C3a and CF pathology, Spearman rank correlation analyses were performed between C3a and either lung function (FEV₁), age, neutrophil count, or CXCL8 concentration (figure 3-8).

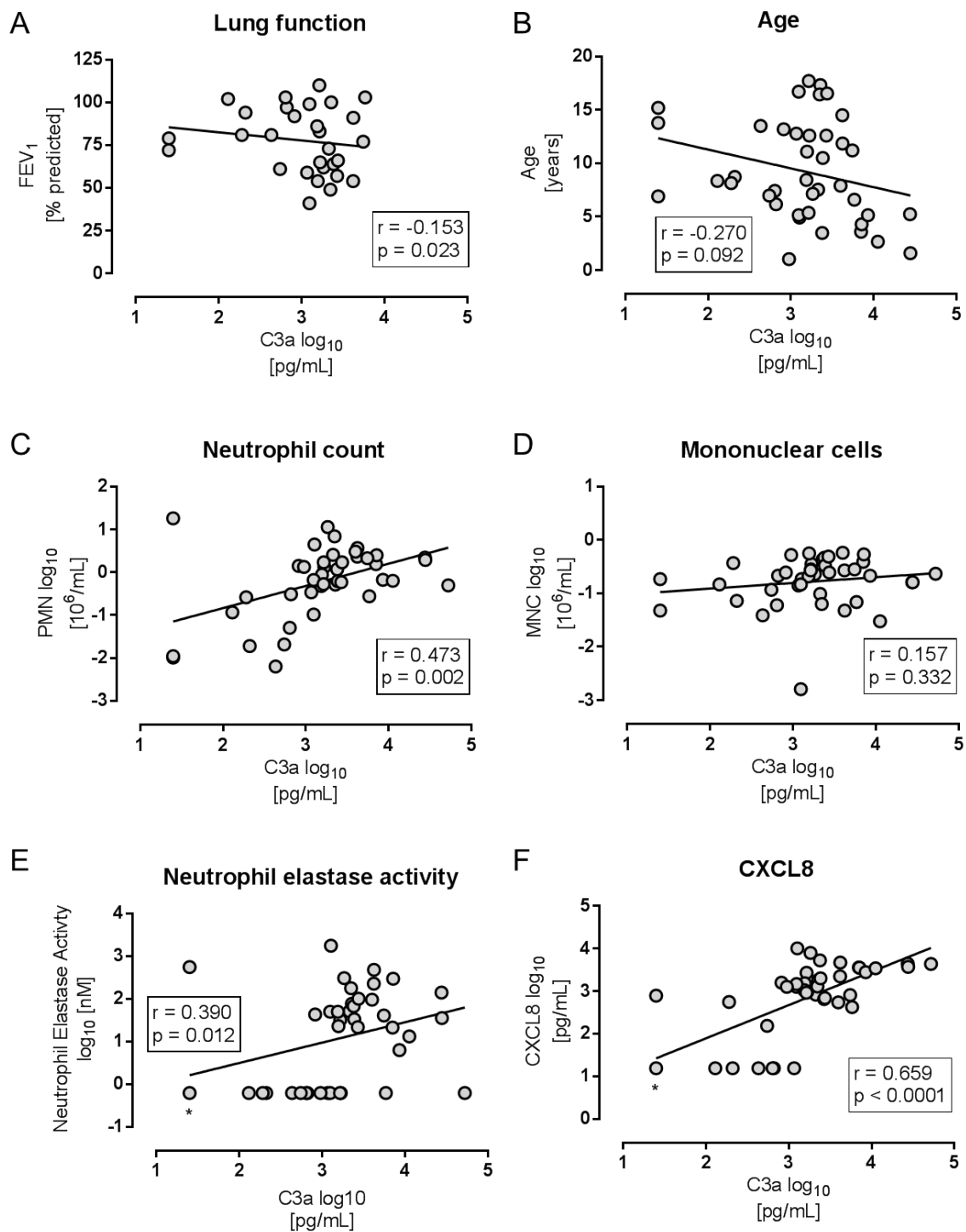


Figure 3-8: The relationship between C3a and neutrophilic inflammation in CF BAL fluid. Spearman rank correlations were performed between C3a concentration and either **A**) FEV₁ (n=29), **B**) Age (n=40), **C**) neutrophil count (n=41), **D**) Mononuclear cell count (n=41), **E**) neutrophil elastase activity (n=41) or, **F**) CXCL8 concentration (n=41). An asterisk (*) marks overlapping data points for n=2 (E) and n=2 (F). Statistical outcomes (r and p values) are annotated in black boxes.

A sensitive commercial C3a ELISA was used to determine the concentration of C3a in CF BAL fluid. The median concentration was 1670 pg/mL with a range between 25 and 52110 pg/mL. There was a statistically significant negative correlation between C3a and lung function (FEV₁) in CF BAL fluid, $r = -0.153$ and $p = 0.023$ (figure 3-8A). Additionally, despite a negative trend, the correlation between C3a concentration and age was not statistically significant (figure 3-8B).

Neutrophil-mediated damage to the CF airway can irreversibly remodel the CF lung reducing pulmonary function. Therefore, additional correlations between C3a and neutrophil count, NE activity or CXCL8 were performed to investigate whether C3a is associated with neutrophilic inflammation (figure 3-8C, E and F). There were statistically significant positive correlations between C3a and either neutrophil count ($r = 0.473$, $p = 0.002$), NE activity ($r = 0.390$, $p = 0.012$) or CXCL8 ($r = 0.659$, $p < 0.0001$). The expression of C3aR on neutrophils is controversial but expression has been shown on monocytes, macrophages and T cells (Klos *et al.* 2013). C3a is chemotactic for monocytes and therefore, the correlation between C3a and mononucleated cells in CF BAL fluid was analysed (figure 3-8D). From my data there was no statistically significant correlation between C3a and mononuclear cells.

As mentioned above, C3a concentrations in CF BAL fluid were measured in a commercial ELISA and the in-house MSD platform; this provides an opportunity to compare the values that were measured by each platform. It has been reported that singleplex and multiplex platforms from the same manufacturers can give different results and as a consequence skew relationships between analytes (de Koning *et al.* 2012). Therefore, C3a concentration, measured by MSD and ELISA, were compared to investigate whether alternative methods of measuring C3a gave different medians and influenced the relationship with other analytes. As mentioned above, the MSD used to measure C3a plate did not give values for all samples and therefore, the comparison of C3a measured by these platforms compared 28 paired samples (figure 3-9).

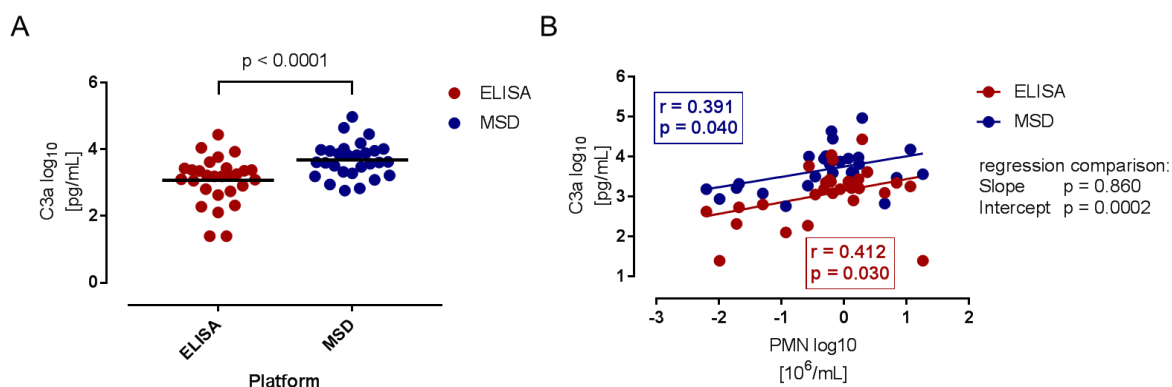


Figure 3-9: Comparing quantification of C3a measured by singleplex (ELISA) and multiplex (MSD) platforms. **A)** C3a concentration in CF BAL fluid samples (n=28) measured by C3a ELISA (red) or MSD platform (blue), medians are indicated by black bars. Statistical comparison of medians was performed using Wilcoxon paired t-test ($p < 0.0001$). **B)** Correlation between neutrophil count (PMN, y-axis) and C3a (x-axis) measured by ELISA (red) and MSD platform (blue), best-fit linear regressions were fitted for both plots. Outcomes (r and p values) of Spearman rank analysis are provided in boxes coloured respectively. Comparison of regressions was also performed comparing slope or intercept of both regressions, p values are given for each comparison.

The median C3a concentrations measured by each platform were compared by paired t-test (figure 3-9A). C3a measured by the MSD platform was significantly higher ($p < 0.0001$) than when measured by the ELISA (means: 4867 ng/mL and 1186 ng/mL respectively).

Even though the medians are statistically different this does not necessarily infer that correlations with other analytes are different, this is because the correlations are ranked. Therefore, as long as the C3a values for each sample are ranked the same, then correlations with other markers shouldn't be affected; this hypothesis was tested by correlating C3a from each platform with neutrophil count, a correlation that I previously found to be statistically significant (figure 3-8).

When correlating with neutrophil count, C3a measured by ELISA and MSD platforms had statistically significant positive correlations (figure 3-9B). Furthermore, the strength of these correlations (r value) was similar for C3a when measured by both platforms (ELISA: $r = 0.412$, MSD $r = 0.391$). A comparison of the two regressions, plotted for each correlation, was compared to assess whether there was any statistical difference. There was a statistical difference in the intercept ($p = 0.0002$) but not the slope ($p = 0.860$), this analysis supports the fact that there are differences in the C3a values measured by the two platforms, but there is no statistical difference in their correlation with neutrophil count. Therefore, I conclude that either C3a data set could be used for analysis of C3a in CF BAL fluid in my study; however, because the Quidel ELISA quantified levels of C3a in more samples, there would be more power in analyses using this data set.

3.9. Correlating C5a with markers of neutrophilic inflammation in the CF airway

Like C3a, elevated C5a has also been reported in the CF airway. Moreover, C5a has been reported to correlate with markers of neutrophilic inflammation (NE, MPO and DNA) and spike dramatically during pulmonary exacerbation (Fick *et al.* 1986; Sass *et al.* 2015; Hair *et al.* 2017). A sensitive commercial C5a ELISA was used to determine the concentration of C5a in CF BAL fluid. The median concentration was 57.8 pg/mL with a range between 5 and 807.4 pg/mL.

In the correlation matrix analysis in figure 3-7, C5a positively correlated with neutrophil count and CXCL8 concentration; therefore, the role of C5a in CF disease progression was further investigated. Correlations were performed with either lung function (FEV₁) or age to investigate whether C5a was associated with disease progression (figure 3-10). There was no correlation between C5a and lung function; however, there was a statistically significant negative correlation between C5a and age, $r = -0.337$ and $p = 0.034$. The relationship between C5a and markers of neutrophilic inflammation such as neutrophil count, NE activity and, CXCL8 concentration were also investigated. There were statistically significant positive correlations between C5a and both neutrophil count ($r = 0.353$ and $p = 0.024$) and CXCL8 ($r = 0.465$, $p = 0.002$). Despite a positive trend the correlation between C5a and NE activity was not statistically significant ($r = 0.286$, $p = 0.070$). C5a is also chemotactic for monocytes and macrophages and therefore, the correlation between C5a and mononuclear cells was also analysed. There was a statistically significant positive correlation between C5a and mononuclear cells in CF BAL fluid.

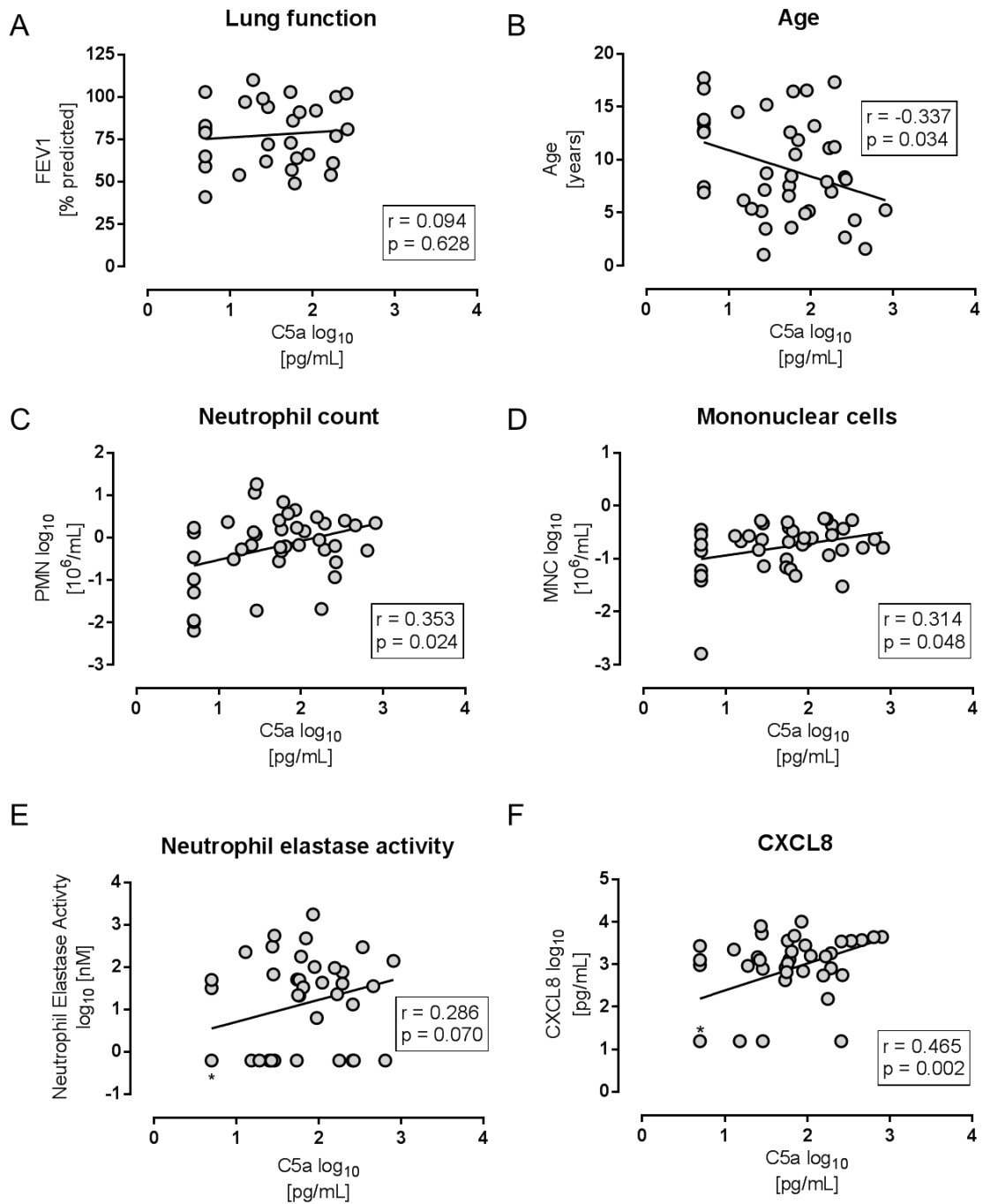


Figure 3-10: The relationship between C5a and neutrophilic inflammation in CF BAL fluid
 Spearman rank correlations were performed between C5a concentration and either **A**) FEV₁ (n=29), **B**) Age (n=40), **C**) neutrophil count (n=41), **D**) mononuclear cells (n=41), **E**) neutrophil elastase activity (n=41) or, **F**) CXCL8 concentration (n=41). An asterisk (*) marks overlapping data points for n=6 (E) and n=5 (F). Statistical outcomes (r and p values) are annotated in black boxes.

3.10. Stratification of the CF cohort for further analysis of C3a and C5a as pathogenic factors

I have found that there were statistically positive correlations between markers of inflammation and both C3a and C5a. Despite previous studies reporting a negative correlation between C5a and lung function, in my study there was a weak negative correlation between C3a with lung function but no correlation with C5a (Sass *et al.* 2015). An explanation for this could be the variation in patients and inflammation at the time when the BAL fluid was taken. As mentioned in the background to this study there are several reasons that the BAL procedure might be performed, such as: portacath insertion (for direct administration of antibiotics to the lungs), surveillance after a course of antibiotics or the patient may have a chronic cough and clinicians may want to identify the pathogen before administering antibiotics. Therefore, despite ongoing disease, CF patients will go through periods of stability where they are relatively well.

I hypothesised that, if I could stratify the cohort using the clinical justification for the BAL procedure, I could test whether C3a or C5a were associated with disease progression. The cohort was stratified into two groups using the notes provided by clinicians at the time the BAL was performed, these groups were: “well” or “unwell”. An example of a “well” sample: one CF patient underwent circumcision and therefore, BAL was performed in parallel, whilst the patient was under general anesthetic. An example of an “unwell” patient would be admission to hospital with pulmonary exacerbation. A tally of the reasons for BAL for each patient has been provided in table 3-6.

Reason for bronchoalveolar lavage	Number of patients
Well (no active infection)	
Portacath	3
Incidental surgery	1
Surveillance but otherwise well	10
Total	14
Unwell (suspected infection)	
Suspected <i>Burkholderia cepacia</i> infection	1
Pulmonary exacerbation	6
Chronic cough / Symptoms of airway infection	5
Identification of <i>Pseudomonas aeruginosa</i> strain	1
Total	13

Table 3-6: Justification for stratification of well and unwell CF patients

Information facilitating “well” and “unwell” stratification was only available for 27 patients furthermore, only 17 of these patients also have data for lung function. This was because this type of information was recorded by the clinician for medical records but not consistently recorded as part of this study.

Different parameters were investigated using the stratified cohort, these were: age, lung function (FEV_1), neutrophil count, CXCL8, C3a and C5a (figure 3-11). Before comparing markers of lung function, neutrophilic inflammation and complement anaphylatoxins, I compared the ages of the two groups (figure 3-11A). The reason for this was that if the two stratification groups differed in age then this might skew the data sets because lung function and neutrophilic inflammation worsens with age. There was no significant difference in age between the “well” and “unwell” patients and therefore, I was confident that age was not skewing the variables in the following analyses.

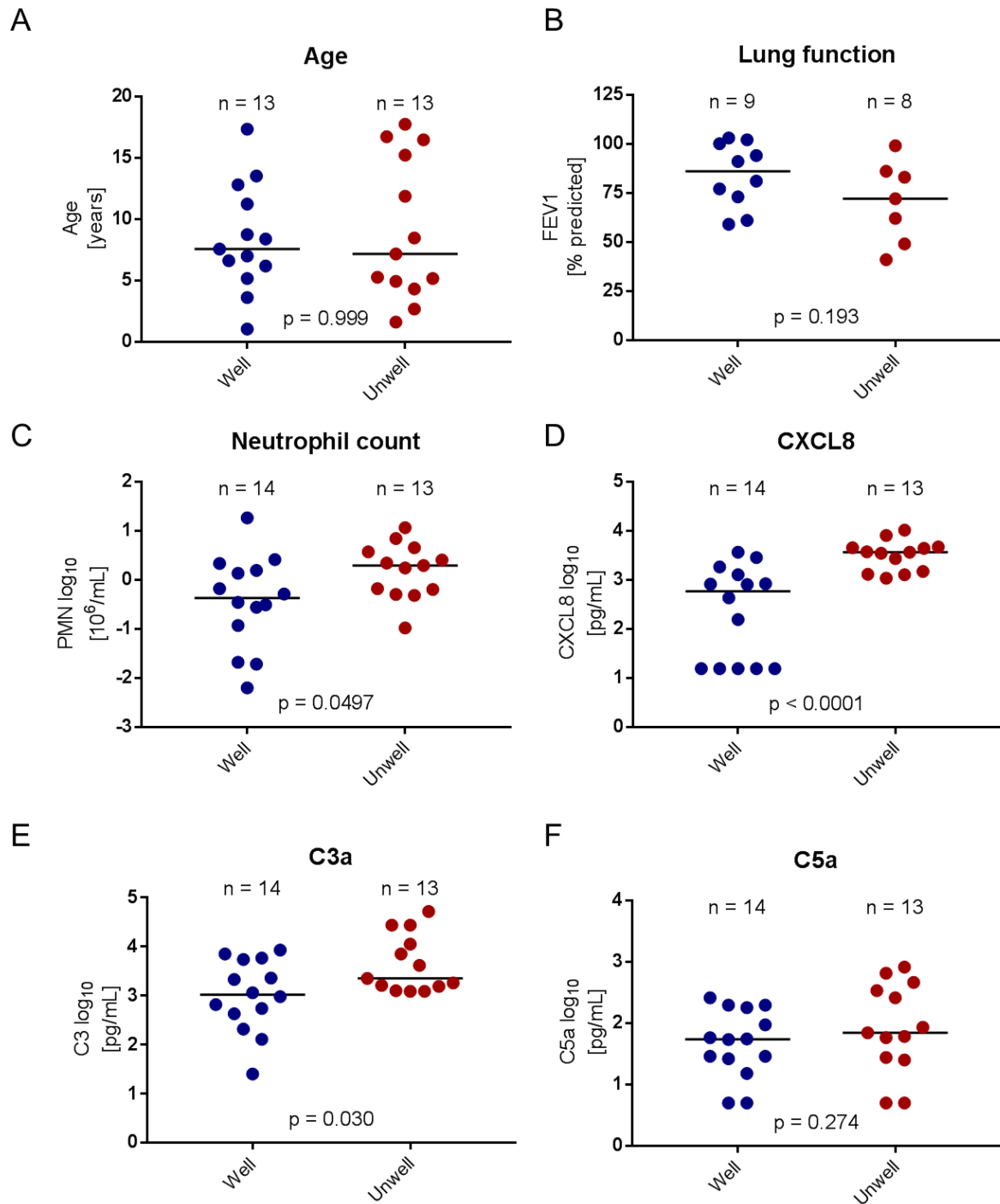


Figure 3-11: Comparing neutrophilic inflammation and complement following stratification of the CF cohort. Non-parametric t-tests (Mann-Whitney) were performed on the medians of “well” (blue) and “unwell” (red) CF patients for **A**) Age (n = 26), **B**) Lung function (FEV₁, n=17), **C**) Neutrophil count (n=27), **D**) CXCL8 (n=27), **E**) C3a (n=27) and **F**) C5a (n=27). Medians are plotted for each variable and condition.

I first tested lung function, neutrophil count and CXCL8 concentration in CF BAL fluid to verify that the stratification I performed reflected disease pathology. I hypothesised that “unwell” patients would have worse lung function and greater neutrophilic inflammation than “well” patients. There was no significant difference in the median lung function between “well” and “unwell” patients however, percentage of predicted FEV₁ data was not available for all the patients stratified (figure 3-11B). The median percentage predicted FEV₁ for “unwell” patients was 72%, compared to 86% for “well” patients. Therefore, there is a trend suggesting that lung function of “unwell” patients is less than “well” patients; however, there may not have been sufficient statistical power in this analysis due to missing data points. It may also be possible that there is no statistical difference.

Despite there being no statistically significant trends in lung function between “well” and “unwell” patients, there was a significant difference between “well” and “unwell” patients when comparing the medians of neutrophil counts, and particularly CXCL8 ($p = 0.0497$ and $p < 0.0001$ respectively)(figure 3-11C and figure 3-11D). Neutrophilic inflammation of the CF airway can permanently reduce lung function. Therefore, neutrophil count and CXCL8 data are in support of lung function data and suggest that, when analysed, “unwell” patients are pathologically unwell. Having performed these analyses I was confident that my stratification reflected that CF disease progression is episodic in that patients go through periods where they are, relatively speaking, “well” or “unwell”.

Having analysed the CF cohort sub-groups for lung function and markers of inflammation, I next investigated whether CF patients had different levels of C3a or C5a during “unwell” periods. Hair *et al* have previously shown that there was a spike in C5a concentration during pulmonary exacerbation in CF patients (Hair *et al.* 2017). The median C3a and C5a levels were compared in “well” and “unwell” patients. The median C3a concentration was significantly higher in CF patients that were “unwell” compared those that were “well” (figure 3-11E, $p = 0.030$). The median C5a concentration was also higher in “unwell” patients compared to “well” patients however, the difference was not statistically significant (figure 3-11F) (69.2 pg/mL compared to 55.0 pg/mL respectively).

3.11. Discussion

In this section I have used BAL fluid from a cohort of CF patients to characterise complement components and the complement anaphylatoxins, C3a and C5a, in the CF airway. I have performed analyses with markers of disease progression and neutrophilic inflammation to investigate whether there is evidence that either C3a or C5a promote CF pathogenesis. I have found that both C3a and C5a correlate with neutrophilic inflammation; however, there was a significant negative correlation between lung function and C3a, but not C5a. To further investigate whether C3a and C5a are linked to worsening disease I stratified the cohort into “well” and “unwell” patients. There were statistically higher levels of C3a in “unwell” CF patient BAL fluid compared to “well” BAL fluid. The median C5a concentration in BAL fluid from “unwell” patients was higher than “well” patients but the difference was not statistically significant

I initially performed analyses to determine whether the CF cohort I was using for my study reflected the national (UK) CF population and therefore, any pathologically relevant outcomes may also be applicable to the wider CF population (UK CF registry 2016). First, I described the clinical characteristics of my cohort such as age, sex, *cftr* genotype, BMI and percentage predicted lung function (FEV₁). The median age of the patients used in my study, at the time the sample was taken (with respect to repeated measures), was 8.3 years, this is less than the UK median (20 years)(UK CF registry 2016). Furthermore, the oldest patient in my study was 17.7 years, reflecting that the population I am characterising is paediatric and therefore, importantly, highlights that the cohort in this study is appropriate for investigating the initial stages of chronic neutrophilic inflammation.

The *cftr* genotype of the patients in the cohort used in this study was also similar to the national trend; 90.2% had at least one F508del allele compared to 90.9% across the UK. It is important that the *cftr* genotype in my cohort reflects the UK population because each mutation has a different phenotype that influences the severity of disease; these have been classed from 1-6 (figure 1-1) (Elborn 2016). Therefore, 90.9% of the UK CF population have at least one allele for a severe disease phenotype. If my cohort significantly differed from this then the outcomes from my study may not be applicable to the more severe disease forms.

I also assessed the correlation between lung function and age in my CF cohort; neutrophilic inflammation of the CF airways causes remodeling, bronchiectasis and loss of lung function (Schafer *et al.* 2018). Therefore, there is a negative trend in percentage predicted FEV₁ over

time, this has been well illustrated by the UK CF registry who have collated all lung function data for UK patients (figure 3-12)(UK CF registry 2016).

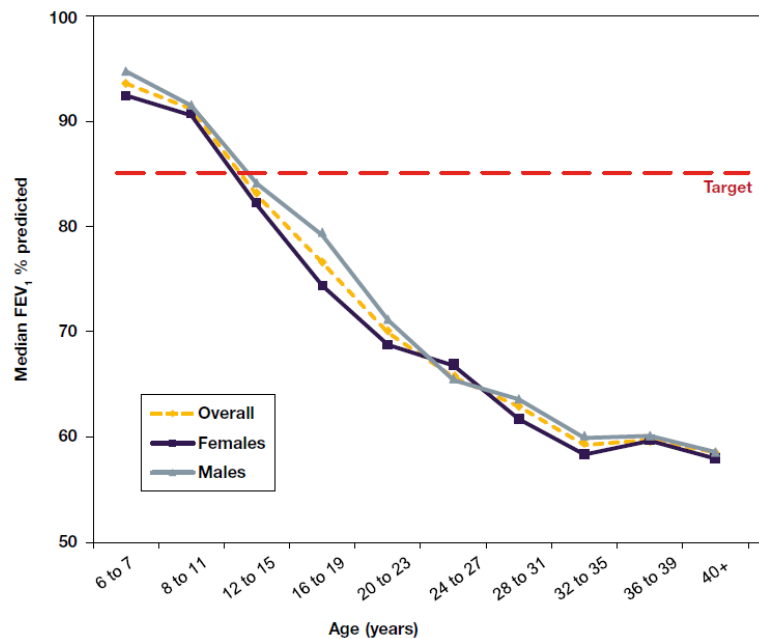


Figure 3-12: Median percentage predicted FEV1 in CF patients over 6 years. Data from the UK CF registry, FEV₁ of patients, excluding those who are younger than 6 years and who have had lung transplants, n=7830. Red dashed line is the target FEV₁ that would be in the near-normal lung function range (UK CF registry 2016).

In support of the national trend, analysis of clinical information available from 29 CF patients in this study, at the time that BAL was performed, showed a statistically significant negative trend between percentage predicted FEV₁ and age. I initially investigated whether the cohort clinical data used in this study reflected the UK CF population. In conclusion, I found that my data reproduced trends that have been reported nationally and therefore my cohort was representative of the UK CF population, as shown in figure 3-12 (UK CF registry 2016).

As well as assessing clinical data from my CF cohort, I also investigated markers of neutrophilic inflammation; this would allow me to investigate whether complement or complement anaphylatoxins, C3a and C5a, are associated with neutrophilic inflammation. I first assessed whether my cohort supported what has previously been reported. Neutrophil counts, NE activity and, CXCL8 are well established markers of neutrophilic inflammation in the CF BAL fluid and sputum (Sagel *et al.* 2007; McElvaney *et al.* 2018). In table 3-7, I have reviewed the literature for reported measurements of the above markers in CF BAL fluid.

Neutrophil count (10 ⁶ /mL)	Neutrophil elastase activity (nM)	CXCL8 (pg/mL)	Median age (decimal years)	Reference
1.93	114	1948	8.3	Current study
0.62	81 (56.3%)	1122	6.4	(McGreal <i>et al.</i> 2010)
-	1100	-	28.2	(McElvaney <i>et al.</i> 2018)
-	8200	-	28.0	(McElvaney <i>et al.</i> 1991)
-	10600	243	27.0	(McElvaney <i>et al.</i> 1992)
7.14	-	-	25.1	(Roum <i>et al.</i> 1999)
0.0039*	-	~3000	6.0	(Wojtczak <i>et al.</i> 2001)
0.0041*	4000 (29.7%)	320	0.25	(Sly <i>et al.</i> 2009)
2.33	-	-	3.2	(Sly <i>et al.</i> 2013)
0.8	1040	1198	3.2	(Ringholz <i>et al.</i> 2014)
-	~2000 (37.7%)	878	4.9	(McNally <i>et al.</i> 2017)
1.15	-	1614	22.1	(Gutierrez <i>et al.</i> 2001)
2.81	-	1153	19.1	(Armstrong <i>et al.</i> 2005)

Table 3-7: Reported means of neutrophil count, NE activity and CXCL8 in CF BAL fluid.

Data was collated from studies investigating markers of inflammation in CF BAL fluid and efficacy of therapeutics. Data from another study from the same centre as my study that used the same BAL fluid processing and analyte quantification methods (grey highlight). Data from some studies was collated from selected populations that might be skewed, such as: unwell (positive for pathogens) or newborn screening (*). In most studies NE activity is only reported for samples where there are detectable levels, these are given as percentage positive (%) for NE activity. For studies that did not report numerical values, levels were estimated from graphs (~).

Reviewing the reported levels of the markers of neutrophilic inflammation used in my study, I found that the neutrophil counts and levels of CXCL8 I recorded are similar to those reported by others (table 3-7). Despite this, the mean NE activity in my study was generally less than what has been reported by others. Importantly, a study from the same centre as my cohort, that was characterised using the same protocols, reported similar NE activity (McGreal *et al.* 2010). Low NE activity in my study compared to other reports could be accounted for by the fact that some groups only report samples that are positive for NE activity (Sly *et al.* 2009; McNally *et al.* 2017). Another difference and advantage to my study is the age of my cohort (8.3 decimal years); this is lower than other reports and is significant because CF disease get progressively worse with age. Therefore, in a more paediatric cohort, markers of neutrophilic inflammation could be lower; however, a more paediatric cohort allows the initial stages of neutrophilic inflammation in the CF airway to be studied.

In my study, I confirmed that there are strong positive correlations between neutrophil count, NE activity and CXCL8 verifying their use as markers of neutrophilic inflammation in this is

study. This was important because in order to investigate the role of C3a and C5a in promoting neutrophilic inflammation I required good reference markers to compare with. Despite my choice (and others) to compare analytes with these markers (see references in table 3-7), neutrophil count, NE activity and CXCL8 are not the only biomarkers of inflammation and disease progression in CF. Sagel *et al.* performed a multivariate analysis of cytokines, proteases and protease inhibitors in sputum (Sagel *et al.* 2012). The authors found that as well as NE activity and CXCL8 other markers such as IL-6 and IL-1 β improved the overall predictive value when monitoring the decline in lung function (Sagel *et al.* 2012). Considering the other candidate markers of inflammation and disease progression that have been reported in the CF airway, I am confident that the three markers of neutrophilic inflammation used in my study were the most appropriate for investigating the role of complement anaphylatoxins in promoting neutrophilic inflammation (Sagel *et al.* 2007; Sagel *et al.* 2012; McElvaney *et al.* 2018).

In the next part of my study, I measured an array of complement components using a multiplex platform that has previously been used to report on complement involvement in various diseases such as epilepsy, psychosis, multiple sclerosis and neuromyelitis optica (Hakobyan *et al.* 2017; Kopczynska *et al.* 2017; Kopczynska *et al.* 2018). C3a and C5a were measured by commercial ELISAs and C5 was measured using an in-house ELISA that utilised a sensitive commercial mouse anti-C5 antibody (SKY59), not currently available on the market. I recently contributed to a publication on diagnostic uses of this antibody (Zelek *et al.* 2018).

Two groups have previously published proteomic analysis of complement components in CF airway fluid, one of these groups reported that several complement components were less abundant in CF compared the airways of asthmatic patients, these were: C1q, C2, C4b, C5 and C6 (Gharib *et al.* 2009). A more recent study performed proteomic analysis on sputum from CF patients chronically infected with *P. aeruginosa* (Pattison *et al.* 2017). Despite gaining further insight into complement in the CF airway, neither of the two proteomic analyses specifically studied the analytes that were measured by multiplex platform in my experiments. Therefore, my analysis is the first to comprehensively report on complement in the CF airway and its association with neutrophilic inflammation.

Interestingly, in my analysis, many of the complement components measured as part of this study positively correlated with neutrophil count and CXCL8. Despite this, relationships with NE activity were weak and not statistically significant. An explanation of weaker associations between complement and NE activity maybe be that these components are susceptible to degradation by NE and therefore their relationships maybe be more complex. Proteolysis of

C3, C5, C3a and C5a by NE has been reported and will be discussed in depth in the next chapter (Huber-Lang *et al.* 2006). A literature search using the terms “neutrophil elastase” and “complement”, “factor B”, “factor H” or “factor D” did not provide any information about NE degradation of the other complement components measured in this study and could be an interesting research topic.

Of interest to the other components that positively correlated with neutrophil counts, factor B has been shown to be elevated during sepsis, a condition where neutrophil dysfunction also contributes to pathogenesis (Zou *et al.* 2013). Factor B, along with factor D (figure 1-19), are important mediators of the amplification loop (alternative pathway) and complement activation, leading to the generation of C3a and C5a, and consequently neutrophil recruitment (Hajishengallis *et al.* 2017). Zou *et al.* have shown that factor B is released by macrophages upon stimulation of TLR-4 in response to infection and suggest that factor B is a pathogenic factor in sepsis (Zou *et al.* 2013). This therefore, could also be an interesting mediator of neutrophilic inflammation in the CF airway during infection.

Factor H did not correlate with either neutrophil count or NE activity but did positively correlate with CXCL8. Factor H is a complement inhibitor that binds to the alternative pathway C3 and C5 convertases (C3b,Bb and C3b,Bb,C3b) causing the release of the catalyst, Bb preventing activation (de Cordoba and de Jorge 2008). Factor H is also a co-factor for factor I, a serine protease that cleaves C3b into iC3b, a form which retains opsonic activity but cannot form convertases (figure 1-19). Factor H has been shown to bind complement receptor 3 (CR3) on neutrophils. Furthermore, fungal pathogens such as *A. fumigatus* and *C. albicans* (opportunistic pathogens in the CF airway), have also been shown to bind factor H, a mechanism that reduces complement activation (Losse *et al.* 2010). Furthermore, it has been shown by Losse *et al.* that interaction between CR3, factor H and pathogen surfaces enhances neutrophil response to these pathogens causing increased release of ROS and CXCL8.

The focus of this study was on the role of C3a and C5a in promoting neutrophilic inflammation. The concentration of C5a, but not C3a, has previously been reported in CF BAL fluid. Both C3a and C5a concentrations have been reported in CF sputum; the median C5a levels in these reports were 258 ng/mL and approximately 1.0 ng/mL (from graph) respectively (Fick *et al.* 1986; Sass *et al.* 2015). In my study I found that the median concentration was 57.8 pg/mL, almost 2000-fold less than Fick *et al.* reported in CF BAL fluid and approximately 20-fold less than what has been reported in sputum by Sass *et al.* There are three reasons that may account for these differences:

1. *Age.* CF disease progresses with age and therefore, chronic neutrophilic inflammation will be less severe in a more paediatric cohort. The median age of the cohort used in this study was 8.3 whereas Fick *et al.* and Sass *et al.* report on C5a and C3a levels in populations with a median age of 19 years in smaller cohorts (9 and 15 CF patients respectively).
2. *Quantification method.* Fick *et al.* use a radioimmunoassay (Upjohn Diagnostics, now Thermo through several mergers) to measure C5a in CF BAL fluid however, this kit is no longer available. Radioimmunoassays use radio-labelled antibodies to bind targets, complexes are then precipitated and the radioactivity in the pellet is measured. Using an appropriate antibody is critical here because any cross-reactivity with C5 will skew the data, this could also be an issue for the kit used by Sass *et al.* for quantification of C5a in sputum. It is unclear from the manuscript by Sass *et al.* whether the kit they use is from BD bioscience or R&D systems however, both manufacturers report cross-reactivity for C5 in their C5a kits (0.89% (mole/mole) and 25% (mole/mole) respectively, <http://www.bdbiosciences.com/> and <https://www.rndsystems.com/>). In my study, CF BAL fluid had a maximum C5 concentration of 250 ng/mL therefore, in a worse-case scenario, using the above kits for C5a quantification in BAL fluid from my study would skew C5a levels by 62.5 ng/mL (R&D systems) and 2.2 ng/mL (BD bioscience).
3. *Sample processing.* In my analysis I processed BAL fluid by removing the cellular component through centrifugation at 500 x g for 5 minutes at 4°C, the supernatant was aliquoted and stored at -80°C within 60 minutes. In contrast, Fick *et al.* concentrated BAL fluid 10-fold using positive pressure ultrafiltration and stored fluid at -78°C (Fick *et al.* 1986). Due to difficulty in standardising airway fluid samples (as mentioned in section 3.1.1a), I think it would be difficult to measure fluid concentration accurately and therefore, concentrating BAL fluid would introduce error when reporting C5a concentration by weight per millilitre. A different method for sample processing was also used by Sass *et al.*, they report that sputum was centrifugated at 14,000 x g for 60 minutes at 4°C (Sass *et al.* 2015). A reason for this vigorous centrifugation step is that the authors were using a similar method to a previous report investigating mucins in CF sputum, which may require a more mechanical extraction method (Davies *et al.* 1999). My concern here is that C5a may bind to soluble GAGs present in the sputum, ultracentrifugation may separate larger C5a-GAG complexes and therefore, complexed C5a may not be included in the quantification but may be relevant to pathogenesis, this will be explored in more depth in chapter 6.

The above reasons may explain the discrepancies observed between our studies. In summary of quantification of C5a in my study, I have carefully selected an appropriate commercial C5a ELISA that has no reported cross-reactivity for C5 (<https://www.quidel.com/>). I have also used a gentle method of sample processing that maintains a more native state than compared to the processing methods described by Fick *et al.* and Sass *et al.* (Fick *et al.* 1986; Sass *et al.* 2015)

C3a in sputum was also quantified by Sass *et al.*; they report a median concentration of approximately 40 ng/mL (from graph) whereas, in CF BAL fluid I measured a median of 1.67 ng/mL by commercial ELISA and 4.1 ng/mL in-house MSD multiplex platform. Like C5a, there are also issues with C3 cross-reacting with C3a ELISA kits; BD bioscience, but not R&D systems, manufacture C3a ELISAs. The manual from the manufacturer's website (<http://www.bdbiosciences.com/>) states that weight for weight there is <0.0384% cross-reactivity with C3 in their kit. C3 is almost 20-fold heavier than C3a; therefore, on a mole for mole basis this cross-reactivity could be 0.77% (0.0384% multiplied by 20). Furthermore, C3 is vastly more abundant than C3a when measured in plasma (20,000 fold) (Barnum and Schein 2018), and CF BAL fluid (>36,000 fold) as quantified by my own study. Crucially, even a small degree of cross-reactivity in this assay would significantly skew C3a quantification.

I found that there were positive correlations between either C3a or C5a and neutrophil count, NE activity (C5a non-significant) or CXCL8 concentration. This is the first study to correlate C3a and C5a in CF BAL fluid with neutrophil counts and CXCL8 however, it has previously been shown in CF sputum that both C3a and C5a significantly correlate with NE concentration, MPO activity and DNA concentration (Hair *et al.* 2017). In my study, the correlation between C5a and NE activity in CF BAL fluid was not significant compared to Hair *et al.* where a strong positive correlation was demonstrated. However, Hair *et al.* quantified total NE not NE activity; the difference here is that serine protease inhibitors such as AAT and SLPI are also present in the airway and therefore, NE concentration alone does not indicate enzyme activity. AAT and SLPI have been measured in CF sputum as measures of neutrophilic inflammation and neutrophilic mediated damage (Sagel *et al.* 2012). Hair *et al.* go further than testing correlations between C3a or C5a and markers of neutrophilic inflammation; they also perform linear models with confidence intervals for each of the analytes tested. The analysis in my study fitted best-fit lines but did not establish direct relationships between analytes. This because Spearman rank analysis does not demonstrate causal relationships.

In my analysis I performed correlations between measures of disease progression (lung function (FEV₁) and age) and C3a or C5a. In contrast to my data, the same group has twice

reported positive correlations between C3a (sputum) and lung function (Sass *et al.* 2015; Hair *et al.* 2017). This group suggested that C3a has a protective role in the CF airway, this follows reports that C3a has an inhibitory role in preventing neutrophil migration from the bone marrow during ischemia-reperfusion injury (Wu *et al.* 2013). An explanation for this discrepancy is that the cohort used in my study is paediatric whereas, in the Sass *et al.* and Hair *et al.* studies the cohort age is older (19 and 24 years respectively). It has been reported that C3a is a biomarker of inflammation and disease progression in several pathologies such as: kidney disease, cardiovascular disease and arthritis as well as airway conditions such as asthma and pneumonia (*P. aeruginosa*); Klos *et al.* has reviewed an extensive list for reference (Mueller-Ortiz *et al.* 2006; Dillard *et al.* 2007; Klos *et al.* 2013). Therefore, it is not clear whether the presence of C3a (and C3a desArg) in the CF airway has a causal relationship with lung function, or whether it is a marker of inflammation and complement activation.

Despite there being no evidence of a correlation between C5a and lung function in my data, others have reported negative correlations. In CF BAL fluid, Fick *et al.* demonstrated that C5a correlated with a worse clinical score and poorer lung function; however, the population size for that study was nine and therefore small (Fick *et al.* 1986). Sass *et al.* and Hair *et al.* both describe negative correlations with between C5a and lung function (Sass *et al.* 2015; Hair *et al.* 2017). Interestingly, Hair *et al.* also perform a longitudinal study on C5a (and C3a) and demonstrate for 3 CF patients that C5a spikes simultaneously with decline in lung function (Hair *et al.* 2017). Furthermore, for 3 different CF patients Hair *et al.* show that an increase in sputum C5a also precedes a decline in lung function. They conclude that C5a in sputum is not only a marker of disease progression but could also be used as a predictor for pulmonary exacerbation (Hair *et al.* 2017).

I also performed correlations between C3a or C5a with age and found negative relationships for both anaphylatoxins however, this association was not statically significant for C3a. Hair *et al.* also describe negative correlations between C3a in CF sputum with age, in contrast to my study, the same group demonstrate a positive relationship between C5a and age in an earlier report on 9 patients (Sass *et al.* 2015; Hair *et al.* 2017). Unfortunately, they do not report the correlation between C5a and age in the more recent manuscript describing 34 patients (Hair *et al.* 2017).

The CF airway is a dynamic and complex environment and, sampling of airway is not always performed during pulmonary exacerbation. Therefore, the population in my study reflects a number of scenarios within the disease in addition to exacerbation, such as periods of relative stability or inflammatory resolution following a course of antibiotics. Consequently, this

episodic nature of infection in the CF airway is reflected in my data, particularly by the markers of neutrophilic inflammation that showed both extremes of high and low levels of inflammation.

A disadvantage of this study was that I did not have a control population. These are difficult to access because the BAL procedure is invasive and requires sedation therefore, making it unethical to perform BAL on healthy individuals. Other control populations can be used such as patients undergoing tonsillectomy however, it is not always clear, despite being “healthy”, how well their airways reflect normality (Brennan *et al.* 2008). Instead of comparing against a control population I stratified my data into two groups “well” and “unwell”; this stratification revealed statistically significant differences between neutrophil count, CXCL8 and C3a.

An advantage to this study was that the population size was greater (n=41) than previous reports investigating C3a and C5a in the CF airway (n= 9, 15 and 34 respectively)(Fick *et al.* 1986; Sass *et al.* 2015; Hair *et al.* 2017). Furthermore, because airway fluid was sampled by BAL, I was able to assess a more paediatric CF cohort; this is essential for investigating the early stages of neutrophilic inflammation in the CF airway. An additional critical advantage was the use of a sensitive commercial C5a (and C3a) ELISA that had no reported cross-reactivity to C5. It is important that we understand initial mechanisms that promote chronic neutrophilic inflammation, so we can more effectively target causative molecules or pathways.

3.12. Conclusion to the chapter

In this chapter I have analysed complement components (C3, C5, C3a and C5a) and revealed that the level of many components is low and, relative to C3 there are significant differences compared to normal plasma. Focusing on the complement anaphylatoxins, I have shown that C3a and C5a are associated with neutrophilic inflammation, supporting findings that have previously been reported (Fick *et al.* 1986; Sass *et al.* 2015; Hair *et al.* 2017). Despite showing positive correlations between C3a or C5a with neutrophilic inflammation the relationship with lung function and disease progression was not clear. The mechanisms by which these two molecules promote chronic airway disease, particularly CF, is not fully understood. In the next sections I will explore the mechanisms by which C3a and C5a could promote CF pathogenesis; I will investigate how C3a and C5a interact with the CF lung environment and, as a consequence, whether their activity is modified. Specifically, I will investigate the generation and proteolysis of C3a and C5a by NSPs that are present in the CF airway. I will also investigate whether C5a interacts with soluble GAGs and, if so, whether these interactions modify function.

4. Generation of C5a and C3a by neutrophil serine proteases in the CF airway

4.1. Background to the study

The complement cascade is not a closed system, it can be regulated by other pathways such as metabolic pathways (Barbu *et al.* 2015), pathogen virulence factors (Hovingh *et al.* 2016), and crosstalk with the coagulation system (Foley 2016).

In particular, the coagulation system has co-evolved with the complement cascade to enable quick response to wounds and systemic infection. Consequently, several coagulation system proteases are able to generate functional C5a from C5, independently of C5-convertase; these are thrombin, Factor IX, Factor Xa, Factor XI, plasmin and kallikrein (Huber-Lang *et al.* 2006; Foley 2016). It has been proposed that generation (in addition to complement activation) of functional C5a by these enzymes facilitates leukocyte recruitment to the wound or infection site, accumulating and facilitating coagulation. Furthermore, plasmin and factor Xa can also cleave C5 into functional C5b, enabling terminal complement activation and the formation of MAC (Huber-Lang *et al.* 2006). Therefore, the crosstalk between the coagulation and complement cascades can be beneficial for wound responses; however, without tight regulation this may also lead to thrombosis (Foley *et al.* 2016).

4.1.1. Atypical generation of C3a and C5a by non-complement proteases

Atypical cleavage of C3 and C5 into functional C3a-like and C5a-like fragments is not unique to the coagulation pathway and has been demonstrated for a growing list of non-complement proteases (see table 4-1). Endogenous C3a and C5a-generating proteases have been identified as pathogenic factors in several inflammatory diseases such as rheumatoid arthritis and asthma, these will be discussed later (Giles *et al.* 2015; Yuan *et al.* 2015). Exogenous non-complement proteases expressed by bacteria, fungi, parasites and venomous animals such as snakes and insects have evolved to deplete or evade the complement system; facilitating colonisation, parasitic living or death of the host (Reed *et al.* 1995; Luo *et al.* 2018). Also, proteases expressed in peanuts have been shown to generate C3a and C5a-like forms; these anaphylatoxins could

Protease	Anaphylatoxins Generated	Associated pathology	Reference
Endogenous			
Neutrophil proteases: Neutrophil serine proteases – (neutrophil elastase and cathepsin G)	C3a	CNS pathology COPD	(Huber-Lang <i>et al.</i> 2012; Yuan <i>et al.</i> 2015; Hooshmand <i>et al.</i> 2017)
	C5a	COPD Rheumatoid Arthritis	(Brozna <i>et al.</i> 1977; Wetsel and Kolb 1983; Robbins <i>et al.</i> 1991; Giles <i>et al.</i> 2015)
Matrix metalloproteinase 12			
Neutrophil MPO-generated hypochlorite	C5a	Inflammation	(Vogt 1996)
Coagulation Proteases (thrombin, plasmin, Factors IX, X, XI and kallikrein)	C5a	Thrombus formation Asbestos	(Wetsel and Kolb 1983; Governa <i>et al.</i> 2000; Huber-Lang <i>et al.</i> 2006)
	C3a	<i>C. albicans</i> invasion	(Irmischer <i>et al.</i> 2018)
Apoptosis pathways (Granzyme B, cathepsin D)	C5a	Trauma	(Huber-Lang <i>et al.</i> 2012; Perl <i>et al.</i> 2012)
Trypsin	C3a and C5a	Acute pancreatitis	(Wetsel and Kolb 1983)
Beta-tryptase	C3a, C4a and C5a	Asthma	(Fukuoka <i>et al.</i> 2008)
Bacterial			
<i>Pseudomonas aeruginosa</i> Pseudomonas elastase	C5a	Cystic fibrosis	(Fick <i>et al.</i> 1986)
<i>Porphyromonas gingivalis</i> gingipain-1	C3a (inactive) and C5a	Periodontal disease	(Wingrove <i>et al.</i> 1992)
<i>Streptococcal spp.</i> ScpA	C3a and C5a	Bacterial invasion	(Lynskey <i>et al.</i> 2017)
Parasite			
<i>Entamoeba histolytica</i> cysteine proteinase	C3a and C5a	Parasite colonisation	(Reed <i>et al.</i> 1995)
Dust mite (<i>Dermataphagoides farina</i>) Derp1	C3a and C5a	Asthma	(Maruo <i>et al.</i> 1997)
Fungal			
<i>Aspergillus fumigatus</i> Alp1	C3a and C5a generation	Fungal colonisation	(Behnsen <i>et al.</i> 2010; Shende <i>et al.</i> 2018)
<i>Candida albicans</i> Pra1	C3a (inactive)	Fungal colonisation	(Luo <i>et al.</i> 2018)
Animal toxins			
(<i>Bothrops pirajal</i>) Batroxase	C3a, C4a, and C5a	Complement depletion	(Menaldo <i>et al.</i> 2016)
Inc. Cobra venom factor (<i>Naja naja</i>)	C3a and C5a	Complement depletion	(Tambourgi and van den Berg 2014)
Plants			
Peanut proteases	C3a and C5a	Peanut allergy	(Javaux <i>et al.</i> 2016)

Table 4-1: List of exogenous and endogenous proteases that have been reported to generate C3a-like and C5a-like fragments.

contribute to pathology during peanut allergenic response; this phenomenon is probably a result of proteases broad substrate specificity rather than co-evolution (Javaux *et al.* 2016).

4.1.2. Generation of functional forms of C3a and C5a by NSPs

The generation of C3a and C5a by NSPs was initially investigated in the 1970s and 1980s; it was demonstrated that NE and CG were both able to cleave C3 and C5, producing fragments with chemotactic activity (Venge and Olsson 1975; Brozna *et al.* 1977; Wetsel and Kolb 1983). After a review of the literature, C5a generation by NSPs proteases has generally been more widely explored than C3a. This likely reflects the potency of the C5a/C5aR1 axis as a driver of inflammatory disease. Despite building on knowledge of non-canonical generation of C3a and C5a for the past four decades, the significance of atypically generated C5a and C3a in pathogenesis is still not fully understood.

The pathogenic roles of NSP-generated C3a and C5a in rheumatoid arthritis and COPD will be discussed in-turn below. These are both diseases where neutrophils have been shown to contribute to pathology and therefore, could be relevant for studying atypical generation of C3a and C5a in the CF airway.

The role of C5a generation by NE has been investigated with respect to rheumatoid arthritis (Giles *et al.* 2015). A single nucleotide polymorphism coding a mutation (V802I) in C5 has been previously identified as a risk factor for the disease, as well as other inflammatory diseases such as periodontitis and poor outcome in pneumococcal meningitis, cardiovascular diseases and stroke (Kurreeman *et al.* 2007; Giles *et al.* 2015). Giles *et al.* demonstrate using V802I mutant C5 constructs, that the substitution of valine for isoleucine at position 802 increases C5 turnover by NE leading to increased C5a production. The authors suggested that this phenomenon could contribute to disease pathology by increasing neutrophil recruitment to joints, a hallmark of disease pathology (Wright *et al.* 2014). Giles *et al.* also observed that NE-generated C5a-like fragments from both C5 constructs were 1 KDa larger than C5 convertase-generated C5a (Giles *et al.* 2015). The authors concluded by speculating that NE cleaved C5 at an alternative site compared to C5-convertase. Valine at position 760 was speculated as this alternative site, based on cleavage preferences of NE.

4.1.3. Generation of C3a and C5a by proteases present during airway disease

C3a and C5a generation by NE has also been reported in a study investigating cigarette smoke-mediated emphysema in COPD (Robbins *et al.* 1991; Yuan *et al.* 2015). Exposing normal serum to cigarette smoke, Robbins *et al.* observed an increase in chemotactic activity towards monocytes and neutrophils (Robbins *et al.* 1991). Furthermore, inhibition of canonical complement activation, by addition of EDTA (a metal chelator that sequesters calcium preventing calcium dependant assembly of the C1 complex), did not completely arrest the generation of chemotactic activity in the serum (Robbins *et al.* 1991). MMPs are also sensitive to EDTA, as they require co-factors such as zinc (or similarly charged ions like cobalt). Further characterisation by the authors demonstrated that C5a generation could be inhibited by addition of EDTA therefore, suggesting that C3a generation by non-complement protease (other than MMPs) may be responsible for chemotactic activity (Robbins *et al.* 1991).

Yuan *et al.* investigated C3a generation by NE in smoke-mediated lung disease (Yuan *et al.* 2015). In particular, they demonstrated that C3 deficient mice were less susceptible to lung disease induced by cigarette smoke inhalation. Moreover, Yuan *et al.* demonstrated that purified NE, CG and MMP12 but not PR3 was able to generate a C3a-like fragment from purified C3. The authors also showed that the C3a fragment produced by NE but not MMP12 was active and induced chemotaxis of bone marrow-derived dendritic cells and myeloid-derived dendritic cells; dendritic cell-induced differentiation of Th1 and Th17 cells has been shown to be a feature of smoke induced emphysema in mice (Kurimoto *et al.* 2013). Yuan *et al.* linked C3a generation and C3 proteolysis to the human disease by demonstrating that C3 cleavage fragments could be visualised on *ex vivo* lung tissue from smokers with emphysema (Yuan *et al.* 2015). Yuan *et al.* suggested that atypical C3a generation by the above proteases creates a feedback loop of C3aR upregulation, immune activation and recruitment that leads to collateral lung tissue damage.

4.1.4. Generation of C5a by proteases present in the CF airway

With relevance to the CF airway, non-canonical generation of C5a by pseudomonas elastase (from the bacterium *P. aeruginosa*) and proteases released by *S. aureus* have been reported (Fick *et al.* 1986; Sass *et al.* 2015). As discussed in the previous chapter Fick *et al.* reported elevated C5a in the CF airway, they further demonstrate that complement-mediated chemotactic activity, induced by adding C5 to zymosan activated CF BAL fluid, could not be completely arrested by EDTA. EDTA is an inhibitor of complement activity and

metalloprotease activity such as MMPs and pseudomonas elastase, a metalloprotease, released by opportunistic CF pathogen *P. aeruginosa*. (Fick *et al.* 1986). Additionally, a serine protease inhibitor, PMSF, also did not fully arrest C5a generation (Fick *et al.* 1986). From here, Fick *et al.* investigated C5a-generating components of CF BAL fluid such as pseudomonas elastase by resolving proteolytic fragments of C5 by SDS-PAGE. In addition, they demonstrate using a radioimmunoassay, that pseudomonas elastase can generate C5a from purified C5. Furthermore, in a scenario more relevant to the CF airway, they show that C5a is generated when alveolar macrophages from normal lungs (a source of C5 in the lung) are incubated with pseudomonas elastase (Fick *et al.* 1986).

Almost 30 years later, Sass *et al.* investigated C5a generation by proteolytic factors released by *S. aureus* and *P. aeruginosa*. They demonstrated that C5a was generated when dead and live forms of both bacteria species were incubated with CF sputum (Sass *et al.* 2015). Furthermore, they also show that generation of C5a could be inhibited by a classical/lectin pathway inhibitor developed by their group (Mauriello *et al.* 2013). Therefore, Sass *et al.* suggest that complement activation by canonical proteases, rather than pathogen-proteases, are responsible for C5a generation in these experiments (Sass *et al.* 2015).

In summary, it is well-established that non-complement proteases can generate functional C3a-like and C5a-like fragments. Furthermore, noncanonical production of complement anaphylatoxins has been associated with inflammatory disease progression including airway disorders such as asthma, COPD and CF. NSPs have been reported to generate active C3a and C5a in the airway (Fick *et al.* 1986; Robbins *et al.* 1991; Yuan *et al.* 2015); however, the significance of NSP-mediated anaphylatoxin generation in the CF airway is not fully understood.

4.2. Hypothesis

I hypothesise that, NSPs generate alternative forms of C3a and C5a that are functionally different to their native counterparts and that these *de novo* forms promote pathogenesis in the CF airway.

4.3. Chapter aims

1. Assess evidence for non-canonical C3a and C5a generation in BAL fluid from CF patients.
2. Investigate and confirm C5a and C3a generation by proteases present in CF BAL fluid.
3. Use purified NSPs to comprehensively characterise the generation of C3a-like and C5a-like fragments.
4. Investigate functional differences between NSP-generated C3a and C5a and their native, convertase-generated counterparts.

4.4. Evidence of C3a and C5a generation by NSPs in the CF airway.

Before investigating the mechanisms of non-canonical C3a and C5a generation in the CF airway, evidence for C3a and C5a generation was assessed in CF BAL fluid. Data from the chapter 3 suggested that C3 expression in the CF lung was over 2000-fold that of C5, whereas in blood a 10-fold difference is expected (Barnum and Schein 2018). I also investigated in the previous section how these different ratios impacted on complement activity in terms of levels of terminal pathway components and the relative abundance of C3a and C5a. Visual analysis revealed that the C3 to C3a or C5a ratios were different in the CF airway compared to normal plasma and therefore, could suggest an abnormality in the generation of these anaphylatoxins in the CF airway.

4.4.1. Evidence of complement activation and generation of C3a and C5a

Initially, I analysed the data from the CF BAL fluid for evidence of C3a and C5a generation in the CF airway, this was investigated by correlating C3a and C5a levels with their respective parent molecules, C3 and C5 (figure 4-1). C3a strongly correlated with C3 (figure 4-1A), Spearman rank analysis gave r and p values of 0.853 and <0.0001 respectively. A significant but weaker positive correlation was also observed between C5 and C5a ($r = 0.389$, $p = 0.014$)(Figure 4-1B).

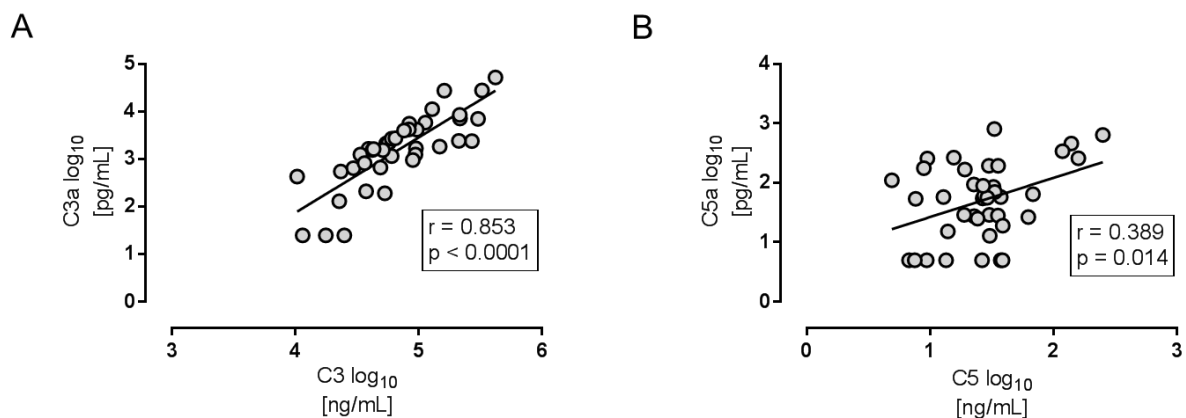


Figure 4-1: Evidence of C3a and C5a generation in BAL fluid from the CF airway.

Data from chapter 3. Spearman rank analysis of correlations between **A**) C3 (MSD) and C3a (ELISA) $n = 41$ **B**) C5 (ELISA) and C5a (ELISA), $n=40$. Best-fit linear regressions were fitted to the data (solid black lines). Statistical outcomes r and p values and in black boxes.

A stronger correlation between C3/C3a than C5/C5a suggested that there are differences in the generation of C3a compared to C5a in the CF airway. If complement activation was “normal” in the CF airway strong positive correlations might be expected between terminal complement components (C5b-9) and C3a or C5a. The correlations between C3a or C5a with terminal complement components (C5b-9) were investigated as an indication of canonical complement activation (figure 4-2).

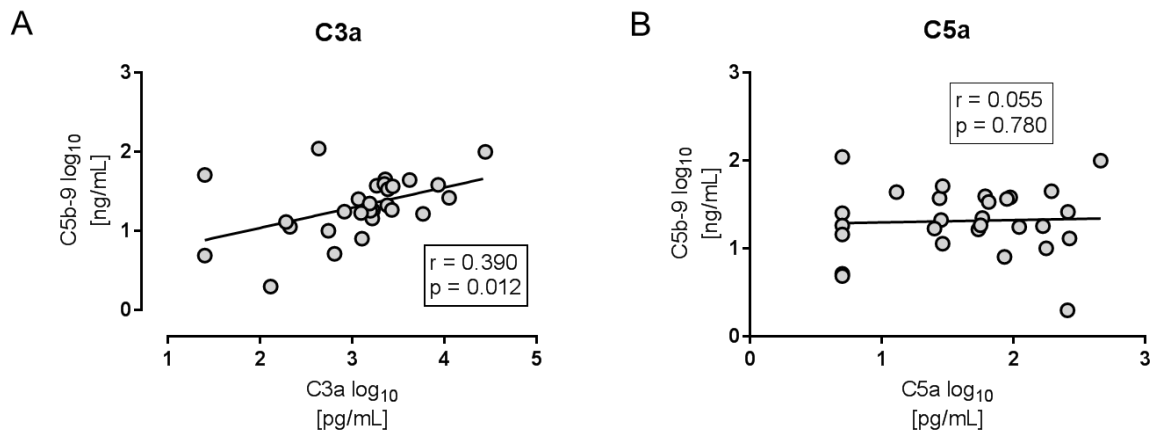


Figure 4-2: Evidence of normal complement activity in BAL fluid from the CF cohort
 Correlations between C5b-9 and **A**) C3a or **B**) C5a. Spearman rank analysis was performed on data from CF BAL fluid with best-fit linear regressions (solid black lines). Statistical outcomes r and p values and in black boxes. $n=28$.

As mentioned in section 3.7.2, there were technical difficulties when performing one of the MSD plates therefore, there was C5b-9 data for 28 out of 40 CF BAL fluid samples. C3a positively correlated with C5b-9 (figure 4-2A) ($r = 0.494$, $p = 0.008$); however, a correlation between C5a and C5b-9 was not significant (figure 4-2B). Data from figure 4-1 and figure 4-2 suggested that there are differences between C3a and C5a generation in the CF airway. An explanation for the difference between C3a and C5a generation could be the differential influence of NSPs within the CF airway. Therefore, the CF cohort was analysed for evidence of NE-mediated generation of C3a and C5a.

4.4.2. Evidence for the generation of C3a and C5a by NE in the CF airway

It has been shown that NSPs are able to generate C3a-like and C5a-like fragments from the respective parent molecules (Wetsel and Kolb 1983; Yuan *et al.* 2015). I analysed the data from the CF cohort for evidence of C3 or C5 proteolysis; for instance lower C3/C5 concentrations in samples with higher NE activity. Cohort data was analysed to explore whether any correlation existed between NE activity and levels of C3 or C5 (figure 4-3).

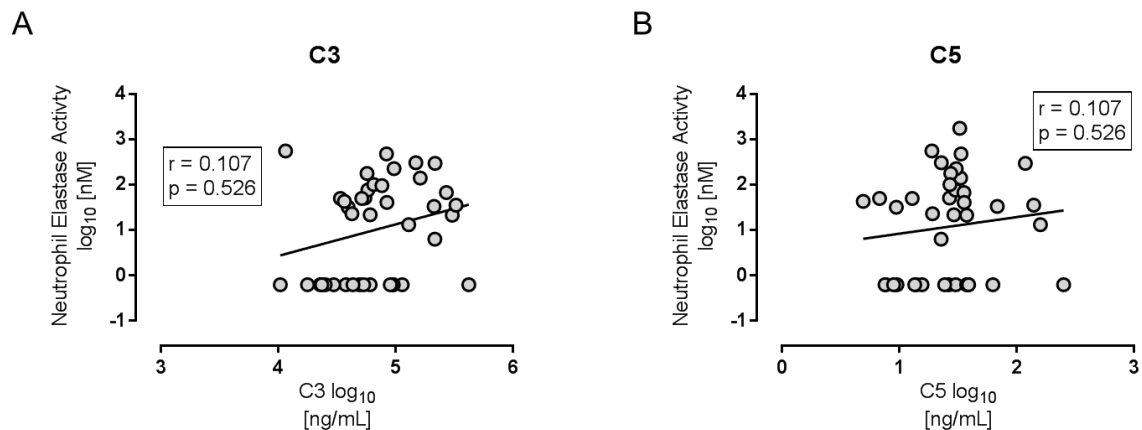


Figure 4-3: Correlation of C3 and C5 proteolysis by NE in BAL fluid from CF patients. Correlations between NE activity and **A)** C3 or **B)** C5. Spearman rank correlation analysis performed on data from CF BAL fluid with best-fit linear regressions (solid black lines). Statistical outcomes r and p values and in black boxes. $n=40$.

Correlations between NE and either C3 or C5 were not significant, suggesting either that NE does not degrade C3 or C5 or, a more likely explanation, given the literature on C3 and C5 proteolysis and C3a/C5a generation, is that, CF is a complex disease and that relationships between NE and either C3 or C5 are not directly related (Huber-Lang *et al.* 2012). NSP-mediated generation of C3a and C5a has previously been reported (Wetsel and Kolb 1983; Yuan *et al.* 2015) and therefore, evidence supporting C3a and C5a generation by NE in the CF airway was investigated.

There was a weak but significant positive relationship between NE and C3a (figure 4-4A) ($r = 0.390$, $p = 0.012$) however, despite a positive trend, the correlation between NE and C5a was not significant (figure 4-4B) ($r = 0.286$, $p = 0.070$). As I mentioned above in explanation of data in figure 4-3, although there was not any strong evidence from analysis of the cohort to support C3a and C5a generation by NE, the relationships between these components may not be simple and further investigation is required to elucidate the mechanism involved.

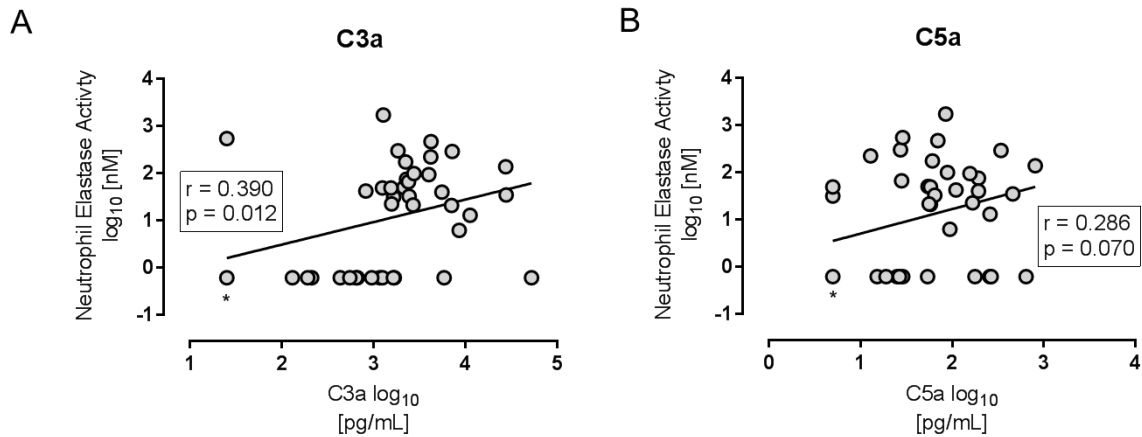


Figure 4-4: Evidence of C3a and C5a generation by NE in BAL fluid from CF patients.

Correlations between NE activity and **A)** C3a or **B)** C5a. Spearman rank correlations performed on data from CF BAL fluid with linear regressions (solid black lines). Asterisks (*) mark overlapping data (A*) n = 2 and (B*) n = 6. Statistical outcomes r and p values and in black boxes. n=41.

Data from CF BAL fluid showed that C3a and C5a were present in the CF airway and that NE correlated with elevated expression of these complement anaphylatoxins. As well as C5a generation, it has been reported that C5a can be degraded by NSPs, reducing activity *in vitro* (Brozna *et al.* 1977). Furthermore, it has been shown that CXCL8, a potent neutrophil chemoattractant in the CF airway is also susceptible to degradation by NSPs (Leavell *et al.* 1997). Like CXCL8, C3a and C5a may also be susceptible to degradation by NSPs which, may explain the weak correlations observed above (figure 4-4). Therefore, although the main aims of this chapter were to characterise generation of C3a and C5a in CF airway I also investigated further proteolysis of C3a and C5a by NSPs.

4.5. Degradation of C5a and C3a by proteases present in the in the CF airway

Recombinant C5a (rhC5a) has been used by others in previous investigations of C5a function (Miyabe *et al.* 2017). There are structural differences between “native”, C5 convertase-generated C5a (nC5a) compared to rhC5a, such differences might affect proteolysis. In particular, rhC5a is expressed in *E. coli*, therefore rhC5a could be alternatively folded compared to nC5a; X-ray diffraction of the two forms have not been compared. Due to expression in a prokaryotic system, rhC5a is not N-glycosylated at asparagine residue at position 64 (see figure 1-21). In addition, a “His-tag” containing sequence (amino acid sequence: MRGSHHHHHHGSDYDIPTTENLYFQGGS (see page 286)) is incorporated into the N-terminal of rhC5a to facilitate purification. For these reasons, nC5a and rhC5a were compared to investigate whether structural differences affected susceptibility to proteolysis.

4.5.1. Optimising the visualisation of C5a on SDS-PAGE.

SDS-PAGE and western blotting was chosen as a method of detecting C3a and C5a proteolysis because it enables visualisation of cleavage fragments. Before performing degradation experiments, separation and detection of rhC5a and nC5a by SDS-PAGE and Western blot was optimised (figure 4-5).

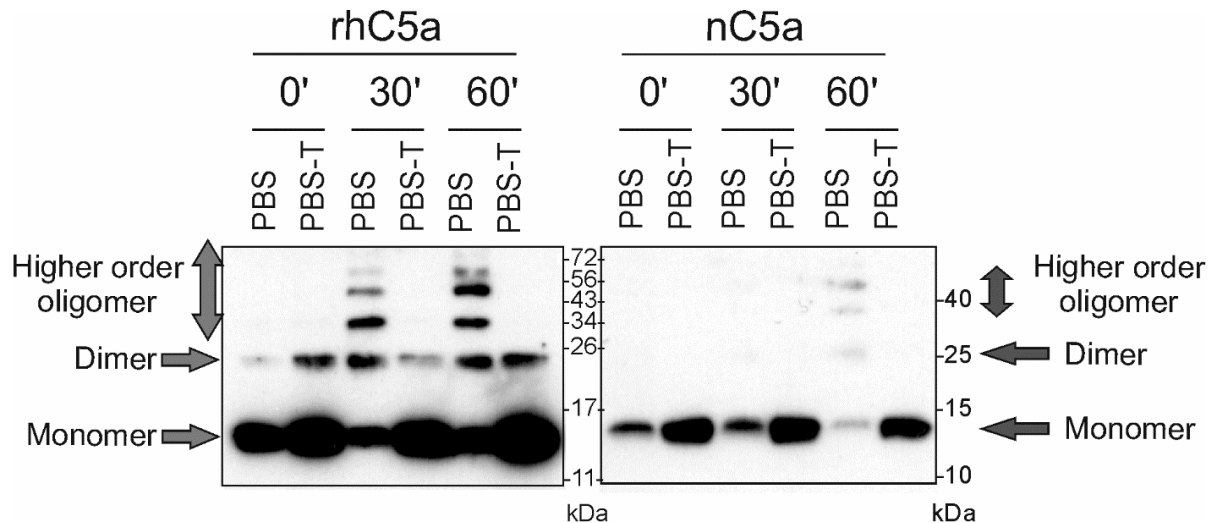


Figure 4-5: Recombinant C5a and native C5a separation and detection by SDS-PAGE and Western blot. Recombinant C5a and native C5a (5 µg/mL) diluted in PBS or PBS-tween-20 (0.05%, v/v) were incubated at 37°C for 30 minutes “30’ ” or 60 minutes “60’ ” or stored on ice “0’ ”. Both C5a forms were resolved under non-reducing conditions on 15% bis-tris polyacrylamide gels by electrophoresis, then transferred to nitrocellulose. C5a was visualised by mouse anti-C5/C5a monoclonal antibody and goat anti-mouse HRP conjugate antibody. Annotation of possible dimers or higher oligomeric structures are marked by arrows. The above blot is from a single gel with a reference ladder resolved between the left and right sides. Representative of n=3.

Recombinant C5a and nC5a forms were incubated at 37°C following dilution in PBS or PBS/Tween-20. C5a and C3a have been reported to be sticky molecules and therefore a detergent, tween-20, was used to reduce aggregation (Klos *et al.* 2013). For western blots, C5a was separated under non-reducing conditions detected using a mouse anti-C5/C5a monoclonal antibody that binds to the c-terminal signaling domain of C5a (see figure 1-21) (Klos *et al.* 1988). The first observation from western blotting was that nC5a had a molecular weight approximately 1 kDa greater than rhC5a, 14 and 13 kDa respectively (figure 4-5). Yet, when the combined mass of each of the constituent amino acids is calculated, the rhC5a sequence has a molecular weight of 11.3 kDa and nC5a has a molecular weight of 8.2 kDa. An explanation could be that nC5a may differ depending of N-glycosylation composition which increases the molecular mass by up to 25%, depending on the variable composition of the N-glycosylation (Fernandez and Hugli 1976). It was also observed that both C5a forms assembled in higher oligomeric structures when diluted in PBS and incubated at 37°C; this

was evident from the molecular weight of the oligomeric bands. For example, rhC5a bands were visualised at ~13 kDa (monomeric), ~25 kDa (dimer), ~36 kDa (trimer), and ~50 kDa (tetramer). The addition of a detergent, tween-20, reduced oligomer formation, increasing band intensity of the monomeric C5a band; however, dimeric rhC5a was still evident at 60 minutes even in the presence of tween-20. The NMR structure of nC5a has been determined; interestingly, the structure was solved using dimeric nC5a, but the relevance of dimeric C5a *in vivo* is not fully understood (Cook *et al.* 2010). For this reason, I modified my experimental procedures to reduce oligomerisation by adding tween-20 to my dilution buffers, this was so that experimentation on C5a was performed when in a monomeric state.

4.5.2. Proteolysis of C5a by purified NSPs

Having optimised C5a resolution by SDS-PAGE, proteolysis of C5a by NSPs was investigated by exposing purified C5a to NE, CG and PR3 and visualising cleavage by western blot (figure 4-6). Degradation of nC5a by NE was observed over a 6 h period, this was evident from a reduction in band intensity, suggesting the loss of the epitope for the mouse anti-C5a c-terminal monoclonal antibody (figure 4-6A). However, some bands did not completely transfer from the gel to the blot given the appearance of reduced signal. Native C5a appeared more resistant to proteolysis by CG and PR3 than NE over 24 h. It is also possible that nC5a was not degraded and nC5a signal was reduced due to sticking of C5a to plastic tubing. Proteolysis of nC5a and rhC5a was compared using a dilution series of NE, CG and PR3 over 1h (figure 4-6B). In support of data from figure 4-6A, there was no observable degradation of nC5a by any of the three proteases over the 1 h at 37°C. Interestingly, rhC5a was more susceptible to degradation by each of the three NSPs than its native counterpart (figure 4-6B and figure 4-6C).

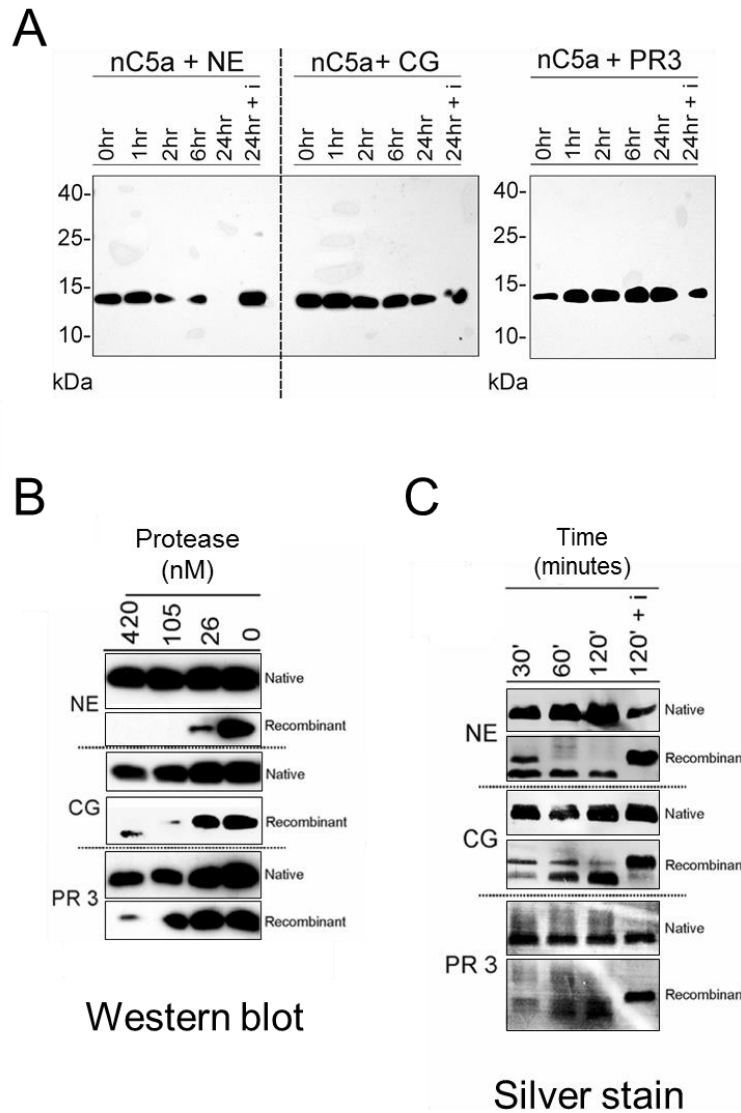


Figure 4-6: Proteolysis of C5a by purified NSPs. **A)** Native C5a (5 $\mu\text{g/mL}$) was exposed to 420 nM of each protease at 37°C for up to 24 h, at 1, 2, 6 and 24 h a sample was removed, and protease activity was arrested by adding 5 mM PMSF. Each protease was also incubated with PMSF “i” prior to incubation with nC5a to show that loss was due protease degradation. Proteins were resolved on 15% bis-tris poly-acrylamide gels and transferred to nitrocellulose for western blotting using mouse anti-C5/C5a monoclonal Ab and detection by goat anti-mouse HRP-conjugate. **B)** Degradation of nC5a “native” was compared to rhC5a “recombinant” when exposed to NSPs over a 4-fold dilution series (420 to 26 nM) for 1 h at 37°C. Proteins were resolved and visualised as for “A”. **C)** Comparing degradation of nC5a and rhC5a using silver staining. C5a was exposed 420 nM of three NSPs for up to 2h, samples were taken at 30', 60' and 120'. As for “A” PMSF was pre-incubated to show degradation was specific to proteases. For “C” blots were cut to only show C5a bands, but NSPs were also visible and can be seen in figure 4-8B (with respect to C3a) n=3 for each figure.

Furthermore, rhC5a exposed to each NSP generated a lower molecular weight fragment when detecting all resolved proteins by silver staining (figure 4-6C). The same lower molecular weight fragments of rhC5a were detected by Western blot when rhC5a was incubated with CG (figure 4-6B). The lower molecular weight fragments generated from rhC5a by NE or PR3

were not detected by Western blot and therefore, reflects that the rhC5a C-terminal epitope for the detection antibody is being cleaved by these proteases. Whereas, for CG the epitope is still present and therefore suggests that the N-terminal is cleaved. None the less, the main observation from these experiments is that nC5a is more resistant to proteolysis by NSPs compared to rhC5a and reveals that the structural differences have implications when investigating C5a exposure to NSPs. Quantification by ELISA would provide further information into the comparable rate of degradation of these two C5a forms.

4.5.3. Degradation of C5a by proteases in CF BAL fluid

The above experiments have shown that rhC5a and, to a lesser extent, nC5a were susceptible to proteolysis by purified NSPs. To investigate the hypothesis that C5a in the CF airway is susceptible to degradation, both C5a forms were incubated with CF BAL fluid (figure 4-7). Three BAL fluid samples were chosen that had increasing NE activity. Additionally, BAL 3, that had the highest NE activity, was pre-incubated with a serine protease inhibitor (PMSF) to investigate whether NSPs were responsible for degradation.

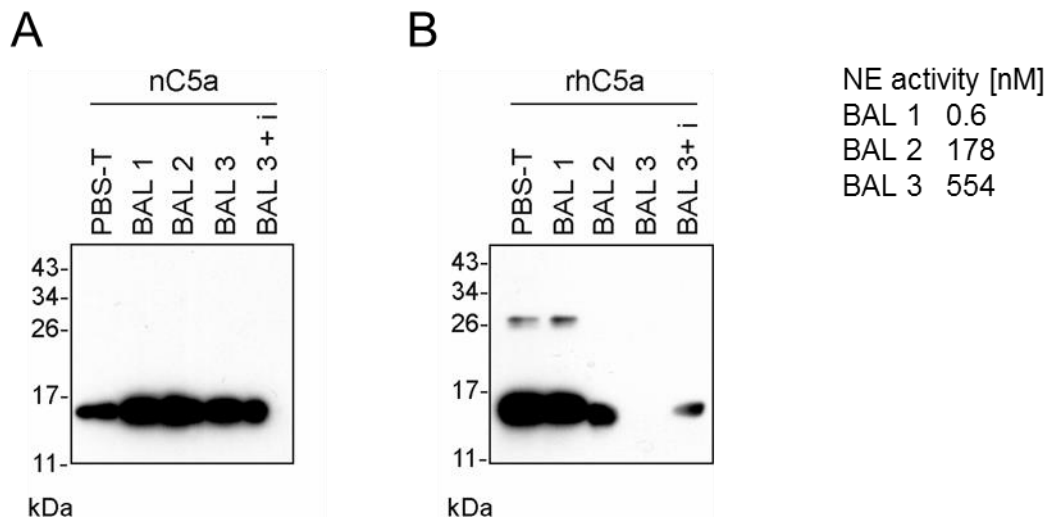


Figure 4-7: Degradation of C5a by proteases present in BAL fluid from CF patients. Native C5a (A) or rhC5a (B) (5 µg/mL) was incubated with PBS-T or one of three BAL fluid (BAL1, 2, or 3) for 1 h at 37°C. After incubation 5 mM PMSF was added. BAL 3 was also incubated with PMSF “i” prior to incubation with C5a to show that serine proteases were responsible for degradation. Proteins were resolved on 15% bis-tris poly-acrylamide gels and transferred to nitrocellulose for western blotting using mouse anti-C5/C5a monoclonal Ab and detection by goat anti-mouse HRP-conjugate, n=2.

From western blots in figure 4-6B it was observed that rhC5a was susceptible to proteolysis by proteases present in CF BAL fluid when exposed for 1 h at 37°C. In support of experiments performed with purified proteases, there was evidence of rhC5a degradation when exposed to BAL 2 and BAL 3, these BAL fluid samples had 178 nM and 554 nM NE activity respectively.

Inhibition of serine protease activity in BAL 3, the sample with highest NE activity, partially prevented degradation, suggesting that serine proteases are at least partly responsible for proteolysis of rhC5a. There was no evidence of nC5a degradation following exposure to any of the CF BAL fluids tested (figure 4-7A); however, part of the "BAL3 + I" is missing due to inefficient transfer from the gel. These data further supported data from experiments where nC5a was incubated with purified NSPs and showed that nC5a was resistant to degradation (figure 4-6A). The above experiments show that the structural difference in rhC5a compared to nC5a has implications when exposing to purified NSPs and those present in CF BAL fluid. Furthermore, despite reports that C5a is susceptible to proteolysis by these proteases, in my experiments nC5a was resistant to degradation (Brozna *et al.* 1977).

4.5.4. C3a proteolysis by purified NSPs

Proteolysis of native C3a by NSPs was also investigated. Initial observations (not shown) suggested that native C3a did not aggregate as observed with C5a; however, C3a cleavage experiments were still performed in PBS-tween20 so that a comparison with C5a could still be made. Replicating C5a experiments, C3a was exposed to purified NE, CG or PR3.

Degradation of C3a was visualised by western blot using a mouse anti-C3/C3a monoclonal antibody that recognises the C3a C-terminal signaling region (figure 4-8). C3a was readily degraded by NE and PR3 but not CG following 1 h exposure when detecting degradation by western blot. Proteolysis of C3a by NE and PR3 was prevented by pre-incubating each NSP with PMSF. To visualise break-down products that do not possess the epitope for the monoclonal antibody, gels were stained for protein using silver nitrate (figure 4-8B). Interestingly, the extent of C3a degradation observed in figure 4-8A was less pronounced when visualised by silver stain suggesting that the antibody epitope used for western blotting was susceptible to degradation. Moreover, cleavage of C3a did not clearly reduce molecular weight suggesting that degradation may be minor and only cleave the C-terminal signaling domain. Further analysis by mass spectrometry would help compare the molecule weights of C3a following exposure to NSPs. C3a exposed to CG appeared more susceptible to degradation than when fragments were visualised by western blotting. This phenomenon suggested that there was a subtle cleavage site for this protease within the epitope for the monoclonal antibody used in this stain.

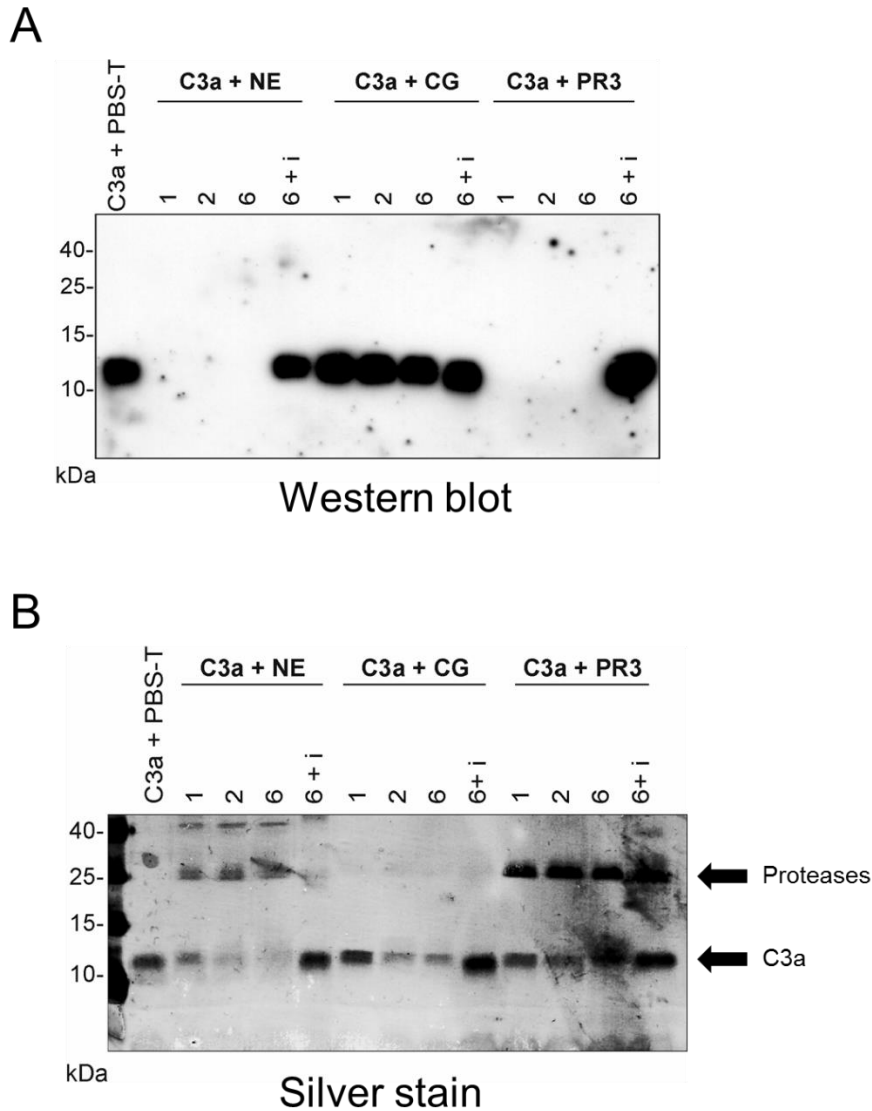


Figure 4-8: Proteolysis of C3a by purified NSPs. C3a (5 $\mu\text{g/mL}$) was exposed to 420 nM of each NSP at 37°C for up to 24 h, at 1, 2 and 6 h a sample was removed, and protease activity was arrested by adding 5 mM PMSF. NSPs were also pre-incubated with PMSF “i” prior to incubation with C3a, to show that loss was due serine protease degradation. Proteins were resolved on 15% bis-tris polyacrylamide gels and visualised **(A)** proteins were transferred to nitrocellulose for western blotting using mouse anti-C5/C3a monoclonal Ab and detection by goat anti-mouse HRP-conjugate. **(B)** Gels were stained with silver nitrate for visualise total protein. n=3 for both sets of experiments.

In section 4.4.2 I reported weak correlations between NE and C3a or C5a. I hypothesised that C3a and C5a could be susceptible to degradation by NSPs present in the CF airway. In this section it was observed that C3a was more susceptible to degradation by NSPs than nC5a, when exposed to the same protease concentration over the same time period. As well as hypothesising that C3a and C5a could be susceptible to proteolysis, I also hypothesised that NSPs generate C3a and C5a from parental C3 and C5. In the next section, atypical generation of C3a and C5a by NSPs was investigated.

4.6. Generation of C3a and C5a by proteases present in CF BAL fluid.

To investigate C3a and C5a generation in the CF airway, C3 or C5 was incubated with CF BAL fluid samples from five patients (figure 4-9). BAL fluid was selected by level of NE activity so that there was a range from high (1.74 μM) to low (0.01 μM) activity. Each BAL fluid sample was also pre-incubated with or without serine protease inhibitor, PMSF, to determine if serine proteases were responsible for any C3a or C5a generation observed.

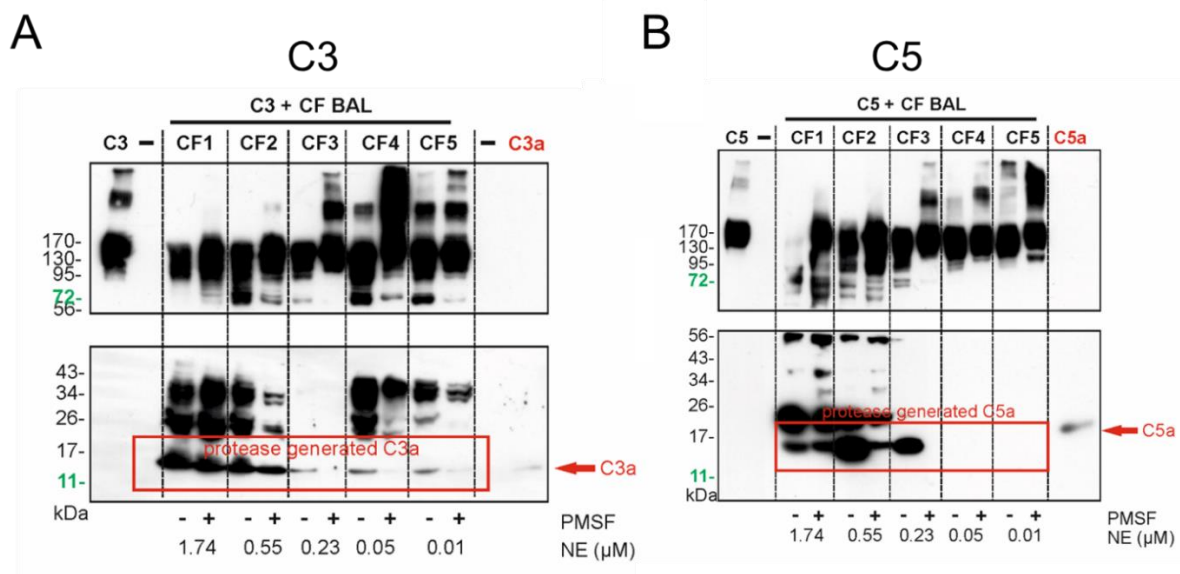


Figure 4-9: C3a and C5a generation by proteases expressed in BAL fluid from the CF cohort. C3 (A) and C5 (B) were incubated at 37°C for 1 h with five CF BAL fluid samples (CF1 to 5) that had a range of NE activity. CF BAL fluid was also pre-incubated with (+) or without (-) 5mM PMSF. Proteins were resolved by SDS-PAGE on 4-20% tris-glycine gradient polyacrylamide gels. Generation of C3a and C5a was visualised by western blot using mouse anti-C3/C3a or mouse anti-C5/C5a monoclonal antibodies respectively with detection by goat anti-mouse HRP conjugate secondary antibody. For staining, blots were cut at 56 kDa reference maker and stained identically. For developing top blots (containing C3 and C5) were incubated in low sensitivity ECL, bottom blots (containing C3a and C5a) were incubated with high sensitivity ECL. C3, C3a, C5, nC5a (red) without CF BAL fluid were also resolved for reference. Red boxes indicate suspected C3a-like and C5a-like fragments, red arrow indicates molecular weight of C3a or C5a respectively. Blots representative of n=2.

Interestingly, C3a-like or C5a-like fragments of similar molecular weight to their convertase-generated counterparts were produced when C3 or C5 were incubated with CF BAL fluid that had the highest NE activity. Unfortunately, a comparison of molecular weight between C5a-like fragments and nC5a was difficult to make due to a “smile” in gel used to resolve C5. Generation of C3a-like fragments was observed even when C3 was incubated with CF5, that had low NE activity (figure 4-9A), suggesting that C3 is labile and that C3a is readily generated by protease in CF BAL fluid. Unlike C3a, C5a-like forms were not detected when C5 was incubated with CF4 or CF5 (figure 4-9B).

Pre-incubating CF1 with PMSF did not appear to prevent generation of C3a-like and C5a-like fragments. Addition of PMSF to CF2 and CF3 had a more obvious effect on C3a and C5a generation. Visually, band intensity for C5a-like fragments was greater when C5 was incubated with CF2 and CF3 compared to CF1, despite less NE activity in these samples. These data suggest that C3 may be more susceptible than C5 to degradation by proteases present in CF BAL fluid. Moreover, it has been shown that both C3 and C5 are susceptible to proteolysis by non-serine proteases however, pre-incubation of BAL fluid with PMSF demonstrated that serine proteases are predominantly responsible for C3a-like and C5a-like generation.

C5a-like fragments, with similar molecular weight to nC5a, were generated when C5 was exposed to each of the three NSPs (figure 4-10A). Despite previous reports of C5a generation by NE and CG, this is the first time that PR3 has been shown to generate C5a-like fragments (Brozna *et al.* 1977; Kolb *et al.* 1981; Giles *et al.* 2015). I observed that NE-generated C5a was subject to further degradation when incubated over 6 hours; this was visually evident by reduced band intensity of NE-generated fragments at 6 h compared to 2 h.

Pre-incubating the separate NSPs with PMSF prevented C5 degradation, demonstrating that the NSPs were responsible for C5a generation. Interestingly, the band pattern of C5 breakdown products differed for each protease, highlighting the variation in cleavage site specificity and potential for the generation of alternative forms of C5a.

Giles *et al.* reported a 1 kDa difference between nC5a and C5a-like fragments generated by NE (Giles *et al.* 2015). It was not clear from my own 4-20% tris-glycine gels whether there were any minor differences in molecular weight between nC5a and the C5a-like fragments generated by NSPs (figure 4-10A). To make a comparison of NSP-generated C5a-like forms easier, fragments were resolved on a 20% bis-tris polyacrylamide gel. C5 was exposed to serially diluted NSPs from 420 to 105 nM for 1 h at 37°C (figure 4-10B). The generation of C5a-like fragments (band intensity) was titratable with the concentration of each protease. Interestingly, higher molecular weight C5a-like bands were produced following exposure of C5 to 105 nM CG compared to 420 nM. On closer inspection, the band generated by 420 nM CG appeared to be of a lower molecular weight than nC5a. Even when resolving C5a-like fragments with 20% acrylamide gels, I could not confirm data from Giles *et al.* that showed that NE-generated C5a had a higher molecular weight than nC5a (Giles *et al.* 2015). I also could not detect a difference in molecular weight between PR3-generated C5a and nC5a.

In the above experiments I have shown that each NSP can generate C5a-like fragments that are of similar molecular weight to nC5a however these data did not indicate whether these fragments are functional. The monoclonal antibody used for detection in the above experiment (figure 4-10) binds to an epitope on the C5a signaling domain in the C-terminal and therefore, suggests that the C5a-like fragments generated by NSPs possess the signaling domain and could be functional. The activity of C5a-like fragments generated by NSPs was investigated using a U937 monocyte reporter cell line that had been stably transfected with C5aR1.

4.7.2. Assessing the functional activity of NSP-generated C5a-like fragments using a U937-C5aR1 reporter cell line

Intracellular calcium signaling in U937-C5aR1 has previously been used to investigate the activity of C5a-like fragments generated by NE (Giles *et al.* 2015). As discussed in section 1.4.3a, calcium flux is important for G-protein coupled receptors, such as C5aR1, to signal and induce a cellular response like ROS production and chemotaxis. Monitoring intracellular calcium flux enables real-time observation of receptor activation and cell stimulation. In this assay, a fluorochrome (Fura-2-acetoxymethyl ester) is incubated with U937-C5aR1 cells whereby, it diffuses through the cell membrane. Once inside the cells, acetoxymethyl ester is cleaved from Fura-2 by cytoplasmic esterases preventing Fura-2 from diffusing back out. Fura-2 binds to intracellular calcium, fluorescence of Fura-2 is measured at 340 and 380 nm and the ratio 340/380 is calculated to give an approximation of the intracellular calcium concentration. Monocytes use extracellular calcium to initiate intracellular flux. Therefore, in the calcium signaling assay the calcium concentration in assay buffers was known and enabled the calculation of intracellular calcium concentration during signaling events.

4.7.2.a. Optimisation of an intracellular calcium signalling assay for measuring the activity of C5a-like fragments.

Initially, a titration of nC5a was performed to assess the sensitivity of U937-C5aR1 cells (Figure 4-11A). Native C5a induced a concentration dependent increase in intracellular calcium U937-C5aR1, and calcium release could still be detected at 25 ng/mL nC5a (figure 4-11A). A potent C5aR1 antagonist was titrated to determine the concentration required to prevent intracellular calcium release in U937-C5aR1 stimulated by 250 ng/mL of nC5a (Figure 4-11B). This preliminary experiment was to confirm that U937-C5aR1 activity in this and future experiments was a result of C5aR1 stimulation, rather than non-specific activation of another G-protein coupled receptor expressed on the surface leading to intracellular calcium release. These experiments indicated that 25 μ M antagonist was sufficient to prevent U937-C5aR1 activation by 250 ng/mL nC5a. Therefore, this concentration of antagonist was used in future experiments.

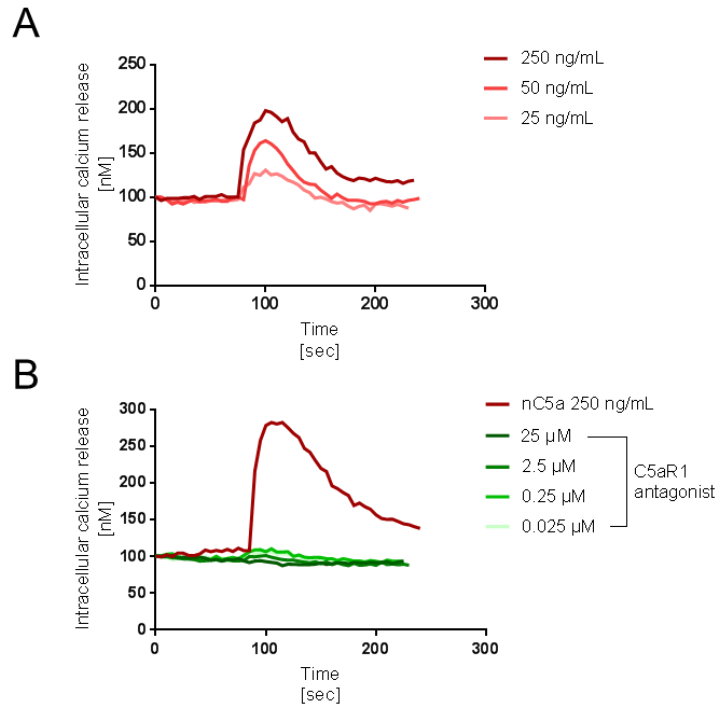


Figure 4-11: Optimising a U937-C5aR1 C5a reporter assay. (A) U937-C5aR1 loaded with Fura-2 were stimulated with 250, 50 and 25 ng/mL nC5a. **(B)** U937-C5aR1 cells were also stimulated with 250 ng/mL nC5a following pre-incubating cells with Krebs-HEPES buffer or a 10-fold dilution series from 25 to 0.025 μM of C5aR1-specific antagonist NDT9513727 for 15 minutes at room temperature (green shades). Fluorescence of calcium-bound Fura-2 was measured every five seconds until signaling event plateaued. Data are from single experiments.

4.7.2.b. Assessing the activity of C5a-like fragments generated by purified NSPs.

To investigate the activity of C5a-like fragments, C5 cleavage experiments were performed as they were for the SDS-PAGE analysis (figure 4-10) and samples used to stimulate intracellular calcium release from U937-C5aR1 (figure 4-12). Purified C5 was exposed to individual NSPs for 2 and 6 h at 37°C, protease activity was arrested using a native serine protease inhibitor, AAT. C5 was also exposed to individual NSPs that had been pre-incubated with AAT to verify that U937-C5aR1 signalling was a consequence of C5a generation by NSPs. In addition, U937-C5aR1 cells were pre-incubated with the C5aR1 antagonist tested in the previous section (figure 4-11b), this was to verify that any calcium signaling events observed were a result of C5aR1 activation.

C5 cleavage fragments generated following exposure to either NE, CG or PR3 induced intracellular calcium release within U937-C5aR1 (figure 4-12A – C). Confirming data from western blots, prolonged incubation with each protease reduced the activity of C5a-like fragments, diminishing calcium response at the 6 h time point. Furthermore, pre-incubating each protease with AAT, prevented signaling, confirming that calcium release is mediated by protease degradation of C5.

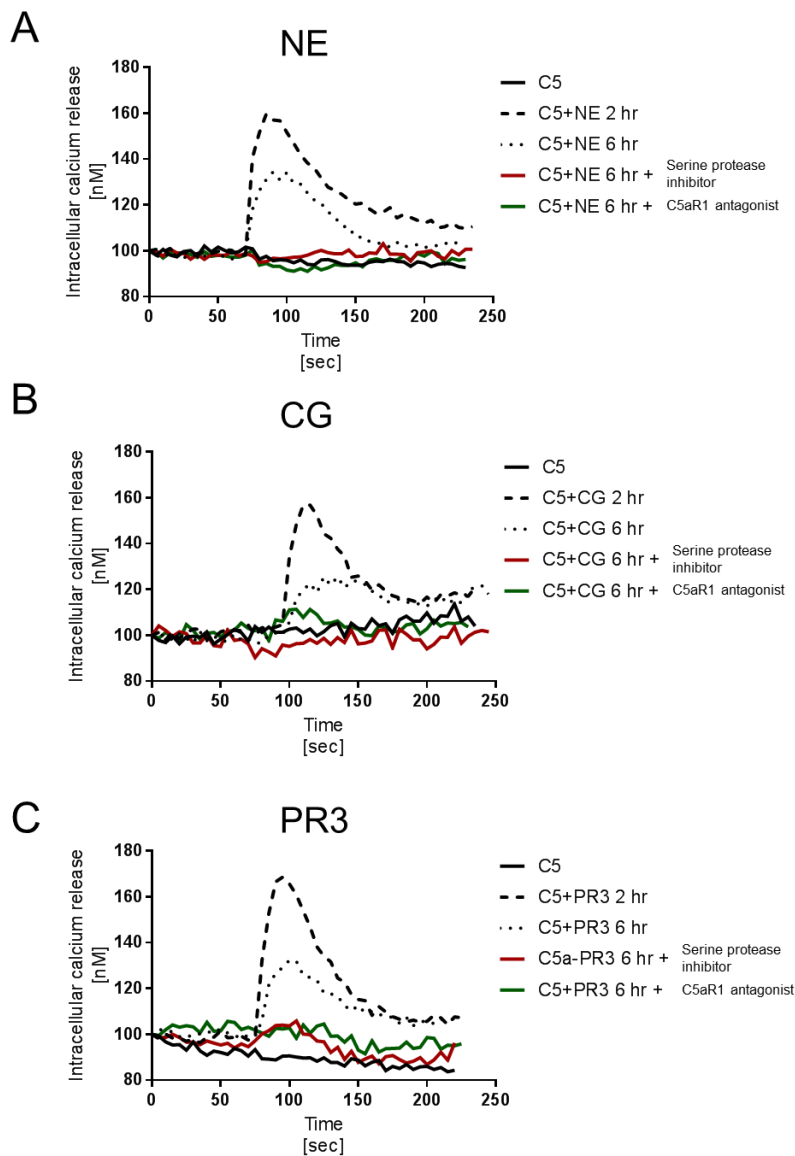


Figure 4-12: Assessing the activity of NSP-generated C5a using U937-C5aR1 cells. C5 was incubated with 420nM (A) NE (B) CG, or (C) PR3 for 2 h (black dashed line) or 6 h (black dotted line) at 37°C. C5 was also exposed for 6 h with each protease pre-incubated with AAT (solid red line). To show C5aR1-specific stimulation cells were pre-incubated with C5aR1 antagonist for 15' at room temperature (solid green line). Samples were diluted 1/20 in Krebs-HEPES buffer prior to cell stimulation and kept on ice. Fluorescence of calcium-bound Fura-2 (y-axis) was measured every five seconds (x-axis) until signaling event plateaued. Data is representative of 2 experiments for each protease.

Cells were incubated with a potent C5aR1 antagonist to verify that the signal induced by NSP-generated C5a-like fragments was a consequence of C5aR1 activation. Pre-incubating cells with NDT9513727 prevented calcium release under all NSP conditions, confirming C5a-like signaling is mediated through C5aR1. C5a-like fragments, generated by each protease, induced comparable calcium response after 2 hours, ~160-170 nM. Calcium response in U937-C5aR1 was variable over different days and therefore, graphs in figure 4-12 are representative of responses observed from two experiments.

4.7.3. Comprehensive analysis of C5a-like fragments generated by NSPs

In the previous sections I have investigated the generation of C5a by NSPs and shown that each NSP is able to generate a C5a-like fragment that is biologically active and induces calcium flux in U937-C5aR1 monocytes. In the next section, I will further characterise NSP-mediated C5a generation and C5 degradation by quantifying C5a and C5 concentrations after exposing C5 to individual NSPs for 15, 30, 60 and 120 minutes at 37°C. In addition, samples from the same experiments were used to measure C5 activity in a complement hemolysis assay. This was to investigate the effects of NSPs on the function of C5. Samples from each experiment were diluted for each assay type to allow accurate measurement on each platform, for example; 1/5000 for C5a ELISA, 1/5000 for C5 ELISA and 1/47 for haemolysis assays. The remaining sample was diluted in loading buffer and loaded on to 4-20% polyacrylamide gels.

4.7.3.a. Quantifying the rate of C5a-like fragment generation by NSPs.

The rate of C5a generation by NSPs was measured by commercial C5a ELISA (Quidel) that has no reported cross-reactivity for C5 (figure 4-13).

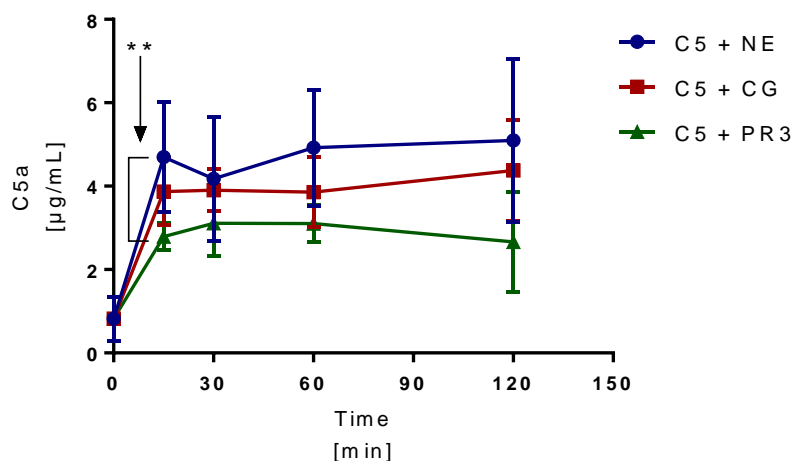


Figure 4-13: Quantification of C5a generation by NSP proteolysis of C5. C5 was exposed to each NSP for 15, 30, 60 and 120 minutes at 37°C (x-axis). Cleavage fragments were diluted 1 in 5000 in sample buffer provided by the manufacturer, C5a was quantified by C5a ELISA (commercial). C5a concentration in each sample was interpolated from a standard curve provided by the manufacturer. Obtained values were multiplied by the dilution factor and plotted above (y-axis). At t=0, C5 was measured without NSP (untreated). Data plotted as mean \pm SEM. Statistical analysis by Two-way ANOVA with Tukey's test for multiple comparisons, n=3.

Interestingly, detectable C5a was generated within 15 minutes of exposing C5 to each NSP. At the same time point, NE generated 4.7 ± 1.3 $\mu\text{g/mL}$ C5a, statistically more, than PR3 (2.8 ± 0.3 $\mu\text{g/mL}$, $p=0.0014$) but not significantly more than CG (3.9 ± 0.8 $\mu\text{g/mL}$, $p=0.463$). After the first 15 minutes there was no statistically significant change in C5a concentration, irrespective of the NSPs that C5 was exposed to. After 2 h there was no statistical difference in C5a concentration when comparing each NSP. Visually, C5a concentration, when C5 was incubated with PR3, appeared to increase over 30 minutes then decrease after 120 minutes; however, there was not enough evidence to support this observation statistically. In summary of figure 4-13, the majority of C5a is generated by each of the NSPs within 15 minutes with NE having the highest C5a-generating activity. As well as characterising C5a generation, I also investigated C5 degradation by measuring C5 concentration in the same samples.

4.7.3.b. Quantifying the rate of C5 proteolysis by NSPs.

C5 degradation by NSPs was also quantified by in-house C5 ELISA, as used for quantification of C5 in CF BAL fluid in section 3.7.1. In section 3.7.1, I used a combination of antibodies (SKY59-Hycult) in the C5 ELISA to enable the quantification of intact C5. In this ELISA SKY59 binds the C5 β chain and the Hycult anti-C5 antibody binds the C5 α chain (figure 4-14). Additionally, a second in-house C5 ELISA (SKY59-2D5) was also performed in section 3.7.1. This alternative C5 ELISA uses an in-house mouse anti-C5 antibody specific to the C5 α chain for detection. Therefore, following exposure of C5 to NSPs, the two different C5 ELISAs could potentially detect different C5 fragments, with the SKY59:Hycult pairing detecting more intact C5 and the SKY59:2D5 pairing potentially detecting partially degraded C5.

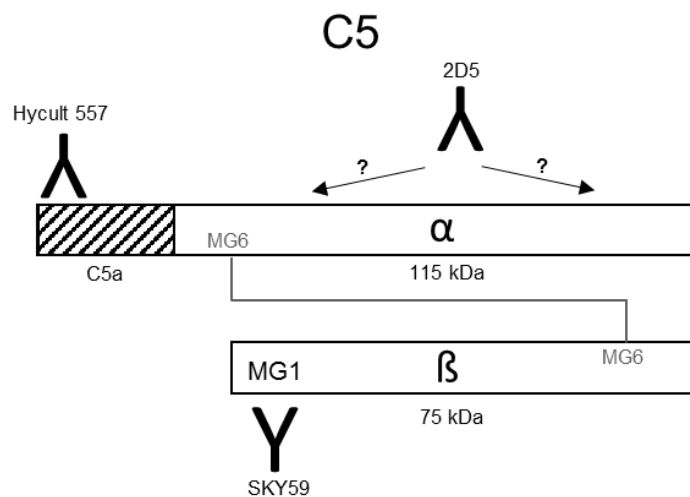


Figure 4-14: Simplified structural diagram of C5, adapted from Barnum *et al.* 2018. C5 comprises of two chains α and β , these are joined by a single disulphide bond (MG6-MG6). C5a (hashed box) is cleaved from C5 α . Hycult 557 antibody binds to the C-terminal pentapeptide. SKY59 binds to α -2-macroglobulin 1 (MG1) on C5 β . The suspected binding site of 2D5 (in-house) monoclonal is on C5 α .

C5 was quantified in the same samples used for the quantification of C5a, from the experiments performed in the previous section (figure 4-15).

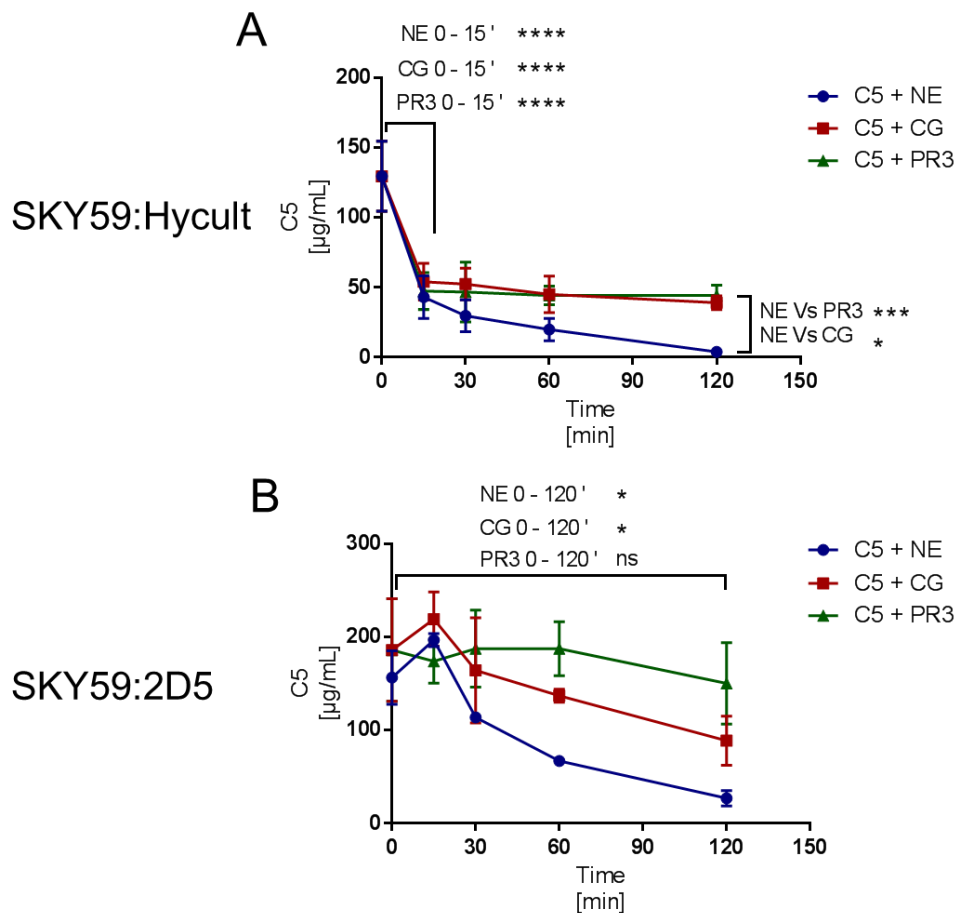


Figure 4-15: Quantification of C5 following exposure to NSPs. C5 was exposed to each NSP for 15, 30, 60 and 120 minutes at 37°C (x-axis). Cleavage fragments were diluted 1 in 5000 in 1% BSA, C5 was quantified by in-house C5 ELISA using either **A)** SKY59-Hycult antibody pairing or **B)** SKY59-2D5 pairing. C5 concentration in each sample was interpolated from a standard curve (same for both antibody pairings). Obtained values were multiplied by the dilution factor and plotted above (y-axis). At t=0, C5 was measured without NSP. Data plotted as mean ± SEM, statistical analysis by Two-way ANOVA with Tukey's test for multiple comparisons, n=3.

When C5 was measured using SKY59-Hycult C5 ELISA antibody pairing, there was a statistically significant difference in mean C5 concentration between C5 ($129.5 \pm 25.1 \mu\text{g/mL}$) and C5 exposed to either NE ($42.9 \pm 15.2 \mu\text{g/mL}$), CG ($53.9 \pm 13.3 \mu\text{g/mL}$) or PR3 ($47.3 \pm 13.1 \mu\text{g/mL}$) after 15 minutes ($p < 0.0001$ in each case, figure 4-15A). From the same data, there was also a statistically significant difference in mean C5 concentration when C5 was exposed to NE ($3.6 \pm 1.9 \mu\text{g/mL}$) over 120 minutes than when exposed to CG ($38.9 \pm 4.9 \mu\text{g/mL}$) or PR3 ($44.1 \pm 7.4 \mu\text{g/mL}$) over the same time period; $p = 0.023$ and $p = 0.008$ respectively.

Interestingly, different trends were observed using the SKY-2D5 antibody pairing; a statistically significant difference in C5 concentration was demonstrated for NE and CG

between 0 and 120 minutes; $p=0.020$ and $p = 0.035$ respectively (figure 4-15B). The difference in C5 concentration when exposed to PR3 was not significant between 0 and 120 minutes. There was also no significant difference between each protease at each time point. These data further highlight difficulties in accurately measuring C5 in diseases characterised by neutrophilic inflammation. This is because the C5 ELISA being used for quantification may detect partially degraded C5 that may not be functional (C5b-9 (MAC) formation), this will be investigated later in section 4.7.3e.

4.7.3.c. Combining data from C5a generation and C5 degradation experiments.

Further analysis of C5a generation was performed by converting the concentration of C5a and C5 measured by ELISAs to molar concentrations. This enabled the calculation of percentage conversion from C5 to C5a and other non-C5a intermediate breakdown products (figure 4-16).

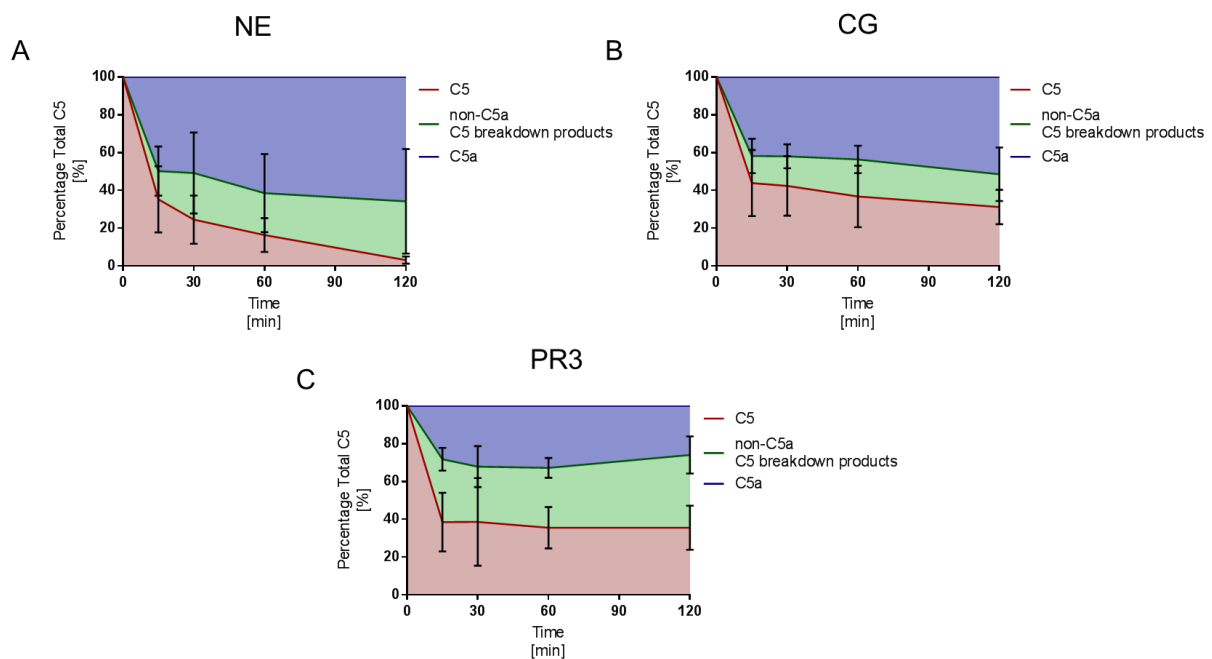


Figure 4-16: Percentage conversion of C5 to C5a and other non-C5a intermediates. Data from figure 4-13 and figure 4-15 (SKY59:Hycult ELISA pairing data) were converted to molar concentrations for A) NE B) CG and, C) PR3. C5a (blue) was calculated as a percentage of C5 (red). Other non-C5a intermediates (green) were calculated by subtracting percentage C5a from percentage C5 ($C5 - C5a = \text{non-C5a intermediates}$) (y-axis). Data is plotted against time (x-axis) Data plotted as mean \pm SEM, $n = 3$.

NE converted approximately 60% of C5 to C5a over 120 minutes, whereas in comparison CG converted approximately 50% of C5 to C5a and PR3 converted approximately 30% (figure 4-

16). Therefore, NE is the most potent at generating C5a-like fragments however, these data do not take into consideration subsequent simultaneous degradation of C5a-like fragments, as discussed earlier in this section.

As well as characterising NSP-mediated C5a generation, the effects of C5 degradation on activity were also investigated. In figure 4-15, it was observed that intact C5 concentration, measured by the C5 ELISA (SKY59-Hycult), decreased by almost 70% within 15 minutes exposure to NE. Further evidence of rapid C5 degradation was also visualised by western blot (section 4.7.1), yet it is not known what effect this has on the ability to contribute to terminal complement pathway activation and MAC formation. To address this, C5 activity following exposure to NSPs was measured using a haemolysis assay.

4.7.3.d. Optimising the complement haemolysis assay for measuring C5 activity following exposure to purified NSPs.

The haemolysis assay measures complement activity by lysing sheep erythrocytes that have been sensitised with rabbit anti-sheep erythrocyte antibodies. Human serum is added to the erythrocytes as a source of complement components. Complement activation is triggered by the anti-sheep antibodies, forming MAC on the erythrocytes causing lysis. Consequently, haemoglobin from the erythrocytes is released into the supernatant, giving a red hue. Measuring absorbance of the supernatant at 405 nm enables calculation of percentage lysis compared to maximum lysis, induced by incubating the erythrocytes with water.

The haemolysis assay was optimised to investigate the effects of NSP exposure on C5 function. C5-depleted serum was used as a complement source in haemolysis assays. This allowed me to undertake experiments C5, which then could be added back to investigate the impact of C5 modification. Furthermore, normal serum contains protease inhibitors, such as AAT, that would make performing these experiments on whole serum difficult. This is because these inhibitors would prevent the generation of C5a-like fragments by the NSPs, as shown in the previous experiments.

It has previously been shown that atypical cleavage of C5 by NE may be a mechanism for complement activation through the generation of functional C5b (Vogt 2000). Testing the

generation of functional C5b is complex and requires purifying individual complement components to “build-up” the terminal complement cascade and MAC formation. In my project I am interested in alternative activation of complement by non-complement proteases but have focused on C5a (and C3a generation) by NSPs. Despite this, I am aware that NSPs could generate functional C5b as well as C5a. Therefore, a single preliminary experiment was performed whereby C5 was titrated to a concentration that could induce 50 % lysis when added back to C5-depleted serum. This was to enable the detection of reduced or potentially increased complement activity mediated via C5 cleavage by NSPs. In these experiments 1% C5-depleted serum was used so that less C5 and serum was required, both precious resources. In order to establish the concentration of C5 required for 50% lysis, C5 was serially diluted in 4-fold increments from 2660 ng/mL to 0.14 ng/mL (final concentration) and added to C5-depleted serum (figure 4-17).

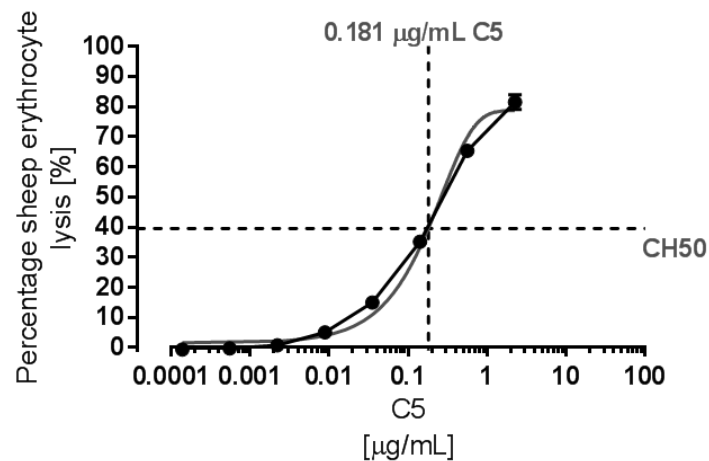


Figure 4-17: Determining the concentration of C5 required for 50% lysis in 1 % C5-depleted serum. C5 was diluted 4-fold serially from 2660 ng/mL to 0.14 ng/mL (x-axis) and added to C5-depleted serum. Complement activity was compared by measuring lysis of sensitized sheep erythrocytes (y-axis). Non-linear dose-response curve was fitted on triplicate values from a single experiment and final C5 concentration at 50% lysis calculated (dashed cross-hair).

I observed that erythrocyte lysis, as a measure of complement activity, decreased as C5 was diluted. A dose-response curve was fitted by GraphPad prism®, assuming maximum lysis at 2.66 µg/mL C5. It should be noted that 100% erythrocyte lysis, induced by incubation of sheep cells with water, was not achieved through complement activation using this protocol. Therefore, 50% on the dose-response curve was achieved at approximately 39.5% sheep erythrocyte lysis. Interpolating 39.5% lysis value from the fitted curve gave a final C5 concentration of 0.181 µg/mL. This meant that samples from the C5 cleavage experiments were diluted by 1/47, a factor that equated to 0.181 µg/mL C5.

4.7.3.e. Measuring C5 activity following exposure to purified NSPs

Samples from the above C5 cleavage experiments, used to characterise C5a generation and C5 degradation by NSPs, were also used to measure C5 activity in the optimised haemolysis assay. Based on the analysis in figure 4-17, C5 samples were diluted 1/47 so that untreated C5 led to approximately 50% sheep erythrocyte lysis (figure 4-18). This was to allow the detection of increased or decreased C5 activity.

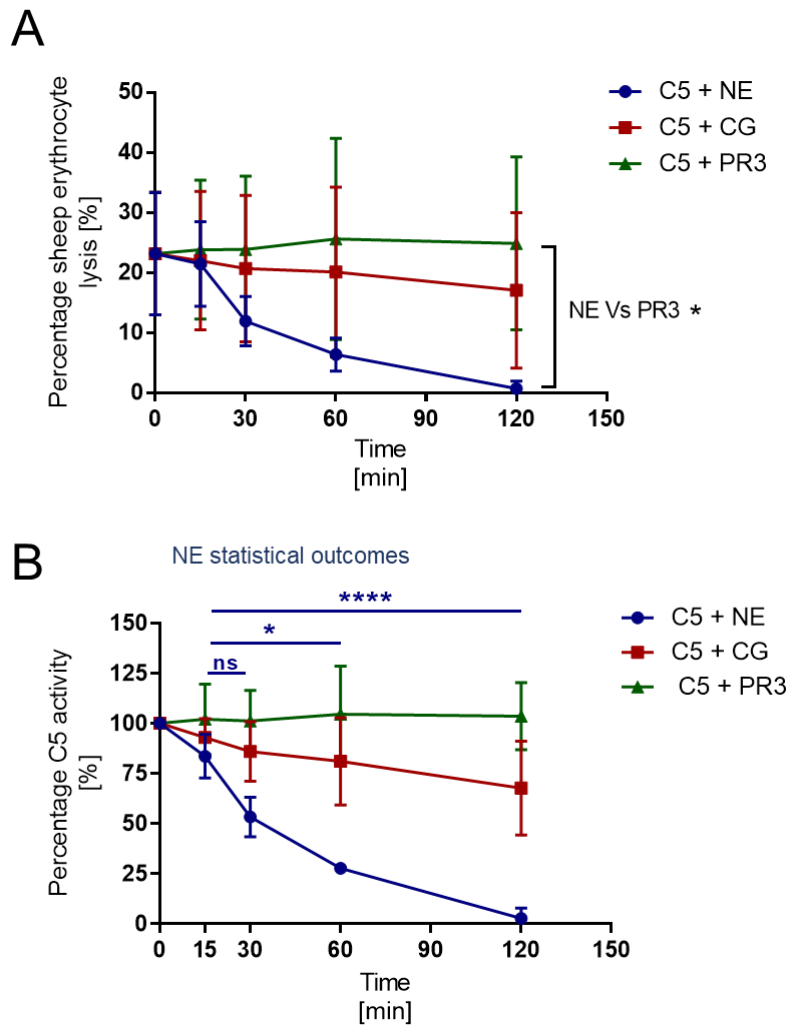


Figure 4-18: Assessing C5 activity following exposure to NSP. A) Haemolysis assay was performed using samples from the above experiment series. C5 was exposed to NE (blue), CG (red), and PR3 (green) over 15, 30, 60, and 120 minutes at 37°C (x-axis). Samples were diluted (1 in 47) so that C5 was limited to give 50% sheep erythrocyte lysis (y-axis). **B)** Data from “A” was standardised by calculating percentage C5 activity using t=0 as 100%. Statistical comparisons for both plots were by Two-way ANOVA with Tukey’s test for multiple comparisons. For “B” statistical outcomes are for NE only (blue) and compare activity between 15 mins and all other later time points, all other comparisons were not significant, Data plotted as mean ± SEM, n=3.

Despite diluting samples so that untreated C5 gave a theoretical value of 50% lysis, in the current experiment I observed values that gave a mean of 23.2%. This is probably because the calculation of C5 required for 50 % was made from a single experiment. None the less, an increase or decrease would still be able to be detected because this value was still on the exponential part of the curve from figure 4-17. C5 exposed to NE rapidly lost activity, as shown by a reduction in sheep erythrocyte lysis. At t=120 minutes, there was a statistically significant difference in erythrocyte lysis when C5 had been exposed to NE compared to PR3 (p=0.032). Interestingly, despite C5 concentration (SKY59:Hycult) decreasing by over 60% when exposed to PR3 (figure 4-15A), C5 function was retained between t=0 and t=120 minutes. This contrast in ELISA and activity data reveals differences in cleavage site preference between the different PR3. Furthermore, C5 may retain function despite susceptibility to cleavage by PR3.

To reduce variation in these data erythrocyte lysis was standardised; this was done by calculating percentage C5 activity based on C5 at t=0 (figure 4-18B); percentage activity = ((percentage lysis due to sample) / (percentage lysis at t=0) x 100). As for figure 4-18A, there was no significant difference in percentage activity between t=0 and t=120 when C5 was exposed to either CG or PR3. In contrast, there was a significant difference in percentage C5 activity when C5 was exposed to NE between t=15 and t=60 or t=120 (p=0.011, and p<0.0001 respectively).

From these sets of experiments that measured C5a generation, C5 degradation and C5 activity, I observed that there is evidence of differential cleavage of C5 by individual NSPs. In particular, I found that exposure of C5 to NE has the most detrimental effect on C5 function and is also most potent in C5a generation (figure 4-16).

Despite previous reports of C3a and C5a generation by NE and CG by other groups, it is not clear whether such NSP-generated C5a is functionally identical to nC5a produced by C5 convertase. The functional differences in NSP-generated C5a will be investigated in section 4.9.4. In this section I have investigated C5a-generation by three NSPs; however, C3a generation by NE and CG has also been previously reported (Yuan *et al.* 2015). I also investigated the generation of C3a by NSPs, but because the expression of C3aR on neutrophils is a controversial topic the characterisation of C3a generated by NSPs was less comprehensive (Klos *et al.* 2013)

4.8. C3a generation by NSPs

Atypical C3a generation by NE in the emphysematous airway has previously been reported (Robbins *et al.* 1991; Yuan *et al.* 2015). In the previous chapter I found that C3a positively correlated with neutrophil count in CF; however, this does not necessarily imply a causative relationship. In the current chapter I also found a statistically significant positive correlation between C3a and NE (figure 4-4A). Furthermore, C3a-like fragments generated by proteases in CF BAL fluid were visualised by Western blot. To confirm data from previous reports and further characterise generation of C3a by NE (and other the NSPs) C3 was exposed to a 2-fold dilution series of each protease for 30 minutes at 37°C. C3 cleavage fragments were resolved by SDS-PAGE and visualised by western blotting using a mouse anti-C3/C3a monoclonal antibody that targets the C3a C-terminal signalling domain (figure 4-19).

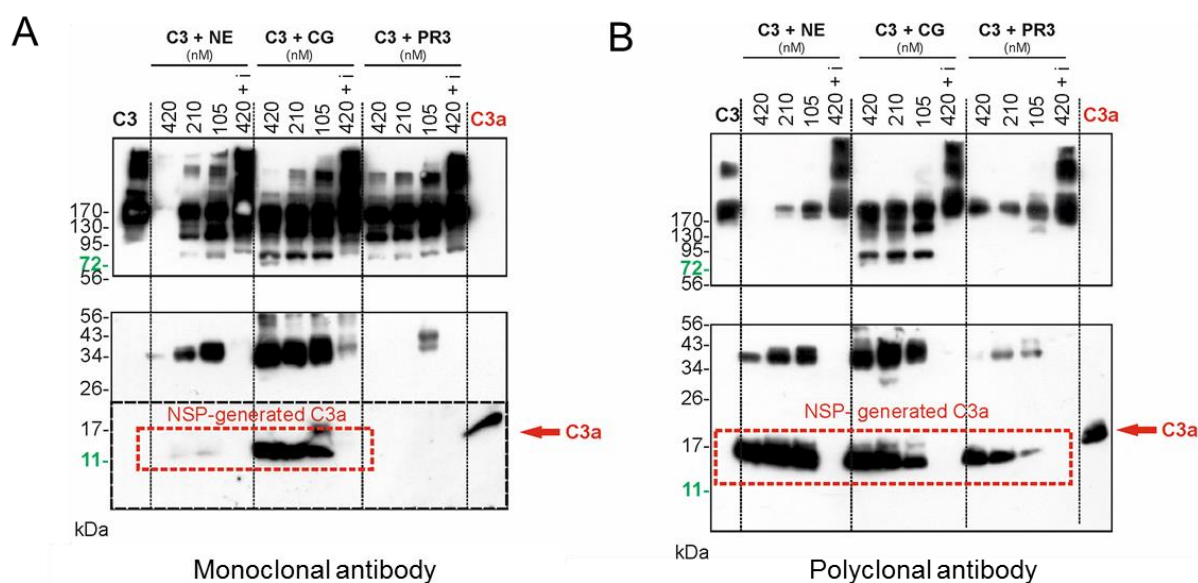


Figure 4-19: Generation of C3a-like fragments by purified NSPs. C3 was incubated with a 2-fold dilution series (420 to 105 nM) of either NE, CG or PR3 at 37°C for 1 h. In addition, each protease at 420nM was pre-incubated with 5 mM PMSF “i”. Proteins were resolved under non-reducing conditions by SDS-PAGE on 4-20% tris-glycine gradient polyacrylamide gels. Generation of C3a was visualised by western blot using mouse anti-C3/C3a monoclonal (A) or goat anti-C3a polyclonal antibodies (B) with detection by goat anti-mouse or donkey anti-rabbit HRP-conjugate secondary antibodies respectively. For staining blots were cut at 56 kDa reference marker and stained identically. For developing, top blots (containing C3) were incubated in low sensitivity ECL, bottom blots (containing C3a) were incubated with high sensitivity ECL. For “A” the lower part (dashed black box) was developed over a longer exposure time for visualisation of band. C3a was resolved for reference (green). Red boxes indicate suspected C3a-like fragments, red arrow indicates molecular weight of C3a, n=3.

C3a-like fragments generated by CG had a similar molecular weight to native C3a, produced by C3 convertase (figure 4-19A). Unfortunately, a smile in the gel made it difficult to compare the molecular weight of C3a-like fragments with native C3a. In contrast to previous reports (Yuan *et al.* 2015), only faint C3a-like bands were visualised when C3 was exposed to NE in my experiments. C3a-like bands could not be detected when C3 was exposed to PR3, yet it was apparent that C3 was degraded because other break-down products were present and the intact C3 band was less intense than the negative control (untreated C3).

I hypothesised that the C3a-like fragments, generated by each of the NSPs, were subject to further degradation of the C-terminus, preventing detection by the monoclonal antibody. I hypothesised that this could be because the epitope for anti-C3/C3a antibody is in the C-terminal signaling domain of C3a. Therefore, the same samples were resolved by SDS-PAGE but detected using anti-C3a polyclonal antibody, a commercial antibody made by immunising rabbits with the entire native C3a protein (figure 4-19B). Interestingly, C3a-like bands were observed in C3 break-down products produced by individual NSPs. For CG and PR3 C3a-like band intensity was dependent on protease concentration. Unfortunately, as with figure 4-19A, a smile in the gel made it difficult to compare molecular weights of C3a-like bands with convertase-generated C3a. For this reason, greater resolution was sought by resolving C3 degradation products using single-concentration 20% bis-tris polyacrylamide gels (figure 4-20).

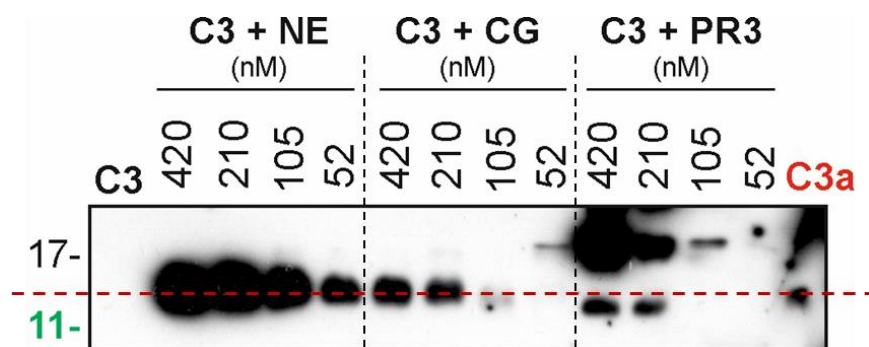


Figure 4-20: Resolving NSP-generated C3a fragments on 20% polyacrylamide gels. C3 was incubated with a 2-fold dilution series (420 to 52 nM) of either NE, CG or PR3 at 37°C for 1 h. Proteins were resolved under non-reducing conditions by SDS-PAGE on 20% bis-tris polyacrylamide gels. Generation of C3a was visualised by western blot using a rabbit anti-C3a polyclonal antibody with detection by donkey anti-rabbit HRP-conjugate secondary antibody. For staining blots were cut at 56 kDa reference maker and stained identically. Due to separation using high-density gels, only low molecular weight bands could be identified. Red dashed line indicates molecular weight of C3a based on the reference protein, n=1.

As visualised using gradient gels, C3a-like fragments, generated by each of the three NSPs, could be detected using the goat anti-C3a polyclonal antibody. In addition to figure 4-19B, further dilution of each protease to 52 nM enabled a titratable effect to be observed for each

protease whereas before an effect was only found with CG exposure to PR3. There was no apparent smiling in the gel and therefore, a comparison of molecular weights could be made; NE and CG generated a C3a-like band with a similar molecular weight to C3 convertase generated C3a. Interestingly, C3a-like bands generated by PR3 had a lower molecular weight than C3a, this could reflect loss of the C-terminal signaling domain preventing detection by the monoclonal antibody used in figure 4-19A. Due to technical difficulties repeating this experiment, there is only one blot comparing the molecular weights of NSP-generated C3a with native C3a and therefore, further confirmation by mass spectrometry is required to more accurately compare difference in molecular weight.

In replication of previous reports, I have shown that NE and CG were able to generate C3a-like fragments through cleavage of C3 (Yuan *et al.* 2015). Furthermore, in contrast to the previous account by Yuan *et al.* I have also shown that PR3 can also generate a C3a-like fragment. Despite this, only C3a-like fragments generated by CG, and to a lesser extent NE, could be visualised using a monoclonal antibody that binds to the C3a signaling domain. Therefore, I hypothesised that only C3a-like fragments that stained positively for the monoclonal antibody would be active. To test the activity of NSP-generated C3a I used a reported cell line transfected with C3aR.

4.8.1. Optimisation of a C3a activity assay for measuring the activity of C3-like fragments

RBL-2H3 cells stably transfected with the C3aR were used to investigate the function of C3a-like fragments. In brief, stimulation of the RBL cells, via the C3aR, induces degranulation, releasing enzymes into the media. The extent of degranulation, or stimulation, can be quantified by measuring the release of β -hexosaminidase, an enzyme that, in a physiological setting, breaks down ganglioside through cleavage of N-acetyl galactosamine. β -hexosaminidase activity is quantified by incubation with a specific chromogenic substrate (4-Nitrophenyl N-acetyl- β -D-glucosaminide), that turns yellow when cleaved, allowing absorbance measurement at 405 nm. Data can be calculated as a percentage of total β -hexosaminidase release, achieved by lysing cells with triton X-100. C3a activity can also be calculated using a standard curve of known concentrations of C3a; an example is given in figure 4-21.

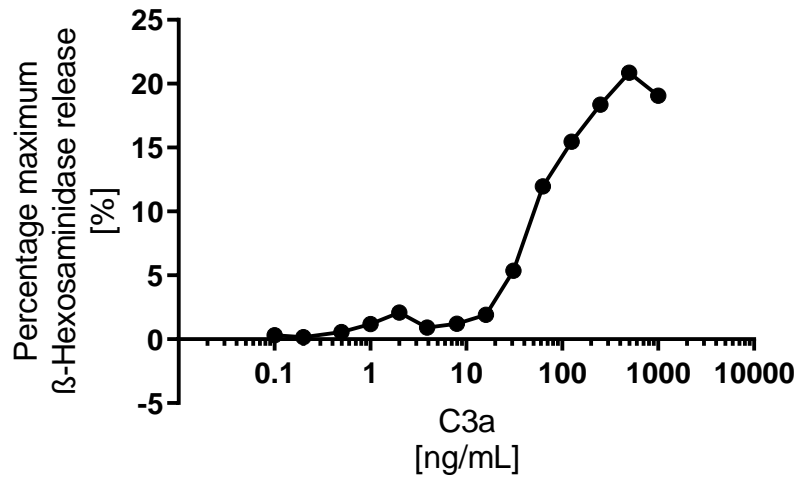


Figure 4-21: Example of a standard curve for RBL-C3aR β -hexosaminidase reporter assay.

A 2-fold dilution series of C3a from 1000 ng/mL to 0.12 ng/mL (x-axis). RBL-C3aR cells were stimulated for 30 minutes at 37°C 5% CO₂, supernatant was transferred to a 96-well plate and substrate was added to each well and incubated for 3 h at 37°C. Stimulation was measured as a percentage of total β -hexosaminidase release (y-axis). Mean values from assay duplicates were plotted. N=1

4.8.2. Activity of C3a-like fragments generated by NSPs

To investigate the activity of C3a-like fragments generated by NSPs, C3 cleavage experiments were performed as for the western blot analyses in figure 4-19; C3 was exposed to a 2-fold dilution series of individual NSPs for 1 h at 37°C (figure 4-22).

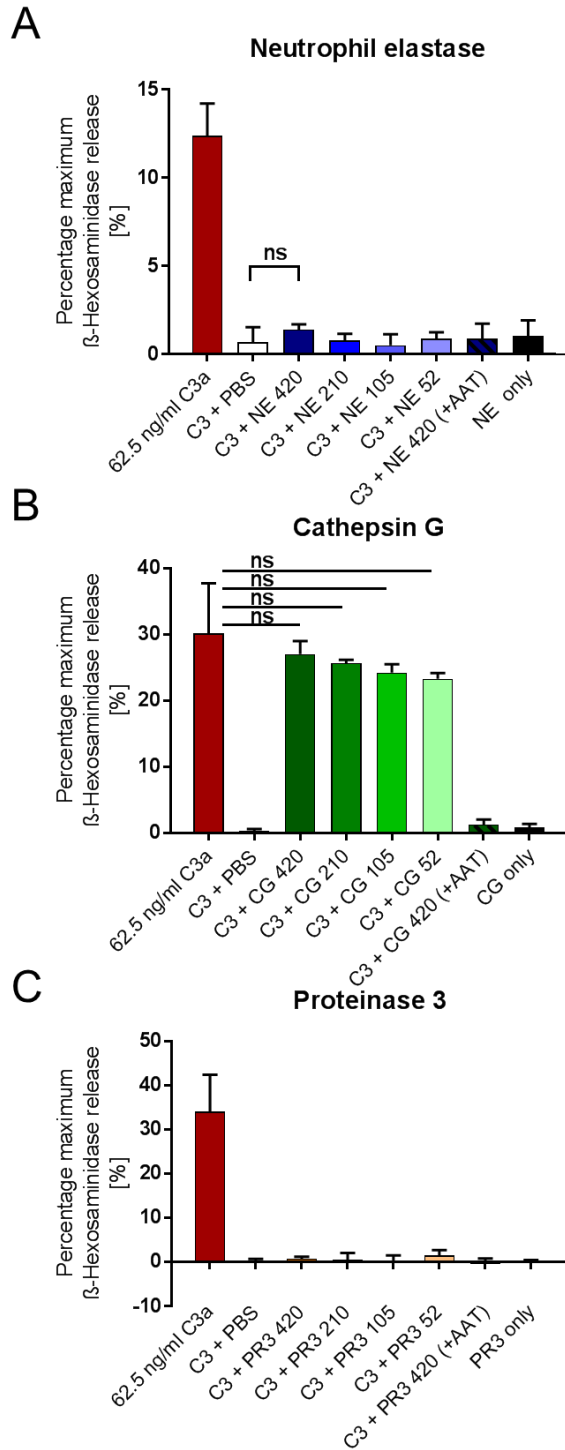


Figure 4-22 Assessing the activity of C3a-like fragments generated by NSP.

C3 was incubated with a 2-fold dilution series (420 to 52 nM) of either (A) NE (blue shades), (B) CG (green shades) (C) or PR3 (orange shades) at 37°C for 1 h. C3a 62.5 ng/mL was used as a reference (red). A native serine protease inhibitor, AAT, was also pre-incubated with the highest concentration of each protease (diagonal stripe). Non-specific degradation of the β -hexosaminidase substrate was assessed by adding protease only (black). RBL-C3aR cells were stimulated for 30 minutes at 37°C 5% CO₂, supernatant was transferred to a 96-well plate and substrate was added to each well and incubated for 3 h at 37°C. Data was plotted as mean \pm SEM, statistical analyses by Two-way ANOVA with Tukey's test for multiple comparisons (n=3).

A small modification to the protocol was that the proteolytic activity of NSPs was arrested using AAT rather than PMSF, this is due to the cytotoxic effects of PMSF on cells. NSPs diluted in PBS-T to a concentration of 420 nM (but not added to C3) were included as a negative control and confirmed that each NSP was not able to cleave β -hexosaminidase substrate and generate a false-positive (even though protease activity was arrested with AAT). Interestingly, CG, but not NE or PR3, generated functionally active C3a-like fragments that could stimulate degranulation of RBL-C3aR cells. The difference in the activity between these C3a-like fragments further demonstrate the alternative cleavage site preferences for these proteases. For instance, cleavage of the C-terminal signaling domain that is required for C3aR activation. Activity of C3a-like fragments generated by 420 nM CG had mean β -hexosaminidase release similar to that induced by 62.5 ng/mL C3a ($p = 0.787$) (figure 4-22B). It was shown in figure 4-19A, that NE-generated C3a-like fragments that were faint but visible by western blot. There was also minor residual activity in NE-generated C3a-like fragments; however, activity was not statistically different to C3 incubated with PBS ($p = 0.705$) (figure 4-22A). Data from the C3a activity assay support my hypothesis that cleavage of the C-terminal epitope for the monoclonal antibody coincides with the loss of activity in these fragments.

C3a standards in experiments performed with NE (figure 4-22A) had lower β -hexosaminidase release compared to CG and PR3 experiments (figure 4-22B and figure 4-22C). This was particularly evident when comparing β -hexosaminidase release following stimulation by purified C3a across each set of experiments. This was probably due to fluctuation in the capacity of the cells to signal from week to week however, total β -hexosaminidase release, measured from lysed cells, remained the same (not shown). Therefore, this phenomenon may have reduced the ability to detect low levels of C3a activity.

So far, I have shown that C5a and C3a can be generated by proteases present in CF BAL fluid. I have confirmed and expanded on previous reports of functionally active C5a and C3a generation by purified NSPs; however, it is not known whether functional differences exist between NSP-generated anaphylatoxins and their convertase-generated counterparts; this will be explored in the next section.

4.9. Functional differences in alternatively generated forms of C3a and C5a

C3a and C5a are potent pro-inflammatory mediators and therefore require tight regulation. In blood, C3a and C5a are rapidly inactivated by CPB and CPN; these cleave the C-terminal arginine, producing C3a-desArg and C5a-desArg respectively. Expression of CPB and CPN in the normal and CF airway has not been described. Therefore, inactivation of NSP-generated C3a-like and C5a-like fragments by CPB and CPN was investigated.

4.9.1. Measuring CPB and CPN activity in CF BAL fluid.

Before investigating CPB and CPN inactivation of C3a and C5a, expression of these inhibitors was measured in the CF airway as this has not previously been reported. Carboxypeptidase activity was measured using a chromogenic substrate specific for CPN and CPB, Furylacryloyl-Ala-Lys. As for the NE activity assay, CF BAL fluid sample is added to the carboxypeptidase substrate and the mean change in absorbance (336nm) over time is calculated using a best-fit linear regression. To quantify CPN and CPB expression, purified porcine CPB was used as a standard curve, an example is given in figure 4-23A.

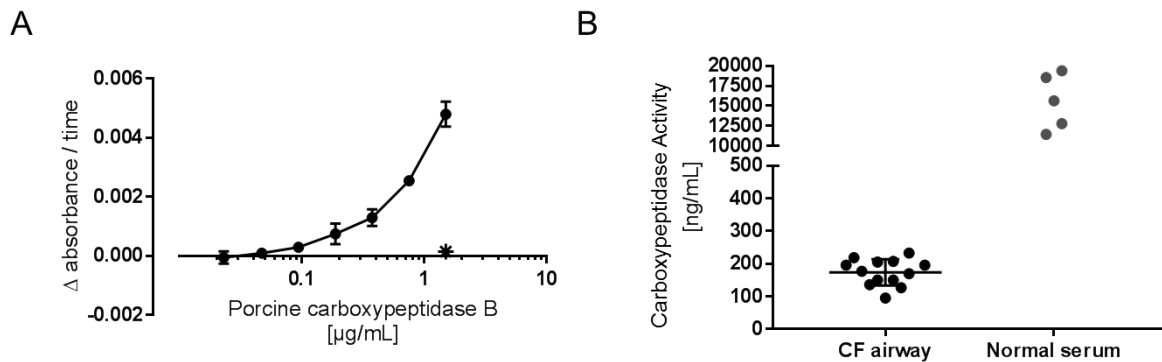


Figure 4-23: Quantifying CPB and CPN activity in CF BAL fluid. A) A standard curve of carboxypeptidase activity was established by diluting purified porcine CPB 2-fold serially from 1.5 to 0.023 $\mu\text{g/mL}$ (black line). CPB (1.5 $\mu\text{g/mL}$) was also pre-incubated with 5mM 1,10 phenanthroline (black star “*”). Activity was quantified using a chromogenic substrate, Furylacryloyl-Ala-Lys, by measuring change in absorbance (336nm) every minute for 20 minutes. Mean change was calculated by line of best fit over 20 minutes. **B)** 13 CF BAL fluid were diluted 1 in 4 and added to substrate (median annotated by black bars). Normal human serum was diluted 1 in 15 for comparison. Carboxypeptidase activity was calculated by interpolating values from the standard curve in “A” and multiplying by the corresponding dilution factors. n=13 for CF BAL fluid, n=5 of the same normal serum sample.

Human sources of CPB are available but are significantly more expensive. Furthermore, it has been reported that there is no difference in function between porcine and human CPB (Marinkovic *et al.* 1977). Porcine CPB was diluted serially 2-fold from 1.5 to 0.023 µg/mL and change in absorbance was measured upon exposure to the chromogenic substrate. CPN requires zinc as a co-factor for activity, a chelator of metal ions, 1,10 phenanthroline was also pre-incubated with the highest standard (1.5 µg/mL) to show that substrate breakdown was specific to porcine CPB (figure 4-23B).

The rate of chromogenic substrate breakdown was titratable with porcine CPB concentration between 1.5 and 0.023 µg/mL. A metal chelator, 1,10 phenanthroline was effective at preventing substrate breakdown when pre-incubated with 1.5 µg/mL showing that activity is specific to the CPB in this experiment. Similar porcine CPB standard curves as shown in figure 4-23A were used to interpolate CPB activity in 13 CF BAL fluid samples and serum from a single healthy donor (figure 4-23B). The mean CPB activity in CF BAL fluid was 174 ng/mL (range: 95 – 233 µg/mL) compared to 15.56 µg/mL in serum from a single healthy donor. Due to the sensitivity of this assay, CPN and CPB activity was measured using the lower part of the standard curve. It should be noted that Furylacryloyl-Ala-Lys is not specific to CPB and will also be cleaved by CPN therefore, carboxypeptidase activity in the above figure is relative to porcine CPB.

Analysing data from figure 4-23B, the carboxypeptidase activity in the CF airway is over 70-fold less than in circulation; however, I did not yet know whether C5a (or C3a) could still be inactivated by this amount of activity.

4.9.2. A RBL-C5aR1 reporter cell line for measuring C5a activity

A RBL-C5aR1 reported cell line was used to investigate inactivation of C5a by CPB. As for RBL-C3aR, β-hexosaminidase release is used to measure receptor stimulation. In section 4.7.2 I assessed the activity of C5a-like fragments using an U937-C5aR1 reporter cell line. The RBL-C5aR1 reporter assay became available later on during my project and was chosen over the U937-C5aR1 calcium signalling because it enables simultaneous testing of different conditions. The protocol for the U937-C5aR1 activity assay only allowed for one condition to be tested at a time. By this I mean that U937-C5aR1 cells were loaded with Fura-2-AM and

then there was a two-hour window to perform cell stimulations. Beyond this, leakage of Fura-2 from the cells affects the data. Each test would take 10-15 minutes and therefore, only a set amount of conditions could be tested in one sitting. RBL cell reporter assays were performed in 96-well plates with all conditions tested simultaneously. Before investigating the inactivation of NSP-generated C5a (and C3a), the sensitivity of RBL-C5aR1 reporter assay was tested.

To quantify activity of C5a-like fragments generated by NSPs and measure inactivation of C5a by CPB, a standard curve was established using purified nC5a by performing a 10-fold serial dilution series from 250 to 0.0025 ng/mL in PBS-T. A variable slope was fitted by GraphPad prism®, $r = 0.984$ (figure 4-24). β -hexosaminidase was detectable when nC5a was diluted to 0.4 ng/mL therefore, for future experiments a standard curve would range from 250 to 0.4 ng/mL in a 5-fold dilution series.

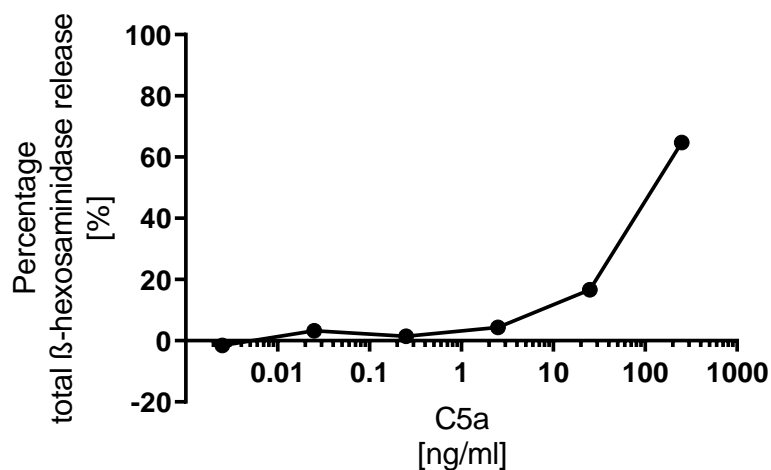


Figure 4-24: Optimisation of RBL-C5aR1 C5a reporter assay. RBL-C5aR1 cells were stimulated for 30 minutes at 37°C 5% CO₂, supernatant was removed and added to an equal volume of chromogenic substrate, 4-Nitrophenyl N-acetyl- β -D-glucosaminide and incubated for 3 h at 37°C. Tris (1 M) was added and absorbance measured at 405 nm. Data were calculated as a percentage of total β -hexosaminidase release induced by incubating cells with 0.1% triton X-100 (y-axis). Background signal measured by stimulating cell with phenol-red free media only was subtracted from all data points. C5a was diluted 10-fold from 250 to 0.0025 ng/mL (x-axis) in PBS-T (0.00125 % (final concentration)), data was plotted as mean values from assay duplicates. Data from a single experiment.

4.9.3. Inactivation of native C3a and C5a by porcine CPB

Having optimised the RBL-C5aR1 reporter assay, porcine CPB was used to briefly investigate whether levels of carboxypeptidases observed in CF BAL fluid, from figure 4-23B, were able to inactivate nC5a or C3a. In preliminary experiments, nC5a and C3a were incubated with a series of porcine CPB dilutions from 15 $\mu\text{g}/\text{mL}$ to 192 pg/mL for 1 h at 37°C and, the exposed anaphylatoxins were used to stimulate RBL-C5aR1 or RBL-C3aR respectively. Complete inactivation of nC5a was not achieved at the highest porcine CPB concentration used (figure 4-25A), this concentration was similar to the CPB activity observed in serum from a single healthy donor (15.56 $\mu\text{g}/\text{mL}$) (figure 4-23B). C3a was more readily inactivated by porcine CPB than C5a furthermore, additional dilution of CPB (to 38.4 pg/mL) was required before inactivation of C3a was no longer detectable (figure 4-25B).

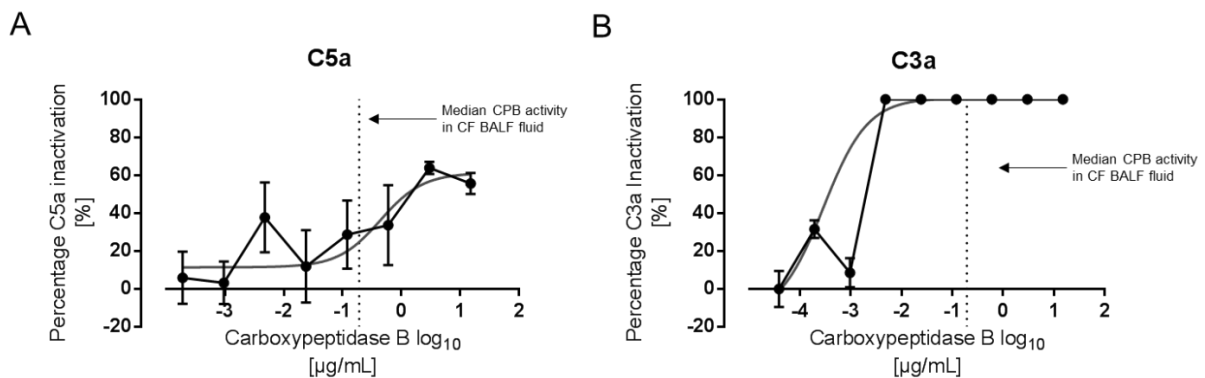


Figure 4-25: Inactivation of native C5a and C3a by porcine CPB. **A)** C5a (1 $\mu\text{g}/\text{mL}$) or **B)** C3a (0.5 $\mu\text{g}/\text{mL}$) was incubated with a 5-fold dilution series of porcine CPB from 15 $\mu\text{g}/\text{mL}$ to 192 pg/mL (38. pg/mL) for C3a for 1 h at 37°C (x-axis). Samples were diluted 1 in 10 using phenol red-free media prior to cell stimulation. RBL-C5aR1 or RBL-C3aR cells were stimulated for 30 minutes at 37°C 5% CO₂, and β -hexosaminidase release was measured using chromogenic substrate). C5a and C3a activity were quantified by interpolating values from a standard curve produces using purified nC5a and C3a. Percentage inactivation was calculated by dividing the activity of each condition by the activity of untreated C5a or C3a and subtracting from 100. Data points are triplicates from a single experiment (mean and standard deviation). A four-variable non-linear least squares regression was fitted on triplicate values from a single experiment by Graphpad prism® (red). Median carboxypeptidase activity in CF BAL fluid was annotated by a dotted line.

4.9.4. CPB inactivation of C3a and C5a forms generated by NSPs

CPB/N activity was found in CF BAL fluid. Furthermore, the equivalent concentration of porcine CPB could reduce C5a activity and completely inactivate C3a. I have shown that NSPs can generate functionally active C5a-like and C3a-like fragments, but it is not known whether CPB/N can inactivate these alternative forms. Active C3a-like and C5a-like fragments were generated by exposing C3 to 420nM CG and C5 to 420nM of each NSPs for 1 h at 37°C. NSP-generated C3a and C5a fragments were subsequently exposed to 15 $\mu\text{g}/\text{mL}$ porcine

CPB for 1 h at 37°C and activity was compared with the respective convertase-generated counterparts (C3a and C5a).

4.9.4.a. Assessing CPB inactivation of NSP-generated C5a

I first investigated inactivation of NSP-generated C5a by CPB (figure 4-26). Interestingly, there was no statistical difference in C5a activity when C5a-like fragments generated by NE and PR3 were exposed to porcine CPB, suggesting resistance to inactivation ($p > 0.999$ and $p > 0.999$ respectively, figure 4-26A).

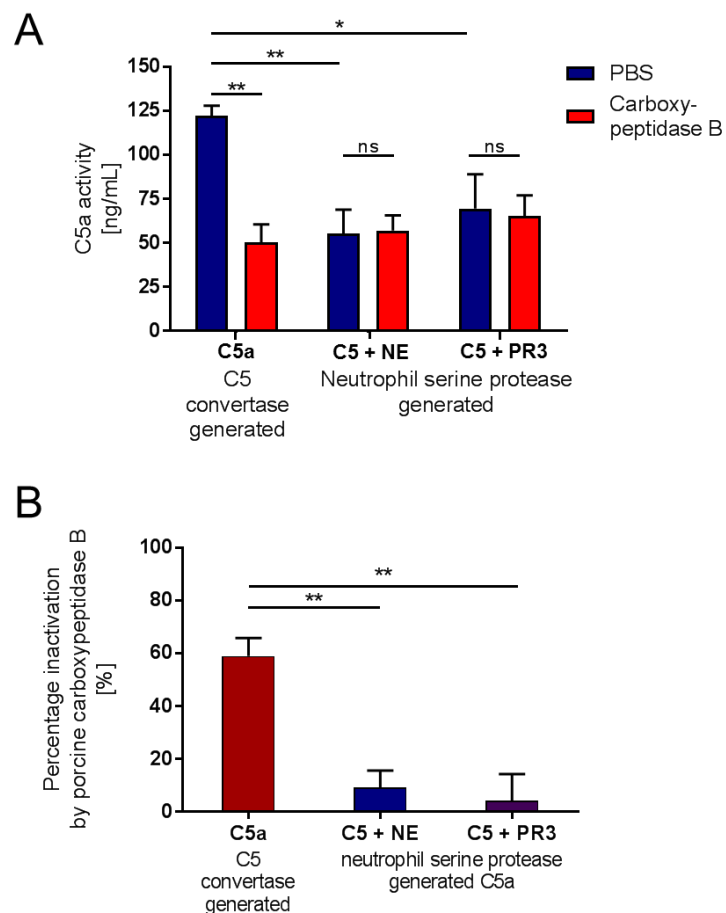


Figure 4-26: Inactivation of NSP-generated C5a-like fragments by porcine CPB. **A)** C5 was exposed to NE or PR3 for 1 h at 37°C, AAT was added subsequently added to inhibit protease activity. Purified C5a (125 µg/mL) or C5 cleavage fragments were exposed to PBS (blue) or 15 µg/mL (uquivalent to activity in serum) porcine CPB (red) for 1 h at 37°C then used to stimulate RBL-C5aR1. C5a activity was interpolated from a standard curve of purified C5a (y-axis). Data was presented as mean ± SEM, Two-way ANOVA (Tukey’s multiple comparison) was performed to compare means, n=3. **B)** Data from “A” was calculated as percentage inactivation, by dividing the activity of each condition by the activity of their respective untreated control (no CPB), this value was multiplied by 100 then, subtracted from 100. Mean inactivation for each condition were compared by One-way ANOVA, n=3.

As shown in figure 4-25A, porcine CPB reduced nC5a activity significantly ($p < 0.006$) but did not completely abolish function; it was unclear from these experiments why nC5a retained function after exposure to CPB. There was a significant difference in C5a activity between C5 convertase-generated C5a and the C5a-like fragments generated by NE and PR, without exposure to porcine CPB ($p = 0.008$ and $p = 0.020$ respectively). This difference in activity between nC5a and protease-generated C5a was due to the concentration of nC5a that I used for reference in these experiments. Therefore, because the activity of nC5a and C5a-like forms was different, data from figure 4-26A was re-calculated as percentage inactivation in relation to the untreated control (figure 4-26B). Analysing these standardised data, there was a significant difference in the percentage inactivation of nC5a compared to C5a generated by NE and PR3 ($p < 0.01$).

Previous quantification of C5a activity was performed by measuring intracellular calcium flux in U937-C5aR1. Despite demonstrating activity from CG-generated C5a-like fragments using U937-C5aR1, no detectable activity was detected from these fragments when measuring β -hexosaminidase release from RBL-C5aR1 (shown in figure 5-6 in a similar type of experiment). None-the-less, C5a activity was detected in C5a-like fragments generated by NE and PR3.

4.9.4.b. Assessing CPB inactivation of NSP-generated C3a

A similar set of experiments was also performed comparing CPB inactivation of C3a-like fragments generated by CG (figure 4-27).

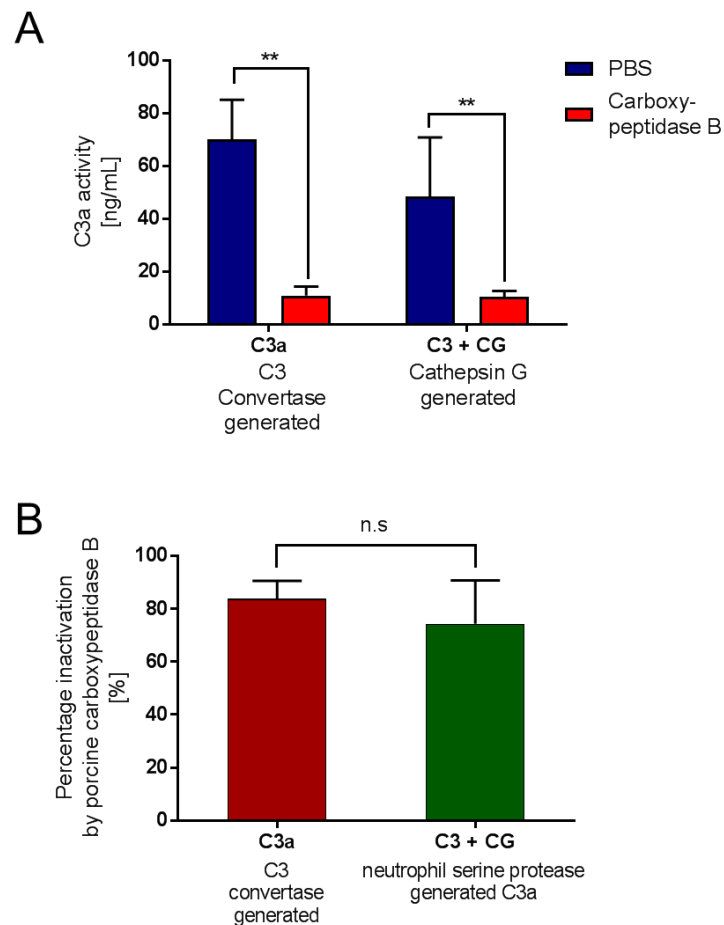


Figure 4-27: Inactivation of CG-generated C3a-like fragments by porcine CPB. A) C3 was exposed to CG for 1 h at 37°C, AAT was added subsequently added to inhibit protease activity. Purified C3a (75 ng/mL) or C3 cleavage fragments were exposed to PBS (blue) or 15 µg/mL porcine CPB (red) for 1 h at 37°C then used to stimulate RBL-C5aR1. C3a activity was interpolated from a standard curve of purified C3a (y-axis). One-way ANOVA was performed to compare means, n=3. **B)** Data from “A” was calculated as percentage inactivation, by dividing the activity of each condition by the activity of their respective untreated control (no CPB), this value was multiplied by 100 then subtracted from 100. Mean inactivation for each condition were compared by One-way ANOVA with Dunnett’s test for multiple comparisons, n=3.

There was a statistically significant reduction in C3a activity when either purified C3a or CG-generated C3a-like fragments were exposed to 15 µg/mL porcine CPB ($p = 0.001$ and $p = 0.009$ respectively, figure 4-27A). Furthermore, re-calculating data as percentage activation

confirmed that there was no statistical difference in inactivation of CG-generated C3a compared to native, C3 convertase-generated C3a ($p = 0.500$, figure 4-27B). These data suggest that there is no difference in susceptibility to inactivation by porcine CPB between C3a and the C3a-like fragments generated by CG. Data from CPB C3a and C5a inactivation experiments were the first to find that the C5a-like fragments generated by NE and PR3 are resistant to inactivation compared to native C5 convertase-generated C5a.

4.10. Discussion

The complement anaphylatoxins, C3a and C5a, are elevated during chronic neutrophilic inflammation of the CF airway and there is evidence from my study (chapter 3) and other reports that they contribute to neutrophilic inflammation and pathogenesis (Fick *et al.* 1986; Sass *et al.* 2015; Hair *et al.* 2017). Non-canonical generation of C3a and C5a by pathogen-derived proteases has been reported in the CF airway and may contribute to elevated C5a expression during infection (Fick *et al.* 1986; Sass *et al.* 2015). NSP-mediated C3a and C5a generation has previously been reported in inflammatory airway disease such as COPD however, this mechanism has not been fully explored in the CF airway (Kolb *et al.* 1981; Fick *et al.* 1986; Robbins *et al.* 1991; Yuan *et al.* 2015). I hypothesised that NSPs in the CF airway generate alternative forms of C5a and C3a that are functionally different to their native counterparts.

4.10.1. Evidence for C3a and C5a generation by NSPs in the CF airway

Initially, I assessed data from CF BAL fluid in chapter 3 for evidence of non-canonical C3a and C5a generation. Interestingly, C3a but not C5a correlated with terminal complement pathway activation (C5b-9). A study of canonical complement activation using zymosan (a complement activating fungal glucan) has previously demonstrated that cleavage of one C3 molecule does not necessarily equate to one C5a (after assembly of C5-convertase) (Morad *et al.* 2015). Furthermore, the same group show that the C3a:C5a ratio is not linear and the C3a:C5a ratio increases as complement becomes more active, suggesting dynamic kinetics within the complement system (Morad *et al.* 2015). Despite improving our understanding of complement activation and anaphylatoxin generation, the above study does not simulate complex environments such as the CF airway. I think that there may be alternative fates for C5a compared to C3a in the CF airway that could account for the difference in their relationships with C5b-9. A possible explanation is that there could be higher C5aR1 expression on cells present in the CF airway compared to C3aR and therefore C5a is more readily removed by

receptor internalisation. During infection, the CF airway is dominated by neutrophils that have high expression of C5aR1 whereas there is ongoing controversy over whether neutrophils express C3aR (Ember *et al.* 1991; Norgauer *et al.* 1993). Moreover, it has been shown that neutrophils from patients with sepsis had reduced C5aR1 expression as result of C5aR1 stimulation and internalisation however, C5aR1 degradation by NSPs (reported by our group) may also reduce expression (Unnewehr *et al.* 2013; van den Berg *et al.* 2014). As well as differences in internalisation of C5a and C3a, it has been shown that C5a is susceptible to degradation by NE and CG; this was further characterised in my study (Brozna *et al.* 1977). I have shown that, under similar conditions, C3a was more susceptible to degradation than C5a which may be contrary to my argument for why C3a correlates with C5b-9 but not C5a. Despite this, I have observed that C3 is present at concentrations 1000-fold greater than C5, whereas in circulation this difference is more like 10-fold (Barnum and Schein 2018). In summary the CF airway is a complex environment that cannot be fully understood by simple two-way relationships.

4.10.2. Comparing NSP proteolysis of recombinant and native C5a forms

In initial experiments, I compared functional differences between rhC5a and nC5a. Recombinant C5a has been used by other groups in substitute for nC5a however, there are structural differences, such as glycosylation of nC5a, that may be important when performing investigations on C5a (Miyabe *et al.* 2017). In this study, I have shown that rhC5a is more susceptible to degradation by NSPs than nC5a; this has not previously been reported. The N-glycosylation of asparagine-64 of C5a accounts for 25% of total C5a molecular weight therefore, a large glycosylation residue could sterically hinder NSPs access to cleavage sites (see figure 4-29)(Fernandez and Hugli 1976). Sareneva *et al.* have reported that two N-glycosylation sites on interferon- γ are important for protection against plasmin, NE and CG (Sareneva *et al.* 1995). I attempted to de-glycosylate nC5a in order to investigate whether the n-glycosylation site did indeed protect nC5a from degradation; however, I was unable to confirm successful de-glycosylation (not shown).

4.10.3. Generation of C3a-like and C5a-like fragments by proteases present in CF BAL fluid

NSPs have been reported to generate functional C3a-like and C5a-like fragments (Wetsel and Kolb 1983; Robbins *et al.* 1991; Yuan *et al.* 2015). In my study, evidence of C3a and C5a

generation by NSPs in CF BAL fluid was initially investigated by correlating NE activity with either C3a or C5a. C5a is a potent activator of neutrophils that induces the release of NE, further driving C5a generation; however, as mentioned above, NE can also in turn degrade C5a (Goldstein and Weissmann 1974; Brozna *et al.* 1977). None the less, Fick *et al.* demonstrate a strong correlation ($r = 0.97$, $p = 0.03$) between C5a concentration and elastolytic activity in BAL fluid from 7 CF patients (Fick *et al.* 1986). It should be noted that elastolytic activity in the above study may originate from pseudomonas elastase and other proteases as well as NE. This is because radiolabeled elastin was used as a substrate and elastin can be degraded by a range of proteases and not just pseudomonas elastase (Fick *et al.* 1986; Cowland and Borregaard 2016). Without specific antibodies that can differentiate between different C5a forms such as native C5a, C5a-desArg and alternatively generated C5a-like fragments, I think it will be difficult to conclusively demonstrate C3a and C5a generation in complex samples such as CF BAL fluid.

To further investigate C3a and C5a generation by NSPs in the CF airway, purified C3 and C5 were incubated with CF BAL fluid. C3a and C5a-like molecules of similar molecular weight to nC5a were produced. Furthermore, a serine protease inhibitor (PMSF) was sufficient to block the majority of C3a and C5a generating activity indicating that it was due to serine proteases. Fick *et al.* have also demonstrated C5a generation by CF BAL using SDS-PAGE however, ^{125}I -C5 was used to visualise cleavage fragments rather than western blotting (Fick *et al.* 1986). They observed different molecular weight C5a-like bands when CF BAL fluid was pre-incubated with PMSF, suggesting alternative forms of C5a were generated by serine and non-serine proteases. The addition of C5-convertase generated C5a was not resolved on their gels for comparison but would improve identification of C5a-like fragments. Furthermore, the use of ^{125}I -C5 to visualise C5a generation means that non-C5a fragments of similar molecular weight to nC5a may produce false positives. An advantage of my study was the use of a monoclonal antibody with an epitope in the c-terminal signaling domain to visualise C5a-like fragments.

In support of my data, Fick *et al.* also demonstrated that serine proteases were predominantly responsible for C5a-generation in their experiments; they found that PMSF reduced C5a-generation by 32-48% (Fick *et al.* 1986). Moreover, they also show that a different serine protease inhibitor, AAT, reduced C5a-generation by 49-66%.

After a review of the literature, my study is the first to show and visualise non-canonical generation of C3a by proteases expressed in CF airway; however, some of these data were preliminary and therefore further characterisation is required. In my study, C3a-generation

was not completely arrested when CF BAL fluid was pre-incubated with PMSF. Others have observed that C3a-like fragments, whilst not active (as measured by monocyte chemotaxis assays), can be generated by MMP12 a protease also released during neutrophil degranulation (Yuan *et al.* 2015).

4.10.4. Generation of functional C3a-like forms by purified NSPs

I demonstrated that C3a could be generated by purified NSPs. My results confirm generation of C3a-like fragments by NE and CG reported by Yuan *et al.* (Yuan *et al.* 2015). In addition, I detected C3a-like generation by PR3, a fragment not found by Yuan *et al.* This is likely to be because they stained their C3a-like fragments using a different monoclonal antibody (R&D systems, clone 354113) against C3a. It is not clear from the manufacturer's website (<https://resources.rndsystems.com/>) where on C3a the epitope for this antibody is located. An advantage to my study, was the use of two anti-C3a antibodies for the detection of C3a-like fragments; these were a monoclonal antibody for the C3a C-terminal signaling domain and, a polyclonal antibody against native C3a. PR3-generated C3a was detected using the polyclonal antibody but not the monoclonal antibody. PR3-generated C3a fragments had a lower molecular weight but these data were from a single experiment and require confirmation using mass spectrometry. I also show that C3a-like fragments generated by CG, that stained positive for the C3a C-terminus, were active and stimulated the release of β -hexosaminidase from RBL-C3aR. The anti-C3a polyclonal antibody demonstrated generation of C3a-like peptides by all three proteases but only CG generated C3a had detectable activity. By comparison, Yuan *et al.* showed that NE-generated C3a induced chemotaxis of bone-marrow derived and monocyte derived dendritic cells (Yuan *et al.* 2015). In explanation, the authors use 1:1000 ratio of NE to C3, whereas in my own experiments the greatest ratio of NE to C3 was 1:150. Therefore, there may be intermediate NE-derived C3a-like species during limited proteolysis that are active. Subsequent minor degradation, removing residues from the signaling domain could inactivate these fragments explaining why their activity was not detected in my experiments. From my observations of the CF airway the median ratio of NE to C3 was 1:263 however, the smallest ratio, in samples with the greatest inflammation, was 1:0.7. Therefore, with a ratio of between 1:10 and 1:150 my experiments may be more representative of C3a generation by NSPs in the inflamed airway, or at least the CF airway.

4.10.5. Generation of functional C5a-like forms by purified NSPs

C5a-generation by NE and CG has previously been shown (Brozna *et al.* 1977; Wetsel and Kolb 1983; Huber-Lang *et al.* 2002; Giles *et al.* 2015) yet, to my knowledge, this is the first time C5a-like fragments cleaved from C5 by PR3 has been documented. Despite, the above reports on C5a-generation, a more comprehensive characterisation was performed on each protease. A time-course experiment of C5 proteolysis by each protease was carried out over 2 h; C5a was quantified by ELISA, C5 was quantified by two in-house C5 ELISAs and C5 activity was measured by haemolysis assay. It was found that the majority of C5a-like fragments were generated within 15 minutes of exposure to each NSP.

Giles *et al.* have also reported a time-course experiment by exposing C5 to NE; however, the rate of C5a generation that they demonstrate appears to be less than my experiments (Giles *et al.* 2015). This could be explained by the ratios of C5 to NE; in my experiments I used a ratio of 1:10 whereas Giles *et al.* report using 1:20, double my own cleavage assays.

4.10.6. Assessing C5 function following exposure to purified NSPs

I also quantified C5 degradation in cleavage experiments using two ELISAs that detected C5 using alternative antibody pairings. The two alternative C5 ELISAs enabled the measurement of theoretically intact (SKY59-Hycult pairing) and partially cleaved C5 (SKY59-2D5 pairing). Interestingly, intact C5 concentration decreased dramatically within the first 15 minutes, mirroring C5a-generation. Only NE degraded C5 to near-zero concentrations over the 2 h period observed. The SKY59-2D5 pairing demonstrated a less-severe loss of C5 when exposed to each NSP. These data further support observations of low intact C5 concentrations in CF BAL fluid reported in the cohort characterisation in the previous chapter. In addition, C5 activity was quantified by measuring sheep erythrocyte lysis in a classical pathway haemolysis assay. Interestingly, visually, C5 function mapped more closely to the C5 concentration by the C5 ELISA that can detect partially cleaved C5. This observation suggests that complement activation can occur with C5 that has been partially cleaved by each NSP however, further experimentation would be required to test this theory. The most striking result was that the function of C5 exposed to PR3 did not significantly change over 2 hours despite the generation of C5a and evidence of degradation by western blots. The generation of functional C5b-like fragments by NE but not CG or PR3 has been reported (Vogt 2000). Although my experiments have been designed to investigate C5b-like generation, there is evidence to suggest that PR3, more so than NE and CG, may also cleave functional C5b. A

comprehensive experiment using C5-depleted serum and purified complement components would be required to definitively demonstrate function C5b-like generation.

4.10.7. Investigating CPB inactivation of C3a-like and C5a-like fragments

The most interesting finding from this chapter was that NE and PR3-generated C5a was resistant to inactivation by porcine CPB. CPN and CPB are crucial for regulating C3a and C5a in circulation (Skidgel and Erdos 2007). It has recently been demonstrated using acute and subacute systemic disease models that, despite functional similarities, CPB and CPN have different roles. CPN is constantly expressed in circulation; however, CPB is upregulated via thrombin during acute challenge (Morser *et al.* 2018). With relevance to the CF airway, I measured carboxypeptidase activity in CF BAL fluid to assess whether carboxypeptidase inactivation of C3a and C5a was still an important mechanism for regulation of activity in the CF airway. CPB and CPN activity was measured in 13 CF BAL fluid samples and a serum sample from a single healthy donor; serum CPB activity was over 70-fold higher than that found in CF BAL fluid. A disadvantage to my study was that I did not differentiate CPB and CPN activity. Commercial ELISAs are available for CPN and CPB. Alongside activity data, these would provide comprehensive insight into C3a and C5a regulation in the CF airway. Carboxypeptidases are expressed by hepatic cells, it is not clear whether non-liver cells, such as airway epithelial cells or alveolar macrophages, can produce carboxypeptidases locally (Skidgel and Erdos 2007). CPB activity in sera has previously been measured in CF patients; this was to investigate whether pancreatic deficiency, caused by bile duct blockage, reduced carboxypeptidases in circulation (Koheil *et al.* 1979). The authors did not observe any significant difference between CPB activity in CF sera compared to age and gender matched control subjects with ciliary dyskinesia.

In my experiments, porcine CPB was used to inactivate C3a and C5a. A comparison of porcine and human CPB by Erdos *et al.* showed that CPB from both species have identical substrate specificity (terminal lysine and arginine) (Marinkovic *et al.* 1977). A dissimilarity was that human but not porcine CPB activity was fully arrested by EDTA (Marinkovic *et al.* 1977). Reviewing the literature, I did not find any reports that compared inactivation of C5a (or C3a) by human and porcine CPB.

The role of carboxypeptidases and C5a inactivation has been reported in a mouse model of asthma (Fujiwara *et al.* 2012). The authors observed that CPB knock-out mice were more sensitive to ovalbumin-induction of airway hyperresponsiveness. Furthermore, symptoms of

hyperresponsiveness were reduced when CPB knock-out mice were administered a C5aR antagonist. The authors concluded that carboxypeptidases are important for regulating C5a activity in the asthmatic airway; however, they did not comment on the non-canonical generation of C5a by NSPs.

4.10.7.a. Resistance of NE- and PR3-generated C5a to inactivation by CPB

For the first time, I have demonstrated that NE and PR3-generated C5a-like forms are resistant to inactivation by porcine CPB. This means that NSPs are not only important for elevating levels of C5a in the CF airway but the C5a that NSPs produce is functionally different. I propose a model whereby NSP-generation of functionally different C5a promotes neutrophilic inflammation but, these neutrophils infiltrating the airway become desensitised through NSP-cleavage of C5aR1, as previously reported by our group (van den Berg *et al.* 2014). Due to the critical role of C5a in orchestrating inflammation, cleavage of C5aR1 renders neutrophils ineffective at clearing pathogens (Hunniger *et al.* 2015). A vicious cycle is established whereby NSP release, C5a generation and inefficient pathogen clearance drives CF airway pathology (figure 4-28).

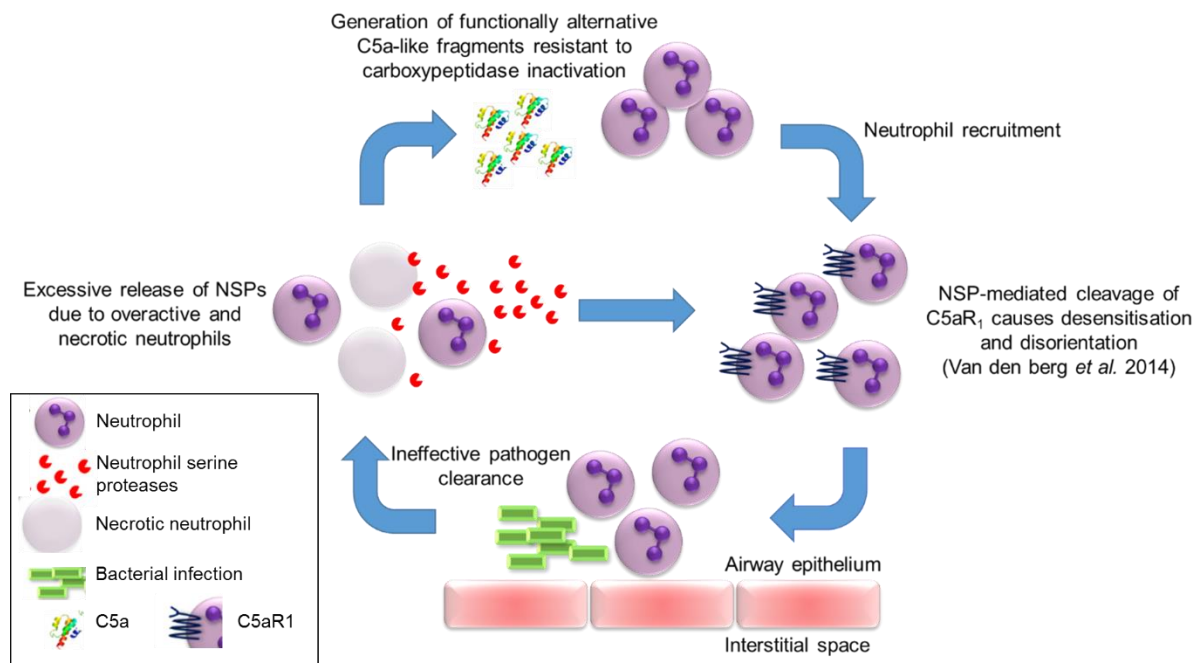


Figure 4-28: Diagram of the role of NSP-generated C5a in the CF airway.

Activated and necrotic neutrophils release NSPs into the airway. NSPs generate C5a-like fragments that are resistant to carboxypeptidase regulation. NSP-generated C5a facilitates further neutrophil recruitment to the CF airway. Upon infiltrating the airway, C5aR1 is cleaved by NSPs from the neutrophil surface preventing C5a-mediated function. Without C5a communication neutrophils are less effective at clearing pathogens driving a vicious cycle.

This model shows how C5a could promote neutrophilic inflammation in the CF airway may also be relevant for diseases where NSP-generation of C5a has also been reported such as rheumatoid arthritis, asthma and COPD (Robbins *et al.* 1991; Giles *et al.* 2015; Verschoor *et al.* 2016).

A possible explanation of why NE and PR3-generated C5a is resistant to inactivation by CPB is the site where the C5a-like fragment is cleaved from the C5-alpha chain. It has been speculated that the NE cleavage site is at C5 position valine-760, 9 amino acids downstream of the C5-convertase cleave site, arginine-751 (see figure 4-29) (Giles *et al.* 2015). Despite this, neither C-terminal sequencing nor mass spectrometry has been performed on NE-generated C5a to confirm this cleavage site. Figure 4-29 demonstrates a number of NE and PR3 cleavage sites upstream and downstream of the C5-convertase site on C5. These have been predicted using a database that collates all reported cleavage site preferences for these proteases (<https://www.ebi.ac.uk/merops/>). For instance, NE is more likely to cleave after leucine, valine and isoleucine. Additionally, the MEROPS website suggests that there are different site specificities for recombinant NE and NE purified from human blood. NE data collated by MEROPS was from two separate publications (Harris *et al.* 2000; Wysocka *et al.* 2008).

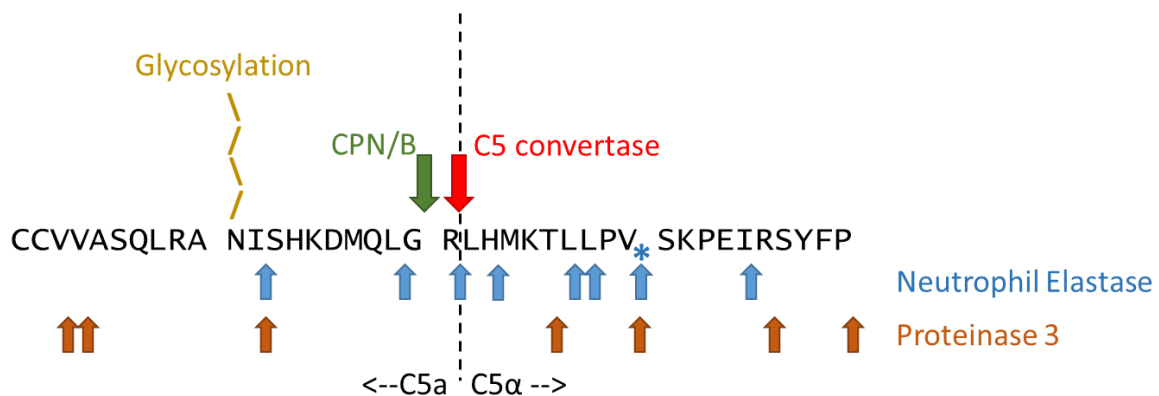


Figure 4-29: Amino acid sequence of C5a and predicted preferential cleavage sites for NE and PR3. Predicted cleavage sites for NE (blue) and PR3 (orange) (<https://www.ebi.ac.uk/merops/database>). Blue asterisk is the NE-cleavage site suspected by Giles *et al.* (Giles *et al.* 2015). Red arrows annotate C5-cleavage site after C5 arginine-751 and green arrow is the site for subsequent CPB or CPB cleavage of arginine-751 to produce the inactivated form C5a-desArg. The N-glycosylation site at C5 Asparagine-742 (C5a-64) is annotated in yellow. The black dashed line represents canonical C5/C5a cleavage, C5a from C5α chain.

Despite no reported protein sequence data, Giles *et al.* observed that NE-generated C5a was 1 kDa bigger than convertase-generated C5a therefore, a cleavage site downstream of the C5-convertase is plausible (Giles *et al.* 2015). CPB and CPN are endopeptidases that cleave terminal lysine or arginine residues therefore, obstruction of the C5a C-terminal arginine by

an extension of C5a sequence would theoretically prevent cleavage and inactivation (Skidgel and Erdos 2007).

4.10.7.b. Inactivation of CG-generated C3a by CPB

Only CG generated detectable functional C3a-like fragments in my study; this C3a form was not resistant to inactivation by porcine CPB. Again (as for C5a), reviewing the MEROPS database, there are multiple predicted cleavage sites, many of which are shared with NE, but my data did not show that NE-generated C3a was active (figure 4-30). These predicted sites are based on probability, I have selected sites with the highest probability, but because CG has broad specificity it is possible that CG also cleaves at the same position as C3-convertase. In support of the CG C3a cleavage site being the same as C3 convertase, my own resolution of CG-generated C3a by SDS-PAGE did suggest that the molecular weight of these fragments were similar to native C3a.

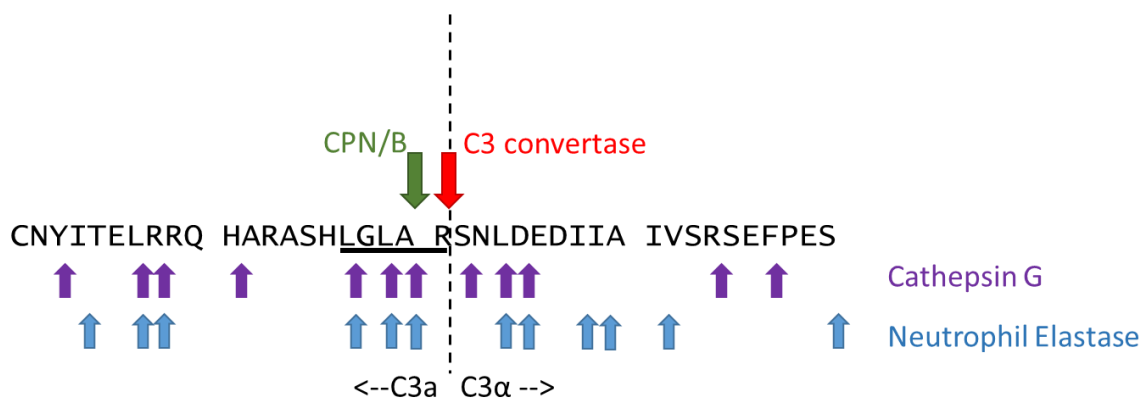


Figure 4-30: Amino acid sequence C3a and predicted preferential cleavage site of CG and PR3. Predicted cleavage sites for NE (blue) and CG (purple) (<https://www.ebi.ac.uk/merops/> database). Red arrows annotate C3-cleavage site and green arrow is the site for subsequent CPN or CPB cleavage of arginine to produce the inactivated form C3a-desArg. The black dashed line represents canonical C3/C3a cleavage, C3a from C3-alpha chain.

To my knowledge, none of the groups in table 4-1 that investigated atypical C3a or C5a-generation also assessed whether these fragments could be inactivated by CPB or CPN. Despite this, Riedemann *et al.* performed peptide sequencing of trypsinised C5 and observed that trypsin cleaved C5a-like fragments of identical length to native C5a (Riedemann *et al.* 2017). Therefore, given my hypothesis that elongated C5a-like fragments are protected from CPB inactivation by additional amino acids, I would predict that trypsin-generated C5a is inactivated similarly to nC5a. Mass spectrometry of β -tryptase has also confirmed the generation of C3a and C5a that are identical in mass to their convertase-generated counterparts (Fukuoka *et al.* 2008). I assume, again, that these fragments are also susceptible

to CPB inactivation. Therefore, although I have extensively listed (table 4-1) non-complement proteases that can generate functional C3a and C5a, it is possible that not all are resistant to inactivation, as I have shown for NE and PR3-generated C5a.

	Neutrophil elastase	Cathepsin G	Proteinase 3
C3a	degradation	degradation	degradation
nC5a	Limited degradation (24hr)	No degradation	No degradation
rhC5a	degradation	degradation	degradation
C3	C3a-like fragment No activity	C3a-like fragment Active Inactivated by CPB	C3a-like fragment No activity
C5	C5a-like fragment Active Resistant to CPB inactivation	C5a-like fragment Some activity CPB inactivation not tested	C5a-like fragment Active Resistant to CPB inactivation

Table 4-2 Summary of experiments exposing complement components to NSPs

4.11. Conclusion to the chapter

The complement anaphylatoxins, C3a and C5a, are elevated in the CF airway however, their roles in disease progression are unclear. Over the past 40 years numerous non-complement proteases have been shown to generate functional C3a and C5a forms, including NSPs. In this section I have investigated C5a and C3a generation by NSPs, with particular focus on C5a. Most intriguingly, I have demonstrated that NE and PR3 can generate functionally different C5a that is resistant to inactivation by CPB. Therefore, in the CF airway not only do NSPs contribute to C5a (and C3a) generation but these forms bypass regulation by carboxypeptidases and therefore, could potentially drive chronic neutrophilic inflammation. Importantly, CF represents a case of neutrophilic inflammation that is representative of other inflammatory diseases such as asthma, COPD, rheumatoid arthritis and sepsis. Therefore, mechanisms of C5a-mediated inflammation will also apply to these diseases; however, more investigation is required to differentiate the contribution by different C5a forms. In the next section I will investigate whether therapeutic complement inhibitors that bind C5 and prevent the generation of C5a (and C5b) are also effective at blocking atypical generation of C5a by NSPs.

5. Generation of C5a-like fragments by neutrophil serine proteases in the presence of C5 cleavage inhibitors

5.1. Background to the chapter

The complement system is critical for removal of pathogens and foreign bodies. Furthermore, complement is integral in promoting inflammation, clearing apoptotic cells and promoting tissue regeneration (Ricklin *et al.* 2010). Despite this, the reliance on complement for the above mechanisms means that dysregulation can contribute to disease pathology (de Cordoba *et al.* 2012). This is the case for numerous inflammatory and autoimmune disorders throughout the body such as sepsis, rheumatoid arthritis and systemic lupus erythematosus (de Cordoba *et al.* 2012).

Due to the wide-reaching effects in disease, controlling complement activity has become an attractive therapeutic target; however, deciding how and where in the cascade is a challenge (Morgan and Harris 2015). This is because simply dampening complement activity in order to reduce symptoms of a disease may leave a patient more susceptible to infection. Academic institutions and pharmaceutical companies have developed a range of therapeutics targeting initiation, alternative pathway (amplification loop), MAC assembly and the anaphylatoxins (C3a and C5a) (figure 5-1) (Morgan and Harris 2015). Complement based therapeutics are undergoing clinical trials in kidney disease (aHUS, glomerulopathy and PNH), autoimmune diseases (rheumatoid arthritis, lupus nephritis and myasthenia gravis), ischaemia-reperfusion (stroke, by-pass and organ transplantation) as well as inflammation (AMD and sepsis) (Morgan and Harris 2015). The airway has also been suggested as a target for complement inhibition, particularly in diseases such as asthma and COPD (Marc *et al.* 2010; Khan *et al.* 2014).

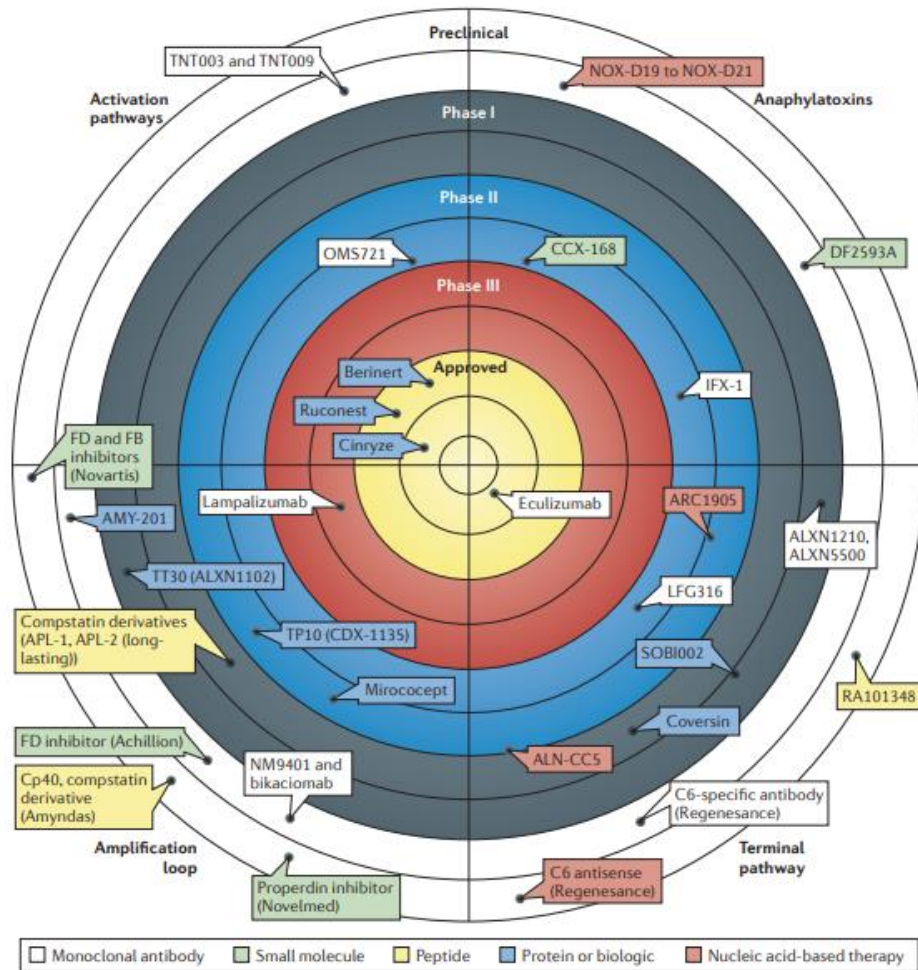


Figure 5-1: Complement therapeutics, their target pathway and phase in clinical trial, Figure extracted from Morgan and Harris 2015. Complement therapeutics have been developed to target the three complement activation pathways as well as the anaphylatoxins. A range of different inhibitory mediators have been produced such as monoclonal antibodies (white), small molecules (green), peptides (yellow), proteins (blue) or nucleic acids (red). The current phase in clinical trial is dictated by their proximity to the centre of the target (diagram), phase I-II, preclinical and approved for use in clinical is labelled at the top.

In particular, two diseases have been controlled using C5 cleavage inhibitors these are; PNH and aHUS. Both diseases are rare (1-2 and 3.3 cases per million respectively), they have different disease mechanisms (discussed in section 1.6.5) but have been successfully managed by blocking the cleavage of C5 by C5 convertase using the drug Eculizumab (Solaris) (Hillmen *et al.* 2006; Zuber *et al.* 2012). Following positive outcomes in PNH and aHUS, Eculizumab is undergoing clinical trials for numerous other diseases, these include: AMD, neuromyelitis optica, mild allergic asthma, refractory myasthenia gravis and Guillain-Barre syndrome (Morgan and Harris 2015).

Eculizumab is a mouse monoclonal antibody that recognises a linear epitope in the C-terminus of C5 between residues 884 and 890 (Thomas *et al.* 1996). Eculizumab has been

“humanised”, meaning that the mouse complementarity-determining regions (CDR) are grafted onto human IgG heavy and light chains (Thomas *et al.* 1996). Eculizumab does not bind chimpanzee or baboon C5 though the sequence is highly homologous to human C5 (including the epitope for Eculizumab). This discrepancy led to the discovery of an additional Eculizumab binding site, a hairpin loop at residues 913-922 on human C5 (Brachet *et al.* 2016). These residues are not conserved between humans and non-human primates, accounting for the lack of Eculizumab cross-reactivity (Brachet *et al.* 2016). Interestingly, these interactions between Eculizumab and C5 still permits C5 to bind with C5-convertase; however, it prevents cleavage of C5 (into C5a and C5b) (Jore *et al.* 2016). The precise mechanisms by which C5 cleavage inhibitors function is difficult to investigate due to the short half-life of C5-convertases (Jore *et al.* 2016).

Despite its successes, Eculizumab is not perfect and several issues leave opportunities for additional therapeutic approaches. One of the issues with targeting C5 is that it is expressed at approximately 75-100 µg/mL in serum, requiring high levels (900-1200 mg/person) of plasma antibody for full inhibition of C5 activity (Fukuzawa *et al.* 2017; Barnum and Schein 2018). For this reason, Eculizumab is one of the world’s most expensive drugs with a cost of £340,000 per patient per year (Jore *et al.* 2016). A second issue is that patients with a mutation in C5 arginine-885 (R885H) do not respond to Eculizumab treatment (Nishimura *et al.* 2014). This is because the polymorphism lies within the linear epitope described above (Nishimura *et al.* 2014). The R885H mutation has a prevalence of 3.5% in the healthy Japanese population (Nishimura *et al.* 2014). Further analysis of C5 constructs found five more mutations that may reduce response to Eculizumab, although no PNH or aHUS patients bearing these alternative forms have been discovered (Volk *et al.* 2016).

With these issues in mind, several competitor C5 cleavage inhibitors have been developed and are undergoing clinical trials. As well as other monoclonal antibodies, different strategies include aptamers (protein-binding oligonucleotides; ARC1905) and naturally occurring inhibitors (Nunn *et al.* 2005; Ni and Hui 2009; Jore *et al.* 2016). The tick C5 cleavage inhibitors, OmCI and RaCI, have been isolated from two different tick species, *Ornithodoros moubata* and *Rhipicephalus appendiculatus* respectively (Nunn *et al.* 2005; Jore *et al.* 2016). Their normal role is to prevent immune activation upon ticks feeding on their hosts by inhibiting activation of host C5. The mechanism by which OmCI and RaCI block C5 cleavage is that they bind and prevent a conformational change upon C5 interaction with C5 convertase (figure 5-2) (Jore *et al.* 2016).

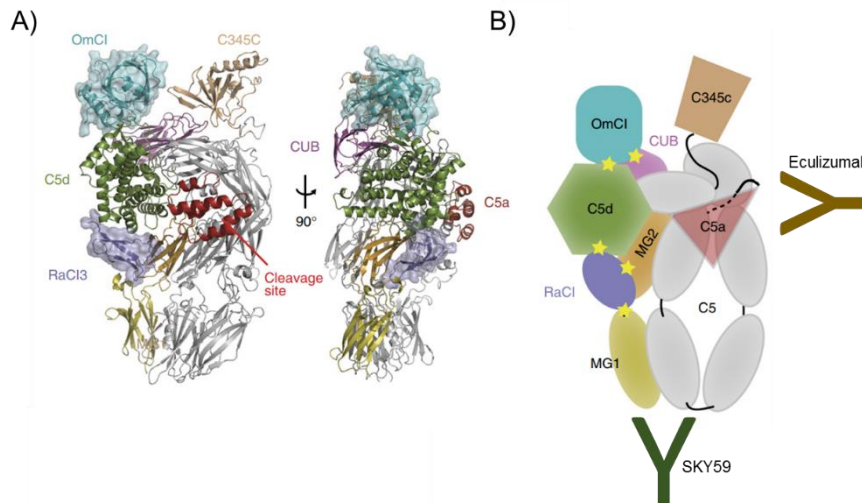


Figure 5-2: Structures of OmCl and RaCl complexes and reported binding sites of Eculizumab and SKY59. Adapted from Jore *et al.* (Jore *et al.* 2016) **A)** Crystal structure of OmCl-C5 and RaCl3 (RaCl variant) complexes. Tick inhibitors bind in different locations, in both cases preventing conformational change of C5, particularly a flexible C345c region stopping cleavage of C5a (red). OmCl also binds via a CUB domain, common in complement peptidases **B)** Cartoon representing C5 structure with binding sites for OmCl (cyan), RaCl (purple), SKY59 (dark green), and eculizumab (orange).

Recombinant OmCl (Coversin) is currently undergoing clinical trials in PNH and sepsis (<https://www.akaritx.com/coversin/>). Encouraging results using OmCl were also observed in a porcine model of sepsis when co-administered with an anti-CD14 antibody (Skjeflo *et al.* 2015). RaCl has only recently been isolated and it has been shown that the C5 binding site is distinct to that of OmCl and eculizumab (figure 5-2) (Jore *et al.* 2016). Due to a low molecular weight (<20 kDa), the authors hypothesised that the tick inhibitors will have a longer half-life than eculizumab and therefore require a reduced dosage and reducing the cost per patient. Immunoglobulins have a short half-life of approximately 7-21 days (Wang *et al.* 2018). They are degraded following internalisation by Fc receptors and trafficking to endosomal compartments (Wang *et al.* 2018). The neonatal Fc receptor is important for cycling internalised IgGs whilst facilitating the degradation of their ligands (Wang *et al.* 2018). Short half-life of IgGs is an issue for their use as a therapeutic, again this is exaggerated with Eculizumab because large doses are already required to overcome the high concentrations of C5 in serum (Fukuzawa *et al.* 2017). To solve the issue of short half-life therapeutic antibodies *in vivo*, Igawa *et al.* have engineered antibody CDR regions to disassociate from the ligand at pH 6, preventing degradation in endosomal compartments and allowing cycling of antigen-free IgG via neonatal Fc receptors (Igawa *et al.* 2010). They show in mice that modification

of Tocilizumab (anti-IL-6R) in this manner increased concentration of the antibody in serum 40-fold compared to the unmodified drug over a 4-day period. The same technology has been integrated into a humanised rabbit-anti human C5 monoclonal antibody that has inhibitory activity, SKY59 (Fukuzawa *et al.* 2017). SKY59 not only inhibits C5 cleavage with similar kinetics to eculizumab but can be recycled *in vivo* (Fukuzawa *et al.* 2017). In addition, SKY59 can inhibit terminal pathway activation in patients that have the R885H variant in C5 (Fukuzawa *et al.* 2017). It should be noted that a second-generation version of Eculizumab, Ravulizumab, engineered to enable cycling is currently undergoing phase II trials in PNH and aHUS (Ricklin *et al.* 2018).

The efficacy of Eculizumab and the tick C5 cleavage inhibitors to block terminal complement activation has been well characterised; however, the mechanism behind SKY59-mediated inhibition are not clear (Jore *et al.* 2016; Fukuzawa *et al.* 2017). I have recently contributed to a report showing that SKY59 not only binds C5 but it can also bind C5b-6 preventing MAC formation and cell lysis (Zepek *et al.* 2018). Despite characterisation of these therapeutic inhibitors, little is known about their capacity to prevent endogenous and exogenous protease generation of C5a, as investigated and discussed in the previous chapter. Riedemann *et al.* have documented the first initial evidence that C5a can be generated by thrombin in the presence of Eculizumab (Riedemann *et al.* 2017). Furthermore, by optimising an in-house C5a ELISA, the authors report elevated C5a/C5adesArg in aHUS patients undergoing treatment, suggesting C5 inhibition by Eculizumab is not complete. Riedemann *et al.* attribute C5a generation to thrombin and demonstrate that their own anti-C5a therapeutic antibody, IFX-1, is required for full protection for immune activation.

If thrombin can generate C5a in the presence of Eculizumab, is this also true for the NSP-generated C5a-like fragments that I investigated in chapter 4? Moreover, do other C5 cleavage inhibitors offer any greater or lesser protection from non-canonical C5a generation? In attempt to answer these questions the inhibitory function of four cleavage inhibitors against NSP-mediated C5a generation was investigated. These include; Eculizumab, SKY59, OmCI and RaCI.

5.2. Hypothesis

I hypothesise that eculizumab is unable to prevent the generation of functionally active C5a-like fragments by NSPs. Investigation will also include three other C5 cleavage inhibitors: SKY59, OmCI and, RaCI.

5.3. Aims

1. Compare complement inhibition of four C5 cleavage inhibitors: Eculizumab, SKY59, OmCI, and RaCI.
2. Investigate and compare NSP-generation of C5a-like fragments in the presence of the above four inhibitors using SDS-PAGE, a commercial C5a ELISA and the RBL-C5aR1 reporter assay.
3. Explore mechanisms by which NSPs potentially bypass C5 cleavage inhibitor protection

5.4. Comparison of the activity of four therapeutic C5 cleavage inhibitors using a haemolysis assay

Before investigating the main aim of this chapter, a haemolysis assay was optimised to enable comparison of the different inhibitors. The haemolysis assay that was used to investigate the different C5 cleavage inhibitors had a similar protocol to that used in section 4.7.3e. Here I used C5-depleted serum as a source of complement and added back experimentally modified C5 to investigate effects of NSP degradation on its function. This was because serine protease inhibitors (such as AAT) are present in the circulation and these could have blocked NSP activity in my experiments. In the following experiments, as before, 1% C5-depleted human serum was used. Based on reports that C5 is approximately 100 µg/mL in normal serum (Barnum and Schein 2018), at 1% the C5 concentration in normal serum would be 1 µg/mL. From this calculation I would need to add back at least 1 µg/mL of C5 to the 1% C5-depleted serum to obtain physiological complement activity.

To confirm the activity of the four therapeutic C5 cleavage inhibitors, 2.5 µg/mL (132 nM) C5 was incubated with the individual therapeutic inhibitors at a range of concentrations from an equivalent 5-fold molar excess of therapeutic to C5 (5:1) to over a 4000-fold excess of C5 to therapeutic (0.006:1 therapeutic to C5). The C5 concentration used (2.5 µg/mL) was higher than the physiological concentration calculated for the serum dilution used (1.0 µg/mL), this is because in later experiments greater C5 concentrations were required to enable visualisation on western blots.

C5 was incubated with each therapeutic inhibitor for 15 minutes at 37°C then added to 1% C5 depleted serum. Sensitised sheep-erythrocytes were added, and lysis was quantified after incubating for 60 minutes at 37°C (figure 5-3).

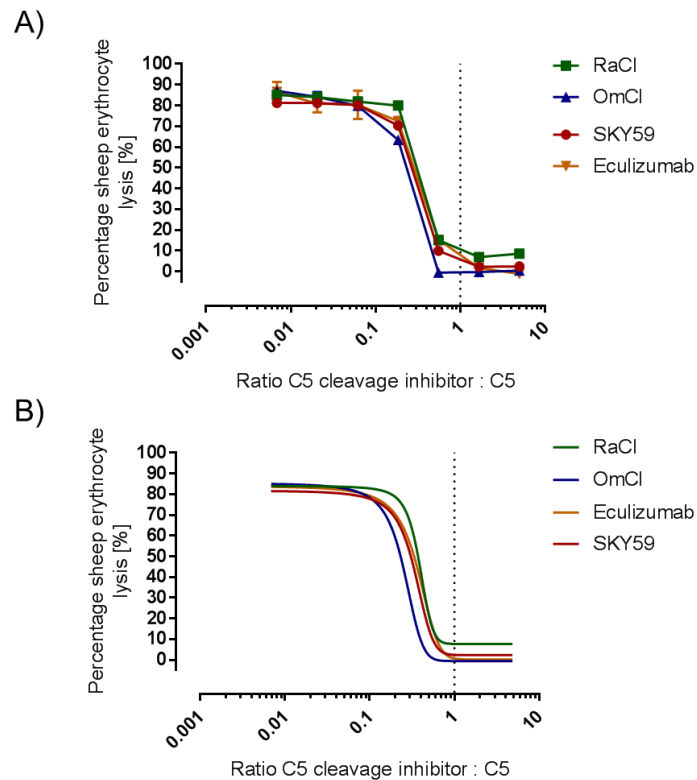


Figure 5-3: Comparing the activity of therapeutic C5 cleavage inhibitors. C5 (132 nM) was incubated for 15 min at 37°C with each cleavage inhibitor, diluted in a 3-fold series so that the inhibitor to C5 ratio ranged from 5 to 0.006 (x-axis). Each condition was diluted 1 in 10 in C5-depleted serum so that the final concentration of C5 was 0.25 µg. Complement activity was measured as a percentage of sheep erythrocyte lysis. Data is presented as **A)** raw data (mean and standard deviation) **B)** Raw data from "A" fitted with sigmoidal curves by GraphPad Prism®. R-squared > 0.99 for each condition. Dotted line marks 1:1 ratio. N=2.

All inhibitors completely prevented sheep lysis at a 1:1 ratio of inhibitor to C5. RaCl did not fully inhibit complement despite a plateau in activity (figure 5-3A). Each sigmoidal curve fitted by GraphPad Prism® had a R-squared greater than 0.99 (figure 5-3B). OmCl was the most potent C5-cleavage inhibitor, evidenced by a lower ratio required for inhibition; however, these data were collated from two experiments therefore, no statistical conclusions can be made. Despite this, the above experiments establish that all the inhibitors are active at a ratio of 1:1, confirming reports on their pharmacokinetics that one molecule of inhibitor binds to one molecule of C5 (Jore *et al.* 2016; Fukuzawa *et al.* 2017). In future assays, therapeutic C5 inhibitors were used in 5-fold excess of C5, this was to ensure complete inhibition.

5.5. Generation of C5a by NSPs in the presence of four C5 cleavage inhibitors

The main aim of this section was to investigate whether C5 cleavage inhibitors were able to prevent non-canonical generation of C5a by NSPs. To test this, a similar protocol to the

experiments performed in chapter 4 was used for generation of C5a-like fragments. In brief, C5 was pre-incubated with the four, individual therapeutic C5 cleavage inhibitors for 15 minutes at room temperature. C5, in complex with therapeutic cleavage inhibitors, was then exposed to either NE, PR3 or CG for 30 minutes at 37°C, NSP activity was arrested with AAT. Samples from the same experiments (n=3) were used to visualise any C5-proteolysis by SDS-PAGE and western blotting, quantify C5a concentration and assess C5a activity.

5.5.1. Visualising C5a-like fragments generated by NSPs

The cleavage fragments of C5 that had been pre-incubated with the therapeutic inhibitors and subsequently exposed to NSPs were visualised by western blot using a monoclonal antibody that recognises the C-terminal of C5a (as used previously in chapter 4). A fifth antibody “4G” was also included but was not part of my investigation (figure 5-4).

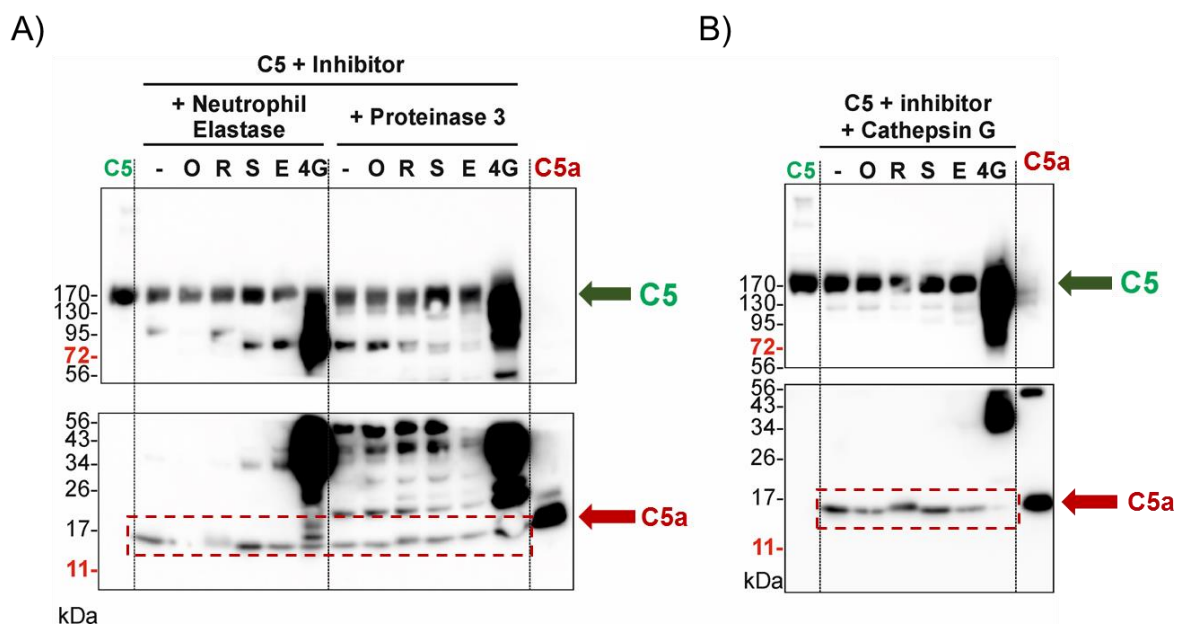


Figure 5-4: Visualising C5a-like fragments generated by NSPs when in the presence of therapeutic C5 cleavage inhibitors. C5 was exposed to **A)** NE, PR3 and, **B)** CG following incubation with cleavage inhibitors (“-” – no inhibitor, “O” – OmCI, “R” – RaCI, “S” – SKY59, “E” – Eculizumab, and “4G” – 4G2). Fragments were resolved by SDS-PAGE on 4-20% tris-glycine gels (non-reducing) and visualised by western blot using a monoclonal anti C5/C5a antibody and goat anti-mouse HRP-conjugate secondary antibody. Following transfer blots were cut at the 56 kDa marker and stained identically. For developing, the top blot was developed in low-sensitivity ECL and the bottom blots in high-sensitivity ECL. Bands representing the molecular weight of reference protein C5 (green arrows) and C5a (red arrows) have been annotated. Bands within dashed red boxes indicate bands of similar molecular weight to nC5a N=1 for eculizumab, n=2 for SKY59, OmCI and RaCI (n=3 NE generated C5a with SKY59, OmCI and RaCI).

As previously shown in chapter 4, C5 exposed to each individual NSP, generated a C5a-like fragment that was a similar molecular weight to nC5a. Interestingly, pre-incubating C5 with therapeutic C5 cleavage inhibitors did not prevent the cleavage of C5 by NSPs. Furthermore, C5a-like bands were generated of similar molecular weight to nC5a and C5a-like bands produced by NSPs from uninhibited C5. Unfortunately, there was evidence of “smiling” in the gel, making absolute determination of C5a molecular weight difficult for NE and CG generated C5a fragments.

On closer inspection neither SKY59 or Eculizumab had any obvious impact on C5a generation by any of the three NSPs. RaCI did not inhibit C5a generation by PR3 or CG but the C5a-like band produced by NE appeared fainter than the positive control (C5 exposed to NE without any cleavage inhibitor, “-”). Furthermore, when C5 was pre-incubated with RaCI, the C5a-like bands generated by each NSP had slightly higher molecular weight (~1 kDa) than the other NSP-generated C5a fragments, including positive controls for each of the respective proteases. As observed for RaCI, OmCI did not inhibit C5a generation by CG or PR3, but only a small part of a NE-generated C5a band was visible. It is possible that a band was resolved but did not transfer to the nitrocellulose membrane completely, probably due to an air bubble between the gel and membrane. Therefore, it is not conclusive from this blot whether OmCI is able to prevent C5a-like fragment generation by NE. Despite repeating this set of experiments three times, a technical issue with the western blots meant that only a single full set of data was available.

5.5.2. Quantifying the generation of C5a by NSPs in the presence of therapeutic C5 cleavage inhibitors

I have shown the first preliminary evidence of C5a generation by NSPs following pre-incubation of C5 with four therapeutic C5 cleavage inhibitors; however, western blots are not sufficiently quantitative to detect any subtle effects of the above C5 cleavage inhibitors on C5a-like generation by NSPs. A sensitive commercial C5a ELISA was performed to quantify C5a from the same samples as were used for western blots (Figure 5-5).

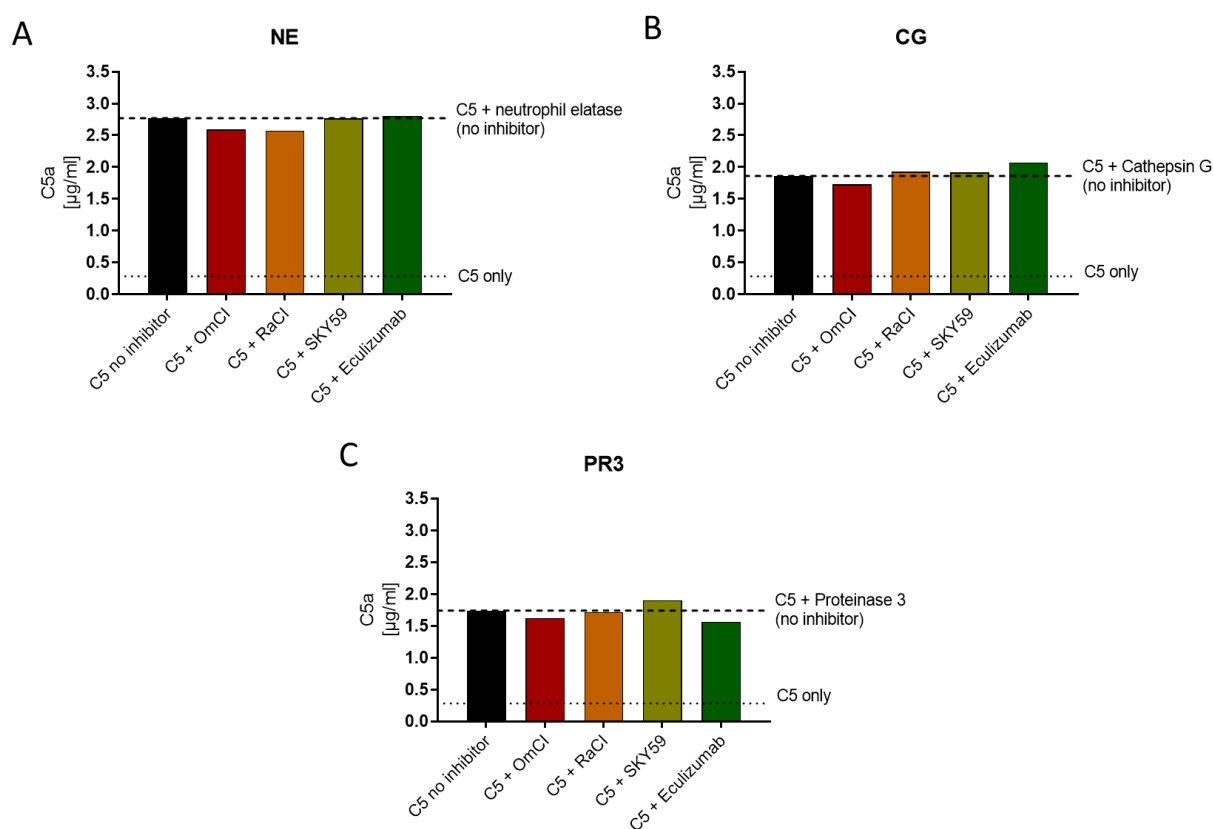


Figure 5-5: Quantifying NSP-generation of C5a-like fragments when in the presence of therapeutic C5 cleavage inhibitors. C5 was exposed to **A) NE**, **B) CG**, and **C) PR33** following incubation with cleavage inhibitors (x-axis). C5a was quantified by commercial C5a ELISA (y-axis). Dashed black lines are the mean concentration of C5a when C5 was exposed to protease without cleavage inhibitor. Dotted black lines are the mean concentration of C5a when (n=2).

A C5a ELISA was performed on samples from two out of three experiments and therefore there were not sufficient replicates to perform statistical analyses. Despite an absence of

statistical evidence, these data can still provide some quantitative information about C5a generated by NSPs when C5 is pre-incubated with C5 cleavage inhibitors. Data from C5a ELISAs reflect preliminary data from the western blot in figure 5-4, that none of the four therapeutic C5 cleavage inhibitors can prevent the generation of C5a-like fragments by NSPs. Data from the C5a ELISA show that the levels of C5a generated by NSPs are similar between untreated C5 and C5 that has been pre-incubated with the therapeutic inhibitors.

The C5a-like fragments generated by NSPs in the presence of C5 cleavage inhibitors were visualised by western blot and quantified by C5a ELISA. It was also important to establish whether these C5a-like fragments are functionally active.

5.5.3. Assessing the activity of C5a-like fragments generated by NSPs in the presence of therapeutic C5-cleavage inhibitors

Activity of C5a-like fragments was measured by stimulating β -hexosaminidase release from RBL-C5aR1, as previously described for experiments in section 4.9.2. C5a activity experiments were performed in parallel with the western blots and C5a ELISA and therefore samples from the same experiments were used (figure 5-6).

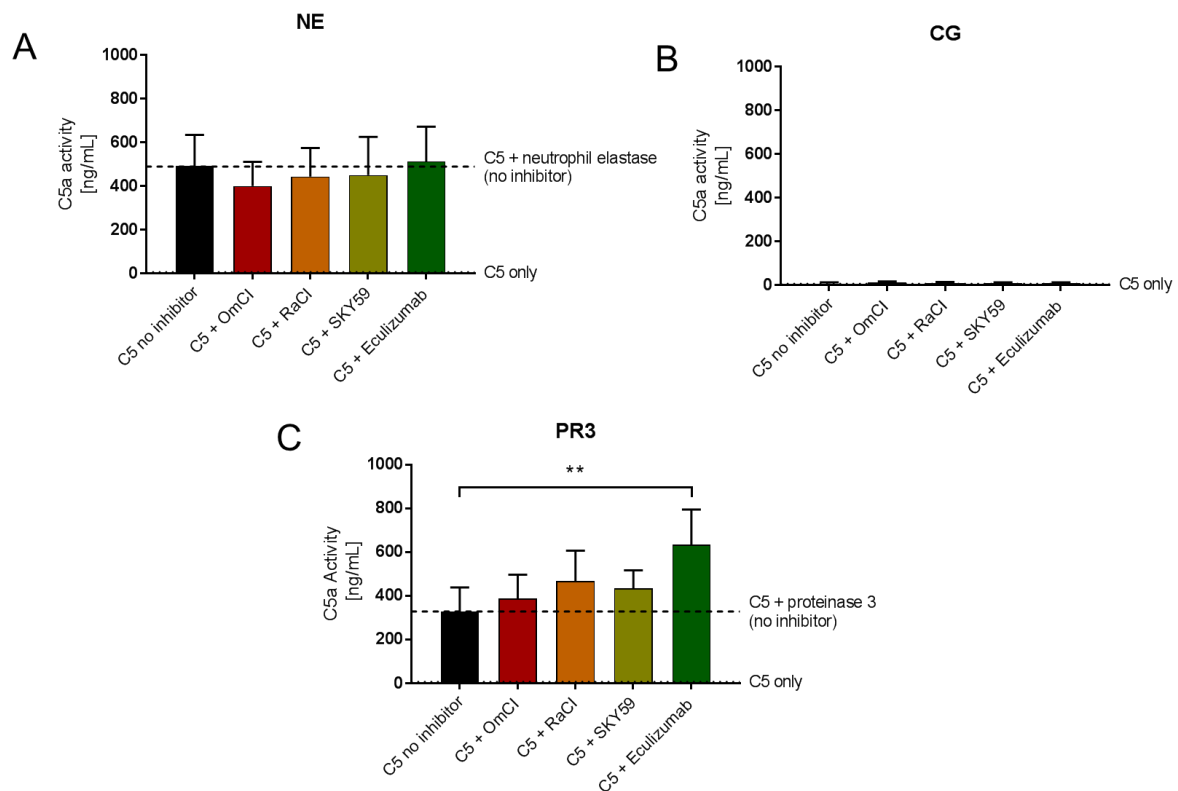


Figure 5-6: Activity of C5a-like fragments generated by NSPs in the presence of therapeutic C5 cleavage inhibitors. C5 was exposed to 420 nM **A)** NE, **B)** CG, and **C)** PR3 following pre-incubation with cleavage inhibitors (x-axis). Fragments were diluted 1 in 20 in phenol red-free media and added to RBL-C5aR1 cells. C5a activity was quantified by measuring β -hexosaminidase release upon stimulation by known concentrations of purified nC5a (y-axis). Dashed black lines are the mean signal from C5 exposed to protease without cleavage inhibitor. Dotted black lines are the mean signal where C5 was not exposed to protease or inhibitor. Data is presented as mean \pm SEM. For each protease a Two-way ANOVA with Tukey's test for multiple comparisons was used to compare C5a generation between samples, n =3.

A statistically significant increase in C5a activity, almost double, was observed for C5a-like fragments generated by PR3 when C5 was pre-incubated with Eculizumab (mean; 634 ng/mL) compared to the untreated positive control (mean; 328.4 ng/mL, p = 0.005) (figure 5-6C). There was no significant difference in C5a activity between all other C5a-like fragments generated by NE and PR3 in the presence of inhibitors, compared to when C5a was generated

without cleavage inhibitors present. The C5a ELISA in figure 5-5 detected small amounts of C5a in the C5 preparations, this would equate to 26.9 nM C5a and therefore 3.6 % of C5 (742 nM) at the beginning of the experiment. However, this concentration of C5a was not reflected in the activity assays (mean C5a activity in C5; 6.7 ng/mL) because the activity assay is not sensitive enough to detect this level of activity

As reported in section 4.9.4, the RBL-C5aR1 reporter assay did not detect activity from CG-generated C5a. C5a activity was a fifth of what would be expected from the concentrations measured by C5a ELISA. For instance, NE generated 2.8 µg/mL of C5a, but this equated to 493 ng/mL C5a activity. Data from westerns blots, C5a ELISAs and C5a activity assays together suggest that neither OmCI, RaCI, SKY59, or Eculizumab prevented C5a-like generation by the three NSPs used. Unfortunately, the activity of CG-generated C5a fragments could not be confirmed using the RBL-C5aR1 reported cell line (figure 5-6B). I also investigated the mechanisms by which C5a can be generated by NSPs from C5 when in the presence of therapeutic inhibitors. I hypothesised that the therapeutic cleavage inhibitors themselves could also be susceptible to degradation by the NSPs. If so, proteolysis may reduce the activity of C5 cleavage inhibitors, allowing cleavage of C5a from C5 by NSPs; this will be addressed in the following section.

5.6. Investigating inactivation of therapeutic C5 cleavage inhibitors by NE

A haemolysis assay similar to that used in section 5.4 was performed to investigate whether NE had any impact on the activity of the therapeutic C5 cleavage inhibitors. All four C5 cleavage inhibitors were exposed to either NE or PBS and then incubated with C5. AAT was added to arrest NE activity (figure 5-7).

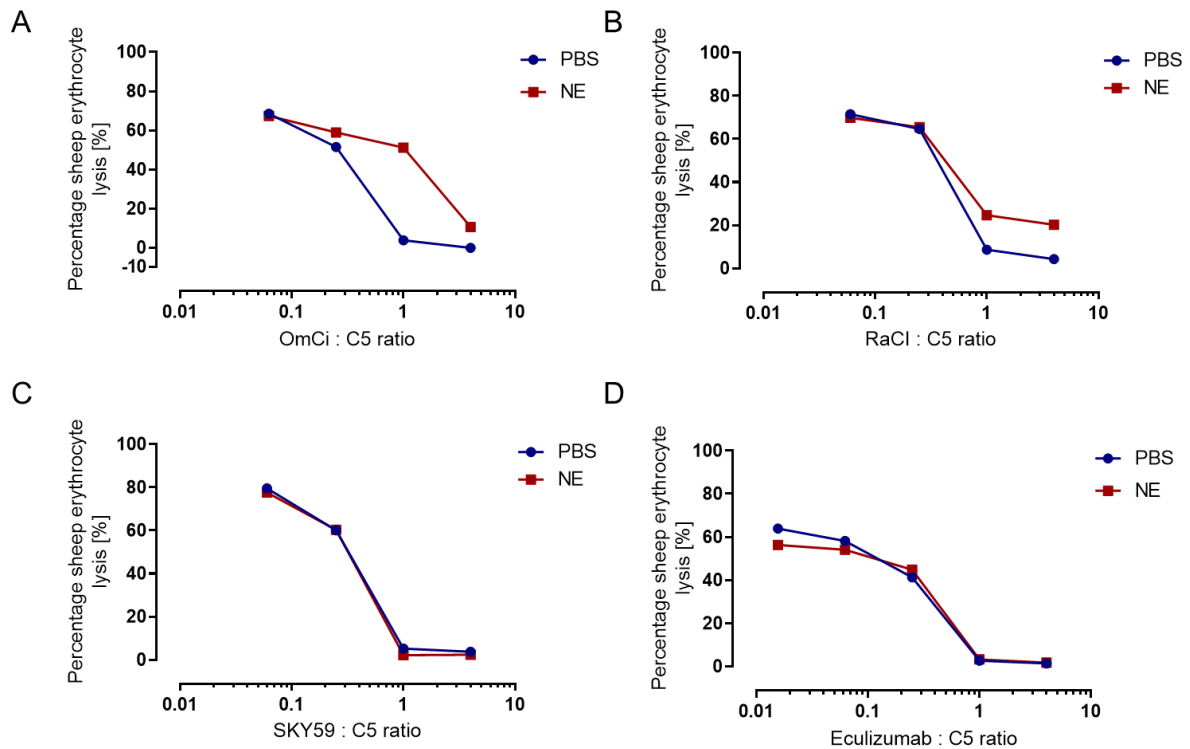


Figure 5-7: Impact of NE on the function of therapeutic C5 cleavage inhibitors. Lysis of sheep erythrocyte was used to measure activity of **A)** OmCi, **B)** RaCl, **C)** SKY59 and **D)** Eculizumab following exposure to 420 nM NE for 60 minutes at 37°C prior to incubating with C5. Mean activity was compared to cleavage inhibitor incubated without NE over a 4-fold dilution series where C5 was constant, n=2.

Data from haemolysis assays revealed that the small tick-derived inhibitors may be susceptible to degradation by NE (figure 5-7A and B). At a ratio of 1:1 (OmCi to C5, there was a reduction in OmCi activity compared to when untreated. Despite this, at a ratio of 4:1 inhibition of complement activity by OmCi could be maintained despite possible degradation by NE. RaCl also had reduced activity at a 1:1 ratio yet, at 4:1 activity began to plateau, suggesting a greater concentration of RaCl is required to prevent complement activation when exposed to NE. Unfortunately, due to the concentration of the RaCl stock solution the ratio of RaCl to C5 could not be increased beyond 5:1. Eculizumab and SKY59 did not show any obvious reduction in activity, indicating that the CDRs (antigen binding domains) were not

affected by NE exposure at the concentrations used. The experiments below were not repeated enough times to allow statistical interpretation.

5.7. Susceptibility of therapeutic C5 cleavage inhibitors to proteolysis by NE

From the above experiments I have shown some preliminary data that could suggest that the activity of OmCI and RaCI may be affected during exposure to NE. To explore inactivation of the therapeutic inhibitors by NE further I assessed their potential proteolysis by SDS-PAGE and silver staining. To visualise degradation, OmCI and RaCI were exposed to a dilution series of NE and proteins were resolved by SDS-PAGE and stained with silver nitrate, a sensitive protein stain (figure 5-8). SKY59 was also included; this was to investigate whether degradation of monoclonal antibody-based therapeutics was occurring despite no apparent impact on inhibitory activity, as shown by haemolysis assays.

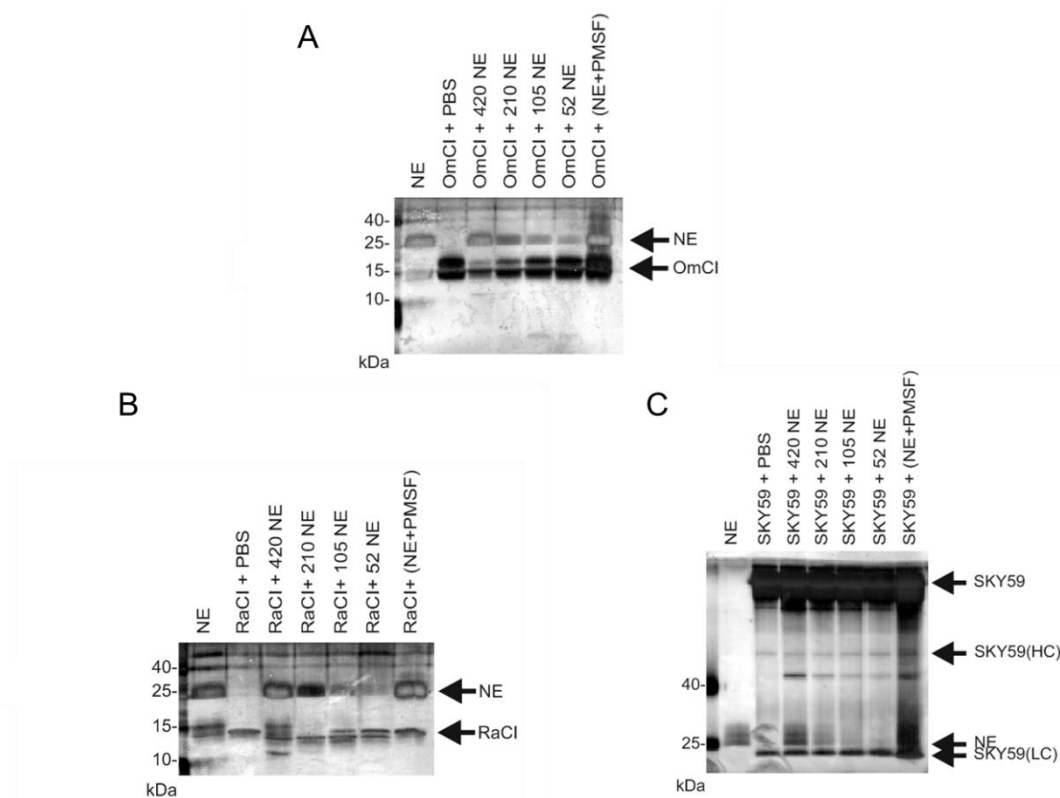


Figure 5-8: Visualising degradation of therapeutic C5 cleavage inhibitors following exposure to NE. A) OmCI B) RaCI and, C) SKY59 were exposed to 2-fold serial dilutions of 420 to 52 nM NE (similar to NE activity in the CF airway, see chapter 3) for 60 minutes at 37°C. Degradation was observed by silver stain following resolution on either 15% (OmCI and RaCI) or 12.5% (SKY59) bis-tris gels under non-reducing conditions. Bands were compared to NE only, cleavage inhibitor only and cleavage inhibitor with NE that had been inactivated by PMSF. “HC” – heavy chain, “LC” light chain. Representative of two experiments.

When separated by SDS-PAGE, RaCI resolved to approximately 14 kDa compared to the reported molecular weight of ~8 kDa (Jore *et al.* 2016). OmCI resolved into paired bands at approximately 15 and 19 kDa, compared to a reported molecular weight of ~17kDa (Hepburn *et al.* 2007). The molecular weight of NE was approximately 25 kDa, similar to the molecular weight specified by the manufacturer (29.5 kDa) (<https://www.athensresearch.com>). Another band at ~15 kDa was visualised when NE was resolved by SDS-PAGE (figure 5-8 A and B) and could represent sample spill over from OmCI and RaCI lanes respectively.

Silver staining the polyacrylamide gels provided some preliminary evidence that all the cleavage inhibitors in this experiment could be susceptible to degradation. This was particularly evident at the maximum NE Concentration (420nM). When OmCI was exposed to NE, the upper bands of the pair contained less protein, indicated by the fading bands (figure 5-8A). Moreover, inhibiting protease activity with PMSF prevented the loss of the upper OmCI band. The reduction in OmCI band intensity was titratable with NE concentration suggesting that protein loss was due to proteolysis.

RaCI was also susceptible to proteolysis; when RaCI was exposed to 420 nM NE there were lower molecular weight bands that had molecular weights of approximately 13 and 11 kDa (figure 5-8B). The generation of a lower molecular weight band was titratable with NE concentration and inhibition of protease activity with PMSF prevented RaCI degradation. Proteolysis of OmCI and RaCI observed in silver stained polyacrylamide gels supports the reduction in inhibitory activity that was shown in haemolysis assays.

Despite resolving SKY59 under non-reducing conditions, suspected IgG light (~25 kDa) and heavy chains (~50 kDa) were detected. None-the-less the majority of the protein was intact at the expected molecular weight of ~150 kDa (measured on a gel separate to the one shown. Both are representative of the same data). Interestingly, an unknown band at ~45 kDa was observed when SKY59 was exposed to NE. Furthermore, generation of this unknown band was dependent on the concentration of NE and was not present when either NE or SKY59 were incubated in PBS. Incubating NE with PMSF in this experiment did not fully inhibit the activity of this protease. PMSF is unstable in solution and therefore, it could be that in this experiment that the PMSF was less effective than when used previously.

In summary, in preliminary experiments I investigated the effect of NE of the activity of therapeutic C5 cleavage inhibitors. In these initial experiments I some evidence that the tick C5 cleavage inhibitors, OmCI and RaCI, could be less active when exposed to NE. I also used

SDS-PAGE to investigate the susceptibility of the therapeutic cleavage inhibitors to proteolysis by NE.

5.8. Discussion

Eculizumab is one of a handful of FDA and EMA approved anti-complement therapeutics. It has been successful in treating patients with PNH and aHUS over the past 10 years and is currently undergoing trials in other diseases (Morgan and Harris 2015). In light of non-canonical mechanisms of activating complement, I hypothesised that NSPs could generate functional C5a-like proteins in the presence of eculizumab, a monoclonal antibody-based C5-cleavage inhibitor. I investigated NSP-mediated generation of C5a following C5 incubation with Eculizumab or three other C5 cleavage inhibitors currently undergoing clinical and pre-clinical trials.

In this chapter it was shown in preliminary experiments that eculizumab and three other therapeutic C5 cleavage inhibitors were unable to fully inhibit C5a generation by three NSPs; NE, CG and PR3. C5a-like protein generation was visualised by western blot, quantified by ELISA and the activity of C5a-like fragments was verified using an RBL-C5aR1 reporter assay.

C5a-like fragment molecular weights were observed by western blot and their activity was confirmed in a β -hexosaminidase assay. In the absence of sequence data, I could only assume that the protein sequences of these fragments are the same as those generated without a cleavage inhibitor present. Nevertheless, mass spectrometry or C-terminal protein sequencing could be performed for better characterisation and comparison of C5a-like fragments generated in the presence of these C5 cleavage inhibitors. This kind of approach has been used to characterise C5a fragments generated by thrombin and protease released by *A. fumigatus* (Riedemann *et al.* 2017; Shende *et al.* 2018). When C5 was pre-incubated with RaCl I observed that the C5a generated by each NSP was slightly larger than those C5a fragments generated in the presence of the other C5 cleavage inhibitors. It is possible that the conformational change induced by RaCl as part of its inhibitory function alters the extent to which C5 exposes C5a for cleavage (Jore *et al.* 2016). None the less, based on the C5a activity assays the increased molecular weight of C5a when generated in the presence of RaCl did not lead to a change in activity for NE and PR3 generated fragments.

As discussed in chapter 4, there is a growing list (table 4-1) of proteases that are able to generate functional C5a-like fragments from degradation of C5. Despite knowledge of non-canonical complement activation and anaphylatoxin generation there are very few reports that

have investigated these alternative activation mechanisms with respect to eculizumab and other therapeutic C5 cleavage inhibitors.

Riedemann *et al.* hypothesised that eculizumab interfered with commercial C5a ELISAs preventing detection of C5a during clinical trials and that the generation of C5a by non-complement proteases was being masked by these issues (Riedemann *et al.* 2017). The authors demonstrated that trypsin and thrombin were able to generate C5a-like fragments in the presence of eculizumab. Furthermore, they used mass spectrometry to show that the fragments generated had a similar amino acid sequence to C5-convertase generated C5a (Riedemann *et al.* 2017). They, as I have in my study, raised concern over the cross-reactivity of commercial C5a ELISAs with C5. Despite raising this concern, their own in-house kit was assessed for cross-reactivity with C3, C3a, C4 and C5b-9 but cross-reactivity with C5 was not reported. Therefore, the reported C5a ELISA format may not be any more advantageous to what is already available on the market. In evidence of possible cross-reactivity with C5, their ELISA detects 45 ng/ml (3.85 nM) C5a in purified 50 nM C5, this is equal to 7.7% cross-reactivity (Riedemann *et al.* 2017). Therefore, although Riedemann *et al.* have shown generation of C5a by trypsin and thrombin in the presence of eculizumab, it is still not clear how important this particular mechanism is *in vivo*.

Riedemann *et al.* also hypothesise that an anti-C5a antibody would be required to provide protection from non-complement protease-generated C5a (Riedemann *et al.* 2017). Co-incubating C5 with eculizumab and their proprietary therapeutic antibody, IFX-1, reduced C5a detection but not generation. None-the-less, IFX-1 inhibited C5a-mediated CD11b upregulation on granulocytes. In summary of their study, C5 and C5a inhibitors may be required to regulate C5a activation by non-complement proteases. An advantage of my study over that of Riedemann *et al.* is that I have compared several pre-clinical and clinical therapeutic C5 cleavage inhibitors. As I have shown in figure 5-1, there are many competitive C5 cleavage inhibitors undergoing clinical trials that offer advantages such as lower dosage and better patient coverage (regarding the R885H mutation). Therefore, although eculizumab is currently the only C5 cleavage inhibitor currently being used in the clinic, it is probable that it will be replaced (Morgan and Harris 2015). Furthermore, it is important that new C5 cleavage inhibitors, undergoing clinical trials, are also assessed for their ability to block generation of C5a by NSPs and other non-complement proteases.

Thrombin-mediated generation of C5a in the presence of OmCI has been investigated by Roversi *et al.* (Roversi *et al.* 2013). Interestingly, OmCI has independent binding sites for C5 and LTB₄, a potent neutrophil chemoattractant discussed in section 1.4.4e (Roversi *et al.*

2013). The dual-inhibitory effects of OmCI were assessed using a murine model of acute lung injury (Roversi *et al.* 2013). The authors reported that OmCI did not prevent C5a-generation by thrombin *in vitro*, despite increasing OmCI to 100-fold excess of C5. They showed that as a therapeutic, OmCI was effective against reducing lung inflammation following ovalbumin insult, significantly decreasing neutrophil infiltration into the airway. Moreover, OmCI also significantly reduced C5a generation in BAL fluid sampled from the treated mice (Roversi *et al.* 2013). Despite these positive results, OmCI did not completely abolish neutrophil-mediated injury or C5a expression implying that other chemoattractants are important. I think that in light of my own work, the ineffectiveness of OmCI in reducing neutrophil mediated injury in their study may reflect an inability of OmCI to inhibit C5a generation by NSPs. The model used in the above study was for acute inflammation and therefore OmCI may be less applicable to chronic inflammatory airway disorders such as asthma, COPD and CF. None-the-less, this model still provides useful information on the mechanisms that lead to chronic inflammation in the airway.

An advantage to the current study was that C5a was accurately quantified by ELISA that has no reported cross-reactivity with C5 (<https://www.quidel.com>). Despite this, I measured 3.6% cross-reactivity between C5 and C5a in this ELISA. Another explanation is that the purified C5 is contaminated C5a; however, there was no evidence of this in western blots. In reflection of western blots observing nC5a in chapter 4, I do not think that western blots would be sensitive enough to detect these low levels of C5a.

Another advantage to this study was that I investigated proteolysis of each inhibitor by NE in order to try and explain why the therapeutic cleavage inhibitors are ineffective at preventing NSP-mediated C5a generation. Haemolysis assays and SDS-PAGE showed that RaCI and OmCI were susceptible to degradation by NE. Despite no loss of inhibitory activity, exposure of SKY59 to NE produced an unidentified fragment. NE degradation of IgG has been previously reported (Prince *et al.* 1979). Prince *et al.* have shown that NE degrades IgG producing a 50 kDa fragment that binds protein A, a virulence factor expressed on the surface of *Staphylococcus aureus* that binds to the Fc region of IgG (Prince *et al.* 1979). Therefore, it is also possible that the 45 kDa molecular band I observed in my own blots could also be a cleaved fragment of the SKY59 IgG Fc region. Prince *et al.* also show that the degraded IgG in their experiments still bound to antigen and was able to bind FcγR on the surface of neutrophils (Prince *et al.* 1979).

The degradation of IgGs by NSPs have been studied in the context of the CF airway and it has been hypothesised that NE burden in the inflamed airway could limit success of vaccines

against bacterial strains (Margaroli and Tirouvanziam 2016). The same principle could also apply to IgG-derived complement therapeutics such as eculizumab and SKY59 if they are to be used in neutrophil driven diseases such as sepsis. To overcome the potential for degradation, all inhibitors in my experiments were used in 5-fold excess of C5, ensuring complete inhibition of canonical complement activation even when exposed to NE. From this, I concluded that C5a generation in the presence of the cleavage inhibitors was a result of protease bypassing the inhibitor and not sequential degradation of the inhibitor followed by C5 (figure 5-9).

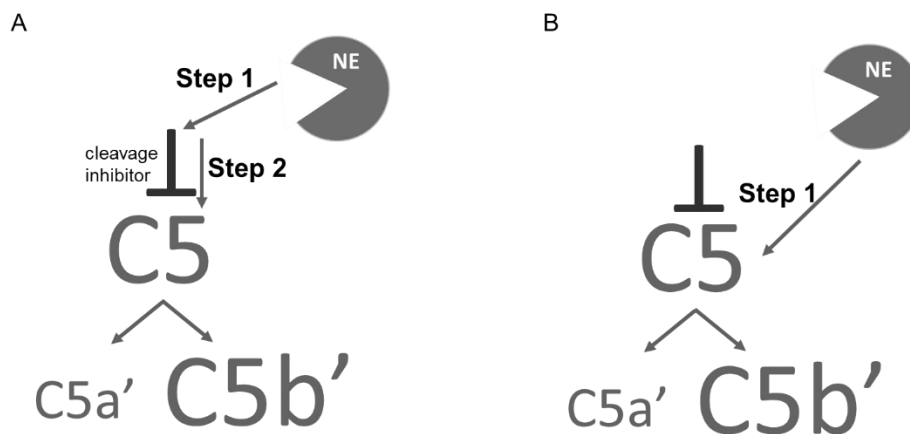


Figure 5-9: Diagram of the mechanisms by which NE could bypass C5 cleavage inhibitors.

A) NE generates C5a' (and other products) in a two-step manner 1) degradation of the C5 cleavage inhibitor and 2) proteolysis of C5. **B)** NE generates C5a' by bypassing the C5-cleavage inhibitor.

C5a generation by NSP was investigated in this chapter; however, I did not explore the generation of functional C5b. Therefore, it is still not fully understood whether terminal pathway activation can be initiated by NSPs, or during inhibition by the therapeutic used in this study.

In chapter 4 it was shown that proteases expressed in CF BAL fluid can generate C5a-like fragments that may promote disease progression. Therapeutic inhibition of complement in the CF airway has not been explored, this is likely to be due a lack of understanding of how much complement contributes to disease progression. Despite this, C5a and C3a generation have also been associated with disease progression in airway hyperresponsiveness in asthma (Khan *et al.* 2014). As well as NSPs, dust mite proteases have been reported to generate C5a-like fragments in asthma (Maruo *et al.* 1997). Complement inhibitors have been investigated as a method to reduce airway hyperresponsiveness in asthma: A chimeric IgG with complement receptor related gene y (CRRY), a molecule analogous to human soluble-

CR1 (a receptor for C3b and complement inhibitor), was used to reduce complement activation and consequent airway inflammation in mice exposed to ovalbumin (Taube *et al.* 2003). However, as discussed above with regards to OmCI, if C5 cleavage inhibitors were to be considered as a viable option to prevent C5a generation then the ability of non-complement proteases to bypass current C5 cleavage inhibitors needs to be investigated further. In this case, inhibitors specific to C5a (IFX-1) or C5aR1 (PMX53) may be more appropriate for the control of C5a-mediated inflammation and smooth muscle contraction (Subramanian *et al.* 2011; Sun *et al.* 2015).

As well as in the CF airway, neutrophilic inflammation is also a pathogenic factor in sepsis. Patients receiving eculizumab already receive a course of antibiotics and meningitis vaccines to counteract reduced protection via the complement system (Wong *et al.* 2013). A hypothetical scenario could occur whereby a patient, administered with eculizumab, upon contracting systemic infection could be at risk of developing sepsis mediated by C5a activation of neutrophils. C5a generation and neutrophil dysfunction are associated with disease severity in sepsis, however the contribution of NSP-generated C5a has not been investigated (Conway Morris *et al.* 2009; Xu *et al.* 2016).

OmCI, co-administered with an anti-CD14 antibody, has been used to reduce inflammation in a porcine model of sepsis (Skjeflo *et al.* 2015). The authors observed a significant reduction in complement terminal pathway components and inflammatory cytokines but C5a concentration was not measured. RA101295, a small peptide (2 kDa) C5 cleavage inhibitor has also been investigated in a non-human primate model of *E. coli* induced sepsis (Keshari *et al.* 2017). It was observed that C5a levels in baboon blood were significantly reduced at 2 and 4 hours timepoints when animals were given subcutaneous injections of the inhibitor (Keshari *et al.* 2017). Despite this, the authors found that C5a levels continued to increase up to 72 hours after administration; however, no untreated animals survived past 36 hours for comparison of C5a concentration in serum. As with the other inhibitors tested in my study it is unclear whether RA101295 is effective at preventing C5a generation by NSPs.

The present study was limited to *in vitro* studies and therefore it would be interesting to study these mechanisms *in vivo*. Further *ex vivo* and *in vivo* studies could be carried out to investigate this mechanism further. For instance, I could have tested the ability of proteases in CF BAL fluid to generate C5a in the presence of these therapeutic inhibitors. As discussed in chapter 3, antibodies specific to NSP, thrombin and other non-complement-generated C5a would enhance quantification of alternative forms of C5a that are generated during disease manifestation.

5.9. Conclusion to the chapter

In addition to reports investigating thrombin and trypsin, it has been demonstrated in this study that NE, CG and PR3 can generate C5a-like fragments despite pre-incubation of C5 with eculizumab. Furthermore, three additional C5 cleavage inhibitors were also ineffective against NSP-mediated C5a generation. Expression of NSPs is upregulated during chronic neutrophilic inflammation and therefore, non-canonical C5a activation should be considered when new therapeutic inhibitors are being explored for use in inflammatory diseases. Further investigation is required to determine the contribution of non-complement proteases towards C5a generation.

6. Characterising interactions between C5a and glycosaminoglycans

6.1. Background to the chapter

The characterisation of interactions between GAGs and pro-inflammatory molecules has significantly changed understanding of neutrophilic inflammation in the CF airway (Reeves *et al.* 2011a). In testament to this enhanced understanding, therapeutics targeting GAGs (in particular CXCL8-GAG interactions) are being developed for use in CF clinics (Furnari *et al.* 2012; McElvaney *et al.* 2015; Brivio *et al.* 2016). The following section will give a brief overview of the literature that supports our current understanding how GAGs can promote CF pathogenesis and is the basis for the investigations in this chapter.

6.1.1. Structure of GAGs and their diversity

GAGs are ubiquitous. They are negatively charged, long chains of repeating disaccharides and important structural components of the ECM (Reeves *et al.* 2011a; Lindahl *et al.* 2015). There are five well-characterised GAGs; (HA, dermatan sulphate, CS, HS and heparin (figure 6-1). There are two categories of GAGs, these are sulphated and non-sulphated; HA is non-sulphated whereas, heparin and other “sulphate” GAGs are sulphated (Lindahl *et al.* 2015). A further distinction is that sulphated GAGs are synthesised in the Golgi apparatus whereas HA is produced at the inner surface of the cell membrane (Lindahl *et al.* 2015). Synthesis of sulphated GAGs is catalysed by polymerisation enzymes. For example, the carbohydrate transferases glucuronosyltransferase and N-acetylgalactosaminyltransferase are essential for the production of CS (Lindahl *et al.* 2015). O-sulphation groups are added to sulphated GAGs by sulfotransferases which depend on the carbohydrate substrate, N-acetyl-D-glucosamine has a 4-O-sulphation whereas iduronic acid has a 2-Osulphation (see figure 6-1) (Lindahl *et al.* 2015).

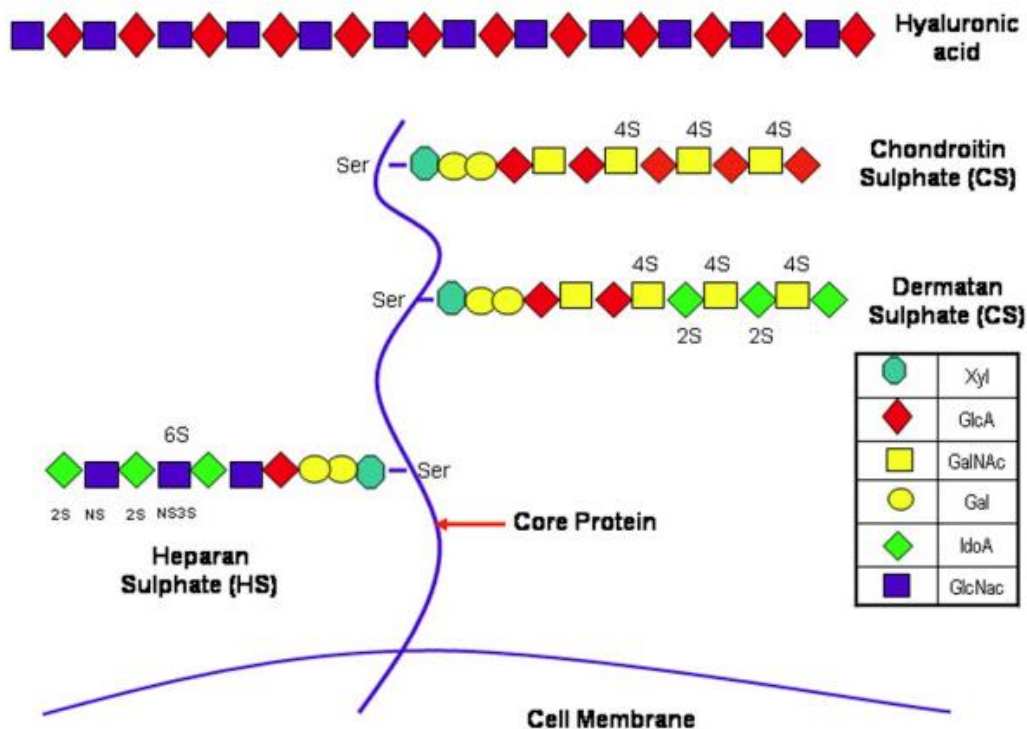


Figure 6-1: Diagram of the carbohydrate composition of GAGs, extracted from Souza-Fernandes et al. (Souza-Fernandes et al. 2006). Hyaluronic acid does not interact with a protein core, it is composed of alternating repeats of D-glucuronic acid (GlcA) and N-Acetylglucosamine (GlcNAc). Sulphated GAGs interact with protein cores through bonds between serine on the core and GlcA – galactose (Gal) - xylose (Xyl) on the sulphated GAG. CS is a disaccharide repeat of N-acetyl-D-glucosamine (GalNAc) and GlcA. Dermatan is a disaccharide repeat of GalNAc and iduronic acid (IdoA). HS is a disaccharide repeat of IdoA and GlcNAc. Sulphated GAGs are differentially sulphated depending on carbohydrate annotated with “S” and number of carbon atom within the corresponding sugar.

Following synthesis from the Golgi apparatus GAGs form proteoglycans, assembling around a protein cores that can be membrane bound, for example syndecan, or protein cores can be secreted, such as perlecan, an integral part of ECM assembly (figure 6-2) (Lindahl *et al.* 2015). Furthermore, not all GAGs interact with the same protein cores and moreover, HA does not require a protein core, and is synthesised at the cell membrane not the Golgi (Pichert *et al.* 2012b). There are three membrane-associated enzymes that generate HA. These are called HA synthases-1, -2 and -3, and have different functions; HA synthase-1 and -2 generate high-molecular weight HA and HA synthase-3 produces low-molecular weight HA (Itano *et al.* 1999).

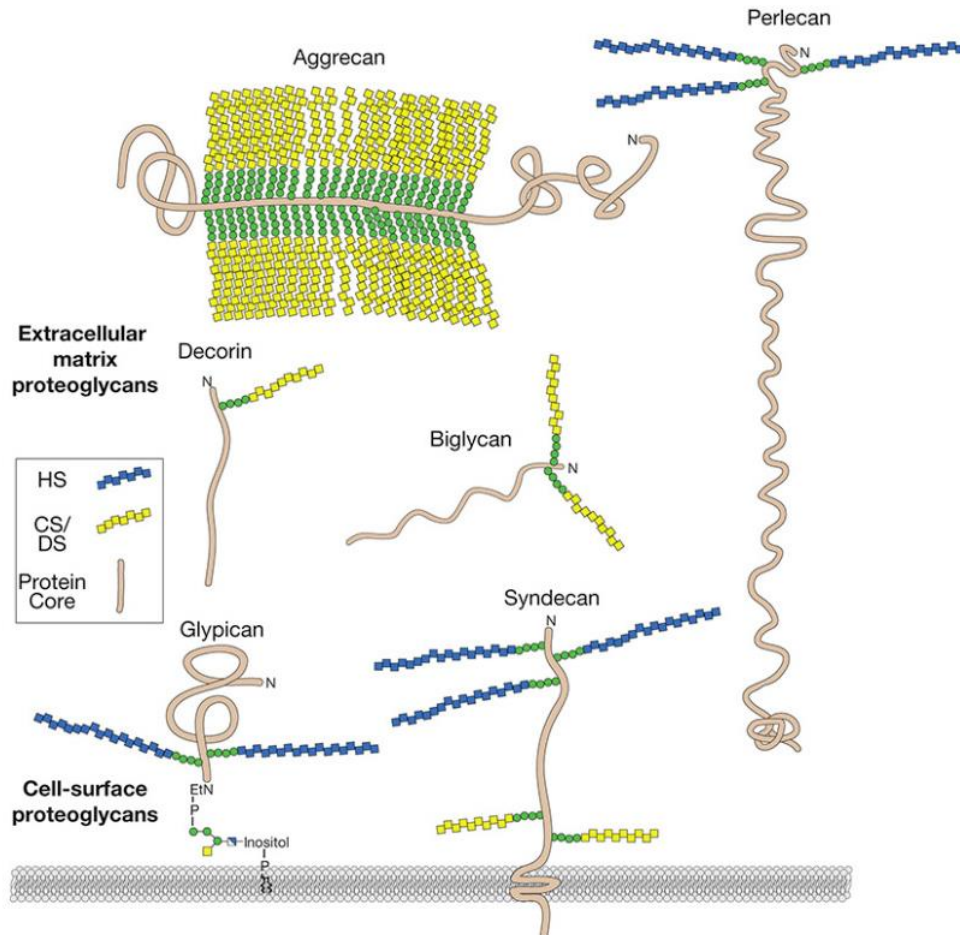


Figure 6-2: Proteoglycan cores and associated GAGs, extracted from Lindahl et al. (Lindahl et al. 2015). Proteoglycan cores can be membrane bound via GPI anchors (glypican) or transmembrane domains (syndecan). Proteoglycans can also be secreted; secreted proteoglycan cores are important for extracellular matrix structure. Proteoglycans can be bound by different sulphated GAG species; CS and dermatan sulphate (yellow) or, HS (blue).

The physio-chemical properties of GAGs are derived from heterogenous polysaccharides that have varied length as well as dynamic states of sulphation and acetylation, governed by N-sulphotransferase and N-deacetylase, present in the Golgi (Humphries *et al.* 1997). As an example of GAG diversity, it has been estimated that HS has 48 different disaccharide forms of structurally modified iduronic acid (Parish 2006).

6.1.2. Functional roles of GAGs in inflammation

The diverse chemical properties of GAGs mean that they have a wide-range of roles in cellular functions such as communication, differentiation, adhesion, antigen presentation and cell migration (Whitelock and Iozzo 2005; Reeves *et al.* 2011a). For example, the addition of sulphate groups to carbon-3 of N-acetylglucuronic acid within HS produces a non-coagulant surface on endothelial cells facilitating free movement of cells within the vasculature

(Whitelock and Iozzo 2005). In addition, surface-GAG expression and sulphation can be dynamically regulated during inflammation, this can promote leukocyte adhesion by binding chemoattractants (Parish 2006). Wang *et al.* have shown *in vivo* that HS proteoglycan interacts with L-selectin, promoting L-selectin-mediated leukocyte adhesion to endothelial cells via PSGL-1 (Wang *et al.* 2005). In these experiments, the authors used knockout mice that conditionally expressed endothelial N-sulphotransferase and showed that sulphation of HS was required for migration of leukocytes towards gradients of chemokines.

Furthermore, although HA is not sulphated, it has been shown that HA length can alter its immunomodulatory function and has been shown to promote inflammation in airway disease (Matuska *et al.* 2016). Short chain HA (150-300 kDa) has been reported to be proinflammatory whereas long chain HA (1000 kDa) has been demonstrated to be anti-inflammatory (Matuska *et al.* 2016). HA is modified by the transfer of heavy chains from inter- α -inhibitor, a serine protease inhibitor, to carbon-6 hydroxyl groups of N-acetyl-glucosamine, that make up the structure of hyaluronic acid (Dyer *et al.* 2016a). The above reaction is catalysed by an enzyme called TNF-stimulated gene 6. This complex modification induces crosslinking of HA that promotes leukocyte adherence and release of enzymes that in turn degrade HA into the short, pro-inflammatory fragments that are recognised in a DAMP-like manner by TLR-4 (figure 6-3) (Matuska *et al.* 2016).

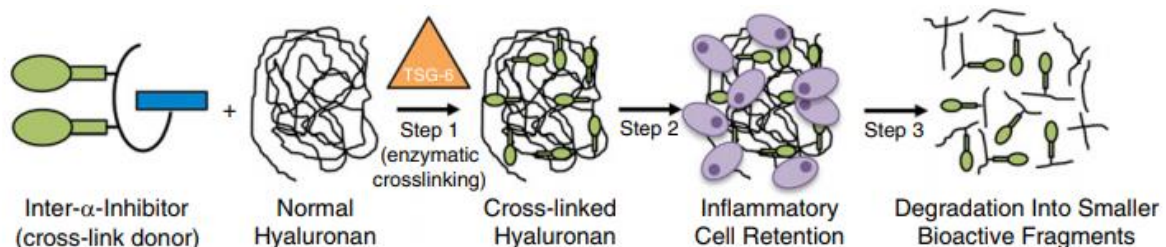


Figure 6-3: Processing of HA during inflammation, extracted from Matuska *et al.* (Matuska *et al.* 2016). The heavy chain (blue box) of inter- α -inhibitor binds to HA, this facilitates TSG-6 mediated cross-linking. HA matrices promote leukocyte migration and clumping, leukocytes release enzymes that break down HA into smaller fragments that act as DAMPs and signal via TLR4.

6.1.3. The role of GAGs in the CF airway

GAGs are an important constituent of the ECM interstitium and sub-epithelial tissue that provide structural support, maintain hydration and facilitate migration of leukocytes during an inflammatory response (Souza-Fernandes *et al.* 2006). The role of GAGs in the CF airway has an added layer of complexity compared to their normal function; degradation and remodelling of the ECM in CF airway by neutrophil and pathogen-derived proteases releases

soluble GAGs into the airway surface liquid (Reeves *et al.* 2011a). In particular, three soluble GAGs have been reported to be elevated in the CF airway compared to healthy controls; HS, CS and the non-sulphated GAG, HA (Reeves *et al.* 2011a). The properties and reported roles of these GAGs have been described in the overleaf (table 6-1).

Summarising table 6-1, a diverse range of techniques has been employed to detect and quantify soluble GAGs in the CF airway; these include restricted digestion of GAGs using GAGases, immunohistochemistry and electrophoresis. Therefore, it is difficult to compare the expression of soluble GAGs between different CF patient cohorts. Furthermore, groups have made different observations about which GAGs are elevated, with each study suggesting one GAG is more important for disease progression than the other. None the less, the studies summarised in table-6-1 have shown elevated soluble GAG concentrations in BAL fluid compared to non-CF controls, such as non-CF bronchiectasis. The immunomodulatory role of GAGs is not necessarily dependent on higher expression but, the level of sulphation (HS and CS), length (HA) and solubilisation following degradation of the ECM. Simply measuring GAGs does not inform us about their structural diversity. For instance, diversity of HA chain length and association with heavy chains donated by inter- α -inhibitor has been investigated in the CF airway (Matuska *et al.* 2016).

	Heparan Sulphate	Chondroitin Sulphate	Hyaluronic Acid
Saccharide Components	β -D-glucuronic acid N-acetyl- α - D-glucosamine	D-galactosamine D-glucuronic acid	D-Glucuronic acid N-acetylglucosamine
Functions	<p>HS is a constituent part of the ECM scaffold by binding laminin supports</p> <p>HS interacts with Collagen V in the ECM adhering the ECM to the basement membrane.</p> <p>Cytokine interaction (CXCL8, IL-5, IL-6, IL-10, IL-18, TNFα and, platelet factor 4). CXCL8 Interaction with GAGs protects CXCL8 from degradation by neutrophil serine proteases</p>	<p>CS interacts with several cell-signaling molecules that have roles in growth and differentiation cytokines, chemokine and enzymes. Binding to these molecules can be augmented by the degree of sulphation.</p>	<p>Long HA form (1000 kDa) is anti-inflammatory and possess bacteriostatic properties</p> <p>HA interact with inter-α-inhibitor heavy chains, a reaction catalysed by TNF-stimulated gene 6. Promotes leukocytes recruitment (see figure 6-3).</p> <p>Short HA form (150-300 kDa) cleaved from long by hyaluronidases. Short HA has pro-inflammatory roles through interaction with; CD44 – leukocyte rolling/activation; RHAMM (receptor for HA-mediated motility) – leukocyte rolling/activation/inflammation Signaling via TLR2 and TLR4 (DAMP-like)</p>
Expression in CF	<p>Elevated expression of intact HS and epithelial and endothelial basement membranes in CF and COPD compared to non-CF controls</p> <p>Soluble HS fragments also elevated in the CF airway due to degradation of the ECM</p>	<p>Digestion by GAGases and agarose electrophoresis identified CS in CF and chronic bronchitis patients</p> <p>Expression of CS proteoglycan cores in CF and non-CF bronchiectasis has been shown by western blot</p>	<p>Crude chemical separation of saccharides in CF BAL fluid demonstrate that HA acid was the only detectable GAG.</p> <p>Fluorophore assisted carbohydrate electrophoresis demonstrated elevated heavy chain-hyaluronic acid complexes in CF sputum.</p>
Roles in CF	<p>Binding of CXCL8 to HS prevents proteolysis increasing half-life of HS in the airway and promoting neutrophilic inflammation</p> <p>HS can be used as an adherence molecule for <i>P. aeruginosa</i> (opportunistic pathogen in the CF airway).</p>	<p>CFTR mutation alters intracellular organelle pH, altering activity of glycosyltransferase and may be responsible for increased CS polymerisation.</p> <p>CS increases turbidity of mucus and can induce plug forming.</p>	<p>CFTR facilitates HA transport across epithelial cell membranes, reduced function due to lack of CFTR could lead to accumulation in epithelial cells.</p>
References	(Solic et al. 2005; Reeves et al. 2011a)	(Rahmoune et al. 1991; Bhaskar et al. 1998; Khatri et al. 2003)	(Sahu 1980; Garantziotis et al. 2016; Matuska et al. 2016)

Table 6-1: Comparison of structure and function of GAGs expressed in the CF airway.

6.1.4. Interaction between CXCL8 and GAGs in the CF airway

Chemokine-GAG interaction is one of the most well-documented mechanisms of immune-modulation by GAGs and, has been suggested to be a contributing factor to pathogenesis in the CF airway (Reeves *et al.* 2011a). It has been proposed that chemokine-GAG interaction has multiple roles during inflammation such as ligand-receptor presentation and establishing chemotactic gradients within tissue (figure 6-4) (Tanino *et al.* 2010; Pichert *et al.* 2012b; Dyer *et al.* 2016b).

CXCL8-GAG interaction has been studied intensely and precise binding sites for heparin, HS, CS, dermatan sulphate and, HA have been mapped on NMR structures (Spillmann *et al.* 1998; Krieger *et al.* 2004; Pichert *et al.* 2012a). Interestingly, there is a core region of CXCL8 (amino acids 57-77) that binds strongly to all the above GAGs. In particular, lysine-59, valine-66, valine-67, lysine-69, alanine-74, and glutamine-75. The latter, glutamine, was observed to have the largest chemical shifts when analysed using NMR indicating strong interaction (Pichert *et al.* 2012a).

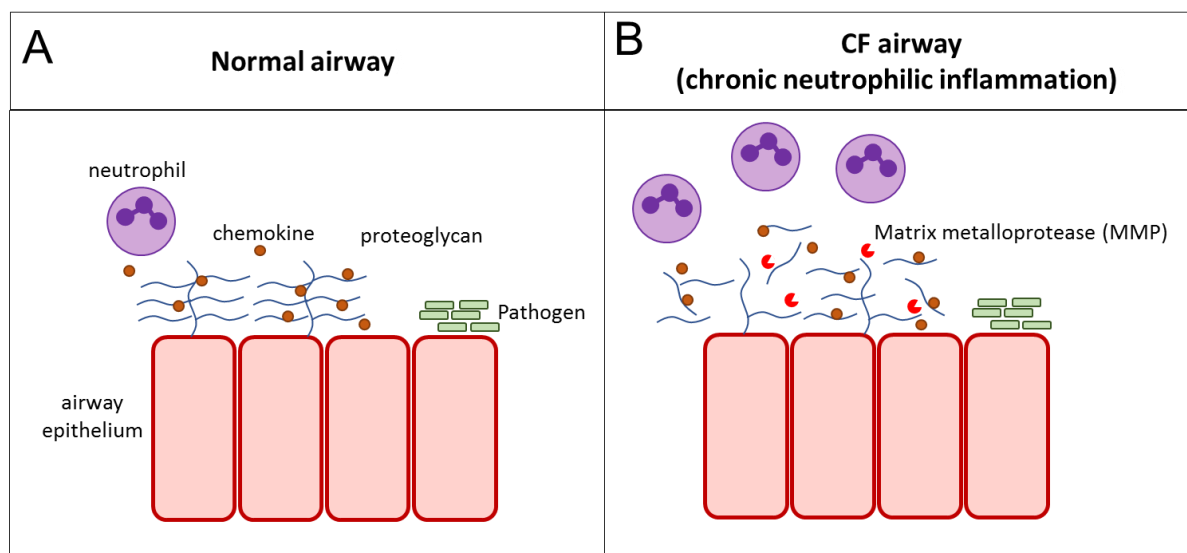


Figure 6-4: Chemotactic role of GAGs in the airway. **A)** Chemokines establish chemotactic gradients using proteoglycans and hyaluronic acid (not shown). **B)** Excessive neutrophilic degranulation releases NSPs and MMPs that breakdown ECM and structural GAGs disrupting chemotactic gradients, hampering pathogen clearance.

As well as understanding the chemistry behind chemokine-GAG binding, the influence of GAG interaction on chemokine function has also been investigated (Kuschert *et al.* 1999; Culley *et al.* 2003). Several groups have used Boyden chamber cell migration assays to investigate the functional consequences of CXCL8-GAG complexes, with some conflicting data. Webb *et al.* demonstrate that HS but neither heparin nor CS increased CXCL8 potency as a neutrophil chemoattractant (Webb *et al.* 1993). Whereas, Ramdin *et al.* report reduced neutrophil migration when heparin, HS or, dextran sulphate were incubated with CXCL8, compared to CXCL8 without GAGs (Ramdin *et al.* 1998). In addition, Schlorke *et al.* observed reduced chemotaxis to CXCL8 with heparin but not CS or HS (Schlorke *et al.* 2012). In the same study it was shown that CS and heparin induced increased oxidative burst in neutrophils when co-incubated with CXCL8. To add further complexity, CXCL8 forms dimers that have altered affinity for GAGs; the significance of oligomerisation and GAG interaction on CXCL8 function is not fully understood (Gangavarapu *et al.* 2012; Joseph *et al.* 2015).

With greater relevance to CF, CXCL8 is susceptible to proteolysis by NE, but when in complex with GAGs it has been demonstrated that CXCL8 becomes resistant to degradation by NE (Leavell *et al.* 1997; Reeves *et al.* 2011b). Reeves *et al.* use western blots to show that CXCL8 in the CF airway is present in both native and GAG-complexed forms. Furthermore, by exposing CF BAL fluid to GAG lyases the authors observe that CXCL8 can be liberated from GAG complexes and is consequently degraded if also exposed to NE. The authors also show that degradation of CXCL8 also occurs when NaCl concentration in BAL fluid is increased. The mechanism behind this phenomenon is that at NaCl concentrations between 300 and 450 mM, the ionic bonds binding CXCL8 and GAGs are disrupted, freeing and exposing CXCL8 to degradation by NE. Nebulised hypertonic saline is routinely administered to CF patients to facilitate mucus clearance. Reeves *et al.* also show that increasing NaCl concentration in CF BAL fluid reduces the chemotaxis of neutrophils, with the assumption that CXCL8 is freely degraded (Reeves *et al.* 2011a). However, the authors did not speculate on any other GAG-binding chemokines or chemotactic factors, such as C5a.

6.1.5. Interactions between C5a and GAGs

C5a has similar properties to CXCL8 such as low molecular weight, structure, and charge (isoelectric point). C5a and CXCL8 are chemotactic for neutrophils, stimulate degranulation, and induce oxidative burst through interaction with their respective G-protein coupled receptors. It has been observed that heparin-based sorbent and surfaces pre-coated with heparin reduce C5a concentration in the circulation (Mollnes *et al.* 1991; Sinitsyn *et al.* 1992).

These observations were made when investigating methods to reduce spontaneous complement activation during cardiac bypass surgery (Mollnes *et al.* 1991; Sinitsyn *et al.* 1992). The effect of heparin on rhC5a (recombinant) function has also been investigated; Culley *et al.* assessed the inhibitory effect of heparin on several CCL chemokines and rhC5a (Culley *et al.* 2003). They observed that when incubated with heparin, CCL11 and CCL13 but not rhC5a inhibited shape change, chemotaxis and oxidative burst using HL60 cells, an immortal cell line with neutrophil-like properties. Despite demonstrating that heparin had no effect on rhC5a activity in these assays, the authors observed that rhC5a was retarded on a sepharose-heparin column suggesting that rhC5a does interact with heparin.

In light of the above studies, C5a interaction with other GAGs, such as those expressed in the CF airway, has not been comprehensively characterised. As shown in chapter 4, C5a can be readily generated in the CF airway by complement activation and other non-complement proteases such as NSPs.

6.2. Hypothesis

I hypothesised that C5a binds ionically to soluble GAGs and that these interactions influence C5a activity, a mechanism that could be important for the normal roles of C5a in inflammation. I also hypothesise that in the CF airway, modification of C5a activity by GAGs promotes chronic neutrophilic inflammation.

6.3. Aims for this chapter

1. Investigate the expression of GAGs in the BAL fluid from CF patients.
2. Develop methods to characterise C5a-GAG binding using purified HS, CS and HA.
3. Investigate the functional significance of nC5a-HS interaction on C5a activity using the RBL-C5aR1 reporter cell line.

6.4. Sulphated GAG expression in the CF airway

Before investigating C5a-GAG interaction, GAG expression in the CF airway was measured in CF BAL fluid. This was to confirm that there was expression of soluble GAGs in the CF airway and to assess whether there was any association with the concentration of C5a in those samples.

6.4.1. Quantifying soluble GAGs in CF BAL fluid

GAG expression was detected using dimethyl-methylene blue, a stain that has been described to bind sulphated GAGs (Stone *et al.* 1994). Dimethyl-methylene blue has been used to measure GAG release following cartilage breakdown in response to injury (Jeffrey and Aspden 2007). Visually, when in suspension with GAGs, the colour of dimethyl-methylene blue shift from deep blue (no GAGs) to violet (GAGs present), this change in colour can be detected using a spectrophotometer by measuring absorbance at 570nm. To quantify sulphated GAG concentration in CF BAL fluid, a reference curve was required. A comparison of purified HS and CS over a 2-fold dilution demonstrated similar absorbance curves when incubated with dimethyl-methylene blue (figure 6-5).

When GAGs were not present the optical absorbance is approximately 0.62 absorbance units, whereas when CS was added the optical density was reduced to a minimum of approximately 0.2 absorbance units (figure 6-5).

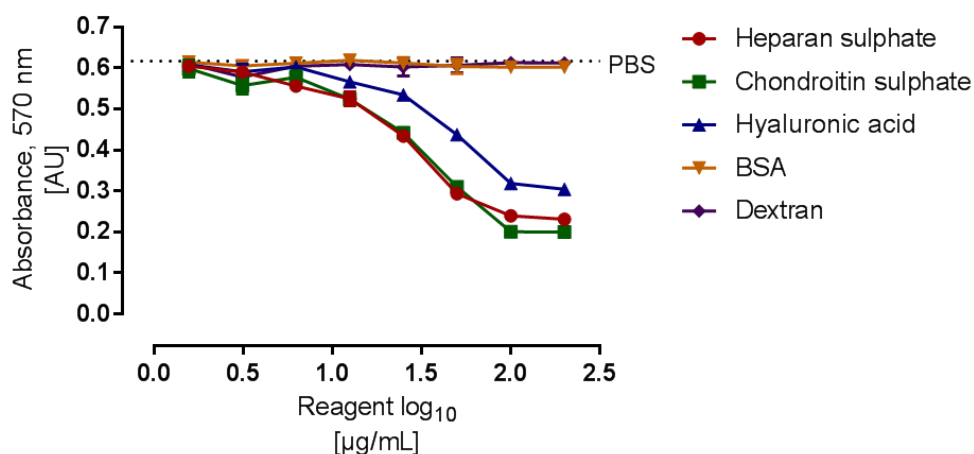


Figure 6-5: Dimethyl-methylene blue stain assay for quantifying sulphated GAGs in CF BAL fluid. Absorbance was measured at 570 nm. Comparison of GAGs; HS (red), CS (green), and HA (blue) in a 2-fold dilution series from 200 to 0.78 µg/mL. BSA (orange) and dextran (purple) were used as negative controls and diluted in the same series. PBS, without GAG, is represented by the dotted black line, Mean of two experiments plotted.

Despite reports that dimethyl-methylene blue binds sulphated GAGs, a naturally non-sulphated GAG, HA, was also positive for the stain (Stone *et al.* 1994). To further assess the specificity of the dimethyl-methylene blue stain, BSA and dextran were included as generic examples of protein and carbohydrate respectively. Neither BSA nor dextran stained positively when diluted to the same concentrations (mass/volume) as HS and CS. Given the purpose of the stain was to enable quantification of GAGs in the CF airway, this assay was still suitable to give an indication of GAG concentration in CF BALF fluid.

A standard curve of HS in 2-fold dilution series from 200 to 0.78 $\mu\text{g}/\text{mL}$ was used for quantification of GAGs in CF BAL fluid (figure 6-6). A preliminary experiment was performed to ascertain what dilution factor of CF BAL fluid samples was required for accurate quantification. Using CXCL8 as marker of inflammation, five CF BAL fluid samples were chosen that represented a range of inflammatory states. GAG expression was detected in four out of five samples when BAL fluid was diluted 2-fold in PBS (not shown) therefore, a 1 in 2 dilution factor was used for the remaining cohort samples. GAG expression in CF BAL fluid samples from 39 patients was measured, in one patient quantification was below the detection limit (0.78 $\mu\text{g}/\text{mL}$). The median expression was 37.2 $\mu\text{g}/\text{mL}$ with a range of 0.39 to 389 $\mu\text{g}/\text{mL}$ relative to a HS curve. To my knowledge, this is the first time that soluble GAGs concentration in CF BAL fluid has been quantified using dimethyl-methylene blue stain.

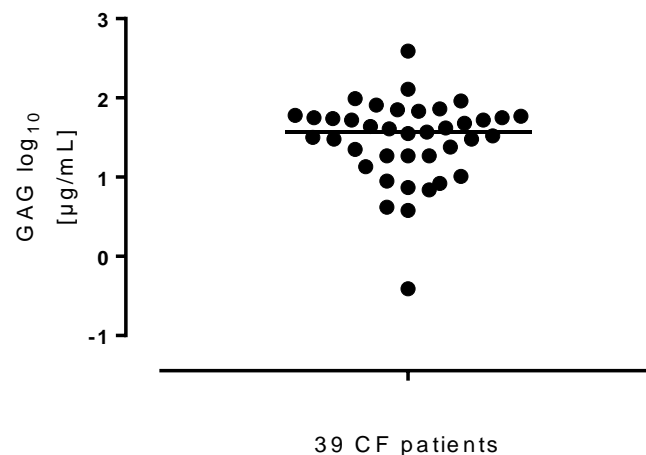


Figure 6-6: Soluble GAG concentration in CF BAL fluid. CF BAL fluid was diluted 1 in 2 in PBS and incubated with dimethyl-methylene blue. Absorbance at 570 nm was read immediately using a spectrophotometer. GAG concentration (y-axis) was quantified by interpolating absorbance values from a standard curve of purified HS (200 to 0.78 $\mu\text{g}/\text{mL}$). Black bar represents cohort median for n=39.

6.4.2. Correlations between GAGs and markers of neutrophilic inflammation in CF BAL fluid

As discussed in the background to the study, it has been shown that GAG expression correlates with neutrophilic inflammation in the CF airway (Solic *et al.* 2005). A correlation was performed on my data to assess the relationships between GAGs and markers of neutrophilic inflammation (neutrophil count, CXCL8 and NE activity) in CF patients (figure 6-7).

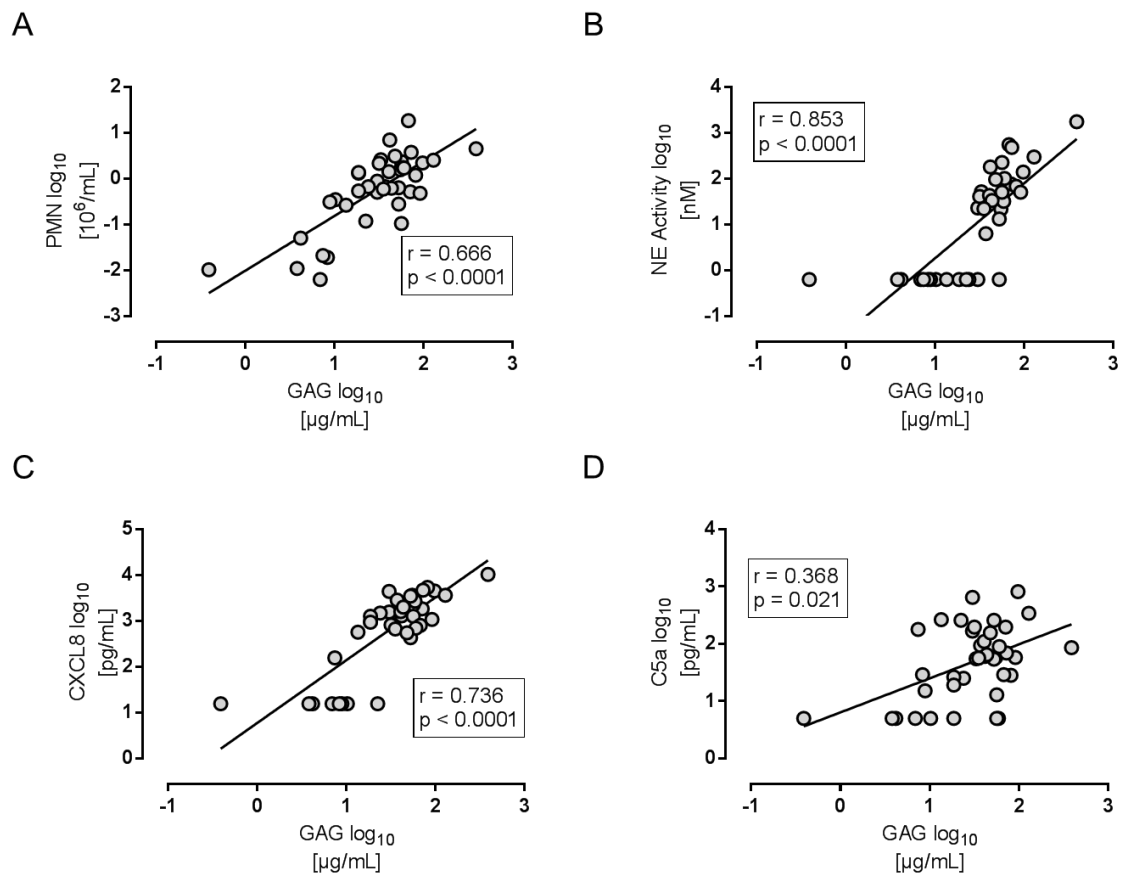


Figure 6-7: Spearman rank correlation analysis of GAGs and markers of neutrophilic inflammation in CF BAL fluid. Correlations between GAGs (y-axis) and **A)** PMN count, **B)** NE Activity, **C)** CXCL8, and **D)** C5a (x-axis). A “line of best fit” was plotted (black line) using linear regression analysis. Correlation outcomes, r and p , for each analysis are in boxes. $N=39$ for each analysis.

In this study, there was a statistically significant positive correlation with PMN count (figure 6-7A: $r = 0.666$, $p < 0.0001$). Soluble GAGs are liberated by degradation of ECM by neutrophil derived proteases such as NE. Therefore, evidence for the liberation of soluble GAGs in the CF cohort was assessed by correlating GAG expression with NE activity. There was a significant positive correlation between NE and GAG expression in CF BAL fluid (figure 6-7B: $r = 0.853$, $p < 0.0001$). The interaction between CXCL8 and GAGs has been well

characterised (Pichert *et al.* 2012b). In this study, there was a significant positive correlation between CXCL8 and GAGs (figure 6-7C: $r = 0.736$, $p < 0.0001$). To obtain initial evidence of C5a-GAG interaction in the CF airway, the correlation between C5a and GAGs was tested. There was a significant positive correlation between C5a and GAGs (figure 6-7D: $r = 0.368$, $p = 0.021$).

Analysis of CF BAL fluid confirmed that GAG expression correlates with markers of neutrophilic inflammation. There was a correlation between C5a and GAGs in the CF airway and therefore this relationship required further investigation. This is the first time GAG concentration has been correlated with C5a in pathological samples. Despite a significant positive relationship, these data are not conclusive evidence of interaction. Therefore, in the following section the interaction between C5a and GAGs was investigated.

6.5. Characterisation of C5a-GAG interactions by PAGE

In the literature several methods have been used to visualise and characterise GAG interaction with proteins; these include PAGE, affinity chromatography and solid phase plate-based assays (Culley *et al.* 2003; Clark *et al.* 2006; Reeves *et al.* 2011b).

6.5.1. Resolving nC5a and rhC5a by native-PAGE and BN-PAGE

Reeves *et al.* demonstrate CXCL8-GAG interactions in CF BAL using native PAGE, a technique that exploits the native charge (isoelectric point, pI) of the target protein and running buffer pH for gel migration, rather than a charge carrier such as SDS (Fiala *et al.* 2011; Reeves *et al.* 2011b). To optimise this technique for resolution of C5a and potential C5a-complexes, rhC5a was compared to nC5a in a dilution series (figure 6-8A). Functional differences were observed between nC5a and rhC5a in chapter 4 and therefore, further differences may also persist in their interactions with GAGs. This is important because previously published analysis of C5a-GAG interaction has been performed using rhC5a rather than nC5a (Culley *et al.* 2003; Miyabe *et al.* 2017).

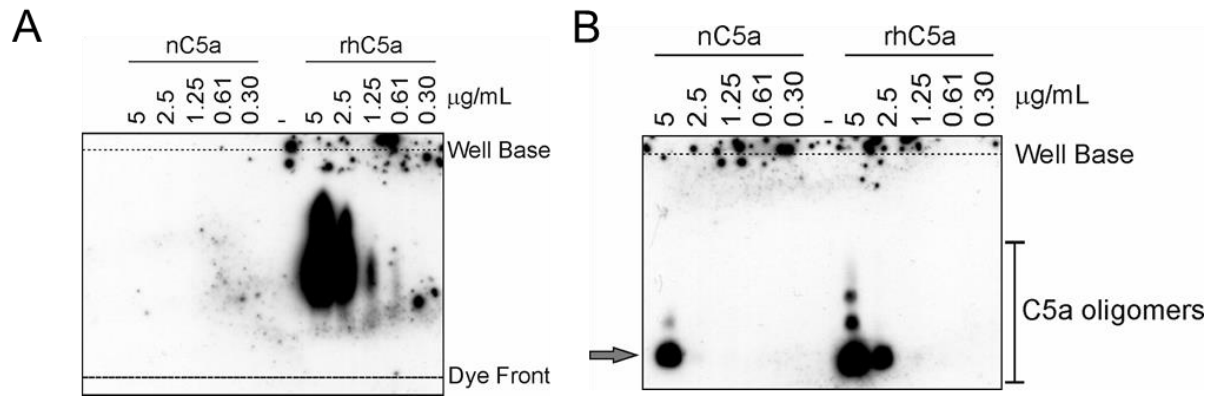


Figure 6-8: Comparing PAGE techniques for resolution of C5a and C5a-GAG complexes. Two-fold dilutions of nC5a and rhC5a in PBS were resolved by **A)** native-PAGE (n=1) or **B)** BN-PAGE (n=1) on 4-20% tris-glycine gels, detection by monoclonal anti-human C5/C5a antibody and goat-anti-mouse HRP conjugated antibody. Arrow indicates C5a molecular weight.

Recombinant C5a, but not nC5a, was visualised on SDS-free gels when resolved by native-PAGE (figure 6-8A); however, the rhC5a band was not well-defined as SDS-PAGE in section 4.5. Native PAGE utilises native charge of protein for mobilisation through a polyacrylamide matrix. A possible explanation for the detection of rhC5a but not nC5a could be that the His-tag incorporated into rhC5a increases the native charge allowing it to be mobilised in this system. Detection of rhC5a but not nC5a continues to highlight structural differences in the two forms that were discussed in chapter 4.

An inability to detect nC5a by native-PAGE meant that to investigate nC5a-GAG complexes an alternative method was required. A compromise between native PAGE and SDS-PAGE is to resolve proteins by blue native PAGE (BN-PAGE) whereby coomassie blue R-250 is used as a charge carrier (Fiala *et al.* 2011). Moreover, coomassie blue is not a detergent and therefore, unlike SDS-PAGE, does not alter protein structure potentially disassociating C5a-GAG complexes.

With similarities to the experiment shown in figure 6-8A, rhC5a and nC5a were diluted in series and resolved using a SDS-free system by adding coomassie blue into loading buffer and running buffers. When visualised by western blot, both nC5a and rhC5a were detected at a concentration of 5 µg/mL (figure 6-8B). A stronger signal was observed with rhC5a compared to nC5a, further demonstrated by the presence of a rhC5a band when 2.5 µg/mL was loaded. Moreover, multiple rhC5a bands could be detected at the highest concentration suggesting the formation of higher oligomeric structures of rhC5a; this was previously observed by SDS-

PAGE (section 4.5). The same oligomeric banding phenomenon was also observed for nC5a. I concluded that BN-PAGE could be suitable for visualising C5a-GAG interactions.

6.5.2. Separating C5a and C5a-GAG complexes using BN-PAGE

C5a-GAG interaction was investigated by incubating nC5a with a 10-fold dilution series of three purified GAGs; HS, CS and HA (Figure 6-9A).

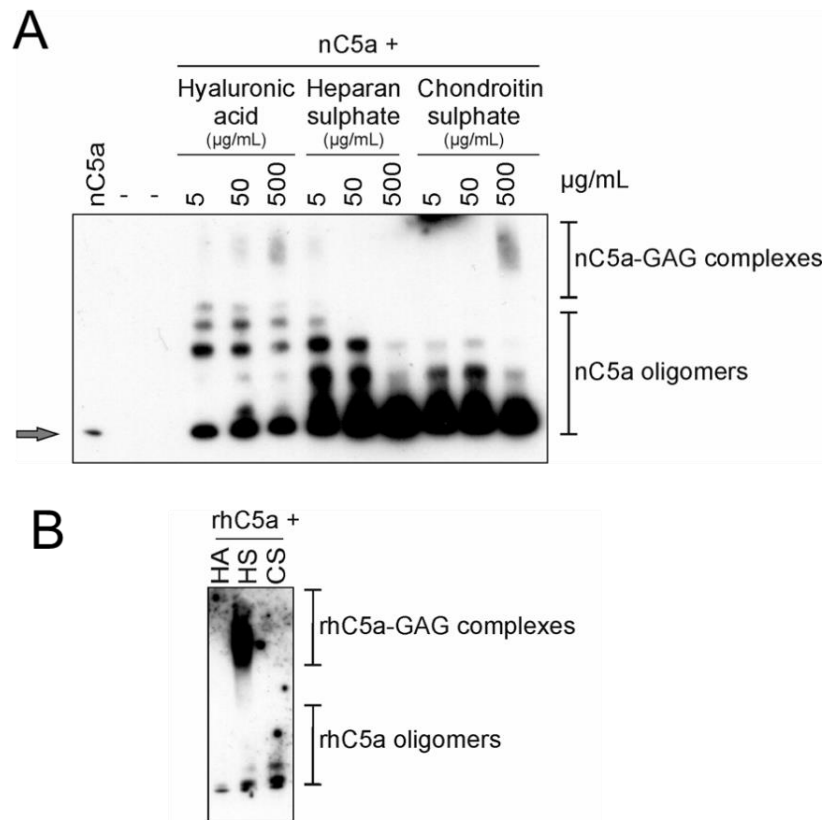


Figure 6-9: C5a and C5a-GAG complexes resolved by BN-PAGE. A) BN-PAGE, resolving of 5 µg/mL nC5a incubated with 10-fold dilution series of each GAG from 5 to 500 µg/mL for 1 h at 37°C. Arrow indicates nC5a molecular weight. **B)** BN-PAGE, resolving of 5 µg/mL rhC5a incubated with 500 µg/mL of each GAG for 1 h at °37C. In both experiments C5a-GAG complexes were separated on 4-20% tris-glycine gels; detection by monoclonal anti-human C5/C5a antibody and goat-anti-mouse HRP conjugated antibody. N=1.

As observed in Figure 6-8B, the anti-C5/C5a antibody detected multiple C5a bands indicative of higher oligomeric structures; however, only a single band was observed when nC5a was incubated with PBS, a negative control. Interestingly, broad smeared bands were observed when nC5a was incubated with the 500 µg/mL CS or HA, indicating possible C5a-GAG interaction. Moreover, a titratable effect was observed when nC5a was incubated with HA whereby the suspected nC5a-HA band intensity increased with HA concentration. A faint

band, indicating nC5a-HS interaction, could only be detected when nC5a was incubated with 5 µg/mL HS.

In comparison, for rhC5a, bands indicative of GAG interaction could only be observed when rhC5a was incubated with 500 µg/mL HS (figure 6-9B). Despite encouraging and original observations, both blots with rhC5a and nC5a could not be consistently replicated and therefore, no strong conclusions can be drawn from these data. To continue this investigation and build on evidence from these data, an alternative method for characterising C5a-GAG interaction was required.

6.6. Using size exclusion chromatography to characterise C5a-GAG complexes

Size exclusion chromatography was identified as a possible method for detecting C5a-GAG interaction; this technique has not previously been used to detect C5a-GAG interactions. This method uses a glass column packed with chemically modified agarose matrix that contains pores that facilitate selective separation of different sized molecules under physiological conditions. Separation is carried out in the fluid phase and a continuous flow is collected in fractions. The different parameters in this technique could potentially enable the separation of C5a and larger C5a-GAGs complexes. Continuous parameters can be measured such as flow rate, pressure, conductivity, and protein concentration (ultra-violet). Due to the small concentrations of C5a used in the following experiments, the spectrophotometer was not sensitive enough to detect C5a in the fractions (not shown). For this reason, an in-house C5a ELISA was developed and optimised to accurately quantify C5a.

6.6.1. Optimising an in-house ELISA for detection of C5a in column eluate

In this project I have used a sensitive commercial ELISA to quantify C5a in CF BAL fluid and in experiments where C5 is also present. The advantage of the C5a ELISA manufactured by Quidel is that it has no reported cross-reactivity with C5, this property is not required for measuring C5a in systems without C5. The commercial C5a ELISA is expensive therefore, a sandwich ELISA for C5a/C5a-desArg was developed using two mouse-anti-C5a monoclonal antibodies (figure 6-10).

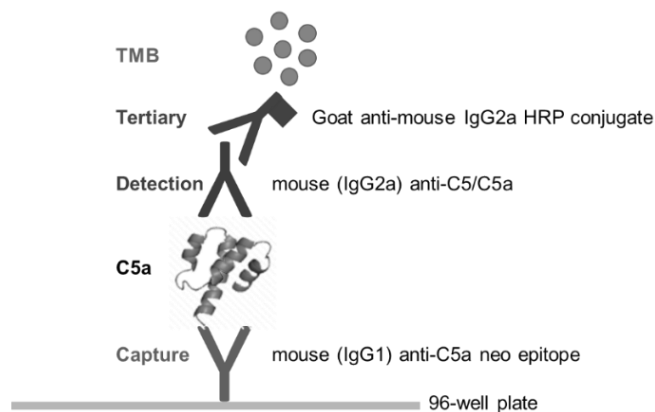


Figure 6-10: Diagram C5a ELISA and the antibodies used. “Capture” antibody is coated overnight on plastic. C5a standard or column fraction is incubated. “Detection” antibody recognises capture-bound C5a. Detection antibody is quantified using HRP-conjugated “tertiary” antibody and TMB substrate.

The capture antibody, Hycult mouse anti-C5a/C5a desArg-neo clone 2952 (IgG1 isotype), binds a neo-epitope that is exposed following cleavage of C5a from C5-alpha chain by C5 convertase. The detection antibody, the same used for western blots in chapters 4 and 5, binds to the C-terminal of C5a (IgG2a isotype). Both anti-C5a antibodies were developed by immunising mice therefore, for detection of binding a “tertiary” goat-anti-mouse IgG2a-HRP conjugated isotype specific antibody was used.

To verify that there was no cross reactivity of the goat-anti-mouse IgG2a-HRP to the mouse-anti-C5a neo-epitope capture antibody (IgG1), both capture and detection antibodies were coated onto a 96-well Maxisorb™ plate (figure 6-11A.). Cross-reactivity of the goat-anti-mouse IgG2a HRP was tested over a dilution series from 80 to 20 ng/mL. A positive control of goat-anti-mouse IgG HRP conjugate, picking up all IgG was used at 80 ng/mL to show equal coating of capture and detection antibodies.

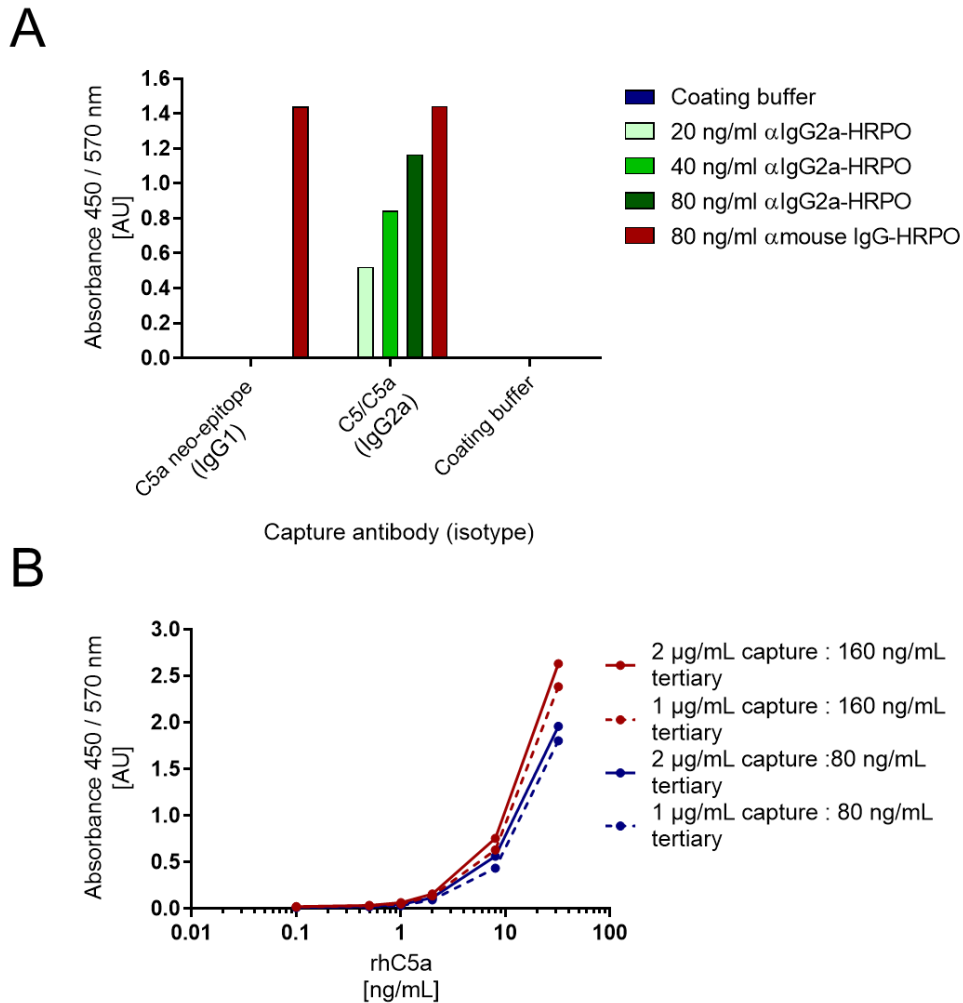


Figure 6-11: Optimisation of C5a ELISA to quantify C5a in column chromatography fractions.

A) Wells of a 96-well plate were coated overnight with either 1 µg/mL anti-C5a neo epitope monoclonal antibody (Hycult clone 2952), anti-C5/C5a monoclonal antibody (Hycult clone 557) or coating buffer. Plates were washed and a dilution series (20 to 80 ng/mL) of goat anti-mouse IgG2a HRP-conjugate antibody (green shades), 80 ng/mL goat anti-mouse IgG1 HRP-conjugate antibody (red), or 1% milk/PBS was added and incubated for 1 h at 37°C. Wells were washed and TMB added, colour was allowed to develop and stopped with HCl. Absorbance was measured at 450 nm with 570 nm reference filter. Mean values from duplicates in a single experiment. **B)** Dilution of capture and tertiary antibodies to detect a dilution series from 32 to 0.1 ng/mL rhC5a, detection antibody kept constant at 1 µg/mL. Absorbance was measured as for “A”. Mean values from duplicates in a single experiment

There was no cross-reactivity between the goat-anti-mouse IgG2a and capture antibody, validating the use of these antibodies in this combination. A dilution of the capture and tertiary antibodies was carried out to improve sensitivity of the C5a ELISA (figure 6-11B). I determined from these data that neither increasing the capture or detection antibody concentration substantially improved detection of C5a. Therefore, the capture and detection antibodies were to be used at 1 µg/ml. The concentration of tertiary antibody improved detection and therefore the goat-anti-mouse HRP-conjugated antibody to be used at 160 ng/mL. Having optimised a C5a ELISA, I could accurately detect C5a in column chromatography fractions.

6.6.2. Separating C5a-GAG complexes using a SD75 column

C5a-GAG complexes have not previously been characterised using size exclusion chromatography. A Superdex 75 10/300 GL column (SD75) was initially selected because the manufacturer specifies that it has a resolution range between 3 and 70 kDa. Therefore, it would be able to separate unbound C5a (10.4 kDa) and GAG-bound C5a (>50 kDa). It should be noted that the GAGs used in these experiments are heterogenous and the molecular weight was not specified by the manufacturer.

In a preliminary experiment 2 µg nC5a in PBS was loaded onto the column, the first observation made was that total yield of C5a in the collected fractions was low, less than 5% of the start material (not shown). C5a, and C3a, are “sticky” proteins due to their charge and can bind to plastic and other surfaces (Klos *et al.* 2013). I hypothesised that the low yield was due to incomplete elution from the column and binding of C5a to the polystyrene fraction tubes after elution.

6.6.3. Investigating low C5a recovery from SD75 column

To investigate C5a binding non-specifically to the column, 1 column volume of 1 M NaCl in PBS was flowed through the column to disrupt any ionic bonds between C5a and the column matrix. A broad peak suspected to be C5a, large enough to be detected by the UV spectrometer was eluted by 1 M NaCl; this could not be quantified by C5a ELISA because the high salt concentration interfered with the ELISA. I concluded for this that C5a was retarded on the column and was not being eluted in the column run-through. I also hypothesised that C5a was binding to the collection tubes throughout the experiment; each run would typically take 2 hours to complete.

To investigate non-specific binding of C5a to the polystyrene fraction tubes, an ELISA-style assay was performed using the same antibodies as the in-house C5a ELISA figure 6-12A. Briefly, 100 µL 2 ng/mL nC5a was incubated in two sizes of Eppendorf tubes or polystyrene fraction tubes for 1 h at 37°C. Unbound C5a was removed by pipette and tubes washed with PBS-tween (0.05%, v/v). The tubes were incubated with 100 µL 2 µg/mL mouse-anti-C5/C5a antibody for 1 h at 37°C. Antibody bound to C5a was detected using 160 ng/mL goat-anti-mouse HRP-conjugated antibody. Following washes, TMB was added and colour change was observed. After 5 minutes, 50 µL developed TMB solution was transferred to a 96-well plate,

reaction stopped with an equal volume of HCl and absorbance measured at 450nm. Signal was detected from all plastic tested, indicating non-specific binding of C5a (figure 6-12B).

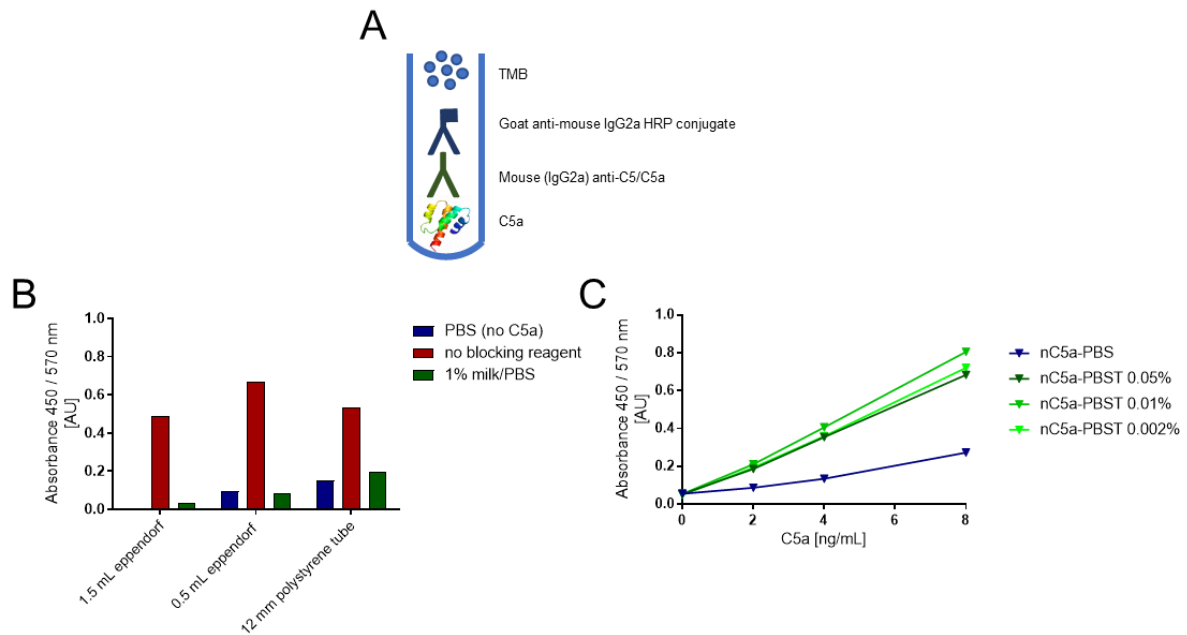


Figure 6-12: A tube-based ELISA to detect C5a. **A)** Diagram of ELISA-style in-situ assay to determine whether C5a binds to plastics. **B)** 2 ng/mL nC5a/PBS incubated in plastic vessels 1 h at room temperature, washed and 2 μ g/mL mouse-anti-C5/C5a antibody added for 1 h at room temperature. Unbound antibody was washed, and 160 ng/mL goat-anti-mouse HRP-conjugate antibody added and incubated for 1 h at room temperature. Tubes were washed, TMB added and allowed to develop for 5 minutes then transferred to a 96-well plate. Reaction was stopped with HCl. Absorbance read at 450 nm / 570 nm reference filter. **C)** In-house C5a ELISA comparing the use of tween-20 concentrations in the sample buffer. Trouble-shooting experiments were only performed once (n=1).

There was no signal from PBS coated (no C5a) vessels, verifying that there was no non-specific binding of the antibodies. Additionally, pre-coating the plastics with 1% milk/PBS reduced signal from bound C5a to similar levels to PBS for each respective vessel.

To improve recovery of C5a from the chromatography column, I hypothesised that collecting fractions in tubes containing a PBS tween-20 buffer would prevent further binding to plastic however, the effect of tween-20 on the C5a ELISA needed to be validated. A series of tween-20 concentrations in the sample buffer (1% milk/PBS) were assessed to determine the effect on the ELISA (figure 6-12C). Adding tween-20 to the sample buffer dramatically improved ELISA signal and therefore it was concluded that using tween-20 in collection tubes would not be detrimental to detecting C5a in the ELISA. In both SDS-PAGE and ELISA I have found that tween-20 improves detection by the antibodies used. It is not clear why this is but this phenomenon could suggest that aggregated C5a (in PBS, no tween) obscures the antibody epitope, reducing signal. The following adaptations were made to the column protocol and

fraction collection; future column fractions were collected in tubes pre-blocked in 1% milk/PBS and also contained 0.5 mL 2% milk/PBS-tween 20 (0.1% v/v). Therefore, collecting a 0.5 mL fraction would dilute the fraction 2-fold and give a final concentration of 1% milk/PBS-tween 20 (0.05%).

6.6.3.a. SD75 separation of C5a-GAG complexes

Even though the monoclonal anti-C5a antibody only detected faint nC5a-HS interaction in western blots (figure 6-9A), rhC5a binding to HS proteoglycan was reported as part of a larger study investigating the roles of C5a in promoting inflammation in rheumatoid arthritis (Miyabe *et al.* 2017). This was published during the course of my own experiments. To further characterise nC5a interaction with HS, nC5a was pre-incubated with HS for 1 h at 37°C and loaded on to a SD75 column (figure 6-13). Native C5a collected in each fraction was measured using the in-house C5a ELISA described above. Data was calculated as a percentage of total eluted C5a.

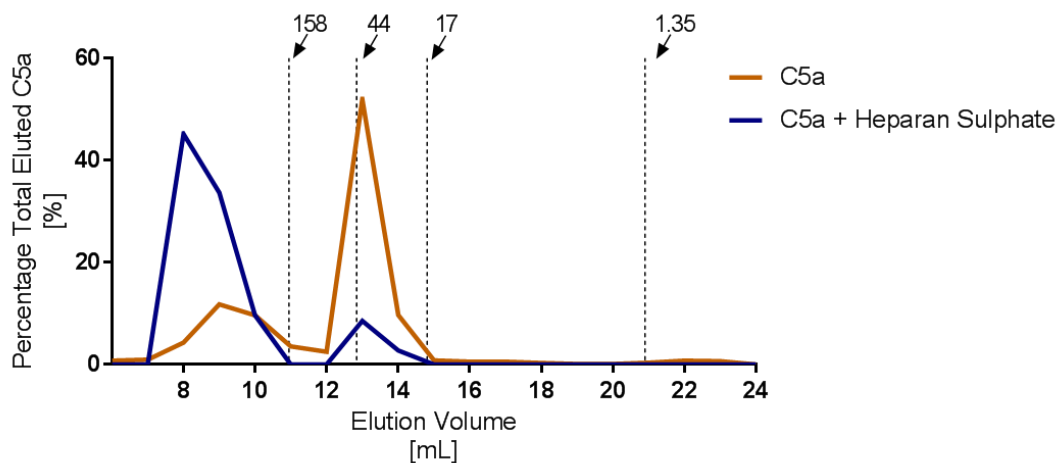


Figure 6-13: Separation of nC5a and nC5a-HS complexes on SD75 column.

2 µg nC5a in 200 µL PBS was loaded onto a SD75 column and eluted using PBS running buffer. 0.5 mL fractions were collected from 6 to 23 mL (x-axis), pooled in pairs to 1 mL and nC5a measured by C5a ELISA. C5a is plotted as a percentage of the total C5a eluted (y-axis). Native C5a was pre-incubated with PBS (orange) or 500 µg/ml HS (blue line) for 1 h at 37°C. On a separate run, protein molecular weight markers were loaded for reference (vertical dashed lines represent peak mid-points for each marker including respective molecular weights (kDa)). Graph is representative of n=2 for nC5a and nC5a + HS.

Untreated nC5a eluted in two peaks: a sharp peak, containing 80% total nC5a, eluted between 12 and 14 mL. Comparing to protein standards the molecular weight of this material was between 17 and 44 kDa. The remaining material eluted in a smaller, broad peak elute between 8 and 11 mL (>150 kDa). Interestingly, incubating nC5a with HS reduced the sharp peak that previously eluted between 12 and 14 mL. Instead, the majority of the material, presumably

nC5a complexed with HS, eluted in 4 mL following the void volume of the column (7mL), this is the volume that is not occupied by agarose matrix. These data suggest that nC5a-HS complexes are heterogenous in size, demonstrated by a broad peak. Additionally, these complexes are greater than 150 kDa, the maximum range of the resolution for the SD75 column.

The experiments shown in figure 6-13 provide preliminary evidence that C5a binds HS and that these complexes are likely to be greater than 150 kDa. Therefore, to improve resolution and enable characterisation of the size C5a-GAG complexes, a column that could resolve a greater range molecular weights was required. I selected a Superose 6 column because it has physiochemical properties that allow separation of particles that are between 5 and 5,000 kDa. The volume of the column is the same as SD75 and therefore the same separation protocol was used.

6.6.4. Separating C5a-GAG complexes on a Superose 6 column

In separate experiments nC5a, nC5a incubated with HS, and nC5a incubated with CS were loaded on to a Superose 6 column (figure 6-14).

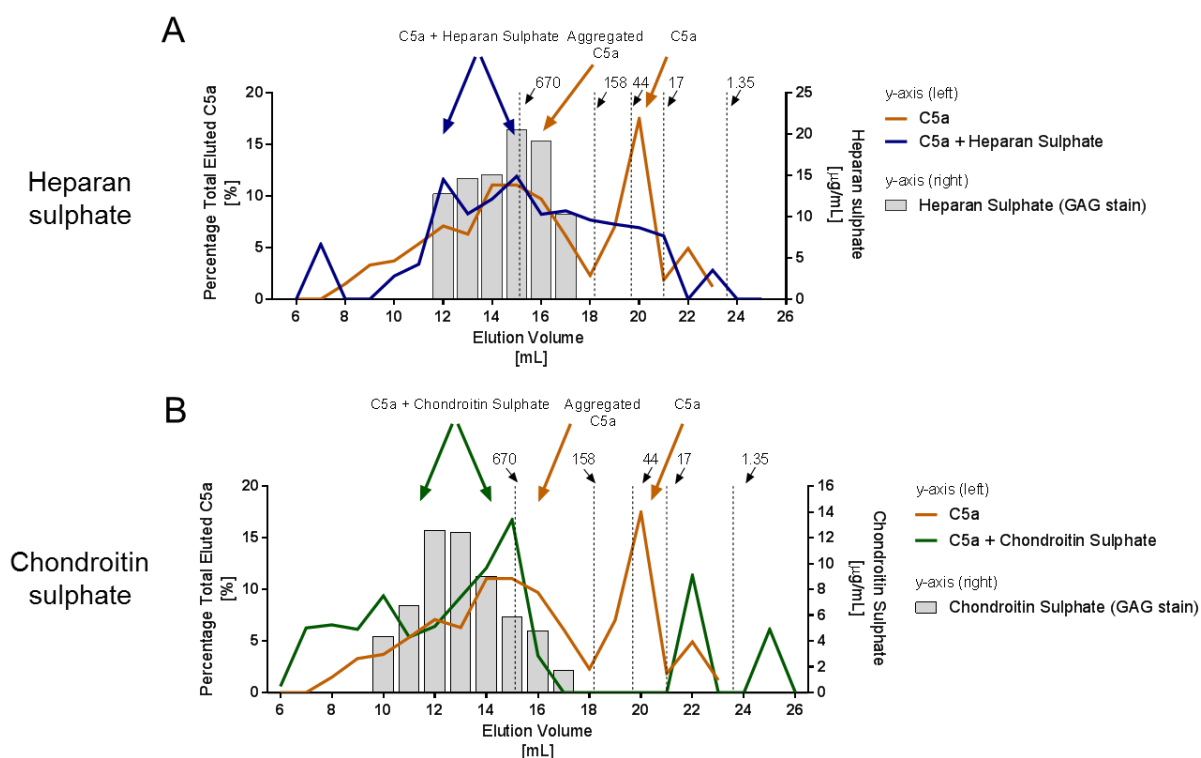


Figure 6-14: Separation of C5a and C5a-GAG complexes by a Superose 6 column. 2 µg nC5a in 200 µL PBS was loaded onto a superose 6 column and eluted using PBS running buffer. 0.5 mL fractions were collected from 6 to 26 mL (x-axis), pooled in pairs (1 mL) and nC5a was measured by C5a ELISA. C5a was plotted as a percentage of the total C5a eluted (y-axis (left)). C5a was pre-incubated with PBS (orange), **A**) 500 µg/mL HS (blue) or **B**) 500 µg/mL CS (green) for 1 h at 37°C. With conditions where GAGs were incubated with nC5a, GAG concentration was also measured in each fraction using dimethyl methylene blue stain (y-axis (right)). Protein molecular weight markers were loaded separately for reference (vertical dashed lines represent peak mid-points for each marker and include respective molecular weights (kDa)). Peaks of interest are annotated with arrows that are the colour of the respective condition. Graphs are representative of n=2 for C5a+PBS and C5a + HS, n=1 for C5a + CS.

The same experiments performed with the SD75 column (figure 6-13) were replicated on the Superose 6 column and C5a concentration was quantified by C5a ELISA as before. Additionally, GAG concentration was also measured in the eluted fractions using the dimethyl-methylene blue stain used for GAG quantification in the CF cohort. GAG concentration was measured in fractions to investigate whether C5a and GAGs eluted in the same fractions, suggesting possible interaction.

Using the Superose 6 column, a sharp peak, suspected to be monomeric nC5a, eluted between 44 and 17 kDa. In contrast to the SD75 column, the majority of C5a material eluted in a broad peak between elution volume 6 and 18 mL. According to the protein reference makers, C5a in this broad peak could have a molecular weight between 158 and 5000 kDa (maximum resolution limit). I speculated that this high molecular weight material is likely to be aggregated nC5a, evidence of oligomerisation was shown in western blots in a previous chapter (figure 4-5).

Incubating nC5a with HS reduced the “monomeric C5a” peak and instead, a broad peak of C5a material eluted between elution volumes 9 to 22 mL (figure 6-14A). Interestingly, this broad peak contained two C5a spikes, observed in fractions 12 mL and 15 mL. Moreover, these increases in C5a elution at volumes 12 and 15 mL coincided with the elution of HS, as measured by staining samples with dimethyl methylene blue. Therefore, I speculated that these two peaks represented C5a-HS complexes.

In experiments where nC5a was pre-incubated with CS, a diminished “monomeric C5a” peak was also observed (figure 6-14B). Large molecular weight C5a was eluted over a broad peak, between 6 and 17mL, additionally, a spike in eluted C5a was measured in fraction 15. The same peak coincided with what is suspected to be aggregated C5a but not where majority of CS was detected. By measuring CS in fractions using the dimethyl-methylene blue stain, a peak in CS eluted between 11 and 14 mL.

Separation of nC5a incubated with GAGs using the Superose 6 column has built on evidence of the formation of nC5a-GAG complexes established by the SD75 column. Due to the similarity in molecular weights between suspected nC5a aggregates and nC5a-GAG complexes, I decided that alternative experimental approaches were required.

6.7. Characterising C5a-GAG interaction using a heparin-sepharose affinity column.

Affinity chromatography, using a sepharose-heparin column, has been previously used to investigate rhC5a-heparin interaction (Culley *et al.* 2003). Heparin is structurally analogous to HS; however, heparin differs in disaccharide composition whereby N-acetylglucosamine in HS is substituted by α -L-iduronic acid. Due to their physio-chemical similarities, evidence of C5a-heparin interactions could suggest that HS can also form complexes with C5a.

To replicate data published by Culley *et al.*, using rhC5a, 2 μ g nC5a in 200 μ l PBS was loaded onto a 1 mL heparin-sepharose affinity column. The column was washed with five column

volumes (5mL) PBS, 154 mM NaCl, then NaCl concentration in PBS was increased to 1 M over a gradient of approximately 84.6 mM (10%) / minute; after 25 mL the NaCl concentration in PBS was theoretically 1 M. The hypothesis behind this was that hypertonic solution would disrupt ionic bonds between nC5a and heparin. Fractions (0.5 mL) were collected in milk blocked tubes to improve C5a recovery, as for size exclusion chromatography experiments.

I first tested to see whether nC5a was retarded on a heparin affinity column, as reported by Culley *et al.* for rhC5a (Culley *et al.* 2003). Native C5a was incubated at 37°C for 1 h and loaded onto a 1 mL heparin affinity column (figure 6-15A).

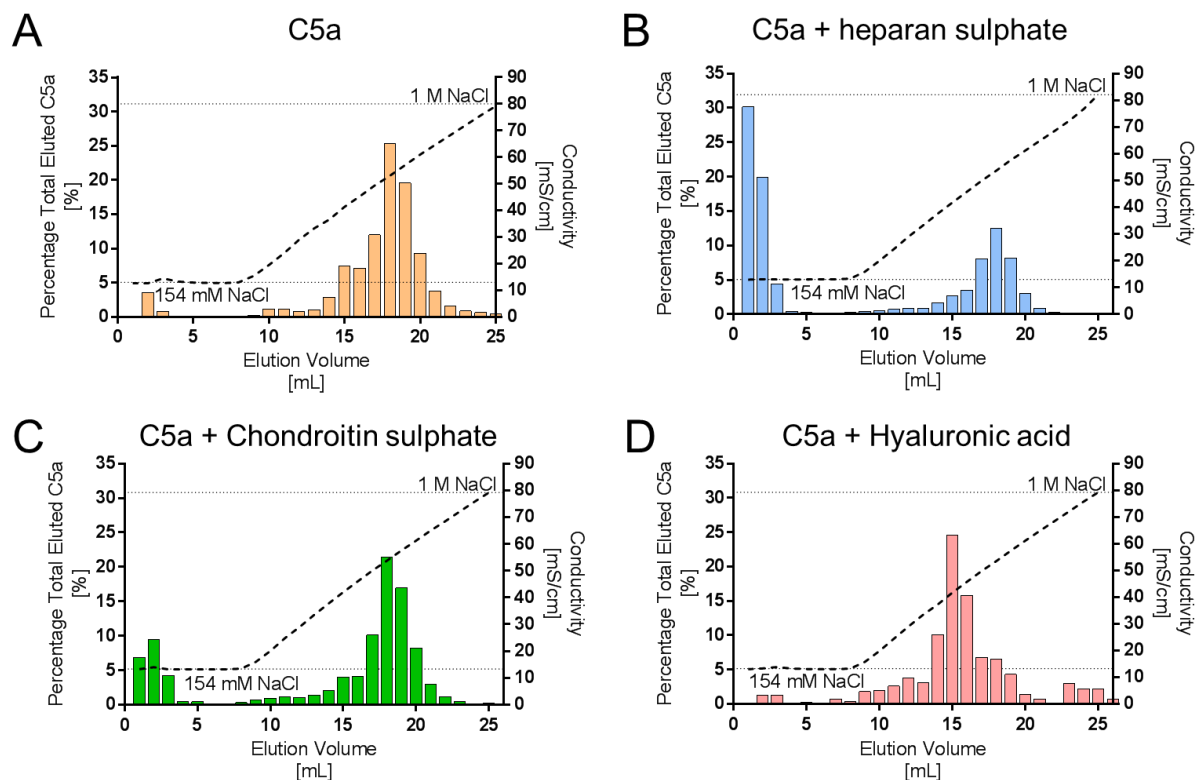


Figure 6-15: Assessing binding of nC5a and nC5a-GAG complexes to a heparin affinity column. Binding of nC5a pre-incubated with **A)** PBS **B)** HS, **C)** CS, or **D)** HA to a heparin affinity column. 2 µg nC5a in PBS incubated with 100 µg each GAG for 1 h at 37°C. Bound nC5a was eluted with a concentration gradient of NaCl in PBS from 154 mM to 1 M (indicated by dotted lines), increase in gradient was observed by the increase in conductivity during elution, dashed black line (y-axis (right)). 0.5 mL fractions were collected from 1 to 25 mL elution volume (x-axis). C5a in fractions was measured by C5a ELISA and plotted as percentage total C5a, solid bars (y-axis (left)). Graphs representative of n=2 experiments (C5a + HA, n=1).

When a gradient of NaCl in PBS from 154 mM to 1000 mM was applied, a sharp C5a peak eluted between elution volumes 15 and 20 mL. I calculated, given the conductivity at 154 mM and 1000 mM NaCl, that the NaCl concentration between 15 and 20 mL would have been

approximately 488 mM to 670 mM NaCl. In this first experiment I found that nC5a could be retarded on a heparin affinity column and eluted with a gradient of NaCl. In the next set of experiments, I investigated whether pre-incubating nC5a with different GAGs could inhibit C5a from binding to the heparin matrix within the column.

As mentioned above, the similarities in heparin and HS mean that they have been shown to bind similar, if not the same, residues on the target protein (CXCL8) (Pichert *et al.* 2012a). Therefore, to investigate binding of C5a to heparin and other GAGs, I hypothesised that pre-incubating nC5a with other GAGs would inhibit anaphylatoxin binding to the heparin affinity column.

Native C5a was incubated with either HS, CS or HA and loaded on to the heparin affinity column. Interestingly, when nC5a was pre-incubated with HS (figure 6-15B) over 50% of total C5a material eluted in the run-through, suggesting that it was prevented from binding to heparin within the matrix of the column. The remaining material, presumably nC5a not bound to HS, eluted with the increasing NaCl concentration between elution volumes 15 to 21 mL, as observed in figure 6-15A. A similar but less pronounced shift could also be observed when nC5a was incubated with CS (figure 6-15C). Approximately 20% of C5a material eluted in the run-through, with the remaining C5a eluting in a single peak between elution volume 15 to 21 mL. Incubating nC5a with HA produced a similar profile to untreated nC5a however, the sharp C5a peak eluted by the NaCl gradient eluted earlier than untreated C5a (figure 6-15D).

Experiments using a heparin affinity column provided conclusive evidence that C5a binds to heparin, HS and to a lesser extent CS. Additionally, an approximate strength of these interactions has been observed using a NaCl gradient. Nevertheless, a second platform was sought to support these data.

6.8. Solid phase plate assay for detection of C5a-GAG binding

Solid phase plate-based assays were considered as a potential platform for characterising C5a-GAG interaction; this technique would require coating plastic with either GAGs or C5a. Coating plastic plates with GAGs can be challenging due to their strong negative charge. Plates chemically rendered capable of binding GAGs were purchased, but initial observations using CXCL8 as a positive control did not reliably differentiate between binding to GAGs and non-specific binding to the plate (not shown). Despite this, Miyabe *et al.* used HS proteoglycan-coated plates to investigate rhC5a interaction and to test competition using heparin (Miyabe *et al.* 2017). Binding the target protein to plastic and measuring GAG

interaction using biotinylated-GAGs has been reported in investigations on CXCL8 and other chemokines (Clark *et al.* 2006; Dyer *et al.* 2016b). Coating plates with C5a and assessing GAG-binding has not previously been reported therefore, the protocols for investigating chemokines were adapted for use with C5a.

6.8.1. Optimisation of solid phase C5a-GAG binding assay

In brief, a 96-well plate is coated with purified C5a overnight. The next day, unbound C5a is discarded and the plate is blocked with BSA. Following block, biotinylated-HS was added to each well and incubated for 3 h at 37°C. Unbound GAGs were discarded, and bound GAGs were detected using streptavidin-HRP and TMB (figure 6-16A).

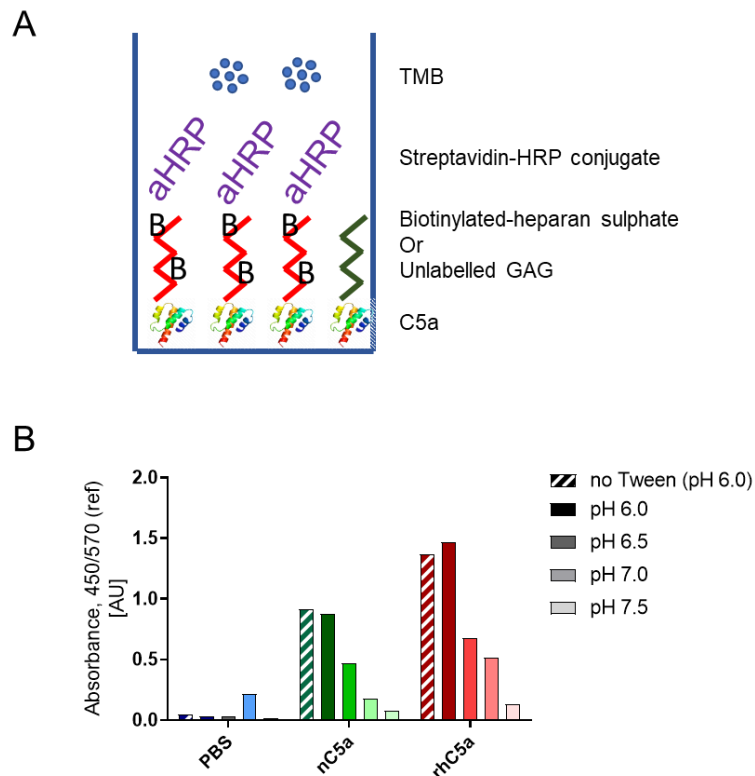


Figure 6-16: Optimisation of solid phase binding assay. A) Diagram of the principle behind detecting C5a-GAG interaction using solid phase platform. **B)** Investigating necessity of assay buffer pH during biotinylated-HS incubation step. Wells were coated with PBS (blue), nC5a (green) or, rhC5a (red). Assay buffer with a range of pH from 6.0 to 7.5 (dark to light shades), increasing in 0.5 increments. Assay buffer pH was increased by additional of NaOH. An assay buffer at pH 6.0 with tween-20 omitted was also compared (diagonal stripes (colour/white)), n=1.

In the literature, groups have reported using assay buffers containing high concentrations of tween-20 (up to 1%) and a lower than physiological pH (pH 6). These conditions are not physiological for CF airway (Schultz *et al.* 2017) and therefore, I investigated whether these

conditions were necessary for the performance of the assay. Assay buffers with increasing pH and a buffer without tween-20 (at pH 6.0) were assessed during the biotinylated-HS incubation step of the protocol (figure 6-16B).

When tween-20 was omitted from the assay buffer for all steps, absorbance measurements of wells coated with either PBS or nC5a were above the detection limit of the spectrophotometer (not shown because data could not be measured). Additionally, omitting tween-20 from the buffer during the biotinylated-HS incubation step had no visible effect when comparing to the pH 6 assay buffer with tween (used by Clark *et al.* (Clark *et al.* 2006)). Therefore, tween-20 was used at 0.1% throughout the assay in future experiments.

Different pH buffers were made to test the influence of pH on binding of biotinylated-HS to C5a. Increasing the assay buffer pH, reduced the absorbance measured and therefore, the amount of biotinylated-HS bound to nC5a. It has recently been shown that the CF airway pH is approximately pH 7.0 therefore, a pH 6.0 buffer is not necessarily physiological (Schultz *et al.* 2017). Even though these conditions are not representative of the CF airway they still enable investigation of C5a-GAG interaction that may have a wider non-pathological role not just in the inflamed airway. Despite using non-physiological conditions, investigating nC5a-GAG interaction in assays with low absorbance would reduce the ability to detect subtle effects and therefore, the assay buffer was kept at pH 6.0, in line with previous reports (Clark *et al.* 2006). These preliminary experiments optimised assay conditions as follows; plates were blocked with 1% BSA and the assay buffer used was 50 mM sodium acetate, 100 mM NaCl, 0.1% tween-20, pH 6.0.

6.8.2. Characterisation of C5a-GAG binding using solid phase plate assay

Characterisation of nC5a-GAG complexes using affinity chromatography revealed that nC5a-heparin interaction can be perturbed using a NaCl gradient (figure 6-15A). These experiments were replicated using the solid phase binding assay to assess whether these observations could be supported by a different platform.

Experiments performed using the heparin affinity column revealed that nC5a could be eluted from the column when the NaCl concentration was greater than 450 mM (figure 6-15A). Dissociation of biotinylated-HS and nC5a was investigated using hypertonic assay buffers with NaCl at concentrations from 0.154 up to 1 M (figure 6-17). Increasing the NaCl concentration to 200mM reduced absorbance of nC5a-biotinylated-HS by approximately 80%. Further increase to 400 mM NaCl reduced signal to near background levels, controlled by coating wells with PBS only.

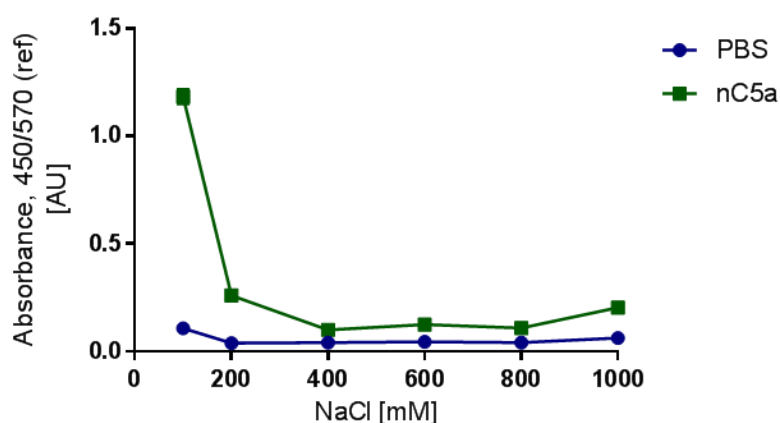


Figure 6-17: Influence of NaCl on C5a-HS interaction. Wells of a 96-well plate were coated with 1 $\mu\text{g/mL}$ nC5a or PBS overnight. Biotinylated-HS binding was measured in assay buffers with increasing NaCl concentration from 100 to 800 mM. Representative of two experiments.

Experiments using the heparin affinity column also revealed that HS and to a lesser extent CS could compete for heparin binding sites on nC5a (figure 6-15B-C). I hypothesised that if the different GAGs bound nC5a at the same amino acid residues then the relative affinity of each GAG for nC5a could be assessed in a competition assay. A competition assay was developed using unlabelled (not biotinylated) GAGs to compete for biotinylated-HS binding sites on nC5a (figure 6-18).

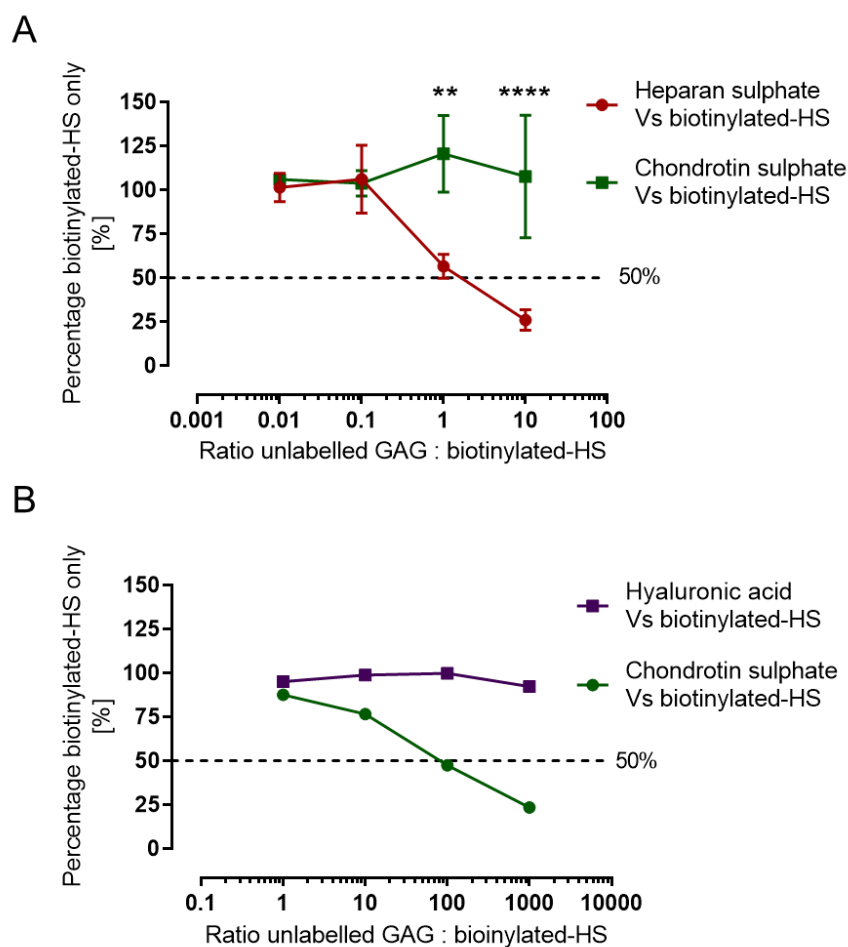


Figure 6-18: Competition for nC5a-biotinylated-HS binding using unlabeled GAGs. Wells were coated with 0.5 $\mu\text{g/mL}$ nC5a. Coated nC5a in wells was incubated with biotinylated-HS in solution with **A**) unlabeled HS or CS at ratios (x-axis) between 0.01 and 10 ($n=3$). Data presented as mean \pm SEM. Two-way ANOVA with Tukey's test for multiple comparisons was performed to compare mean binding at each ratio tested. **B**) Unlabeled CS or HA at ratios (x-axis) between 1 and 1000, mean of two experiments. In both sets of experiments absorbance was measured at 450/570 nm. Data is presented as a percentage of wells incubated with biotinylated-HS only (y-axis).

In the first set of experiments unlabelled HS or CS was added in solution with biotinylated-HS at ratios between 0.01:1 and 10:1 (unlabelled GAG to biotinylated-HS). The unlabelled GAGs and biotinylated-HS were then incubated with C5a pre-coated on the plates, the assay was

performed as described in section 6.8.1. The molecular weight of the GAGs used in these experiments is unverified and therefore, ratios were calculated by mass rather molar equivalence. Due to the natural variation in absorbance between assays, data is presented as percentage absorbance of wells incubated with biotinylated-HS alone.

An important result was that at a ratio of 1:1 unlabelled-HS to biotinylated-HS the absorbance was approximately 50% compared to signal of wells incubated with biotinylated-HS (figure 6-18A). This means that biotinylated-HS binding to nC5a can be inhibited by an equimolar (approximately) amount of unlabelled HS. Additionally, there was no strong evidence to suggest that unlabelled-CS could compete for binding at these ratios. At 1:1 and 10:1 ratios of unlabelled-GAG to biotinylated-HS there was statistically significant difference in biotinylated-HS binding to C5a when competing with unlabelled HS compared to unlabelled-CS ($p = 0.001$ and $p < 0.0001$ respectively).

In figure 6-18A, there was no evidence from the data to suggest that unlabelled CS competed with biotinylated-HS for nC5a binding, at the ratios used. In a second set of experiments, the ratio of unlabelled-CS to biotinylated-HS was increased to 1000:1, HA was also compared (figure 6-18B). Increasing the ratio of unlabelled-CS to biotinylated-HS to 100:1 reduced binding of biotinylated-HS to 50%. Therefore, CS has approximately a 100-fold lower affinity (based on mass) for the binding site of biotinylated-HS; however, despite increasing HA concentration to 1000-fold that of biotinylated-HS there was no detectable competition for the HS binding site.

6.8.3. Investigating binding of HS to other complement components

Having characterised nC5a and biotinylated-HS interaction it was hypothesised that C5, with a 20-fold greater mass than C5a and potential for more binding sites may also bind GAGs. Furthermore, C3a is homologous to C5a and may also interact with GAGs, and therefore, C3 also. The aforementioned complement components were diluted in series and binding of biotinylated-HS measured (figure 4-19).

Data was calculated as a percentage of the absorbance of the highest concentration of each respective complement component. This was due to the variation in absorbances at the highest dilution, possibly owing to the affinity of each component to the plastic plate.

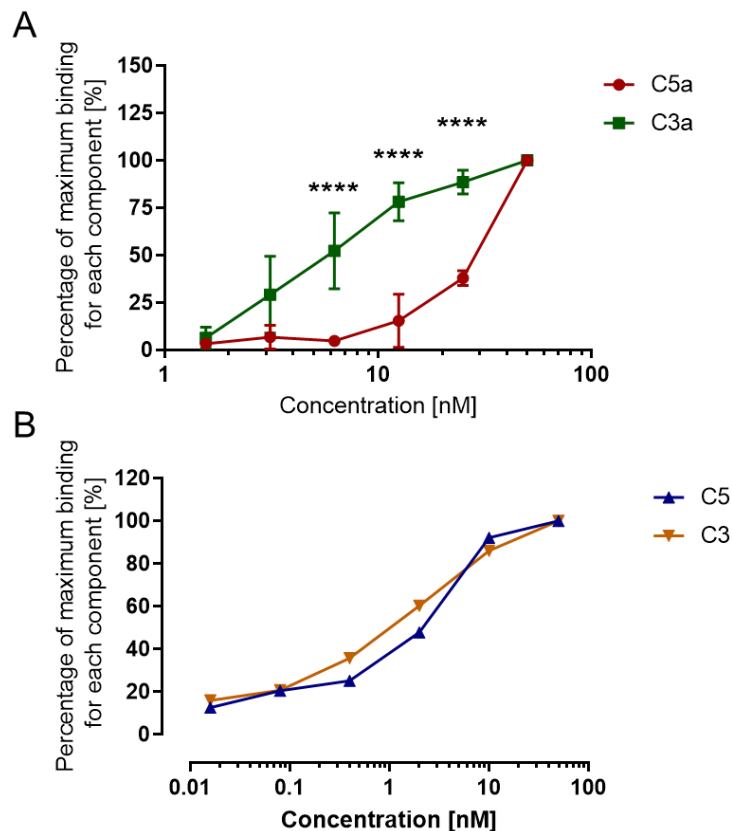


Figure 6-19: Comparing the binding of different complement components to HS. Plates were coated with a concentration gradient of **A**) C3a (green, n=3) and nC5a (red, n=3), Two-way ANOVA with Tukey's test for multiple comparisons was performed to compare percentage binding at each molar concentration tested. Data was plotted as means \pm SEM **B**) C3 (orange, n=2) and C5 (blue, n=2) over a dilution series (x-axis). Data is presented as means from two experiments. For both **A** and **B** Solid phase binding assay was performed as previously described. Data points are percentage absorbance at the highest concentration for each respective component (y-axis).

Interestingly, observations using this platform suggested that biotinylated-HS had a higher affinity for C3a than C5a; there was a significant difference in percentage binding at 25, 12.5 and 6.25 nM of coated anaphylatoxin ($p < 0.0001$, $p < 0.0001$ and $p < 0.0001$ respectively) (figure 4-19A). Additionally, biotinylated-HS also bound C5 and C3 (figure 4-19B). Additionally, interactions between C3 or C5 and biotinylated-HS were stronger than their respective cleaved anaphylatoxins and required further dilution for a full curve to be observed. In a visual comparison, there was no apparent difference between biotinylated-HS binding to C5 or C3. Therefore, from these data HS binds complement components in a hierarchy $C3=C5>C3a>C5a$. Despite intriguing results, this path of investigation was not continued due to a lack of available time left in this project. If this line of investigation were to be continued it would be interesting to perform surface plasmon resonance for more accurate quantification of the affinities between the above complement components and GAGs.

In this section a hypothesis driven selection of different methods was used to show evidence that C5a interacts with GAGs, in particular, heparin and HS. Despite this, these data do not provide insight into how C5a-HS interaction influences C5a function. At the beginning of this chapter I hypothesised that binding of C5a to soluble GAGs in the CF airway may modify function, promoting neutrophilic inflammation.

6.9. Functional significance of C5a-HS interaction

In the above experiments it has been consistently observed that HS has a higher affinity for nC5a than CS and HA. Therefore, because there was stronger evidence for C5a-HS interaction, I focused my investigation on the influence of HS interaction on C5a function. It has previously been shown that rhC5a incubated with heparin (analogous to HS) did not inhibit function of rhC5a when used to stimulate oxidative burst in HL60 cells (Culley *et al.* 2003). In my thesis, the effect of HS binding to nC5a was investigated using the RBL-C5aR1 transfected cell-line (activity assay previously described in section 4.9).

6.9.1. Effects of HS binding on C5a function

Native C5a was incubated with HS for up to 3 h, mirroring the solid phase binding platform biotinylated-HS incubation step (figure 6-16A). C5a activity was measured at hourly time points by quantifying β -hexosaminidase release from RBL-C5aR1 following stimulation with samples (figure 4-20).

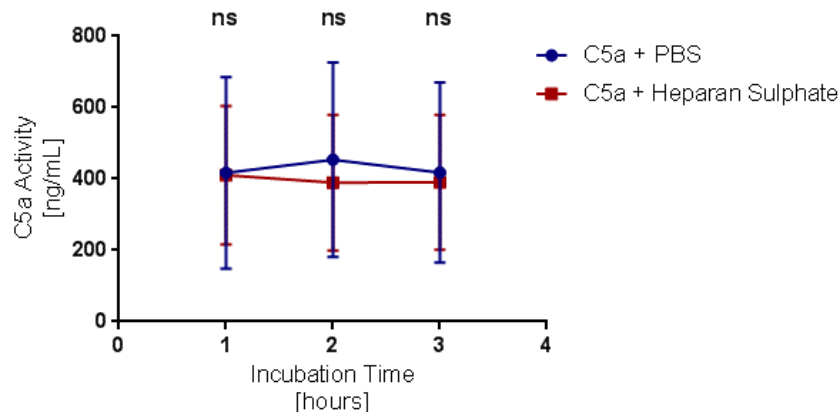


Figure 6-20: Influence of HS on C5a activity. 1 μ g/mL nC5a was incubated with 500 μ g/mL HS or PBS for up to 3 h at 37°C (x-axis). Samples were diluted 1 in 10 in phenol red-free media and added to cells for 30 minutes at 37°C 5% CO₂. C5a activity (y-axis) was calculated using a standard curve of C5a and measuring β -hexosaminidase in supernatant following stimulation of RBL-C5aR1 cells. One-way ANOVA was used to test whether there was any difference in activity between the two conditions at each time point (n=6).

Reflecting data published by Culley *et al.* on rhC5a, there was also no significant difference in activity between nC5a and nC5a incubated with HS at any of the time points (Culley *et al.* 2003). As C5a activity is not affected by HS binding, this data could provide insight into the binding site for HS on C5a. For instance, the C5a C-terminal is important for activity and therefore because C5a is still active these data suggest that the HS binding site is located elsewhere.

6.9.2. Testing the ability of HS to protect C5a from degradation by NE.

It has been reported that CXCL8 interaction with GAGs protects against degradation by NE in the CF airway, prolonging half-life (Reeves *et al.* 2011b). The authors stated that this mechanism could promote neutrophilic inflammation in the CF lung. I hypothesised that the same phenomenon is applicable to C5a when in complex with HS. In chapter 4 (figure 4-6) I showed that C5a was susceptible to degradation by proteases in CF BAL fluid and by purified

NSPs. Here, I tested the ability of HS to protect C5a from NE-mediated inactivation; C5a activity was measured using RBL-C5aR1 cells (figure 6-21).

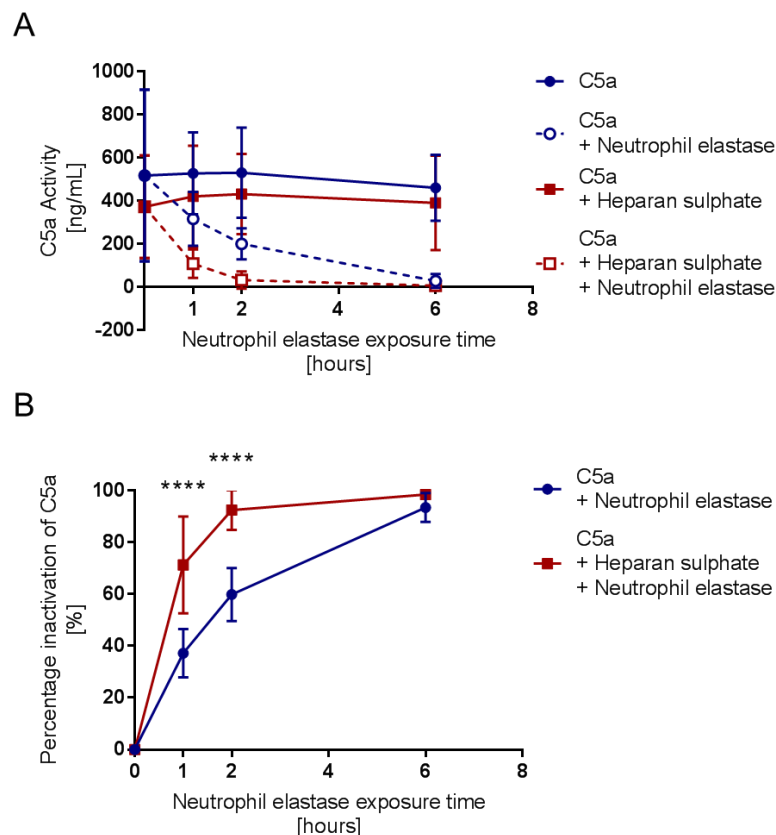


Figure 6-21: Influence of HS of C5a inactivation by NE. A) C5a activity was determined by measuring stimulation of RBL-C5aR1. nC5a (1 $\mu\text{g}/\text{mL}$) was pre-incubated with HS (500 $\mu\text{g}/\text{mL}$) or PBS for 1 h at 37°C then exposed to NE (25 $\mu\text{g}/\text{mL}$) or PBS for up to 6 h (n=4). Samples were taken at 0, 1, 2 and 6 h (x-axis). Samples were diluted 1 in 10 in phenol red-free media and added to cells for 30 minutes at 37°C 5% CO_2 . C5a activity was calculated using a standard curve of C5a (y-axis). **B)** Data from “A” was calculated as percentage inactivation (y-axis, 100 – percentage of C5a without neutrophil elastase) for each respective time point. Data for both plots is presented as mean \pm SEM, Two-way ANOVA with Tukey’s test for multiple comparison was used to compare means at each time point, n=4.

In support of data from figure 6-20, there was no significant difference in activity between nC5a and nC5a incubated with HS. Interestingly, there was a visible difference in activity between C5a and C5a incubated with HS when exposed to NE over a 6-hour time course; however, these observations were not statistically significant (figure 6-21A).

To normalise the impact of day to day natural variation from my experiments, data was standardised by calculating the percentage inactivation of C5a (figure 6-21B). Following standardisation, I found that nC5a incubated with HS, was significantly more susceptible to degradation by NE (t=1; $p < 0.001$, t=2; $p < 0.001$). Following 6-hour exposure to NE, activity of nC5a, with and without HS, was completely abolished.

To confirm that inactivation of C5a was due to NE-mediated proteolysis, the concentration of nC5a from the above experiments was quantified by a sensitive commercial C5a ELISA. This experiment was repeated three times; however, due to technical difficulties only two data sets were measured and unfortunately there was not enough time at the later stages of my project to repeat the experiment (figure 6-22).

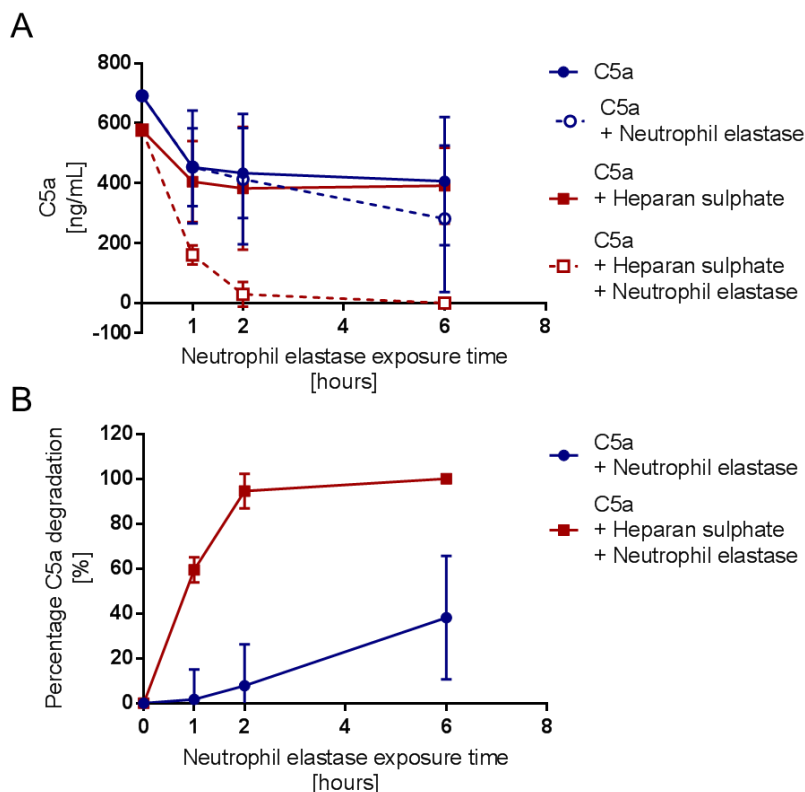


Figure 6-22: Quantifying NE proteolysis of C5a when in complex with HS. **A)** HS (500 $\mu\text{g}/\text{mL}$) or PBS for was incubated with 5 $\mu\text{g}/\text{mL}$ nC5a at 1 h at 37°C then exposed to NE (25 $\mu\text{g}/\text{mL}$) or PBS for up to 6 h (n=2). Samples were taken at 0, 1, 2 and 6 h (x-axis). At t=0 nC5a (or nC5a with HS) and C5a incubated with NE gave the same measurement. **B)** Data from “A” was calculated as percentage degradation (y-axis, 100 minus the percentage of C5a without NE) for each respective time point. Data for both plot are presented as means for two experiments.

Data from the C5a ELISA had visually similar trends to figure 6-21, in that nC5a incubated with HS was more susceptible to degradation by NE than nC5a that was not incubated with HS. Interestingly, nC5a without HS was susceptible to degradation by NE, but the rate of nC5a concentration loss (proteolysis) appeared to be less than the rate of inactivation from figure 6-22A. Moreover, when the data was calculated as percentage degradation, the difference between inactivation (figure 6-21B) and degradation (figure 6-22B) became more apparent. The difference in the rate of concentration loss and inactivation suggested that there may be subtle differences in the way C5a is degraded by NE when C5a is in complex with HS.

6.9.3. Influence of HS on the inactivation of C5a by CPB

In chapter 4, I showed that NSP-generated C5a is resistant to inactivation by CPB, an important mechanism for regulating C5a activity in circulation. I am also interested in whether interaction with GAGs can also modify the activity of C5a by preventing inactivation by CPB. I hypothesised that HS complexed with nC5a may prevent inactivation by CPB. The susceptibility of nC5a to inactivation by CPB when in complex with HS was investigated. As for the above experiments, nC5a was incubated with HS over 3 h. At 1, 2, and 3-hour time points nC5a was exposed to either porcine CPB or PBS for 1 h at 37°C. C5a activity was quantified by measuring β -hexosaminidase release from RBL-C5aR1 cells (figure 6-23).

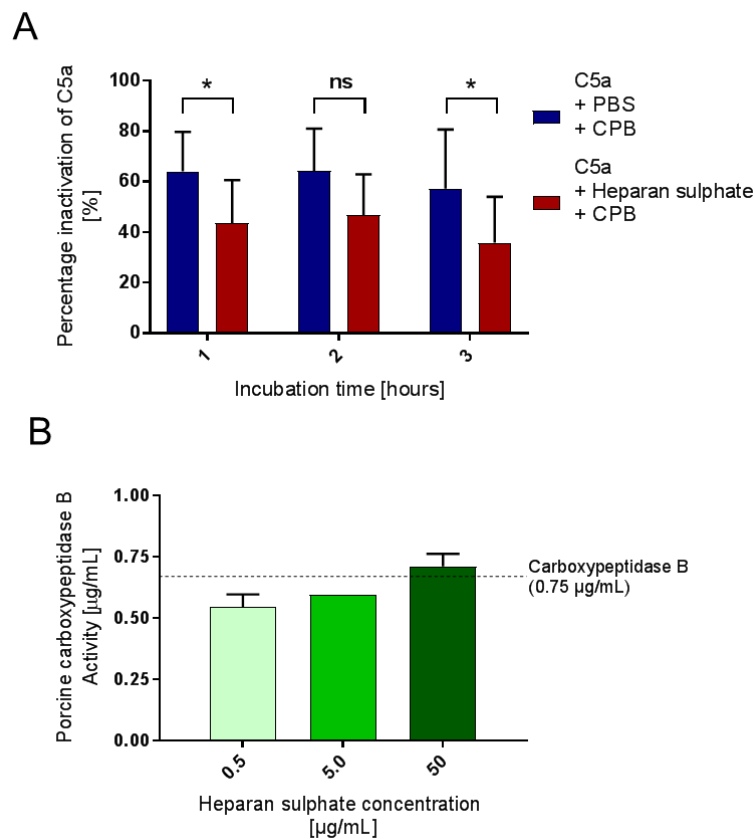


Figure 6-23: Influence of HS on inactivation of C5a by CPB. **A)** 1 μ g/mL nC5a was incubated with HS (red) or PBS (blue) for 1, 2 and 3 at 37°C, samples were then either exposed to CPB or PBS for 1 h at 37°C. C5a activity in samples was measured by stimulation of β -hexosaminidase release from RBL-C5aR1. Percentage inactivation was calculated by dividing the activity of C5a (or C5a-HS) exposed to CPB by the samples that were incubated with PBS, this value was subtracted from 1 and multiplied by 100 to give percentage inactivation. Data was represented as mean \pm SEM, Two-way ANOVA (with Tukey's test for multiple comparisons) was performed to test whether there was any difference in activity between the two conditions at each time point (n=4). **B)** Inhibitory activity of three HS dilutions (x-axis) on porcine CPB was assessed using the carboxypeptidase activity assay and chromogenic substrate, Furylacryloyl-Ala-Lys. Activity was calculated using a standard curve of porcine CPB (y-axis), n=1.

In chapter 4, I demonstrated that there was statistically significant inactivation of nC5a by porcine CPB. To standardise the normal variability encountered in assay repeats, percentage inactivation was calculated for each time point for C5a incubated with and without HS (figure 6-23A). Interestingly, a statistically significant difference in inactivation by CPB was observed when C5a was incubated with HS for 1 h ($p = 0.039$). From these data at the 1 h time point nC5a-HS was 32% more active than nC5a following exposure to CPB. There was also a significant difference at $t = 3$ ($p = 0.032$). Despite a visible difference at $t = 2$, the difference in activation was not statistically significant ($p = 0.071$).

An explanation for the above difference in nC5a inactivation by CPB, was that HS could have an inhibitory effect on porcine CPB activity. In a preliminary experiment to test this hypothesis ($n=1$), HS was incubated with porcine CPB and CPB activity was measured in the carboxypeptidase activity assay (as used in section 4.9.1 to measure carboxypeptidase activity in CF BAL fluid). HS was added to porcine CPB at the same ratios as used for C5a activity experiments. Two further 10-fold dilutions of HS were made to see whether any effect was titratable. Despite a small titratable effect on CPB activity, at 50 $\mu\text{g}/\text{mL}$ HS, there was no obvious difference in porcine CPB activity (figure 6-23B). Therefore, it is unlikely that the reduced inactivation of C5a in (figure 6-23A) is due an inhibitory effect of HS on the activity of porcine CPB. Further replication of this experiment would be required for further assurance that HS does not inhibit CPB activity.

In summary of these experiments investigating the influence of HS on nC5a activity, HS had no effect on C5a activity however, C5a was more susceptible to proteolysis by NE. Interestingly, there was some evidence that HS modestly reduced inactivation of nC5a by porcine CPB.

6.10. Discussion

I hypothesised that in the CF airway soluble GAGs bind C5a, modifying function and promoting neutrophilic inflammation. In this chapter, I have shown that the concentration of soluble GAGs in CF BAL fluid correlated with inflammation in the CF airway, including CXCL8, a chemokine that has well-characterised GAG interactions (Pichert *et al.* 2012a). A correlation between GAGs and C5a was also observed. As for chapter 3, data were not corrected for total protein, following current ERS guide lines for reporting biological factors in CF BAL fluid (de Blic *et al.* 2000). Recombinant C5a and heparin interaction has previously been studied (Culley *et al.* 2003) however, interactions between C5a and soluble GAGs, found in the CF airway, have not been comprehensively characterised.

Western blots and column chromatography were used to investigate C5a-GAG binding. Conclusive evidence of C5a interaction with HS and CS was shown using a heparin affinity column. HS, CS and, HA were used to compete for heparin binding sites on nC5a, revealing strong inhibition of C5a-heparin binding by HS and to a lesser extent CS. Replicating data from the heparin affinity columns, a solid phase binding platform showed that biotinylated-HS bound to nC5a. Furthermore, unlabelled HS competed for nC5a binding at a 1:1 ratio, the affinity of CS for the HS binding site on nC5a was shown to be 100-fold lower. These experiments confirmed C5a-heparin interaction and further characterised C5a interaction with GAGs found elevated in the CF airway. My data showed that HS has affinity for nC5a and therefore, the influence of HS on C5a activity and regulation was investigated. HS interaction had no detectable effect on C5a activity, and unlike what has been reported for CXCL8, HS did not protect nC5a but increased susceptibility to proteolysis by NE. Interestingly, C5a in complex with HS was less susceptible to inactivation by porcine CPB.

Characterisation of C5a binding to a sepharose-heparin column has previously been reported (Culley *et al.* 2003), with observations that rhC5a was eluted by 422 mM NaCl in PBS. Data from this chapter is similar to this finding; I have shown that nC5a could be eluted approximately between 488 and 680 mM NaCl. Culley *et al.* also investigated the impact of heparin on rhC5a function with the hypothesis that heparin may reduce activity. They found that incubating rhC5a with heparin did not affect shape change or oxidative burst of eosinophils and did not prevent migration of HL60 cells, an immortal neutrophil-like cell line (Gallagher *et al.* 1979). In confirmation of data from their experiments, I observed nC5a interaction with HS, known to bind similar sites to heparin, did not affect rat basophil degranulation of β -hexosaminidase.

The second difference is that rhC5a lacks the N-glycosylation at asparagine-64, a result of expression in *E. coli*. In chapter 4, I demonstrated that rhC5a is more susceptible to degradation by NSPs when compared to nC5a. In this chapter, I observed a further difference between the two C5a forms; the solid phase binding assay revealed that rhC5a bound biotinylated-HS with greater affinity than nC5a. It is interesting that neither report by Culley *et al.* or Miyabe *et al.* discussed the structural differences between the two C5a forms and how this might influence their data. Figure 6-24 highlights the primary structural differences between nC5a and rhC5a. I hypothesise that positively charged histidine amino acids within the His-tag of rhC5a might confer higher affinity for GAGs explaining the higher affinity of HS for rhC5a than nC5a. In support of my hypothesis, a modified recombinant form of CXCL8, PA401, has been engineered to have a higher affinity for GAGs (Adage *et al.* 2015). PA401 is a pre-clinical CF therapeutic developed to compete against native CXCL8 for GAG binding, leaving native CXCL8 susceptible to degradation by NSPs in the CF airway (Adage *et al.* 2015; McElvaney *et al.* 2015). CXCL8 was modified by replacing neutrally charged amino acids with positively charged amino acids, such as lysine (Adage *et al.* 2015).

Experiments using de-glycosylated nC5a, by commercially available endoglycosidases, could help assess the significance of the nC5a N-glycosylation site for interaction with HS (and other GAGs). For example, investigating the differential glycosylation of anti-thrombin α and β forms has revealed preferential heparin binding by highly glycosylated β anti-thrombin (Pol-Fachin *et al.* 2011). Interaction with heparin modulates anti-thrombin activity and is important for function (Pol-Fachin *et al.* 2011).

A further advantage of this study to those previously reporting C5a-GAG interactions was that I quantified soluble GAG concentration in the CF airway, giving additional confidence in the GAG to C5a ratio used in my experiments. The GAG to nC5a ratio used in my experiments was less than what I observed in CF BAL fluid. For instance, for chromatography, 100 μg GAG was incubated with 2 μg C5a (50:1). In chapter 3, the greatest expression of C5a in CF BAL fluid was 807 pg/mL and, in this chapter lowest detectable GAG expression was 3.8 $\mu\text{g}/\text{mL}$, a ratio of over 4700:1. Therefore, any observed effects *in vitro*, are underestimates of a *in vivo* CF lung environment. In order to make my experiments more physiologically representative of the CF airway I would need to either decrease the C5a concentration or increase GAG concentration. The platforms used in this chapter would not be able to detect significantly lower concentrations of C5a. Furthermore, the GAGs used in these experiments are not soluble in aqueous solution at concentrations greater than 3 mg/ml and therefore, increasing GAG concentration in my experiments may not have been possible.

Despite previous reports of C5a-heparin interaction, observations made in this chapter more comprehensively characterise nC5a-GAG binding (Mollnes *et al.* 1991; Culley *et al.* 2003; Miyabe *et al.* 2017). The hypotheses for this investigation were initially made following reports of an in-depth characterisation of CXCL8-GAG interaction and the functional implications, particularly for neutrophilic inflammation in the CF airway (Reeves *et al.* 2011a; Reeves *et al.* 2011b). Like C5a, CXCL8 is small and chemotactic for neutrophils and therefore, I hypothesised that similar modifications of CXCL8, through interaction with GAGs, may also apply to C5a.

In comparison to C5a, it has been shown that CXCL8 eluted from a sepharose-heparin column at 510 mM NaCl (Webb *et al.* 1993). Therefore because higher concentrations of NaCl are required to disrupt these ionic interactions, CXCL8 has a higher affinity for this GAG than nC5a (488 to 680 mM NaCl (my data), 422 mM NaCl(Culley *et al.* 2003.) . Unlike nC5a, CXCL8 has also been observed to bind HA however, methods used in my study could not detect C5a-HA complexes and therefore, C5a affinity cannot be ruled out. It should be noted that in the current study both the heparin column and solid phase platform can only test C5a binding of heparin or HS binding sites. This is because, in both the competition assays performed using these platforms, GAGs competed for heparin/HS binding of C5a. However, biotinylation of CS or HA would enable analysis of possible alternative binding sites for these GAGs. In explanation, it has been shown that that HA preferentially binds alternative sites on CXCL8 compared to HS and heparin (Pichert *et al.* 2012a). Therefore, HA might not compete against HS for binding as tested for C5a in the present study.

An important consequence of CXCL8 interaction with GAGs is protection of this chemokine from degradation and inactivation by NSPs (Reeves *et al.* 2011a). However, in my study nC5a incubated with HS was more susceptible to proteolysis by NE. Myself and others have shown that C5a can be degraded by NE (Brozna *et al.* 1977; Huber-Lang *et al.* 2006). I can only speculate on the mechanism that increases C5a proteolysis when in complex with HS. A possible mechanism is that HS induces a conformational change in C5a tertiary structure further exposing the c-terminal signalling domain to degradation. In support of my hypothesis, binding of heparin to anti-thrombin has been reported to induce conformation changes in constituent α -helices that increase activity (Pol-Fachin *et al.* 2011).

Despite revealing increased susceptibility to degradation by NE, another important result was that nC5a in complex with HS was less susceptible to inactivation by porcine CPB; this is the first time it has been shown that GAGs may modify C5a activity. As tested for NE, this

phenomenon did not appear to be due to modified activity of CPB by HS. In blood, regulation of C5a, and other proteins, by CPN and CPB is a crucial mechanism for preventing over-activation of neutrophils and other C5aR1 expressing cells (Matthews *et al.* 2004). In chapter 4, I measured CPN and CPB activity in the CF airway and therefore, interaction of C5a with soluble HS may prevent anaphylatoxin inactivation and promote neutrophilic inflammation. Furthermore, this mechanism may be important for maintaining the normal functional of C5a in inflammation. C5a is a potent chemoattractant and critical for orchestrating the inflammatory response towards pathogens by upregulating opsonic receptors (Hunniger *et al.* 2015).

In this chapter I have built on evidence that C5a interacts with GAGs. A potential weakness to this study is the source and heterogeneity of the GAGs used in the experiments. All GAGs were sourced from Sigma however, this manufacturer does not disclose any information on the size or degree of sulphation of these GAGs. None the less, other published studies discussed in this chapter have also reported on GAG characterisation using GAGs sourced from Sigma (Culley *et al.* 2003). Purity, size and sulphation have a strong influence on GAG binding to the target protein (Pichert *et al.* 2012a). An off-shoot company from the University of Manchester, Iduron, specialises in producing pure GAGs with known levels of sulphation (<http://iduron.co.uk/>). To characterise nC5a-GAG interaction further, de-sulphated HS and CS could be investigated. It has been shown for CXCL8 that the level of sulphation alters GAG binding (Pichert *et al.* 2012a). In light of data from chapter 4, it would also be interesting to investigate the differences in the affinity for GAGs between nC5a and the C5a-like fragments that are readily generated by NSPs. In section 4.9.4; I reported for the first time that, C5a-like fragments generated by NE and PR3 are resistant to inactivation by porcine CPB. Therefore, are the functional differences between nC5a and the NSP-generated C5a-like fragments observed in this study further modified through interaction with GAGs?

Binding of HS to other complement components was also investigated using the solid phase binding platform. Interestingly, C5, C3 and, C3a all bound HS with greater affinity than nC5a. Despite coating plates with equivalent molar concentrations of complement components, the actual concentration of each component bound to the plastic was not determined. Therefore, further investigation is required for a more conclusive comparison at equimolar concentrations. With similarities to C5a, Sinitsyn *et al.* also showed that C3a could be retarded on a heparin-based sorbent suggesting C3a-heparin interaction (Sinitsyn *et al.* 1992). HA and HA subjected to heat treatment and freeze-thawing to alter conformation has also been reported to bind several complement components including C3 and C5 (Hong *et al.* 2007). Interestingly, the authors give evidence that treating HA modifies how it binds and, that these chemically-altered

GAGs inhibit sheep erythrocyte haemolysis by binding C1 and C3. The functional impact of HS on C3a, C3, and C5 was not investigated in the present study.

6.11. Conclusion to the chapter

In summary, the ECM is degraded during neutrophilic inflammation of the CF airway liberating soluble GAGs that disrupt neutrophil function through interaction with chemokines. To date, most interest in GAG-chemokine interaction has been placed on CXCL8, well-documented as a major contributor towards neutrophilic inflammation in the CF airway. CXCL8-mediated neutrophilic inflammation has been reported to be accelerated through interaction with soluble GAGs. I have shown that C5a also binds heparin and HS, with the latter interaction reducing inactivation by carboxypeptidases. Modulation of C5a activity in this manner could contribute towards neutrophilic inflammation and has, until more recently, been overlooked. C5a is a highly potent chemoattractant; moreover, it is crucial for orchestrating the inflammatory response by upregulating opsonic receptors and the release of pro-inflammatory factors. In this chapter I have mainly focused on the pathogenic implications of C5a-GAG interactions; however, these experiments also show that these interactions may play a normal role in the function of C5a by maintaining activity in the presence of carboxypeptidases.

7. Final summary

In this project I have used a cohort of CF patients to investigate the role of the complement anaphylatoxins in promoting chronic neutrophilic inflammation in the CF airway. I found that C5a and C3a positively correlated with makers of neutrophilic inflammation in CF BAL fluid. I used CF BAL fluid to explore the mechanisms by which C5a and C3a promote neutrophilic inflammation. Serine proteases within BAL fluid were able to generate C5a-like and C3a-like fragments of similar molecular weight to convertase-generated C5a and C3a. I characterised the generation of functionally active C5a-like and C3a-like fragments using purified NSPs. I also assessed whether NSP-generated C5a and C3a could be inactivated by carboxypeptidases, a critical mechanism for regulating native C5a and C3a activity. An important outcome of these experiments was that NE and PR3-generated C5a was resistant to activation. I suggest that this mechanism of generating alternatively functioning C5a-like fragments could contribute to neutrophilic inflammation and the CF airway and in other diseases that are characterised by chronic inflammation, such as COPD, rheumatoid arthritis and sepsis.

I also investigated mechanisms by which C5a is influenced by the local lung environment in CF. In particular, I explored the influence of GAGs interaction on C5a function. I found that nC5a interacted with heparin and HS and that these interactions had two consequences for C5a activity. The first is that when C5a was incubated with HS it was more susceptible to NE-mediated proteolysis. The second consequence of C5a interaction with HS was that C5a was more resistant to inactivation by CPB. The interactions between C5a and GAGs may be important for the normal roles of C5a in inflammation such as; neutrophil recruitment, degranulation and the up regulation of opsonic receptors (Hunniger *et al.* 2015). The abundance of soluble GAGs in the CF airway mean that these mechanisms by which GAGs modify C5a activity may also be a contributor towards chronic neutrophilic inflammation in CF.

7.1. Limitations to the study

In this study I used BAL fluid from CF patients to explore the mechanism by which C5a (and C3a) promote chronic neutrophilic inflammation. As previously mentioned BAL fluid sampling is the gold standard for identifying pathogens during pulmonary exacerbation and during routine surveillance (Ronchetti *et al.* 2018). Analysis of BAL fluid rather than sputum is also more advantageous when reporting on immunomodulatory factors (cytokines, lipids etc.)

within the airway due the way these samples are processed (McElvaney *et al.* 2018). Despite this, there are limitations to using BAL fluid for studying pathogenic factors in CF. For instance, BAL requires sedation and is invasive and therefore the ERS considers it unethical to perform BAL on healthy volunteers (Brennan *et al.* 2008). Consequently, because BAL cannot be performed on healthy volunteers other non-CF disease controls are sometimes used for healthy controls (Brennan *et al.* 2008). These include asthma, ciliary dyskinesia, tonsillectomy surgery and non-CF bronchiectasis (Brennan *et al.* 2008). In my study I did not have access to a control population however, in chapter 3 I stratified my patient cohort by reasons for performing BAL to separate well and unwell patients. This was successful when comparing neutrophil count and levels of CXCL8.

Another limitation to analysing BAL fluid is that it is from a single site, a ERS consensus recommends that the first sample site is the right middle lobe of the lungs (de Blic *et al.* 2000). An issue here could be that, if inflammation is localised in the airway then analytes from this single site may not correlate with disease scores (McNally *et al.* 2017). The consensus for surveillance of pathogens in the CF airway using BAL is to sample from the right middle lobe followed by the left lower lobe or most infected lobe as identified by chest X-ray (Brennan *et al.* 2008). A pool of these two sites is also analysed. A recent report was the first to compare inflammation (CXCL8) in a single site with a pool of two sites (McNally *et al.* 2017). McNally *et al.* report using a cohort of 32 CF patients showed that there was no statistical difference between a single site and a pooled sample. In my study, three samples were collected: right middle lobe, left lower lobe and a pool of the two sites. All analyses in my study were performed on the samples from the right middle lobe. Measuring and comparing inflammation and complement in the other sites would have been interesting to investigate but there was not enough time to perform these experiments. Although I have discussed BAL sampling from a single site as a limitation, I have also described it as an advantage over sputum sampling therefore, all factors should be considered when weighing up advantages and disadvantages of reporting on airway fluid samples.

In this study I have used immortal cell lines such as U937 and RBL-2H3. These were transfected with C3aR or C5aR1 to investigate functional activity of C3a-like and C5a-like fragments generated by NSPs. These cell lines were informative about the activity of these fragments; however, I did not assess C5a and C3a-like fragments in primary neutrophils. Neutrophils are notoriously difficult to work with as they have a short life-span *in vitro* and they are sensitive to stimulation by non-specific factors. Despite these difficulties it is still possible to work with primary neutrophils and our group has previously reported on C5a signaling in these cells (van den Berg *et al.* 2014). In my study I investigated the molecular characteristics

of C5a (and C3a) and therefore it was more appropriate to use stably transfected cell lines, rather than primary cells. As a compromise to working with blood neutrophils some groups use HL60 cells, a leukemia cell line that displays a neutrophil-like morphology. HL60 cells have been used to study the influence of heparin interaction with chemokines or C5a (Culley *et al.* 2003). A disadvantage of using HL60 cell lines to study the normal function of neutrophils is that due to disruption of granulopoiesis they do not produce secondary granules and therefore, they do not truly reflect neutrophils (Gallagher *et al.* 1979). A second cell line NB-4 also has a neutrophil-like phenotype, and has similar disadvantages to HL60 as these also not possess secondary granules (Pass *et al.* 2007). Therefore, HL60 and NB4 cell lines are acceptable for investigating neutrophil chemotaxis and ROS production but not suitable for studying neutrophil maturation (Pass *et al.* 2007).

I have investigated the role of C5a (and C3a) in promoting neutrophilic inflammation in the CF airway. Despite intriguing results, experiments investigating C5a and C3a were performed in simple *ex vivo* or *in vitro* systems. This does not invalidate my data, but the CF airway is a complex environment containing a plethora of self and pathogen-derived factors and therefore, we must be careful when translating findings from *in vitro* experiments. None the less, models of CF are not straightforward, particularly as neutrophils are terminally differentiated cells with a short life-span. A promyelocytic immortal cell line (PLB-985) that can be differentiated into neutrophil-like phenotypes with $\Delta F508\text{Del}$ *cftr* have been used to investigate defective phagosome function in neutrophils (Zhou *et al.* 2013b). PLB-985, like HL-60 and NB-4, are immature in terms of granulopoiesis and do not fully reflect the morphology of mature neutrophils (Tucker *et al.* 1987).

Animal models of the CF airway are also not straightforward. Mice models with mutations in *cftr*, that reflect mutations characterised in humans, do not develop severe airway disease; this is because of physiological differences between mice and humans (Lavelle *et al.* 2016). At the tissue level, the murine upper airways are representative of humans; however, there are fewer mucus-producing goblet cells in the mouse lower airway meaning that they do not spontaneously develop lung obstruction when lacking the CFTR (Lavelle *et al.* 2016). Porcine models of CF have been more successful in replicating human CF airway pathology (Lavelle *et al.* 2016). Pigs with the $\Delta F508\text{del}$ *cftr* genotype had similar neutrophil influx and CXCL8 levels observed in the human disease (Rogers *et al.* 2008). Furthermore, the porcine airway had recurrent *S. aureus* infections, mimicking early microbiology in paediatric CF patients (Stoltz *et al.* 2010). A disadvantage to porcine CF models is the majority of newborn piglets are born with obstructive meconium ileum, a blockage of the GI tract that requires surgical intervention, which increases the cost of maintaining this animal model (Lavelle *et al.* 2016).

A more suitable but unusual animal used to model CF airway disease is ferrets. *Cftr*^{-/-} ferrets have a phenotype that is representative of CF in humans however, pathology in the GI tract is much more severe with 75% of developing meconium ileum (Lavelle *et al.* 2016). In summary, modelling CF disease in cell lines and animals is difficult and reflects the importance of CFTR in homeostasis.

7.2. What does my research mean for CF?

The fact that we are still unable to control neutrophilic inflammation in the CF airway suggests that there are fundamental aspects of disease pathogenesis that we do not understand. In this study, I investigated how C5a and mechanisms of C5a generation could promote neutrophilic inflammation. One of the key papers behind this rationale was written by Mackerness *et al.* who identified that in CF sputum, C5a (as well as other factors) was an important neutrophil chemotactic factor (Mackerness *et al.* 2008). The aim of this project was not to pursue C5a as a therapeutic target, but to improve understanding of another factor in the CF airway, beyond CXCL8, that contributes to neutrophilic inflammation. I do not doubt that CXCL8 is a major contributor to neutrophilic inflammation in the airway; however, I do feel that other factors such as LTB₄, fMLP and C5a are overlooked, given their potency and roles in neutrophil stimulation (Brink *et al.* 2003; Ye *et al.* 2009; Klos *et al.* 2013). I do not think that C5a is any more or less pathogenic in the CF airway than CXCL8; however, C5a has many functions that are important for orchestrating inflammation and clearance of pathogens. These include neutrophil priming and upregulation of opsonic receptors (Hunniger *et al.* 2015). Furthermore, CXCL8 and C5a have distinctive roles. For instance, CXCL8 may be more important for neutrophil recruitment to the airway lumen but C5a may be more critical for the over-activation of neutrophils by promoting degranulation and ROS production (Kim and Haynes 2012; Hunniger *et al.* 2015). CF is not the only disease where C5a has been identified as a pathogenic factor. Other airway diseases include COPD and asthma but C5a has also been identified as a pathogenic factor in sepsis. Consequently, C5a has been suggested to be an appropriate therapeutic target in these diseases (Khan *et al.* 2013; Huber-Lang *et al.* 2014; Khan *et al.* 2014).

Would C5a be an appropriate target in CF? Sass *et al.* used a C1 inhibitor as part of their study to investigate atypical generation of C5a in CF sputum (Sass *et al.* 2015). From their data they suggest that C5a generation is predominantly through complement activation and not mediated by non-complement proteases. Their single *ex vivo* study does not conclusively mean that non-canonical generation of C5a in the airway is not a significant mechanism for promoting pathogenesis. Specifically targeting C5a in the CF airway could be achieved by

directly blocking C5a by antibody such as IFX-1 developed by inflaRx GmbH (Riedemann *et al.* 2017). C5a function could also be abrogated by PMX53, a hexapeptide antagonist of C5aR1 (Tamamis *et al.* 2014). As well as considering the methods of inhibiting C5a function, when to block C5a should be carefully thought out. It has been reported that C5a has both protective and pathogenic roles in developing hyperallergic asthma and therefore, the protective roles of C5a, as mediator of normal inflammation should be considered (Kohl *et al.* 2006). Particularly in light of BIIL284, a BLT₁R antagonist that had serious adverse effects when administered in a CF trial (Konstan *et al.* 2014). In this case, BLT₁R inhibition reduced neutrophil recruitment but increased susceptibility to infection by *P. aeruginosa*. I think that blocking C5a (or C5aR1) would be more appropriate during pulmonary exacerbation; this is because C5a has been reported to spike during pulmonary exacerbation in CF patients (Hair *et al.* 2017). If C5a is pathogenic during these episodes, then inhibition may prevent airway remodeling and irreversible loss of lung function. I would also advocate further research into NSP-generated C5a and the effectiveness of the above C5a/C5aR1 inhibitors in reducing the activity of alternative C5a forms that I have investigated in this project.

In chapter 5, I investigated the generation of C5a by NSPs in the presence of C5 cleavage inhibitors. I reported that three pre-clinical therapeutics and eculizumab, a successful clinical complement inhibitor, were ineffective against NSP-mediated C5a generation. As I discussed in chapter 5, given these data, I do not think these C5 cleavage inhibitors would be appropriate for use in CF and, I have concerns over their use in diseases characterised by neutrophilic inflammation. This is because my research has shown that during neutrophilic inflammation the inhibitory function of these therapies can be bypassed by NSPs. Therefore, they might only be effective against terminal complement activation and MAC formation but not the generation of C5a. Furthermore, MAC mediated lysis is an important mechanism for the elimination of pathogens that you may not want to attenuate during pulmonary exacerbation (Savoia *et al.* 2008).

In summary, I think that this research could continue to raise awareness of other important neutrophil stimulants in the CF airway as well as CXCL8. C5a, is a multi-faceted pro-inflammatory molecule as well as a potent neutrophil chemoattractant; furthermore, these functions are crucial for orchestrating a normal inflammatory response as well as contributing to pathogenesis in chronic conditions. Further understanding is needed of how each of these C5a-mediated functions contributes to chronic neutrophil inflammation before therapeutic intervention is considered.

7.3. CF therapeutics – what is the future?

For CF patients, the greatest gains in life expectancy over the last couple of decades have been through disease management and improvements in pathogen surveillance (Elborn 2016). An issue with testing many new CF therapeutics is that they may have long-term benefits that are not detected in short-term trials. Furthermore, trials are often performed in older patients (Mayer-Hamblett *et al.* 2016). Therapeutics that correct CFTR function would be more beneficial in paediatric patients, to prevent lung function decline in the earlier stages of the disease before chronic neutrophilic inflammation is established. The issue with long term trials in paediatric cohorts is that given the short life expectancy of CF patients, it is unethical to have a placebo control group for such a long period. The other ethical consideration is the desire to stop other medications so that the effect size of the therapeutic under trial can be accurately measured.

Currently CF disease is managed by regular physiotherapy and inhalation of nebulized hypertonic saline as well as corticosteroids and administration of antibiotics upon contracting pulmonary infection (Elborn 2016). There have been several different therapeutic approaches to preserve lung function and improve life expectancy in CF. Two clinically approved therapeutics, Ivacaftor and Lumacaftor have been developed to increase CFTR activity (G551D *cftr* patients) and facilitate intracellular trafficking (Δ 508Del *cftr* patients)(Wainwright *et al.* 2015). A combined therapy using both drugs, Orkambi, has been shown to marginally reduce the decline in lung function in CF patients (Wainwright *et al.* 2015). Despite modest improvements, these drugs are one of the most successful approaches to preserving lung function. It is likely that the long-term benefits, not observed in short 2-year trials, will become more apparent in the next few years. Furthermore, in paediatric CF patients these drugs will maintain healthy lung function prior to the decline in lung function that is observed as CF patients age. Despite this potential, Orkambi is expensive (over £140,000/patient/year) and the National Health Service has restricted its availability, a controversial issue that has recently been reported in the national news <https://www.bbc.co.uk/news/uk-wales-45215134>).

Gene therapy using liposomal delivery of wild type CFTR (rather than correcting gene mutation) to the airway epithelium has been trialed in CF patients and was found to modestly stabilise lung function (Alton *et al.* 2015). More specifically, a double blind, placebo-controlled phase IIb trial was conducted with 140 patients over a 12-month period. Absolute change in lung function over this period was 3.7% (0.1-7.3), greater than placebo control (Alton *et al.* 2015). Gene therapy has long been thought to be the “gold bullet” for CF; however, issues such as delivery vector (viral or liposomal in a complex environment) and epithelial turn-over

has slowed development of therapeutics correcting *cftr* mutation (Fajac and De Boeck 2017). None-the-less, other mechanisms of genetically correcting *cftr* mutation are being developed such as mRNA repair, whereby single-stranded anti-sense RNA is used to guide the repair of abnormal mRNA prior to translation (Zamecnik *et al.* 2004).

The limited success of gene therapy and benefits of potentiators/activators does not mean that gene therapy will not be an important therapeutic in the future. One of the first CF therapeutics was the supplementation of pancreatic enzymes that are deficient in CF patients due to blockage of bile ducts (Somaraju and Solis-Moya 2015). Before this, most people with mutations in *cftr* did not live through childhood, before airway chronic inflammation became established (Somaraju and Solis-Moya 2015). Only after intervention did airway inflammation become the predominant factor in mortality. Therefore, if drugs like Orkambi restore airway function, CF patients will live longer but another aspect of the disease could manifest; for instance, CF-related diabetes, osteopenia and distal intestinal obstruction syndrome (Elborn 2016). Gene therapy could be a more appropriate therapeutic approach for correcting CF pathology not just in the airway.

Neutrophilic inflammation of the airway is a major characteristic of CF pathology yet, therapeutic approaches to reduce inflammation have been largely unsuccessful. In some cases, anti-inflammatory drugs have been detrimental, particularly in the case of BIIL284, a BLT₁R antagonist (Konstan *et al.* 2014). Ibuprofen remains one of the only modestly effective anti-inflammatory drugs prescribed to CF patients (Konstan *et al.* 2007). Targeting CXCL8-mediated neutrophilic inflammation in the CF airway has also been approached. As previously mentioned, a decoy CXCL8, PA401, has been developed that has no activity but has greater affinity for GAGs (McElvaney *et al.* 2015). The mechanism of PA401 in reducing CXCL8 levels in the CF airway, is that PA401 competes with CXCL8 for GAG binding sites (McElvaney *et al.* 2015). GAGs have been shown to protect CXCL8 from degradation by NSPs and therefore, preventing CXCL8-GAG interaction would leave CXCL8 susceptible to inactivation (McElvaney *et al.* 2015; Reeves *et al.* 2015). PA401 is currently undergoing pre-clinical trials (McElvaney *et al.* 2015).

7.4. Do we need to research the roles C5a (and C3a) in CF pathogenesis?

Above I briefly discussed the different therapeutic approaches to restoring CFTR function in the CF airway. Given that these therapeutics are being improved and the benefits of taking them are becoming more apparent, why do we need to investigate C5a (and C3a) in the CF airway? Chronic neutrophilic inflammation is not unique to the CF airway and is a

characteristic of other airway diseases such as COPD and neutrophilic asthmas (Hoenderdos and Condliffe 2013; Lambrecht and Hammad 2015). Neutrophilic inflammation is also a pathogenic factor in sepsis and rheumatoid arthritis (Delano and Ward 2016; Sadik *et al.* 2018). Despite differences in the way these diseases manifest and progress, neutrophils and neutrophil dysfunction contribute to their pathogenesis. Furthermore, complement and in particular the C5a-C5aR1 axis, has been reported to be significant in promoting neutrophilic inflammation in these diseases (Conway Morris *et al.* 2009; Marc *et al.* 2010; Khan *et al.* 2015; Miyabe *et al.* 2017). Therefore, as well as investigating new mechanisms that promote neutrophilic inflammation in CF, this disease can be used as a case study of extreme neutrophilic inflammation. This means that the mechanisms that I have investigated in this project could also be translated to other inflammatory diseases.

The generation of C5a-like forms by non-complement proteases such as NSPs as a mechanism of promoting pathogenesis has previously been reported in pathologies including rheumatoid arthritis, COPD and asthma (Robbins *et al.* 1991; Giles *et al.* 2015; Verschoor *et al.* 2016). Therefore, the NSP-generated C5a that I found to be resistant to inactivation by carboxypeptidases could also be an important for driving neutrophilic inflammation in these other diseases.

7.5. The importance of Complement

Complement contributes to a variety of different diseases: however, there are less than handful that are directly linked to complement dysregulation or deficiency. Does this mean that complement is not an important aspect of our immune system? Persons deficient in C3, a component central to complement activity, are susceptible to recurrent bacterial infections (Botto *et al.* 2009). C5 deficient persons are also susceptible to meningococcal infection, further demonstrating a central role for complement in preventing infection (Arnaout *et al.* 2013). Despite these case studies, complement deficiencies are rare (1-5 cases per million), but they are more prevalent in communities where there is consanguineous marriage (Arnaout *et al.* 2013; Nanthapaisal *et al.* 2018).

Beyond immunity, complement has also been hypothesised to have roles in fertilization, embryogenesis and neural development (Hawksworth *et al.* 2018); protecting sperm from elimination by complement, guiding stem cells into the appropriate areas and pruning redundant neurons (Hawksworth *et al.* 2018). Do these critical roles in reproduction and development explain the rarity of complement deficiency? Particularly with development, the discrepancy between the reported developmental functions of complement and what we

observed in the population are intriguing; however, these discrepancies may highlight that animal models do not completely reflect the human complement system (Hawksworth *et al.* 2018).

Complement is ancient, and pre-dates adaptive immunity. Furthermore, complement C3 genes have been discovered in primitive organisms such as ascidians (sea squirts) and sea anemones (Nonaka and Yoshizaki 2004; Hawksworth *et al.* 2018). Injecting LPS into the pharynx of *Ciona intestinalis* (sea squirt), has demonstrated that C3 and its cleavage fragments are part of this organism's immune defense (Giacomelli *et al.* 2012). None the less, if complement was sufficient for immune protection in complex mammals then the adaptive immune system may not have evolved. Interestingly, C3 deficient individuals are particularly vulnerable to bacterial infections during childhood, as adaptive immunity is developing its antigen repertoire (Botto *et al.* 2009). Therefore, the complement system provides vital protection whilst the adaptive immune system matures.

I have discussed the necessity of complement in immunity using examples of complete complement deficiency for justification. In an era of GWAS (genome-wide association studies) to search for genetic evidence of an individual's susceptibility to disease, mutations in complement genes have been identified as risk factors (Harris *et al.* 2012). Examples of diseases where complement genes are risk factors are AMD, rheumatoid arthritis and aHUS (Harris *et al.* 2012). Combining all the identified single nucleotide polymorphisms in C3, factor B and factor I in a Spanish population Harris *et al.* have developed a "complotype" (Harris *et al.* 2012). An individual's complotype could indicate that they are more at risk from infection due to single nucleotide polymorphisms that reduce complement activity. Or, at the other end of the scale, a patient may be at risk of inflammation as a consequence of increased complement activity (Harris *et al.* 2012).

Given the developmental and protective role of complement how important is it for immunity and pathogen clearance in the airway? In asthma the C5a/C5aR1 axis has been reported to have both protective or pathogenic roles during sensitisation and hyperresponsiveness respectively (Laumonnier *et al.* 2017). Polymorphisms in C3, C5 and C5aR1 genes have also been associated with different levels of risk for developing bronchial asthma (Hasegawa *et al.* 2004). In particular, the authors found that a C4896T mutation in C3 was associated with developing bronchial asthma in adults. A C1632T polymorphism in C5 was found to be protective against developing asthma in adults. Despite identification of these polymorphisms, no mechanisms were explored in their study. Complement is important for eliminating pathogens in the airway. It has been demonstrated that airways infected with *P. aeruginosa*

and *B. cepacia* had high levels of pathogen-specific IgG; furthermore, antibacterial activity was complement mediated (Savoia *et al.* 2008). Therefore, complement in the airway is important for responding to allergens and pathogens.

7.6. Immune modulation by NSPs

In section 1.4.7, I discussed the reported roles that NSPs have in immune modulation, such as proteolytic activation of PARs, pro-IL-1 β and CXCL8-77 (Joosten *et al.* 2009; Chakraborty *et al.* 2014; Mercer *et al.* 2014). As part of this project, I have characterised the alternative generation of functionally different C5a (and C3a). With the above diverse mechanisms in mind, are these functions coincidental or a result of intricate evolution between NSPs and the innate immune system?

My first thought is that many of the reported mechanisms of immune modulation by NSPs are coincidental and, are a result of the broad specificity of NSPs. A database of NSPs substrates (recombinant and native) can be viewed on the MEROPs website (<https://merops.sanger.ac.uk/>). In response to the broad specificity of NSPs, our immune system has evolved to regulate the activity of these proteases through the production of serine protease inhibitors, such as; AAT, SLPI and elafin (Korkmaz *et al.* 2010). These inhibitors prevent excessive tissue damage or remodeling as a result of neutrophilic inflammation (Korkmaz *et al.* 2010). Therefore, NSP-mediated immunomodulation would need to occur in close proximity to neutrophils, where proteases activity is highest. Immune modulation by NSPs may also be more prevalent in diseases where there is chronic neutrophilic inflammation that overwhelms their regulation, such as the CF airway (Hentschel *et al.* 2015). Taking this all into account, do these NSP-mediated functions offer a great enough selective advantages to suggest that these mechanisms evolved?

Another reason why I suggest these mechanisms are coincidental is that the canonical activation of these immune functions is mediated by serine proteases. The normal reported activation mechanism of PAR-1 is through cleavage by thrombin (Mercer *et al.* 2014), a serine protease. Furthermore C5 convertase is a proteolytic complex of serine proteases C4bC2b (C3 convertase), that has cleavage site specificity modified by binding of C3b (Barnum and Schein 2018). Although the serine protease family is large, it is not inconceivable that these proteases share site specificity. In support of this statement, cleavage of identical C5a fragments to native C5a has been reported by thrombin and trypsin (Riedemann *et al.* 2017). Therefore, C5 convertase and thrombin share the same cleavage site on C5. I have hypothesised that the cleavage of NE-generated C5a is not the same as C5 convertase

generated C5a. Furthermore Giles *et al.* speculated that the NE cleavage site is 10-amino acids downstream and therefore a similar sized C5a fragments produced (Giles *et al.* 2015). If serine proteases share some degree of site-specificity, then we might expect to see more cases of immunomodulation, where there is atypical activation of protease-activated immune functions by NSPs. Although, many NSP mediated immunomodulatory functions have been reported, there could be many more that have not been discovered.

My approach to the question of whether NSP-mediated immune modulation is coincidence has been binary. I think that it is more likely that some of these NSP-mediated functions have evolved and others are coincidence. Furthermore, some of these mechanisms may only be applicable to cases where there is extreme neutrophilic inflammation (such as CF), and others may be “normal” roles for these proteases. For instance, until the 1930s CF patients did not live to a reproductive age (Somaraju and Solis-Moya 2015); therefore, the selective pressure for NSP-mediated immune modulation in CF may not be very high. In summary, it seems unlikely that the generation of C5a-like (and C3a-like) fragments by NSPs in the CF airway has been driven by evolution. On the other hand, the pathogenic role that these mechanisms of C5a (and C3a) generation may not be a large enough negative selective pressure for them to be more tightly regulated.

7.7. Conclusion to the chapter

From my data I think that the generation of alternatively functioning C5a by NSPs could be an important mechanism for promoting neutrophilic inflammation in the CF airway. Interactions between GAGs that modify the regulation of C5a could also be significant for the normal roles of C5a in inflammation and its pathogenic roles during chronic inflammation. CF is an extreme case of neutrophilic inflammation that can be used to study the molecular characteristics of C5a (and C3a). Further understanding of the pathogenic roles of complement anaphylatoxins in CF can be translated to other diseases characterised by neutrophilic inflammation.

7.8. Key findings from my study

1. C5a and C3a positively correlate with markers of neutrophilic inflammation in CF BAL fluid.
2. C5a-like and C3a-like fragments are generated by proteases present in CF BAL fluid.
3. NE and PR3 generate functionally alternative C5a that is resistant to inactivation by CPB.
4. Complement therapeutics that inhibit cleavage of C5 by C5 convertase are ineffective against NSP-mediated C5a generation.
5. C5a binds heparin, HS and CS. C5a-HS interaction protects C5a from inactivation by CPB

7.9. Future Work

- Comprehensively characterise NSP-generated C5a-like and C3a-like fragments using mass spectrometry.
- Develop a specific antibody to quantify generation of C5a-like and C3a-like fragments in CF BAL fluid (and other samples from diseases characterised by neutrophilic inflammation).
- Investigate other proteases (as well as NSPs) that can generate C5a-like fragments in the presence of therapeutic C5 cleavage inhibitors.
- Use purified GAG species and surface plasmon resonance to measure C5a affinity for different GAGs.

8. References

Abdul Roda, M., Fernstrand, A. M., Redegeld, F. A., Blalock, J. E., Gaggar, A. and Folkerts, G. (2015). The matrikine PGP as a potential biomarker in COPD. *Am J Physiol Lung Cell Mol Physiol* **308**(11): 1095-1101.

Adage, T., Del Bene, F., Fiorentini, F., Doornbos, R. P., Zankl, C., Bartley, M. R. and Kungl, A. J. (2015). PA401, a novel CXCL8-based biologic therapeutic with increased glycosaminoglycan binding, reduces bronchoalveolar lavage neutrophils and systemic inflammatory markers in a murine model of LPS-induced lung inflammation. *Cytokine* **76**(2):433-441.

Ahmad, A., Ahmed, A. and Patrizio, P. (2013). Cystic fibrosis and fertility. *Curr Opin Obstet Gynecol* **25**(3):167-172.

Al-Mohanna, F. A. and Hallett, M. B. (1988). The use of fura-2 to determine the relationship between cytoplasmic free Ca²⁺ and oxidase activation in rat neutrophils. *Cell Calcium* **9**(1):17-26.

Alexander, J. J., Chaves, L. D., Chang, A., Dighe, S., Jacob, A. and Quigg, R. J. (2015). Abrogation of immune complex glomerulonephritis by native carboxypeptidase and pharmacological antagonism of the C5a receptor. *Cell Mol Immunol* **13**: 651-657

Alton, E. W., Armstrong, D. K., Ashby, D., Bayfield, K. J., Bilton, D., Bloomfield, E. V., . . . Wolstenholme-Hogg, P. (2015). Repeated nebulisation of non-viral CFTR gene therapy in patients with cystic fibrosis: a randomised, double-blind, placebo-controlled, phase 2b trial. *Lancet Respir Med* **3**(9):684-691.

Amitani, R., Wilson, R., Rutman, A., Read, R., Ward, C., Burnett, D., . . . Cole, P. J. (1991). Effects of human neutrophil elastase and *Pseudomonas aeruginosa* proteinases on human respiratory epithelium. *Am J Respir Cell Mol Biol* **4**(1):26-32.

An, L. L., Mehta, P., Xu, L., Turman, S., Reimer, T., Naiman, B., . . . Fung, M. (2014). Complement C5a potentiates uric acid crystal-induced IL-1beta production. *Eur J Immunol* **44**(12):3669-3679.

Andersson, C. K., Andersson-Sjoland, A., Mori, M., Hallgren, O., Pardo, A., Eriksson, L., . . . Erjefalt, J. S. (2011). Activated MCTC mast cells infiltrate diseased lung areas in cystic fibrosis and idiopathic pulmonary fibrosis. *Respir Res* **12**:139.

Armstrong, D. S., Hook, S. M., Jansen, K. M., Nixon, G. M., Carzino, R., Carlin, J. B., . . . Grimwood, K. (2005). Lower airway inflammation in infants with cystic fibrosis detected by newborn screening. *Pediatr Pulmonol* **40**(6):500-510.

Arnaout, R., Al Shorbaghi, S., Al Dhekri, H., Al-Mousa, H., Al Ghonaium, A., Al Saud, B., . . . Hawwari, A. (2013). C5 complement deficiency in a Saudi family, molecular characterization of mutation and literature review. *J Clin Immunol* **33**(4):871-875.

Asgari, E., Le Friec, G., Yamamoto, H., Perucha, E., Sacks, S. S., Kohl, J., . . . Kemper, C. (2013). C3a modulates IL-1beta secretion in human monocytes by regulating ATP efflux and subsequent NLRP3 inflammasome activation. *Blood* **122**(20):3473-3481.

Bakare, N., Rickerts, V., Bargon, J. and Just-Nubling, G. (2003). Prevalence of *Aspergillus fumigatus* and other fungal species in the sputum of adult patients with cystic fibrosis. *Mycoses* **46**(1-2):19-23.

Balfour-Lynn, I. M. and Welch, K. (2016). Inhaled corticosteroids for cystic fibrosis. *Cochrane Database Syst Rev* (8): 1915 - 1920

Barbu, A., Hamad, O. A., Lind, L., Ekdahl, K. N. and Nilsson, B. (2015). The role of complement factor C3 in lipid metabolism. *Mol Immunol* **67**(1):101-107.

Barnaby, R., Koeppen, K., Nymon, A., Hampton, T. H., Berwin, B., Ashare, A. and Stanton, B. A. (2018). Lumacaftor (VX-809) restores the ability of CF macrophages to phagocytose and kill *Pseudomonas aeruginosa*. *Am J Physiol Lung Cell Mol Physiol* **314**(3):L432-L438.

Barnum, S. and Schein, T. (2018). *The complement facts book*. Second Edition ed. 125 London Wall, London EC2Y 5AS, United Kingdom: Academic Press, p. 471.

Bayes, H. K., Bicknell, S., MacGregor, G. and Evans, T. J. (2014). T helper cell subsets specific for *Pseudomonas aeruginosa* in healthy individuals and patients with cystic fibrosis. *PLoS One* **9**(2):e90263.

Bazzoni, F., Tamassia, N., Rossato, M. and Cassatella, M. A. (2010). Understanding the molecular mechanisms of the multifaceted IL-10-mediated anti-inflammatory response: lessons from neutrophils. *Eur J Immunol* **40**(9):2360-2368.

Behnsen, J., Lessing, F., Schindler, S., Wartenberg, D., Jacobsen, I. D., Thoen, M., . . . Brakhage, A. A. (2010). Secreted *Aspergillus fumigatus* protease Alp1 degrades human complement proteins C3, C4, and C5. *Infect Immun* **78**(8):3585-3594.

Bekker, P., Dairaghi, D., Seitz, L., Leleti, M., Wang, Y., Ertl, L., . . . Schall, T. J. (2016). Characterization of Pharmacologic and Pharmacokinetic Properties of CCX168, a Potent and Selective Orally Administered Complement 5a Receptor Inhibitor, Based on Preclinical Evaluation and Randomized Phase 1 Clinical Study. *PLoS One* **11**(10):e0164646.

Belaouaj, A., Kim, K. S. and Shapiro, S. D. (2000). Degradation of outer membrane protein A in *Escherichia coli* killing by neutrophil elastase. *Science* **289**(5482):1185-1188.

Belaouaj, A., McCarthy, R., Baumann, M., Gao, Z., Ley, T. J., Abraham, S. N. and Shapiro, S. D. (1998). Mice lacking neutrophil elastase reveal impaired host defense against gram negative bacterial sepsis. *Nat Med* **4**(5):615-618.

Bellemare, A., Vernoux, N., Morin, S., Gagne, S. M. and Bourbonnais, Y. (2010). Structural and antimicrobial properties of human pre-elafin/trappin-2 and derived peptides against *Pseudomonas aeruginosa*. *BMC Microbiol* **10**:253.

Bergsson, G., Reeves, E. P., McNally, P., Chotirmall, S. H., Greene, C. M., Grealley, P., . . . McElvaney, N. G. (2009). LL-37 complexation with glycosaminoglycans in cystic fibrosis lungs inhibits antimicrobial activity, which can be restored by hypertonic saline. *J Immunol* **183**(1):543-551.

Berton, G., Mocsai, A. and Lowell, C. A. (2005). Src and Syk kinases: key regulators of phagocytic cell activation. *Trends Immunol* **26**(4):208-214.

Bhaskar, K. R., Turner, B. S., Grubman, S. A., Jefferson, D. M. and LaMont, J. T. (1998). Dysregulation of proteoglycan production by intrahepatic biliary epithelial cells bearing defective (delta-f508) cystic fibrosis transmembrane conductance regulator. *Hepatology* **27**(1):7-14.

Birke, F. W., Meade, C. J., Anderskewitz, R., Speck, G. A. and Jennewein, H. M. (2001). In vitro and in vivo pharmacological characterization of BIIL 284, a novel and potent leukotriene B(4) receptor antagonist. *J Pharmacol Exp Ther* **297**(1):458-466.

Boackle, S. A., Morris, M. A., Holers, V. M. and Karp, D. R. (1998). Complement opsonization is required for presentation of immune complexes by resting peripheral blood B cells. *J Immunol* **161**(12):6537-6543.

Bolger, M. S., Ross, D. S., Jiang, H., Frank, M. M., Ghio, A. J., Schwartz, D. A. and Wright, J. R. (2007). Complement levels and activity in the normal and LPS-injured lung. *Am J Physiol Lung Cell Mol Physiol* **292**(3):L748-759.

Bonfield, T. L., Panuska, J. R., Konstan, M. W., Hilliard, K. A., Hilliard, J. B., Ghnaim, H. and Berger, M. (1995). Inflammatory cytokines in cystic fibrosis lungs. *Am J Respir Crit Care Med* **152**(6 Pt 1):2111-2118.

Borregaard, N. (2010). Neutrophils, from marrow to microbes. *Immunity* **33**(5):657-670.

Botto, M., Kirschfink, M., Macor, P., Pickering, M. C., Wurzner, R. and Tedesco, F. (2009). Complement in human diseases: Lessons from complement deficiencies. *Mol Immunol* **46**(14):2774-2783.

Brachet, G., Bourquard, T., Gallay, N., Reiter, E., Gouilleux-Gruart, V., Poupon, A. and Watier, H. (2016). Eculizumab epitope on complement C5: Progress towards a better understanding of the mechanism of action. *Mol Immunol* **77**:126-131.

- Braga, T. T., Agudelo, J. S. and Camara, N. O. (2015). Macrophages During the Fibrotic Process: M2 as Friend and Foe. *Front Immunol* **6**:602.
- Branzk, N., Lubojemska, A., Hardison, S. E., Wang, Q., Gutierrez, M. G., Brown, G. D. and Papayannopoulos, V. (2014). Neutrophils sense microbe size and selectively release neutrophil extracellular traps in response to large pathogens. *Nat Immunol* **15**(11):1017-1025.
- Brennan, S., Gangell, C., Wainwright, C. and Sly, P. D. (2008). Disease surveillance using bronchoalveolar lavage. *Paediatr Respir Rev* **9**(3):151-159.
- Brink, C., Dahlen, S. E., Drazen, J., Evans, J. F., Hay, D. W., Nicosia, S., . . . Yokomizo, T. (2003). International Union of Pharmacology XXXVII. Nomenclature for leukotriene and lipoxin receptors. *Pharmacol Rev* **55**(1):195-227.
- Brinkmann, V. (2018). Neutrophil Extracellular Traps in the Second Decade. *J Innate Immun*:1-8.
- Brivio, A., Conese, M., Gambazza, S., Biffi, A., Tirelli, A. S., Russo, M., . . . Colombo, C. (2016). Pilot Randomized Controlled Trial Evaluating the Effect of Hypertonic Saline With and Without Hyaluronic Acid in Reducing Inflammation in Cystic Fibrosis. *J Aerosol Med Pulm Drug Deliv* **29**(6):482-489.
- Brozna, J. P., Senior, R. M., Kreutzer, D. L. and Ward, P. A. (1977). Chemotactic factor inactivators of human granulocytes. *J Clin Invest* **60**(6):1280-1288.
- Bruscia, E. M. and Bonfield, T. L. (2016). Cystic Fibrosis Lung Immunity: The Role of the Macrophage. *J Innate Immun* **8**(6):550-563.
- Burns, J. L. and Rolain, J. M. (2014). Culture-based diagnostic microbiology in cystic fibrosis: can we simplify the complexity? *J Cyst Fibros* **13**(1):1-9.
- Butler, M. W., Robertson, I., Greene, C. M., O'Neill, S. J., Taggart, C. C. and McElvaney, N. G. (2006). Elafin prevents lipopolysaccharide-induced AP-1 and NF-kappaB activation via an effect on the ubiquitin-proteasome pathway. *J Biol Chem* **281**(46):34730-34735.
- Cain, S. A. and Monk, P. N. (2002). The orphan receptor C5L2 has high affinity binding sites for complement fragments C5a and C5a des-Arg(74). *J Biol Chem* **277**(9):7165-7169.
- Campbell, W. D., Lazoura, E., Okada, N. and Okada, H. (2002). Inactivation of C3a and C5a octapeptides by carboxypeptidase R and carboxypeptidase N. *Microbiol Immunol* **46**(2):131-134.
- Cantin, A. M., Hartl, D., Konstan, M. W. and Chmiel, J. F. (2015). Inflammation in cystic fibrosis lung disease: Pathogenesis and therapy. *J Cyst Fibros* **14**(4): 419-430

Caporale, L. H., Tippet, P. S., Erickson, B. W. and Hugli, T. E. (1980). The active site of C3a anaphylatoxin. *J Biol Chem* **255**(22):10758-10763.

Chakraborty, M., McGreal, E. P., Williams, A., Davies, P. L., Powell, W., Abdulla, S., . . . Kotecha, S. (2014). Role of serine proteases in the regulation of interleukin-8 during the development of bronchopulmonary dysplasia in preterm ventilated infants. *PLoS One* **9**(12):e114524.

Chmiel, J. F., Konstan, M. W. and Elborn, J. S. (2013). Antibiotic and anti-inflammatory therapies for cystic fibrosis. *Cold Spring Harb Perspect Med* **3**(10):a009779.

Chotirmall, S. H., Greene, C. M., Oglesby, I. K., Thomas, W., O'Neill, S. J., Harvey, B. J. and McElvaney, N. G. (2010). 17Beta-estradiol inhibits IL-8 in cystic fibrosis by up-regulating secretory leucoprotease inhibitor. *Am J Respir Crit Care Med* **182**(1):62-72.

Chotirmall, S. H. and McElvaney, N. G. (2014). Fungi in the cystic fibrosis lung: bystanders or pathogens? *Int J Biochem Cell Biol* **52**:161-173.

Chotirmall, S. H., Smith, S. G., Gunaratnam, C., Cosgrove, S., Dimitrov, B. D., O'Neill, S. J., . . . McElvaney, N. G. (2012). Effect of estrogen on pseudomonas mucoidy and exacerbations in cystic fibrosis. *N Engl J Med* **366**(21):1978-1986.

Cianflone, K. (2003). Acylation stimulating protein and triacylglycerol synthesis: potential drug targets? *Curr Pharm Des* **9**(17):1397-1410.

Clark, S. J., Higman, V. A., Mulloy, B., Perkins, S. J., Lea, S. M., Sim, R. B. and Day, A. J. (2006). His-384 allotypic variant of factor H associated with age-related macular degeneration has different heparin binding properties from the non-disease-associated form. *J Biol Chem* **281**(34):24713-24720.

Clarke, L. L., Grubb, B. R., Yankaskas, J. R., Cotton, C. U., McKenzie, A. and Boucher, R. C. (1994). Relationship of a non-cystic fibrosis transmembrane conductance regulator-mediated chloride conductance to organ-level disease in Cftr(-/-) mice. *Proc Natl Acad Sci U S A* **91**(2):479-483.

Clemens, R. A. and Lowell, C. A. (2015). Store-operated calcium signaling in neutrophils. *J Leukoc Biol* **98**(4):497-502.

Colotta, F., Re, F., Muzio, M., Bertini, R., Polentarutti, N., Sironi, M., . . . Mantovani, A. (1993). Interleukin-1 type II receptor: a decoy target for IL-1 that is regulated by IL-4. *Science* **261**(5120):472-475.

Condon, T. V., Sawyer, R. T., Fenton, M. J. and Riches, D. W. (2011). Lung dendritic cells at the innate-adaptive immune interface. *J Leukoc Biol* **90**(5):883-895.

Conway Morris, A., Kefala, K., Wilkinson, T. S., Dhaliwal, K., Farrell, L., Walsh, T., . . . Simpson, A. J. (2009). C5a mediates peripheral blood neutrophil dysfunction in critically ill patients. *Am J Respir Crit Care Med* **180**(1):19-28.

Cook, W. J., Galakatos, N., Boyar, W. C., Walter, R. L. and Ealick, S. E. (2010). Structure of human desArg-C5a. *Acta Crystallogr D Biol Crystallogr* **66**(Pt 2):190-197.

Coulthard, L. G. and Woodruff, T. M. (2015). Is the complement activation product C3a a proinflammatory molecule? Re-evaluating the evidence and the myth. *J Immunol* **194**(8):3542-3548.

Cowland, J. B. and Borregaard, N. (2016). Granulopoiesis and granules of human neutrophils. *Immunol Rev* **273**(1):11-28.

Culley, F. J. (2009). Natural killer cells in infection and inflammation of the lung. *Immunology* **128**(2):151-163.

Culley, F. J., Fadlon, E. J., Kirchem, A., Williams, T. J., Jose, P. J. and Pease, J. E. (2003). Proteoglycans are potent modulators of the biological responses of eosinophils to chemokines. *Eur J Immunol* **33**(5):1302-1310.

Dalle-Donne, I., Rossi, R., Giustarini, D., Milzani, A. and Colombo, R. (2003). Protein carbonyl groups as biomarkers of oxidative stress. *Clin Chim Acta* **329**(1-2):23-38.

Das, S. T., Rajagopalan, L., Guerrero-Plata, A., Sai, J., Richmond, A., Garofalo, R. P. and Rajarathnam, K. (2010). Monomeric and dimeric CXCL8 are both essential for in vivo neutrophil recruitment. *PLoS One* **5**(7):e11754.

David, A., Fridlich, R. and Aviram, I. (2005). The presence of membrane Proteinase 3 in neutrophil lipid rafts and its colocalization with FcγRIIIb and cytochrome b558. *Exp Cell Res* **308**(1):156-165.

Davies, J. R., Svitacheva, N., Lannefors, L., Kornfalt, R. and Carlstedt, I. (1999). Identification of MUC5B, MUC5AC and small amounts of MUC2 mucins in cystic fibrosis airway secretions. *Biochem J* **344 Pt 2**:321-330.

de Benedictis, F. M. and Bush, A. (2012). Corticosteroids in respiratory diseases in children. *Am J Respir Crit Care Med* **185**(1):12-23.

de Blic, J., Midulla, F., Barbato, A., Clement, A., Dab, I., Eber, E., . . . Rossi, G. (2000). Bronchoalveolar lavage in children. ERS Task Force on bronchoalveolar lavage in children. European Respiratory Society. *Eur Respir J* **15**(1):217-231.

de Cordoba, S. R. and de Jorge, E. G. (2008). Translational mini-review series on complement factor H: genetics and disease associations of human complement factor H. *Clin Exp Immunol* **151**(1):1-13.

- de Cordoba, S. R., Tortajada, A., Harris, C. L. and Morgan, B. P. (2012). Complement dysregulation and disease: from genes and proteins to diagnostics and drugs. *Immunobiology* **217**(11):1034-1046.
- de Koning, L., Liptak, C., Shkreta, A., Bradwin, G., Hu, F. B., Pradhan, A. D., . . . Kellogg, M. D. (2012). A multiplex immunoassay gives different results than singleplex immunoassays which may bias epidemiologic associations. *Clin Biochem* **45**(10-11):848-851.
- de Vrankrijker, A. M., Wolfs, T. F. and van der Ent, C. K. (2010). Challenging and emerging pathogens in cystic fibrosis. *Paediatr Respir Rev* **11**(4):246-254.
- Dean, T. P., Dai, Y., Shute, J. K., Church, M. K. and Warner, J. O. (1993). Interleukin-8 concentrations are elevated in bronchoalveolar lavage, sputum, and sera of children with cystic fibrosis. *Pediatr Res* **34**(2):159-161.
- Defea, K. (2008). Beta-arrestins and heterotrimeric G-proteins: collaborators and competitors in signal transduction. *Br J Pharmacol* **153 Suppl 1**:S298-309.
- Delano, M. J. and Ward, P. A. (2016). Sepsis-induced immune dysfunction: can immune therapies reduce mortality? *J Clin Invest* **126**(1):23-31.
- Desai, A. P., Stanley, T., Atuan, M., McKey, J., Lipuma, J. J., Rogers, B. and Jerris, R. (2012). Use of matrix assisted laser desorption ionisation-time of flight mass spectrometry in a paediatric clinical laboratory for identification of bacteria commonly isolated from cystic fibrosis patients. *J Clin Pathol* **65**(9):835-838.
- Devaney, J. M., Greene, C. M., Taggart, C. C., Carroll, T. P., O'Neill, S. J. and McElvaney, N. G. (2003). Neutrophil elastase up-regulates interleukin-8 via toll-like receptor 4. *FEBS Lett* **544**(1-3):129-132.
- Di, A., Brown, M. E., Deriy, L. V., Li, C., Szeto, F. L., Chen, Y., . . . Nelson, D. J. (2006). CFTR regulates phagosome acidification in macrophages and alters bactericidal activity. *Nat Cell Biol* **8**(9):933-944.
- Di Pietro, C., Zhang, P. X., O'Rourke, T. K., Murray, T. S., Wang, L., Britto, C. J., . . . Bruscia, E. M. (2017). Ezrin links CFTR to TLR4 signaling to orchestrate anti-bacterial immune response in macrophages. *Sci Rep* **7**(1):e10882.
- Dillard, P., Wetsel, R. A. and Drouin, S. M. (2007). Complement C3a regulates Muc5ac expression by airway Clara cells independently of Th2 responses. *Am J Respir Crit Care Med* **175**(12):1250-1258.
- Dinarello, C. A. (2018). Overview of the IL-1 family in innate inflammation and acquired immunity. *Immunol Rev* **281**(1):8-27.

Dittrich, A. S., Kuhbandner, I., Gehrig, S., Rickert-Zacharias, V., Twigg, M., Wege, S., . . . Mall, M. A. (2018). Elastase activity on sputum neutrophils correlates with severity of lung disease in cystic fibrosis. *Eur Respir J* **51**(3): 170-191

Donaldson, S. H. and Boucher, R. C. (2007). Sodium channels and cystic fibrosis. *Chest* **132**(5):1631-1636.

Doni, A., Garlanda, C. and Mantovani, A. (2016). Innate immunity, hemostasis and matrix remodeling: PTX3 as a link. *Semin Immunol* **28**(6):570-577.

Doring, G., Bragonzi, A., Paroni, M., Akturk, F. F., Cigana, C., Schmidt, A., . . . Ulrich, M. (2014). BIL284 reduces neutrophil numbers but increases *P. aeruginosa* bacteremia and inflammation in mouse lungs. *J Cyst Fibros* **13**(2):156-163.

Dri, P., Haas, E., Cramer, R., Menegazzi, R., Gasparini, C., Martinelli, R., . . . Patriarca, P. (1999). Role of the 75-kDa TNF receptor in TNF-induced activation of neutrophil respiratory burst. *J Immunol* **162**(1):460-466.

du Bois, R. M., Bernaudin, J. F., Paakko, P., Hubbard, R., Takahashi, H., Ferrans, V. and Crystal, R. G. (1991). Human neutrophils express the alpha 1-antitrypsin gene and produce alpha 1-antitrypsin. *Blood* **77**(12):2724-2730.

Durstin, M., Gao, J. L., Tiffany, H. L., McDermott, D. and Murphy, P. M. (1994). Differential expression of members of the N-formylpeptide receptor gene cluster in human phagocytes. *Biochem Biophys Res Commun* **201**(1):174-179.

Duvoix, A., Mackay, R. M., Henderson, N., McGreal, E., Postle, A., Reid, K. and Clark, H. (2011). Physiological concentration of calcium inhibits elastase-induced cleavage of a functional recombinant fragment of surfactant protein D. *Immunobiology* **216**(1-2):72-79.

Dyer, D. P., Salanga, C. L., Johns, S. C., Valdambrini, E., Fuster, M. M., Milner, C. M., . . . Handel, T. M. (2016a). The Anti-inflammatory Protein TSG-6 Regulates Chemokine Function by Inhibiting Chemokine/Glycosaminoglycan Interactions. *J Biol Chem* **291**(24):12627-12640.

Dyer, D. P., Salanga, C. L., Volkman, B. F., Kawamura, T. and Handel, T. M. (2016b). The dependence of chemokine-glycosaminoglycan interactions on chemokine oligomerization. *Glycobiology* **26**(3):312-326.

El-Benna, J., Hurtado-Nedelec, M., Marzaioli, V., Marie, J. C., Gougerot-Pocidallo, M. A. and Dang, P. M. (2016). Priming of the neutrophil respiratory burst: role in host defense and inflammation. *Immunol Rev* **273**(1):180-193.

Elborn, J. S. (2016). Cystic fibrosis. *Lancet* **388**(10059):2519-2531.

Elborn, J. S., Ramsey, B. W., Boyle, M. P., Konstan, M. W., Huang, X., Marigowda, G., . . . Wainwright, C. E. (2016). Efficacy and safety of lumacaftor/ivacaftor combination therapy in

patients with cystic fibrosis homozygous for Phe508del CFTR by pulmonary function subgroup: a pooled analysis. *Lancet Respir Med* **4**(8):617-626.

Ellis, T. N. and Beaman, B. L. (2004). Interferon-gamma activation of polymorphonuclear neutrophil function. *Immunology* **112**(1):2-12.

Eltboli, O., Bafadhel, M., Hollins, F., Wright, A., Hargadon, B., Kulkarni, N. and Brightling, C. (2014). COPD exacerbation severity and frequency is associated with impaired macrophage efferocytosis of eosinophils. *BMC Pulm Med* **14**:112.

Ember, J. A., Johansen, N. L. and Hugli, T. E. (1991). Designing synthetic superagonists of C3a anaphylatoxin. *Biochemistry* **30**(15):3603-3612.

Engelke, C., Wiese, A. V., Schmutde, I., Ender, F., Strover, H. A., Vollbrandt, T., . . . Kohl, J. (2014). Distinct roles of the anaphylatoxins C3a and C5a in dendritic cell-mediated allergic asthma. *J Immunol* **193**(11):5387-5401.

Equi, A. C., Pike, S. E., Davies, J. and Bush, A. (2001). Use of cough swabs in a cystic fibrosis clinic. *Arch Dis Child* **85**(5):438-439.

Esther, C. R., Jr., Hill, D. B., Button, B., Shi, S., Jania, C., Duncan, E. A., . . . Boucher, R. C. (2017). Sialic acid-to-urea ratio as a measure of airway surface hydration. *Am J Physiol Lung Cell Mol Physiol* **312**(3):L398-L404.

Fajac, I. and De Boeck, K. (2017). New horizons for cystic fibrosis treatment. *Pharmacol Ther* **170**:205-211.

Farrar, C. A., Tran, D., Li, K., Wu, W., Peng, Q., Schwaeble, W., . . . Sacks, S. H. (2016). Collectin-11 detects stress-induced L-fucose pattern to trigger renal epithelial injury. *J Clin Invest* **126**(5):1911-1925.

Feinberg, H., Jegouzo, S. A. F., Rex, M. J., Drickamer, K., Weis, W. I. and Taylor, M. E. (2017). Mechanism of pathogen recognition by human dectin-2. *J Biol Chem* **292**(32):13402-13414.

Felton, J. M., Lucas, C. D., Rossi, A. G. and Dransfield, I. (2014). Eosinophils in the lung - modulating apoptosis and efferocytosis in airway inflammation. *Front Immunol* **5**:302.

Fernandez, H. N. and Hugli, T. E. (1976). Partial characterization of human C5a anaphylatoxin. I. Chemical description of the carbohydrate and polypeptide portions of human C5a. *J Immunol* **117**(5 Pt 1):1688-1694.

Fiala, G. J., Schamel, W. W. and Blumenthal, B. (2011). Blue native polyacrylamide gel electrophoresis (BN-PAGE) for analysis of multiprotein complexes from cellular lysates. *J Vis Exp* **48**: e2164

- Fick, R. B., Jr., Robbins, R. A., Squier, S. U., Schoderbek, W. E. and Russ, W. D. (1986). Complement activation in cystic fibrosis respiratory fluids: in vivo and in vitro generation of C5a and chemotactic activity. *Pediatr Res* **20**(12):1258-1268.
- Fiore, S., Maddox, J. F., Perez, H. D. and Serhan, C. N. (1994). Identification of a human cDNA encoding a functional high affinity lipoxin A4 receptor. *J Exp Med* **180**(1):253-260.
- Fisette, A., Munkonda, M. N., Oikonomopoulou, K., Paglialunga, S., Lambris, J. D. and Cianflone, K. (2013). C5L2 receptor disruption enhances the development of diet-induced insulin resistance in mice. *Immunobiology* **218**(1):127-133.
- Fogarty, A. W., Britton, J., Clayton, A. and Smyth, A. R. (2012). Are measures of body habitus associated with mortality in cystic fibrosis? *Chest* **142**(3):712-717.
- Foley, J. H. (2016). Examining coagulation-complement crosstalk: complement activation and thrombosis. *Thromb Res* **141 Suppl 2**:S50-54.
- Foley, J. H., Walton, B. L., Aleman, M. M., O'Byrne, A. M., Lei, V., Harrasser, M., . . . Conway, E. M. (2016). Complement Activation in Arterial and Venous Thrombosis is Mediated by Plasmin. *EBioMedicine* **5**:175-182.
- Fortin, C. F., Ear, T. and McDonald, P. P. (2009). Autocrine role of endogenous interleukin-18 on inflammatory cytokine generation by human neutrophils. *Faseb j* **23**(1):194-203.
- Forton, J. (2015). Induced sputum in young healthy children with cystic fibrosis. *Paediatr Respir Rev* **16 Suppl 1**:6-8.
- Freeman, S. A. and Grinstein, S. (2014). Phagocytosis: receptors, signal integration, and the cytoskeleton. *Immunol Rev* **262**(1):193-215.
- Frost, F., Dyce, P., Nazareth, D., Malone, V. and Walshaw, M. J. (2018). Continuous glucose monitoring guided insulin therapy is associated with improved clinical outcomes in cystic fibrosis-related diabetes. *J Cyst Fibros* **1**(1): 798-803.
- Fuchs, T. A., Abed, U., Goosmann, C., Hurwitz, R., Schulze, I., Wahn, V., . . . Zychlinsky, A. (2007). Novel cell death program leads to neutrophil extracellular traps. *J Cell Biol* **176**(2):231-241.
- Fujinaga, M., Chernaia, M. M., Halenbeck, R., Koths, K. and James, M. N. (1996). The crystal structure of PR3, a neutrophil serine proteinase antigen of Wegener's granulomatosis antibodies. *J Mol Biol* **261**(2):267-278.
- Fujiwara, A., Taguchi, O., Takagi, T., D'Alessandro-Gabazza, C. N., Boveda-Ruiz, D., Toda, M., . . . Gabazza, E. C. (2012). Role of thrombin-activatable fibrinolysis inhibitor in allergic bronchial asthma. *Lung* **190**(2):189-198.

Fukuoka, Y., Xia, H. Z., Sanchez-Munoz, L. B., Dellinger, A. L., Escribano, L. and Schwartz, L. B. (2008). Generation of anaphylatoxins by human beta-tryptase from C3, C4, and C5. *J Immunol* **180**(9):6307-6316.

Fukuzawa, T., Sampei, Z., Haraya, K., Ruike, Y., Shida-Kawazoe, M., Shimizu, Y., . . . Nezu, J. (2017). Long lasting neutralization of C5 by SKY59, a novel recycling antibody, is a potential therapy for complement-mediated diseases. *Sci Rep* **7**(1):1080.

Fumagalli, L., Zhang, H., Baruzzi, A., Lowell, C. A. and Berton, G. (2007). The Src family kinases Hck and Fgr regulate neutrophil responses to N-formyl-methionyl-leucyl-phenylalanine. *J Immunol* **178**(6):3874-3885.

Furnari, M. L., Termini, L., Traverso, G., Barrale, S., Bonaccorso, M. R., Damiani, G., . . . Collura, M. (2012). Nebulized hypertonic saline containing hyaluronic acid improves tolerability in patients with cystic fibrosis and lung disease compared with nebulized hypertonic saline alone: a prospective, randomized, double-blind, controlled study. *Thorax* **67**(6):315-322.

Futosi, K., Fodor, S. and Mocsai, A. (2013). Reprint of Neutrophil cell surface receptors and their intracellular signal transduction pathways. *Int Immunopharmacol* **17**(4):1185-1197.

Gallagher, R., Collins, S., Trujillo, J., McCredie, K., Ahearn, M., Tsai, S., . . . Gallo, R. (1979). Characterization of the continuous, differentiating myeloid cell line (HL-60) from a patient with acute promyelocytic leukemia. *Blood* **54**(3):713-733.

Gangavarapu, P., Rajagopalan, L., Kolli, D., Guerrero-Plata, A., Garofalo, R. P. and Rajarathnam, K. (2012). The monomer-dimer equilibrium and glycosaminoglycan interactions of chemokine CXCL8 regulate tissue-specific neutrophil recruitment. *J Leukoc Biol* **91**(2):259-265.

Garantziotis, S., Brezina, M., Castelnovo, P. and Drago, L. (2016). The role of hyaluronan in the pathobiology and treatment of respiratory disease. *Am J Physiol Lung Cell Mol Physiol*:ajplung.00168.02015.

Gazi, U. and Martinez-Pomares, L. (2009). Influence of the mannose receptor in host immune responses. *Immunobiology* **214**(7):554-561.

Gaziano, R., Bozza, S., Bellocchio, S., Perruccio, K., Montagnoli, C., Pitzurra, L., . . . Romani, L. (2004). Anti-*Aspergillus fumigatus* efficacy of pentraxin 3 alone and in combination with antifungals. *Antimicrob Agents Chemother* **48**(11):4414-4421.

Geering, B. and Simon, H. U. (2011). Peculiarities of cell death mechanisms in neutrophils. *Cell Death Differ* **18**(9):1457-1469.

Gerard, C. and Hugli, T. E. (1981). Identification of classical anaphylatoxin as the des-Arg form of the C5a molecule: evidence of a modulator role for the oligosaccharide unit in human des-Arg74-C5a. *Proc Natl Acad Sci U S A* **78**(3):1833-1837.

Gerber, N., Lowman, H., Artis, D. R. and Eigenbrot, C. (2000). Receptor-binding conformation of the "ELR" motif of IL-8: X-ray structure of the L5C/H33C variant at 2.35 Å resolution. *Proteins* **38**(4):361-367.

Gernez, Y., Walters, J., Mirkovic, B., Lavelle, G. M., Colleen, D. E., Davies, Z. A., . . . Moss, R. B. (2016). Blood basophil activation is a reliable biomarker of allergic bronchopulmonary aspergillosis in cystic fibrosis. *Eur Respir J* **47**(1):177-185.

Gharib, S. A., Vaisar, T., Aitken, M. L., Park, D. R., Heinecke, J. W. and Fu, X. (2009). Mapping the lung proteome in cystic fibrosis. *J Proteome Res* **8**(6):3020-3028.

Giacomelli, S., Melillo, D., Lambris, J. D. and Pinto, M. R. (2012). Immune competence of the *Ciona intestinalis* pharynx: complement system-mediated activity. *Fish Shellfish Immunol* **33**(4):946-952.

Giles, J. L., Choy, E., van den Berg, C., Morgan, B. P. and Harris, C. L. (2015). Functional analysis of a complement polymorphism (rs17611) associated with rheumatoid arthritis. *J Immunol* **194**(7):3029-3034.

Goldstein, I. M. and Weissmann, G. (1974). Generation of C5-derived lysosomal enzyme-releasing activity (C5a) by lysates of leukocyte lysosomes. *J Immunol* **113**(5):1583-1588.

Governa, M., Amati, M., Valentino, M., Visona, I., Fubini, B., Botta, G. C., . . . Carmignani, M. (2000). In vitro cleavage by asbestos fibers of the fifth component of human complement through free-radical generation and kallikrein activation. *J Toxicol Environ Health A* **59**(7):539-552.

Grailer, J. J., Canning, B. A., Kalbitz, M., Haggadone, M. D., Dhond, R. M., Andjelkovic, A. V., . . . Ward, P. A. (2014). Critical role for the NLRP3 inflammasome during acute lung injury. *J Immunol* **192**(12):5974-5983.

Greally, P., Hussein, M. J., Cook, A. J., Sampson, A. P., Piper, P. J. and Price, J. F. (1993). Sputum tumour necrosis factor- α and leukotriene concentrations in cystic fibrosis. *Arch Dis Child* **68**(3):389-392.

Greenlee-Wacker, M. C. (2016). Clearance of apoptotic neutrophils and resolution of inflammation. *Immunol Rev* **273**(1):357-370.

Griffith, J. W., Sokol, C. L. and Luster, A. D. (2014). Chemokines and chemokine receptors: positioning cells for host defense and immunity. *Annu Rev Immunol* **32**:659-702.

Griffiths, J. S., Thompson, A., Stott, M., Benny, A., Lewis, N. A., Taylor, P. R., . . . McGreal, E. P. (2018). Differential susceptibility of Dectin-1 isoforms to functional inactivation by neutrophil and fungal proteases. *Faseb j*:201701145R.

Gross, O., Gewies, A., Finger, K., Schafer, M., Sparwasser, T., Peschel, C., . . . Ruland, J. (2006). Card9 controls a non-TLR signalling pathway for innate anti-fungal immunity. *Nature* **442**(7103):651-656.

Gutierrez, J. P., Grimwood, K., Armstrong, D. S., Carlin, J. B., Carzino, R., Olinsky, A., . . . Phelan, P. D. (2001). Interlobar differences in bronchoalveolar lavage fluid from children with cystic fibrosis. *Eur Respir J* **17**(2):281-286.

Guyot, N., Bergsson, G., Butler, M. W., Greene, C. M., Weldon, S., Kessler, E., . . . McElvaney, N. G. (2010). Functional study of elafin cleaved by *Pseudomonas aeruginosa* metalloproteinases. *Biol Chem* **391**(6):705-716.

Guyot, N., Butler, M. W., McNally, P., Weldon, S., Greene, C. M., Levine, R. L., . . . McElvaney, N. G. (2008). Elafin, an elastase-specific inhibitor, is cleaved by its cognate enzyme neutrophil elastase in sputum from individuals with cystic fibrosis. *J Biol Chem* **283**(47):32377-32385.

Hair, P. S., Sass, L. A., Vazifedan, T., Shah, T. A., Krishna, N. K. and Cunnion, K. M. (2017). Complement effectors, C5a and C3a, in cystic fibrosis lung fluid correlate with disease severity. *PLoS One* **12**(3):e0173257.

Hajishengallis, G., Reis, E. S., Mastellos, D. C., Ricklin, D. and Lambris, J. D. (2017). Novel mechanisms and functions of complement. *Nat Immunol* **18**(12):1288-1298.

Hakobyan, S., Luppe, S., Evans, D. R., Harding, K., Loveless, S., Robertson, N. P. and Morgan, B. P. (2017). Plasma complement biomarkers distinguish multiple sclerosis and neuromyelitis optica spectrum disorder. *Mult Scler* **23**(7):946-955.

Hamon, Y., Jaillon, S., Person, C., Ginies, J. L., Garo, E., Bottazzi, B., . . . Delneste, Y. (2013). Proteolytic cleavage of the long pentraxin PTX3 in the airways of cystic fibrosis patients. *Innate Immun* **19**(6):611-622.

Haq, I. J., Gray, M. A., Garnett, J. P., Ward, C. and Brodlie, M. (2016). Airway surface liquid homeostasis in cystic fibrosis: pathophysiology and therapeutic targets. *Thorax* **71**(3):284-287.

Harris, C. L., Heurich, M., Rodriguez de Cordoba, S. and Morgan, B. P. (2012). The complotype: dictating risk for inflammation and infection. *Trends Immunol* **33**(10):513-521.

Harris, J. L., Backes, B. J., Leonetti, F., Mahrus, S., Ellman, J. A. and Craik, C. S. (2000). Rapid and general profiling of protease specificity by using combinatorial fluorogenic substrate libraries. *Proc Natl Acad Sci U S A* **97**(14):7754-7759.

Hartl, D., Gaggar, A., Bruscia, E., Hector, A., Marcos, V., Jung, A., . . . Doring, G. (2012). Innate immunity in cystic fibrosis lung disease. *J Cyst Fibros* **11**(5):363-382.

- Hartl, D., Griese, M., Kappler, M., Zissel, G., Reinhardt, D., Rebhan, C., . . . Krauss-Etschmann, S. (2006). Pulmonary T(H)2 response in *Pseudomonas aeruginosa*-infected patients with cystic fibrosis. *J Allergy Clin Immunol* **117**(1):204-211.
- Hasegawa, K., Tamari, M., Shao, C., Shimizu, M., Takahashi, N., Mao, X. Q., . . . Suzuki, Y. (2004). Variations in the C3, C3a receptor, and C5 genes affect susceptibility to bronchial asthma. *Hum Genet* **115**(4):295-301.
- Hawthornth, O. A., Coulthard, L. G., Mantovani, S. and Woodruff, T. M. (2018). Complement in stem cells and development. *Semin Immunol* **37**:74-84.
- Hayashi, F., Means, T. K. and Luster, A. D. (2003). Toll-like receptors stimulate human neutrophil function. *Blood* **102**(7):2660-2669.
- Hebert, C. A., Vitangcol, R. V. and Baker, J. B. (1991). Scanning mutagenesis of interleukin-8 identifies a cluster of residues required for receptor binding. *J Biol Chem* **266**(28):18989-18994.
- Heit, B., Tavener, S., Raharjo, E. and Kubes, P. (2002). An intracellular signaling hierarchy determines direction of migration in opposing chemotactic gradients. *J Cell Biol* **159**(1):91-102.
- Hentschel, J., Fischer, N., Janhsen, W. K., Markert, U. R., Lehmann, T., Sonnemann, J., . . . Mainz, J. G. (2015). Protease-antiprotease imbalances differ between Cystic Fibrosis patients' upper and lower airway secretions. *J Cyst Fibros* **14**(3):324-333.
- Hepburn, N. J., Williams, A. S., Nunn, M. A., Chamberlain-Banoub, J. C., Hamer, J., Morgan, B. P. and Harris, C. L. (2007). In vivo characterization and therapeutic efficacy of a C5-specific inhibitor from the soft tick *Ornithodoros moubata*. *J Biol Chem* **282**(11):8292-8299.
- Hetland, G., Johnson, E. and Aasebo, U. (1986). Human alveolar macrophages synthesize the functional alternative pathway of complement and active C5 and C9 in vitro. *Scand J Immunol* **24**(5):603-608.
- Hidalgo, A., Peired, A. J., Wild, M., Vestweber, D. and Frenette, P. S. (2007). Complete identification of E-selectin ligands on neutrophils reveals distinct functions of PSGL-1, ESL-1, and CD44. *Immunity* **26**(4):477-489.
- Hillmen, P., Young, N. S., Schubert, J., Brodsky, R. A., Socie, G., Muus, P., . . . Luzzatto, L. (2006). The complement inhibitor eculizumab in paroxysmal nocturnal hemoglobinuria. *N Engl J Med* **355**(12):1233-1243.
- Hoegger, M. J., Fischer, A. J., McMenimen, J. D., Ostedgaard, L. S., Tucker, A. J., Awadalla, M. A., . . . Welsh, M. J. (2014). Impaired mucus detachment disrupts mucociliary transport in a piglet model of cystic fibrosis. *Science* **345**(6198):818-822.

Hoenderdos, K. and Condliffe, A. (2013). The neutrophil in chronic obstructive pulmonary disease. *Am J Respir Cell Mol Biol* **48**(5):531-539.

Holm, S. (1979). A simple sequentially rejective multiple test procedure. *Scandinavian Journal of Statistics* **6**(2):65-70.

Hong, Q., Kuo, E., Schultz, L., Boackle, R. J. and Chang, N. S. (2007). Conformationally altered hyaluronan restricts complement classical pathway activation by binding to C1q, C1r, C1s, C2, C5 and C9, and suppresses WOX1 expression in prostate DU145 cells. *Int J Mol Med* **19**(1):173-179.

Hong, S., Beja-Glasser, V. F., Nfonoyim, B. M., Frouin, A., Li, S., Ramakrishnan, S., . . . Stevens, B. (2016). Complement and microglia mediate early synapse loss in Alzheimer mouse models. *Science* **352**(6286):712-716.

Hooshmand, M. J., Nguyen, H. X., Piltti, K. M., Benavente, F., Hong, S., Flanagan, L., . . . Anderson, A. J. (2017). Neutrophils Induce Astroglial Differentiation and Migration of Human Neural Stem Cells via C1q and C3a Synthesis. *J Immunol* **199**(3): 1069-1085.

Hopken, U. E., Lu, B., Gerard, N. P. and Gerard, C. (1996). The C5a chemoattractant receptor mediates mucosal defence to infection. *Nature* **383**(6595):86-89.

Hovingh, E. S., van den Broek, B. and Jongerius, I. (2016). Hijacking Complement Regulatory Proteins for Bacterial Immune Evasion. *Front Microbiol* **7**:2004.

Huber-Lang, M., Barratt-Due, A., Pischke, S. E., Sandanger, O., Nilsson, P. H., Nunn, M. A., . . . Mollnes, T. E. (2014). Double blockade of CD14 and complement C5 abolishes the cytokine storm and improves morbidity and survival in polymicrobial sepsis in mice. *J Immunol* **192**(11):5324-5331.

Huber-Lang, M., Denk, S., Fulda, S., Erler, E., Kalbitz, M., Weckbach, S., . . . Perl, M. (2012). Cathepsin D is released after severe tissue trauma in vivo and is capable of generating C5a in vitro. *Mol Immunol* **50**(1-2):60-65.

Huber-Lang, M., Sarma, J. V., Zetoune, F. S., Rittirsch, D., Neff, T. A., McGuire, S. R., . . . Ward, P. A. (2006). Generation of C5a in the absence of C3: a new complement activation pathway. *Nat Med* **12**(6):682-687.

Huber-Lang, M., Younkin, E. M., Sarma, J. V., Riedemann, N., McGuire, S. R., Lu, K. T., . . . Ward, P. A. (2002). Generation of C5a by phagocytic cells. *Am J Pathol* **161**(5):1849-1859.

Huey, R., Erickson, B. W., Bloor, C. M. and Hugli, T. E. (1984). Contraction of guinea pig lung by synthetic oligopeptides related to human C3a. *Immunopharmacology* **8**(1):37-45.

Hughes, C. E., Pollitt, A. Y., Mori, J., Eble, J. A., Tomlinson, M. G., Hartwig, J. H., . . . Watson, S. P. (2010). CLEC-2 activates Syk through dimerization. *Blood* **115**(14):2947-2955.

Humbles, A. A., Lu, B., Nilsson, C. A., Lilly, C., Israel, E., Fujiwara, Y., . . . Gerard, C. (2000). A role for the C3a anaphylatoxin receptor in the effector phase of asthma. *Nature* **406**(6799):998-1001.

Humphries, D. E., Sullivan, B. M., Aleixo, M. D. and Stow, J. L. (1997). Localization of human heparan glucosaminyl N-deacetylase/N-sulphotransferase to the trans-Golgi network. *Biochem J* **325** (Pt 2):351-357.

Hunniger, K., Bieber, K., Martin, R., Lehnert, T., Figge, M. T., Loffler, J., . . . Kurzai, O. (2015). A second stimulus required for enhanced antifungal activity of human neutrophils in blood is provided by anaphylatoxin c5a. *J Immunol* **194**(3):1199-1210.

Hussell, T. and Bell, T. J. (2014). Alveolar macrophages: plasticity in a tissue-specific context. *Nat Rev Immunol* **14**(2):81-93.

Huttenrauch, F., Pollok-Kopp, B. and Oppermann, M. (2005). G protein-coupled receptor kinases promote phosphorylation and beta-arrestin-mediated internalization of CCR5 homo- and hetero-oligomers. *J Biol Chem* **280**(45):37503-37515.

Ibrahim, F. B., Pang, S. J. and Melendez, A. J. (2004). Anaphylatoxin signaling in human neutrophils. A key role for sphingosine kinase. *J Biol Chem* **279**(43):44802-44811.

Igawa, T., Ishii, S., Tachibana, T., Maeda, A., Higuchi, Y., Shimaoka, S., . . . Hattori, K. (2010). Antibody recycling by engineered pH-dependent antigen binding improves the duration of antigen neutralization. *Nat Biotechnol* **28**(11):1203-1207.

Irmscher, S., Doring, N., Halder, L. D., Jo, E. A. H., Kopka, I., Dunker, C., . . . Skerka, C. (2018). Kallikrein Cleaves C3 and Activates Complement. *J Innate Immun* **10**(2):94-105.

Itano, N., Sawai, T., Yoshida, M., Lenas, P., Yamada, Y., Imagawa, M., . . . Kimata, K. (1999). Three isoforms of mammalian hyaluronan synthases have distinct enzymatic properties. *J Biol Chem* **274**(35):25085-25092.

Janciauskiene, S., Wrenger, S., Immenschuh, S., Olejnicka, B., Greulich, T., Welte, T. and Chorostowska-Wynimko, J. (2018). The Multifaceted Effects of Alpha1-Antitrypsin on Neutrophil Functions. *Front Pharmacol* **9**:341.

Javaux, C., Stordeur, P., Azarkan, M., Mascart, F. and Baeyens-Volant, D. (2016). Isolation of a thiol-dependent serine protease in peanut and investigation of its role in the complement and the allergic reaction. *Mol Immunol* **75**:133-143.

Jeffrey, J. E. and Aspden, R. M. (2007). Cyclooxygenase inhibition lowers prostaglandin E2 release from articular cartilage and reduces apoptosis but not proteoglycan degradation following an impact load in vitro. *Arthritis Res Ther* **9**(6):R129.

Jensen, T. J., Loo, M. A., Pind, S., Williams, D. B., Goldberg, A. L. and Riordan, J. R. (1995). Multiple proteolytic systems, including the proteasome, contribute to CFTR processing. *Cell* **83**(1):129-135.

Jia, N., Semba, U., Nishiura, H., Kuniyasu, A., Nsiama, T. K., Nishino, N. and Yamamoto, T. (2010). Pivotal Advance: Interconversion between pure chemotactic ligands and chemoattractant/secretagogue ligands of neutrophil C5a receptor by a single amino acid substitution. *J Leukoc Biol* **87**(6):965-975.

Jones, A. W., Robinson, R., Mohamed, P., Davison, G., Izzat, H. J. and Lewis, K. E. (2016a). Impaired Blood Neutrophil Function in the Frequent Exacerbator of Chronic Obstructive Pulmonary Disease: A Proof-of-Concept Study. *Lung* **194**(6):881-887.

Jones, H. R., Robb, C. T., Perretti, M. and Rossi, A. G. (2016b). The role of neutrophils in inflammation resolution. *Semin Immunol* **28**(2):137-145.

Joosten, L. A., Netea, M. G., Fantuzzi, G., Koenders, M. I., Helsen, M. M., Sparrer, H., . . . van den Berg, W. B. (2009). Inflammatory arthritis in caspase 1 gene-deficient mice: contribution of proteinase 3 to caspase 1-independent production of bioactive interleukin-1beta. *Arthritis Rheum* **60**(12):3651-3662.

Jore, M. M., Johnson, S., Sheppard, D., Barber, N. M., Li, Y. I., Nunn, M. A., . . . Lea, S. M. (2016). Structural basis for therapeutic inhibition of complement C5. *Nat Struct Mol Biol* **23**(5):378-386.

Jose, P. J., Moss, I. K., Maini, R. N. and Williams, T. J. (1990). Measurement of the chemotactic complement fragment C5a in rheumatoid synovial fluids by radioimmunoassay: role of C5a in the acute inflammatory phase. *Ann Rheum Dis* **49**(10):747-752.

Joseph, P. R., Mosier, P. D., Desai, U. R. and Rajarathnam, K. (2015). Solution NMR characterization of chemokine CXCL8/IL-8 monomer and dimer binding to glycosaminoglycans: structural plasticity mediates differential binding interactions. *Biochem J* **472**(1):121-133.

Jung, A., Kleinau, I., Schonian, G., Bauernfeind, A., Chen, C., Griese, M., . . . Paul, K. (2002). Sequential genotyping of *Pseudomonas aeruginosa* from upper and lower airways of cystic fibrosis patients. *Eur Respir J* **20**(6):1457-1463.

Kaetzel, C. S., Robinson, J. K., Chintalacharuvu, K. R., Vaerman, J. P. and Lamm, M. E. (1991). The polymeric immunoglobulin receptor (secretory component) mediates transport of immune complexes across epithelial cells: a local defense function for IgA. *Proc Natl Acad Sci U S A* **88**(19):8796-8800.

- Karsten, C. M. and Kohl, J. (2012). The immunoglobulin, IgG Fc receptor and complement triangle in autoimmune diseases. *Immunobiology* **217**(11):1067-1079.
- Karsten, C. M., Laumonier, Y., Eurich, B., Ender, F., Broker, K., Roy, S., . . . Kohl, J. (2015). Monitoring and cell-specific deletion of C5aR1 using a novel floxed GFP-C5aR1 reporter knock-in mouse. *J Immunol* **194**(4):1841-1855.
- Karsten, C. M., Pandey, M. K., Figge, J., Kilchenstein, R., Taylor, P. R., Rosas, M., . . . Kohl, J. (2012). Anti-inflammatory activity of IgG1 mediated by Fc galactosylation and association of FcγRIIB and dectin-1. *Nat Med* **18**(9):1401-1406.
- Kauppinen, A., Paterno, J. J., Blasiak, J., Salminen, A. and Kaarniranta, K. (2016). Inflammation and its role in age-related macular degeneration. *Cell Mol Life Sci* **73**(9):1765-1786.
- Kelly, E., Greene, C. M. and McElvaney, N. G. (2008). Targeting neutrophil elastase in cystic fibrosis. *Expert Opin Ther Targets* **12**(2):145-157.
- Kerem, E., Viviani, L., Zolin, A., MacNeill, S., Hatziaorou, E., Ellemunter, H., . . . Olesen, H. (2014). Factors associated with FEV1 decline in cystic fibrosis: analysis of the ECFS patient registry. *Eur Respir J* **43**(1):125-133.
- Keshari, R. S., Silasi, R., Popescu, N. I., Patel, M. M., Chaaban, H., Lupu, C., . . . Lupu, F. (2017). Inhibition of complement C5 protects against organ failure and reduces mortality in a baboon model of Escherichia coli sepsis. *Proc Natl Acad Sci U S A*.
- Khan, M. A., Assiri, A. M. and Broering, D. C. (2015). Complement mediators: key regulators of airway tissue remodeling in asthma. *J Transl Med* **13**:272.
- Khan, M. A., Maasch, C., Vater, A., Klussmann, S., Morser, J., Leung, L. L., . . . Nicolls, M. R. (2013). Targeting complement component 5a promotes vascular integrity and limits airway remodeling. *Proc Natl Acad Sci U S A* **110**(15):6061-6066.
- Khan, M. A., Nicolls, M. R., Surguladze, B. and Saadoun, I. (2014). Complement components as potential therapeutic targets for asthma treatment. *Respir Med* **108**(4):543-549.
- Khatri, I. A., Bhaskar, K. R., Lamont, J. T., Sajjan, S. U., Ho, C. K. and Forstner, J. (2003). Effect of chondroitinase ABC on purulent sputum from cystic fibrosis and other patients. *Pediatr Res* **53**(4):619-627.
- Kidd, T. J., Ramsay, K. A., Vidmar, S., Carlin, J. B., Bell, S. C., Wainwright, C. E. and Grimwood, K. (2015). Pseudomonas aeruginosa genotypes acquired by children with cystic fibrosis by age 5-years. *J Cyst Fibros* **14**(3):361-369.
- Kim, D. and Haynes, C. L. (2012). Neutrophil chemotaxis within a competing gradient of chemoattractants. *Anal Chem* **84**(14):6070-6078.

Kim, D. and Haynes, C. L. (2013). The role of p38 MAPK in neutrophil functions: single cell chemotaxis and surface marker expression. *Analyst* **138**(22):6826-6833.

Kim, S. D., Lee, H. Y., Shim, J. W., Kim, H. J., Yoo, Y. H., Park, J. S., . . . Bae, Y. S. (2011). Activation of CXCR2 by extracellular matrix degradation product acetylated Pro-Gly-Pro has therapeutic effects against sepsis. *Am J Respir Crit Care Med* **184**(2):243-251.

Kim, S. Y., Son, M., Lee, S. E., Park, I. H., Kwak, M. S., Han, M., . . . Shin, J. S. (2018). High-Mobility Group Box 1-Induced Complement Activation Causes Sterile Inflammation. *Front Immunol* **9**:705.

Kirby, A. C., Coles, M. C. and Kaye, P. M. (2009). Alveolar macrophages transport pathogens to lung draining lymph nodes. *J Immunol* **183**(3):1983-1989.

Klos, A., Ihrig, V., Messner, M., Grabbe, J. and Bitter-Suermann, D. (1988). Detection of native human complement components C3 and C5 and their primary activation peptides C3a and C5a (anaphylatoxic peptides) by ELISAs with monoclonal antibodies. *J Immunol Methods* **111**(2):241-252.

Klos, A., Wende, E., Wareham, K. J. and Monk, P. N. (2013). International Union of Basic and Clinical Pharmacology. [corrected]. LXXXVII. Complement peptide C5a, C4a, and C3a receptors. *Pharmacol Rev* **65**(1):500-543.

Knutsen, A. P., Hutchinson, P. S., Albers, G. M., Consolino, J., Smick, J. and Kurup, V. P. (2004). Increased sensitivity to IL-4 in cystic fibrosis patients with allergic bronchopulmonary aspergillosis. *Allergy* **59**(1):81-87.

Koheil, A., Corey, M. and Forstner, G. (1979). Deficiency of serum carboxypeptidase B-like (anaphylatoxin inactivator, carboxypeptidase N) activity in sera from patients with cystic fibrosis. *Clin Invest Med* **2**(2-3):99-103.

Kohl, J., Baelder, R., Lewkowich, I. P., Pandey, M. K., Hawlisch, H., Wang, L., . . . Wills-Karp, M. (2006). A regulatory role for the C5a anaphylatoxin in type 2 immunity in asthma. *J Clin Invest* **116**(3):783-796.

Koizumi, M., Fujino, A., Fukushima, K., Kamimura, T. and Takimoto-Kamimura, M. (2008). Complex of human neutrophil elastase with 1/2SLPI. *J Synchrotron Radiat* **15**(Pt 3):308-311.

Kolb, W. P., Kolb, L. M., Wetsel, R. A., Rogers, W. R. and Shaw, J. O. (1981). Quantitation and stability of the fifth component of complement (C5) in bronchoalveolar lavage fluids obtained from non-human primates. *Am Rev Respir Dis* **123**(2):226-231.

Koller, B., Bals, R., Roos, D., Korting, H. C., Griese, M. and Hartl, D. (2009). Innate immune receptors on neutrophils and their role in chronic lung disease. *Eur J Clin Invest* **39**(7):535-547.

- Koller, B., Kappler, M., Latzin, P., Gaggar, A., Schreiner, M., Takyar, S., . . . Hartl, D. (2008). TLR expression on neutrophils at the pulmonary site of infection: TLR1/TLR2-mediated up-regulation of TLR5 expression in cystic fibrosis lung disease. *J Immunol* **181**(4):2753-2763.
- Koller, D. Y., Gotz, M., Eichler, I. and Urbanek, R. (1994). Eosinophilic activation in cystic fibrosis. *Thorax* **49**(5):496-499.
- Konstan, M. W., Doring, G., Heltshe, S. L., Lands, L. C., Hilliard, K. A., Koker, P., . . . Hamilton, A. (2014). A randomized double blind, placebo controlled phase 2 trial of BIIL 284 BS (an LTB4 receptor antagonist) for the treatment of lung disease in children and adults with cystic fibrosis. *J Cyst Fibros* **13**(2):148-155.
- Konstan, M. W., Hilliard, K. A., Norvell, T. M. and Berger, M. (1994). Bronchoalveolar lavage findings in cystic fibrosis patients with stable, clinically mild lung disease suggest ongoing infection and inflammation. *Am J Respir Crit Care Med* **150**(2):448-454.
- Konstan, M. W. and Ratjen, F. (2012). Effect of dornase alfa on inflammation and lung function: potential role in the early treatment of cystic fibrosis. *J Cyst Fibros* **11**(2):78-83.
- Konstan, M. W., Schluchter, M. D., Xue, W. and Davis, P. B. (2007). Clinical use of Ibuprofen is associated with slower FEV1 decline in children with cystic fibrosis. *Am J Respir Crit Care Med* **176**(11):1084-1089.
- Konstan, M. W., Walenga, R. W., Hilliard, K. A. and Hilliard, J. B. (1993). Leukotriene B4 markedly elevated in the epithelial lining fluid of patients with cystic fibrosis. *Am Rev Respir Dis* **148**(4 Pt 1):896-901.
- Kopczynska, M., Zelek, W., Touchard, S., Gaughran, F., Di Forti, M., Mondelli, V., . . . Morgan, B. P. (2017). Complement system biomarkers in first episode psychosis. *Schizophr Res.*
- Kopczynska, M., Zelek, W. M., Vespa, S., Touchard, S., Wardle, M., Loveless, S., . . . Morgan, B. P. (2018). Complement system biomarkers in epilepsy. *Seizure* **60**:1-7.
- Korkmaz, B., Horwitz, M. S., Jenne, D. E. and Gauthier, F. (2010). Neutrophil elastase, proteinase 3, and cathepsin G as therapeutic targets in human diseases. *Pharmacol Rev* **62**(4):726-759.
- Kotecha, S., Doull, I., Davies, P., McKenzie, Z., Madsen, J., Clark, H. W. and McGreal, E. P. (2013). Functional heterogeneity of pulmonary surfactant protein-D in cystic fibrosis. *Biochim Biophys Acta* **1832**(12):2391-2400.
- Kovacs, A., Szabo, L., Longstaff, C., Tenekedjiev, K., Machovich, R. and Kolev, K. (2014). Ambivalent roles of carboxypeptidase B in the lytic susceptibility of fibrin. *Thromb Res* **133**(1):80-87.

Kreda, S. M., Davis, C. W. and Rose, M. C. (2012). CFTR, mucins, and mucus obstruction in cystic fibrosis. *Cold Spring Harb Perspect Med* **2**(9):a009589.

Krieger, E., Geretti, E., Brandner, B., Goger, B., Wells, T. N. and Kungl, A. J. (2004). A structural and dynamic model for the interaction of interleukin-8 and glycosaminoglycans: support from isothermal fluorescence titrations. *Proteins* **54**(4):768-775.

Krug, N., Tschernig, T., Erpenbeck, V. J., Hohlfeld, J. M. and Kohl, J. (2001). Complement factors C3a and C5a are increased in bronchoalveolar lavage fluid after segmental allergen provocation in subjects with asthma. *Am J Respir Crit Care Med* **164**(10 Pt 1):1841-1843.

Kruger, P., Saffarzadeh, M., Weber, A. N., Rieber, N., Radsak, M., von Bernuth, H., . . . Hartl, D. (2015). Neutrophils: Between host defence, immune modulation, and tissue injury. *PLoS Pathog* **11**(3):e1004651.

Ku, C. J., Wang, Y., Weiner, O. D., Altschuler, S. J. and Wu, L. F. (2012). Network crosstalk dynamically changes during neutrophil polarization. *Cell* **149**(5):1073-1083.

Kuckleburg, C. J. and Newman, P. J. (2013). Neutrophil proteinase 3 acts on protease-activated receptor-2 to enhance vascular endothelial cell barrier function. *Arterioscler Thromb Vasc Biol* **33**(2):275-284.

Kurimoto, E., Miyahara, N., Kanehiro, A., Waseda, K., Taniguchi, A., Ikeda, G., . . . Tanimoto, M. (2013). IL-17A is essential to the development of elastase-induced pulmonary inflammation and emphysema in mice. *Respir Res* **14**:5: e5.

Kuroda, H., Fujihara, K., Takano, R., Takai, Y., Takahashi, T., Misu, T., . . . Aoki, M. (2013). Increase of complement fragment C5a in cerebrospinal fluid during exacerbation of neuromyelitis optica. *J Neuroimmunol* **254**(1-2):178-182.

Kurreeman, F. A., Padyukov, L., Marques, R. B., Schrodi, S. J., Seddighzadeh, M., Stoeken-Rijsbergen, G., . . . Toes, R. E. (2007). A candidate gene approach identifies the TRAF1/C5 region as a risk factor for rheumatoid arthritis. *PLoS Med* **4**(9):e278.

Kuschert, G. S., Coulin, F., Power, C. A., Proudfoot, A. E., Hubbard, R. E., Hoogewerf, A. J. and Wells, T. N. (1999). Glycosaminoglycans interact selectively with chemokines and modulate receptor binding and cellular responses. *Biochemistry* **38**(39):12959-12968.

Lai, H. C., FitzSimmons, S. C., Allen, D. B., Kosorok, M. R., Rosenstein, B. J., Campbell, P. W. and Farrell, P. M. (2000). Risk of persistent growth impairment after alternate-day prednisone treatment in children with cystic fibrosis. *N Engl J Med* **342**(12):851-859.

Lambrecht, B. N. and Hammad, H. (2015). The immunology of asthma. *Nat Immunol* **16**(1):45-56.

Lamkanfi, M. (2011). Emerging inflammasome effector mechanisms. In: *Nat Rev Immunol*. Vol. 11. England, pp. 213-220.

- Lämmerman, T. (2015). In the eye of the neutrophil swarm-navigation signals that bring neutrophils together in inflamed and infected tissues. *J Leukoc Biol* **100**(1): 55-63
- Laumonier, Y., Wiese, A. V., Figge, J. and Karsten, C. (2017). Regulation and function of anaphylatoxins and their receptors in allergic asthma. *Mol Immunol* **84**:51-56.
- Lavelle, G. M., White, M. M., Browne, N., McElvaney, N. G. and Reeves, E. P. (2016). Animal Models of Cystic Fibrosis Pathology: Phenotypic Parallels and Divergences. *Biomed Res Int* **1**: 1-14.
- Lawrence, R. H. and Sorrelli, T. C. (1992). Decreased polymorphonuclear leucocyte chemotactic response to leukotriene B4 in cystic fibrosis. *Clin Exp Immunol* **89**(2):321-324.
- Le Bourgeois, M., Goncalves, M., Le Clainche, L., Benoist, M. R., Fournet, J. C., Scheinmann, P. and de Blic, J. (2002). Bronchoalveolar cells in children < 3 years old with severe recurrent wheezing. *Chest* **122**(3):791-797.
- Le Cabec, V., Calafat, J. and Borregaard, N. (1997). Sorting of the specific granule protein, NGAL, during granulocytic maturation of HL-60 cells. *Blood* **89**(6):2113-2121.
- Le, Y., Murphy, P. M. and Wang, J. M. (2002). Formyl-peptide receptors revisited. *Trends Immunol* **23**(11):541-548.
- Leavell, K. J., Peterson, M. W. and Gross, T. J. (1997). Human neutrophil elastase abolishes interleukin-8 chemotactic activity. *J Leukoc Biol* **61**(3):361-366.
- Lee, J. S., Frevert, C. W., Thorning, D. R., Segerer, S., Alpers, C. E., Cartron, J. P., . . . Goodman, R. B. (2003). Enhanced expression of Duffy antigen in the lungs during suppurative pneumonia. *J Histochem Cytochem* **51**(2):159-166.
- Leffler, J., Bengtsson, A. A. and Blom, A. M. (2014). The complement system in systemic lupus erythematosus: an update. *Ann Rheum Dis* **73**(9):1601-1606.
- LeGrys, V. A., Yankaskas, J. R., Quittell, L. M., Marshall, B. C. and Mogayzel, P. J., Jr. (2007). Diagnostic sweat testing: the Cystic Fibrosis Foundation guidelines. *J Pediatr* **151**(1):85-89.
- Lehman, N., Di Fulvio, M., McCray, N., Campos, I., Tabatabaian, F. and Gomez-Cambronero, J. (2006). Phagocyte cell migration is mediated by phospholipases PLD1 and PLD2. *Blood* **108**(10):3564-3572.
- Lekstrom-Himes, J. A., Dorman, S. E., Kopar, P., Holland, S. M. and Gallin, J. I. (1999). Neutrophil-specific granule deficiency results from a novel mutation with loss of function of the transcription factor CCAAT/enhancer binding protein epsilon. *J Exp Med* **189**(11):1847-1852.

- Lethem, M. I., James, S. L., Marriott, C. and Burke, J. F. (1990). The origin of DNA associated with mucus glycoproteins in cystic fibrosis sputum. *Eur Respir J* **3**(1):19-23.
- Leung, B. P., Culshaw, S., Gracie, J. A., Hunter, D., Canetti, C. A., Campbell, C., . . . McInnes, I. B. (2001). A role for IL-18 in neutrophil activation. *J Immunol* **167**(5):2879-2886.
- Li, D., Dong, B., Tong, Z., Wang, Q., Liu, W., Wang, Y., . . . Duan, Y. (2012). MBL-mediated opsonophagocytosis of *Candida albicans* by human neutrophils is coupled with intracellular Dectin-1-triggered ROS production. *PLoS One* **7**(12):e50589.
- Li, K., Sacks, S. H. and Zhou, W. (2007). The relative importance of local and systemic complement production in ischaemia, transplantation and other pathologies. *Mol Immunol* **44**(16):3866-3874.
- Li, Z., Jiang, H., Xie, W., Zhang, Z., Smrcka, A. V. and Wu, D. (2000). Roles of PLC-beta2 and -beta3 and PI3Kgamma in chemoattractant-mediated signal transduction. *Science* **287**(5455):1046-1049.
- Lin, F., Nguyen, C. M., Wang, S. J., Saadi, W., Gross, S. P. and Jeon, N. L. (2005). Neutrophil migration in opposing chemoattractant gradients using microfluidic chemotaxis devices. *Ann Biomed Eng* **33**(4):475-482.
- Lindahl, U., Couchman, J., Kimata, K. and Esko, J. D. (2015). Proteoglycans and Sulfated Glycosaminoglycans. In: rd, Varki, A., Cummings, R.D., Esko, J.D., Stanley, P., Hart, G.W., . . . Seeberger, P.H. (eds.) *Essentials of Glycobiology*. Cold Spring Harbor (NY): Cold Spring Harbor Laboratory Press
- Copyright 2015-2017 by The Consortium of Glycobiology Editors, La Jolla, California. All rights reserved., pp. 207-221.
- Lindmark, A., Gullberg, U. and Olsson, I. (1994). Processing and intracellular transport of cathepsin G and neutrophil elastase in the leukemic myeloid cell line U-937-modulation by brefeldin A, ammonium chloride, and monensin. *J Leukoc Biol* **55**(1):50-57.
- Liu, M., Saeki, K., Matsunobu, T., Okuno, T., Koga, T., Sugimoto, Y., . . . Yokomizo, T. (2014). 12-Hydroxyheptadecatrienoic acid promotes epidermal wound healing by accelerating keratinocyte migration via the BLT2 receptor. *J Exp Med* **211**(6):1063-1078.
- Lloyd, C. M. and Hessel, E. M. (2010). Functions of T cells in asthma: more than just T(H)2 cells. *Nat Rev Immunol* **10**(12):838-848.
- Lloyd, C. M. and Saglani, S. (2013). T cells in asthma: influences of genetics, environment, and T-cell plasticity. *J Allergy Clin Immunol* **131**(5):1267-1274; quiz 1275.
- Lopez-Boado, Y. S., Espinola, M., Bahr, S. and Belaaouaj, A. (2004). Neutrophil serine proteinases cleave bacterial flagellin, abrogating its host response-inducing activity. *J Immunol* **172**(1):509-515.

Losse, J., Zipfel, P. F. and Jozsi, M. (2010). Factor H and factor H-related protein 1 bind to human neutrophils via complement receptor 3, mediate attachment to *Candida albicans*, and enhance neutrophil antimicrobial activity. *J Immunol* **184**(2):912-921.

Luo, S., Dasari, P., Reiher, N., Hartmann, A., Jacksch, S., Wende, E., . . . Zipfel, P. F. (2018). The secreted *Candida albicans* protein Pra1 disrupts host defense by broadly targeting and blocking complement C3 and C3 activation fragments. *Mol Immunol* **93**:266-277.

Lynskey, N. N., Reglinski, M., Calay, D., Siggins, M. K., Mason, J. C., Botto, M. and Sriskandan, S. (2017). Multi-functional mechanisms of immune evasion by the streptococcal complement inhibitor C5a peptidase. *PLoS Pathog* **13**(8):e1006493.

Mackerness, K. J., Jenkins, G. R., Bush, A. and Jose, P. J. (2008). Characterisation of the range of neutrophil stimulating mediators in cystic fibrosis sputum. *Thorax* **63**(7):614-620.

Magalhaes, A. C., Dunn, H. and Ferguson, S. S. (2012). Regulation of GPCR activity, trafficking and localization by GPCR-interacting proteins. *Br J Pharmacol* **165**(6):1717-1736.

Maiya, S., Desai, M., Baruah, A., Weller, P., Clarke, J. R. and Gray, J. (2004). Cough plate versus cough swab in patients with cystic fibrosis; a pilot study. *Arch Dis Child* **89**(6):577-579.

Mantovani, A., Sica, A., Sozzani, S., Allavena, P., Vecchi, A. and Locati, M. (2004). The chemokine system in diverse forms of macrophage activation and polarization. *Trends Immunol* **25**(12):677-686.

Marasco, W. A., Phan, S. H., Krutzsch, H., Showell, H. J., Feltner, D. E., Nairn, R., . . . Ward, P. A. (1984). Purification and identification of formyl-methionyl-leucyl-phenylalanine as the major peptide neutrophil chemotactic factor produced by *Escherichia coli*. *J Biol Chem* **259**(9):5430-5439.

Marc, M. M., Korosec, P., Kosnik, M., Kern, I., Flezar, M., Suskovic, S. and Sorli, J. (2004). Complement factors c3a, c4a, and c5a in chronic obstructive pulmonary disease and asthma. *Am J Respir Cell Mol Biol* **31**(2):216-219.

Marc, M. M., Kristan, S. S., Rozman, A., Kern, I., Flezar, M., Kosnik, M. and Korosec, P. (2010). Complement factor C5a in acute exacerbation of Chronic Obstructive Pulmonary Disease. *Scand J Immunol* **71**(5):386-391.

Marcy, T. W., Merrill, W. W., Rankin, J. A. and Reynolds, H. Y. (1987). Limitations of using urea to quantify epithelial lining fluid recovered by bronchoalveolar lavage. *Am Rev Respir Dis* **135**(6):1276-1280.

Margaroli, C. and Tirouvanziam, R. (2016). Neutrophil plasticity enables the development of pathological microenvironments: implications for cystic fibrosis airway disease. *Mol Cell Pediatr* **3**(1):38.

Marinkovic, D. V., Marinkovic, J. N., Erdos, E. G. and Robinson, C. J. (1977). Purification of carboxypeptidase B from human pancreas. *Biochem J* **163**(2):253-260.

Maruo, K., Akaike, T., Ono, T., Okamoto, T. and Maeda, H. (1997). Generation of anaphylatoxins through proteolytic processing of C3 and C5 by house dust mite protease. *J Allergy Clin Immunol* **100**(2):253-260.

Mathis, S. P., Jala, V. R., Lee, D. M. and Haribabu, B. (2010). Nonredundant roles for leukotriene B4 receptors BLT1 and BLT2 in inflammatory arthritis. *J Immunol* **185**(5):3049-3056.

Matthews, K. W., Mueller-Ortiz, S. L. and Wetsel, R. A. (2004). Carboxypeptidase N: a pleiotropic regulator of inflammation. *Mol Immunol* **40**(11):785-793.

Matuska, B., Comhair, S., Farver, C., Chmiel, J., Midura, R. J., Bonfield, T. and Lauer, M. E. (2016). Pathological Hyaluronan Matrices in Cystic Fibrosis Airways and Secretions. *Am J Respir Cell Mol Biol* **55**(4):576-585.

Mauriello, C. T., Pallera, H. K., Sharp, J. A., Woltmann, J. L., Jr., Qian, S., Hair, P. S., . . . Krishna, N. K. (2013). A novel peptide inhibitor of classical and lectin complement activation including ABO incompatibility. *Mol Immunol* **53**(1-2):132-139.

Mayer-Hamblett, N., Boyle, M. and VanDevanter, D. (2016). Advancing clinical development pathways for new CFTR modulators in cystic fibrosis. *Thorax* **71**(5):454-461.

McAllister, F., Henry, A., Kreindler, J. L., Dubin, P. J., Ulrich, L., Steele, C., . . . Kolls, J. K. (2005). Role of IL-17A, IL-17F, and the IL-17 receptor in regulating growth-related oncogene-alpha and granulocyte colony-stimulating factor in bronchial epithelium: implications for airway inflammation in cystic fibrosis. *J Immunol* **175**(1):404-412.

McElvaney, N. G., Hubbard, R. C., Birrer, P., Chernick, M. S., Caplan, D. B., Frank, M. M. and Crystal, R. G. (1991). Aerosol alpha 1-antitrypsin treatment for cystic fibrosis. *Lancet* **337**(8738):392-394.

McElvaney, N. G., Nakamura, H., Birrer, P., Hebert, C. A., Wong, W. L., Alphonso, M., . . . Crystal, R. G. (1992). Modulation of airway inflammation in cystic fibrosis. In vivo suppression of interleukin-8 levels on the respiratory epithelial surface by aerosolization of recombinant secretory leukoprotease inhibitor. *J Clin Invest* **90**(4):1296-1301.

McElvaney, O. J., Gunaratnam, C., Reeves, E. P. and McElvaney, N. G. (2018). A specialized method of sputum collection and processing for therapeutic interventions in cystic fibrosis. *J Cyst Fibros in press*.

McElvaney, O. J., O'Reilly, N., White, M., Lacey, N., Pohl, K., Gerlza, T., . . . McElvaney, N. G. (2015). The effect of the decoy molecule PA401 on CXCL8 levels in bronchoalveolar lavage fluid of patients with cystic fibrosis. *Mol Immunol* **63**(2):550-558.

McEver, R. P. (2002). Selectins: lectins that initiate cell adhesion under flow. *Curr Opin Cell Biol* **14**(5):581-586.

McGrath, L. T., Mallon, P., Dowey, L., Silke, B., McClean, E., McDonnell, M., . . . Elborn, S. (1999). Oxidative stress during acute respiratory exacerbations in cystic fibrosis. *Thorax* **54**(6):518-523.

McGreal, E. P., Davies, P. L., Powell, W., Rose-John, S., Spiller, O. B., Doull, I., . . . Kotecha, S. (2010). Inactivation of IL-6 and soluble IL-6 receptor by neutrophil derived serine proteases in cystic fibrosis. *Biochim Biophys Acta* **1802**(7-8):649-658.

McNally, P., O'Rourke, J., Fantino, E., Chacko, A., Pabary, R., Turnbull, A., . . . Sly, P. D. (2017). Pooling of bronchoalveolar lavage in children with cystic fibrosis does not adversely affect the microbiological yield or sensitivity in detecting pulmonary inflammation. *J Cyst Fibros* **17**(3): 391-399.

Menaldo, D. L., Bernardes, C. P., Jacob-Ferreira, A. L., Nogueira-Santos, C. G., Casare-Ogasawara, T. M., Pereira-Crott, L. S. and Sampaio, S. V. (2016). Effects of Bothrops atrox venom and two isolated toxins on the human complement system: Modulation of pathways and generation of anaphylatoxins. *Mol Immunol* **80**:91-100.

Mercer, P. F., Williams, A. E., Scotton, C. J., Jose, R. J., Sulikowski, M., Moffatt, J. D., . . . Chambers, R. C. (2014). Proteinase-activated receptor-1, CCL2, and CCL7 regulate acute neutrophilic lung inflammation. *Am J Respir Cell Mol Biol* **50**(1):144-157.

Michaelis, J., Vissers, M. C. and Winterbourn, C. C. (1990). Human neutrophil collagenase cleaves alpha 1-antitrypsin. *Biochem J* **270**(3):809-814.

Middleton, P. G., Chen, S. C. and Meyer, W. (2013). Fungal infections and treatment in cystic fibrosis. *Curr Opin Pulm Med* **19**(6):670-675.

The UK Cystic Fibrosis Trust Microbiology Laboratory Standards Working Group (2010). *Laboratory Standards for Processing Microbiological Samples from People with Cystic Fibrosis* **1**: 1 – 40.

Minghetti, L., Nicolini, A., Polazzi, E., Greco, A., Perretti, M., Parente, L. and Levi, G. (1999). Down-regulation of microglial cyclo-oxygenase-2 and inducible nitric oxide synthase expression by lipocortin 1. *Br J Pharmacol* **126**(6):1307-1314.

Mitroulis, I., Kourtzelis, I., Kambas, K., Rafail, S., Chrysanthopoulou, A., Speletas, M. and Ritis, K. (2010). Regulation of the autophagic machinery in human neutrophils. *Eur J Immunol* **40**(5):1461-1472.

Mittal, S. K. and Roche, P. A. (2015). Suppression of antigen presentation by IL-10. *Curr Opin Immunol* **34**:22-27.

Miyabe, Y., Miyabe, C., Murooka, T. T., Kim, E. Y., Newton, G. A., Kim, N. D., . . . Luster, A. D. (2017). Complement C5a receptor is the key initiator of neutrophil adhesion igniting immune complex-induced arthritis. *Science Immunology* **2**(7): e2195.

Moalli, F., Paroni, M., Veliz Rodriguez, T., Riva, F., Polentarutti, N., Bottazzi, B., . . . Garlanda, C. (2011). The therapeutic potential of the humoral pattern recognition molecule PTX3 in chronic lung infection caused by *Pseudomonas aeruginosa*. *J Immunol* **186**(9):5425-5434.

Mocsai, A., Abram, C. L., Jakus, Z., Hu, Y., Lanier, L. L. and Lowell, C. A. (2006). Integrin signaling in neutrophils and macrophages uses adaptors containing immunoreceptor tyrosine-based activation motifs. *Nat Immunol* **7**(12):1326-1333.

Mocsai, A., Jakus, Z., Vantus, T., Berton, G., Lowell, C. A. and Ligeti, E. (2000). Kinase pathways in chemoattractant-induced degranulation of neutrophils: the role of p38 mitogen-activated protein kinase activated by Src family kinases. *J Immunol* **164**(8):4321-4331.

Mocsai, A., Ligeti, E., Lowell, C. A. and Berton, G. (1999). Adhesion-dependent degranulation of neutrophils requires the Src family kinases Fgr and Hck. *J Immunol* **162**(2):1120-1126.

Mocsai, A., Walzog, B. and Lowell, C. A. (2015). Intracellular signalling during neutrophil recruitment. *Cardiovasc Res* **107**(3):373-385.

Mogayzel, P. J., Jr., Naureckas, E. T., Robinson, K. A., Mueller, G., Hadjiliadis, D., Hoag, J. B., . . . Marshall, B. (2013). Cystic fibrosis pulmonary guidelines. Chronic medications for maintenance of lung health. *Am J Respir Crit Care Med* **187**(7):680-689.

Mollnes, T. E., Brekke, O. L., Fung, M., Fure, H., Christiansen, D., Bergseth, G., . . . Lambris, J. D. (2002). Essential role of the C5a receptor in E coli-induced oxidative burst and phagocytosis revealed by a novel lepirudin-based human whole blood model of inflammation. *Blood* **100**(5):1869-1877.

Mollnes, T. E., Videm, V., Gotze, O., Harboe, M. and Oppermann, M. (1991). Formation of C5a during cardiopulmonary bypass: inhibition by precoating with heparin. *Ann Thorac Surg* **52**(1):92-97.

Monk, P. N. and Partridge, L. J. (1993). Characterization of a complement-fragment-C5a-stimulated calcium-influx mechanism in U937 monocytic cells. *Biochem J* **295** (Pt 3):679-684.

Morad, H. O., Belete, S. C., Read, T. and Shaw, A. M. (2015). Time-course analysis of C3a and C5a quantifies the coupling between the upper and terminal Complement pathways in vitro. *J Immunol Methods* **427**:13-18.

Morgan, B. P. and Harris, C. L. (2015). Complement, a target for therapy in inflammatory and degenerative diseases. *Nat Rev Drug Discov* **14**(12):857-877.

- Moriceau, S., Lenoir, G. and Witko-Sarsat, V. (2010). In cystic fibrosis homozygotes and heterozygotes, neutrophil apoptosis is delayed and modulated by diamide or roscovitine: evidence for an innate neutrophil disturbance. *J Innate Immun* **2**(3):260-266.
- Morser, J., Shao, Z., Nishimura, T., Zhou, Q., Zhao, L., Higgins, J. and Leung, L. L. K. (2018). Carboxypeptidase B2 and N play different roles in regulation of activated complements C3a and C5a in mouse. *J Thromb Haemost* **16**(5): 991-1002.
- Moss, R. B., Mistry, S. J., Konstan, M. W., Pilewski, J. M., Kerem, E., Tal-Singer, R. and Lazaar, A. L. (2013). Safety and early treatment effects of the CXCR2 antagonist SB-656933 in patients with cystic fibrosis. *J Cyst Fibros* **12**(3):241-248.
- Mueller-Ortiz, S. L., Hollmann, T. J., Haviland, D. L. and Wetsel, R. A. (2006). Ablation of the complement C3a anaphylatoxin receptor causes enhanced killing of *Pseudomonas aeruginosa* in a mouse model of pneumonia. *Am J Physiol Lung Cell Mol Physiol* **291**(2):L157-165.
- Mueller-Ortiz, S. L., Wang, D., Morales, J. E., Li, L., Chang, J. Y. and Wetsel, R. A. (2009). Targeted disruption of the gene encoding the murine small subunit of carboxypeptidase N (CPN1) causes susceptibility to C5a anaphylatoxin-mediated shock. *J Immunol* **182**(10):6533-6539.
- Muto, Y., Fukumoto, Y. and Arata, Y. (1987). Solution conformation of carboxy-terminal fragments of the third component of human complement C3: proton nuclear magnetic resonance study of C3a, des-Arg-C3a, and C3a Arg69. *J Biochem* **102**(3):635-641.
- Nanthapaisal, S., Eleftheriou, D., Gilmour, K., Leone, V., Ramnath, R., Omoyinmi, E., . . . Brogan, P. A. (2018). Cutaneous Vasculitis and Recurrent Infection Caused by Deficiency in Complement Factor I. *Front Immunol* **9**:735-742.
- Nataf, S., Davoust, N., Ames, R. S. and Barnum, S. R. (1999). Human T cells express the C5a receptor and are chemoattracted to C5a. *J Immunol* **162**(7):4018-4023.
- Navarro, J., Rainisio, M., Harms, H. K., Hodson, M. E., Koch, C., Mastella, G., . . . McKenzie, S. G. (2001). Factors associated with poor pulmonary function: cross-sectional analysis of data from the ERCF. European Epidemiologic Registry of Cystic Fibrosis. *Eur Respir J* **18**(2):298-305.
- Neeli, I., Dwivedi, N., Khan, S. and Radic, M. (2009). Regulation of extracellular chromatin release from neutrophils. *J Innate Immun* **1**(3):194-201.
- Netea, M. G., Brown, G. D., Kullberg, B. J. and Gow, N. A. (2008). An integrated model of the recognition of *Candida albicans* by the innate immune system. *Nat Rev Microbiol* **6**(1):67-78.

- Nguyen, G. T., Green, E. R. and Meccas, J. (2017). Neutrophils to the ROScue: Mechanisms of NADPH Oxidase Activation and Bacterial Resistance. *Front Cell Infect Microbiol* **7**:373-399 .
- Ni, Z. and Hui, P. (2009). Emerging pharmacologic therapies for wet age-related macular degeneration. *Ophthalmologica* **223**(6):401-410.
- Nichols, D. P. and Chmiel, J. F. (2015). Inflammation and its genesis in cystic fibrosis. *Pediatr Pulmonol* **50 Suppl 40**:S39-56.
- Nikiforovich, G. V., Marshall, G. R. and Baranski, T. J. (2008). Modeling molecular mechanisms of binding of the anaphylatoxin C5a to the C5a receptor. *Biochemistry* **47**(10):3117-3130.
- Nilsson, B. and Nilsson Ekdahl, K. (2012). The tick-over theory revisited: is C3 a contact-activated protein? *Immunobiology* **217**(11):1106-1110.
- Nimrichter, L., Burdick, M. M., Aoki, K., Laroy, W., Fierro, M. A., Hudson, S. A., . . . Schnaar, R. L. (2008). E-selectin receptors on human leukocytes. *Blood* **112**(9):3744-3752.
- Nishimura, J., Yamamoto, M., Hayashi, S., Ohyashiki, K., Ando, K., Brodsky, A. L., . . . Kanakura, Y. (2014). Genetic variants in C5 and poor response to eculizumab. *N Engl J Med* **370**(7):632-639.
- Nonaka, M. and Yoshizaki, F. (2004). Primitive complement system of invertebrates. *Immunol Rev* **198**:203-215.
- Norgauer, J., Dobos, G., Kownatzki, E., Dahinden, C., Burger, R., Kupper, R. and Gierschik, P. (1993). Complement fragment C3a stimulates Ca²⁺ influx in neutrophils via a pertussis-toxin-sensitive G protein. *Eur J Biochem* **217**(1):289-294.
- Nunn, M. A., Sharma, A., Paesen, G. C., Adamson, S., Lissina, O., Willis, A. C. and Nuttall, P. A. (2005). Complement inhibitor of C5 activation from the soft tick *Ornithodoros moubata*. *J Immunol* **174**(4):2084-2091.
- O'Donnell, J. A., Kennedy, C. L., Pellegrini, M., Nowell, C. J., Zhang, J. G., O'Reilly, L. A., . . . Croker, B. A. (2015). Fas regulates neutrophil lifespan during viral and bacterial infection. *J Leukoc Biol* **97**(2):321-326.
- O'Donoghue, A. J., Jin, Y., Knudsen, G. M., Perera, N. C., Jenne, D. E., Murphy, J. E., . . . Hermiston, T. W. (2013). Global substrate profiling of proteases in human neutrophil extracellular traps reveals consensus motif predominantly contributed by elastase. *PLoS One* **8**(9):e75141.
- O'Dwyer, C. A., O'Brien, M. E., Wormald, M. R., White, M. M., Banville, N., Hurley, K., . . . Reeves, E. P. (2015). The BLT1 Inhibitory Function of alpha-1 Antitrypsin Augmentation Therapy Disrupts Leukotriene B4 Neutrophil Signaling. *J Immunol* **195**(8):3628-3641.

O'Neill, L. A. (2008). The interleukin-1 receptor/Toll-like receptor superfamily: 10 years of progress. *Immunol Rev* **226**:10-18.

O'Shea, J. J. and Plenge, R. (2012). JAK and STAT signaling molecules in immunoregulation and immune-mediated disease. *Immunity* **36**(4):542-550.

Oakley, R. H., Laporte, S. A., Holt, J. A., Caron, M. G. and Barak, L. S. (2000). Differential affinities of visual arrestin, beta arrestin1, and beta arrestin2 for G protein-coupled receptors delineate two major classes of receptors. *J Biol Chem* **275**(22):17201-17210.

Okuno, T., Iizuka, Y., Okazaki, H., Yokomizo, T., Taguchi, R. and Shimizu, T. (2008). 12(S)-Hydroxyheptadeca-5Z, 8E, 10E-trienoic acid is a natural ligand for leukotriene B4 receptor 2. *J Exp Med* **205**(4):759-766.

Padrines, M., Wolf, M., Walz, A. and Baggiolini, M. (1994). Interleukin-8 processing by neutrophil elastase, cathepsin G and proteinase-3. *FEBS Lett* **352**(2):231-235.

Painter, R. G., Valentine, V. G., Lanson, N. A., Jr., Leidal, K., Zhang, Q., Lombard, G., . . . Wang, G. (2006). CFTR Expression in human neutrophils and the phagolysosomal chlorination defect in cystic fibrosis. *Biochemistry* **45**(34):10260-10269.

Pandya, P. H. and Wilkes, D. S. (2014). Complement system in lung disease. *Am J Respir Cell Mol Biol* **51**(4):467-473.

Papayannopoulos, V., Metzler, K. D., Hakkim, A. and Zychlinsky, A. (2010). Neutrophil elastase and myeloperoxidase regulate the formation of neutrophil extracellular traps. *J Cell Biol* **191**(3):677-691.

Papayianni, A., Serhan, C. N. and Brady, H. R. (1996). Lipoxin A4 and B4 inhibit leukotriene-stimulated interactions of human neutrophils and endothelial cells. *J Immunol* **156**(6):2264-2272.

Parish, C. R. (2006). The role of heparan sulphate in inflammation. *Nat Rev Immunol* **6**(9):633-643.

Parkins, M. D. and Floto, R. A. (2015). Emerging bacterial pathogens and changing concepts of bacterial pathogenesis in cystic fibrosis. *J Cyst Fibros* **14**(3):293-304.

Parkos, C. A. (2016). Neutrophil-Epithelial Interactions: A Double-Edged Sword. *Am J Pathol* **186**(6):1404-1416.

Parks, Q. M., Young, R. L., Poch, K. R., Malcolm, K. C., Vasil, M. L. and Nick, J. A. (2009). Neutrophil enhancement of *Pseudomonas aeruginosa* biofilm development: human F-actin and DNA as targets for therapy. *J Med Microbiol* **58**(Pt 4):492-502.

Pass, M. B., Borregaard, N. and Cowland, J. B. (2007). Derangement of transcription factor profiles during in vitro differentiation of HL60 and NB4 cells. *Leuk Res* **31**(6):827-837.

Pattison, S. H., Gibson, D. S., Johnston, E., Peacock, S., Rivera, K., Tunney, M. M., . . . Elborn, J. S. (2017). Proteomic profile of cystic fibrosis sputum cells in adults chronically infected with *Pseudomonas aeruginosa*. *Eur Respir J* **50**(1):e1601569.

Pease, J. E., Burton, D. R. and Barker, M. D. (1994). Generation of chimeric C5a/formyl peptide receptors: towards the identification of the human C5a receptor binding site. *Eur J Immunol* **24**(1):211-215.

Peng, Q., Li, K., Smyth, L. A., Xing, G., Wang, N., Meader, L., . . . Zhou, W. (2012). C3a and C5a promote renal ischemia-reperfusion injury. *J Am Soc Nephrol* **23**(9):1474-1485.

Perl, M., Denk, S., Kalbitz, M. and Huber-Lang, M. (2012). Granzyme B: a new crossroad of complement and apoptosis. *Adv Exp Med Biol* **946**:135-146.

Pichert, A., Samsonov, S. A., Theisgen, S., Thomas, L., Baumann, L., Schiller, J., . . . Pisabarro, M. T. (2012a). Characterization of the interaction of interleukin-8 with hyaluronan, chondroitin sulfate, dermatan sulfate and their sulfated derivatives by spectroscopy and molecular modeling. *Glycobiology* **22**(1):134-145.

Pichert, A., Schlorke, D., Franz, S. and Arnhold, J. (2012b). Functional aspects of the interaction between interleukin-8 and sulfated glycosaminoglycans. *Biomatter* **2**(3):142-148.

Pignatti, P., Delmastro, M., Perfetti, L., Bossi, A., Balestrino, A., Di Stefano, A., . . . Moscato, G. (2002). Is dithiothreitol affecting cells and soluble mediators during sputum processing? A modified methodology to process sputum. In: *J Allergy Clin Immunol*. Vol. 110. United States, pp. 667-668.

Pimplikar, S. W. (2014). Neuroinflammation in Alzheimer's disease: from pathogenesis to a therapeutic target. *J Clin Immunol* **34 Suppl 1**:S64-69.

Pol-Fachin, L., Franco Becker, C., Almeida Guimaraes, J. and Verli, H. (2011). Effects of glycosylation on heparin binding and antithrombin activation by heparin. *Proteins* **79**(9):2735-2745.

Postle, A. D., Mander, A., Reid, K. B., Wang, J. Y., Wright, S. M., Moustaki, M. and Warner, J. O. (1999). Deficient hydrophilic lung surfactant proteins A and D with normal surfactant phospholipid molecular species in cystic fibrosis. *Am J Respir Cell Mol Biol* **20**(1):90-98.

Prince, H. E., Folds, J. D. and Spitznagel, J. K. (1979). Proteolysis of human IgG by human polymorphonuclear leucocyte elastase produces an Fc fragment with in vitro biological activity. *Clin Exp Immunol* **37**(1):162-168.

Prince, L. R., Prosseda, S. D., Higgins, K., Carling, J., Prestwich, E. C., Ogryzko, N. V., . . . Sabroe, I. (2017). NR4A orphan nuclear receptor family members, NR4A2 and NR4A3, regulate neutrophil number and survival. *Blood* **130**(8):1014-1025.

Punchard, N. A., Whelan, C. J. and Adcock, I. (2004). The Journal of Inflammation. *J Inflamm (Lond)* **1**(1):1-4.

Rabiet, M. J., Huet, E. and Boulay, F. (2007). The N-formyl peptide receptors and the anaphylatoxin C5a receptors: an overview. *Biochimie* **89**(9):1089-1106.

Rabiet, M. J., Huet, E. and Boulay, F. (2008). Complement component 5a receptor oligomerization and homologous receptor down-regulation. *J Biol Chem* **283**(45):31038-31046.

Raby, A. C., Holst, B., Davies, J., Colmont, C., Laumonnier, Y., Coles, B., . . . Labeta, M. O. (2011). TLR activation enhances C5a-induced pro-inflammatory responses by negatively modulating the second C5a receptor, C5L2. *Eur J Immunol* **41**(9):2741-2752.

Rahmoune, H., Lamblin, G., Lafitte, J. J., Galabert, C., Filliat, M. and Roussel, P. (1991). Chondroitin sulfate in sputum from patients with cystic fibrosis and chronic bronchitis. *Am J Respir Cell Mol Biol* **5**(4):315-320.

Ramdin, L., Perks, B., Sheron, N. and Shute, J. K. (1998). Regulation of interleukin-8 binding and function by heparin and alpha2-macroglobulin. *Clin Exp Allergy* **28**(5):616-624.

Raptis, S. Z., Shapiro, S. D., Simmons, P. M., Cheng, A. M. and Pham, C. T. (2005). Serine protease cathepsin G regulates adhesion-dependent neutrophil effector functions by modulating integrin clustering. *Immunity* **22**(6):679-691.

Ratjen, F., Paul, K., van Koningsbruggen, S., Breitenstein, S., Rietschel, E. and Nikolaizik, W. (2005). DNA concentrations in BAL fluid of cystic fibrosis patients with early lung disease: influence of treatment with dornase alpha. *Pediatr Pulmonol* **39**(1):1-4.

Ratjen, F., Waters, V., Klingel, M., McDonald, N., Dell, S., Leahy, T. R., . . . Grasemann, H. (2016). Changes in airway inflammation during pulmonary exacerbations in patients with cystic fibrosis and primary ciliary dyskinesia. *Eur Respir J* **47**(3):829-836.

Reed, S. L., Ember, J. A., Herdman, D. S., DiScipio, R. G., Hugli, T. E. and Gigli, I. (1995). The extracellular neutral cysteine proteinase of *Entamoeba histolytica* degrades anaphylatoxins C3a and C5a. *J Immunol* **155**(1):266-274.

Reeves, E. P., Bergin, D. A., Murray, M. A. and McElvaney, N. G. (2011a). The involvement of glycosaminoglycans in airway disease associated with cystic fibrosis. *ScientificWorldJournal* **11**:959-971.

Reeves, E. P., McCarthy, C., McElvaney, O. J., Vijayan, M. S., White, M. M., Dunlea, D. M., . . . McElvaney, N. G. (2015). Inhaled hypertonic saline for cystic fibrosis: Reviewing the

potential evidence for modulation of neutrophil signalling and function. *World J Crit Care Med* **4**(3):179-191.

Reeves, E. P., Williamson, M., O'Neill, S. J., Grealley, P. and McElvaney, N. G. (2011b). Nebulized hypertonic saline decreases IL-8 in sputum of patients with cystic fibrosis. *Am J Respir Crit Care Med* **183**(11):1517-1523.

Ren, B., McCrory, M. A., Pass, C., Bullard, D. C., Ballantyne, C. M., Xu, Y., . . . Szalai, A. J. (2004). The virulence function of *Streptococcus pneumoniae* surface protein A involves inhibition of complement activation and impairment of complement receptor-mediated protection. *J Immunol* **173**(12):7506-7512.

Richman-Eisenstat, J. B., Jorens, P. G., Hebert, C. A., Ueki, I. and Nadel, J. A. (1993). Interleukin-8: an important chemoattractant in sputum of patients with chronic inflammatory airway diseases. *Am J Physiol* **264**(4 Pt 1):L413-418.

Ricklin, D., Hajishengallis, G., Yang, K. and Lambris, J. D. (2010). Complement: a key system for immune surveillance and homeostasis. *Nat Immunol* **11**(9):785-797.

Ricklin, D. and Lambris, J. D. (2013). Complement in immune and inflammatory disorders: pathophysiological mechanisms. *J Immunol* **190**(8):3831-3838.

Ricklin, D., Mastellos, D. C., Reis, E. S. and Lambris, J. D. (2018). The renaissance of complement therapeutics. *Nat Rev Nephrol* **14**(1):26-47.

Riedemann, N. C., Habel, M., Ziereisen, J., Hermann, M., Schneider, C., Wehling, C., . . . Guo, R. (2017). Controlling the anaphylatoxin C5a in diseases requires a specifically targeted inhibition. *Clin Immunol* **180**:25-32.

Riedl, M. (2015). Recombinant human C1 esterase inhibitor in the management of hereditary angioedema. *Clin Drug Investig* **35**(7):407-417.

Ringholz, F. C., Buchanan, P. J., Clarke, D. T., Millar, R. G., McDermott, M., Linnane, B., . . . Urbach, V. (2014). Reduced 15-lipoxygenase 2 and lipoxin A4/leukotriene B4 ratio in children with cystic fibrosis. *Eur Respir J* **44**(2):394-404.

Robb, C. T., Regan, K. H., Dorward, D. A. and Rossi, A. G. (2016). Key mechanisms governing resolution of lung inflammation. *Semin Immunopathol* **38**(4):425-448.

Robbins, R. A., Nelson, K. J., Gossman, G. L., Koyama, S. and Rennard, S. I. (1991). Complement activation by cigarette smoke. *Am J Physiol* **260**(4 Pt 1):L254-259.

Rock, K. L., Lai, J. J. and Kono, H. (2011). Innate and adaptive immune responses to cell death. *Immunol Rev* **243**(1):191-205.

Rogers, C. S., Stoltz, D. A., Meyerholz, D. K., Ostedgaard, L. S., Rokhlina, T., Taft, P. J., . . . Welsh, M. J. (2008). Disruption of the CFTR gene produces a model of cystic fibrosis in newborn pigs. *Science* **321**(5897):1837-1841.

Ronchetti, K., Tame, J. D., Paisey, C., Thia, L. P., Doull, I., Howe, R., . . . Forton, J. T. (2018). The CF-Sputum Induction Trial (CF-SpIT) to assess lower airway bacterial sampling in young children with cystic fibrosis: a prospective internally controlled interventional trial. *Lancet Respir Med* **6**(6):461-471.

Roos, D. and de Boer, M. (2014). Molecular diagnosis of chronic granulomatous disease. *Clin Exp Immunol* **175**(2):139-149.

Ross, G. D., Newman, S. L., Lambris, J. D., Devery-Pocius, J. E., Cain, J. A. and Lachmann, P. J. (1983). Generation of three different fragments of bound C3 with purified factor I or serum. II. Location of binding sites in the C3 fragments for factors B and H, complement receptors, and bovine conglutinin. *J Exp Med* **158**(2):334-352.

Roth, M. D. and Golub, S. H. (1993). Human pulmonary macrophages utilize prostaglandins and transforming growth factor beta 1 to suppress lymphocyte activation. *J Leukoc Biol* **53**(4):366-371.

Roum, J. H., Borok, Z., McElvaney, N. G., Grimes, G. J., Bokser, A. D., Buhl, R. and Crystal, R. G. (1999). Glutathione aerosol suppresses lung epithelial surface inflammatory cell-derived oxidants in cystic fibrosis. *J Appl Physiol (1985)* **87**(1):438-443.

Roversi, P., Ryffel, B., Togbe, D., Mailliet, I., Teixeira, M., Ahmat, N., . . . Nunn, M. A. (2013). Bifunctional lipocalin ameliorates murine immune complex-induced acute lung injury. *J Biol Chem* **288**(26):18789-18802.

Rubio, F., Cooley, J., Accurso, F. J. and Remold-O'Donnell, E. (2004). Linkage of neutrophil serine proteases and decreased surfactant protein-A (SP-A) levels in inflammatory lung disease. *Thorax* **59**(4):318-323.

Sadik, C. D. and Luster, A. D. (2012). Lipid-cytokine-chemokine cascades orchestrate leukocyte recruitment in inflammation. *J Leukoc Biol* **91**(2):207-215.

Sadik, C. D., Miyabe, Y., Sezin, T. and Luster, A. D. (2018). The critical role of C5a as an initiator of neutrophil-mediated autoimmune inflammation of the joint and skin. *Semin Immunol* **37**:21-29.

Saffar, A. S., Ashdown, H. and Gounni, A. S. (2011). The molecular mechanisms of glucocorticoids-mediated neutrophil survival. *Curr Drug Targets* **12**(4):556-562.

Sagel, S. D., Chmiel, J. F. and Konstan, M. W. (2007). Sputum biomarkers of inflammation in cystic fibrosis lung disease. *Proc Am Thorac Soc* **4**(4):406-417.

- Sagel, S. D., Kapsner, R., Osberg, I., Sontag, M. K. and Accurso, F. J. (2001). Airway inflammation in children with cystic fibrosis and healthy children assessed by sputum induction. *Am J Respir Crit Care Med* **164**(8 Pt 1):1425-1431.
- Sagel, S. D., Khan, U., Jain, R., Graff, G., Daines, C. L., Dunitz, J. M., . . . Shaffer, M. L. (2018). Effects of an Antioxidant-enriched Multivitamin in Cystic Fibrosis: Randomized, Controlled, Multicenter Trial. *Am J Respir Crit Care Med* **198**(5):639-647.
- Sagel, S. D., Wagner, B. D., Anthony, M. M., Emmett, P. and Zemanick, E. T. (2012). Sputum biomarkers of inflammation and lung function decline in children with cystic fibrosis. *Am J Respir Crit Care Med* **186**(9):857-865.
- Sahoo, A. R., Mishra, R. and Rana, S. (2018). The Model Structures of the Complement Component 5a Receptor (C5aR) Bound to the Native and Engineered (h)C5a. *Sci Rep* **8**(1):2955.
- Sahu, S. C. (1980). Hyaluronic acid. An indicator of pathological conditions of human lungs? *Inflammation* **4**(1):107-112.
- Saitoh, H., Masuda, T., Shimura, S., Fushimi, T. and Shirato, K. (2001). Secretion and gene expression of secretory leukocyte protease inhibitor by human airway submucosal glands. *Am J Physiol Lung Cell Mol Physiol* **280**(1):L79-87.
- Salam, M. T., Bastain, T. M., Rappaport, E. B., Islam, T., Berhane, K., Gauderman, W. J. and Gilliland, F. D. (2011). Genetic variations in nitric oxide synthase and arginase influence exhaled nitric oxide levels in children. *Allergy* **66**(3):412-419.
- Sareneva, T., Pirhonen, J., Cantell, K. and Julkunen, I. (1995). N-glycosylation of human interferon-gamma: glycans at Asn-25 are critical for protease resistance. *Biochem J* **308** (Pt 1):9-14.
- Sass, L. A., Hair, P. S., Perkins, A. M., Shah, T. A., Krishna, N. K. and Cunnion, K. M. (2015). Complement Effectors of Inflammation in Cystic Fibrosis Lung Fluid Correlate with Clinical Measures of Disease. *PLoS One* **10**(12):e0144723.
- Savoia, D., Deplano, C. and Zucca, M. (2008). Pseudomonas aeruginosa and Burkholderia cenocepacia infections in patients affected by cystic fibrosis: serum resistance and antibody response. *Immunol Invest* **37**(1):19-27.
- Scannell, M. and Maderna, P. (2006). Lipoxins and annexin-1: resolution of inflammation and regulation of phagocytosis of apoptotic cells. *ScientificWorldJournal* **6**:1555-1573.
- Schafer, J., Griese, M., Chandrasekaran, R., Chotirmall, S. H. and Hartl, D. (2018). Pathogenesis, imaging and clinical characteristics of CF and non-CF bronchiectasis. *BMC Pulm Med* **18**(1):79.

- Schalkwijk, J., Wiedow, O. and Hirose, S. (1999). The trappin gene family: proteins defined by an N-terminal transglutaminase substrate domain and a C-terminal four-disulphide core. *Biochem J* **340** (Pt 3):569-577.
- Schatz-Jakobsen, J. A., Yatime, L., Larsen, C., Petersen, S. V., Klos, A. and Andersen, G. R. (2014). Structural and functional characterization of human and murine C5a anaphylatoxins. *Acta Crystallogr D Biol Crystallogr* **70**(Pt 6):1704-1717.
- Schlorke, D., Thomas, L., Samsonov, S. A., Huster, D., Arnhold, J. and Pichert, A. (2012). The influence of glycosaminoglycans on IL-8-mediated functions of neutrophils. *Carbohydr Res* **356**:196-203.
- Schultz, A., Puvvadi, R., Borisov, S. M., Shaw, N. C., Klimant, I., Berry, L. J., . . . Stick, S. M. (2017). Airway surface liquid pH is not acidic in children with cystic fibrosis. *Nature Communications* **8**(1):1409-1418.
- Scola, A. M., Higginbottom, A., Partridge, L. J., Reid, R. C., Woodruff, T., Taylor, S. M., . . . Monk, P. N. (2007). The role of the N-terminal domain of the complement fragment receptor C5L2 in ligand binding. *J Biol Chem* **282**(6):3664-3671.
- Scola, A. M., Johswich, K. O., Morgan, B. P., Klos, A. and Monk, P. N. (2009). The human complement fragment receptor, C5L2, is a recycling decoy receptor. *Mol Immunol* **46**(6):1149-1162.
- Serna, M., Giles, J. L., Morgan, B. P. and Bubeck, D. (2016). Structural basis of complement membrane attack complex formation. *Nat Commun* **7**:10587.
- Shapouri-Moghaddam, A., Mohammadian, S., Vazini, H., Taghadosi, M., Esmaeili, S. A., Mardani, F., . . . Sahebkar, A. (2018). Macrophage plasticity, polarization, and function in health and disease. *J Cell Physiol* **233**(9):6425-6440.
- Shawar, S. M., Rich, R. R. and Becker, E. L. (1995). Peptides from the amino-terminus of mouse mitochondrially encoded NADH dehydrogenase subunit 1 are potent chemoattractants. *Biochem Biophys Res Commun* **211**(3):812-818.
- Shende, R., Wong, S. S. W., Rapole, S., Beau, R., Ibrahim-Granet, O., Monod, M., . . . Sahu, A. (2018). *Aspergillus fumigatus* conidial metalloprotease Mep1p cleaves host complement proteins. *J Biol Chem* **293**(40):15538-15555.
- Shevchenko, A., Wilm, M., Vorm, O. and Mann, M. (1996). Mass spectrometric sequencing of proteins silver-stained polyacrylamide gels. *Anal Chem* **68**(5):850-858.
- Singh, A., Ralhan, A., Schwarz, C., Hartl, D. and Hector, A. (2018). Fungal Pathogens in CF Airways: Leave or Treat? *Mycopathologia* **183**(1):119-137.
- Sinitsyn, V. V., Bokchubaev, E. T., Mamontova, A. G., Ovtrakht, N. V., Nasonov, E. L., Konovalov, G. A. and Kukharchuk, V. V. (1992). C3a and C5a anaphylatoxins bind to

heparin-based sorbent in low density lipoprotein apheresis: in vitro and in vivo investigations. *Artif Organs* **16**(3):291-293.

Skidgel, R. A. and Erdos, E. G. (2007). Structure and function of human plasma carboxypeptidase N, the anaphylatoxin inactivator. *Int Immunopharmacol* **7**(14):1888-1899.

Skjeflo, E. W., Christiansen, D., Espevik, T., Nielsen, E. W. and Mollnes, T. E. (2014). Combined inhibition of complement and CD14 efficiently attenuated the inflammatory response induced by *Staphylococcus aureus* in a human whole blood model. *J Immunol* **192**(6):2857-2864.

Skjeflo, E. W., Sagatun, C., Dybwik, K., Aam, S., Urvig, S. H., Nunn, M. A., . . . Mollnes, T. E. (2015). Combined inhibition of complement and CD14 improved outcome in porcine polymicrobial sepsis. *Crit Care* **19**:415-423.

Skov, M., Pressler, T., Lykkesfeldt, J., Poulsen, H. E., Jensen, P. O., Johansen, H. K., . . . Ciofu, O. (2015). The effect of short-term, high-dose oral N-acetylcysteine treatment on oxidative stress markers in cystic fibrosis patients with chronic *P. aeruginosa* infection -- a pilot study. *J Cyst Fibros* **14**(2):211-218.

Sly, P. D., Brennan, S., Gangell, C., de Klerk, N., Murray, C., Mott, L., . . . Ranganathan, S. C. (2009). Lung disease at diagnosis in infants with cystic fibrosis detected by newborn screening. *Am J Respir Crit Care Med* **180**(2):146-152.

Sly, P. D., Gangell, C. L., Chen, L., Ware, R. S., Ranganathan, S., Mott, L. S., . . . Stick, S. M. (2013). Risk factors for bronchiectasis in children with cystic fibrosis. *N Engl J Med* **368**(21):1963-1970.

Smith, W. D., Bardin, E., Cameron, L., Edmondson, C. L., Farrant, K. V., Martin, I., . . . Davies, J. C. (2017). Current and future therapies for *Pseudomonas aeruginosa* infection in patients with cystic fibrosis. *FEMS Microbiol Lett* **364**(14):e121.

Smrcka, A. V. and Sternweis, P. C. (1993). Regulation of purified subtypes of phosphatidylinositol-specific phospholipase C beta by G protein alpha and beta gamma subunits. *J Biol Chem* **268**(13):9667-9674.

Smyth, A. R. and Walters, S. (2014). Prophylactic anti-staphylococcal antibiotics for cystic fibrosis. *Cochrane Database Syst Rev* (11):Cd001912.

Snelgrove, R. J., Jackson, P. L., Hardison, M. T., Noerager, B. D., Kinloch, A., Gaggar, A., . . . Blalock, J. E. (2010). A critical role for LTA4H in limiting chronic pulmonary neutrophilic inflammation. *Science* **330**(6000):90-94.

Sogawa, Y., Ohyama, T., Maeda, H. and Hirahara, K. (2011). Inhibition of neutrophil migration in mice by mouse formyl peptide receptors 1 and 2 dual agonist: indication of cross-desensitization in vivo. *Immunology* **132**(3):441-450.

Solic, N., Wilson, J., Wilson, S. J. and Shute, J. K. (2005). Endothelial activation and increased heparan sulfate expression in cystic fibrosis. *Am J Respir Crit Care Med* **172**(7):892-898.

Somaraju, U. R. and Solis-Moya, A. (2015). Pancreatic enzyme replacement therapy for people with cystic fibrosis (Review). *Paediatr Respir Rev* **16**(2):108-109.

Sonnenberg, G. F. and Artis, D. (2015). Innate lymphoid cells in the initiation, regulation and resolution of inflammation. *Nat Med* **21**(7):698-708.

Sosnay, P. R., Siklosi, K. R., Van Goor, F., Kaniecki, K., Yu, H., Sharma, N., . . . Cutting, G. R. (2013). Defining the disease liability of variants in the cystic fibrosis transmembrane conductance regulator gene. *Nat Genet* **45**(10):1160-1167.

Souza-Fernandes, A. B., Pelosi, P. and Rocco, P. R. (2006). Bench-to-bedside review: the role of glycosaminoglycans in respiratory disease. *Crit Care* **10**(6):237-253.

Spencer, J. L., Stone, P. J. and Nugent, M. A. (2006). New insights into the inhibition of human neutrophil elastase by heparin. *Biochemistry* **45**(30):9104-9120.

Spillmann, D., Witt, D. and Lindahl, U. (1998). Defining the interleukin-8-binding domain of heparan sulfate. *J Biol Chem* **273**(25):15487-15493.

Staab, E. B., Sanderson, S. D., Wells, S. M. and Poole, J. A. (2014). Treatment with the C5a receptor/CD88 antagonist PMX205 reduces inflammation in a murine model of allergic asthma. *Int Immunopharmacol* **21**(2):293-300.

Starosta, V., Rietschel, E., Paul, K., Baumann, U. and Griese, M. (2006). Oxidative changes of bronchoalveolar proteins in cystic fibrosis. *Chest* **129**(2):431-437.

Steele, C., Rapaka, R. R., Metz, A., Pop, S. M., Williams, D. L., Gordon, S., . . . Brown, G. D. (2005). The beta-glucan receptor dectin-1 recognizes specific morphologies of *Aspergillus fumigatus*. *PLoS Pathog* **1**(4):e42.

Stillie, R., Farooq, S. M., Gordon, J. R. and Stadnyk, A. W. (2009). The functional significance behind expressing two IL-8 receptor types on PMN. *J Leukoc Biol* **86**(3):529-543.

Stokell, J. R., Gharaibeh, R. Z., Hamp, T. J., Zapata, M. J., Fodor, A. A. and Steck, T. R. (2015). Analysis of changes in diversity and abundance of the microbial community in a cystic fibrosis patient over a multiyear period. *J Clin Microbiol* **53**(1):237-247.

Stoltz, D. A., Meyerholz, D. K., Pezzulo, A. A., Ramachandran, S., Rogan, M. P., Davis, G. J., . . . Welsh, M. J. (2010). Cystic fibrosis pigs develop lung disease and exhibit defective bacterial eradication at birth. *Sci Transl Med* **2**(29):29ra31.

- Stone, J. E., Akhtar, N., Botchway, S. and Pennock, C. A. (1994). Interaction of 1,9-dimethylmethylene blue with glycosaminoglycans. *Ann Clin Biochem* **31** (Pt 2):147-152.
- Stover, C. K., Pham, X. Q., Erwin, A. L., Mizoguchi, S. D., Warrenner, P., Hickey, M. J., . . . Olson, M. V. (2000). Complete genome sequence of *Pseudomonas aeruginosa* PAO1, an opportunistic pathogen. *Nature* **406**(6799):959-964.
- Strainic, M. G., Liu, J., Huang, D., An, F., Lalli, P. N., Muqim, N., . . . Medof, M. E. (2008). Locally produced complement fragments C5a and C3a provide both costimulatory and survival signals to naive CD4+ T cells. *Immunity* **28**(3):425-435.
- Strey, C. W., Siegmund, B., Rosenblum, S., Marquez-Pinilla, R. M., Oppermann, E., Huber-Lang, M., . . . Bechstein, W. O. (2009). Complement and neutrophil function changes after liver resection in humans. *World J Surg* **33**(12):2635-2643.
- Subramanian, H., Kashem, S. W., Collington, S. J., Qu, H., Lambris, J. D. and Ali, H. (2011). PMX-53 as a dual CD88 antagonist and an agonist for Mas-related gene 2 (MrgX2) in human mast cells. *Mol Pharmacol* **79**(6):1005-1013.
- Sun, S., Zhao, G., Liu, C., Fan, W., Zhou, X., Zeng, L., . . . Zhou, Y. (2015). Treatment with anti-C5a antibody improves the outcome of H7N9 virus infection in African green monkeys. *Clin Infect Dis* **60**(4):586-595.
- Taggart, C. C., Cryan, S. A., Weldon, S., Gibbons, A., Greene, C. M., Kelly, E., . . . McElvaney, N. G. (2005). Secretory leucoprotease inhibitor binds to NF-kappaB binding sites in monocytes and inhibits p65 binding. *J Exp Med* **202**(12):1659-1668.
- Taggart, C. C., Lowe, G. J., Greene, C. M., Mulgrew, A. T., O'Neill, S. J., Levine, R. L. and McElvaney, N. G. (2001). Cathepsin B, L, and S cleave and inactivate secretory leucoprotease inhibitor. *J Biol Chem* **276**(36):33345-33352.
- Takeuchi, O. and Akira, S. (2010). Pattern recognition receptors and inflammation. *Cell* **140**(6):805-820.
- Tamamis, P., Kieslich, C. A., Nikiforovich, G. V., Woodruff, T. M., Morikis, D. and Archontis, G. (2014). Insights into the mechanism of C5aR inhibition by PMX53 via implicit solvent molecular dynamics simulations and docking. *BMC Biophys* **7**:5-21.
- Tambourgi, D. V. and van den Berg, C. W. (2014). Animal venoms/toxins and the complement system. *Mol Immunol* **61**(2):153-162.
- Tan, H. L., Regamey, N., Brown, S., Bush, A., Lloyd, C. M. and Davies, J. C. (2011). The Th17 pathway in cystic fibrosis lung disease. *Am J Respir Crit Care Med* **184**(2):252-258.
- Tang, D., Kang, R., Coyne, C. B., Zeh, H. J. and Lotze, M. T. (2012). PAMPs and DAMPs: signal 0s that spur autophagy and immunity. *Immunol Rev* **249**(1):158-175.

- Tanino, Y., Coombe, D. R., Gill, S. E., Kett, W. C., Kajikawa, O., Proudfoot, A. E., . . . Frevert, C. W. (2010). Kinetics of chemokine-glycosaminoglycan interactions control neutrophil migration into the airspaces of the lungs. *J Immunol* **184**(5):2677-2685.
- Taube, C., Rha, Y. H., Takeda, K., Park, J. W., Joetham, A., Balhorn, A., . . . Gelfand, E. W. (2003). Inhibition of complement activation decreases airway inflammation and hyperresponsiveness. *Am J Respir Crit Care Med* **168**(11):1333-1341.
- Thomas, T. C., Rollins, S. A., Rother, R. P., Giannoni, M. A., Hartman, S. L., Elliott, E. A., . . . Evans, M. J. (1996). Inhibition of complement activity by humanized anti-C5 antibody and single-chain Fv. *Mol Immunol* **33**(17-18):1389-1401.
- Thornton, B. P., Vetvicka, V., Pitman, M., Goldman, R. C. and Ross, G. D. (1996). Analysis of the sugar specificity and molecular location of the beta-glucan-binding lectin site of complement receptor type 3 (CD11b/CD18). *J Immunol* **156**(3):1235-1246.
- Tian, W., Dewitt, S., Laffafian, I. and Hallett, M. B. (2004). Ca(2+), calpain and 3-phosphorylated phosphatidyl inositides; decision-making signals in neutrophils as potential targets for therapeutics. *J Pharm Pharmacol* **56**(5):565-571.
- Tosi, M. F. and Berger, M. (1988). Functional differences between the 40 kDa and 50 to 70 kDa IgG Fc receptors on human neutrophils revealed by elastase treatment and antireceptor antibodies. *J Immunol* **141**(6):2097-2103.
- Tosi, M. F., Zakem, H. and Berger, M. (1990). Neutrophil elastase cleaves C3bi on opsonized pseudomonas as well as CR1 on neutrophils to create a functionally important opsonin receptor mismatch. *J Clin Invest* **86**(1):300-308.
- Triantafilou, K., Hughes, T. R., Triantafilou, M. and Morgan, B. P. (2013). The complement membrane attack complex triggers intracellular Ca²⁺ fluxes leading to NLRP3 inflammasome activation. *J Cell Sci* **126**(Pt 13):2903-2913.
- Tucker, K. A., Lilly, M. B., Heck, L., Jr. and Rado, T. A. (1987). Characterization of a new human diploid myeloid leukemia cell line (PLB-985) with granulocytic and monocytic differentiating capacity. *Blood* **70**(2):372-378.
- Tunney, M. M., Klem, E. R., Fodor, A. A., Gilpin, D. F., Moriarty, T. F., McGrath, S. J., . . . Wolfgang, M. C. (2011). Use of culture and molecular analysis to determine the effect of antibiotic treatment on microbial community diversity and abundance during exacerbation in patients with cystic fibrosis. *Thorax* **66**(7):579-584.
- Twigg, M. S., Brockbank, S., Lowry, P., FitzGerald, S. P., Taggart, C. and Weldon, S. (2015). The Role of Serine Proteases and Antiproteases in the Cystic Fibrosis Lung. *Mediators Inflamm* **2015**:293053.
- UK CF registry. (2016). UK Cystic Fibrosis Registry 2016 Annual Data Report.

Unnewehr, H., Rittirsch, D., Sarma, J. V., Zetoune, F., Flierl, M. A., Perl, M., . . . Huber-Lang, M. (2013). Changes and regulation of the C5a receptor on neutrophils during septic shock in humans. *J Immunol* **190**(8):4215-4225.

Urban, C. F., Ermert, D., Schmid, M., Abu-Abed, U., Goosmann, C., Nacken, W., . . . Zychlinsky, A. (2009). Neutrophil extracellular traps contain calprotectin, a cytosolic protein complex involved in host defense against *Candida albicans*. *PLoS Pathog* **5**(10):e1000639.

van den Berg, C. W., Tambourgi, D. V., Clark, H. W., Hoong, S. J., Spiller, O. B. and McGreal, E. P. (2014). Mechanism of neutrophil dysfunction: neutrophil serine proteases cleave and inactivate the C5a receptor. *J Immunol* **192**(4):1787-1795.

van Ewijk, B. E., van der Zalm, M. M., Wolfs, T. F., Fler, A., Kimpen, J. L., Wilbrink, B. and van der Ent, C. K. (2008). Prevalence and impact of respiratory viral infections in young children with cystic fibrosis: prospective cohort study. *Pediatrics* **122**(6):1171-1176.

Van Pottelberge, G. R., Bracke, K. R., Pauwels, N. S., Vermassen, F. E., Joos, G. F. and Brusselle, G. G. (2012). COPD is associated with reduced pulmonary interstitial expression of pentraxin-3. *Eur Respir J* **39**(4):830-838.

Vandivier, R. W., Fadok, V. A., Hoffmann, P. R., Bratton, D. L., Penvari, C., Brown, K. K., . . . Henson, P. M. (2002a). Elastase-mediated phosphatidylserine receptor cleavage impairs apoptotic cell clearance in cystic fibrosis and bronchiectasis. *J Clin Invest* **109**(5):661-670.

Vandivier, R. W., Fadok, V. A., Ogden, C. A., Hoffmann, P. R., Brain, J. D., Accurso, F. J., . . . Henson, P. M. (2002b). Impaired clearance of apoptotic cells from cystic fibrosis airways. *Chest* **121**(3 Suppl):89-89.

Venereau, E., Casalgrandi, M., Schiraldi, M., Antoine, D. J., Cattaneo, A., De Marchis, F., . . . Bianchi, M. E. (2012). Mutually exclusive redox forms of HMGB1 promote cell recruitment or proinflammatory cytokine release. *J Exp Med* **209**(9):1519-1528.

Venge, P. and Olsson, I. (1975). Cationic proteins of human granulocytes. VI. Effects on the complement system and mediation of chemotactic activity. *J Immunol* **115**(6):1505-1508.

Verschoor, A., Karsten, C. M., Broadley, S. P., Laumonier, Y. and Kohl, J. (2016). Old dogs-new tricks: immunoregulatory properties of C3 and C5 cleavage fragments. *Immunol Rev* **274**(1):112-126.

Vethanayagam, R. R., Almyroudis, N. G., Grimm, M. J., Lewandowski, D. C., Pham, C. T., Blackwell, T. S., . . . Segal, B. H. (2011). Role of NADPH oxidase versus neutrophil proteases in antimicrobial host defense. *PLoS One* **6**(12):e28149.

Vibhuti, A., Gupta, K., Subramanian, H., Guo, Q. and Ali, H. (2011). Distinct and shared roles of beta-arrestin-1 and beta-arrestin-2 on the regulation of C3a receptor signaling in human mast cells. *PLoS One* **6**(5):e19585.

- Vogt, W. (1996). Complement activation by myeloperoxidase products released from stimulated human polymorphonuclear leukocytes. *Immunobiology* **195**(3):334-346.
- Vogt, W. (2000). Cleavage of the fifth component of complement and generation of a functionally active C5b6-like complex by human leukocyte elastase. *Immunobiology* **201**(3-4):470-477.
- Voisin, M. B. and Nourshargh, S. (2013). Neutrophil transmigration: emergence of an adhesive cascade within venular walls. *J Innate Immun* **5**(4):336-347.
- Volk, A. L., Hu, F. J., Berglund, M. M., Nordling, E., Stromberg, P., Uhlen, M. and Rockberg, J. (2016). Stratification of responders towards eculizumab using a structural epitope mapping strategy. *Sci Rep* **6**:e31365.
- Wainwright, C. E., Elborn, J. S., Ramsey, B. W., Marigowda, G., Huang, X., Cipolli, M., . . . Boyle, M. P. (2015). Lumacaftor-Ivacaftor in Patients with Cystic Fibrosis Homozygous for Phe508del CFTR. *N Engl J Med* **373**(3):220-231.
- Walz, A., Peveri, P., Aschauer, H. and Baggiolini, M. (1987). Purification and amino acid sequencing of NAF, a novel neutrophil-activating factor produced by monocytes. *Biochem Biophys Res Commun* **149**(2):755-761.
- Wang, H., Ricklin, D. and Lambris, J. D. (2017). Complement-activation fragment C4a mediates effector functions by binding as untethered agonist to protease-activated receptors 1 and 4. *Proc Natl Acad Sci U S A* **114**(41):10948-10953.
- Wang, H., Wang, C., Zhao, M. H. and Chen, M. (2015a). Neutrophil extracellular traps can activate alternative complement pathways. *Clin Exp Immunol* **181**(3):518-527.
- Wang, L., Fuster, M., Sriramarao, P. and Esko, J. D. (2005). Endothelial heparan sulfate deficiency impairs L-selectin- and chemokine-mediated neutrophil trafficking during inflammatory responses. *Nat Immunol* **6**(9):902-910.
- Wang, R., Xiao, H., Guo, R., Li, Y. and Shen, B. (2015b). The role of C5a in acute lung injury induced by highly pathogenic viral infections. *Emerg Microbes Infect* **4**(5):e28.
- Wang, X., Mathieu, M. and Brezski, R. J. (2018). IgG Fc engineering to modulate antibody effector functions. *Protein Cell* **9**(1):63-73.
- Watts, C. L. and Bruce, M. C. (1995). Comparison of secretory component for immunoglobulin A with albumin as reference proteins in tracheal aspirate from preterm infants. *J Pediatr* **127**(1):113-122.
- Webb, L. M., Ehrenguber, M. U., Clark-Lewis, I., Baggiolini, M. and Rot, A. (1993). Binding to heparan sulfate or heparin enhances neutrophil responses to interleukin 8. *Proc Natl Acad Sci U S A* **90**(15):7158-7162.

Weldon, S., McNally, P., McElvaney, N. G., Elborn, J. S., McAuley, D. F., Wartelle, J., . . . Taggart, C. C. (2009). Decreased levels of secretory leucoprotease inhibitor in the *Pseudomonas*-infected cystic fibrosis lung are due to neutrophil elastase degradation. *J Immunol* **183**(12):8148-8156.

Werfel, T., Kirchhoff, K., Wittmann, M., Begemann, G., Kapp, A., Heidenreich, F., . . . Zwirner, J. (2000). Activated human T lymphocytes express a functional C3a receptor. *J Immunol* **165**(11):6599-6605.

Westwood, J. P., Mackay, A. J., Donaldson, G., Machin, S. J., Wedzicha, J. A. and Scully, M. (2016). The role of complement activation in COPD exacerbation recovery. *ERJ Open Res* **2**(4):27-30.

Wetsel, R. A. and Kolb, W. P. (1983). Expression of C5a-like biological activities by the fifth component of human complement (C5) upon limited digestion with noncomplement enzymes without release of polypeptide fragments. *J Exp Med* **157**(6):2029-2048.

Whitelock, J. M. and Iozzo, R. V. (2005). Heparan sulfate: a complex polymer charged with biological activity. *Chem Rev* **105**(7):2745-2764.

Wingrove, J. A., DiScipio, R. G., Chen, Z., Potempa, J., Travis, J. and Hugli, T. E. (1992). Activation of complement components C3 and C5 by a cysteine proteinase (gingipain-1) from *Porphyromonas* (*Bacteroides*) *gingivalis*. *J Biol Chem* **267**(26):18902-18907.

Wojtczak, H. A., Kerby, G. S., Wagener, J. S., Copenhaver, S. C., Gotlin, R. W., Riches, D. W. and Accurso, F. J. (2001). Beclomethasone dipropionate reduced airway inflammation without adrenal suppression in young children with cystic fibrosis: a pilot study. *Pediatr Pulmonol* **32**(4):293-302.

Wong, E. K., Goodship, T. H. and Kavanagh, D. (2013). Complement therapy in atypical haemolytic uraemic syndrome (aHUS). *Mol Immunol* **56**(3):199-212.

Wright, A. J., Higginbottom, A., Philippe, D., Upadhyay, A., Bagby, S., Read, R. C., . . . Partridge, L. J. (2007). Characterisation of receptor binding by the chemotaxis inhibitory protein of *Staphylococcus aureus* and the effects of the host immune response. *Mol Immunol* **44**(10):2507-2517.

Wright, H. L., Moots, R. J. and Edwards, S. W. (2014). The multifactorial role of neutrophils in rheumatoid arthritis. *Nat Rev Rheumatol* **10**(10):593-601.

Wright, S. D. and Silverstein, S. C. (1983). Receptors for C3b and C3bi promote phagocytosis but not the release of toxic oxygen from human phagocytes. *J Exp Med* **158**(6):2016-2023.

Wu, M. C., Brennan, F. H., Lynch, J. P., Mantovani, S., Phipps, S., Wetsel, R. A., . . . Woodruff, T. M. (2013). The receptor for complement component C3a mediates protection

from intestinal ischemia-reperfusion injuries by inhibiting neutrophil mobilization. *Proc Natl Acad Sci U S A* **110**(23):9439-9444.

Wysocka, M., Lesner, A., Guzow, K., Mackiewicz, L., Legowska, A., Wiczek, W. and Rolka, K. (2008). Design of selective substrates of proteinase 3 using combinatorial chemistry methods. *Anal Biochem* **378**(2):208-215.

Xu, R., Lin, F., Bao, C., Huang, H., Ji, C., Wang, S., . . . Wang, F. S. (2016). Complement 5a receptor-mediated neutrophil dysfunction is associated with a poor outcome in sepsis. *Cell Mol Immunol* **13**(1):103-109.

Xue, R., Gu, H., Qiu, Y., Guo, Y., Korteweg, C., Huang, J. and Gu, J. (2016). Expression of Cystic Fibrosis Transmembrane Conductance Regulator in Ganglia of Human Gastrointestinal Tract. *Sci Rep* **6**:30926.

Yamamoto, T. (2000). Molecular mechanism of monocyte predominant infiltration in chronic inflammation: mediation by a novel monocyte chemotactic factor, S19 ribosomal protein dimer. *Pathol Int* **50**(11):863-871.

Yamasaki, S., Matsumoto, M., Takeuchi, O., Matsuzawa, T., Ishikawa, E., Sakuma, M., . . . Saito, T. (2009). C-type lectin Mincle is an activating receptor for pathogenic fungus, *Malassezia*. *Proc Natl Acad Sci U S A* **106**(6):1897-1902.

Yang, D., Chen, Q., Gertz, B., He, R., Phulsuksombati, M., Ye, R. D. and Oppenheim, J. J. (2002). Human dendritic cells express functional formyl peptide receptor-like-2 (FPRL2) throughout maturation. *J Leukoc Biol* **72**(3):598-607.

Yang, H., Antoine, D. J., Andersson, U. and Tracey, K. J. (2013). The many faces of HMGB1: molecular structure-functional activity in inflammation, apoptosis, and chemotaxis. *J Leukoc Biol* **93**(6):865-873.

Ye, R. D., Boulay, F., Wang, J. M., Dahlgren, C., Gerard, C., Parmentier, M., . . . Murphy, P. M. (2009). International Union of Basic and Clinical Pharmacology. LXXIII. Nomenclature for the formyl peptide receptor (FPR) family. *Pharmacol Rev* **61**(2):119-161.

Yipp, B. G., Petri, B., Salina, D., Jenne, C. N., Scott, B. N., Zbytnuik, L. D., . . . Kubes, P. (2012). Infection-induced NETosis is a dynamic process involving neutrophil multitasking in vivo. *Nat Med* **18**(9):1386-1393.

Yokomizo, T. (2011). Leukotriene B4 receptors: novel roles in immunological regulations. *Adv Enzyme Regul* **51**(1):59-64.

Yokomizo, T., Izumi, T., Chang, K., Takawa, Y. and Shimizu, T. (1997). A G-protein-coupled receptor for leukotriene B4 that mediates chemotaxis. *Nature* **387**(6633):620-624.

Yokomizo, T., Kato, K., Terawaki, K., Izumi, T. and Shimizu, T. (2000). A second leukotriene B(4) receptor, BLT2. A new therapeutic target in inflammation and immunological disorders. *J Exp Med* **192**(3):421-432.

Yoshimura, K., Nakamura, H., Trapnell, B. C., Chu, C. S., Dalemans, W., Pavirani, A., . . . Crystal, R. G. (1991). Expression of the cystic fibrosis transmembrane conductance regulator gene in cells of non-epithelial origin. *Nucleic Acids Res* **19**(19):5417-5423.

Yuan, X., Shan, M., You, R., Frazier, M. V., Hong, M. J., Wetsel, R. A., . . . Kheradmand, F. (2015). Activation of C3a receptor is required in cigarette smoke-mediated emphysema. *Mucosal Immunol* **8**(4):874-885.

Zamecnik, P. C., Raychowdhury, M. K., Tabatadze, D. R. and Cantiello, H. F. (2004). Reversal of cystic fibrosis phenotype in a cultured Delta508 cystic fibrosis transmembrane conductance regulator cell line by oligonucleotide insertion. *Proc Natl Acad Sci U S A* **101**(21):8150-8155.

Zanetti, M. (2004). Cathelicidins, multifunctional peptides of the innate immunity. *J Leukoc Biol* **75**(1):39-48.

Zani, M. L., Baranger, K., Guyot, N., Dallet-Choisy, S. and Moreau, T. (2009). Protease inhibitors derived from elafin and SLPI and engineered to have enhanced specificity towards neutrophil serine proteases. *Protein Sci* **18**(3):579-594.

Zarbock, A., Ley, K., McEver, R. P. and Hidalgo, A. (2011). Leukocyte ligands for endothelial selectins: specialized glycoconjugates that mediate rolling and signaling under flow. *Blood* **118**(26):6743-6751.

Zelek, W. M., Stott, M., Walters, D., Harris, C. L. and Morgan, B. P. (2018). Characterising a pH-switch anti-C5 antibody as a tool for human and mouse complement C5 purification and cross-species inhibition of classical and reactive lysis. *Immunology* **155**(3):396-403.

Zhang, T., Garstka, M. A. and Li, K. (2017). The Controversial C5a Receptor C5aR2: Its Role in Health and Disease. *J Immunol Res* **2017**:8193932.

Zhang, Z. and Schluesener, H. J. (2006). Mammalian toll-like receptors: from endogenous ligands to tissue regeneration. *Cell Mol Life Sci* **63**(24):2901-2907.

Zhou, J., Nefedova, Y., Lei, A. and Gaborilovich, D. (2018). Neutrophils and PMN-MDSC: Their biological role and interaction with stromal cells. *Semin Immunol* **35**:19-28.

Zhou, J., Perelman, J. M., Kolosov, V. P. and Zhou, X. (2013a). Neutrophil elastase induces MUC5AC secretion via protease-activated receptor 2. *Mol Cell Biochem* **377**(1-2):75-85.

Zhou, Y., Song, K., Painter, R. G., Aiken, M., Reiser, J., Stanton, B. A., . . . Wang, G. (2013b). Cystic fibrosis transmembrane conductance regulator recruitment to phagosomes in neutrophils. *J Innate Immun* **5**(3):219-230.

Zimmer, M., Medcalf, R. L., Fink, T. M., Mattmann, C., Lichter, P. and Jenne, D. E. (1992). Three human elastase-like genes coordinately expressed in the myelomonocyte lineage are organized as a single genetic locus on 19pter. *Proc Natl Acad Sci U S A* **89**(17):8215-8219.

Zou, L., Feng, Y., Li, Y., Zhang, M., Chen, C., Cai, J., . . . Chao, W. (2013). Complement factor B is the downstream effector of TLRs and plays an important role in a mouse model of severe sepsis. *J Immunol* **191**(11):5625-5635.

Zuber, J., Fakhouri, F., Roumenina, L. T., Loirat, C. and Fremeaux-Bacchi, V. (2012). Use of eculizumab for atypical haemolytic uraemic syndrome and C3 glomerulopathies. *Nat Rev Nephrol* **8**(11):643-657.

Zwirner, J., Fayyazi, A. and Gotze, O. (1999). Expression of the anaphylatoxin C5a receptor in non-myeloid cells. *Mol Immunol* **36**(13-14):877-884.